Landolt-Börnstein
Numerical Data and Functional Relationships in Science and Technology
New Series / Editor in Chief: W. Martienssen

Group I: Elementary Particles, Nuclei and Atoms
Volume 17

Photon and Electron Interactions with Atoms, Molecules and Ions

Subvolume C
Interactions of Photons and Electrons with Molecules

M. Brunger, R.S. Brusa, S.J. Buckman, M.T. Elford,
Y. Hatano, Y. Itikawa, K. Kameta, G.P. Karwasz,
N. Kouchi, B.G. Lindsay, M.A. Mangan, A. Zecca

Edited by Y. Itikawa

Springer

ISSN 1615-1844 (Elementary Particles, Nuclei and Atoms)

ISBN 3-540-44338-X Springer-Verlag Berlin Heidelberg New York

Library of Congress Cataloging in Publication Data
Zahlenwerte und Funktionen aus Naturwissenschaften und Technik, Neue Serie
Editor in Chief: W. Martienssen
Vol. I/17C: Editor: Y. Itikawa
At head of title: Landolt-Börnstein. Added t.p.: Numerical data and functional relationships in science and technology.
Tables chiefly in English.
Intended to supersede the Physikalisch-chemische Tabellen by H. Landolt and R. Börnstein of which the 6th ed. began publication in 1950 under title:
Zahlenwerte und Funktionen aus Physik, Chemie, Astronomie, Geophysik und Technik.
Vols. published after v. 1 of group I have imprint: Berlin, New York, Springer-Verlag
Includes bibliographies.
1. Physics--Tables. 2. Chemistry--Tables. 3. Engineering--Tables.
I. Börnstein, R. (Richard), 1852-1913. II. Landolt, H. (Hans), 1831-1910.
III. Physikalisch-chemische Tabellen. IV. Title: Numerical data and functional relationships in science and technology.
QC61.23 502'.12 62-53136

Springer-Verlag Berlin Heidelberg New York
a member of BertelsmannSpringer Science+Business Media GmbH

Printed in Germany

Cover layout: Erich Kirchner, Heidelberg
Typesetting: Redaktion Landolt-Börnstein, Darmstadt
Printing and Binding: WB-Druck, Rieden / Allgäu

SPIN: 1087 4891 63/3020 - 5 4 3 2 1 0 – Printed on acid-free paper

Editor

Y. Itikawa
Institute of Space and Astronautical Science
3-1-1 Yoshinodai, Sagamihara, Kanagawa 229-8510, Japan
e-mail: itikawa@pub.isas.ac.jp

Contributors

M. Brunger
Department of Physics
Flinders University of South Australia
GPO Box 2100
Adelaide, 5001, Australia
e-mail: Michael.Brunger@flinders.edu.au
Excitation, *integral elastic cross sections*, *elastic momentum transfer*

R.S. Brusa
Dipartimento di Fisica
Università di Trento
I-38050 Povo, Italy
e-mail: brusa@science.unitn.it
Total scattering cross sections

S.J. Buckman
Atomic and Molecular Physics Laboratories
Research School of Physical Sciences
The Australian National University
Canberra, ACT 0200, Australia
e-mail: stephen.buckman@anu.edu.au
Integral elastic cross sections, *elastic momentum transfer*, *excitation*

M.T. Elford
Atomic and Molecular Physics Laboratories
Research School of Physical Sciences
The Australian National University
Canberra, ACT 0200, Australia
e-mail: mte107@rsphysse.anu.edu.au
Elastic momentum transfer, *integral elastic cross sections*, *excitation*

Y. Hatano
Department of Molecular and Materials Sciences
Kyushu University
Kasuga-Koen 6-1, Kasuga-shi
Fukuoka 816-8580, Japan
e-mail: yhatano@mm.kyushu-u.ac.jp
Photoabsorption, *photoionization*, *neutral dissociation*

Y. Itikawa
Institute of Space and Astronautical Science
3-1-1 Yoshinodai, Sagamihara
Kanagawa 229-8510, Japan
e-mail: itikawa@pub.isas.ac.jp
Electron attachment, index by molecular species

K. Kameta
Institute of Physics Publishing
7th Floor Maruzen Building
Nihonbashi 2-3-10, Chuo-ku
Tokyo 103-8245, Japan
email: kosei.kameta@iop.org
Photoabsorption, *photoionization*, *neutral dissociation*

G.P. Karwasz
Dipartimento di Fisica
Università di Trento
I-38050 Povo, Italy
and
Instytut Fizyki
Pomorska Akademia Pedagogiczna
76200 Słupsk, Poland
e-mail: karwasz@science.unitn.it
Total scattering cross sections

N. Kouchi
Department of Chemistry
Tokyo Institute of Technology
2-12-1 Ookayama, Meguroku
Tokyo 152-8551, Japan
e-mail: nkouchi@chem.titech.ac.jp
Photoabsorption, *photoionization*, *neutral dissociation*

B.G. Lindsay
Physics and Astronomy, MS 108
Rice University
6100 Main Street
Houston, TX 77005-1892, U.S.A.
e-mail: lindsay@rice.edu
Electron-impact ionization

M.A. Mangan
Physics and Astronomy, MS 108
Rice University
6100 Main Street
Houston, TX 77005-1892, U.S.A.
present address:
Sandia National Laboratories
P.O. Box 5800 MS-0871
Albuquerque, NM 87185-0871, U.S.A.
e-mail: mamanga@sandia.gov
Electron-impact ionization

A. Zecca
Dipartimento di Fisica
Università di Trento
I-38050 Povo, Italy
e-mail: zecca@science.unitn.it
Total scattering cross sections

Landolt-Börnstein

Editorial Office
Gagernstr. 8, D-64283 Darmstadt, Germany
fax: +49 (6151) 171760
e-mail: lb@springer.de

Internet
http://www.landolt-boernstein.com/

Preface

Subvolume C of Volume I/17 deals with the interaction of photons and electrons with molecules. Molecules, as a collision partner, behave in almost the same way as atoms, which are dealt with in the subvolume A. Only, but notable, difference between the two kinds of targets is the existence of nuclear degrees of motion in the molecule. The nuclear motion induces additional processes in the photon/electron collisions with molecules, i.e., excitations of rotational and vibrational states and molecular dissociation. It should be noted that the dissociation process results in many different products (atoms, molecules, radicals and ions). Another feature of molecules is their diversity. Their size, shape and composition are varied widely. For these reasons, it is difficult to prepare a comprehensive database for the molecular targets. The subvolume C presents the data compilation that has been made comprehensive as far as possible with an intensive effort of the authors.

Chapter 4 compiles cross sections for the photoabsorption, photoionization and neutral dissociation upon photon interaction with molecules. Considering the importance and the availability of the cross section data, the photon energy is limited to be lower than 60 eV in the chapter. Chapter 5 presents the cross sections for ion production by electron collision with molecules. Productions of positive and negative ions are dealt with separately in the Sections 5.1 and 5.2, respectively. Dissociative collision plays a main part in the ion production. Chapter 6 gives the cross sections for the electron scattering from molecules and the electron-impact excitation of molecules. Section 6.1 gives the total scattering cross section. Sections 6.2-4, respectively, present the cross sections for the elastic scattering, momentum transfer and excitation processes.

As in the previous subvolumes, the style of the presentation of numerical data is not uniform over the subchapters. In all the cases, however, one set of recommended values of the cross section is presented for each process and each molecular species. The quality of the recommended data depends on the process and molecule. For the details, attached comments should be consulted. The molecular species included are different depending on the subchapter. This reflects the availability of the reliable data to be included in the compilation. For the readers' convenience, an index by molecule is given at the end of the subvolume. The present compilation is based mainly on the data available as of early summer of 2000, but additional information, when available, is taken into account as late as spring of 2003.

I thank all the authors for their enormous efforts to survey uncounted number of publications and to critically compile data from them to be assembled here.

Sagamihara, April 2003 **The Editor**

Contents

4 Cross sections for photoabsorption, photoionization, and neutral dissociation of molecules

4.1 Introduction

The interactions of photons with molecules are classified into absorption, scattering, and pair production. In this article, photons of moderate energies particularly in the vacuum ultraviolet (VUV) region are discussed, and therefore only the absorption process is considered. The absorption of a single photon by a molecule in the electronically ground state changes its electronic state from the ground state 0 to a final excited or ionized state j. Its transition probability is expressed in terms of the optical oscillator strength f_j [86Ino1, 95Hat1, 99Hat1].

It is in turn expressed in terms of E_j/R, the transition energy measured in units of the Rydberg energy $R = me^4/(2\hbar^2) = 13.6$ eV, and of M_j^2, the dipole matrix element squared as measured in a_0^2, where the Bohr radius $a_0 = \hbar^2/me^2 = 0.0529$ nm, and m is the electron mass, e the electron charge, and $\hbar$ the Planck's constant divided by 2π, as

$$f_j(E_j) = (E_j / R)M_j^2 \tag{1}$$

A set of E_j and f_j characterizes a discrete spectrum. To discuss a continuous spectrum, one expresses the oscillator strength in a small region of the excitation energy between E and $E + \mathrm{d}E$ as $(\mathrm{d}f/\mathrm{d}E)\mathrm{d}E$, and calls $\mathrm{d}f/\mathrm{d}E$ the oscillator-strength distribution, or, more precisely, the spectral density of the oscillator strength. The total sum of the oscillator strength including discrete and continuous spectra is equal to the total number Z of electrons in the molecule, viz.,

$$\sum_j f_j(E_j) + \int_I^\infty (\mathrm{d}f / \mathrm{d}E)\mathrm{d}E = Z \tag{2}$$

where I represents the (first) ionization potential. Equation (2) is called the Thomas-Kuhn-Reiche (TKR) sum rule.

The oscillator-strength distribution is proportional to the cross section σ_a for the absorption of a photon of energy E. Explicitly one may write

$$\begin{aligned}\sigma_a &= 4\pi^2 \alpha a_0^2 R \frac{\mathrm{d}f}{\mathrm{d}E} \\ &= 8.067 \cdot 10^{-18} \frac{\mathrm{d}f}{\mathrm{d}(E/R)} (\mathrm{cm}^2) \\ &= 109.8 \cdot 10^{-18} \frac{\mathrm{d}f}{\mathrm{d}E} (\mathrm{eV}^{-1}\mathrm{cm}^2)\end{aligned} \tag{3}$$

where $\alpha = e^2/\hbar c = 1/137.04$, the fine structure constant, and c is the velocity of light.

A decisive step in the physical and physicochemical stages of the action of any ionizing radiation on matter is collisions of secondary electrons in a wide energy range with molecules. Ionization and excitation of molecules in collisions with electrons in the energy range higher than about 10^2 eV are well elucidated by the Born-Bethe theory [71Ino1, 83Ino1] and the cross section $Q_j(T)$ at the electron energy T to form the state j at least for optically-allowed transitions is given by

$$Q_j(T) = \frac{4\pi a_0^2 R}{T} M_j^2 \ln\frac{4C_j T}{R} \tag{4}$$

where C_j is a constant and M_j^2 is given by

$$M_j^2 = \int_J^\infty \phi_j(E) \frac{R}{E} \frac{\mathrm{d}f}{\mathrm{d}E} \mathrm{d}E \tag{5}$$

where J is the threshold energy of the state j formation and $\phi_j(E)$ the probability of the state j formation upon photoexcitation of the energy E. Using eq. (4) and further assumptions, Platzman showed that the number of product species j formed per 100 eV absorbed, G_j, is approximately proportional to M_j^2 [62Pla1, 76Shi1]. With the use of the W value, viz., the mean energy, measured in eV, for the production of an ion pair, one may write

$$G_j = \frac{100}{W} \frac{M_j^2}{M_i^2} \tag{6}$$

where M_i^2 is the dipole matrix element squared for ionization, viz.,

$$M_i^2 = \int_I^\infty \eta(E) \frac{R}{E} \frac{\mathrm{d}f}{\mathrm{d}E} \mathrm{d}E \tag{7}$$

where $\eta(E)$ is the quantum yield for photoionization. Since

$$\eta(E) = \sigma_\mathrm{i}(E)/\sigma_\mathrm{a}(E) \tag{8}$$

where $\sigma_\mathrm{i}(E)$ and $\sigma_\mathrm{a}(E)$ are, respectively, the photoionization cross section and the photoabsorption cross section, eq. (6) means that the radiation chemical yield G_j is obtained from optical cross section data. Equation (6) is therefore called the optical approximation. Optical cross section data are, thus, of fundamental importance in understanding not only the interactions of photons with molecules, but also the actions of any ionizing radiation with matter.

Oscillator-strength values have long been measured for various molecules in the wavelength regions at least longer than the near-ultraviolet (UV) region, whereas until recently measurements in the wavelength region shorter than the LiF cutoff at 105 nm (at which the photon energy is 11.8 eV) were relatively few because of experimental difficulties in obtaining appropriate photon sources and because no suitable window materials were available [99Hat1, 87Hat1, 94Hat1, 95Hat2, 95Hat3]. The cutoff energy of 11.8 eV corresponds, roughly speaking, to the ionization potentials of commonly occurring molecules. The sum of the oscillator strengths below 11.8 eV amounts to only a few percent [99Hat1, 87Hat1, 94Hat1, 95Hat2, 95Hat3] of the total sum, which is equal to the total number of electrons in a molecule according to the Thomas-Kuhn-Reiche sum rule. The absorption in the vacuum ultraviolet and soft X-ray (VUV-SX) region is much stronger than in all other wavelength regions. Since there have been remarkable advances in synchrotron radiation (SR) research and related experimental techniques in the VUV-SX region, many measurements in this region are now available [99Hat1, 87Hat1, 94Hat1, 95Hat2, 95Hat3]. Such a situation of SR as a photon source is summarized in Fig. 4.1.1.

Figure 4.1.1 shows the wavelengths of electromagnetic radiation, λ (nm), from the infrared to the γ-ray regions and corresponding photon energies, E (eV) [87Hat1, 94Hat1].

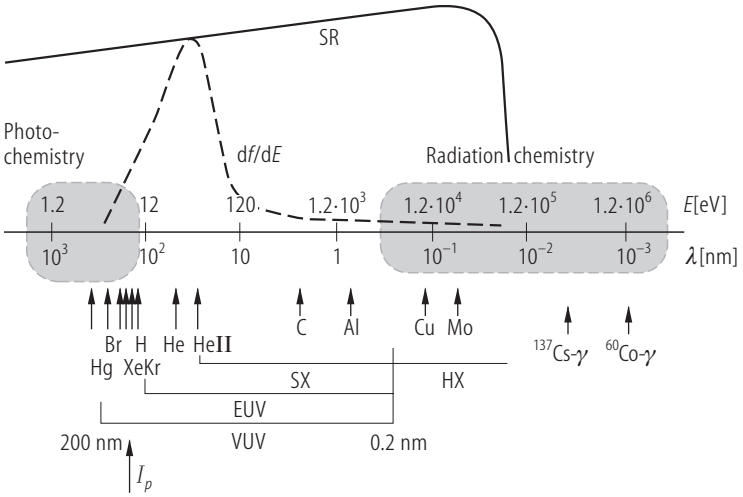

Fig. 4.1.1. Synchrotron radiation (SR) chemistry as a bridge between radiation chemistry and photochemistry. The oscillator strength d*f*/d*E* is shown as a function of wavelength λ and photon energy E. Note the relation $E \cdot \lambda = 1.24 \cdot 10^3$ eV·nm. The intensity of SR is shown as well as the energies of photons from several line sources. VUV, EUV, SX, and HX stand for vacuum ultraviolet, extreme ultraviolet, soft X-ray, and hard X-ray, respectively [87Hat1, 94Hat1]. I_p is the first ionization potential, of which value is in the range 10 – 15 eV for commonly occurring molecules.

Note the relation $E \cdot \lambda = 1.24 \cdot 10^3$ eV·nm. Characteristic X-rays, ^{60}Co-γ rays, and VUV light from discharge lamps are indicated by the arrows. The shaded areas indicate regions for which photon sources, apart from SR, are available and correspond to photochemistry and radiation chemistry. Figure 4.1.1 clearly demonstrates that SR bridges the wide gap in the photon energy between photochemistry and radiation chemistry, i.e., "photon-collision chemistry" and "electron-collision chemistry", respectively.

When a molecule AB absorbs a photon whose energy is larger than its I, AB is not necessarily ionized. In general, there are other decay channels. They are schematically represented as follows:

$AB + h\nu$	$\rightarrow AB^+ + e^-$	direct ionization	(9)
	$\rightarrow AB'$	superexcitation	(10)
AB'	$\rightarrow AB^+ + e^-$	auto-ionization	(11)
	$\rightarrow A + B$	neutral dissociation	(12)
	$\rightarrow AB''$	processes other than (11) and (12).	(13)

In this mechanism, AB is directly ionized (9) and excited (10) to form a superexcited molecule AB' [99Hat1]. The superexcited AB' can ionize (11) or dissociate into neutral fragments (12). The cross section, σ_i, is the sum of the cross sections for both direct and auto-ionization processes, while σ_a is the sum of the cross sections for direct ionization and superexcitation. Since η is defined by eq. (8), the value of $1 - \eta$ shows the importance of the neutral-dissociation processes in the total decay channels of AB' because the process (13) seems not to be important in the decay of such extremely highly excited states. Thus $\sigma_a - \sigma_i = (1 - \eta) \times \sigma_a$ gives the neutral-dissociation cross section, σ_d. As one of the processes (13), ion-pair formation, $AB' \rightarrow A^+ + B^-$, has been extensively studied to clarify the dynamics of superexcited molecules although its cross section is much smaller than those of the processes (11) and (12). The value of η may therefore be smaller than unity in the energy range even above I, which means that the molecules excited into this energy range are not always ionized but use this energy for processes other than ionization. To express the neutral-dissociation processes (12), therefore, the dipole matrix element squared for the neutral-dissociation, M_d^2, is given by

$$M_d^2 = \int_I^\infty [1-\eta(E)]\frac{R}{E}\frac{\mathrm{d}f}{\mathrm{d}E}\mathrm{d}E \tag{14}$$

which corresponds to eq. (5) with

$$\phi_j(E) = 1-\eta(E)$$

and $J = I$. (15)

The electronic structures and dissociation dynamics of molecular superexcited states have been clearly substantiated by electron impact spectroscopy and more recently by spectroscopy combined with SR [99Hat1, 94Hat1, 95Hat2, 83Hat1, 97Kou1, 96Uka1]. It is concluded that a major part of the superexcited states of molecules involves molecular high-Rydberg states which are vibrationally (and/or rotationally), doubly, or inner-core excited, and converge to each of ion states. In some cases non-Rydberg superexcited states are observed.

In electron energy loss experiments of molecules extrapolation of energy loss intensities for incident electron energies much higher than 10^2 eV to zero momentum transfer, i.e., an intensity at the forward scattering, should give, according to the Born-Bethe theory, the corresponding optical oscillator strength [99Hat1]. Brion and coworkers [81Bri1, 85Bri1, 87Gal1, 88Gal1] have extensively investigated such an experimental approach using fast electrons as the virtual photon source, which van der Wiel named "the poor man's synchrotron". They have pointed out some expected characteristics of SR in comparison with virtual photons in understanding ionization and excitation of molecules and made clearly some necessary assumptions to virtual photons instead of real photons. It should be noted here that these two methods, real- and virtual-photon experiments, have complementary roles with each other to substantiate the dynamics of superexcited molecules as well as to understand essential features of the interaction of VUV photons with molecules [95Hat2].

Brion's approach to real-photon experiments using the virtual photon source is also called the electron impact dipole-simulation method, in which some coincidence techniques have been developed for measurements of electronic partial photoionization and ionic photofragmentation cross sections. These measurements are summarized in Table 4.1.1, in comparison with those in real-photon experiments. These simulation techniques have provided a large body of data in comparison with photon experiments of absolute cross sections [87Gal1, 88Gal1]. The photon experiments using synchrotron radiation, which are greatly in progress, can be compared with the simulation measurements [95Hat2].

Table 4.1.1. Photon and electron-impact experiment [88Gal1, 99Hat1].

Photon experiment	Equivalent electron-impact experiment
Total photoabsorption	Electron-energy-loss spectroscopy, dipole (e, e)
Total photoionization	Dipole (e, 2e) or (e, e + ion) (from sums of partial)
Photoelectron spectroscopy	Electron energy loss-ejected electron coincidence, dipole (e, 2e)
Photoionization mass spectrometry	Electron-ion coincidence, dipole (e, e + ion)

4.2 General comments

4.2.1 Scope of the compilation

In this compilation we have restricted our efforts to the absolute cross sections for photoabsorption (σ_a), photoionization (σ_i), and neutral dissociation (σ_d) in the incident photon energy range of 10 – 60 eV or

the energy range of valence-shell excitation and ionization because of the following reasons: (1) the photoabsorption cross section curves of most molecules have their maximum around the energy of 15 – 20 eV, (2) the ionization thresholds of most molecules are located roughly around the energy of 10 – 15 eV, and therefore the photoionization cross section curves should rise at these energies, (3) the absolute measurements of those cross sections in this energy range in particular for polyatomic molecules have still been limited while detailed spectroscopic data have already been obtained bellow the LiF cutoff energy at 11.8 eV, and (4) recent progress in the photoabsorption cross section measurements in this energy range using synchrotron radiation has been remarkable.

Partial photoionization cross sections for the formation of each fragment ion measured by mass spectroscopy have been reported for some molecules. It should be noted, however, that such partial photoionization cross sections are, in general, not so reliable in comparison with the total photoionization cross sections measured by the ionization chamber method because (1) the partial photoionization cross sections are largely affected by the collection efficiency of the spectrometers for their measurements which depends on detected ionic species, their kinetic energies and so on, and thus there are often large discrepancies in measured cross section values between different experiments, and (2) it is necessary for obtaining absolute cross section values to assume that the photoionization quantum yields are unity in the energy range above about 20 eV.

The partial neutral-dissociation cross sections for the formation of each neutral fragment have never been measured so far except excitation spectra of neutral fragments, mainly emissive ones, as far as we know.

The results of the electron impact dipole-simulation method such as those obtained by dipole (e, e), (e, 2e), or (e, e + ion) experiments are adopted instead of real-photon data, only in such a case that they give more reliable cross section data than real-photon experiments or there are no data by real-photon experiments.

The molecules of interest of which cross sections are plotted against the incident photon energy and tabulated are listed below.

diatomic molecules: H_2, N_2, O_2, Cl_2, CO, NO, HF, and HCl
triatomic and relatively simple molecules: H_2O, CO_2, H_2S, N_2O, CS_2, OCS, SO_2, NH_3, and SF_6
silanes: SiH_4 and Si_2H_6
hydrocarbons: CH_4, C_2H_6, C_2H_4, C_2H_2, C_3H_4, cyclo-C_3H_6, C_3H_8, and C_6H_6
halocarbones: CF_4 and CCl_4
alcohols and ethers: CH_3OH, CH_3OCH_3, and $CH_3OC_2H_5$

4.2.2 Evaluation of data

In this compilation we have adopted the most reliable sets of cross sections, σ_a, σ_i, and σ_d, as recommended sets. To do that we have followed the criteria:

(i) data are published in peer reviewed literature,
(ii) data are determined in absolute scale in a direct way,
(iii) data are consistent with others, and
(iv) taking account of inherent accuracy in experimental methods, i.e. the ionization chamber method, electron impact dipole-simulation method, and photoionization mass spectrometric method.

The adopted data are presented in a graphical form. They are also given in a tabular form, if no sharp structures exist in the energy range.

We have not carried out the fitting procedure to determine the recommended values of the cross sections, since two or more data sets in the same energy range were often measured in different ways and thus they have different qualities, i.e. energy resolution, accuracy of cross sections and photon energies, and so on. We have not also combined the σ_a and σ_i to obtain the σ_d following the equation, $\sigma_d = \sigma_a - \sigma_i$, when σ_a and σ_i have different qualities as mentioned above.

In the case of simple diatomic molecules such as H_2 and N_2, sharp peaks are observed with large photoabsorption cross sections, especially in the lower energy range. In real-photon experiments, if the peak shape is narrower than the bandwidth of a monochromator for its measurements the measured photoabsorption cross section suffers from the serious "line saturation effect" [91Cha1]. In such cases, we have adopted the result by the virtual-photon experiments or the dipole-simulation experiments because the integrated photoabsorption cross sections as a function of the photon energy give the correct values of the oscillator strengths of the transitions even if the measured shapes are affected by the energy resolution [91Cha1]. It should be noted, however, that the results of the dipole-simulation experiments are obtained with rather poor energy resolutions, i.e. larger than several tens of meV, in comparison with the real-photon experiments, especially in the lower energy range. It means that some important spectral features in the cross section curves may be sometimes missed in the dipole-simulation experiments. Since, in the case of most polyatomic molecules, besides the simple molecules, sharp peaks with large cross section values have not been seen in their spectra, the line saturation effect may be, in general, not so important in the real-photon data.

In most cases, except those in earlier comparative studies between the real-photon method and the dipole-simulation method, the absolute cross section values obtained by both methods agree with each other [94Hat1]. Comparison of obtained cross section values between the two methods has been discussed in detail [94Hat1, 95Hat1, and references therein] and summarized in conclusion [99Hat1]. It should be noted at least briefly that it is essentially difficult to obtain accurately the absolute values of photoabsorption cross sections in the dipole-simulation experiments and is necessary to use indirect ways for obtaining those as the application of the TKR sum rule to relative values of the cross sections obtained partly with theoretical assumptions. In some cases, further, in relatively earlier dipole-simulation experiments particularly of corrosive molecules upon their electron optics with poorer energy resolutions serious discrepancy from the real-photon experiments has been clearly pointed out in the obtained absolute values of photoabsorption cross sections [91Kam1, 94Hat1, 95Hat2, 95Coo1, 97Oln1, 99Hat1].

As for the absolute values of photoionization quantum yields, i.e., photoionization cross sections, a situation of the dipole-simulation method in comparison with the real-photon experiments is much more serious and controversial because their absolute scales are determined by the assumption that the photoionization quantum yields should be unity around 20 eV, in addition to the above-mentioned difficulty to obtain absolute cross section values in the dipole-simulation experiments.

The real-photon method is essentially more direct and easier as compared with the dipole-simulation method in obtaining absolute values of photoabsorption cross sections, photoionization cross sections, and photoionization quantum yields. In the real-photon method, however, it is needed practically to use big and dedicated facilities of SR in often cases by changing beam-lines there with different types of monochromators depending on used photon-wavelengths and to develop some specific new experimental techniques in the VUV-SX region.

In conclusion as summarized elsewhere [99Hat1], however, these two methods have complementary roles in understanding the interaction of photons with molecules as well as in obtaining the absolute values of the cross sections (σ_a, σ_i, and σ_d).

4.2.3 Other reference books

There have been since last two decades several compilations of photoabsorption and photoionization cross sections. Among them Gallagher et al. [87Gal1, 88Gal1] most comprehensively collected the photoabsorption and partial photoionization cross sections of some 20 molecules. However, most of the data were obtained through the dipole-simulation experiments and the molecules were still limited to simple ones. In the present compilation we intend to collect more real-photon data if they are available, and to extend the range of the molecules. Recent progress in the dipole-simulation method has been summarized by Olney et al. [97Oln1]. The importance of the absolute measurements was well emphasized in the monograph by Berkowitz [79Ber1]. He collected the cross section data until late 1970s and evaluated them by using sum rules including the TKR sum rule.

A review by Koch and Sonntag [79Koc1] devoted several pages to valence-shell excitation and ionization of molecules by synchrotron radiation.

Those who wish to see the detailed discussion on spectral assignments below the LiF cutoff energy should refer to a series of the books by Robin [74Rob1, 75Rob1, 85Rob1] which deals with the molecular spectra above 6 eV. As for oxygen and nitrogen molecules, there are tabulations of photoabsorption and photoionization cross sections in 1979 and 1992 [79Kir1, 92Fen1].

4.3 Glossary and abbreviation

σ_a :	[cm^2]	photoabsorption cross section
σ_i :	[cm^2]	photoionization cross section
σ_d :	[cm^2]	neutral-dissociation cross section
η:		photoionization quantum yield (defined as $\eta = \sigma_i / \sigma_a$, therefor $\sigma_i = \eta \times \sigma_a$ and $\sigma_d = (1 - \eta) \times \sigma_a$)
E:	[eV]	photon energy or excitation energy (E (eV) = $1.24 \cdot 10^3 / \lambda$ (nm), where λ is photon wavelength)
dipole:		electron impact dipole-simulation method

4.4 Cross section data

4.4.1 CCl_4

After the compilation by Gallagher et al. [87Gal1, 88Gal1] in 1987 and 1988, a few sets of photoabsorption cross sections (σ_a) were reported in the valence excitation energy range. Burton et al. [94Bur1] measured the values of σ_a in the photon energy range of 5 - 400 eV by the dipole-simulation method, and these values were then evaluated through the sum rules by Olney et al. [97Oln1], who showed that the results by Burton et al.[94Bur1] should be corrected and put the corrected σ_a values on the web site, ftp://ftp.chem.ubc.ca/pub/cooper. The recommended values of σ_a which were measured with the resolution of 48 meV in the energy range below 30 eV and those with the resolution of 1 eV in the range above 30 eV have been obtained from the web site and adopted as recommended values.

Table 4.4.1.1. Cross section data for CCl_4. Only references mentioned in the present compilation are listed.

Ref.	Method	Cross sections	Photon energy range	Energy resolution
87Gal1, 88Gal1	compilation			
94Bur1	dipole	σ_a, σ_i, partial ion	5 - 400 eV	48 meV or 1 eV
97Oln1	review, dipole	σ_a		

Table 4.4.1.2. Photoabsorption cross sections (σ_a) of CCl_4.

E [eV]	σ_a [10^{-18} cm^2]	E [eV]	σ_a [10^{-18} cm^2]	E [eV]	σ_a [10^{-18} cm^2]
9.1	33.8	15.5	186.5	28.0	67.7
9.4	131.3	16.0	181.0	29.0	57.9
9.5	113.0	16.5	178.9	30.0	46.1
9.7	136.0	17.0	167.7	32.0	29.8
10.0	67.4	17.5	156.7	34.0	20.4
10.0	64.8	17.9	143.2	36.0	14.1
11.0	96.9	19.0	146.4	38.0	10.1
11.3	67.7	20.0	144.4	40.0	8.54
12.0	94.9	21.0	140.1	45.0	6.47
12.5	108.0	22.0	134.6	50.0	6.32
13.0	142.5	23.0	122.3	55.0	6.03
13.5	184.6	24.0	109.7	60.0	5.97
14.2	199.4	25.0	97.3	65.0	5.70
14.5	185.3	26.0	87.5	70.0	5.49
15.0	185.7	27.0	77.2		

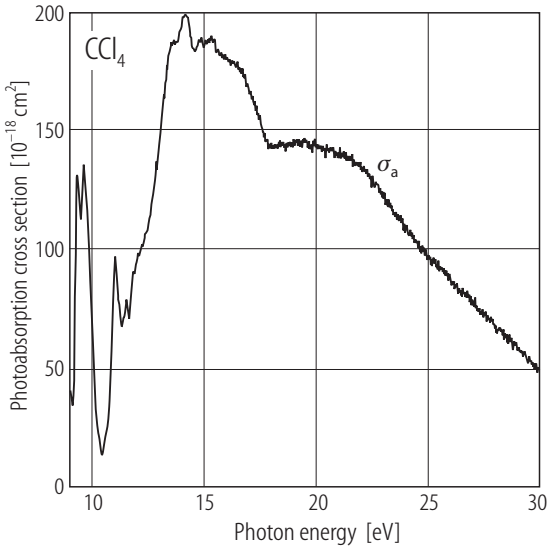

Fig. 4.4.1.1. Photoabsorption cross sections (σ_a) of CCl_4 in the energy range up to 30 eV measured with the energy resolution of 48 meV. See the text as for the data source.

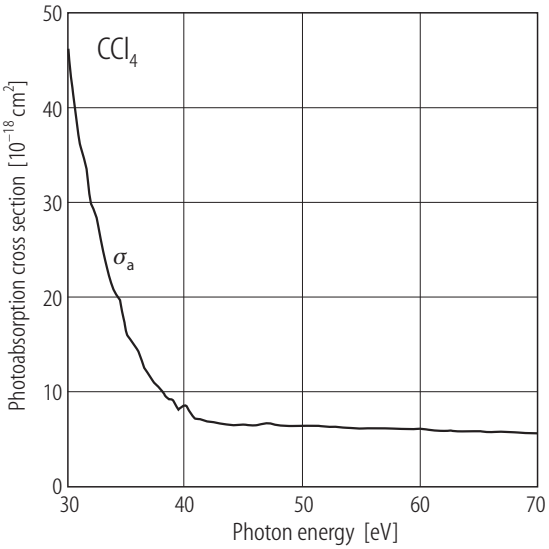

Fig. 4.4.1.2. Photoabsorption cross sections (σ_a) of CCl_4 in the energy range of 30 - 70 eV measured with the energy resolution of 1eV. See the text as for the data source.

4.4.2 CF_4

The most recent values of the photoabsorption cross sections (σ_a) of CF_4 were measured by Au et al. [97Au1] with the dipole-simulation method. Their σ_a values measured with the energy resolution of 48 meV have been adopted. The σ_a curves are plotted in Figs. 4.4.2.1 and 4.4.2.2.

Zhang et al.[89Zha1] measured the values of σ_a and σ_i as well as those of partial photoionization cross sections for the formation of fragment ions through the dipole-simulation method. Au et al. [97Au1], however, showed that the values of Zhang et al. [89Zha1] were seriously in error.

Table 4.4.2.1. Cross section data for CF_4. Only references mentioned in the present compilation are listed.

Ref.	Method	Cross sections	Photon energy range	Energy resolution
97Au1	dipole	σ_a	5 - 200 eV	48 meV or 1 eV
89Zha1	dipole	σ_a, σ_i, partial ion	12 - 200 eV	1 eV

Table 4.4.2.2. Photoabsorption cross sections (σ_a) of CF_4.

E [eV]	σ_a [10^{-18} cm^2]	E [eV]	σ_a [10^{-18} cm^2]	E [eV]	σ_a [10^{-18} cm^2]
12.0	0.38	18.0	48.9	24.0	63.3
12.5	3.86	18.5	52.3	25.0	57.2
13.0	3.56	19.0	50.0	27.0	50.7
13.7	52.0	19.5	59.3	30.0	49.5
14.0	46.0	20.0	52.9	35.0	47.8
14.5	17.3	20.5	63.1	40.1	47.5
14.9	8.48	21.0	64.6	45.0	36.9
15.5	23.5	21.5	67.6	50.0	29.4
15.9	56.0	22.0	70.5	55.0	24.7
16.3	30.7	22.5	70.6	59.9	23.3
17.0	43.3	22.8	64.7		
17.5	45.4	23.1	68.7		

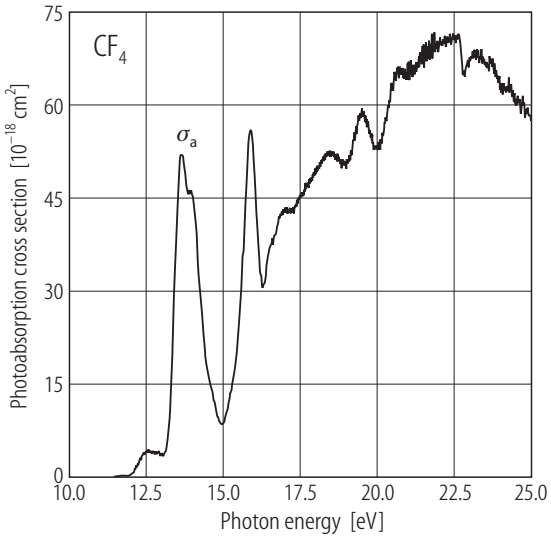

Fig. 4.4.2.1. Photoabsorption cross sections (σ_a) of CF_4 in the energy range of 10 - 25 eV. The data used are from Au et al. [97Au1] with the energy resolution of 48 meV.

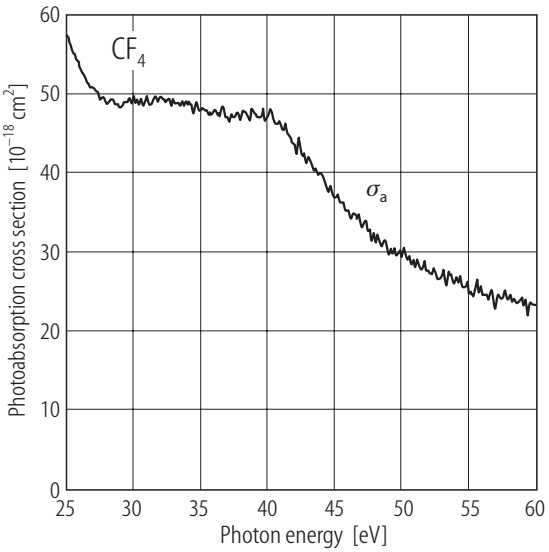

Fig. 4.4.2.2. Photoabsorption cross sections (σ_a) of CF_4 in the energy range of 25 - 60 eV. The data used are from Au et al. [97Au1] with the energy resolution of 48 meV.

4.4.3 CH_3OCH_3

Table 4.4.3.1. Cross section data for CH_3OCH_3.

Ref.	Method	Cross sections	Photon energy range	Energy resolution
92Kam1	photon	σ_a, σ_i, σ_d	13.5 - 24 eV	4 Å (130 meV at 20 eV)

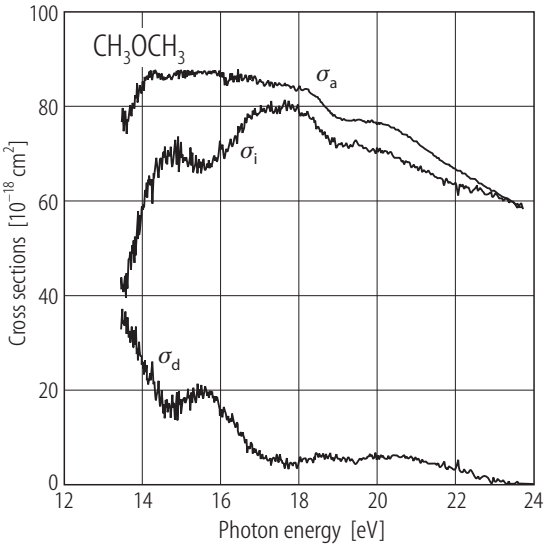

Fig. 4.4.3.1. Photoabsorption (σ_a), photoionization (σ_i), and neutral-dissociation (σ_d) cross sections of CH_3OCH_3 in the energy range of 13.5 - 24 eV. All the data are from [92Kam1].

Table 4.4.3.2. Photoabsorption cross sections (σ_a), photoionization cross sections (σ_i), and neutral-dissociation cross sections (σ_d) of CH_3OCH_3.

E [eV]	σ_a [10^{-18} cm^2]	σ_i [10^{-18} cm^2]	σ_d [10^{-18} cm^2]
13.5	78.8	44.1	34.8
14.0	83.3	58.5	24.9
14.5	86.5	69.8	16.7
15.0	87.1	69.2	18.0
15.5	87.0	66.0	21.0
16.0	86.3	71.2	15.1
16.5	86.2	75.7	10.5
17.0	85.0	78.3	6.71
17.5	84.5	79.9	4.55
18.0	83.5	78.7	4.78
18.5	81.9	75.5	6.41
19.0	77.4	71.8	5.63
19.5	76.9	72.6	4.24
20.0	76.6	70.0	6.62
20.5	75.0	69.0	6.02
21.0	72.5	67.0	5.48
21.5	69.4	65.2	4.26
22.0	66.7	63.7	3.04
22.5	64.6	62.2	2.37
23.0	62.2	60.8	1.37
23.5	59.5	59.5	0.00

4.4.4 $CH_3OC_2H_5$

Table 4.4.4.1. Cross section data for $CH_3OC_2H_5$.

Ref.	Method	Cross sections	Photon energy range	Energy resolution
92Kam1	photon	σ_a, σ_i, σ_d	13.5 - 24 eV	4 Å (130 meV at 20 eV)

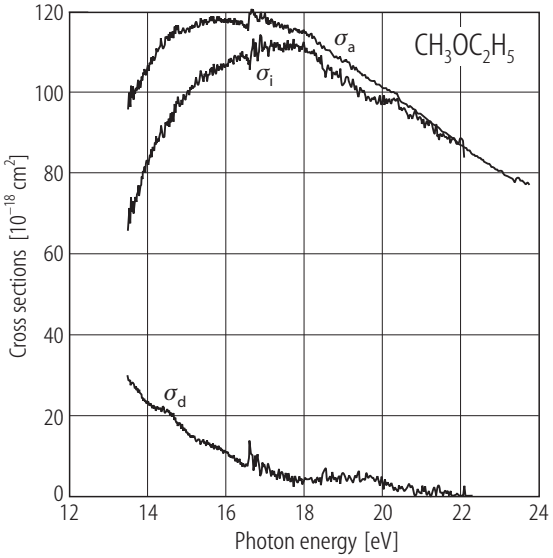

Fig. 4.4.4.1. Photoabsorption (σ_a), photoionization (σ_i), and neutral-dissociation (σ_d) cross sections of $CH_3OC_2H_5$ in the energy range of 13.5 - 24 eV. All the data are from [92Kam1].

Table 4.4.4.2. Photoabsorption cross sections (σ_a), photoionization cross sections (σ_i), and neutral-dissociation cross sections (σ_d) of $CH_3OC_2H_5$.

E [eV]	σ_a [10^{-18} cm^2]	σ_i [10^{-18} cm^2]	σ_d [10^{-18} cm^2]
13.5	99.8	70.9	28.8
14.0	105.7	82.3	23.4
14.5	113.4	92.1	21.3
15.0	115.6	99.9	15.7
15.5	117.9	105.3	12.6
16.0	118.0	106.8	11.2
16.3	117.5	109.1	8.48
17.2	117.5	112.0	5.50
17.5	116.4	112.2	4.19
18.0	115.3	112.2	3.11
18.5	111.2	105.6	5.66
19.0	107.7	102.0	5.64
19.5	104.5	100.3	4.14
20.0	101.5	98.0	3.56
20.5	97.9	95.7	2.15
21.0	94.9	93.9	0.98
21.5	91.0	89.8	1.21

4.4.5 CH_3OH

Photoabsorption cross sections

The photoabsorption cross sections (σ_a) of CH_3OH (methyl alcohol, or methanol) reported until late 1970s were evaluated by Berkowitz [79Ber1] by using the sum rules for the oscillator-strength distribution. The most recent data set which have been adopted in this compilation is that by Burton et al. as shown in Figs. 4.4.5.1 and 4.4.5.2 [92Bur1]. In the energy range below 30 eV, their σ_a values measured with the energy resolution of 48 meV have been adopted, whereas in the energy range above 30 eV, adopted are those measured with the resolution of 1 eV [92Bur1].

Photoionizaton cross sections

Burton et al. [92Bur1] also measured the photoionization cross sections (σ_i), photoionization quantum yields (η), and partial photoionization cross sections for the formation of ionic fragments by the dipole-simulation method with the energy resolution of 1 eV. We have adopted their σ_i and partial photoionization cross sections as recommended values as shown in Figs. 4.4.5.3 - 4.4.5.5. In the energy range of 10 - 12 eV, however, σ_i (and η) curves were measured by Person and Nicole [71Per1] with a much better resolution (1 Å, or 8 meV at 10 eV photon energy) and small scan steps. Thus, those who wish to know the detailed shape of the σ_i curve near the ionization threshold should refer to this reference [71Per1].

Neutral-dissociation cross sections

We have not calculated the σ_d (= σ_a – σ_i) values by using the σ_a and σ_i measured by Burton et al. [92Bur1], which we have adopted as mentioned above. The reasons are: (1) the σ_i values measured by Burton et al. [92Bur1] were obtained providing that $\sigma_i = \sigma_a$ in the energy range above 19.5 eV, which should be confirmed by other experiments, and (2) the present recommended values of σ_a and σ_i were measured with different energy resolutions, therefore, it is not appropriate to combine them to get the σ_d.

Table 4.4.5.1. Cross section data for CH_3OH. Only references mentioned in the present compilation are listed.

Ref.	Method	Cross sections	Photon energy range	Energy resolution
79Ber1	compilation	σ_a	6 eV- 20 keV	
92Bur1	dipole	σ_a, σ_i, partial ion	5 - 360 eV	48 meV or 1 eV
71Per1	photon	σ_a, σ_i, σ_d	10 - 12 eV	1 Å (8 meV at 10 eV)

Table 4.4.5.2. Photoabsorption cross sections (σ_a) of CH_3OH.

E [eV]	σ_a [10^{-18} cm^2]	E [eV]	σ_a [10^{-18} cm^2]	E [eV]	σ_a [10^{-18} cm^2]
10.0	14.6	18.0	49.9	35.0	17.5
11.0	18.4	20.0	47.9	40.0	14.0
12.1	36.7	22.0	42.6	45.0	11.0
12.7	34.0	24.0	36.5	50.0	9.19
14.1	56.4	26.0	31.2	55.0	7.57
15.3	49.3	28.0	26.6	60.0	6.52
16.1	52.5	30.0	23.6		

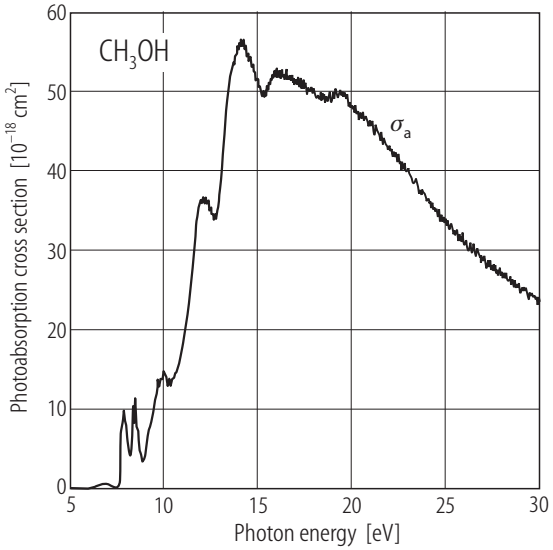

Fig. 4.4.5.1. Photoabsorption cross sections (σ_a) of CH_3OH. The data used are those by Burton et al. [92Bur1] in the energy range of 5 - 30 eV with the resolution of 48 meV.

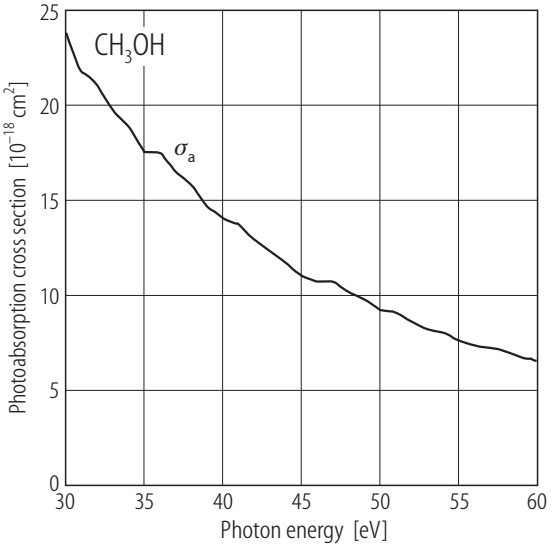

Fig. 4.4.5.2. Photoabsorption cross sections (σ_a) of CH_3OH. The data used are those by Burton et al. [92Bur1] in the energy range of 30 - 60 eV with the resolution of 1 eV.

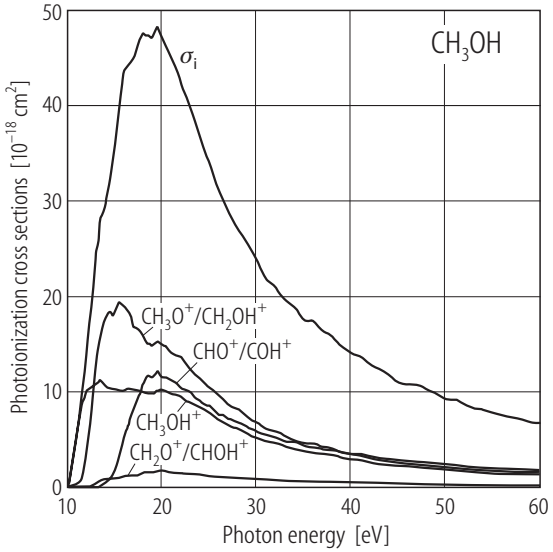

Fig. 4.4.5.3. The partial photoionization cross sections for CH_3OH^+, CH_3O^+/CH_2OH^+, $CH_2O^+/CHOH^+$, and CHO^+/COH^+ along with the σ_i values measured by Burton et al. [92Bur1] with the energy resolution of 1 eV.

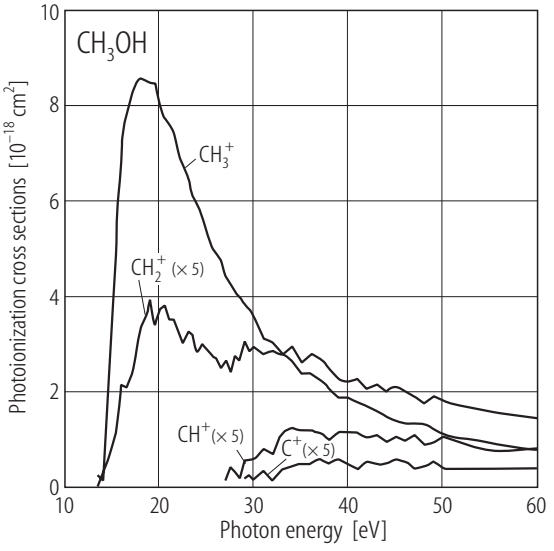

Fig. 4.4.5.4. The partial photoionization cross sections for CH_3^+, CH_2^+, CH^+, and C^+ measured by Burton et al. [92Bur1] with the energy resolution of 1 eV.

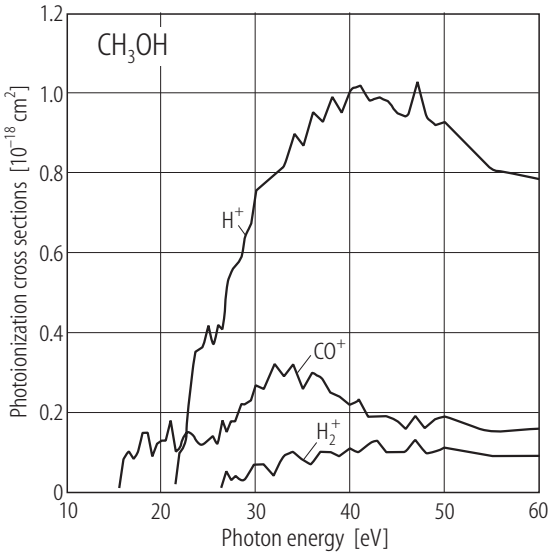

Fig. 4.4.5.5. The partial photoionization cross sections for CO^+, H_2^+, and H^+ measured by Burton et al. [92Bur1] with the energy resolution of 1 eV.

4.4.6 CH_4

After the compilation of photoabsorption (σ_a) and photoionization (σ_i) cross sections by Gallagher et al. in 1987 and 1988 [87Gal1, 88Gal1], there have been a few cross section measurements of CH_4. The most recent and reliable real-photon data of σ_a and σ_i are those by Samson et al. [89Sam1] which have been adopted in the present compilation for the energy range above 13 eV. In the energy range below 13 eV the data of σ_a by dipole-simulation method [93Au1] with the resolution of 48 meV have been adopted because they are the most recent and well determined data from the viewpoint of absolute values within the dipole-simulation experiments. We have calculated the neutral-dissociation cross sections (σ_d) from the σ_a and σ_i by Samson et al [89Sam1]. The recommended values are tabulated in Table 4.4.6.2 and plotted in Fig. 4.4.6.1.

Table 4.4.6.1. Cross section data for CH_4. Only references mentioned in the present compilation are listed.

Ref.	Method	Cross sections	Photon energy range	Energy resolution
87Gal1, 88Gal1	compilation			
89Sam1	photon	σ_a, σ_i, partial ion	13 - 113 eV	1Å (34 meV at 20 eV)
93Au1	dipole	σ_a	7 - 220 eV	48 meV or 1 eV

Table 4.4.6.2. Photoabsorption cross sections (σ_a), photoionization cross sections (σ_i), and neutral-dissociation cross sections (σ_d) of CH_4.

E [eV]	σ_a [10^{-18} cm^2]	σ_i [10^{-18} cm^2]	σ_d [10^{-18} cm^2]
8.6	0.0		
8.7	0.1		
9.1	3.9		
9.1	6.1		
9.4	14.0		
9.7	18.9		
10.1	17.9		
10.4	19.5		
10.9	17.4		
11.4	24.0		
11.9	29.9		
12.7	40.3		
13.0	44.3		
13.1	45.4	3.6	41.8
14.1	49.0	25.5	23.5
15.1	48.1	42.8	5.3
16.1	45.7	44.8	0.9
17.0	43.3	43.3	0
18.0	40.0	40.0	0
19.1	36.9	36.9	0
20.0	34.4	34.4	0
21.0	31.4	31.4	0
22.1	28.6	28.6	0
23.0	26.4	26.4	0
24.3	23.7	23.7	0
25.3	21.4	21.4	0
26.4	19.2	19.2	0
27.0	18.3	18.3	0
28.2	16.7	16.7	0
30.2	13.7	13.7	0
31.8	11.9	11.9	0
34.4	9.60	9.60	0
36.5	8.18	8.18	0
38.7	7.01	7.01	0
40.0	6.42	6.42	0
45.9	4.42	4.42	0
49.6	3.61	3.61	0
56.4	2.53	2.53	0
62.0	1.94	1.94	0

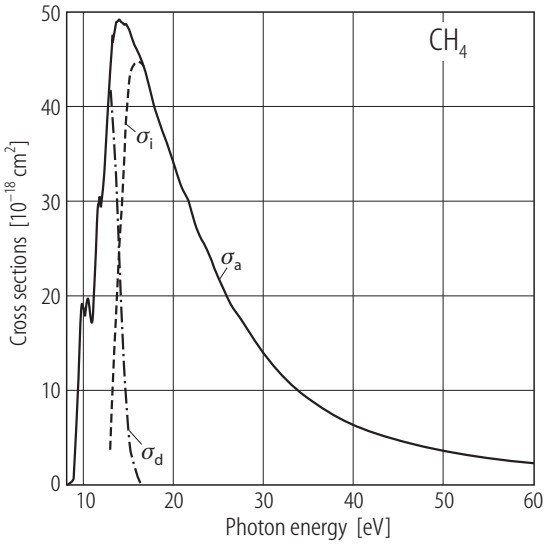

Fig. 4.4.6.1. Photoabsorption (σ_a), photoionization (σ_i), and neutral-dissociation (σ_d) cross sections of CH_4. The data used are the σ_a in 8 - 13 eV by Au et al. [93Au1] with the resolution of 48 meV; the σ_a , σ_i , and σ_d in 13 - 60 eV by Samson et al. [89Sam1] (see text and Table 4.4.6.1).

4.4.7 CO

Photoabsorption cross sections

The photoabsorption cross sections (σ_a) and photoionization quantum yields (η) of CO until late 1970s were reviewed by Berkowitz [79Ber1]. Then Gallagher et al. [87Gal1, 88Gal1] also compiled the photoabsorption (σ_a), photoionization (σ_i), and partial photoionization cross sections.

Chan et al. [93Cha4] measured the values of σ_a in the photon energy range of 7 - 200 eV by the dipole-simulation method, and these values were then evaluated through the sum rules by Olney et al. [97Oln1], who showed that the results by Chan et al. [93Cha4] should be corrected and put the corrected σ_a values on the web site, i.e., ftp://ftp.chem.ubc.ca/pub/cooper. We have hence adopted the corrected σ_a values obtained from the web site, those with the resolution of 48 meV in the energy range below 20 eV and those with the resolution of 1 eV in the range above 20 eV.

Photoionization cross sections and partial photoionization cross sections

Masuoka and Samson [81Mas1] measured the partial photoionization cross sections for the formation of fragment ions, i.e., CO^+, C^+, and O^+, in the energy range of 22 - 138 eV by their real photon experiment. In this energy range the photoionization quantum yields are unity [76Sam1], and therefore the σ_i is equal to the σ_a . They used the σ_a values (= σ_i) by Samson and Haddad [81Sam1] to obtain the absolute values of the partial photoionization cross sections for each fragment ion from the corresponding branching ratios which they measured. The σ_a values by Samson and Haddad [81Sam1] agree well with the recommended values of σ_a mentioned above.

Table 4.4.7.1. Cross section data for CO. Only references mentioned in the present compilation are listed.

Ref.	Method	Cross sections	Photon energy range	Energy resolution
79Ber1	compilation	σ_a, η		
87Gal1, 88Gal1	compilation	σ_a, σ_i		
93Cha4	dipole	σ_a	7 - 200 eV	48 meV or 1 eV
97Oln1	review, dipole	σ_a		
81Mas1	photon	partial ion	22 - 138 eV	1.3 Å (170 meV at 40 eV)
76Sam1	photon	σ_a, σ_i	16 - 40 eV	0.1 Å (3.2 meV at 20 eV)

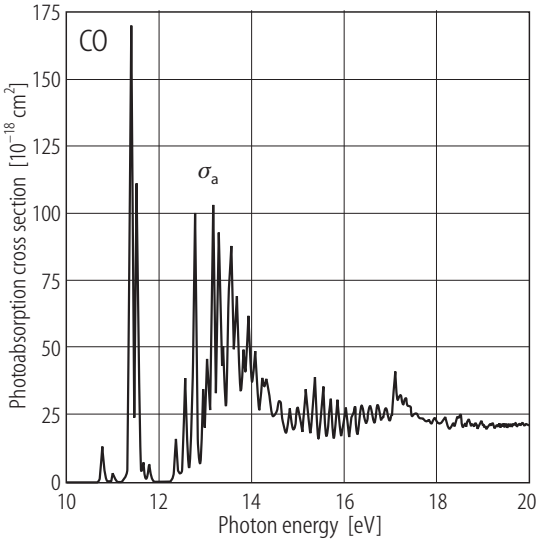

Fig. 4.4.7.1. Photoabsorption cross sections (σ_a) of CO in the energy range of 10 - 20 eV with the resolution of 48 meV. See the text as for the data source.

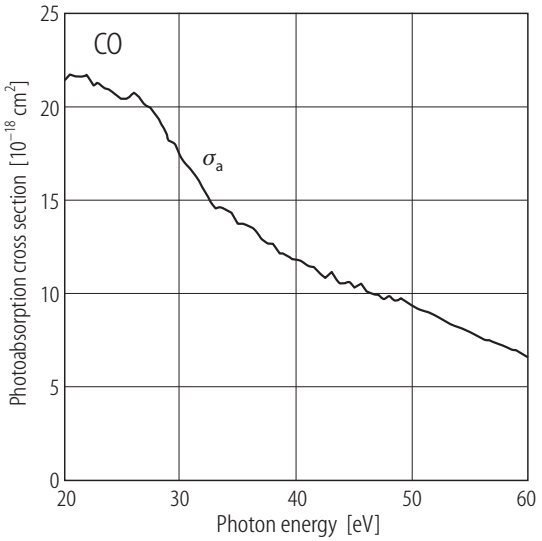

Fig. 4.4.7.2. Photoabsorption cross sections (σ_a) of CO in the energy range of 20 - 60 eV with the resolution of 1 eV. See the text as for the data source.

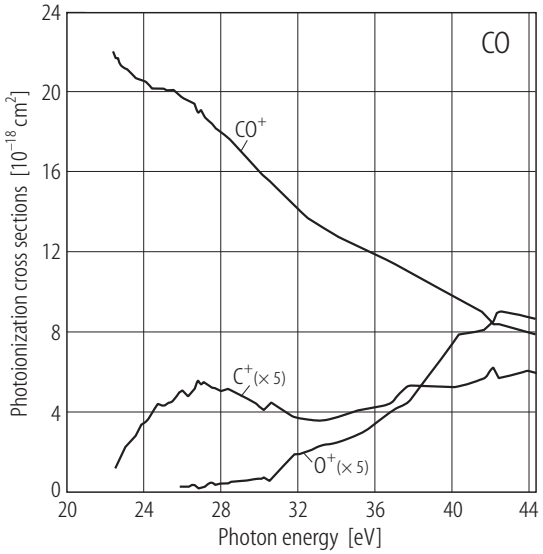

Fig. 4.4.7.3. The partial photoionization cross sections for CO^+, C^+, and O^+ in the energy range of 22 - 44 eV measured by Masuoka and Samson [81Mas1].

4.4.8 CO_2

Table 4.4.8.1. Cross section data for CO_2.

Ref.	Method	Cross sections	Photon energy range	Energy resolution
93Cha6	dipole	σ_a	6 - 203 eV	48 meV or 1 eV
80Hit1	dipole	σ_a, η, partial ion	8 - 75 eV	1 eV
95Sha1	photon	σ_a, σ_i, σ_d	13.7 - 36 eV	0.005 Å (0.16 meV at 20 eV)

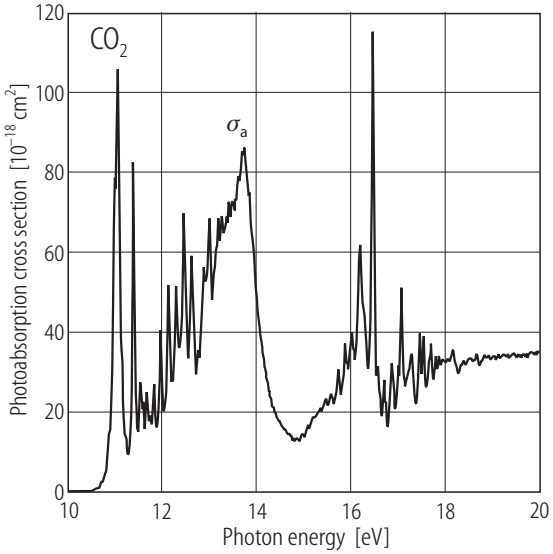

Fig. 4.4.8.1. Photoabsorption cross sections (σ_a) of CO_2 in the energy range of 10 - 20 eV. The data are from [93Cha6] with the resolution of 48 meV.

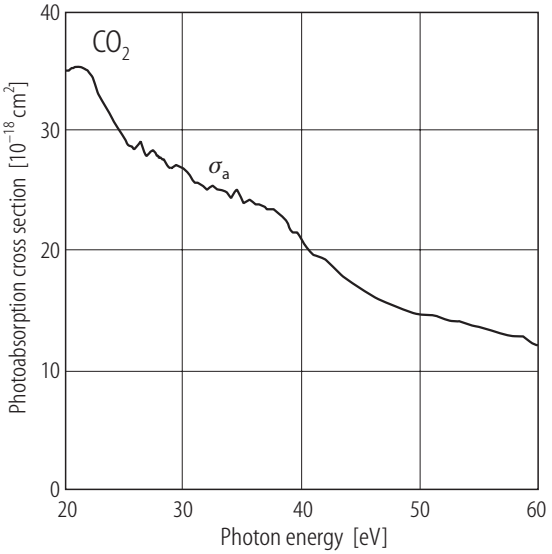

Fig. 4.4.8.2. Photoabsorption cross sections (σ_a) of CO_2 in the energy range of 20 - 60 eV. The data are from [93Cha6] with the resolution of 1 eV.

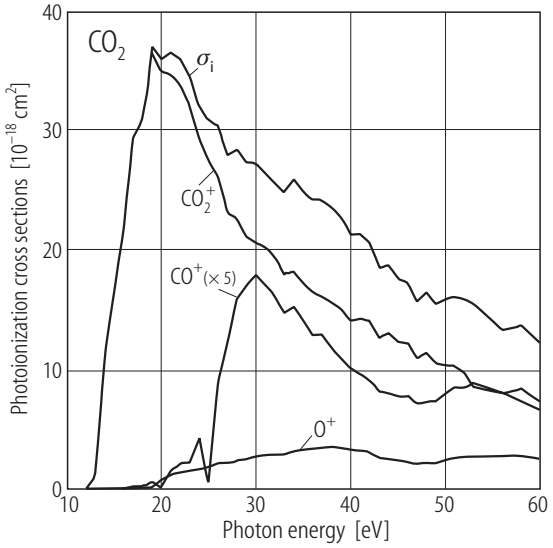

Fig. 4.4.8.3. Photoionization cross sections (σ_i) and the partial photoionization cross sections for the formation of CO_2^+, CO^+, and O^+ from [80Hit1].

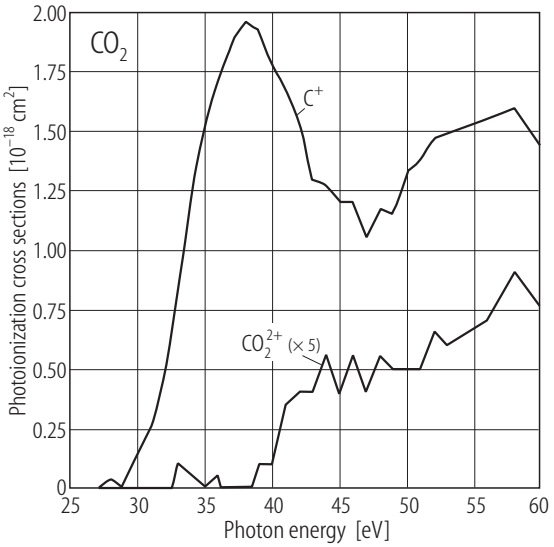

Fig. 4.4.8.4. The partial photoionization cross sections for the formation of C^+ and CO_2^{2+} from [80Hit1].

4.4.9 CS_2

Table 4.4.9.1. Cross section data for CS_2.

Ref.	Method	Cross sections	Photon energy range	Energy resolution
83Wu1	photon	σ_a	16 - 70 eV	1Å (73 meV at 30 eV)

Table 4.4.9.2. Photoabsorption cross sections (σ_a) of CS_2.

E [eV]	σ_a [10^{-18} cm^2]	E [eV]	σ_a [10^{-18} cm^2]	E [eV]	σ_a [10^{-18} cm^2]
16.5	58.5	23.5	29.4	33.0	6.71
16.7	57.1	24.0	26.4	34.0	6.09
17.1	64.4	24.5	23.9	35.0	5.67
17.5	58.8	25.0	22.0	36.0	5.40
17.7	55.2	25.5	20.1	38.0	4.94
17.9	57.6	26.0	18.7	40.0	4.80
18.5	52.6	26.5	17.3	42.0	4.71
19.0	51.3	27.0	15.9	44.0	4.79
19.5	49.0	27.5	14.7	46.0	4.74
20.0	46.9	28.0	13.3	48.0	4.65
20.5	47.0	28.5	12.1	50.0	4.66
21.0	45.2	29.0	11.3	55.0	4.52
21.5	40.4	29.5	10.5	60.0	4.14
22.0	37.3	30.0	9.84	65.1	3.82
22.5	35.9	31.0	8.55		
23.0	32.1	32.0	7.64		

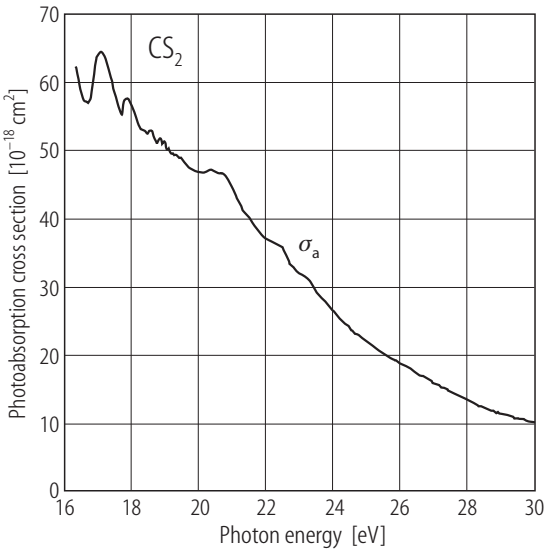

Fig. 4.4.9.1. Photoabsorption cross sections (σ_a) of CS_2 in the energy range of 16 - 30 eV. The data are from [83Wu1].

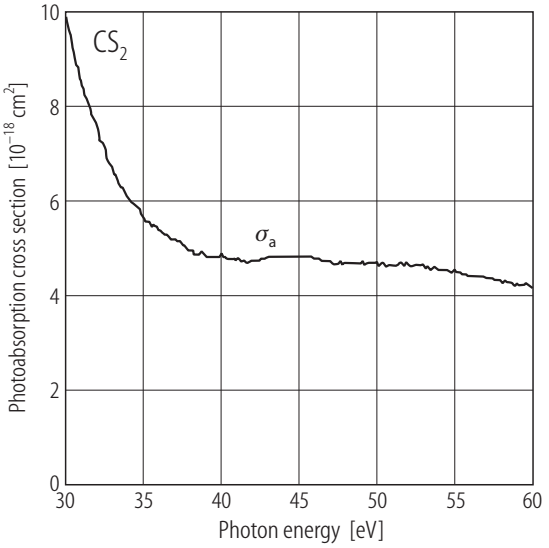

Fig. 4.4.9.2. Photoabsorption cross sections (σ_a) of CS_2 in the energy range of 30 - 60 eV. The data are from [83Wu1].

4.4.10 C_2H_2

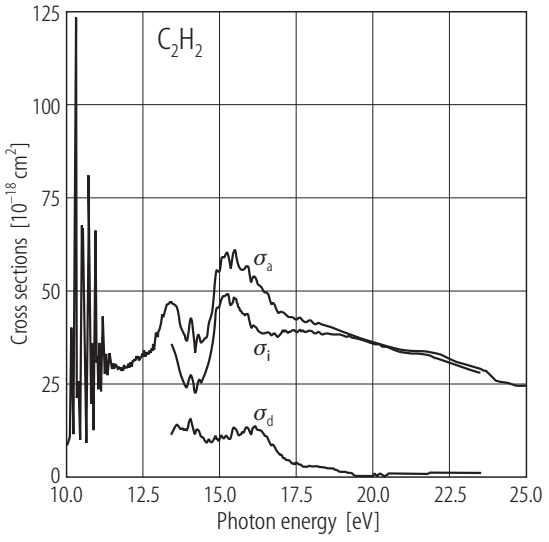

Fig. 4.4.10.1. Photoabsorption (σ_a), photoionization (σ_i), and neutral-dissociation cross sections (σ_d) of C_2H_2 in the energy range of 10 - 25 eV. The data used are the σ_a in the energy range of 10 - 13.5 eV by Cooper et al. [95Coo3] with the resolution of 50 meV; the σ_a in the energy range above 23.5 eV by Cooper et al. [95Coo3] with the resolution of 1 eV; the σ_a, σ_i, and σ_d in the energy range of 13.5 - 23.5 eV by Ukai et al. [91Uka1].

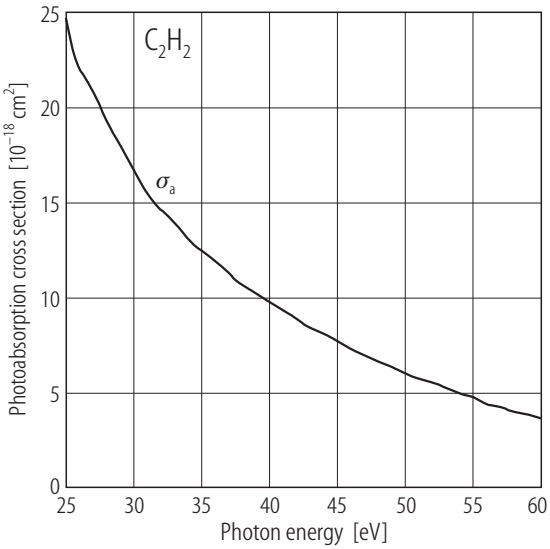

Fig. 4.4.10.2. Photoabsorption cross sections (σ_a) of C_2H_2 in the energy range of 25 - 60 eV. The data are from [95Coo3] with the resolution of 1 eV.

Table 4.4.10.1. Cross section data for C_2H_2.

Ref.	Method	Cross sections	Photon energy range	Energy resolution
91Uka1	photon	σ_a, σ_i, σ_d	13 - 23 eV	4 Å (130 meV at 20 eV)
95Coo3	dipole	σ_a	5.5 - 200 eV	50 meV or 1 eV

Table 4.4.10.2. Photoabsorption cross sections (σ_a), photoionization cross sections (σ_i), and neutral-dissociation cross sections (σ_d) of C_2H_2.

E [eV]	σ_a [10^{-18} cm^2]	σ_i [10^{-18} cm^2]	σ_d [10^{-18} cm^2]
11.5	29.4		
12.0	29.2		
12.5	32.8		
13.0	37.6		
13.5	46.5	34.5	12.1
14.0	36.4	24.0	12.4
14.5	36.7	26.7	10.0
15.0	55.0	45.5	9.48
15.5	61.0	47.9	13.0
16.0	54.3	42.1	12.2
16.5	49.6	38.6	11.0
17.0	44.2	38.3	5.84
18.0	41.9	39.3	2.54
19.0	39.3	38.0	1.26
20.0	36.2	35.9	0.28
21.0	34.1	33.4	0.76
22.0	33.1	32.0	1.07
23.0	30.2	29.3	0.91
24.0	25.8		
25.0	24.4		
27.0	20.7		
30.0	16.7		
35.0	12.4		
40.0	9.8		
45.0	7.7		
50.0	6.0		
55.0	4.7		
60.0	3.7		

4.4.11 C_2H_4

Table 4.4.11.1. Cross section data for C_2H_4.

Ref.	Method	Cross sections	Photon energy range	Energy resolution
97Hol1	photon	σ_a, σ_i, σ_d	10.5 - 24.8 eV	not mentioned
95Coo1	dipole	σ_a	5 - 50 eV	50 meV

Table 4.4.11.2. Photoabsorption cross sections (σ_a), photoionization cross sections (σ_i), and neutral-dissociation cross sections (σ_d) of C_2H_4.

E [eV]	σ_a [10^{-18} cm^2]	E [eV]	σ_a [10^{-18} cm^2]	E [eV]	σ_a [10^{-18} cm^2]
10.5	20.2	17.0	62.3	29.1	24.5
11.0	14.2	17.5	61.4	30.0	22.7
11.5	27.5	18.0	58.1	32.0	19.0
12.0	46.5	19.0	54.7	34.1	16.5
12.5	47.5	20.0	51.6	35.9	14.6
13.0	40.5	21.0	47.6	38.0	13.1
13.5	42.2	22.0	44.1	40.0	11.7
14.0	51.9	23.0	40.9	41.9	10.3
14.5	59.4	24.0	37.5	44.1	8.6
15.0	59.0	25.0	35.6	46.0	8.2
15.5	56.9	26.1	32.1	48.0	7.3
16.0	55.4	27.0	29.5	50.0	6.5
16.5	58.2	28.0	26.7		

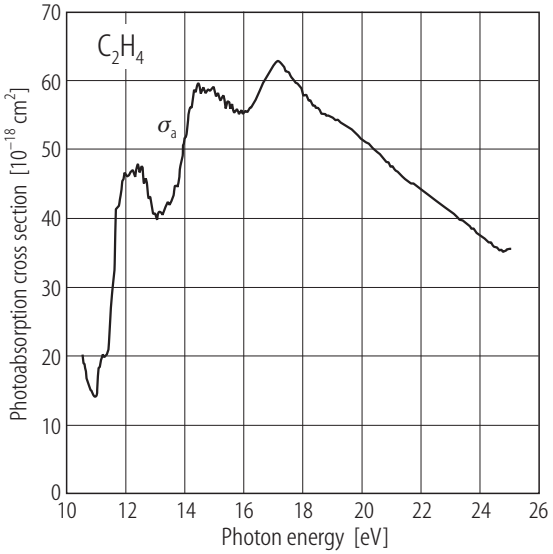

Fig. 4.4.11.1. Photoabsorption cross sections (σ_a) of C_2H_4 in the energy range of 10 - 25 eV. The data used are the those measured by Holland et al.[97Hol1] in the energy range of 10 - 24.8 eV and those by Cooper et al. [95Coo1] in the energy range above 24.8 eV.

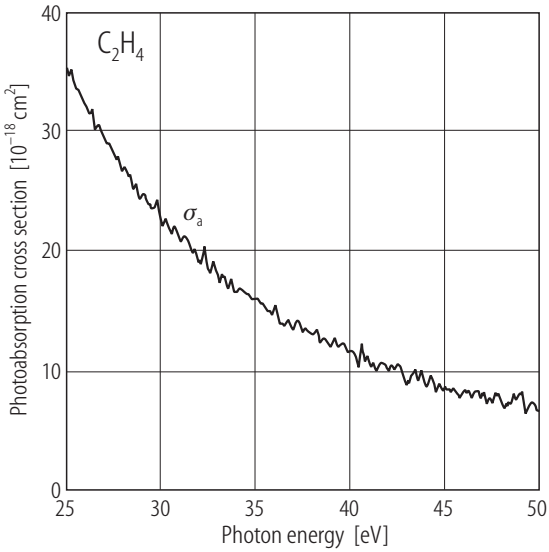

Fig. 4.4.11.2. Photoabsorption cross sections (σ_a) of C_2H_4 in the energy range of 25 - 50 eV. The data are from [95Coo1].

4.4.12 C_2H_6

Table 4.4.12.1. Cross section data for C_2H_6.

Ref.	Method	Cross sections	Photon energy range	Energy resolution
96Kam1	photon	σ_a, σ_i, σ_d	10 - 23 eV	0.9 Å (26 meV at 20 eV)
93Au1	dipole	σ_a	7 - 220 eV	48 meV or 1 eV

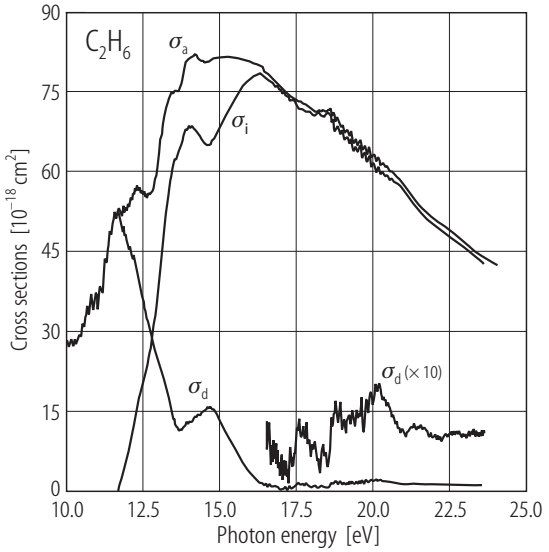

Fig. 4.4.12.1. Photoabsorption (σ_a), photoionization (σ_i), and neutral-dissociation (σ_d) cross sections of C_2H_6 in the energy range of 10 - 24 eV. The data are from [96Kam1].

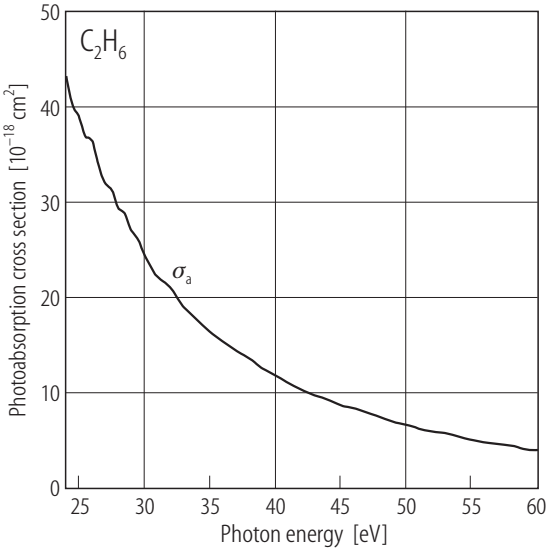

Fig. 4.4.12.2. Photoabsorption cross sections (σ_a) of C_2H_6 in the energy range of 24 - 60 eV. The data are from [93Au1] with the resolution of 1 eV.

Table 4.4.12.2. Photoabsorption cross sections (σ_a), photoionization cross sections (σ_i), and neutral-dissociation cross sections (σ_d) of C_2H_6.

E [eV]	σ_a [10^{-18} cm^2]	σ_i [10^{-18} cm^2]	σ_d [10^{-18} cm^2]
10.0	28.0		
10.5	30.7		
11.0	35.4		
11.5	49.4		
12.0	54.0	6.86	47.2
12.5	56.3	20.6	35.7
13.0	62.5	37.9	24.6
13.5	75.1	61.7	13.5
14.0	81.5	68.6	12.9
14.5	80.9	66.0	14.9
15.0	81.7	68.4	13.4
15.5	81.8	74.2	7.55
16.0	80.9	77.8	3.08
16.5	78.8	77.8	1.01
17.0	75.7	75.2	0.56
17.5	73.6	72.6	1.07
18.0	72.1	71.3	0.81
18.5	71.9	71.4	0.50
19.0	68.9	67.6	1.27
19.5	65.7	64.3	1.44
20.0	63.4	61.7	1.73
20.5	60.5	58.9	1.58
21.0	57.5	56.5	1.05
21.5	53.6	52.4	1.21
22.0	51.0	49.9	1.02
22.5	48.9	47.9	1.09
23.0	46.5	45.4	1.04
23.5	44.2	43.1	1.11
24.0	42.6		
25.0	38.7		
26.0	36.4		
27.0	31.9		
28.0	29.3		
29.0	26.9		
30.0	24.3		
32.0	21.1		
34.0	17.8		
36.0	15.3		
38.0	13.6		
40.0	11.9		
45.0	8.58		
50.0	6.60		
55.0	4.95		
60.0	3.87		

4.4.13 C_3H_4

Table 4.4.13.1. Cross section data for C_3H_4.

Ref.	Method	Cross sections	Photon energy range	Energy resolution
99Hol1	photon	σ_a, σ_i, σ_d	9.7 - 35 eV	1 Å (32 meV at 20 eV)

Table 4.4.13.2. Photoabsorption cross sections (σ_a), photoionization cross sections (σ_i), and neutral-dissociation cross sections (σ_d) of C_3H_4.

E [eV]	σ_a [10^{-18} cm^2]	σ_i [10^{-18} cm^2]	σ_d [10^{-18} cm^2]
10.0	30.7	8.43	22.2
10.5	34.0	22.3	11.7
11.0	50.5	27.2	23.2
11.3	58.1	29.1	29.1
11.5	55.5	29.6	25.9
12.0	43.3	27.9	15.4
12.5	38.7	27.1	11.5
13.0	45.6	35.8	9.78
13.5	56.8	48.0	8.79
14.0	63.1	51.9	11.3
14.5	62.7	49.3	13.4
15.0	58.3	50.5	7.82
15.5	58.4	54.8	3.57
16.0	60.0	59.5	0.47
17.0	62.9	59.3	3.63
18.0	69.0	67.3	1.61
19.0	72.5	71.8	0.70
20.0	71.8		
22.0	60.0		
24.0	47.8		
26.0	40.9		
28.0	35.5		
30.0	30.4		
32.0	26.3		
34.0	23.5		

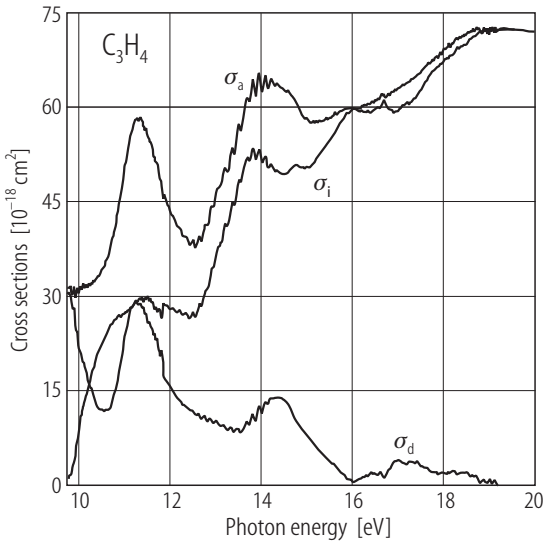

Fig. 4.4.13.1. Photoabsorption (σ_a), photoionization (σ_i), and neutral-dissociation (σ_d) cross sections of C_3H_4 in the energy range of 10 - 20 eV. All the data are from [99Hol1].

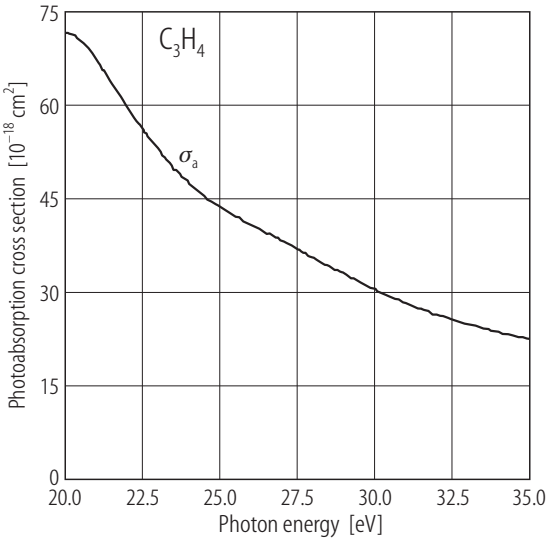

Fig. 4.4.13.2. Photoabsorption cross sections (σ_a) of C_3H_4 in the energy range of 20 - 35 eV. The data are from [99Hol1].

4.4.14 C_3H_8

Table 4.4.14.1. Cross section data for C_3H_8.

Ref.	Method	Cross sections	Photon energy range	Energy resolution
96Kam1	photon	σ_a, σ_i, σ_d	10 - 23 eV	0.9 Å (26 meV at 20 eV)
93Au1	dipole	σ_a	7 - 220 eV	48 meV or 1 eV

Table 4.4.14.2. Photoabsorption cross sections (σ_a), photoionization cross sections (σ_i), and neutral-dissociation cross sections (σ_d) of C_3H_8.

E [eV]	σ_a [10^{-18} cm^2]	σ_i [10^{-18} cm^2]	σ_d [10^{-18} cm^2]
11.0	56.9	0.07	56.9
11.5	58.2	4.73	53.5
12.0	62.9	16.6	46.3
12.5	78.7	34.2	44.5
13.0	84.8	48.6	36.2
13.5	92.5	67.0	25.5
14.0	104	83.3	20.3
14.5	109	93.7	15.4
15.0	112	96.6	15.4
15.5	114	103	10.9
16.0	115	110	4.97
16.5	113	111	1.94
17.0	110	109	1.16
17.5	110	108	1.19
18.0	106	104	1.40
18.5	102	99.9	1.80
19.0	98.2	95.5	2.65
19.5	95.4	92.3	3.11
20.0	91.9	89.7	2.26
20.5	86.3	84.3	1.95
21.0	82.4	80.3	2.12
21.5	78.4	75.9	2.51
22.0	74.1	71.6	2.45
22.5	70.2	68.3	1.88
23.0	66.9	65.6	1.35
23.5	63.7	62.6	1.10
24.0	63.3		
26.0	54.1		
28.0	43.0		
30.0	36.4		
32.0	29.9		
34.0	25.3		
36.0	21.7		
38.0	19.0		
40.0	16.5		
45.0	11.7		
50.0	9.10		
55.0	6.87		
60.0	5.47		

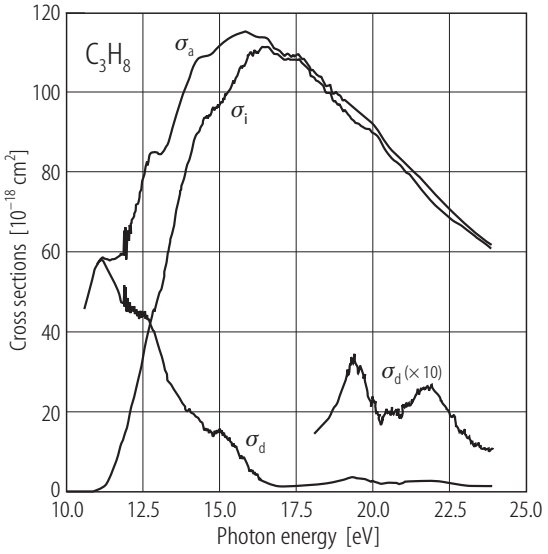

Fig. 4.4.14.1. Photoabsorption (σ_a), photoionization (σ_i), and neutral-dissociation cross sections (σ_d) of C_3H_8 in the energy range of 10 - 24 eV. The data are from [96Kam1].

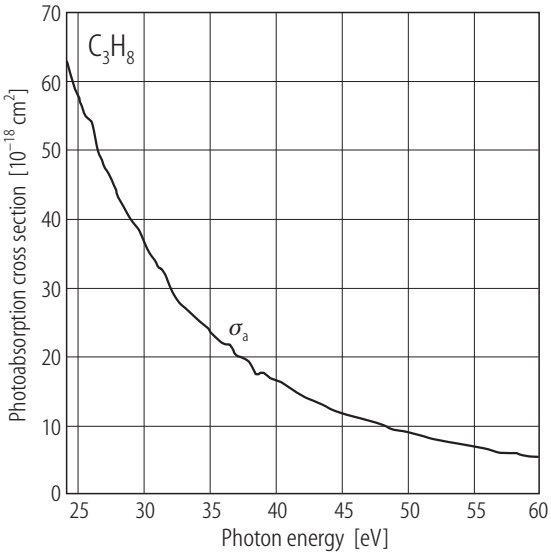

Fig. 4.4.14.2. Photoabsorption cross sections (σ_a) of C_3H_8 in the energy range of 24 - 60 eV. The data are from [93Au1] with the resolution of 1 eV.

4.4.15 C_6H_6

Photoabsorption cross sections

The photoabsorption spectrum of C_6H_6 (benzene) has been extensively studied below the photon energy of 10 eV [67Her1]. However, there have been only a few measurements in the energy range above 10 eV.

Koch and Sonntag [79Koc1] and Berkowitz [79Ber1] reviewed the photoabsorption cross sections (σ_a) published until 1978 in the energy range both higher and lower than 10 eV. The most recent results obtained in the synchrotron radiation experiments are those by Rennie et al. [98Ren1] which have been adopted in the present compilation because their values were reasonably evaluated by the sum rules. Their cross sections are, however, somewhat larger than previous results [76Koc1, 73Yos1].

Photoionizaton cross sections

The photoionization cross sections (σ_i) and photoionization quantum yields of C_6H_6 measured by Rennie et al. [98Ren1] in the energy range of 9 - 20 eV have been adopted in this compilation along with their photoabsorption cross sections as explained above. Only their measurements have been done by means of synchrotron radiation so far, and their photoionization quantum yields are almost consistent with those measured by Yoshino et al. [73Yos1] who used a discharge lamp.

Neutral-dissociation cross sections

The neutral-dissociation cross sections ($\sigma_d = \sigma_a - \sigma_i$) by Rennie et al. [98Ren1] in the energy range of 9 - 20 eV have been adopted as well.

Table 4.4.15.1. Cross section data for C_6H_6. Only references mentioned in the present compilation are listed.

Ref.	Method	Cross sections	Photon energy range	Energy resolution
79Koc1	compilation	σ_a		
79Ber1	compilation	σ_a , η		
76Koc1	photon	σ_a	5 - 35 eV	1 Å (32 meV at 20 eV)
73Yos1	photon	σ_a, η	5.6 - 20.7 eV	2 Å (64.5 meV at 20 eV)
98Ren1	photon	σ_a, σ_i, σ_d	9 - 35.4 eV	not mentioned

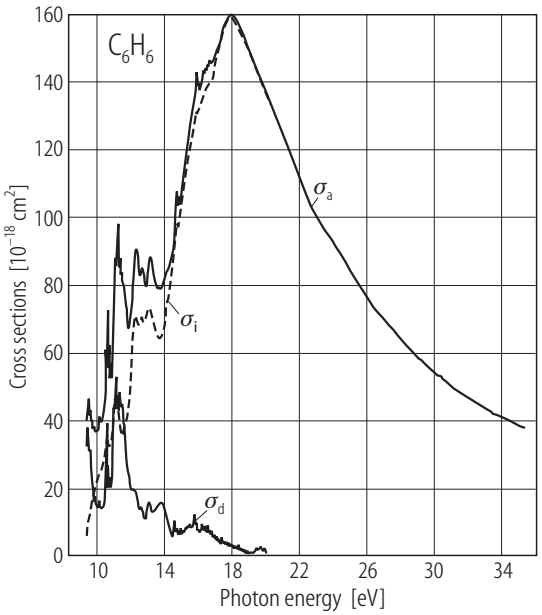

Fig. 4.4.15.1. Photoabsorption (σ_a), photoionization (σ_i), and neutral-dissociation (σ_d) cross sections of C_6H_6. The data are from Rennie et al. [98Ren1].

Table 4.4.15.2. Photoabsorption cross sections (σ_a), photoionization cross sections (σ_i), and neutral-dissociation cross sections (σ_d) of C_6H_6.

E [eV]	σ_a [10^{-18} cm^2]	σ_i [10^{-18} cm^2]	σ_d [10^{-18} cm^2]
10.0	38.2	23.1	14.0
10.5	71.2	38.6	25.8
11.0	87.3	42.1	44.6
11.5	79.1	36.7	40.5
12.0	79.5	63.5	19.2
12.5	83.7	69.7	13.7
12.9	82.6	71.6	11.9
13.5	79.6	65.5	13.2
14.1	84.1	74.4	10.0
14.6	105.4	98.1	9.6
15.1	114.7	111.1	6.4
15.5	129.3	123.5	8.2
16.1	138.9	135.1	6.7
16.5	144.8	139.1	8.4
17.0	148.4	146.8	4.9
17.5	156.2	155.8	4.0
18.0	159.6	158.1	2.5
18.5	154.9	153.2	1.3
19.1	147.1	147.0	0.6
19.4	143.7	143.9	0.7
20.0	136.7	136.5	1.0
21.0	124.3		
22.1	109.1		
23.0	99.9		
24.3	89.7		
25.3	81.0		
26.4	73.2		
27.0	69.8		
28.2	62.6		
29.5	55.7		
30.2	52.9		
31.0	49.6		
32.6	44.3		
33.5	41.8		
34.4	39.7		
35.3	37.7		

4.4.16 Cl_2

Table 4.4.16.1. Cross section data for Cl_2.

Ref.	Method	Cross sections	Photon energy range	Energy resolution
97Oln2	dipole	σ_a	2 - 400 eV	48 meV or 1 eV
87Sam1	photon	σ_a , σ_i , partial ion	12 - 83 eV	

Table 4.4.16.2. Photoabsorption cross sections (σ_a) of Cl_2.

E [eV]	σ_a [10^{-18} cm^2]	E [eV]	σ_a [10^{-18} cm^2]	E [eV]	σ_a [10^{-18} cm^2]
12.0	44.4	18.1	70.1	40.3	2.67
12.5	69.0	18.5	68.0	42.3	2.35
12.8	102	19.0	66.7	44.3	2.21
13.2	79.3	19.6	65.5	46.3	2.24
13.4	88.3	20.0	64.6	48.3	2.29
13.9	60.6	22.0	57.1	50.3	2.41
14.6	86.0	24.0	49.0	52.3	2.54
15.0	70.9	26.0	38.5	54.3	2.48
15.2	75.4	28.0	29.7	56.3	2.55
15.5	72.9	30.0	20.1	58.3	2.58
16.0	74.0	32.0	12.9	60.3	2.61
16.6	74.7	34.3	7.64		
17.0	74.4	36.3	4.91		
17.5	72.6	38.3	3.40		

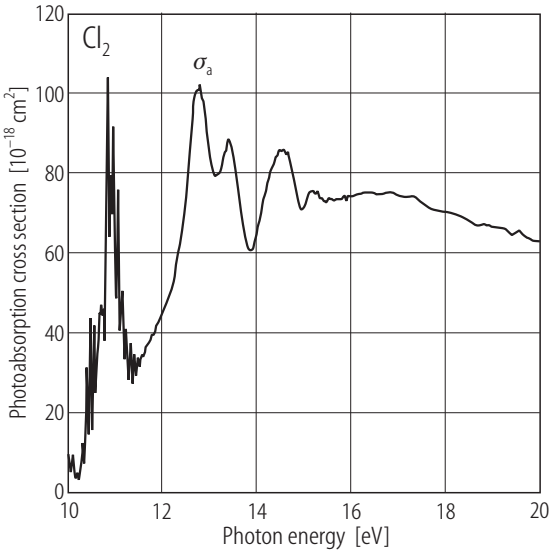

Fig. 4.4.16.1. Photoabsorption cross sections (σ_a) of Cl_2 in the energy range of 10 - 20 eV. The data are from [97Oln2] with the resolution of 48 meV.

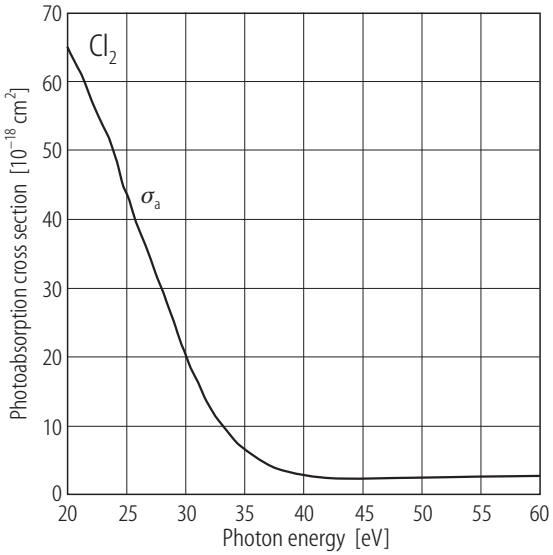

Fig. 4.4.16.2. Photoabsorption cross sections (σ_a) of Cl_2 in the energy range of 20 - 60 eV. The data are from [97Oln2] with the resolution of 1 eV.

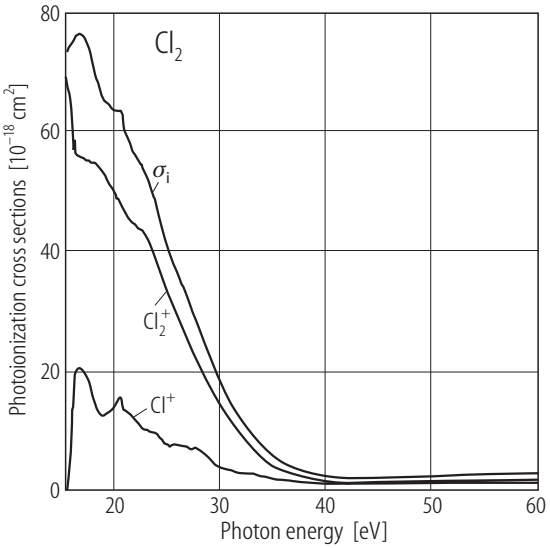

Fig. 4.4.16.3. The partial photoionization cross sections for the formation of Cl_2^+ and Cl^+ along with the photoionization cross sections (σ_i). The data are from [87Sam1].

4.4.17 cyclo-C_3H_6

There have been only several cross section measurements for cyclo-C_3H_6 (cycloparopane) in the energy range of the present interest. The most recent measurement of the σ_a, σ_i, and σ_d above 10 eV are those by Kameta et al. [99Kam1] which we have included in this compilation for the energy range of 10 - 24 eV. In the energy range above 24 eV, the σ_a values by Koizumi et al. [85Koi1] have been adopted. Both data sets were measured by the combination of synchrotron radiation and a double ionization chamber. Kameta et al. [99Kam1] used metallic thin film windows, while Koizumi et al. [85Koi1] measured without any window except an LiF window in the energy range below 11.8 eV. The energy resolutions were 1 Å (32 meV at 20 eV photon energy) [99Kam1] and 8 Å (580 meV at 30 eV photon energy) [85Koi1]. The recommended values are tabulated in Table 4.4.17.2 and plotted in Fig. 4.4.17.1.

Table 4.4.17.1. Cross section data for cyclo-C_3H_6. Only references mentioned in the present compilation are listed.

Ref.	Method	Cross sections	Photon energy range	Energy resolution
99Kam1	photon	σ_a, σ_i, σ_d	10 - 24 eV	1 Å (32 meV at 20 eV)
85Koi1	photon	σ_a	10 - 41 eV	8 Å (580 meV at 30 eV)

Table 4.4.17.2. Photoabsorption cross sections (σ_a), photoionization cross sections (σ_i), and neutral-dissociation cross sections (σ_d) of cyclo-C_3H_6.

E [eV]	σ_a [10^{-18} cm^2]	σ_i [10^{-18} cm^2]	σ_d [10^{-18} cm^2]
10.5	54.0	2.7	51.3
11.0	38.0	6.6	31.4
11.5	40.1	14.1	26.0
12.0	48.4	23.5	24.9
12.5	62.4	30.4	32.0
13.0	105.0	56.8	48.2
13.5	100.9	75.9	25.1
14.0	79.7	71.6	8.11
14.5	86.0	74.1	11.9
15.0	91.5	76.5	15.0
15.5	89.0	75.4	13.7
16.0	88.4	80.2	8.14
16.5	87.6	82.3	5.22
17.0	88.5	85.7	2.82
17.5	91.2	89.2	2.03
18.0	90.5	86.8	3.69
18.5	89.6	84.9	4.73
19.0	87.7	82.4	5.31
19.5	84.8	81.0	3.76
20.0	82.1	79.6	2.46
20.5	79.3	77.6	1.75
21.0	76.5	75.1	1.41
21.5	73.6	71.9	1.77
22.0	70.6	68.9	1.72
22.5	67.2	65.6	1.63
23.0	63.3	61.8	1.54
23.5	60.0	59.1	0.93
24.0	57.5		
25.0	51.6		
26.0	46.4		
27.0	42.4		
28.0	38.6		
29.0	35.1		
30.0	32.2		
31.0	29.7		
32.0	27.5		
33.0	25.9		
34.0	24.3		
35.0	23.0		

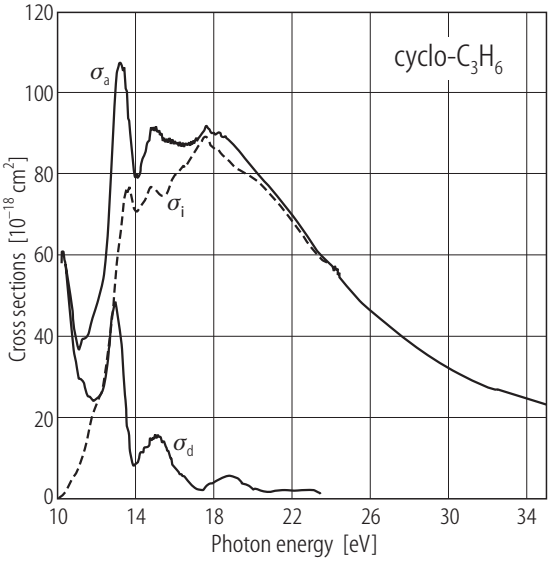

Fig. 4.4.17.1. Photoabsorption (σ_a), photoionization (σ_i), and neutral-dissociation (σ_d) cross sections of cyclo-C_3H_6. The data used are the σ_a , σ_i , and σ_d in the energy range of 10 - 24 eV by Kameta et al. [99Kam1] and the σ_a in the energy range of 24 - 35 eV by Koizumi et al. [85Koi1].

4.4.18 HCl

Table 4.4.18.1. Cross section data for HCl.

Ref.	Method	Cross sections	Photon energy range	Energy resolution
97Dyc1	dipole	σ_a	5 - 280 eV	48 meV or 1 eV

Table 4.4.18.2. Photoabsorption cross sections (σ_a) of HCl.

E [eV]	σ_a [10^{-18} cm^2]	E [eV]	σ_a [10^{-18} cm^2]	E [eV]	σ_a [10^{-18} cm^2]
17.1	44.5	23.0	31.5	33.0	6.00
17.5	45.3	23.5	29.2	34.0	4.79
18.0	44.4	24.0	28.1	35.0	3.69
18.5	44.9	24.5	27.7	36.0	3.14
19.1	42.9	25.0	24.8	38.0	2.22
19.5	41.6	26.0	21.4	40.0	1.62
20.0	39.5	27.0	18.8	45.0	1.23
20.5	39.9	28.0	16.2	50.0	1.25
21.0	36.8	29.0	13.6	55.0	1.22
21.5	36.0	30.0	11.2	60.0	1.24
22.0	34.8	31.0	9.10		
22.5	33.4	32.0	7.57		

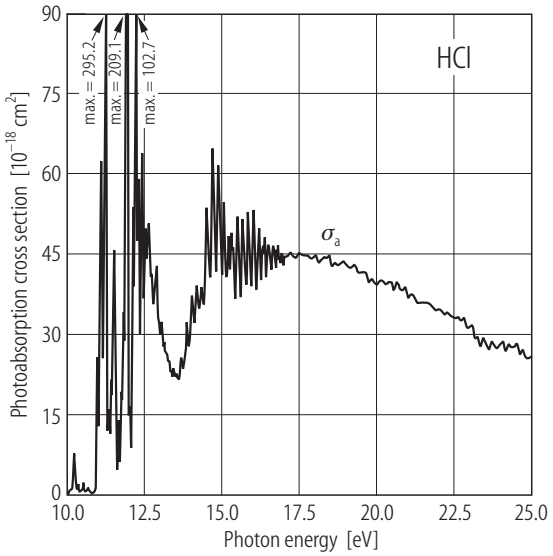

Fig. 4.4.18.1. Photoabsorption cross sections (σ_a) of HCl in the energy range of 10 - 25 eV. The data are from [97Dyc1] with the resolution of 48 meV.

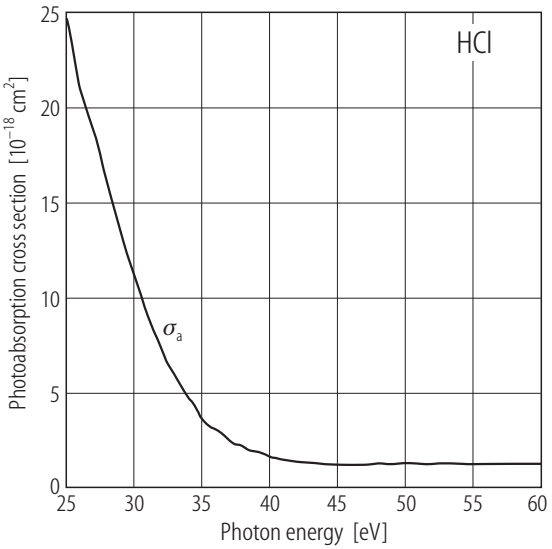

Fig. 4.4.18.2. Photoabsorption cross sections (σ_a) of HCl in the energy range of 25 - 60 eV. The data are from [97Dyc1] with the resolution of 1 eV.

4.4.19 HF

Table 4.4.19.1. Cross section data for HF.

Ref.	Method	Cross sections	Photon energy range	Energy resolution
84Hit1	dipole	σ_a	9 - 40 eV	60 meV or 500 meV
83Car1	dipole	partial ion	16 - 60 eV	1 eV

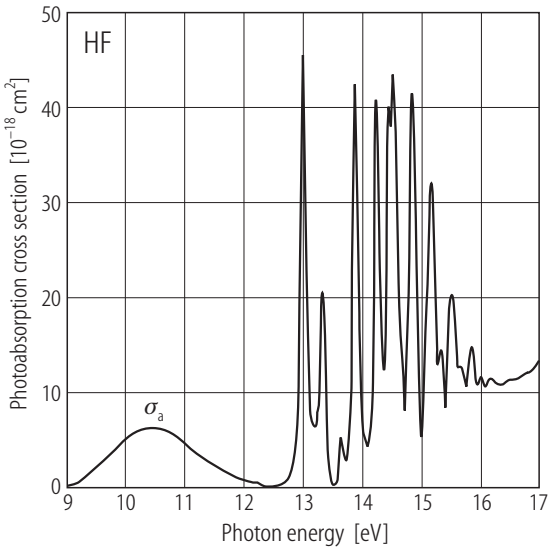

Fig. 4.4.19.1. Photoabsorption cross sections (σ_a) of HF in the energy range of 9 - 17 eV. The data are from [84Hit1] with the resolution of 60 meV.

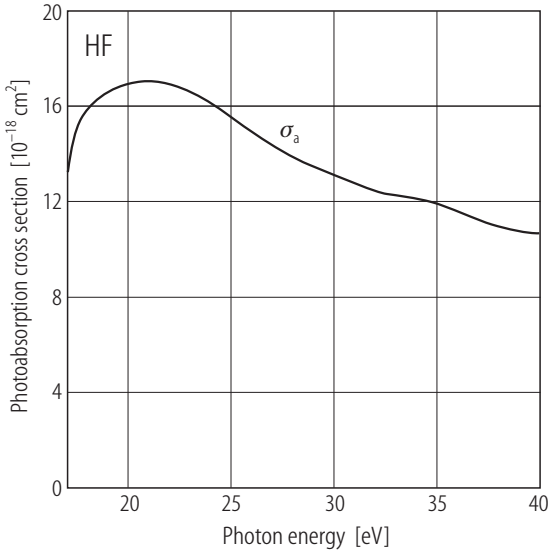

Fig. 4.4.19.2. Photoabsorption cross sections (σ_a) of HF in the energy range of 17 - 40 eV. The data are from [84Hit1] with the resolution of 500 meV.

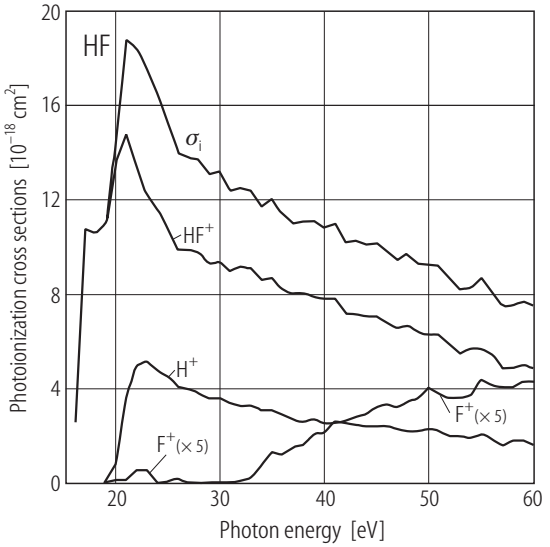

Fig. 4.4.19.3. The partial photoionization cross sections for the formation of HF^+, F^+, and H^+ along with the photoionization cross section (σ_i). The data are from [83Car1].

Table 4.4.19.2. Photoabsorption cross sections (σ_a) of HF.

E [eV]	σ_a [10^{-18} cm^2]	E [eV]	σ_a [10^{-18} cm^2]	E [eV]	σ_a [10^{-18} cm^2]
8.60	0.00	13.9	42.5	17.0	13.2
9.00	0.08	14.1	4.32	18.0	15.9
9.50	1.84	14.2	40.9	19.0	16.6
10.0	4.95	14.4	12.4	20.0	16.9
10.5	6.26	14.5	43.6	21.0	17.0
11.0	4.77	14.7	8.09	22.0	16.9
11.5	2.24	14.9	41.5	23.0	16.7
12.0	0.76	15.0	5.34	24.0	16.1
12.5	0.07	15.2	32.2	26.0	14.9
12.8	1.34	15.4	8.37	28.0	13.8
13.0	45.5	15.5	20.4	30.0	13.0
13.2	6.48	15.8	10.8	35.0	11.8
13.3	20.7	15.9	14.8	39.9	10.6
13.5	0.27	16.0	11.5		
13.7	5.15	16.5	11.4		

4.4.20 H_2

Photoabsorption cross sections

Since the compilation by Gallagher et al. in 1987 and 1988 [87Gal1, 88Gal1], there have been several cross section measurements for hydrogen molecule. As for the photoabsorption cross sections (σ_a), Samson and Haddad [94Sam1] tabulated their recommended values in the photon energy range of 18 - 113 eV, and their values have been adopted above 18 eV range. Because of the rotational and vibrational structures in the photoabsorption cross section curve in the energy range below 17 eV and the line saturation effect discussed in 4.2.2 Evaluation of data, the cross section data available from the ftp site, ftp://ftp.chem.ubc.ca/pub/cooper [97Can1], have been adopted in the energy range below 18 eV.

Photoionization cross sections

The photoionization cross sections (σ_i) in the photon energy range above 18 eV reported by Chung et al. [93Chu1] have been adopted in this compilation. They obtained the σ_i values according to the equation, $\sigma_i = \eta \times \sigma_a$, where the values of η were from Backx et al. [76Bac1] who used the dipole method, and those of σ_a were from [94Sam1] which we have adopted as mentioned above. There have still been no real-photon data of the photoionization quantum yields (η) by now. Except for the energy range of 33 - 41 eV, the photoionization cross sections above 18 eV are equal to the photoabsorption cross sections as shown in Fig. 4.4.20.2.

The photoionization cross sections of energetic H^+ formation from Σ and Π doubly excited states were measured separately [95Lat1].

Neutral-dissociation cross sections

In the energy range above 18 eV, the neutral-dissociation cross sections (σ_d) by Chung et al. [93Chu1] have been adopted.

Table 4.4.20.1. Cross section data for H_2. Only references mentioned in the present compilation are listed.

Ref.	Method	Cross sections	Photon energy range	Energy resolution
87Gal1, 88Gal1	compilation	σ_a, partial ion		
94Sam1	photon	σ_a	18 - 113 eV	
97Can1	dipole	σ_a	11 - 60 eV	48 meV
93Chu1	photon	σ_i, σ_d, partial ion	18 - 124 eV	3 Å (220 meV at 30 eV)
76Bac1	dipole	σ_a , σ_i	10 - 70 eV	500 meV

Table 4.4.20.2. Photoabsorption cross sections (σ_a), photoionization cross sections (σ_i), and neutral-dissociation cross sections (σ_d) of H_2.

E [eV]	σ_a [10^{-18} cm^2]	σ_i [10^{-18} cm^2]	σ_d [10^{-18} cm^2]
18.0	9.85		
19.0	8.68	8.68	0.0
20.0	7.65	7.65	0.0
21.0	6.77	6.77	0.0
22.0	6.03	6.03	0.0
23.0	5.40	5.40	0.0
24.0	4.83	4.83	0.0
25.0	4.31	4.31	0.0
26.0	3.85	3.85	0.0
27.0	3.50	3.50	0.0
28.0	3.20	3.20	0.0
29.0	2.95	2.95	0.0
30.0	2.71	2.71	0.0
31.0	2.41	2.41	0.0
32.0	2.13	2.13	0.0
33.0	1.93	1.91	0.015
34.0	1.74	1.70	0.038
35.0	1.57	1.51	0.063
35.5	1.50	1.43	0.074
36.0	1.42	1.34	0.082
36.5	1.35	1.26	0.089
37.0	1.29	1.20	0.092
37.5	1.23	1.14	0.091
38.0	1.17	1.08	0.085
39.0	1.08	1.02	0.065
40.0	0.990	0.96	0.027
41.0	0.910	0.90	0.007
42.0	0.840	0.84	0.0
44.0	0.722	0.72	0.0
46.0	0.626	0.63	0.0
48.0	0.543	0.54	0.0
50.0	0.477	0.48	0.0
52.0	0.420	0.42	0.0
54.0	0.373	0.37	0.0
56.0	0.331	0.33	0.0
58.0	0.294	0.29	0.0
60.0	0.262	0.26	0.0

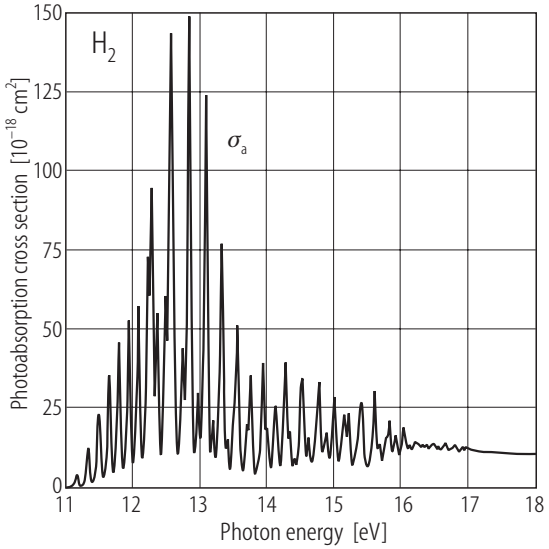

Fig. 4.4.20.1. Photoabsorption cross sections (σ_a) of H_2 in the energy range of 11 - 18 eV. The data used are from [97Can1].

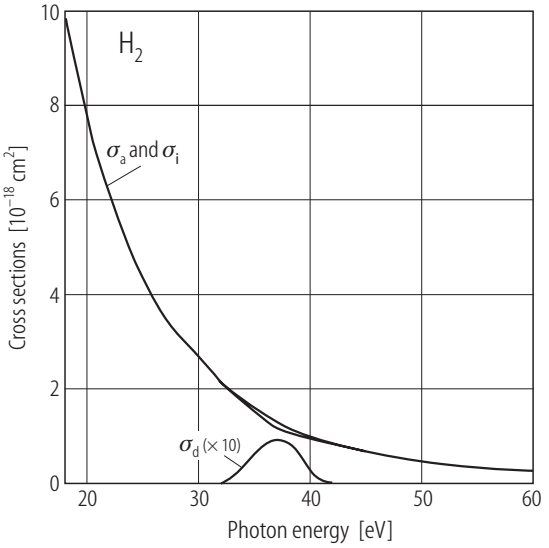

Fig. 4.4.20.2. Photoabsorption (σ_a), photoionization (σ_i), and neutral-dissociation (σ_d) cross sections of H_2 in the energy range of 18 - 60 eV. The σ_a are from 94Sam1, and the σ_i, and σ_d are from [93Chu1].

4.4.21 H_2O

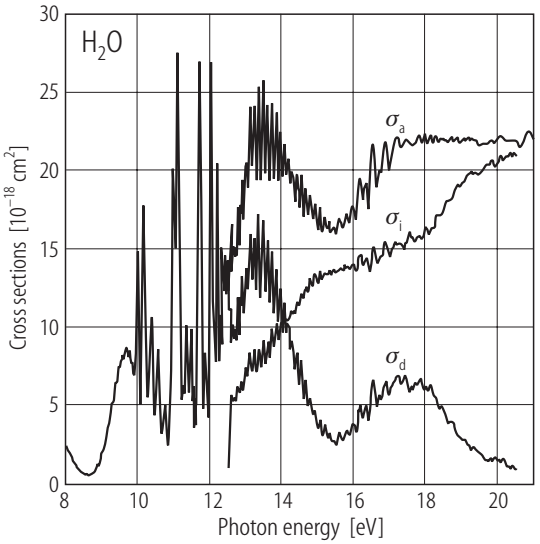

Fig. 4.4.21.1. Photoabsorption (σ_a), photoionization (σ_i), and neutral-dissociation (σ_d) cross sections of H_2O in the energy range of 8 - 21 eV. The σ_a in 8 - 11.5 eV are from Chan et al. [93Cha5] with the resolution of 48 meV; the σ_a, σ_i, and σ_d in the energy range of 11.5 - 21 eV are from Katayama et al.[73Kat1].

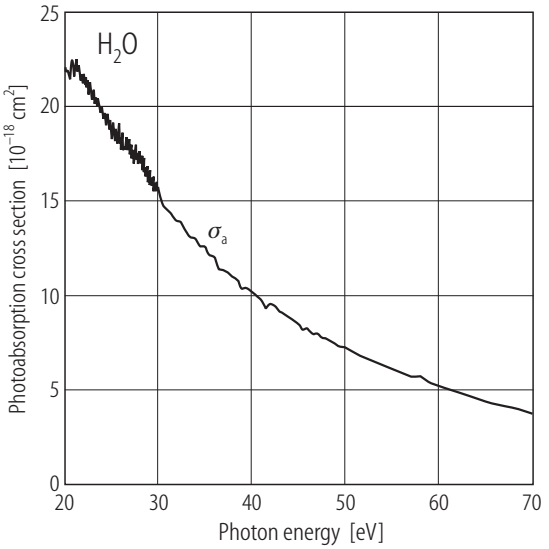

Fig. 4.4.21.2. Photoabsorption cross sections (σ_a) of H_2O in the energy range of 20 - 70 eV. The data are from [93Cha5] with the resolution of 48 meV in the energy range of 21.3 - 30 eV and with the resolution of 1 eV in the range of 30 -70 eV. The σ_a in the energy range of 20 - 21.3 eV are from Katayama et al.[73Kat1].

Table 4.4.21.1. Cross section data for H_2O.

Ref.	Method	Cross sections	Photon energy range	Energy resolution
73Kat1	photon	σ_a, σ_i, σ_d	11.5 - 21.4 eV	0.5 Å (9 meV at 15 eV)
93Cha5	dipole	σ_a	6 - 200 eV	48 meV or 1 eV

4.4.22 H_2S

Table 4.4.22.1. Cross section data for H_2S.

Ref.	Method	Cross sections	Photon energy range	Energy resolution
85Ibu1	photon	σ_a	12 - 26 eV	4 Å (73 meV at 15 eV)
86Bri1	dipole	σ_a, σ_i, partial ion	10 - 90 eV	1 eV

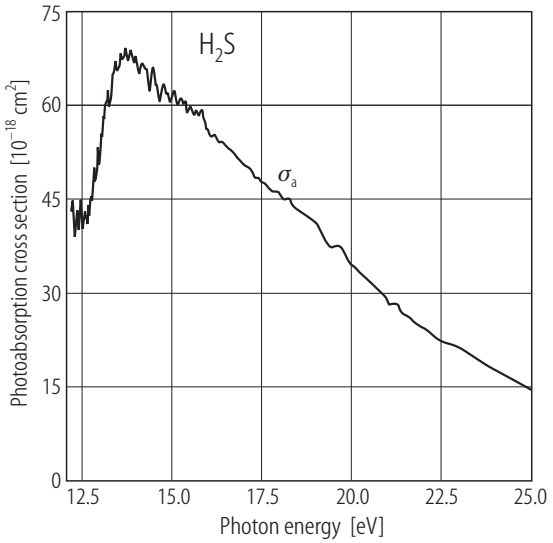

Fig. 4.4.22.1. Photoabsorption cross sections (σ_a) of H_2S in the energy range of 12 - 25 eV. The data are from [85Ibu1].

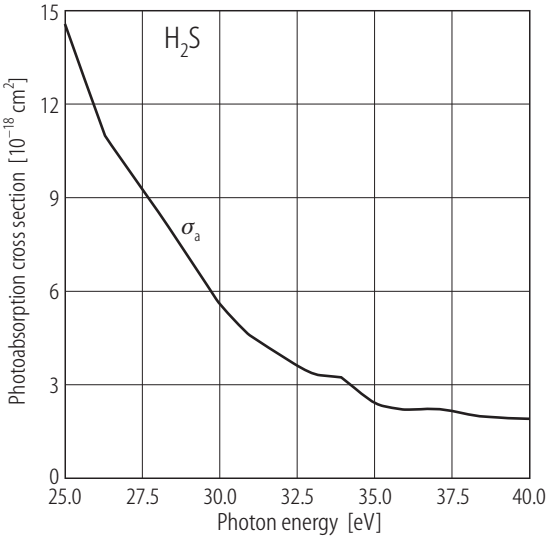

Fig. 4.4.22.2. Photoabsorption cross sections (σ_a) of H_2S in the energy range of 25 - 40 eV. The data are from [85Ibu1] in the energy range of 25 - 26.4 eV and from 86Bri1 in the energy range above 28 eV. The σ_a curve between 26.4 eV and 28 eV was plotted as a straight line.

Table 4.4.22.2. Photoabsorption cross sections (σ_a) of H_2S.

E [eV]	σ_a [10^{-18} cm^2]	E [eV]	σ_a [10^{-18} cm^2]	E [eV]	σ_a [10^{-18} cm^2]
12.5	40.6	17.0	50.7	25.8	12.2
13.0	52.4	18.0	45.7	28.0	8.55
13.5	66.2	19.0	41.3	30.0	5.56
14.0	67.2	20.0	34.7	32.0	3.86
14.5	65.1	21.0	28.8	34.0	3.15
15.0	61.4	22.0	24.4	36.0	2.18
15.5	59.9	23.0	21.5	38.0	2.04
16.0	56.3	23.8	18.2	40.0	1.89
16.5	53.5	24.8	15.2		

4.4.23 NH_3

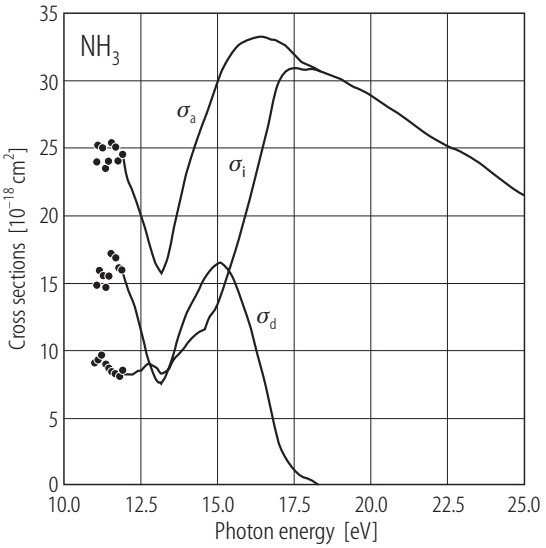

Fig. 4.4.23.1. Photoabsorption (σ_a), photoionization (σ_i), and neutral-dissociation cross sections (σ_d) of NH_3 in the energy range of 10 - 25 eV. All the data are from [87Sam3] with the resolution of 1 Å (32 meV at 20 eV photon energy).

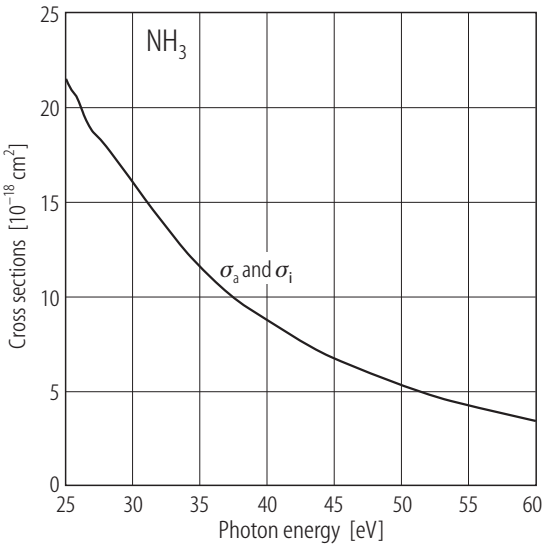

Fig. 4.4.23.2. Photoabsorption (σ_a) and photoionization (σ_i) cross sections of NH_3 in the energy range of 25 - 60 eV. All the data are from [87Sam3]. The values of σ_d in this energy range are equal to zero.

For partial photoionization cross sections see Fig. 4.4.23.3 and Fig. 4.4.23.4.

Table 4.4.23.1. Cross section data for NH_3.

Ref.	Method	Cross sections	Photon energy range	Energy resolution
87Sam3	photon	σ_a, σ_i, σ_d, partial ion	11 - 155 eV	1 Å (32 meV at 20 eV), 0.3 Å (60 meV at 50 eV), 2 Å for partial ion (145 meV at 30 eV)
93Bur1	dipole	σ_a	5 - 200 eV	48 meV or 1 eV
99Edv1	photon	σ_a, σ_i, σ_d	10 - 25 eV	

Table 4.4.23.2. Photoabsorption cross sections (σ_a), photoionization cross sections (σ_i), and neutral-dissociation cross sections (σ_d) of NH_3.

E [eV]	σ_a [10^{-18} cm^2]	σ_i [10^{-18} cm^2]	σ_d [10^{-18} cm^2]
11.6	25.3	8.20	17.1
12.0	23.0	8.20	14.8
12.5	20.0	8.50	11.5
13.2	15.7	8.20	7.50
14.1	23.8	10.7	13.1
14.6	27.0	11.6	15.4
14.9	29.3	13.0	16.3
15.5	32.1	16.7	15.4
16.1	33.1	21.6	11.5
16.5	33.2	25.6	7.60
17.0	32.8	29.8	3.00
17.5	32.0	30.9	1.10
18.0	31.1	30.8	0.30
18.5	30.6	30.6	0
19.1	30.0	30.0	0
20.0	28.8	28.8	0
21.0	27.3	27.3	0
22.1	25.6	25.6	0
23.0	24.7	24.7	0
23.8	23.3	23.3	0
24.8	21.7	21.7	0
25.8	20.5	20.5	0
28.2	17.9	17.9	0
30.2	15.8	15.8	0
35.4	11.2	11.2	0
40.0	8.70	8.70	0
44.3	6.95	6.95	0
49.6	5.38	5.38	0
53.9	4.42	4.42	0
59.0	3.58	3.58	0

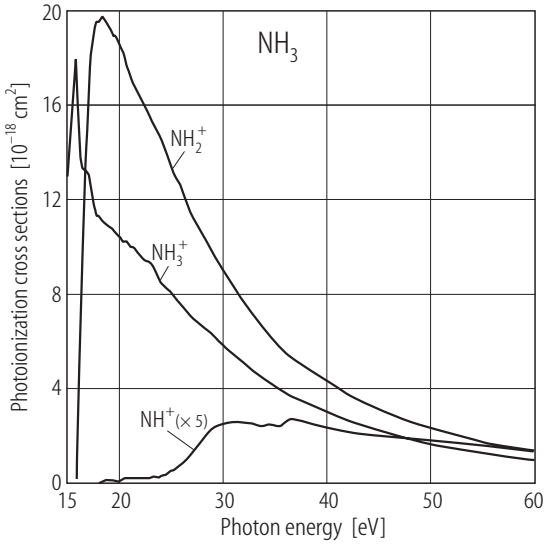

Fig. 4.4.23.3. The partial photoionization cross sections for the formation of NH_3^+, NH_2^+, and NH^+. The data are from [87Sam3] with the resolution of 2 Å (145 meV at 30 eV photon energy).

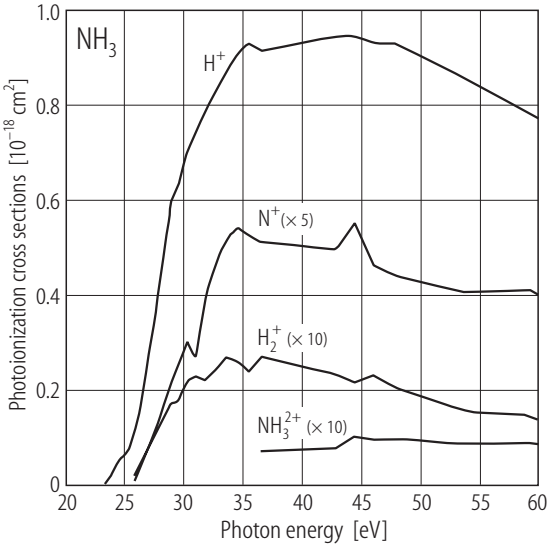

Fig. 4.4.23.4. The partial photoionization cross sections for the formation of H^+, N^+, H_2^+, and NH_3^{2+}. The data are from [87Sam3] with the resolution of 2 Å (145 meV at 30 eV photon energy).

4.4.24 NO

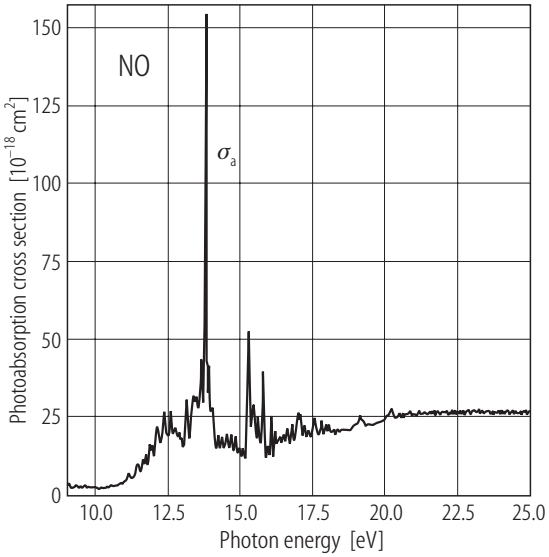

Fig. 4.4.24.1. Photoabsorption cross sections (σ_a) of NO in the energy range of 9 - 25 eV. The data are from [93Cha3].

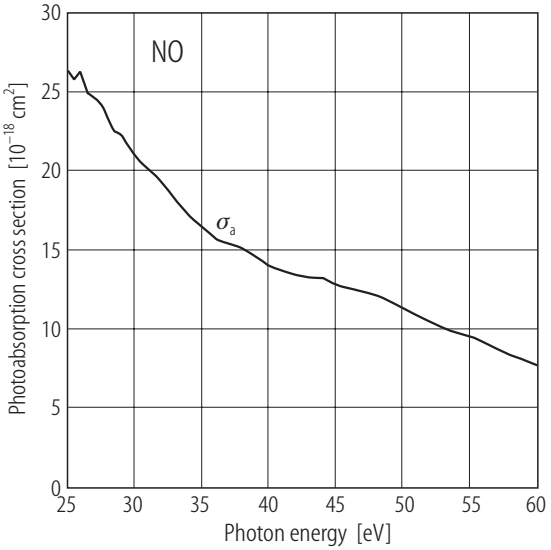

Fig. 4.4.24.2. Photoabsorption cross sections (σ_a) of NO in the energy range of 25 - 60 eV. The data are from [86Iid1].

Table 4.4.24.1. Cross section data for NO.

Ref.	Method	Cross sections	Photon energy range	Energy resolution
93Cha3	dipole	σ_a	5 - 30 eV	48 meV
86Iid1	dipole	σ_a, partial ion	6 - 190 eV	1 eV
67Wat1	photon	σ_a , η	9 - 21 eV	0.2 Å (1.6 meV at 10 eV), 0.4 Å (4.6 meV at 12 eV)

4.4.25 N_2

Photoabsorption cross sections

After the compilation of photoabsorption (σ_a) and photoionization (σ_i) cross sections by Gallagher et al. in 1987 and 1988 [87Gal1, 88Gal1], there have been several cross section measurements for nitrogen molecule.

The most comprehensive compilation of the absolute photoabsorption cross sections was provided by Fennelly and Torr in 1992 [92Fen1], who mainly adopted data by Samson et al. [77Sam1, 87Sam2] for the energy range above 17 eV and those by Carter [72Car1] for the lower energy range. Although the cross section values by Carter were measured with the resolution of 0.04 Å (0.7 meV at the photon energy of 15 eV), they were affected by the line saturation effects as pointed out in 4.2.2 Evaluation of data of this report. Therefore, in the present compilation, in the energy range higher than 20 eV the photoabsorption cross sections measured by Samson et al. [87Sam2] have been adopted, and in the energy range lower than 20 eV the data measured by the dipole-simulation method by Chan et al. [93Cha1].

Photoionization cross sections

The photoionization cross sections are assumed to be equal to the photoabsorption cross sections in the range above 18.8 eV in this compilation according to Samson et al. [77Sam1]. As for the photoionization quantum yields in the energy range below 18.8 eV, there still exist discrepancies between the results as shown in [92Sha2], and we have not adopted any of them in the present compilation from the view point of absolute values. However, those who need photoionization cross sections below 18.8 eV should refer to Shaw et al. [92Sha2]. They gave the photoionization cross sections and photoionization quantum yields with a fairly good resolution (0.1 Å, which is 2 meV at photon energy of 16 eV, or 0.2 Å, which is 6.5 meV at photon energy of 20 eV), although their values were affected by the line saturation effects as mentioned in 4.2.2 Evaluation of data, and have also some ambiguity in absolute scale, e.g., the photoionization quantum yields exceed unity in the energy range around 21 eV.

Neutral-dissociation cross sections

Because of the same reason as mentioned for the photoionization cross sections, we have not provided the recommended values of the neutral-dissociation cross sections in the energy range below 18.8 eV. They are zero in the range above 18.8 eV according as stated above.

Table 4.4.25.1. Cross section data for N_2. Only references mentioned in the present compilation are listed.

Ref.	Method	Cross sections	Photon energy range	Energy resolution
87Gal1, 88Gal1	compilation	σ_a, partial ion		
92Fen1	compilation	σ_a, σ_i	12 - 523 eV	
77Sam1	photon	σ_a, σ_i	16.6 - 124 eV	0.01 Å (0.3 meV at 20 eV)
87Sam2	photon	σ_a, σ_i	15.6 - 109 eV	1 Å (34 meV at 20 eV)
72Car1	photon	σ_a	12.7 - 17 eV	0.04 Å (0.7 meV at 15 eV)
93Cha1	dipole	σ_a	11 - 200 eV	48 meV or 1 eV
92Sha2	photon	σ_a, σ_i, σ_d	15.5 - 25.5 eV	0.1 Å (2 meV at 16 eV) or 0.2 Å (6.5 meV at 20 eV)

Table 4.4.25.2. Photoabsorption cross sections (σ_a) and photoionization cross sections (σ_i) of N_2.

E [eV]	σ_a (= σ_i) [10^{-18} cm^2]	*E* [eV]	σ_a (= σ_i) [10^{-18} cm^2]	*E* [eV]	σ_a (= σ_i) [10^{-18} cm^2]
19.0	25.0	24.6	23.6	30.2	21.0
19.5	23.8	25.0	23.5	35.4	15.3
20.0	23.1	25.6	23.6	40.0	12.0
20.5	22.7	26.1	23.4	45.1	10.6
21.0	22.4	26.4	23.3	50.6	9.8
21.6	22.5	27.0	23.1	55.1	8.3
22.3	24.0	27.6	23.1	60.5	6.6
22.5	24.7	28.2	23.1	65.3	5.5
23.0	25.3	28.5	22.9	68.9	4.8
23.6	24.9	29.2	22.3		
24.0	24.3	29.5	21.9		

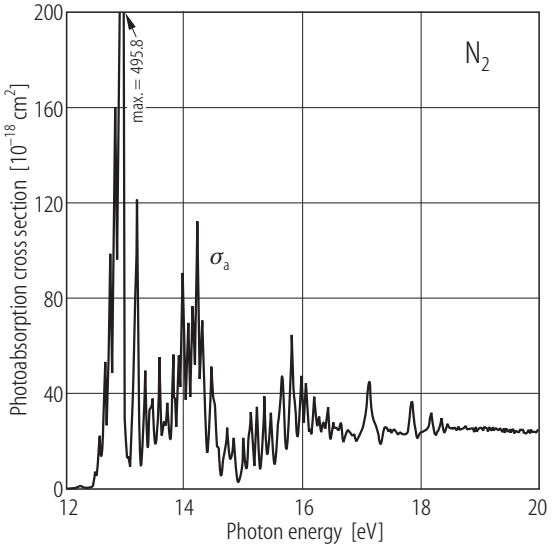

Fig. 4.4.25.1. Photoabsorption cross sections (σ_a) of N_2 in the energy range of 12 - 20 eV. The photoionization cross sections (σ_i) are equal to the photoabsorption cross sections (σ_a) and thus the neutral-dissociation cross sections (σ_d) are zero in the range above 18.8 eV. Only σ_a curve is plotted in this figure. The data used are from Chan et al. [93Cha1].

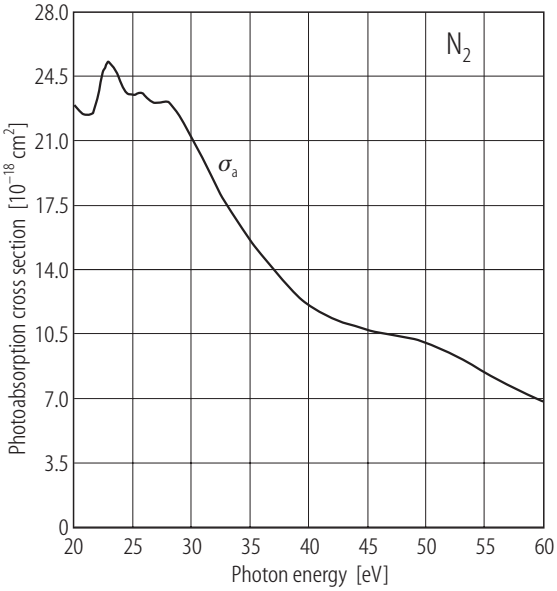

Fig. 4.4.25.2. Photoabsorption cross sections (σ_a) of N_2 in the energy range of 20 - 60 eV. The photoionization cross sections (σ_i) are equal to the photoabsorption cross sections (σ_a) and thus the neutral-dissociation cross sections (σ_d) are zero in the range above 18.8 eV. Only σ_a curve is plotted in this figure. The data used are from Samson et al. [87Sam2].

4.4.26 N_2O

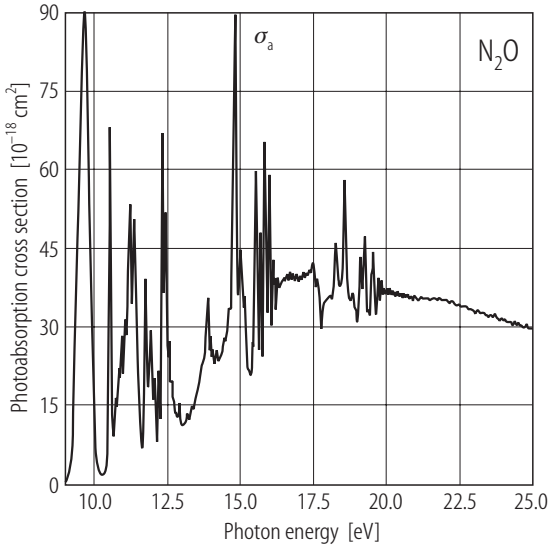

Fig. 4.4.26.1. Photoabsorption cross sections (σ_a) of N_2O in the energy range of 9 - 25 eV. The data are from [94Cha1] with the resolution of 48 meV.

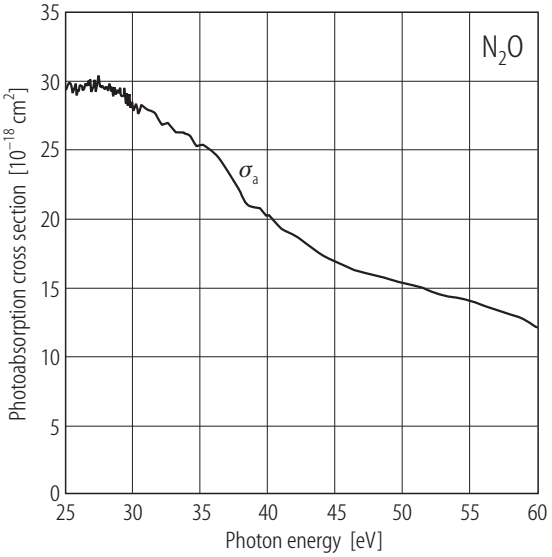

Fig. 4.4.26.2. Photoabsorption cross sections (σ_a) of N_2O in the energy range of 25 - 60 eV. The data are from [94Cha1] with the resolution of 48 meV in the energy range of 25 - 30 eV and with the resolution of 1 eV in the energy range above 30 eV.

Table 4.4.26.1. Cross section data for N_2O.

Ref.	Method	Cross sections	Photon energy range	Energy resolution
94Cha1	dipole	σ_a	5.5 - 203 eV	48 meV or 1 eV
92Sha1	photon	σ_a, σ_i, σ_d	13 - 26 eV	0.2 Å (6 meV at 20 eV)

4.4.27 OCS

The photoabsorption (σ_a), photoionization (σ_i), and partial photoionization cross sections of OCS were compiled by Gallagher et al. [87Gal1, 88Gal1]. The photoabsorption cross sections measured by Wu et al. [82Wu1] using synchrotron radiation have been adopted in the present compilation. The energy resolution of their experiment is 1 Å (129 meV at 40 eV photon energy). Carnovale et al. [82Car1] measured the partial photoionization cross sections for the formation of fragment ions, OCS^+, CS^+, CO^+, S^+, C^+, and O^+, using the dipole-simulation method with the resolution of 1 eV based on the σ_i values measured by White et al.[81Whi1]. We have adopted the σ_i values by White et al.[81Whi1] and the partial photoionization cross sections by Carnovale et al. [82Car1].

Table 4.4.27.1. Cross section data for OCS. Only references mentioned in the present compilation are listed.

Ref.	Method	Cross sections	Photon energy range	Energy resolution
87Gal1, 88Gal1	compilation			
82Wu1	photon	σ_a	16 - 70 eV	1 Å (129 meV at 40 eV)
82Car1	dipole	partial ion	10 - 50 eV	1 eV
81Whi1	dipole	σ_a, σ_i	5 - 50 eV	0.9 eV or 1.3 eV

Table 4.4.27.2. Photoabsorption cross sections (σ_a) of OCS.

E [eV]	σ_a [10^{-18} cm^2]	E [eV]	σ_a [10^{-18} cm^2]	E [eV]	σ_a [10^{-18} cm^2]
18.0	49.8	24.0	28.1	35.0	15.2
18.5	50.2	25.0	24.4	40.0	14.5
19.0	50.3	26.0	22.3	45.0	13.1
19.5	47.2	27.0	20.9	50.0	11.7
20.0	45.0	28.0	20.3	55.0	10.4
21.0	40.0	29.0	20.0	59.9	9.22
22.0	37.0	30.0	19.4		
23.0	33.6	32.0	16.5		

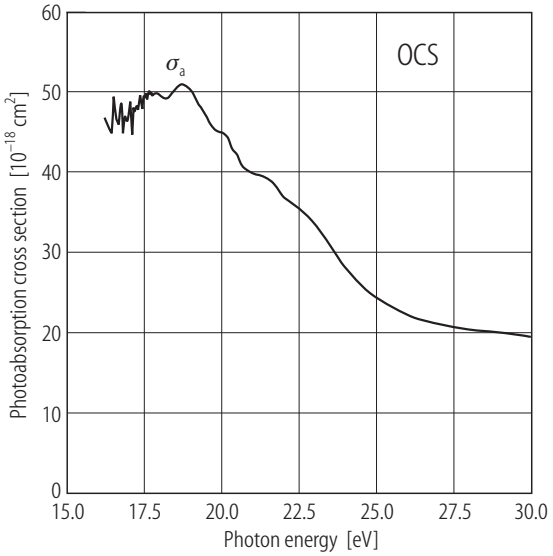

Fig. 4.4.27.1. Photoabsorption cross sections (σ_a) of OCS in the energy range of 16 - 30 eV. The data used are from Wu et al. [82Wu1].

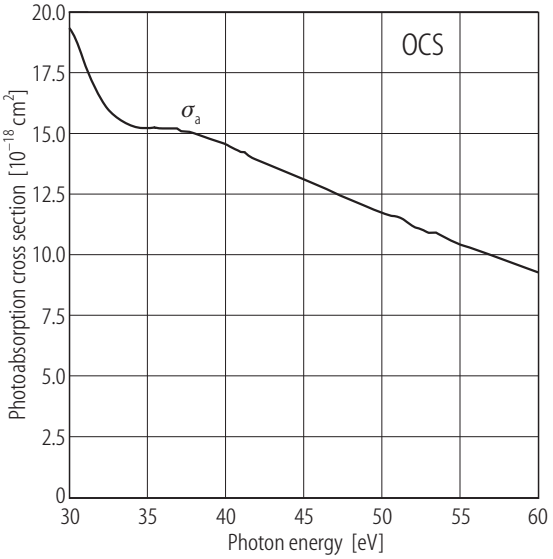

Fig. 4.4.27.2. Photoabsorption cross sections (σ_a) of OCS in the energy range of 30 - 60 eV. The data used are from Wu et al. [82Wu1].

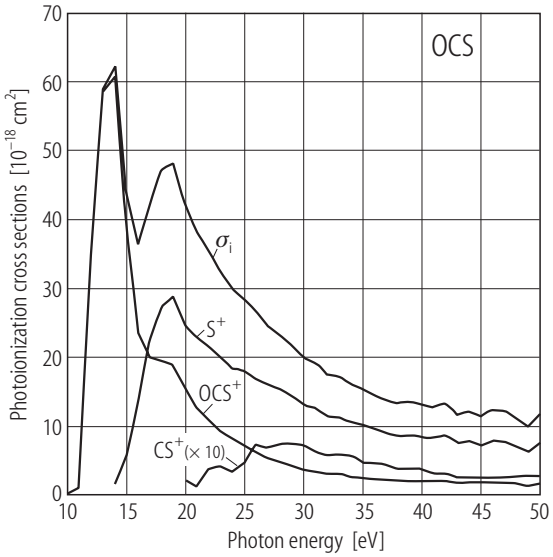

Fig. 4.4.27.3. Photoionization cross sections (σ_i) measured by White et al. [81Whi1] with the resolution of 1.3 eV, and partial photoionization cross sections for OCS^+, CS^+, and S^+ measured by Carnovale et al. with the resolution of 1 eV [82Car1].

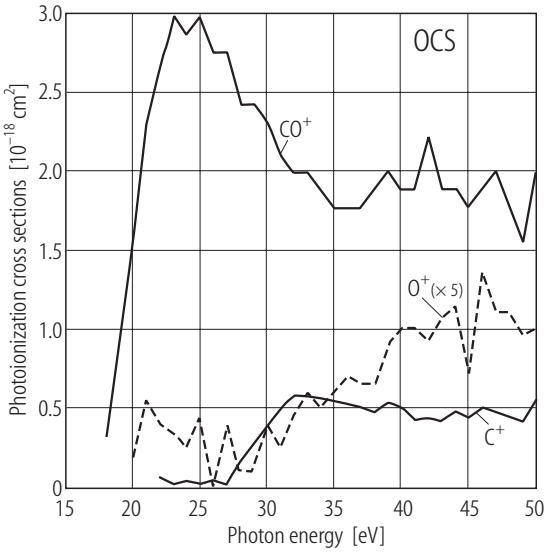

Fig. 4.4.27.4. The partial photoionization cross sections for CO^+, C^+, and O^+ measured by Carnovale et al. with the resolution of 1 eV [82Car1].

4.4.28 O_2

Table 4.4.28.1. Cross section data for O_2.

Ref.	Method	Cross sections	Photon energy range	Energy resolution
93Cha2	dipole	σ_a	5 - 30 eV	48 meV
79Bri1	dipole	σ_a, σ_i, partial ion	5 - 300 eV	0.5 eV
82Sam1	photon	partial ion	19 - 103 eV	
93Hol1	photon	σ_a, σ_i, σ_d	12 - 25 eV	0.2 Å (4 meV at 16 eV) or 0.4 Å (16 meV at 22 eV)

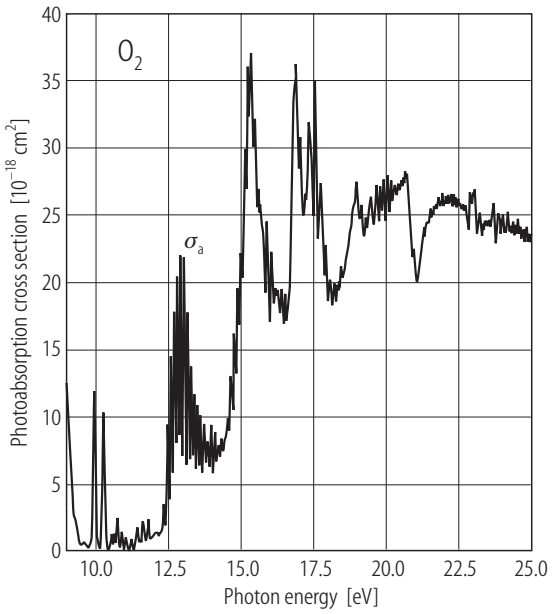

Fig. 4.4.28.1. Photoabsorption cross sections (σ_a) of O_2 in the energy range of 9 - 25 eV. The data are from [93Cha2].

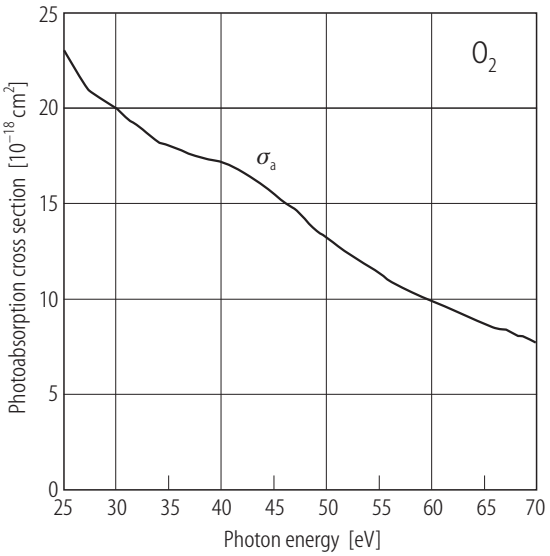

Fig. 4.4.28.2. Photoabsorption cross sections (σ_a) of O_2 in the energy range of 25 - 70 eV. The data are from [79Bri1].

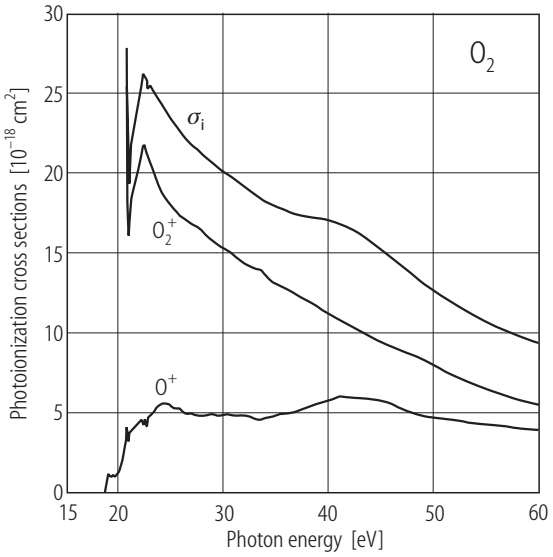

Fig. 4.4.28.3. The partial photoionization cross sections for the formation of O_2^+ and O^+ along with the photoionization cross sections (σ_i). The data are from [82Sam1].

4.4.29 SF_6

Photoabsorption cross sections

The photoabsorption cross sections (σ_a) of SF_6 reported until late 1970s were evaluated by Berkowitz [79Ber1] by using the sum rules for the oscillator-strength distribution. Gallagher et al. [87Gal1, 88Gal1] compiled the photoabsorption (σ_a) and partial photoionization cross sections in 1987 and 1988. The most recent experiment was reported by Holland et al. [92Hol1]. They also made the sum rule analysis by combining their data with the previous ones obtained in other photon energy ranges. In this compilation we have adopted the photoabsorption cross sections (σ_a) which Holland et al. [92Hol1] chose in their sum rule analysis as follows: those by Blechschmidt et al. [72Ble1] in the energy range of 10 - 14.9 eV with the resolution of 1 Å (12 meV at photon energy of 12 eV), those by Holland et al. [92Hol1] in 14.9 - 28.3 eV with the resolution of 0.4 Å (13 meV at photon energy of 20 eV), and those by Lee et al. [77Lee1] in 28.3 - 59.6 eV with the resolution of 1 Å (160 meV at photon energy of 44 eV). All of these three experiments were done by using synchrotron radiation as a light source.

Photoionizaton cross sections and neutral-dissociation cross sections

In addition to the photoabsorption cross sections (σ_a), Holland et al. [92Hol1] measured the photoionization quantum yields (η), and obtained the photoionization cross sections ($\sigma_i = \eta \times \sigma_a$) and neutral-dissociation cross sections ($\sigma_d = (1-\eta) \times \sigma_a$). Although the η values by Holland et al. was rather improved in comparison with those in previous experiments [78Sas1, 79Hit1], their η values around 20 eV exceed unity, and thus the negative values of the neutral-dissociation cross sections (σ_d) were obtained. In the present compilation the σ_i and σ_d values by Holland et al. [92Hol1] have been adopted in the energy range 15.5 - 22.5 eV without any correction. The energy resolution is 0.4 Å (13 meV at the photon energy of 20 eV).

After the compilation by Berkowitz [79Ber1] in 1979 and those by Gallagher et al. [87Gal1, 88Gal1] in 1987 and 1988, the partial photoionization cross sections for the formation of fragment ions were reexamined in a relative scale by Creasey et al. [91Cre1]. The ion-pair formation of this molecule was studied by Mitsuke et al. [90Mit1]. Those who need these cross section values should refer to the corresponding references.

Table 4.4.29.1. Cross section data for SF_6. Only references mentioned in the present compilation are listed.

Ref.	Method	Cross sections	Photon energy range	Energy resolution
79Ber1	compilation	σ_a, η		
87Gal1, 88Gal1	compilation	σ_a, partial ion		
92Hol1	photon	σ_a, σ_i, σ_d, η	13.0 - 29.5 eV	0.4 Å (13 meV at 20 eV)
72Ble1	photon	σ_a	10 - 50 eV	1 Å (12 meV at 12 eV)
77Lee1	photon	σ_a	16.1 - 70.8 eV	1 Å (160 meV at 44 eV)
78Sas1	photon	σ_a, η	15 - 39 eV	2 Å (150 meV at 30 eV)
79Hit1	dipole	σ_a, η, partial ion	15 - 63 eV	1 eV
91Cre1	photon	partial ion (relative)	15.3 - 28.2 eV	< 1 Å (< 32 meV at 20 eV)
90Mit1	photon	ion pair	11.27 - 31.0 eV	0.8 Å (26 meV at 20 eV)

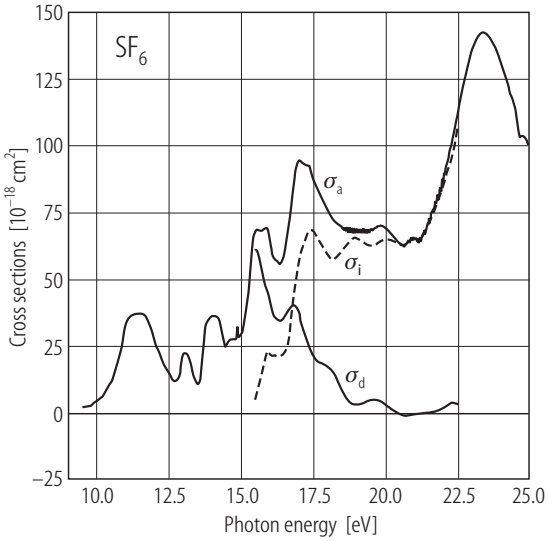

Fig. 4.4.29.1. Photoabsorption (σ_a), photoionization (σ_i), and neutral-dissociation (σ_d) cross sections of SF_6 in the energy range of 10 - 25 eV. The σ_a data used are from Blechschmidt et al. [72Ble1] in the energy range of 10 - 14.9 eV with the resolution of 1 Å (12 meV at photon energy of 12 eV) and Holland et al. [92Hol1] in the range of 14.9 - 25.0 eV with the resolution of 0.4 Å (13 meV at photon energy of 20 eV). The σ_i and σ_d are from Holland et al. [92Hol1] in the range of 15.5 - 22.5 eV with the resolution of 0.4 Å (13 meV at photon energy of 20 eV).

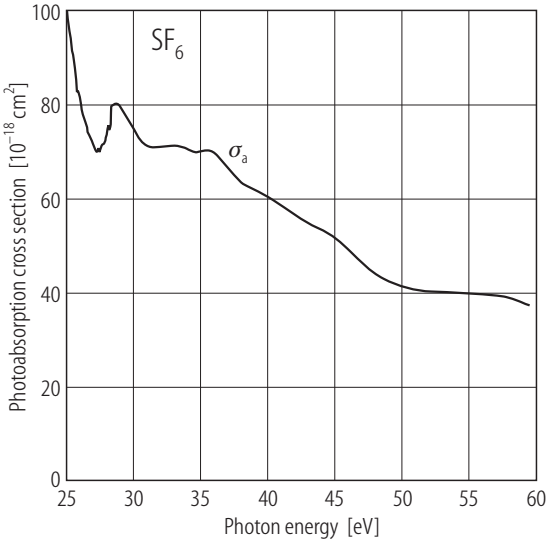

Fig. 4.4.29.2. Photoabsorption cross sections (σ_a) of SF_6 in the energy range of 25 - 60 eV. The σ_a data used are from Holland et al. [92Hol1] in the range of 25.0 - 28.3 eV with the resolution of 0.4 Å (22 meV at photon energy of 26 eV) and Lee et al. [77Lee1] in the range of 28.3 - 59.6 eV with the resolution of 1Å (160 meV at photon energy of 44 eV).

Table 4.4.29.2. Photoabsorption cross sections (σ_a), photoionization cross sections (σ_i), and neutral-dissociation cross sections (σ_d) of SF_6.

E [eV]	σ_a [10^{-18} cm^2]	σ_i [10^{-18} cm^2]	σ_d [10^{-18} cm^2]	E [eV]	σ_a [10^{-18} cm^2]	σ_i [10^{-18} cm^2]	σ_d [10^{-18} cm^2]
10.0	4.1			23.5	141.8		
10.5	11.0			24.0	130.6		
11.0	32.9			24.5	113.6		
11.4	37.4			25.0	99.4		
11.5	37.4			25.5	89.3		
12.0	27.7			26.0	81.1		
12.5	15.1			26.5	75.1		
13.0	22.1			27.0	71.0		
14.0	36.2			27.5	69.7		
14.5	25.0			28.0	72.8		
14.9	28.3			28.5	79.6		
15.0	29.3			29.0	79.1		
15.5	67.6	5.0	61.1	29.5	76.8		
16.0	65.6	22.8	43.1	30.0	74.3		
16.5	58.6	21.9	35.3	31.0	70.8		
17.0	94.4	55.9	38.0	32.0	70.6		
17.5	88.5	68.4	21.3	33.0	70.8		
18.0	76.0	59.2	17.2	34.0	70.3		
18.5	69.7	60.7	8.65	35.0	69.7		
19.0	68.1	65.3	2.73	36.0	69.4		
19.5	68.1	62.3	4.75	37.0	66.4		
20.0	69.5	65.1	2.76	38.0	63.2		
20.5	63.9	63.1	-0.54	39.0	61.5		
20.5	63.6	63.0	-0.58	40.0	60.1		
21.0	65.3	64.8	-0.31	45.0	51.5		
21.5	70.4	70.0	-0.42	50.0	40.9		
22.0	87.3	85.0	1.61	55.0	39.5		
22.5	111.0	107.0	3.01	59.6	36.8		
23.0	135.1						

4.4.30 SO_2

Table 4.4.30.1. Cross section data for SO_2.

Ref.	Method	Cross sections	Photon energy range	Energy resolution
95Hol1	photon	σ_a, σ_i, σ_d	12 - 31 eV	0.4 Å (13 meV at 20 eV)
99Fen1	dipole	σ_a	3.5 - 260 eV	50 meV or 1 eV
98Mas1	photon	partial ion	16 - 120 eV	

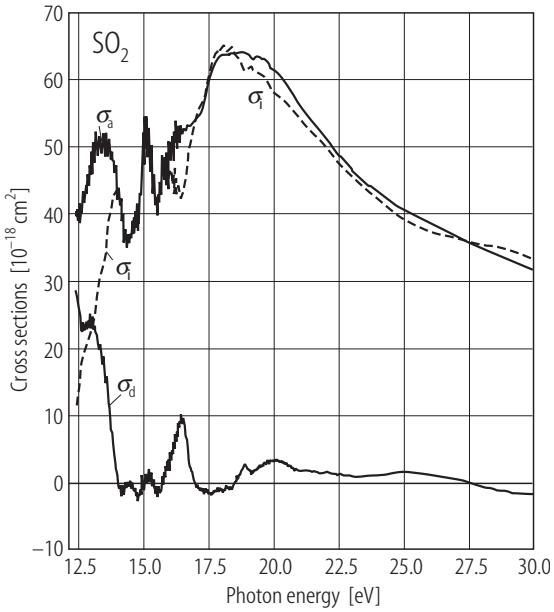

Fig. 4.4.30.1. Photoabsorption (σ_a), photoionization (σ_i), and neutral-dissociation (σ_d) cross sections of SO_2 in the energy range of 12 - 30 eV. All the data are from [95Hol1].

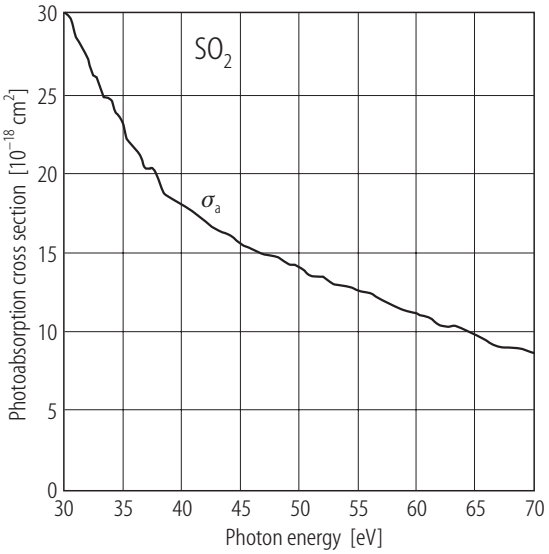

Fig. 4.4.30.2. Photoabsorption cross sections (σ_a) of SO_2 in the energy range of 30 - 70 eV. The data are from [99Fen1] with the resolution of 1 eV.

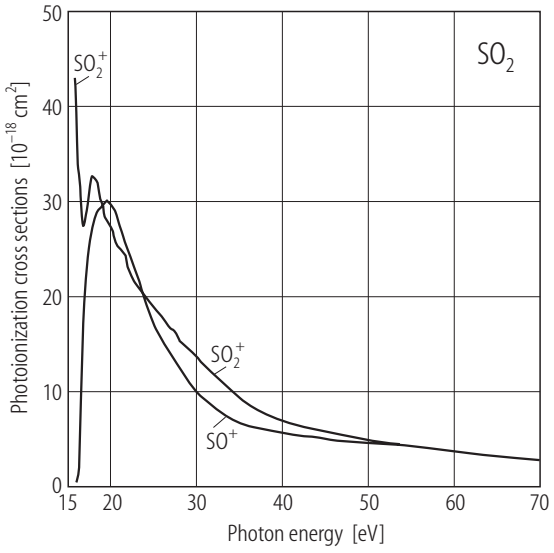

Fig. 4.4.30.3. The partial photoionization cross sections for the formation of SO_2^+ and SO^+. The data are from [98Mas1].

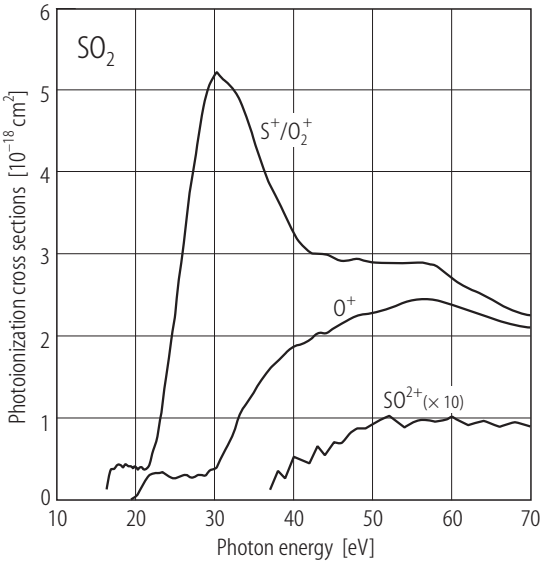

Fig. 4.4.30.4. The partial photoionization cross sections for the formation of S^+/O_2^+, O^+, and SO^{2+}. The data are from [98Mas1].

4.4.31 SiH_4

There have been only a few cross section measurements for SiH_4 molecule. The only real-photon data of the σ_a, σ_i, and σ_d in the energy range of the present interest were obtained by Kameta et al. [91Kam1] which we have included in this compilation for the energy range of 13 - 40 eV. In the energy range below 13 eV and 40 - 60 eV the σ_a values by the dipole-simulation method [95Coo2] have been adopted. The recommended values are tabulated in Table 4.4.31.2 and plotted in Figs. 4.4.31.1 and 4.4.31.2.

Table 4.4.31.1. Cross section data for SiH_4. Only references mentioned in the present compilation are listed.

Ref.	Method	Cross sections	Photon energy range	Energy resolution
91Kam1	photon	σ_a, σ_i, σ_d	13 - 40 eV	1 Å (34 meV at 20 eV)
95Coo2	dipole	σ_a	7.5 - 350 eV	48 meV or 1 eV

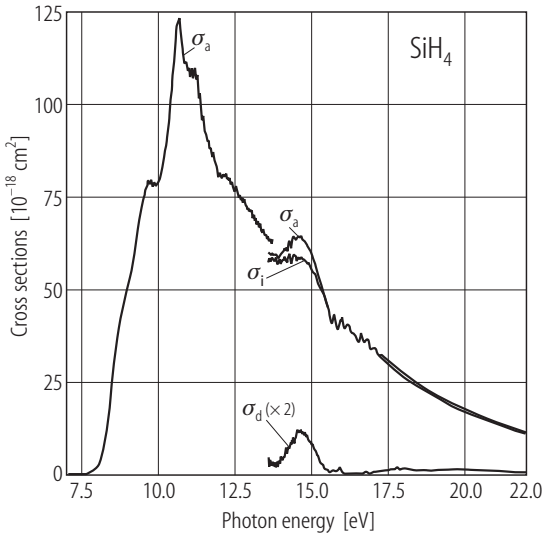

Fig. 4.4.31.1. Photoabsorption (σ_a), photoionization (σ_i), and neutral-dissociation (σ_d) cross sections of SiH_4 in the energy range of 7 - 22 eV. The data used are the σ_a in the range of 7 - 13 eV with the resolution of 48 meV by Cooper et al. [95Coo2]; the σ_a , σ_i , and σ_d in the range of 13 - 22 eV by Kameta et al. [91Kam1].

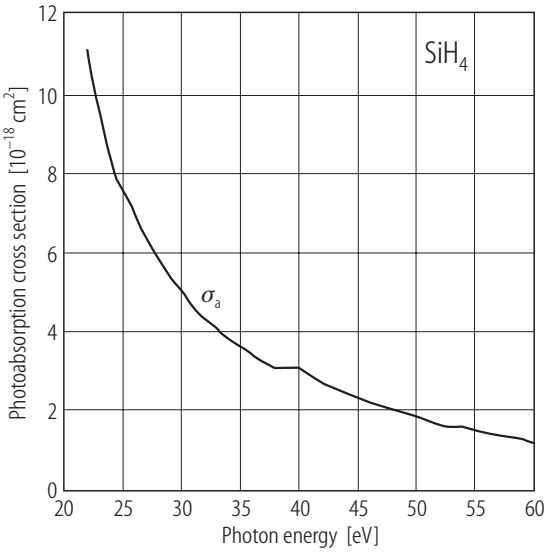

Fig. 4.4.31.2. Photoabsorption cross sections (σ_a) of SiH_4 in the energy range of 22 - 60 eV. The data used are the σ_a in the range of 22 - 40 eV by Kameta et al [91Kam1]; above 40 eV by Cooper et al. [95Coo2] with the resolution of 1 eV.

Table 4.4.31.2. Photoabsorption cross sections (σ_a), photoionization cross sections (σ_i), and neutral-dissociation cross sections (σ_d) of SiH_4.

E [eV]	σ_a [10^{-18} cm^2]	σ_i [10^{-18} cm^2]	σ_d [10^{-18} cm^2]	E [eV]	σ_a [10^{-18} cm^2]	σ_i [10^{-18} cm^2]	σ_d [10^{-18} cm^2]
7.51	0.03			25.00	7.60		
8.00	1.34			26.00	7.07		
8.50	23.8			27.00	6.44		
9.00	50.4			28.00	5.93		
9.50	73.1			29.00	5.43		
10.00	78.9			30.00	5.06		
10.51	109.1			31.00	4.64		
10.70	123.1			32.00	4.36		
11.00	109.2			33.00	4.10		
11.50	94.8			34.00	3.80		
12.00	81.1			35.00	3.65		
12.50	77.6			36.00	3.41		
13.00	71.4			38.00	3.08		
13.51	64.7			40.00	3.07		
13.96	59.2	57.9	1.33	42.00	2.71		
14.45	63.7	59.1	4.58	44.00	2.47		
14.97	60.4	56.0	4.45	46.00	2.21		
15.54	45.3	44.8	0.448	48.00	2.05		
15.94	41.5	41.5	0.000	50.00	1.85		
16.57	37.3	37.2	0.076	52.00	1.64		
17.03	34.2	33.8	0.329	54.00	1.60		
17.51	30.3	29.9	0.444	56.00	1.44		
18.02	27.2	26.6	0.681	58.00	1.33		
18.56	24.2	23.7	0.492	60.00	1.16		
19.13	21.1	20.5	0.572				
19.43	19.7	19.1	0.603				
20.06	17.3	16.6	0.655				
20.39	16.2	15.5	0.624				
21.08	13.8	13.4	0.444				
21.45	12.7	12.3	0.351				
22.22	10.7	10.5	0.224				
24.00	8.41						

4.4.32 Si_2H_6

The only real-photon data of the σ_a, σ_i, and σ_d of Si_2H_6 (disilane) in the energy range of the present interest were obtained by Kameta et al. [91Kam2] and have been adopted. The σ_a, σ_i, and σ_d in the energy range of 13.6 - 22 eV are plotted in Fig. 4.4.32.1, and the σ_a values in the energy range of 22 - 40 eV are in Fig. 4.4.32.2.

Table 4.4.32.1. Cross section data for Si_2H_6. Only references mentioned in the present compilation are listed.

Ref.	Method	Cross sections	Photon energy range	Energy resolution
91Kam2	photon	σ_a, σ_i, σ_d	13.6 - 40 eV	4 Å (130 meV at 20 eV)

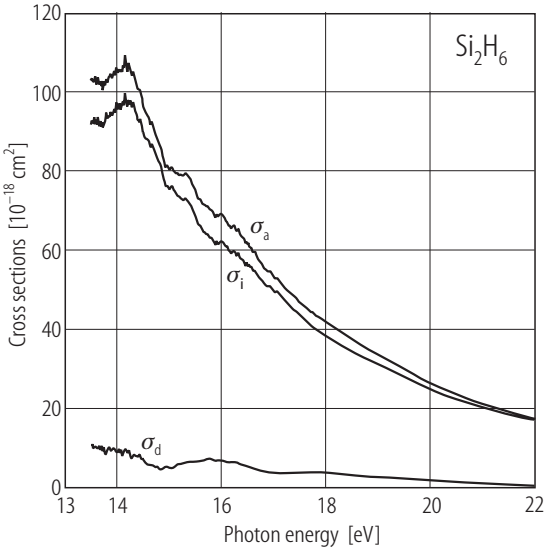

Fig. 4.4.32.1. Photoabsorption (σ_a), photoionization (σ_i), and neutral-dissociation (σ_d) cross sections of Si_2H_6 in the energy range of 13.6 - 22 eV. All the data are from [91Kam2].

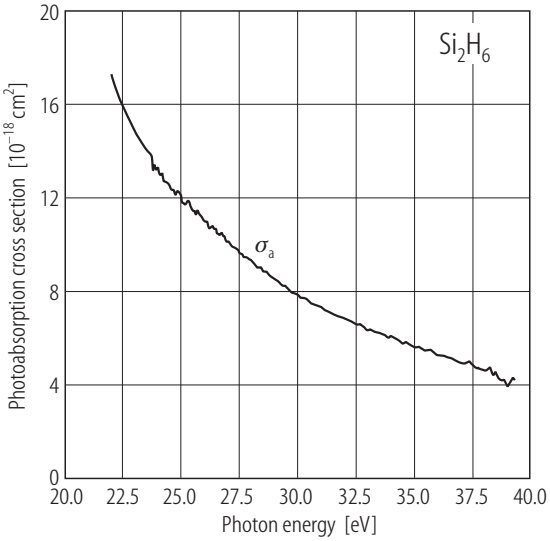

Fig. 4.4.32.2. Photoabsorption cross sections (σ_a) of Si_2H_6 in the energy range of 22 - 40 eV. The data are from [91Kam2].

Table 4.4.32.2. Photoabsorption cross sections (σ_a), photoionization cross sections (σ_i), and neutral-dissociation cross sections (σ_d) of Si_2H_6.

E [eV]	σ_a [10^{-18} cm^2]	σ_i [10^{-18} cm^2]	σ_d [10^{-18} cm^2]
13.5	102.9	92.0	11.0
14.0	105.5	96.5	9.0
14.5	97.1	90.0	7.1
15.0	80.5	75.5	5.0
15.5	75.4	68.9	6.5
16.0	69.0	62.1	6.9
16.5	61.5	56.1	5.3
17.0	53.5	49.9	3.5
17.5	46.8	43.4	3.4
18.0	41.6	38.0	3.6
18.5	37.6	34.4	3.1
19.0	33.6	31.1	2.5
19.5	29.8	27.7	2.0
20.0	26.5	24.7	1.8
20.5	23.6	22.2	1.4
21.0	21.1	20.2	0.9
21.5	19.1	18.6	0.5
22.0	17.3	17.2	0.2
22.5	16.1	16.0	0.1
23.0	14.9		
23.5	14.1		
24.0	13.3		
24.5	12.6		
25.0	12.1		
26.0	11.1		
27.0	10.1		
28.0	9.4		
29.0	8.6		
30.0	7.9		
32.0	6.8		
34.0	6.0		
36.0	5.3		
38.0	4.6		
39.0	3.9		

4.5 References for 4

62Pla1 Platzman, R.L.: Radiat. Res. **17** (1962) 419

67Her1 Herzberg, G.: Molecular Spectra and Molecular Structure, volume III. Electronic Spectra and Electronic Structure of Polyatomic Molecules, Princeton: D. Van Norstrand (1967), p. 555

67Wat1 Watanabe, K., Matsunaga, F.M., Sakai, H.: Applied Optics **6** (1967) 391

71Ino1 Inokuti, M.: Rev. Mod. Phys. **43** (1971) 297

71Per1 Person, J.C., Nicole, P.P.: J. Chem. Phys. **55** (1971) 3390

72Car1 Carter, V.L.: J. Chem. Phys. **56** (1972) 4195

72Ble1 Blechschmidt, D., Haensel, R., Koch, E.E., Nielsen, U., Sagawa, T.: Chem. Phys. Lett. **14** (1972) 33

73Kat1 Katayama, D.H., Huffman, R.E., O'Bryan, C.L.: J. Chem. Phys. **59** (1973) 4309

73Yos1 Yoshino, M., Takeuchi, J., Suzuki, H.: J. Phys. Soc. Jpn. **34** (1973) 1039

74Rob1 Robin, M.B.: Higher Excited States of Polyatomic Molecules, volume I, London: Academic Press (1974)

75Rob1 Robin, M.B.: Higher Excited States of Polyatomic Molecules, volume II, London: Academic Press (1975)

76Bac1 Backx, C., Wight, G.R., Van der Wiel, M.J.: J. Phys. B: At. Mol. Phys. **9** (1976) 315

76Koc1 Koch, E.E, Otto, A.: Int. J. Radiat. Phys. Chem. **8** (1976) 113

76Sam1 Samson, J.A.R., Gardner, J.L.: J. Electron Spectrosc. Relat. Phenom. **8** (1976) 35

76Shi1 Shida, S., Hatano, Y.: Int. J. Radiat. Phys. Chem. **8** (1976) 171

77Lee1 Lee, L.C., Phillips, E., Judge, D.L.: J. Chem. Phys. **67** (1977) 1237

77Sam1 Samson, J.A.R., Haddad, G.N., Gardner, J.L.: J. Phys. B: At. Mol. Phys. **10** (1977) 1749

78Sas1 Sasanuma, M., Ishiguro, E., Masuko, H., Morioka, Y., Nakamura, M.: J. Phys. B: At. Mol. Phys. **11** (1978) 3655

79Ber1 Berkowitz, J.: Photoabsorption, Photoionization, and Photoelectron Spectroscopy, New York: Academic Press (1979)

79Bri1 Brion, C.E., Tan, K.H., Van der Wiel, M.J., Van der Leeuw, Ph.E.: J. Electron Spectrosc. Relat. Phenom. **17** (1979) 101

79Hit1 Hitchcock, A.P., Van der Wiel, M.J.: J. Phys. B: At. Mol. Phys. **12** (1979) 2153

79Kir1 Kirby, K., Constantinides, E.R., Babeu, S., Oppenheimer, M., Victor, G.A.: At. Data Nucl. Data Tables **23** (1979) 63

79Koc1 Koch, E.E., Sonntag, B.F., in: Synchrotron Radiation - Techniques and Applications (Kunz, C., ed.), Berlin: Springer (1979), p. 269

80Hit1 Hitchcock, A.P., Brion, C.E., Van der Wiel, M.J.: Chem. Phys. **45** (1980) 461

81Bri1 Brion, C.E., Hamnett, A.: Adv. Chem. Phys. **45** (1981) 1

81Mas1 Masuoka, T., Samson, J.A.R.: J. Chem. Phys. **74** (1981) 1093

81Sam1 Samson, J.A.R., Haddad, G.: This data set is quoted as unpublished data and tabulated in Ref. [81Mas1]

81Whi1 White, M.G., Leung, K.T., Brion, C.E.: J. Electron Spectrosc. Relat. Phenom. **23** (1981) 127

82Car1 Carnovale, F., Hitchcock, A.P., Cook, J.P.D., Brion, C.E.: Chem. Phys. **66** (1982) 249

82Sam1 Samson, J.A.R., Rayborn, G.H., Pareek, P.N.: J. Chem. Phys. **76** (1982) 393

82Wu1 Wu, C.Y.R., Judge, D.L.: J. Chem. Phys. **76** (1982) 2871

83Car1 Carnovale, F., Brion, C.E.: Chem. Phys. **74** (1983) 253

83Hat1 Hatano, Y.: Comments At. Mol. Phys. **13** (1983) 259

83Ino1 Inokuti, M., in: Applied Atomic Collision Physics, volume IV (Datz, S., ed.), New York: Academic Press (1983), p. 179

83Wu1 Wu, C.Y.R., Judge, D.L.: J. Chem. Phys. **78** (1983) 2180

84Hit1 Hitchcock, A.P., Williams, G.R.J., Brion, C.E., Langhoff, P.W.: Chem. Phys. **88** (1984) 65

85Bri1 Brion, C.E.: Comments At. Mol. Phys. **16** (1985) 249

85Ibu1 Ibuki, T., Koizumi, H., Yoshimi, T., Morita, M., Arai, S., Hironaka, K., Shinsaka, K., Hatano, Y., Yagishita, A., Ito, K.: Chem. Phys. Lett. **119** (1985) 327

85Koi1 Koizumi, H., Yoshimi, T., Shinsaka, K., Ukai, M., Morita, M., Hatano, Y., Yagishita, A., Ito, K.: J. Chem. Phys. **82** (1985) 4856

85Rob1 Robin, M.B.: Higher Excited States of Polyatomic Molecules, volume III, London: Academic Press (1985)

86Bri1 Brion, C.E., Iida, Y., Thomson, J.P.: Chem. Phys. **101** (1986) 449

86Iid1 Iida, Y., Carnovale, F., Daviel, S., Brion, C.E.: Chem. Phys. **105** (1986) 211

86Ino1 Inokuti, M.: Photochem. Photobiol. **44** (1986) 279

87Gal1 Gallagher, J.W., Brion, C.E., Samson, J.A.R., Langhoff, P.W.: JILA Data Center Report, No.32 (1987)

87Hat1 Hatano, Y., in: Radiation Research (Fielden, E.M., Fowler, J.F., Hendry, J.H., Scott, D., eds), London: Taylor & Francis (1987), p. 35

87Sam1 Samson, J.A.R., Angel, G.C.: J. Chem. Phys. **86** (1987) 1814

87Sam2 Samson, J.A.R., Masuoka, T., Pareek, P.N., Angel, G.C.: J. Chem. Phys. **86** (1987) 6128

87Sam3 Samson, J.A.R., Haddad, G.N., Kilcoyne, L.D.: J. Chem. Phys. **87** (1987) 6416

88Gal1 Gallagher, J.W., Brion, C.E., Samson, J.A.R., Langhoff, P.W.: J. Phys. Chem. Ref. Data **17** (1988) 9

89Sam1 Samson, J.A.R., Haddad, G.N., Masuoka, T., Pareek, P.N., Kilcoyne, D.A.L.: J. Chem. Phys. **90** (1989) 6925

89Zha1 Zhang, W., Cooper, G., Ibuki, T., Brion, C.E.: Chem. Phys. **137** (1989) 391

90Mit1 Mitsuke, K., Suzuki, S., Imamura, T., Koyano, I.: J. Chem. Phys. **93** (1990) 8717

91Cha1 Chan, W.F., Cooper, G., Brion, C.E.: Phys.Rev.A **44** (1991) 186

91Cre1 Creasey, J.C., Lambert, I.R., Turkett, R.P., Codling, K., Frasinski, L.J., Hatherly, P.A., Stankiewicz, M.: J. Chem. Soc. Faraday Trans. **87** (1991) 1287

91Kam1 Kameta, K., Ukai, M., Chiba, R., Nagano, K., Kouchi, N., Hatano, Y., Tanaka, K.: J. Chem. Phys. **95** (1991) 1456

91Kam2 Kameta, K., Ukai, M., Terazawa, N., Nagano, K., Chikahiro, Y., Kouchi, N., Hatano, Y., Tanaka, K.: J. Chem. Phys. **95** (1991) 6188

91Uka1 Ukai, M., Kameta, K., Chiba, R., Nagano, K., Kouchi, N., Shinsaka, K., Hatano, Y., Umemoto, H., Ito, Y., Tanaka, K.: J. Chem. Phys. **95** (1991) 4142

92Bur1 Burton, G.R., Chan, W.F., Cooper, G., Brion, C.E.: Chem. Phys. **167** (1992) 349

92Fen1 Fennelly, J.A., Torr, D.G.: Atomic Data and Nuclear Data Tables **51** (1992) 321

92Hol1 Holland, D.M.P., Shaw, D.A., Hopkirk, A., MacDonald, M.A., McSweeney, S.M.: J. Phys. B: At. Mol. Opt. Phys. **25** (1992) 4823

92Kam1 Kameta, K., Ukai, M., Kamosaki, T., Shinsaka, K., Kouchi, N., Hatano, Y., Tanaka, K.: J. Chem. Phys. **96** (1992) 4911

92Sha1 Shaw, D.A., Holland, D.M.P., MacDonald, M.A., Hopkirk, A., Hayes, M.A., McSweeney, S.M.: Chem.Phys. **163** (1992) 387

92Sha2 Shaw, D.A., Holland, D.M.P., MacDonald, M.A., Hopkirk, A., Hayes, M.A., McSweeney, S.M.: Chem. Phys. **166** (1992) 379

93Au1 Au, J.W., Cooper, G., Burton, G.R., Olney, T.N., Brion, C.E.: Chem.Phys. **173** (1993) 209

93Bur1 Burton, G.R., Chan, W.F., Cooper, G., Brion, C.E.: Chem. Phys. **177** (1993) 217

93Cha1 Chan, W.F., Cooper, G., Sodhi, R.N.S., Brion, C.E.: Chem. Phys. **170** (1993) 81

93Cha2 Chan, W.F., Cooper, G., Brion, C.E.: Chem. Phys. **170** (1993) 99

93Cha3 Chan, W.F., Cooper, G., Brion, C.E.: Chem. Phys. **170** (1993) 111

93Cha4 Chan, W.F., Cooper, G., Brion, C.E.: Chem. Phys. **170** (1993) 123

93Cha5 Chan, W.F., Cooper, G., Brion, C.E.: Chem. Phys. **178** (1993) 387

93Cha6 Chan, W.F., Cooper, G., Brion, C.E.: Chem. Phys. **178** (1993) 401

93Chu1 Chung, Y.M., Lee, E.-M., Masuoka, T., Samson, J.A.R.: J. Chem. Phys. **99** (1993) 885

93Hol1 Holland, D.M.P., Shaw, D.A., McSweeney, S.M., MacDonald, M.A., Hopkirk, A., Hayes, M.A.: Chem. Phys. **173** (1993) 315

94Bur1 Burton, G.R., Chan, W.F., Cooper, G., Brion, C.E.: Chem. Phys. **181** (1994) 147

94Cha1 Chan, W.F., Cooper, G., Brion, C.E.: Chem. Phys. **180** (1994) 77

94Hat1 Hatano, Y., in: Dynamics of Excited Molecules (Kuchitsu, K., ed.), Amsterdam: Elsevier (1994), Chapter 6

94Sam1 Samson, J.A.R., Haddad, G.N.: J. Opt. Soc. Am. B **11** (1994) 277

95Coo1 Cooper, G., Olney, T.N., Brion, C.E.: Chem. Phys. **194** (1995) 175

95Coo2 Cooper, G., Burton, G.R., Chan, W.F., Brion, C.E.: Chem. Phys. **196** (1995) 293

95Coo3 Cooper, G., Burton, G.R., Brion, C.E.: J. Electron Spectrosc. Relat. Phenomen. **73** (1995) 139

95Hat1 Hatano, Y., Inokuti, M., in: Atomic and Molecular Data for Radiotherapy and Radiation Research (Inokuti, M., ed.), Vienna: IAEA (1995), Chapter 5

95Hat2 Hatano, Y., in: The Physics of Electronic and Atomic Collisions (Dube, L.J., Mitchell, J.B.A., McConkey, J.W., Brion, C.E., eds.), New York: AIP Press (1995), p. 67

95Hat3 Hatano, Y., in: Radiation Research, volume II (Hagen, U., Harder, D., Jung, H., Streffer, C., eds.), Univ. Würzburg (1995), p. 86

95Hol1 Holland, D.M.P., Shaw, D.A., Hayes, M.A.: Chem. Phys. **201** (1995) 299

95Lat1 Latimer, C.J., Dunn, K.F., O'Neill, F.P., MacDonald, M.A., Kouchi, N.: J. Chem. Phys. **102** (1995) 722

95Sha1 Shaw, D.A., Holland, D.M.P., Hayes, M.A., MacDonald, M.A., Hopkirk, A., McSweeney, S.M.: Chem. Phys. **198** (1995) 381

96Kam1 Kameta, K., Machida, S., Kitajima, M., Ukai, M., Kouchi, N., Hatano, Y., Ito, K.: J. Electron Spectrosc. Relat. Phenom. **79** (1996) 391

96Uka1 Ukai, M.: J. Electron Spectrosc. Relat. Phenom. **79** (1996) 423

97Au1 Au, J.W., Burton, G.R., Brion, C.E.: Chem. Phys. **221** (1997) 151

97Can1 Cann, N., Olney, T.N., Brion, C.E.: in preparation. This paper was cited in the review paper by Olney et al. [97Oln1]. The σ_a values measured with the high resolution (48 meV) are available in the ftp site, ftp://ftp.chem.ubc.ca/pub/cooper, as described in [97Oln1].

97Dyc1 Dyck, M., Cooper, G., Olney, T.N., Brion, C.E.: in preparation. This paper was cited in the review paper by Olney et al. [97Oln1]. The σ_a values measured with both the high resolution (48 meV) and low resolution (1 eV) are available in the anonymous ftp site, ftp://chem.ubc.ca/pub/cooper, as described in [97Oln1]

97Hol1 Holland, D.M.P., Shaw, D.A., Hayes, M.A., Shpinkova, L.G., Rennie, E.E., Karlsson, L., Baltzer, P., Wannberg, B.: Chem. Phys. **219** (1997) 91

97Kou1 Kouchi, N., Ukai, M., Hatano, Y.: J. Phys. B: At. Mol. Opt. Phys. **30** (1997) 2319

97Oln1 Olney, T.N., Cann, N.M., Cooper, G., Brion, C.E.: Chem. Phys. **223** (1997) 59

97Oln2 Olney, T.N., Cooper, G., Brion, C.E.: to be published. This paper was cited in the review paper by Olney et al. [97Oln1]. The σ_a values measured with both the high resolution (48 meV) and low resolution (1 eV) are available in the anonymous ftp site, ftp://chem.ubc.ca/pub/cooper, as described in [97Oln1]

98Mas1 Masuoka, T., Chung, Y., Lee, E-M., Samson, J.A.R.: J. Chem. Phys. **109** (1998) 2246

98Ren1 Rennie, E.E., Johnson, C.A.F., Parker, J.E., Holland, D.M.P., Shaw, D.A., Hayes, M.A.: Chem. Phys. **229** (1998) 107

99Edv1 Edvardsson, D., Baltzer, P., Karlsson, L., Wannberg, B., Holland, D.M.P., Shaw, D.A., Rennie, E.E.: J. Phys. B: At. Mol. Opt. Phys. **32** (1999) 2583

99Fen1 Feng, R., Cooper, G., Burton, G.R., Brion, C.E., Avaldi, L.: Chem. Phys. **240** (1999) 371

99Hat1 Hatano, Y.: Phys. Rep. **313** (1999) 109

99Hol1 Holland, D.M.P., Shaw, D.A.: Chem. Phys. **243** (1999) 333

99Kam1 Kameta, K., Muramatsu, K., Machida, S., Kouchi, N., Hatano, Y.: J. Phys. B: At. Mol. Opt. Phys. **32** (1999) 2719

5 Cross sections for ion production by electron collisions with molecules

5.1 Ionization

5.1.1 Introduction

Ionization of molecules by electron impact is of fundamental importance in many areas of science and technology, consequently it has been the subject of experimental investigation for more than seventy years and the literature abounds with publications on this topic. The accurate determination of absolute electron-impact ionization cross sections for molecules is not a trivial task and inevitably there is often considerable disagreement between various studies. Here we provide, for a large number of molecules, experimental cross section data that we believe to be the most reliable currently available. Theoretical approaches have also been used to determine total electron-impact ionization cross sections and substantial agreement with the recommended experimental values is quite often observed. Calculations of partial cross sections on the other hand are generally much less reliable.

In collisions between electrons and a molecular target AB the following ion production processes may occur:

$e + AB \rightarrow AB^+ + 2e$	single ionization resulting in production of a parent molecular ion
$e + AB \rightarrow A + B^+ + 2e$	dissociative ionization resulting in the production of an, often energetic, fragment molecular ion
$e + AB \rightarrow AB^{2+} + 3e$	ionization resulting in production of a multiply charged product ion; generally much less likely than the other two processes

Most measurements of electron-impact ionization cross sections have been performed by passing a beam of monoenergetic electrons through a gaseous target and collecting the resulting positive ions. If few of the incident electrons collide with target molecules, the cross section $\sigma(X)$ for production of an ion X is given by

$$N(X) = N_e n l \sigma(X)$$

where $N(X)$ is the number of X ions produced by a number N_e of electrons passing a distance l through a uniform gas target of number density n. The cross section defined by this equation is the *partial cross section* for production of X and is normally given in units of m^2 or cm^2.[1] The *total ionization cross section* for a molecular target is then given by the sum of the individual partial ionization cross sections,

$$\sigma(\text{total}) = \sigma(X_1) + \sigma(X_2) + \sigma(X_3) + ...$$

[1] In the literature a variety of units are used; the conversion factors are as follows:
$1\ Å^2 = 1 \cdot 10^{-16}\ cm^2$; $\pi a_0^2 = 0.8797 \cdot 10^{-16}\ cm^2$; $1Mb = 1 \cdot 10^{-18}\ cm^2$.

In much of the earliest work on electron-impact ionization the *total charge production cross section*, which is much less difficult to determine, was measured rather than the partial and total ionization cross sections as defined here. The total charge production cross section is the sum of the partial ionization cross sections weighted by the charges of the respective ions. For molecular targets the total charge production cross section is usually very nearly equal to the total ionization cross section as only a relatively small number of multiply charged product ions are produced.[2] In the literature the total charge production cross section is sometimes referred to as the *gross cross section* or *gross total cross section*, and the total ionization cross section, as defined above, is occasionally referred to as the *counting cross section*. All of these cross sections are integral cross sections in that no account is taken of the details of the collision process, i.e. they are integral over all electron scattering angles, all fragment ion scattering angles and kinetic energies etc.

To arrive at a set of preferred cross section values and in order to understand the evaluation criteria it is necessary first to critically review the various experimental methods that have been used. They can be divided into two very broad categories: those in which the cross sections for total charge production are measured and those in which the partial cross sections for the different product ions are determined. Ultimately it is these partial cross sections that are most important for applications but total cross sections are also helpful in arriving at an accurate picture of the ionization process.

The earliest studies were generally confined to measurements of the total cross section and many of them utilized the parallel plate technique[3] pioneered by Smith [30Smi1] and Tate and Smith [32Tat1]. This approach involves passing an electron beam between a pair of parallel plates in the presence of an ambient target gas. A uniform electric field, perpendicular to the electron beam axis, accelerates ions to a collector and the resulting positive ion current is measured. The major weakness in these early studies concerns the measurement of the target gas pressure using a McLeod Gauge, which although the best instrument available at the time, was subject to error in the case of most gases.[4] Rapp and Englander-Golden [65Rap2] later used the parallel plate geometry, coupled with more reliable pressure measurements, in the study of numerous atoms and molecules and their work has been widely accepted as the *de facto* total cross section standard for quite some time. The parallel plate method is quite straightforward and can lead to extremely reliable results. Consequently, it is occassionally still used today and has provided much valuable and dependable data on total charge production cross sections.

However, for all molecular targets, more than one ionic species may result and primary interest centers on the partial cross sections for production of these different ionic species. The determination of these partial cross sections requires the use of mass spectrometers which substantially increase the complexity of the measurements. The experimental difficulties are further compounded by the fact that the mass spectrometers employed have often not been ideally suited to highly quantitative work. Quadrupole mass spectrometers which are known to have mass transmission issues being a case in point. Numerous studies have also demonstrated that it is extraordinarily difficult to ensure that all product ions are detected specially when mass spectrometers with a long path length are used. This particular problem is exacerbated in those situations where fragment ions are created with considerable kinetic energy and consequently the mass spectrometers used have often discriminated against energetic fragment ions sometimes resulting in underestimation of the cross sections by factors of two or more.

A number of experimental arrangements have commonly been employed to measure partial cross sections. One technique involves passing an electron beam through an effusive molecular beam and extracting the resulting positive ions into a mass spectrometer [90Kri1, 98Tia2]. Relative cross sections obtained in this way are then normalized with reference to a known partial or total cross section. One weakness of this approach is the difficulty of characterizing the overlap between the molecular beam target and the electron beam. Other problems result from the normalization procedures, which are sometimes quite involved, and in cases where normalization is achieved by comparing the sum of the

[2] For example, production of CO_2^{2+} ions by electron-impact on CO_2 is roughly two orders of magnitude less probable than production of the parent CO_2^+ ion.

[3] Sometimes referred to as the condenser technique.

[4] McCloud Gauges can, *if great care is taken*, be used to measure pressure accurately. However, there are numerous sources for potential error including the Ishii effect [85deH1] which was not demonstrated experimentally until 1961.

partial cross sections to a known total cross section any error in the measurement of one partial cross section inevitably results in errors in all of the remaining partial cross sections. Despite these shortcomings, and given complete collection of product ions etc., data obtained using this approach which are carefully normalized to a well established cross section[5] should be reliable.

A second technique incorporates a fast neutral molecular beam obtained by charge transfer of an energetic ion beam which is crossed by an ionizing electron beam. One advantage of this approach is the ease with which product ions may be collected, but, its greatest advantage is that it may be used to study unstable species such as radicals [88Shu1, 93Tar1]. The technique however does present formidable practical difficulties even in the hands of very capable experimenters. It is difficult to precisely ascertain the overlap between the electron beam and the fast neutral beam, and the presence of metastable species, which may be formed in the charge transfer process, is always a possibility. Consequently, the uncertainties in the cross sections determined in this way tend to be large.

An alternative technique in which an electron beam is passed through a static gas target and ions formed along a known path length are extracted and mass analyzed has been pioneered by Stebbings and coworkers [95Str1, 96Str1]. It embodies the simplicity of the parallel plate arrangement discussed earlier coupled with an extremely short path length mass spectrometer together with a detector with which it is possible to demonstrate complete collection of all fragment ions. All quantities needed for the determination of the partial cross sections are directly measured. It overcomes many of the limitations of other techniques and has been shown to produce very accurate independently absolute partial ionization cross sections [01Ste1, 02Rej1]. Its only significant weakness is the relatively low mass resolution achieved which makes it less than ideal for molecules which contain hydrogen atoms.

This brief survey of experimental methods can only cover the most commonly employed techniques. Other methods have been successfully applied in specific cases or have seen only limited use, e.g. fourier transform mass spectrometry [99Jia1].

In evaluating the data for this compilation much stress has been put on the reliability of the experimental techniques employed. Due to the pressure measurement issues outlined above studies prior to that of Rapp and Englander-Golden [65Rap2] are generally not considered very dependable. Among more recent work, studies which have been able to show collection of all product ions are preferred over those where ion discrimination effects are probable. Measurements with small accompanying uncertainties and those which are entirely independent and do not rely on normalization to other work have also been accorded greater weight. By contrast cross section data reported without any uncertainties at all have only been considered when no other data exist.

Other measures of reliability based on comparision of different measurements were also considered. While agreement between two or more independent measurements of the same cross section was generally taken as an endorsement of the accuracy of both measurements, this was not considered conclusive proof of their accuracy as there are many instances where cross sections from different laboratories agree for one process but disagree for others. On the other hand, measurements performed by two different laboratories for many molecular targets which are found to consistently agree must be accorded a higher level of confidence [01Ste1, 02Rej1] and have been recommended where available.

We have attempted to be comprehensive in this compilation. Inevitably, some of the recommended cross sections are of lesser reliability than others but the data presented here are believed to be the best presently available.

[5] Data are often normalized to the Ar^+ partial cross section and often ultimately rely on the accuracy of the Rapp and Englander-Golden [65Rap2] argon total cross section measurement.

5.1.2 Sources

Considerable efforts have been made to examine all relevant publications. A complete list of the articles consulted is given in the bibliography at the end of this compilation. Besides conducting two independent literature searches a number of review articles and bibliographies were also consulted. Comprehensive articles by Zecca and coworkers [01Kar1, 01Kar2, 96Zec1], Märk [85Mar1], Kieffer [67Kie1], and Kieffer and Dunn [66Kie1] were found to be particularly helpful. Useful summaries of recent theoretical work have been given by Harland et al. [98Har1] and Deutsch et al. [00Deu1].

5.1.3 Notes on the data

The following tables and graphs give the recommended ionization cross sections as a function of electron impact energy. Generally, absolute values of the various partial ionization cross sections and the total ionization cross section are given for each species, however, occasionally a complete set of cross sections was unavailable. In several instances the most accurate total cross section measurements reported are those for total charge production. As the total charge production cross section should be essentially equal to the total ionization cross section these total charge production cross sections have been recommended.

Partial cross sections are normally given for production of one specific ion, e.g. $\sigma(O^+)$. However, in some cases it was not possible for the experimenters to distinguish between two species having the same charge-to-mass ratio. The recommended partial cross sections are therefore the sum of the individual partial cross sections, e.g. $\sigma(O^+ + O_2^{2+})$ is equal to the sum of $\sigma(O^+)$ and $\sigma(O_2^{2+})$. For diatomic molecules the cross section for production of the doubly charged parent ion is usually much smaller than that for the singly charged fragment ion and $\sigma(O^+ + O_2^{2+})$, for example, is therefore very nearly equal to $\sigma(O^+)$.

The uncertainties associated with each cross section are given in the text that accompanies the data. In a few cases uncertainties are also given in the data tables, where 1.23(14), for example, indicates 1.23 ± 0.14 and 1.23(4) indicates 1.23 ± 0.04.

Even the most reliable experimental data are subject to some uncertainty, and it is extremely important to bear in mind the accompanying error bars, the general considerations regarding the limitations of the various experimental techniques discussed earlier, and the specific comments regarding each data set.

Acknowledgements

The authors thank Professor Itikawa for the opportunity of contributing to this project, and the staff at Springer-Verlag for their help. We would also like to thank Professor R. F. Stebbings for his expert advice, critical comment, and encouragement during the course of this work.

5.1.4 Cross section data

CH_3Br - Bromomethane [74-83-9]

Recommended data: Rejoub et al. [02Rej2]
Technique used: Parallel plate apparatus with time-of-flight mass spectrometer and position-sensitive detection of product ions; independently absolute.
Comments: The absolute uncertainties in $\sigma(CH_nBr^+)$, $\sigma(CH_n^+)$, $\sigma(Br^+)$, $\sigma(H^+)$ and σ(total) are ±6%, unless otherwise indicated. The uncertainty in the electron beam energy calibration is ±0.5 eV.
Other data reviewed: [97Val1, 69Ber1]

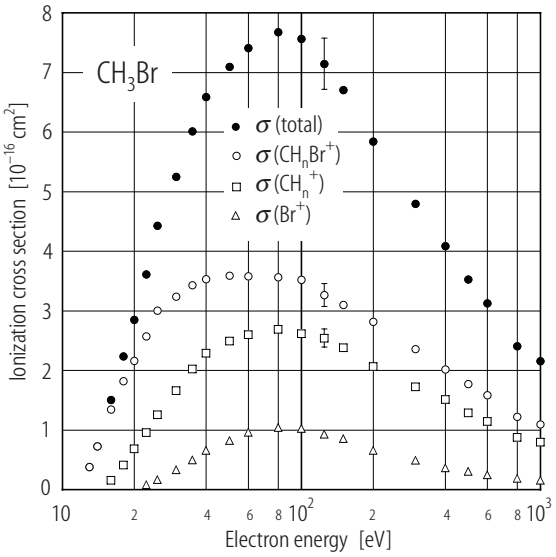

Fig. 5.1.1. CH_3Br electron-impact ionization cross sections.

Table 5.1.1. CH_3Br partial and total electron-impact ionization cross sections.

Energy [eV]	$\sigma(CH_nBr^+)$ [10^{-16} cm^2]	$\sigma(CH_n^+)$ [10^{-16} cm^2]	$\sigma(Br^+)$ [10^{-16} cm^2]	$\sigma(H^+)$ [10^{-17} cm^2]	σ(total) [10^{-16} cm^2]
13	0.382(42)				0.382(42)
14	0.729(66)				0.729(66)
16	1.35(12)	0.158(24)			1.50(14)
18	1.82(13)	0.415(37)			2.23(16)
20	2.16	0.684(48)			2.85
22.5	2.57	0.958(67)	0.080(32)		3.61
25	3.01	1.25	0.167(33)		4.43
30	3.24	1.66	0.334(37)	0.154	5.25
35	3.43	2.02	0.497	0.603	6.01
40	3.53	2.29	0.657	1.04	6.58
50	3.59	2.49	0.824	1.87	7.10
60	3.58	2.60	0.961	2.70	7.41
80	3.57	2.69	1.04	3.79	7.68
100	3.52	2.62	1.02	4.11	7.57
125	3.27	2.54	0.932	4.03	7.14
150	3.10	2.38	0.852	3.67	6.70
200	2.82	2.07	0.657	3.03	5.84
300	2.36	1.72	0.489	2.28	4.80
400	2.02	1.51	0.366	1.89	4.09
500	1.77	1.29	0.302	1.69	3.53
600	1.58	1.14	0.248	1.49	3.12
800	1.22	0.876	0.186	1.25	2.41
1000	1.09	0.799	0.154	1.06	2.15

Br_2 - Bromine [7726-95-6]

Recommended data: Kurepa et al. [81Kur1]
Technique used: Parallel plate apparatus with total ion collection; independently absolute.
Comments: The relative uncertainty in the measured cross section is reported as ± 0.05. The energy scale was calibrated to within 0.05 eV.

Table 5.1.2. Br_2 total electron-impact ionization cross section.[6]

Energy [eV]	σ(total) [10^{-16} cm^2]	Energy [eV]	σ(total) [10^{-16} cm^2]
10.6	0.04	29	6.57
11	0.20	30	6.74
11.6	0.47	32	7.18
12	0.67	34	7.48
12.6	0.94	36	7.74
13	1.11	38	7.99
13.6	1.41	40	8.17
14	1.61	42	8.35
14.6	1.92	44	8.56
15	2.08	46	8.71
15.6	2.38	48	8.84
16	2.59	50	8.97
16.6	2.83	52	9.17
17	2.99	54	9.33
17.6	3.27	56	9.46
18	3.44	58	9.69
19	3.84	60	9.84
20	4.21	62	9.94
21	4.54	66	10.1
22	4.87	70	10.2
23	5.16	76	10.2
24	5.43	80	10.2
25	5.73	86	10.3
26	5.96	90	10.2
27	6.20	96	10.2
28	6.37	100	10.2

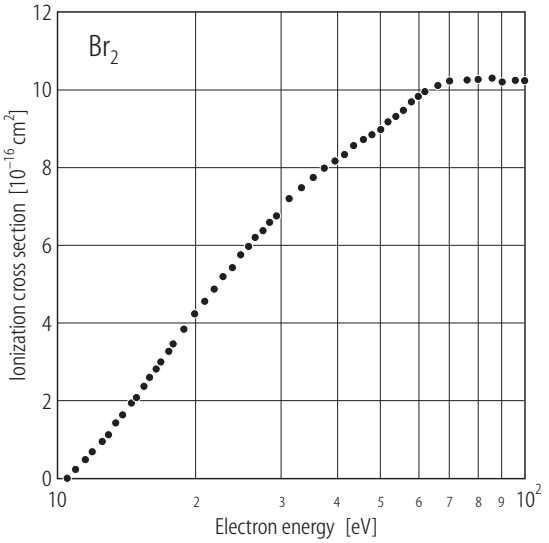

Fig. 5.1.2. Br_2 total electron-impact ionization cross section.

[6] This cross section is for total charge production. For conciseness only representative data points are tabulated.

CCl_2F_2 - Dichlorodifluoromethane [75-71-8]

Recommended data: Leiter et al. [89Lei1]

Technique used: Double focussing mass spectrometer. The data are ultimately normalized to the argon total cross section of Rapp and Englander-Golden [65Rap2].

Comments: The total cross section of Leiter et al. [89Lei1] is in good agreement with the single measurement by Beran and Kevan [69Ber1, 97Chr1] at 70 eV. The maximum relative uncertainty is given as ± 5% for singly charged ions, and ± 10 % for doubly charged ions. The absolute uncertainty is reported as ± 10 % for singly charged ions and ± 20 % for doubly charged ions. However, it should be noted that there are few reliable experimental data with which to compare the results of Leiter et al. [89Lei1] and that the type of apparatus used has often been found to discriminate against energetic fragment ions. The available CCl_2F_2 cross section data have recently been reviewed by Christophorou et al. [97Chr1].

Other data reviewed: [79Pej1]

Table 5.1.3a. CCl_2F_2 partial electron-impact ionization cross sections.

Energy [eV]	$\sigma(CCl_2F_2^+)$ [10^{-18} cm^2]	$\sigma(CCl_2F^+)$ [10^{-17} cm^2]	$\sigma(CClF_2^+)$ [10^{-16} cm^2]	$\sigma(CCl_2^+)$ [10^{-18} cm^2]	$\sigma(Cl_2^+)$ [10^{-18} cm^2]	$\sigma(CClF^+)$ [10^{-17} cm^2]	$\sigma(ClF^+)$ [10^{-19} cm^2]
15	0.09		0.12		0.16		
20	0.63	0.70	1.44	0.01	0.61		0.04
25	0.76	2.25	3.02	0.33	1.01	0.59	0.13
30	0.89	3.52	3.78	1.00	1.75	1.37	0.46
35	0.93	4.11	3.99	1.40	2.68	1.87	0.89
40	0.97	4.47	4.05	1.60	3.29	2.12	1.79
45	1.00	4.82	4.17	1.67	3.60	2.23	2.36
50	1.02	5.10	4.21	1.67	3.78	2.31	2.55
55	1.04	5.31	4.28	1.67	3.83	2.42	2.63
60	1.05	5.56	4.39	1.70	3.83	2.54	2.69
65	1.05	5.73	4.48	1.78	3.81	2.63	2.69
70	1.06	5.98	4.60	1.83	3.80	2.72	2.68
75	1.06	6.12	4.72	1.88	3.81	2.81	2.67
80	1.07	6.26	4.72	1.90	3.83	2.88	2.65
90	1.06	6.37	4.66	1.96	3.76	2.90	2.56
100	1.10	6.40	4.60	2.06	3.70	2.90	2.50
110	1.04	6.44	4.58	2.02	3.76	2.93	2.40
120	1.03	6.51	4.54	1.91	3.83	2.94	2.31
130	1.02	6.54	4.54	1.93	3.75	2.97	2.24
140	1.00	6.61	4.54	1.96	3.70	2.98	2.18
150	0.98	6.68	4.52	1.96	3.56	2.98	2.12
160	0.95	6.68	4.44	1.93	3.43	2.99	2.04
170	0.93	6.61	4.35	1.87	3.29	2.97	1.92
180	0.89	6.58	4.28	1.82	3.11	2.95	1.83

Table 5.1.3b. CCl_2F_2 partial and total electron-impact ionization cross sections.

Energy [eV]	$\sigma(CF_2^+)$ [10^{-17} cm^2]	$\sigma(CCl^+)$ [10^{-17} cm^2]	$\sigma(Cl^+)$ [10^{-16} cm^2]	$\sigma(CF^+)$ [10^{-17} cm^2]	$\sigma(F^+)$ [10^{-18} cm^2]	$\sigma(C^+)$ [10^{-17} cm^2]	σ(total) [10^{-16} cm^2]
15							0.11
20	0.28						1.55
25	2.43		0.05	0.55			3.67
30	4.62	0.59	0.21	3.60	0.03	0.02	5.40
35	5.83	2.35	0.51	5.79	0.27	0.13	6.56
40	6.32	4.03	0.78	6.71	0.87	0.53	7.32
45	6.56	4.75	0.97	6.86	1.89	1.10	7.88
50	6.64	4.81	1.06	6.71	2.57	1.16	8.07
55	6.93	4.70	1.09	6.55	3.01	1.26	8.22
60	7.13	4.63	1.10	6.58	3.36	1.32	8.43
65	7.33	4.55	1.09	6.58	3.66	1.39	8.57
70	7.57	4.53	1.10	6.61	3.88	1.42	8.76
75	7.78	4.49	1.11	6.64	4.10	1.46	8.95
80	7.80	4.44	1.12	6.61	4.24	1.46	8.99
90	8.02	4.36	1.09	6.49	4.51	1.51	8.92
100	8.10	4.20	1.08	6.40	4.70	1.50	8.84
110	8.10	4.08	1.06	6.31	4.81	1.49	8.78
120	8.06	3.94	1.04	6.10	4.84	1.48	8.76
130	8.10	3.80	1.02	6.03	4.81	1.47	8.66
140	8.10	3.75	1.01	6.00	4.81	1.47	8.65
150	8.10	3.66	0.98	5.94	4.81	1.44	8.59
160	8.06	3.58	0.97	5.85	4.75	1.39	8.46
170	8.02	3.49	0.94	5.73	4.67	1.34	8.31
180	7.94	3.37	0.92	5.64	4.59	1.31	8.17

Table 5.1.4. Cross sections for production of mulitply-charged ions from CCl_2F_2 by electron-impact at selected energies.

Energy [eV]	$\sigma(Cl^{2+})$ [10^{-19} cm^2]	$\sigma(CCl^{2+})$ [10^{-18} cm^2]	$\sigma(CCl_2^{2+})$ [10^{-18} cm^2]	$\sigma(CClF^{2+})$ [10^{-19} cm^2]	$\sigma(CClF_2^{2+})$ [10^{-18} cm^2]	$\sigma(CCl_2F^{2+})$ [10^{-18} cm^2]
40			0.06	0.04	0.09	0.34
45			0.45	0.52	0.39	0.99
50			1.07	1.04	0.71	1.50
55	0.06	0.15	1.52	2.21	1.00	1.88
60	0.19	0.31	1.88	2.74	1.23	2.10
65	0.48	0.54	2.08	3.21	1.39	2.29
70	0.91	0.66	2.25	3.58	1.51	2.44
75	1.34	0.74	2.37	3.88	1.60	2.58
80	1.64	0.81	2.46	4.08	1.67	2.66
90	2.15	0.91	2.61	4.43	1.76	2.82
100	2.50	0.99	2.70	4.70	1.80	2.90
120	2.87	1.03	2.81	4.97	1.80	2.92
140	2.96	1.04	2.79	4.97	1.76	2.88
160	2.87	1.02	2.74	4.85	1.69	2.78
180	2.72	0.98	2.62	4.60	1.60	2.64

CCl_4 - Carbon tetrachloride [56-23-5]

Recommended data: Hudson et al. [01Hud1]

Technique used: The apparatus used consisted of a cylindrical collision cell with a magnetically confined electron beam. The cross sections were determined from the total charge collected on the collision cell. These data are independently absolute.

Comments: The experimental accuracy is reported as 4 % or better although this does not necessarily reflect the absolute accuracy [01Hud1, 97Val1]. Comparison of the CH_4 data of Vallance et al. [97Val1], which were obtained using the same apparatus, with the recommended cross section given in this compilation suggests that the absolute accuracy of their CCl_4 data is on the order of ±10 % near the peak of the cross section but lower at other energies. Note that the earlier partial cross section measurments of Leiter et al. [84Lei1] apparently suffer from incomplete ion collection [89Lei1, 01Kar2] which is consistent with the fact that they are significantly lower than the data of Hudson et al. [01Hud1]. Leiter et al. [84Lei1] report that no stable CCl_4^+ ions are formed.

Other data reviewed: [99Lim1, 52Cra1, 61Fox1]

Table 5.1.5. CCl_4 total electron-impact ionization cross sections.[7]

Energy [eV]	σ (total) [10^{-15} cm^2]	Energy [eV]	σ (total) [10^{-15} cm^2]
12	0.177	90	1.52
16	0.283	97	1.50
20	0.500	105	1.47
23	0.738	112	1.44
27	0.935	119	1.42
30	1.06	126	1.40
34	1.16	134	1.36
38	1.24	141	1.34
42	1.32	149	1.33
45	1.37	156	1.30
49	1.42	164	1.26
53	1.46	172	1.23
57	1.50	178	1.21
61	1.52	185	1.20
64	1.54	193	1.18
68	1.54	201	1.16
72	1.56	208	1.14
79	1.54	216	1.13
86	1.53		

[7] These cross sections are for total charge production. The data were digitized from graphs given by Hudson et al. [01Hud1].

CH_3Cl – Chloromethane [74-87-3]

CH_3F – Fluoromethane [593-53-3]

CH_3I – Iodomethane [74-88-4]

Recommended data: Rejoub et al. [02Rej2]

Technique used: Parallel plate apparatus with time-of-flight mass spectrometer and position-sensitive detection of product ions; independently absolute.

Comments: The absolute uncertainties in $\sigma(CH_nCl^+)$, $\sigma(CH_nF^+)$, $\sigma(CH_nI^+)$, $\sigma(CH_n^+)$, $\sigma(I^+)$, $\sigma(H^+)$, and σ(total) are ±6%, unless otherwise indicated. The absolute uncertainties in $\sigma(Cl^+)$ and $\sigma(F^+)$ are ±7% and ±20%, respectively. The uncertainty in the electron beam energy calibration is ±0.5 eV.

Other data reviewed: [01Tor1, 97Val1, 69Ber1]

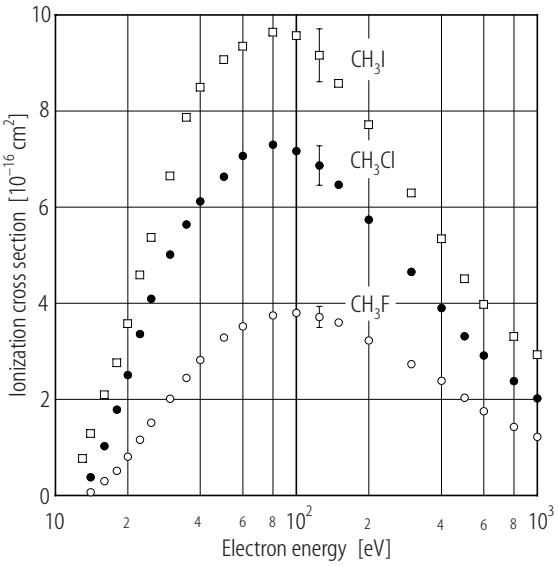

Fig. 5.1.3. CH_3Cl, CH_3F, and CH_3I total electron-impact ionization cross sections.

Table 5.1.6. CH_3Cl partial and total electron-impact ionization cross sections.

Energy [eV]	$\sigma(CH_nCl^+)$ [10^{-16} cm^2]	$\sigma(CH_n^+)$ [10^{-16} cm^2]	$\sigma(Cl^+)$ [10^{-17} cm^2]	$\sigma(H^+)$ [10^{-17} cm^2]	σ(total) [10^{-16} cm^2]
14	0.385(42)				0.385(42)
16	1.03(7)				1.03(7)
18	1.45(10)	0.344(34)			1.79(13)
20	1.81	0.698(56)			2.51
22.5	2.24	1.12(8)			3.36
25	2.51	1.58(11)		0.092(23)	4.10
30	2.71	2.20	0.575	0.502(35)	5.01
35	2.90	2.49	1.87	0.732	5.64
40	2.99	2.67	3.25	1.45	6.12
50	3.06	2.83	4.57	2.97	6.64
60	3.14	2.85	6.38	4.37	7.07
80	3.15	2.92	6.57	5.70	7.30
100	3.12	2.87	5.97	5.76	7.17
125	3.01	2.75	5.55	5.51	6.87
150	2.85	2.62	5.19	4.83	6.47
200	2.61	2.28	4.33	4.18	5.75
300	2.15	1.89	3.14	3.00	4.66
400	1.81	1.63	2.39	2.25	3.90
500	1.56	1.37	1.87	1.93	3.31
600	1.39	1.21	1.55	1.59	2.92
800	1.15	0.986	1.22	1.20	2.38
1000	0.983	0.844	0.959	0.997	2.02

Table 5.1.7. CH_3F partial and total electron-impact ionization cross sections.

Energy [eV]	$\sigma(CH_nF^+)$ [10^{-16} cm^2]	$\sigma(CH_n^+)$ [10^{-16} cm^2]	$\sigma(F^+)$ [10^{-18} cm^2]	$\sigma(H^+)$ [10^{-17} cm^2]	σ(total) [10^{-16} cm^2]
14	0.070(11)				0.070(11)
16	0.300(30)				0.300(30)
18	0.513(41)				0.513(41)
20	0.651	0.160(16)			0.812
22.5	0.852	0.314			1.17
25	1.03	0.488			1.51
30	1.23	0.776		0.123(12)	2.02
35	1.38	1.01		0.497(50)	2.45
40	1.51	1.21		0.989(99)	2.82
50	1.59	1.46	2.99(90)	2.05	3.29
60	1.64	1.57	3.75	2.80	3.52
80	1.68	1.64	5.34	3.79	3.75
100	1.67	1.66	5.77	4.20	3.80
125	1.61	1.60	6.08	4.43	3.72
150	1.56	1.57	5.99	4.17	3.60
200	1.40	1.39	5.24	3.80	3.23
300	1.19	1.21	4.30	2.95	2.73
400	1.06	1.05	3.73	2.39	2.39
500	0.911	0.897	3.07	1.97	2.04
600	0.798	0.780	2.34	1.53	1.75
800	0.645	0.638	1.90	1.25	1.43
1000	0.546	0.558	1.70	1.02	1.22

Table 5.1.8. CH_3I partial and total electron-impact ionization cross sections.

Energy [eV]	$\sigma(CH_nI^+)$ [10^{-16} cm^2]	$\sigma(CH_n^+)$ [10^{-16} cm^2]	$\sigma(I^+)$ [10^{-16} cm^2]	$\sigma(H^+)$ [10^{-17} cm^2]	σ(total) [10^{-16} cm^2]
13	0.77(15)				0.77(15)
14	1.29(26)				1.29(26)
16	2.10(21)				2.10(21)
18	2.77(28)				2.77(28)
20	3.43(27)	0.080(16)	0.061(12)		3.57(29)
22.5	3.95	0.107(11)	0.529(79)		4.59
25	4.14	0.277(28)	0.951(95)		5.37
30	4.36	0.740(59)	1.54(15)		6.65
35	4.56	1.39	1.89(19)	0.376(38)	7.87
40	4.66	1.72	2.03	0.811(81)	8.49
50	4.70	1.98	2.23	1.61(16)	9.07
60	4.67	2.17	2.29	2.25	9.35
80	4.66	2.30	2.33	3.53	9.64
100	4.58	2.25	2.28	4.56	9.57
125	4.31	2.15	2.17	5.31	9.16
150	4.02	2.02	2.02	5.26	8.58
200	3.63	1.84	1.75	4.87	7.72
300	3.03	1.51	1.36	3.95	6.30
400	2.55	1.28	1.15	3.52	5.34
500	2.18	1.08	0.942	3.03	4.51
600	1.92	0.970	0.819	2.69	3.98
800	1.58	0.803	0.689	2.32	3.31
1000	1.41	0.707	0.601	2.11	2.93

CF_4 - Carbon tetrafluoride [75-73-0]

Recommended data: Sieglaff et al. [01Sie1]

Technique used: Parallel plate apparatus with time-of-flight mass spectrometer and position-sensitive detection of product ions; independently absolute.

Comments: The absolute uncertainties in $\sigma(CF_3^+)$, $\sigma(CF_2^+)$, $\sigma(CF^+ + CF_3^{2+})$, and $\sigma(C^+)$ are ± 5 %, unless otherwise indicated. The uncertainties in $\sigma(F^+)$ and $\sigma(CF_2^{2+})$ are ± 8 % and ± 7 % respectively, unless otherwise indicated. The uncertainty in the electron beam energy calibration is ± 0.5 eV. The recommended total cross section is in excellent agreement with the total charge production cross section of Nishimura et al. [99Nis1] and with the data of Rao and Srivastava [97Rao1]. Cross sections for production of pairs of positive ions have been measured by Bruce et al. [92Bru1][8] and Sieglaff et al. [01Sie1]. Most of the available CF_4 data have recently been reviewed by Christophorou et al. [99Chr2, 96Chr1].

Other data reviewed: [95Bru1, 94Bon1, 94Bru1, 93Bru1, 92Ma1, 92Pol1, 91Ma1, 87Pol1, 85Ste1]

Table 5.1.9. CF_4 partial and total electron-impact ionization cross sections.

Energy [eV]	$\sigma(CF_3^+)$ [10^{-16} cm^2]	$\sigma(CF_2^+)$ [10^{-17} cm^2]	$\sigma(CF^+ + CF_3^{2+})$ [10^{-17} cm^2]	$\sigma(C^+)$ [10^{-17} cm^2]	$\sigma(F^+)$ [10^{-17} cm^2]	$\sigma(CF_2^{2+})$ [10^{-18} cm^2]	σ(total) [10^{-16} cm^2]
18	0.041(4)						0.041
20	0.16(1)						0.175
23	0.40	0.021(6)					0.403
27	0.82	0.22(2)					0.847
30	1.20	0.53	0.023(5)				1.25
35	1.65	1.26	0.14(1)	0.005(2)	0.018(9)		1.79
40	1.97	1.42	0.56	0.089(6)	0.092		2.19
45	2.26	1.57	1.08	0.41	0.30	0.02(04)	2.60
50	2.52	1.90	1.59	0.85	0.65	0.32(3)	3.02
60	2.84	2.25	1.97	1.29	1.37	0.91	3.54
70	3.03	2.48	2.57	1.67	2.22	1.86	3.95
80	3.14	2.67	2.93	1.95	3.08	2.76	4.23
90	3.23	2.88	3.20	2.18	3.76	3.35	4.46
100	3.26	2.98	3.56	2.43	4.66	3.93	4.67
120	3.29	3.07	3.91	2.72	5.86	4.64	4.89
140	3.25	3.02	3.89	2.83	6.52	5.01	4.93
160	3.19	3.02	4.03	2.93	7.06	5.02	4.95
200	3.09	2.85	3.79	2.87	7.36	4.97	4.83
250	2.92	2.72	3.58	2.70	6.89	4.49	4.56
300	2.74	2.53	3.23	2.50	6.44	4.41	4.26
400	2.47	2.20	2.59	2.08	5.31	3.52	3.72
500	2.22	1.97	2.20	1.80	4.50	2.91	3.30
600	2.03	1.75	1.94	1.55	3.80	2.69	2.97
800	1.72	1.46	1.52	1.26	2.89	2.10	2.45
1000	1.51	1.24	1.24	1.04	2.47	1.57	2.12

[8] For revisions to the original data see Bonham [94Bon1] and Bruce et al. [95Bru1].

CH_3OH – Methanol [67-56-1]

Recommended data: Rejoub et al. [03Rej1][9]

Technique used: Parallel plate apparatus with time-of-flight mass spectrometer and position sensitive detection of product ions; independently absolute.

Comments: The absolute uncertainties in $\sigma(CH_nO^+)$, $\sigma(CH_n^+ + H_nO^+)$, $\sigma(H^+)$, $\sigma(H_2^+)$, and σ(total) are ±6%, ±6%, ±6%, ±8%, and ±6% respectively. The uncertainty in the electron energy calibration is ±0.5 eV. The recommended total cross section is in good agreement with those of Duric et al. [89Dur1] and Srivastava et al. [96Sri1]. The CH_nO^+ partial cross section agrees well with the sum of the partial cross sections reported by Srivastava et al. [96Sri1].

Table 5.1.10. CH_3OH partial and total electron-impact ionization cross sections.

Energy [eV]	$\sigma(CH_nO^+)$ [10^{-16} cm^2]	$\sigma(CH_n^+ + H_nO^+)$ [10^{-16} cm^2]	$\sigma(H^+)$ [10^{-17} cm^2]	$\sigma(H_2^+)$ [10^{-18} cm^2]	σ(total) [10^{-16} cm^2]
13	0.151(12)				0.151(12)
14	0.335(27)				0.335(27)
16	0.609(43)	0.015(3)			0.624(43)
18	0.913	0.063(6)			0.976
20	1.22	0.115(9)			1.33
22.5	1.60	0.214(17)			1.81
25	1.95	0.298			2.25
30	2.39	0.428	0.379(30)	0.32(8)	2.86
35	2.74	0.563	0.892	0.93(9)	3.41
40	2.98	0.673	1.52	1.59 (13)	3.82
50	3.28	0.821	2.62	3.28(26)	4.40
60	3.39	0.901	3.55	4.72	4.70
80	3.48	0.998	4.88	6.04	5.03
100	3.37	1.01	5.30	6.45	4.98
125	3.30	0.980	5.53	6.02	4.89
150	3.18	0.930	5.40	5.66	4.71
200	2.86	0.847	4.68	4.88	4.22
300	2.41	0.686	3.54	3.55	3.49
400	2.05	0.571	2.70	2.77	2.91
500	1.79	0.488	2.23	2.16	2.52
600	1.62	0.435	1.86	1.89	2.26
800	1.33	0.352	1.42	1.40	1.84
1000	1.14	0.295	1.17	1.13	1.57

[9] Rejoub et al. [03Rej1] also studied ethanol and 1-propanol. Their ethanol total cross section agrees well with that reported by Duric et al. [89Dur1] but their 1-propanol cross section is significantly greater.

CH_4 - Methane [74-82-8]

Recommended data: Straub et al. [97Str1][10]

Technique used: Parallel plate apparatus with time-of-flight mass spectrometer and position-sensitive detection of product ions; independently absolute.

Comments: The absolute uncertainties in $\sigma(CH_4^+)$, $\sigma(CH_3^+)$, $\sigma(CH_2^+)$, $\sigma(CH^+)$, $\sigma(C^+)$, $\sigma(H_2^+)$, $\sigma(H^+)$, and σ(total) are ± 5 %, ± 5 %, ± 6.5 %, ± 6.5 %, ± 8.5 %, ± 7.5 %, ± 5.5 %, and ± 5 % respectively. The uncertainty in the electron energy calibration is ± 1 eV. The recommended total cross section is in very good agreement with those of Rapp and Englander-Golden [65Rap2], Duric et al. [91Dur1], and Nishimura and Tawara [94Nis1]. The partial and total cross sections are in agreement with the data of Tian and Vidal [98Tia1].

Other data reviewed: [97Tia1, 96Tar1, 87Ori1, 84Cha1, 75Win1, 66Ada1, 66Sch1, 58Toz1, 24Hug1]

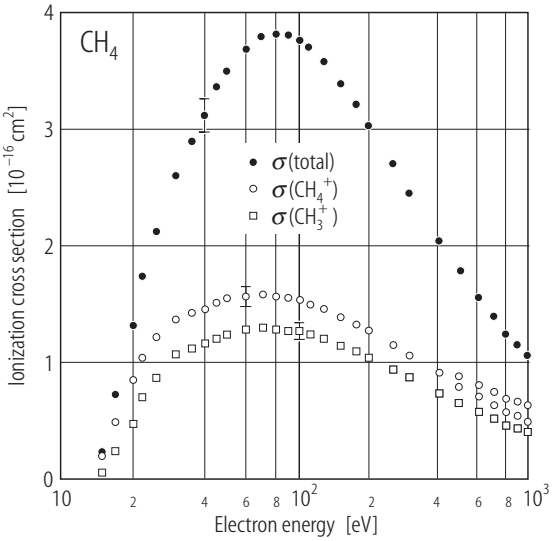

Fig. 5.1.4. CH_4 partial and total electron-impact ionization cross sections.

[10] The data of Straub et al. [97Str1] that are tabulated here reflect a recent recalibration of their apparatus and have been corrected to take account of the production of positive ion pairs [01Lin1].

Table 5.1.11. CH_4 partial electron-impact ionization cross sections.

Energy [eV]	$\sigma(CH_4^+)$ [10^{-16} cm^2]	$\sigma(CH_3^+)$ [10^{-16} cm^2]	$\sigma(CH_2^+)$ [10^{-17} cm^2]	$\sigma(CH^+)$ [10^{-17} cm^2]	$\sigma(C^+)$ [10^{-18} cm^2]	$\sigma(H_2^+)$ [10^{-18} cm^2]	$\sigma(H^+)$ [10^{-17} cm^2]	σ(total) [10^{-16} cm^2]
15	0.182	0.035						0.216
17.5	0.479	0.220	0.050					0.703
20	0.825	0.474	0.157					1.32
22.5	1.03	0.685	0.264					1.74
25	1.20	0.857	0.518	0.041		0.061	0.069	2.12
30	1.36	1.05	1.31	0.292	0.301	0.105	0.287	2.59
35	1.41	1.11	2.03	0.746	1.41	0.602	0.700	2.89
40	1.45	1.14	2.48	1.12	2.74	1.50	1.30	3.12
45	1.50	1.19	2.79	1.36	3.44	2.23	1.96	3.36
50	1.53	1.22	2.88	1.44	4.27	2.68	2.49	3.49
60	1.55	1.25	3.02	1.63	4.92	3.21	3.29	3.67
70	1.56	1.27	3.07	1.73	5.55	3.52	3.80	3.78
80	1.55	1.26	3.11	1.72	5.97	3.64	4.10	3.79
90	1.54	1.26	3.04	1.74	5.94	3.71	4.28	3.78
100	1.52	1.24	3.04	1.67	5.92	3.69	4.30	3.74
110	1.49	1.22	3.00	1.63	5.98	3.59	4.29	3.68
125	1.44	1.19	2.87	1.54	5.78	3.45	4.12	3.56
150	1.38	1.13	2.66	1.40	5.32	3.22	3.81	3.36
175	1.31	1.08	2.46	1.27	4.81	2.84	3.53	3.18
200	1.25	1.03	2.33	1.16	4.44	2.53	3.28	3.02
250	1.13	0.934	1.99	0.981	3.56	2.14	2.68	2.67
300	1.04	0.855	1.77	0.844	3.10	1.89	2.30	2.42
400	0.891	0.719	1.39	0.643	2.13	1.38	1.77	2.02
500	0.778	0.638	1.19	0.524	1.70	1.11	1.43	1.75
600	0.686	0.560	1.03	0.435	1.43	0.991	1.20	1.53
700	0.623	0.507	0.892	0.378	1.25	0.834	1.01	1.37
800	0.552	0.454	0.798	0.327	0.972	0.721	0.871	1.22
900	0.516	0.420	0.726	0.302	0.926	0.588	0.774	1.13
1000	0.476	0.385	0.654	0.272	0.827	0.542	0.688	1.03

CO - Carbon monoxide [630-08-0]

Recommended data: Mangan et al. [00Man1] for $\sigma(CO^+)$, $\sigma(C^+)$, $\sigma(O^+)$, and σ(total)
Tian and Vidal [98Tia1] for $\sigma(CO^{2+})$, $\sigma(O^{2+})$ and $\sigma(C^{2+})$
Rapp and Englander-Golden [65Rap2] for $\sigma(CO^+)$ and σ(total) at energies below 25 eV

Technique used: Mangan et al. [00Man1]: Parallel plate apparatus with time-of-flight mass spectrometer and position-sensitive detection of product ions; independently absolute.
Tian and Vidal [98Tia1]: Time-of-flight mass spectrometer, normalized to the Ar^+ cross section of Straub et al. [95Str1].
Rapp and Englander-Golden [65Rap2]: Parallel plate apparatus, total ion collection, independently absolute.

Comments: The uncertainties in $\sigma(CO^+)$, $\sigma(C^+)$, $\sigma(O^+)$, and σ(total) are ± 5 %, ± 6 %, ± 6 %, and ± 5 %, respectively, for energies of 25 eV and greater. The uncertainties in $\sigma(CO^+)$, and σ(total) are ± 7 % at energies less than 25 eV. The uncertainties in $\sigma(CO^{2+})$, $\sigma(C^{2+})$ and $\sigma(O^{2+})$ are on the order of ± 15 %. The total cross section of Mangan et al. [00Man1] and that of Rapp and Englander-Golden [65Rap2] are in excellent agreement, however, the Mangan et al. [00Man1] data have an uncertainty of ± 1 eV in the electron beam energy and there are few data points near threshold. In this range the data of Rapp and Englander-Golden [65Rap2] is therefore preferred for both $\sigma(CO^+)$ and σ(total). Note that $\sigma(CO^+)$ is equal to σ(total) in this regime.

Other data reviewed: [99Tia1, 90Fre1, 87Ori1, 78Hil1, 76Ada1, 67Sri1, 66Def1, 63Asu1, 62Sch1, 32Tat1, 31Vau1]

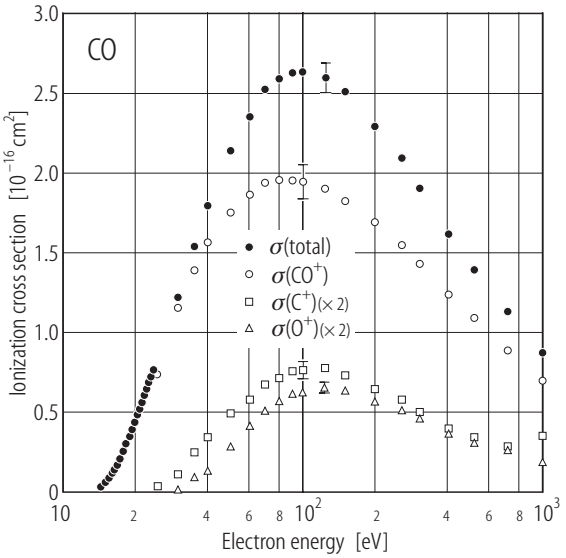

Fig. 5.1.5. CO partial and total electron-impact ionization cross sections.

Table 5.1.12. CO partial and total electron-impact ionization cross sections.

Energy [eV]	$\sigma(CO^+)$ [10^{-16} cm^2]	$\sigma(C^+)$ [10^{-17} cm^2]	$\sigma(O^+)$ [10^{-17} cm^2]	$\sigma(CO^{2+})$ [10^{-19} cm^2]	$\sigma(C^{2+})$ [10^{-18} cm^2]	$\sigma(O^{2+})$ [10^{-19} cm^2]	σ(total) [10^{-16} cm^2]
14.5	0.027						0.027
15	0.051						0.051
15.5	0.077						0.077
16	0.106						0.106
16.5	0.139						0.139
17	0.177						0.177
17.5	0.214						0.214
18	0.254						0.254
18.5	0.297						0.297
19	0.340						0.340
19.5	0.386						0.386
20	0.428						0.428
20.5	0.472						0.472
21	0.516						0.516
21.5	0.560						0.560
22	0.601						0.601
22.5	0.643						0.643
23	0.684						0.684
23.5	0.724						0.724
24	0.766						0.766
25	0.741	0.150					0.756
30	1.15	0.532	0.090				1.21
35	1.38	1.18	0.380				1.54
40	1.56	1.71	0.618				1.79
50	1.75	2.50	1.32	0.85			2.13
60	1.85	2.88	1.99	2.63	0.04		2.35
70	1.93	3.33	2.50	5.34	0.096		2.52
80	1.94	3.51	2.78	6.22	0.243	0.23	2.58
90	1.94	3.74	2.98	7.57	0.444	0.51	2.63
100	1.94	3.76	3.09	8.21	0.539	0.73	2.64
125	1.89	3.80	3.16	8.60	0.944	1.84	2.59
150	1.82	3.58	3.13	7.88	1.16	2.41	2.50
175				8.51	1.24	3.45	
200	1.69	3.17	2.74	6.97	1.25	3.67	2.29
225				7.45	1.21	3.35	
250	1.54	2.84	2.45	6.69	1.19	3.38	2.08
275				5.85	1.16	3.35	
300	1.42	2.44	2.16	5.48	1.10	3.34	1.89
350				4.57	0.978	2.45	
400	1.22	1.98	1.75	4.50	0.904	2.66	1.61
450				3.72	0.816	2.41	
500	1.07	1.67	1.43	3.31	0.762	2.00	1.39
550				3.29	0.757	2.16	
600				3.35	0.708	1.77	
700	0.871	1.25	1.15				1.11
1000	0.683	0.952	0.816				0.863

COS - Carbonyl sulfide [463-58-1]

Recommended data: Srivastava [97Sri2]

Comments: The recommended COS total cross section is quoted by Kim et al. [97Kim1] but has not been published separately. The uncertainty in the cross section is given as ± 15 %. The recommended cross section is approximately 30 % lower than the only other available data, a single measurement of uncertain accuracy at 30 eV reported by Ziesel and Schulz [75Zie1].

Table 5.1.13. COS total electron-impact ionization cross section.[11]

Energy [eV]	σ (total) [10^{-16} cm^2]
15	0.57
20	1.78
25	2.46
30	2.99
35	3.40
40	3.76
50	4.38
60	4.68
70	4.91
80	5.07
90	5.19
100	5.29
120	5.38
140	5.40
160	5.32
180	5.14
200	4.91
250	4.31
300	3.84
400	3.27
500	2.97
600	2.74
700	2.59
800	2.46
900	2.35
1000	2.26

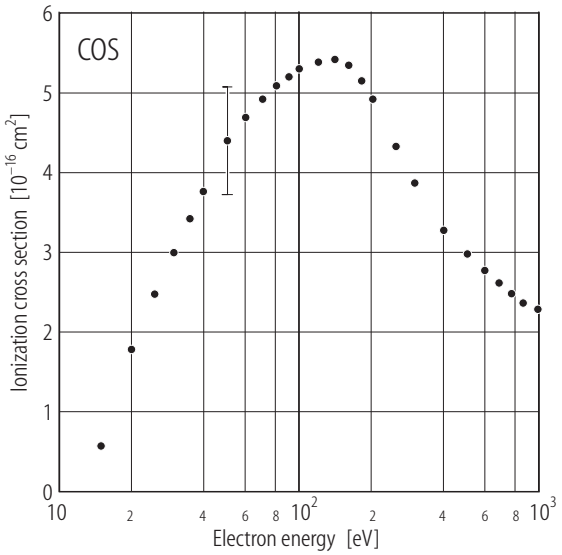

Fig. 5.1.6. COS total electron-impact ionization cross section.

[11] These data were digitized from the graph given by Kim et al. [97Kim1].

CO_2 - Carbon dioxide [124-38-9]

Recommended data: Straub et al. [96Str2][12]
Rapp and Englander-Golden [65Rap2][13] for $\sigma(CO_2^+)$ and σ(total) at energies below 25 eV

Technique used: Straub et al. [96Str2]: Parallel plate apparatus with time-of-flight mass spectrometer and position-sensitive detection of product ions; independently absolute.
Rapp and Englander-Golden [65Rap2]: Parallel plate apparatus with total ion collection; independently absolute.

Comments: The uncertainties in $\sigma(CO_2^+)$, $\sigma(CO^+)$, $\sigma(C^+)$, $\sigma(O^+)$, and σ(total) are ±5% for energies of 25 eV and greater. The uncertainties in $\sigma(CO_2^+)$, and σ(total) are ± 7 % at energies less than 25 eV. The uncertainties in $\sigma(CO_2^{2+})$, $\sigma(C^{2+})$ and $\sigma(O^{2+})$ are ± 6 %, ± 11 %, and ± 11 % respectively. The total cross section of Straub et al. [96Str2] and that of Rapp and Englander-Golden [65Rap2] are in excellent agreement, however, the Straub et al. [96Str2] data have an uncertainty of ± 1 eV in the electron beam energy and there are few data points near threshold. In this range the data of Rapp and Englander-Golden [65Rap2] is therefore preferred for both $\sigma(CO_2^+)$ and σ(total). Note that $\sigma(CO_2^+)$ is equal to σ(total) in this regime.

Other data reviewed: [98Tia2, 90Fre1, 90Kri2, 87Ori1, 78Mar1, 74Cro1, 72Ada1, 65Rap2, 63Asu1]

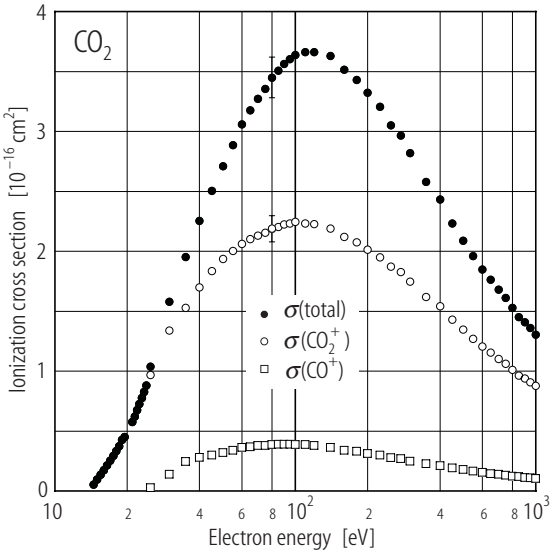

Fig. 5.1.7. CO_2 electron-impact ionization cross sections.

[12] The data of Straub et al. [96Str2] reflect a recent recalibration of their apparatus and thus differ slightly from those given in their original paper.
[13] The data of Rapp and Englander-Golden [65Rap2] are for total charge production.

Table 5.1.14. CO_2 partial and total electron-impact ionization cross sections.

Energy [eV]	$\sigma(CO_2^+)$ [10^{-16} cm^2]	$\sigma(CO^+)$ [10^{-17} cm^2]	$\sigma(C^+)$ [10^{-17} cm^2]	$\sigma(O^+)$ [10^{-17} cm^2]	$\sigma(CO_2^{2+})$ [10^{-18} cm^2]	$\sigma(C^{2+})$ [10^{-19} cm^2]	$\sigma(O^{2+})$ [10^{-19} cm^2]	σ(total) [10^{-16} cm^2]
14.5	0.055							0.055
15	0.097							0.097
15.5	0.135							0.135
16	0.174							0.174
16.5	0.215							0.215
17	0.255							0.255
17.5	0.293							0.293
18	0.333							0.333
18.5	0.373							0.373
19	0.428							0.428
19.5	0.452							0.452
21	0.577							0.577
21.5	0.623							0.623
22	0.676							0.676
22.5	0.727							0.727
23	0.777							0.777
23.5	0.828							0.828
24	0.880							0.880
25	0.969	0.279		0.419				1.04
30	1.34	1.39	0.0240	0.986				1.58
35	1.53	2.47	0.280	1.50				1.95
40	1.70	2.81	0.782	1.95				2.25
45	1.84	2.99	1.21	2.45	0.166			2.50
50	1.94	3.19	1.49	2.99	0.393			2.71
55	2.00	3.39	1.78	3.52	0.686			2.88
60	2.06	3.62	2.08	4.07	1.06			3.06
65	2.10	3.69	2.29	4.52	1.26			3.18
70	2.13	3.79	2.46	4.85	1.59			3.27
75	2.15	3.80	2.61	5.26	1.72			3.36
80	2.19	3.86	2.78	5.56	2.06	0.179		3.45
85	2.20	3.89	2.85	5.84	2.19	0.215		3.51
90	2.22	3.90	2.96	6.06	2.27	0.311		3.56
95	2.23	3.90	3.06	6.22	2.46	0.506	0.169	3.60
100	2.25	3.89	3.10	6.40	2.65	0.520	0.197	3.64
110	2.23	3.86	3.22	6.63	2.85	0.751	0.324	3.66
120	2.23	3.78	3.23	6.71	2.90	1.08	0.721	3.66
140	2.19	3.65	3.31	6.80	2.94	1.57	1.33	3.63
160	2.12	3.40	3.21	6.70	2.90	1.86	1.59	3.52
180	2.08	3.33	3.09	6.47	2.85	2.49	2.17	3.43
200	2.01	3.14	3.01	6.31	2.72	2.79	2.33	3.32
225	1.95	3.00	2.88	6.06	2.57	2.56	2.71	3.21
250	1.87	2.78	2.73	5.72	2.32	2.91	2.86	3.05
275	1.83	2.69	2.60	5.53	2.31	2.47	3.04	2.97
300	1.75	2.50	2.45	5.24	2.03	2.52	2.76	2.82
350	1.62	2.26	2.15	4.70	1.83	2.16	2.49	2.58
400	1.54	2.11	2.02	4.33	1.75	2.24	2.15	2.43
450	1.43	1.93	1.83	3.88	1.65	1.98	1.93	2.23
500	1.35	1.78	1.69	3.61	1.41	1.77	1.92	2.09
550	1.27	1.65	1.54	3.39	1.28	1.84	1.68	1.96
600	1.21	1.54	1.45	3.11	1.25	1.45	1.56	1.85
650	1.16	1.45	1.36	2.99	1.13	1.69	1.42	1.76

Table 5.1.14 (continued)

Energy [eV]	$\sigma(CO_2^+)$ [10^{-16} cm^2]	$\sigma(CO^+)$ [10^{-17} cm^2]	$\sigma(C^+)$ [10^{-17} cm^2]	$\sigma(O^+)$ [10^{-17} cm^2]	$\sigma(CO_2^{2+})$ [10^{-18} cm^2]	$\sigma(C^{2+})$ [10^{-19} cm^2]	$\sigma(O^{2+})$ [10^{-19} cm^2]	σ(total) [10^{-16} cm^2]
700	1.10	1.39	1.27	2.83	1.06	1.47	1.76	1.68
750	1.06	1.32	1.23	2.68	0.986	1.57	1.47	1.61
800	1.01	1.24	1.16	2.52	0.961	1.39	1.27	1.53
850	0.964	1.19	1.08	2.38	0.883	1.29	1.27	1.45
900	0.941	1.13	1.05	2.29	0.823	0.965	1.00	1.41
950	0.909	1.10	1.01	2.22	0.741	0.897	1.16	1.36
1000	0.876	1.03	0.964	2.09	0.723	0.984	1.03	1.30

CS - Carbon monosulfide [2944-05-0]

Recommended data: Freund et al. [90Fre1] for $\sigma(CS^+)$.
Technique used: A beam of molecules was prepared by charge-transfer neutralization of a mass separated ion beam and then ionized by a well-characterized electron beam.
Comments: The absolute uncertainty in these cross sections is reported as ± 10 %.

Table 5.1.15. CS^+ partial electron-impact ionization cross section.

Energy [eV]	$\sigma(CS^+)$ [10^{-16} cm^2]	Energy [eV]	$\sigma(CS^+)$ [10^{-16} cm^2]	Energy [eV]	$\sigma(CS^+)$ [10^{-16} cm^2]
6	0.00	27	3.58	105	3.82
7	0.01	28	3.56	110	3.77
8	0.02	29	3.57	115	3.78
9	0.05	30	3.64	120	3.79
10	0.09	32	3.71	125	3.75
11	0.18	34	3.71	130	3.68
12	0.39	36	3.76	135	3.66
13	0.70	38	3.79	140	3.66
14	1.05	40	3.83	145	3.62
15	1.40	45	3.87	150	3.57
16	1.78	50	3.87	155	3.55
17	2.15	55	3.91	160	3.53
18	2.51	60	3.98	165	3.45
19	2.73	65	3.96	170	3.44
20	2.91	70	3.96	175	3.42
21	3.09	75	3.94	180	3.37
22	3.27	80	3.95	185	3.28
23	3.36	85	3.92	190	3.22
24	3.39	90	3.92	195	3.17
25	3.49	95	3.86	200	3.18
26	3.57	100	3.84		

CS_2 – Carbon disulfide [75-15-0]

Recommended data: Lindsay et al. [03Lin1]

Technique used: Parallel plate apparatus with time-of-flight mass spectrometer and position sensitive detection of product ions; independently absolute.

Comments: The absolute uncertainties in $\sigma(CS_2^+)$, $\sigma(S_2^+)$, $\sigma(CS^+)$, $\sigma(S^+)$, $\sigma(C^+)$, $\sigma(CS_2^{2+})$, and σ(total) are ±6%, ±30%, ±6%, ±6%, ±8%, ±17%, and ±6% respectively. The uncertainty in the electron energy calibration is ±0.5 eV. The CS_2^+ partial cross section data of Freund et al. [90Fre1] and Rao and Srivastava [91Rao1] are in fair agreement with the recommended cross section for energies below about 200 eV.

Other data reviewed: [75Zie1]

Table 5.1.16. CS_2 partial and total electron-impact ionization cross sections.

Energy [eV]	$\sigma(CS_2^+)$ [10^{-16} cm^2]	$\sigma(S_2^+)$ [10^{-17} cm^2]	$\sigma(CS^+)$ [10^{-16} cm^2]	$\sigma(S^+)$ [10^{-16} cm^2]	$\sigma(C^+)$ [10^{-17} cm^2]	$\sigma(CS_2^{2+})$ [10^{-17} cm^2]	σ(total) [10^{-16} cm^2]
11	0.58(9)						0.58(9)
12	1.29(13)						1.29(13)
13	1.84(18)						1.84(18)
14	2.36(18)						2.36(18)
16	3.11(24)						3.11(24)
18	3.68(29)		0.251(43)	0.231(34)			4.16(33)
20	4.14		0.507(86)	0.354(60)			5.00
22.5	3.95		0.89(27)	0.59(18)			5.43
25	4.00	1.0(6)	1.12	0.684(68)			5.91
30	4.04	1.2(6)	1.41	1.19	1.06 (12)		6.86
35	4.16	1.1(6)	1.59	1.63	1.39 (14)	1.06(53)	7.73
40	4.25	1.1(5)	1.64	1.85	1.68 (17)	1.36	8.16
50	4.36	0.81(40)	1.66	2.12	2.09 (21)	1.72	8.60
60	4.47	0.73(36)	1.61	2.25	2.52	1.78	8.83
80	4.51	0.79	1.49	2.29	3.01	1.81	8.85
100	4.44	0.76	1.37	2.32	3.24	1.77	8.71
125	4.23	0.66	1.20	2.20	3.02	1.71	8.17
150	4.00	0.56	1.13	2.02	2.71	1.53	7.63
200	3.51	0.55	0.999	1.63	2.45	1.12	6.55
300	2.99	0.37	0.800	1.16	1.93	0.888	5.28
400	2.65	0.33	0.670	0.937	1.48	0.722	4.51
500	2.37	0.26(18)	0.584	0.813	1.42	0.535	3.99
600	2.18	0.29(20)	0.513	0.726	1.13 (11)	0.502	3.61
800	1.73	0.26(18)	0.445(36)	0.641(64)	1.02 (15)	0.581	3.00
1000	1.50	0.28(20)	0.413(33)	0.615(62)	0.95 (14)	0.46(16)	2.69

C_2F_6 - Hexafluoroethane [76-16-4]

Recommended data: Poll and Meichsner [87Pol1] and Jiao et al. [99Jia1] for the partial cross sections[14]
Nishimura et al. [99Nis1] for σ (total)

Technique used: Poll and Meichsner [87Pol1]: Quadrupole mass spectrometer. The data are normalized to the argon total cross section of Rapp and Englander-Golden [65Rap2].
Jiao et al. [99Jia1]: Fourier transform mass spectrometer. The data are normalized to the Ar^+ cross section of Wetzel et al. [87Wet1].
Nishimura et al.: Parallel plate apparatus with total ion collection; independently absolute.

Comments: The values of σ ($C_2F_5^+$) and σ (CF_3^+) reported by Poll and Meichsner [87Pol1] and Jiao et al. [99Jia1] are in good agreement, however, there are differences on the order of 30 % between their data sets for the other fragment ion cross sections. The sum of the recommended partial cross sections is in reasonable agreement with the recommended total cross section [99Nis1]. The uncertainty in σ ($C_2F_5^+$) and σ (CF_3^+) is on the order of ± 16 %. Given the discrepancy between the two measurements of σ (CF_2^+) and σ (CF^+), the uncertainty in the recommended values is at least ± 20 %. The quoted uncertainty in the recommended total cross section is approximately ± 7 %. The available C_2F_6 cross section data have recently been reviewed by Christophorou and Olthoff [98Chr1].

Other data reviewed: [69Ber1, 63Bib1, 63Kur1]

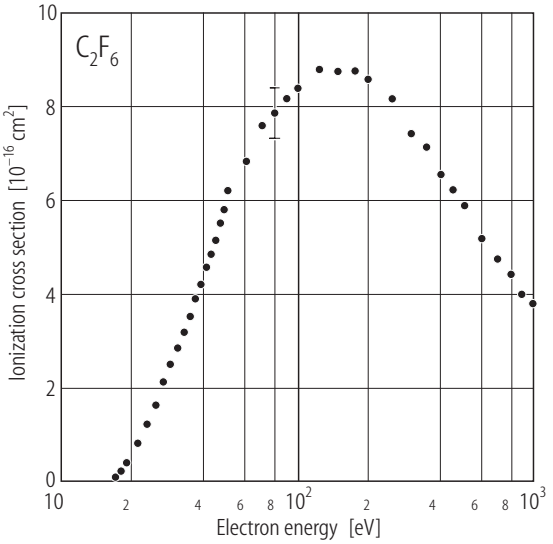

Fig. 5.1.8. C_2F_6 total electron-impact ionization cross section.

[14] The recommended partial cross sections are a simple average of the data of Poll and Meichsner [87Pol1] and Jiao et al. [99Jia1]. Numerical values were obtained by digitizing the graphs given by Poll and Meichsner [87Pol1] and Jiao et al. [99Jia1] and consequently the accuracy of the tabulated data in the near threshold region of the cross section curves is not particularly high.

Table 5.1.17. C_2F_6 total electron-impact ionization cross section. [15]

Energy [eV]	σ (total) [10^{-16} cm^2]	Energy [eV]	σ (total) [10^{-16} cm^2]	Energy [eV]	σ (total) [10^{-16} cm^2]
17	0.0889	41	4.54	176	8.76
18	0.211	43	4.85	201	8.57
19	0.375	45	5.14	251	8.17
21	0.782	47	5.52	301	7.41
23	1.18	49	5.77	351	7.13
25	1.59	51	6.19	401	6.55
27	2.11	61	6.82	451	6.21
29	2.49	71	7.57	501	5.89
31	2.81	81	7.84	601	5.17
33	3.16	91	8.17	701	4.72
35	3.49	101	8.39	801	4.40
37	3.86	126	8.77	901	3.96
39	4.17	151	8.75	1001	3.77

Table 5.1.18. C_2F_6 partial electron-impact ionization cross sections.

Energy [eV]	$\sigma(C_2F_5^+)$ [10^{-16} cm^2]	$\sigma(CF_3^+)$ [10^{-16} cm^2]	$\sigma(CF_2^+)$ [10^{-17} cm^2]	$\sigma(CF^+)$ [10^{-17} cm^2]
16	0.03	0.12		
18	0.17	0.26		
20	0.33	0.42		
22	0.50	0.60		0.21
24	0.68	0.82		0.33
26	0.86	1.06	0.35	0.85
28	1.05	1.37	0.47	1.11
30	1.24	1.67	0.59	1.44
32	1.42	1.93	0.82	1.79
34	1.57	2.14	0.97	2.17
36	1.76	2.36	1.31	2.51
38	1.97	2.62	1.67	3.09
40	2.11	2.83	1.97	3.57
45	2.36	3.23	2.78	4.89
50	2.52	3.51	3.49	6.13
55	2.68	3.70	4.25	7.14
60	2.80	3.92	4.72	7.97
65	2.82	4.01	5.11	8.51
70	2.83	4.06	5.41	8.85

[15] The data of Nishimura et al. [99Nis1] are for total charge production.

C_2H_2 - Acetylene [74-86-2]

Recommended data: Tian and Vidal [98Tia1]

Technique used: Time-of-flight mass spectrometer. The data are normalized to the Ar^+ cross section of Straub et al. [95Str1].

Comments: The uncertainty in these cross sections is on the order of ± 10 % if the magnitude of the cross section is greater than $1 \cdot 10^{-17}$ cm^2, otherwise it is on the order of ± 15 %. Note that the CH^+ cross section includes any $C_2H_2^{2+}$ ions formed as both species have the same mass-to-charge ratio. Likewise σ (C^+) includes a contribution from C_2^{2+} ions.

Other data reviewed: [96Zhe1, 67Gau1]

Table 5.1.19. C_2H_2 partial and total electron-impact ionization cross sections.

Energy [eV]	$\sigma(C_2H_2^+)$ [10^{-16} cm^2]	$\sigma(C_2H^+)$ [10^{-17} cm^2]	$\sigma(C_2^+)$ [10^{-17} cm^2]	$\sigma(CH^+)$ [10^{-17} cm^2]	$\sigma(C^+)$ [10^{-17} cm^2]	$\sigma(H^+)$ [10^{-17} cm^2]	σ(total) [10^{-16} cm^2]
17.5	0.85						0.85
20	1.44	0.75					1.52
25	2.49	3.15	0.22	0.12		0.20	2.86
30	2.90	5.21	0.82	0.78	0.20	0.45	3.65
35	3.15	6.42	1.45	1.45	0.44	0.80	4.21
40	3.30	6.79	1.76	2.03	0.76	1.32	4.57
45	3.38	7.26	1.96	2.49	1.10	1.91	4.85
50	3.50	7.52	2.13	2.99	1.36	2.47	5.15
60	3.54	7.86	2.28	3.57	1.76	3.22	5.41
70	3.54	7.93	2.34	3.87	2.02	3.79	5.53
80	3.59	7.91	2.35	4.08	2.21	4.20	5.66
90	3.58	7.98	2.37	4.05	2.37	4.40	5.70
100	3.47	7.62	2.26	3.95	2.40	4.43	5.54
125	3.28	7.14	2.08	3.65	2.30	4.27	5.22
150	3.17	6.88	1.94	3.37	2.18	4.03	5.01
175	3.04	6.56	1.79	3.12	2.02	3.75	4.76
200	2.95	6.23	1.67	2.89	1.89	3.51	4.57
225	2.84	5.96	1.55	2.63	1.74	3.37	4.36
250	2.69	5.67	1.44	2.45	1.59	3.06	4.11
275	2.54	5.38	1.34	2.25	1.43	2.78	3.86
300	2.46	5.09	1.24	2.13	1.33	2.60	3.70
350	2.26	4.62	1.10	1.86	1.15	2.22	3.36
400	2.09	4.28	0.99	1.64	1.02	1.94	3.08
450	1.95	3.89	0.89	1.48	0.91	1.73	2.84
500	1.85	3.70	0.85	1.34	0.84	1.66	2.69
550	1.75	3.46	0.77	1.23	0.78	1.44	2.52
600	1.64	3.23	0.70	1.12	0.70	1.35	2.35

C_2H_4 - Ethylene [74-85-1]

Recommended data: Tian and Vidal (98Tia4) for the partial cross sections
Rapp and Englander-Golden [65Rap2] and Nishimura and Tawara [94Nis1] for σ (total)

Technique used: Tian and Vidal [98Tia4]: Time-of-flight mass spectrometer. The data are normalized to the Ar^+ cross section of Straub et al. [95Str1].
Rapp and Englander-Golden [65Rap2]: Parallel plate apparatus with total ion collection; independently absolute.
Nishimura and Tawara [94Nis1]: Parallel plate apparatus with total ion collection; independently absolute.

Comments: The uncertainty in the partial cross sections is reported as ± 10 %. The uncertainty in the total cross section is ± 7 % at energies less than 150 eV [65Rapp2] and ± 8 % elsewhere [94Nis1]. All three data sets are in excellent agreement as to the total cross section except very close to threshold.

Other data reviewed: [66Sch1]

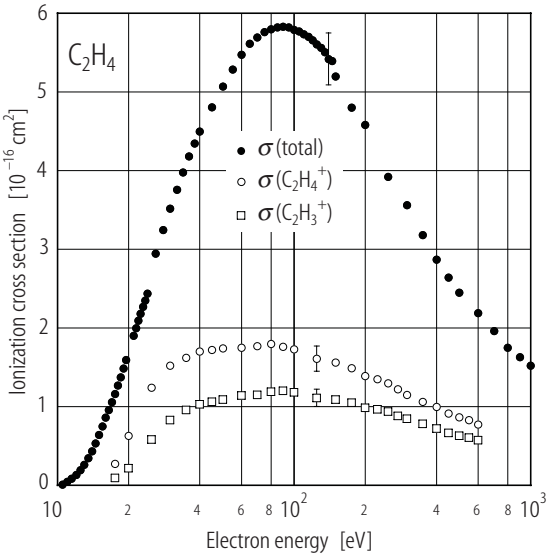

Fig. 5.1.9. C_2H_4 partial and total electron-impact ionization cross sections.

Table 5.1.20. C_2H_4 total electron-impact ionization cross section.[16]

Energy [eV]	σ (total) [10^{-16} cm^2]	Energy [eV]	σ (total) [10^{-16} cm^2]	Energy [eV]	σ (total) [10^{-16} cm^2]
10.5	0.0114	23	2.27	105	5.77
11	0.0449	23.5	2.35	110	5.74
11.5	0.0871	24	2.44	115	5.70
12	0.134	26	2.95	120	5.66
12.5	0.193	28	3.25	125	5.60
13	0.263	30	3.52	130	5.56
13.5	0.345	32	3.76	135	5.51
14	0.431	34	3.98	140	5.42
14.5	0.533	36	4.18	145	5.39
15	0.641	38	4.35	150	5.20
15.5	0.751	40	4.50	175	4.80
16	0.860	45	4.80	200	4.58
16.5	0.959	50	5.07	250	3.92
17	1.06	55	5.29	300	3.56
17.5	1.16	60	5.47	350	3.18
18	1.27	65	5.61	400	2.87
18.5	1.37	70	5.69	450	2.64
19	1.49	75	5.76	500	2.45
19.5	1.59	80	5.80	600	2.19
21	1.90	85	5.82	700	1.96
21.5	2.00	90	5.83	800	1.75
22	2.09	95	5.82	900	1.63
22.5	2.18	100	5.79	1000	1.52

[16] The recommended total cross section is for total charge production.

Table 5.1.21a. C_2H_4 partial electron-impact ionization cross sections.

Energy [eV]	$\sigma(C_2H_4^+)$ [10^{-16} cm^2]	$\sigma(C_2H_3^+)$ [10^{-16} cm^2]	$\sigma(C_2H_2^+)$ [10^{-16} cm^2]	$\sigma(C_2H^+)$ [10^{-17} cm^2]	$\sigma(C_2^+)$ [10^{-18} cm^2]
17.5	0.274	0.0952	0.0929		
20	0.627	0.218	0.201	0.153	
25	1.24	0.579	0.474	0.431	
30	1.52	0.829	0.751	0.688	0.685
35	1.62	0.957	0.909	1.22	1.97
40	1.70	1.03	1.00	1.83	3.28
45	1.72	1.06	1.03	2.03	4.43
50	1.74	1.09	1.06	2.24	5.40
60	1.75	1.14	1.11	2.32	6.48
70	1.77	1.15	1.11	2.55	6.93
80	1.80	1.19	1.14	2.60	7.53
90	1.76	1.20	1.12	2.45	7.92
100	1.73	1.18	1.10	2.35	8.23
125	1.61	1.11	1.03	2.11	7.47
150	1.56	1.09	0.983	2.00	7.36
175	1.49	1.05	0.943	1.78	6.61
200	1.39	0.988	0.890	1.55	5.59
225	1.35	0.965	0.864	1.50	5.15
250	1.30	0.937	0.825	1.37	4.56
275	1.22	0.882	0.772	1.27	4.23
300	1.15	0.845	0.730	1.16	4.07
350	1.06	0.782	0.664	1.02	3.42
400	0.999	0.720	0.617	0.897	2.96
450	0.913	0.665	0.563	0.797	2.55
500	0.865	0.628	0.538	0.726	2.21
550	0.829	0.603	0.504	0.661	1.88
600	0.775	0.573	0.472	0.640	2.06

Table 5.1.21b. C_2H_4 partial electron-impact ionization cross sections.

Energy [eV]	$\sigma(CH_3^+)$ [10^{-18} cm^2]	$\sigma(CH_2^+)$ [10^{-17} cm^2]	$\sigma(CH^+)$ [10^{-17} cm^2]	$\sigma(C^+)$ [10^{-18} cm^2]	$\sigma(H_2^+)$ [10^{-18} cm^2]	$\sigma(H^+)$ [10^{-17} cm^2]
25	0.460	0.512	0.187	0.513		
30	0.800	0.855	0.230	1.15	0.628	0.602
35	0.810	1.18	0.351	1.76	0.771	0.992
40	0.81	1.65	0.536	1.99	1.26	1.57
45	1.01	1.86	0.721	3.41	1.50	1.99
50	1.12	2.11	0.845	4.47	2.12	2.54
60	1.40	2.53	0.107	5.71	2.83	3.53
70	1.54	2.83	1.22	6.82	3.50	4.05
80	1.40	2.89	1.35	7.88	3.57	4.72
90	1.54	2.93	1.43	8.57	3.62	5.03
100	1.25	2.86	1.34	9.01	3.65	5.21
125	1.33	2.71	1.17	8.51	3.46	5.09
150	1.14	2.51	1.16	8.22	3.11	4.71
175	1.09	2.33	1.05	7.81	2.68	4.28
200	1.01	2.13	0.924	6.83	2.35	3.87
225	1.07	1.98	0.877	6.64	2.28	3.59
250	1.10	1.89	0.791	5.82	2.12	3.30
275	0.746	1.72	0.692	5.08	1.91	2.93
300	1.03	1.58	0.661	5.12	1.90	2.74
350	0.580	1.40	0.521	4.01	1.61	2.42
400	0.615	1.27	0.487	3.41	1.33	2.17
450	0.650	1.07	0.410	3.17	1.14	1.79
500	0.544	1.00	0.364	2.88	1.15	1.72
550	0.519	0.990	0.328	2.64	0.929	1.54
600	0.500	0.933	0.297	2.27	0.859	1.38

C_2H_6 - Ethane [74-84-0]

Recommended data: Tian and Vidal [98Tia3] for the partial cross sections.
Nishimura and Tawara [94Nis1] for σ(total).

Technique used: Tian and Vidal [98Tia3]: Time-of-flight mass spectrometer. The data are normalized to the Ar^+ cross section of Straub et al. [95Str1].
Nishimura and Tawara [94Nis1]: Parallel plate apparatus with total ion collection; independently absolute.

Comments: The uncertainty in the partial cross sections is reported as ± 10 %. The uncertainty in the total cross section is reported as ± 8 %. The total cross section of Nishimura and Tawara [94Nis1] is in excellent agreement with that measured by Tian and Vidal [98Tia3] except very close to threshold. The total cross sections of Duric et al. [91Dur1] and Chatham et al. [84Cha1] are also in good agreement with the recommended values.

Other data reviewed: [93Gri1, 66Sch1]

Table 5.1.22. C_2H_6 total electron-impact ionization cross section.[17]

Energy [eV]	σ(total) [10^{-16} cm^2]	Energy [eV]	σ(total) [10^{-16} cm^2]
12	0.074	125	6.53
15	0.618	150	6.32
17	1.39	175	5.98
20	2.24	200	5.68
25	3.48	250	5.01
30	4.45	300	4.60
35	4.94	350	4.18
40	5.41	400	3.86
45	5.84	450	3.47
50	6.04	500	3.33
60	6.67	600	3.03
70	6.93	700	2.71
80	6.86	800	2.38
90	6.84	900	2.25
100	6.89	1000	2.03

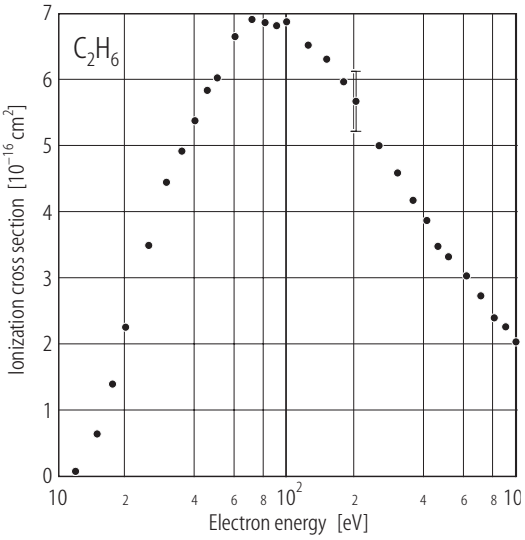

Fig. 5.1.10. C_2H_6 total electron-impact ionization cross section.

[17] The recommended cross section is for total charge production.

Table 5.1.23a. C_2H_6 partial electron-impact ionization cross sections.

Energy [eV]	$\sigma(C_2H_6^+)$ [10^{-17} cm^2]	$\sigma(C_2H_5^+)$ [10^{-17} cm^2]	$\sigma(C_2H_4^+)$ [10^{-16} cm^2]	$\sigma(C_2H_3^+)$ [10^{-17} cm^2]	$\sigma(C_2H_2^+)$ [10^{-17} cm^2]	$\sigma(C_2H^+)$ [10^{-17} cm^2]	$\sigma(C_2^+)$ [10^{-18} cm^2]
17.5	0.80	0.58	0.25	0.65	0.44		
20	1.68	1.22	0.49	1.35	0.80		
25	4.75	3.46	1.43	3.62	2.25		
30	6.64	5.07	2.11	5.32	3.10		
35	6.87	5.58	2.36	7.16	3.99	0.22	
40	7.64	5.81	2.52	8.40	5.26	0.51	
45	7.39	5.73	2.51	8.91	5.89	0.76	0.5
50	7.30	5.70	2.51	9.04	6.33	0.98	1.0
60	7.68	5.93	2.61	9.56	6.66	1.22	1.7
70	7.54	5.92	2.54	9.54	6.73	1.35	2.2
80	7.50	5.83	2.51	9.37	6.64	1.40	2.6
90	7.46	5.93	2.52	9.36	6.67	1.42	2.9
100	7.44	5.83	2.49	9.23	6.55	1.43	3.2
125	7.09	5.60	2.34	8.61	5.97	1.32	3.2
150	6.76	5.33	2.24	8.13	5.48	1.18	3.0
175	6.50	5.17	2.15	7.70	5.09	1.07	2.8
200	6.29	5.03	2.08	7.28	4.77	0.97	2.6
225	6.06	4.80	2.01	6.98	4.45	0.90	2.3
250	5.76	4.62	1.92	6.55	4.14	0.78	2.0
275	5.48	4.42	1.82	6.23	3.82	0.73	1.9
300	5.34	4.24	1.76	5.98	3.67	0.65	1.7
350	4.87	3.91	1.61	5.38	3.26	0.56	1.3
400	4.65	3.75	1.53	5.05	2.96	0.50	1.2
450	4.27	3.47	1.41	4.64	2.67	0.43	1.0
500	4.10	3.31	1.34	4.34	2.48	0.39	0.9
550	3.91	3.13	1.28	4.11	2.34	0.35	0.8
600	3.66	2.93	1.20	3.85	2.17	0.32	0.7

Table 5.1.23b. C_2H_6 partial electron-impact ionization cross sections.

Energy [eV]	$\sigma(CH_3^+)$ [10^{-17} cm^2]	$\sigma(CH_2^+)$ [10^{-17} cm^2]	$\sigma(CH^+)$ [10^{-18} cm^2]	$\sigma(C^+)$ [10^{-18} cm^2]	$\sigma(H_3^+)$ [10^{-18} cm^2]	$\sigma(H_2^+)$ [10^{-18} cm^2]	$\sigma(H^+)$ [10^{-17} cm^2]
17.5	0.19						
20	0.32						
25	0.70					0.2	0.09
30	0.91	0.19				0.7	0.39
35	1.09	0.38			0.2	1.5	0.68
40	1.44	0.66	1.0		0.7	2.5	1.17
45	1.75	0.80	2.3	0.4	1.4	3.4	1.60
50	2.16	1.02	3.2	1.0	2.0	4.8	1.90
60	2.72	1.39	4.5	1.7	3.3	6.8	2.88
70	3.00	1.51	5.6	2.1	3.5	8.6	3.63
80	3.17	1.53	6.1	2.4	4.0	8.9	4.18
90	3.20	1.61	6.6	2.9	3.8	9.6	4.73
100	3.19	1.60	6.7	3.0	3.8	9.8	4.95
125	2.98	1.49	6.3	3.1	3.6	9.0	4.95
150	2.77	1.36	5.5	2.9	3.4	8.2	4.70
175	2.58	1.25	4.8	2.7	3.1	7.6	4.40
200	2.38	1.12	4.4	2.5	2.9	7.1	4.00
225	2.25	1.05	4.1	2.3	2.7	6.5	3.71
250	2.06	0.96	3.7	2.0	2.4	5.7	3.39
275	1.92	0.88	3.2	1.8	2.2	5.3	3.07
300	1.80	0.83	3.0	1.7	2.0	4.9	2.83
350	1.57	0.71	2.4	1.4	1.7	4.1	2.39
400	1.41	0.63	2.0	1.3	1.6	3.8	2.15
450	1.27	0.54	1.7	1.1	1.4	3.3	1.87
500	1.17	0.49	1.5	0.9	1.3	3.0	1.68
550	1.07	0.45	1.3	0.9	1.2	2.7	1.55
600	0.99	0.41	1.1	0.7	1.1	2.4	1.41

C_3F_8 - Octofluoropropane [76-19-7]

Recommended data: Poll and Meichsner [87Pol1] for the partial cross sections[18]
Nishimura et al. [99Nis1] for σ (total)

Technique used: Poll and Meichsner [87Pol1]: Quadrupole mass spectrometer. The data are normalized to the argon total cross section of Rapp and Englander-Golden [65Rap2].
Nishimura et al. [99Nis1]: Parallel plate apparatus with total ion collection; independently absolute.

Comments: The sum of the partial cross sections reported by Poll and Meichsner [87Pol1] is in reasonable agreement with the total cross section reported by Nishimura et al. [99Nis1] at energies less than approximately 70 eV. However, the two cross sections diverge by as much as 20 % at energies greater than 100 eV. The quoted uncertainty in the recommended total cross section is approximately ± 7 %. No uncertainty is given for the partial cross sections. The available C_3F_8 cross section data has recently been reviewed by Christophorou and Olthoff [98Chr2].

Other data reviewed: [89Cha1, 69Ber1, 63Bib1, 63Kur1]

Table 5.1.24. C_3F_8 total electron-impact ionization cross section. [19]

Energy [eV]	σ (total) [10^{-15} cm^2]	Energy [eV]	σ (total) [10^{-15} cm^2]
16	0.0129	60	1.04
17	0.0316	70	1.13
18	0.0562	80	1.19
19	0.0815	90	1.25
20	0.113	100	1.28
22	0.181	125	1.33
24	0.231	150	1.34
26	0.308	175	1.32
28	0.358	200	1.28
30	0.410	250	1.21
32	0.457	300	1.12
34	0.512	350	1.05
36	0.558	400	0.980
38	0.588	450	0.931
40	0.654	500	0.861
42	0.701	600	0.780
44	0.743	700	0.699
46	0.785	800	0.641
48	0.831	900	0.582
50	0.899	1000	0.548

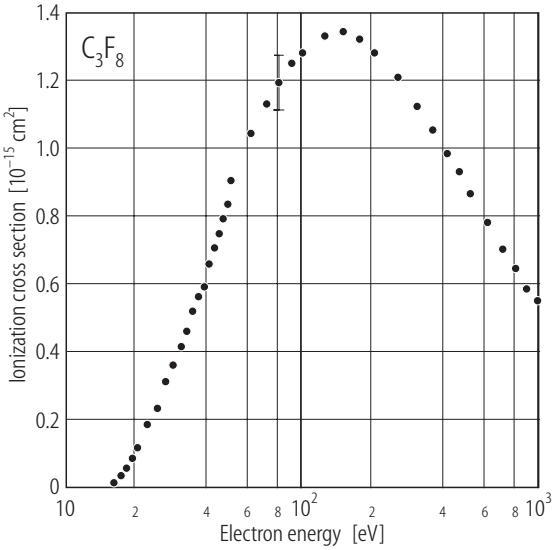

Fig. 5.1.11. C_3F_8 total electron-impact ionization cross section.

[18] The data tabulated here were digitized from graphs given by Poll and Meichsner [87Pol1] and consequently the accuracy of the tabulated data in the near threshold region of the cross section curves is not very high.
[19] The recommended data [99Nis1] are for total charge production.

Table 5.1.25. C_3F_8 partial electron-impact ionization cross sections.

Energy [eV]	$\sigma(C_3F_7^+)$ [10^{-16} cm^2]	$\sigma(C_2F_5^+)$ [10^{-17} cm^2]	$\sigma(C_2F_4^+)$ [10^{-17} cm^2]	$\sigma(CF_3^+)$ [10^{-16} cm^2]	$\sigma(CF_2^+)$ [10^{-17} cm^2]	$\sigma(CF^+)$ [10^{-16} cm^2]
14		0.15	0.07	0.11		
16		0.35	0.28	0.30		
18	0.06	0.62	0.46	0.51		
20	0.13	0.94	0.68	0.79		
22	0.19	1.22	0.84	1.14		
24	0.27	1.54	1.02	1.54		
26	0.34	1.90	1.20	1.90		
28	0.41	2.21	1.37	2.27		
30	0.49	2.54	1.57	2.84	0.09	0.05
35	0.64	3.15	2.01	3.71	0.27	0.15
40	0.80	3.72	2.39	4.58	0.56	0.27
45	0.94	4.27	2.77	5.26	0.96	0.40
50	1.04	4.72	3.12	5.86	1.40	0.52
55	1.13	5.01	3.31	6.30	1.79	0.66
60	1.20	5.23	3.44	6.65	2.10	0.77
65	1.25	5.37	3.49	6.89	2.30	0.86
70	1.26	5.44	3.52	7.06	2.39	0.94
75	1.30	5.49	3.55	7.17	2.49	1.00
80	1.31	5.51	3.55	7.22	2.55	1.01
90	1.31	5.47	3.56	7.27	2.65	1.04
100	1.31	5.38	3.55	7.28	2.70	1.07
110	1.31	5.26	3.52	7.26	2.75	1.08
120	1.30	5.13	3.48	7.23	2.77	1.08
125	1.28	5.05	3.43	7.21	2.77	1.08
130		4.99			2.77	
135		4.92				

C_3H_8 - Propane [74-98-6]

Recommended data: Duric et al. [91Dur1]
Technique used: Parallel plate apparatus with total ion collection; independently absolute.
Comments: The uncertainty in this total cross section is reported as ± 10 %.
Other data reviewed: [66Def1, 66Sch1, 57Lam1]

Table 5.1.26. C_3H_8 total electron-impact ionization cross section.[20]

Energy [eV]	σ (total) [10^{-16} cm^2]	Energy [eV]	σ (total) [10^{-16} cm^2]
12	0.35	45	7.46
13	0.66	50	7.82
14	1.04	55	8.07
15	1.42	60	8.31
16	1.83	65	8.46
17	2.24	70	8.62
18	2.63	75	8.67
19	2.99	80	8.70
20	3.36	85	8.72
22	4.03	90	8.75
24	4.52	95	8.72
26	4.98	100	8.70
28	5.39	120	8.47
30	5.70	140	8.15
32	6.04	160	7.81
34	6.31	180	7.42
36	6.54	200	7.09
38	6.80	220	6.78
40	7.02	240	6.56

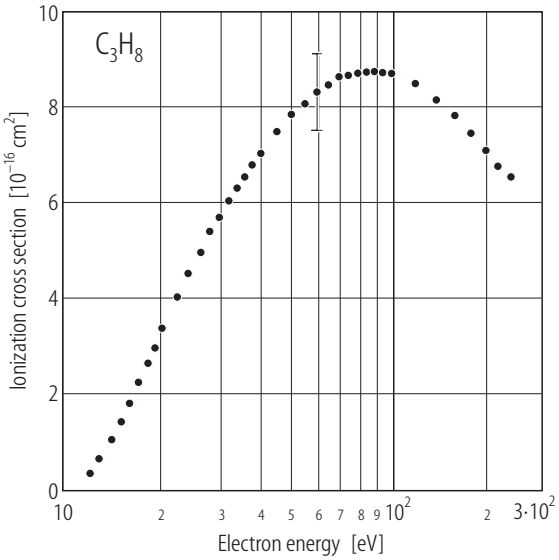

Fig. 5.1.12. C_3H_8 total electron-impact ionization cross section.

[20] The recommended cross section is for total charge production.

C_{60} - Buckminsterfullerene [99685-96-8]

Recommended data: Tarnovsky et al. [98Tar1] for $\sigma(C_{60}^+)$ up to 200 eV.
Matt et al. [96Mat1, 98Fol1, 99Mat1] for the other partial cross sections and the total cross section[21].

Technique used: Tarnovsky et al. [98Tar1]: Fast neutral beam technique; independently absolute.
Matt et al. [96Mat1]: Double focussing Nier-Johnson sector field mass spectrometer; normalized to the $\sigma(C_{60}^-)$ attachment cross section [93Smi1, 95Mat1].

Comments: The C_{60}^+ cross section of Matt et al. [96Mat1, 98Fol1] is in good agreement with the data of Tarnovsky et al. [98Tar1]. As the absolute uncertainty in the measurement of Tarnovsky et al. [98Tar1] is smaller than that in the earlier study the partial and total cross sections reported by Matt et al. [96Mat1, 98Fol1] have been renormalized to the work of Tarnovsky et al. [98Tar1]. The uncertainty in $\sigma(C_{60}^+)$ is reported as ± 15 % by Tarnovsky et al. The uncertainties in $\sigma(C_{60}^{2+})$, $\sigma(C_{60}^{3+})$, and σ(total) should also be on the order of ± 15 %. The uncertainties in the other partial cross sections are probably larger than this as corrections to the original data of up to 100 % were applied by Foltin et al. [98Fol1]. The available C_{60} cross section data have recently been reviewed by Matt et al. [99Mat1].

Other data reviewed: [92Bab1, 95Dun1, 95Vos1, 99Ito1]

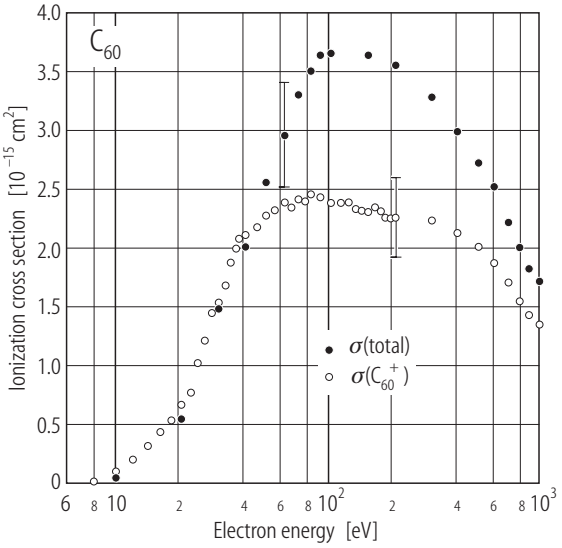

Fig. 5.1.13. C_{60} partial and total electron-impact ionization cross sections.

[21] Matt et al. [96Mat1] performed the original measurement, a correction was then applied by Foltin et al. [98Fol1]. The data given here were digitized from graphs in the article by Matt et al. [99Mat1].

Table 5.1.27. C_{60} partial and total electron-impact ionization cross sections.[22]

Energy [eV]	$\sigma(C_{60}^{+})$ [10^{-15} cm^2]	$\sigma(C_{60}^{2+})$ [10^{-16} cm^2]	$\sigma(C_{60}^{3+})$ [10^{-17} cm^2]	$\sigma(C_{58}^{+})$ [10^{-16} cm^2]	$\sigma(C_{58}^{2+})$ [10^{-16} cm^2]	$\sigma(C_{58}^{3+})$ [10^{-17} cm^2]	σ(total) [10^{-15} cm^2]
8	0.02						
10	0.10						0.05
12	0.20						
14	0.31						
16	0.43						
18	0.53						
20	0.65						0.54
22	0.77						
24	1.02						
26	1.22						
28	1.45						
30	1.52	0.09					1.49
32	1.67						
34	1.87						
36	1.98						
38	2.09						
40	2.12	0.71					2.00
45	2.18						
50	2.26	2.26		0.10			2.56
55	2.32						
60	2.38	4.30	0.19	0.53			2.95
65	2.34						
70	2.41	5.67	0.88	1.06	0.65		3.30
75	2.39						
80	2.44	5.98	2.07	1.01	1.10	0.15	3.51
90	2.42	6.14	3.03	0.99	1.17	0.731	3.63
100	2.37	5.99	3.92	0.85	1.13	1.19	3.65
110	2.37						
120	2.38						
130	2.33						
140	2.31						
150	2.30	5.93	5.47	0.74	0.98	1.85	3.63
160	2.34						
170	2.30						
180	2.25						
190	2.25						
200	2.25	5.81	6.50	0.60	0.89	2.31	3.54
300	2.23	5.33	6.11	0.49	0.72	1.79	3.28
400	2.12	4.62	4.89	0.40	0.57	1.40	2.98
500	2.00	4.12	4.08	0.31	0.48	1.17	2.72
600	1.86	3.69	3.53	0.27	0.40	0.96	2.51
700	1.69	3.07	2.67	0.22	0.31	0.83	2.21
800	1.54	2.61	2.30	0.20	0.26	0.71	1.99
900	1.43	2.22	1.88	0.16	0.23	0.58	1.82
1000	1.34	2.10	1.92	0.13	0.21	0.49	1.70

[22] The C_{60}^{+} cross section data were digitized from the graph given by Tarnovsky et al. [98Tar1].

Cl_2 - Chlorine [7782-50-5]

Recommended data: Average of the Kurepa and Belic [78Kur1] and Stevie and Vasile [81Ste1] cross sections as suggested by Christophorou and Olthoff [99Chr1] for σ (total).

Technique used: Kurepa and Belic [78Kur1]: Parallel plate apparatus with total ion collection; independently absolute.
Stevie and Vasile [81Ste1]: Utilized a modulated molecular beam technique using calibrant gases to determine the ionization cross sections. The data are normalized to those of Rapp and Englander-Golden [65Rap2].

Comments: The uncertainty in the Kurepa and Belic data is ± 15 % and that in the Stevie and Vasile data is ± 10 %. However, as the two data sets do not quite agree to within their combined uncertainties the recommended cross section is probably not accurate to better than ± 15 %.

Other data reviewed: [97Sri1, 92Mor1, 72Cen1, 60Fro1]

Table 5.1.28. Cl_2 total electron-impact ionization cross section.[23]

Energy [eV]	σ (total) [10^{-16} cm^2]	Energy [eV]	σ (total) [10^{-16} cm^2]
11.5	0.03	35	5.26
12	0.11	40	5.49
13	0.25	45	5.68
14	0.43	50	5.87
15	0.69	55	6.03
16	0.99	60	6.15
17	1.32	65	6.25
18	1.67	70	6.32
19	2.06	75	6.33
20	2.47	80	6.31
22	3.25	85	6.28
24	3.79	90	6.25
26	4.17	95	6.22
28	4.51	100	6.19
30	4.80		

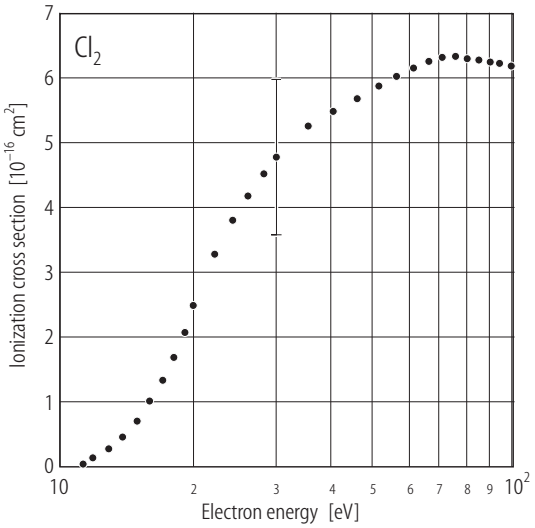

Fig. 5.1.14. Cl_2 total electron-impact ionization cross section.

[23] The recommended cross section is for total charge production.

F_2 - Fluorine [7782-41-4]

Recommended data: Rao and Srivastava [96Rao1] for $\sigma(F_2^+)$, $\sigma(F^+ + F_2^{2+})$, and σ(total)

Technique used: Crossed electron-molecular beam geometry. The ions were analyzed with a quadrupole mass spectrometer and a time-of-flight mass spectrometer. The data are ultimately normalized to the helium total cross section of Rapp and Englander-Golden [65Rap2].

Comments: The uncertainty in these cross sections is reported as ± 15 %. An earlier study performed by Stevie and Vasili [81Ste1] over a limited energy ranges, which also appears reasonably credible, found the total cross section to be approximately 25 % greater than that reported by Rao and Srivastava [96Rao1].

Other data reviewed: [81Ste1, 72Cen1]

Table 5.1.29. F_2 electron-impact ionization cross sections.

Energy [eV]	$\sigma(F_2^+)$ [10^{-17} cm^2]	$\sigma(F^+ + F_2^{2+})$ [10^{-17} cm^2]	σ(total) [10^{-17} cm^2]
20	0.431	0.039	0.47
25	0.958	0.141	1.10
30	1.73	0.332	2.06
35	2.71	0.464	3.18
40	4.02	0.601	4.62
45	5.56	0.752	6.32
50	6.55	0.870	7.42
55	7.38	0.974	8.36
60	7.93	1.07	9.00
65	8.15	1.15	9.31
70	8.27	1.24	9.50
75	8.36	1.29	9.65
80	8.41	1.32	9.73
85	8.46	1.35	9.81
90	8.49	1.37	9.86
95	8.51	1.38	9.89
100	8.49	1.40	9.89
105	8.48	1.41	9.89
110	8.45	1.41	9.87
115	8.41	1.42	9.84
120	8.37	1.42	9.79
125	8.31	1.43	9.73
150	8.03	1.43	9.46
175	7.76	1.40	9.16
200	7.45	1.36	8.82
250	6.85	1.28	8.14
300	6.28	1.21	7.49
400	5.31	1.06	6.37
500	4.53	0.923	5.45
600	3.96	0.827	4.78
700	3.54	0.745	4.28
800	3.21	0.685	3.89
900	2.94	0.640	3.58
1000	2.72	0.605	3.33

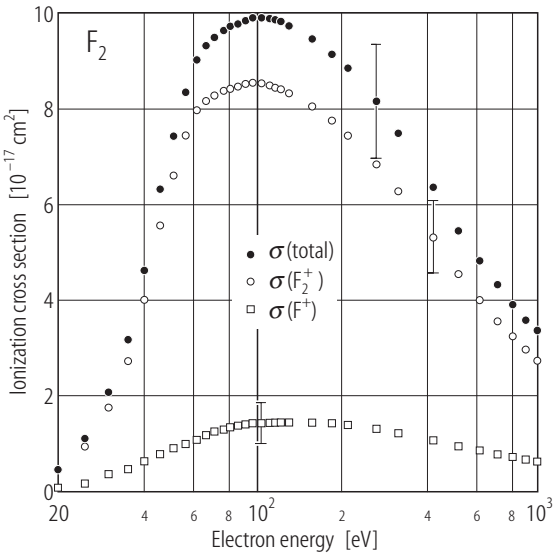

Fig. 5.1.15. F_2 electron-impact ionization cross sections.

NF_3 - Nitrogen trifluoride [7783-54-2]

Recommended data: Average of the Tarnovsky et al. [94Tar1] and Haaland et al. [01Haa1] cross sections.

Technique used: Tarnovsky et al. [94Tar1]: A beam of molecules was prepared by charge-transfer neutralization of a mass separated ion beam and then ionized by a well-characterized electron beam. The data were normalized to the argon total ionization cross section of Rapp and Englander-Golden [65Rap2].[24]
Haaland et al. [01Haa1]: Fourier transform mass spectrometer. The data are normalized to the argon cross section of Wetzel et al. [87Wet1].

Comments: The uncertainty in the Tarnovsky et al. [94Tar1] data is ± 18-20 %[25] and that for the singly-charged ion cross sections reported by Haaland et al. [01Haa1] is ± 16 %. However, because of large discrepancies between these two measurements the uncertainties associated with the recommended values are greater than the figures quoted above. Based on the level of agreement between the two data sets the estimated uncertainties in $\sigma(NF_3^+)$, $\sigma(NF^+)$, and σ(total) are ± 20 %, ± 25 %, and ± 20 % respectively. The uncertainty in $\sigma(NF_2^+)$ is ± 20 % below 50 eV and as great as ± 40 % at higher energies. The tabulated N^+ data and those for the doubly-charged ions are due to Haaland et al. [01Haa1] alone. The N^+ cross section of Haaland et al. [01Haa1] is consistent with the upper limit for $\sigma(N^+)$ of $1 \cdot 10^{-17}$ cm^2 at 70 eV given by Tarnovsky et al. [94Tar1]. No cross section has been recommended for production of F^+ ions as the disagreement between the two studies is very large. Tarnovsky et al. [94Tar1] measured $3 \cdot 10^{-17}$ cm^2 for $\sigma(F^+)$ at 100 eV while Haaland et al. [01Haa1] report a value roughly ten times smaller. The uncertainty in the electron beam energy of Haaland et al. [01Haa1] was ± 0.2 eV.

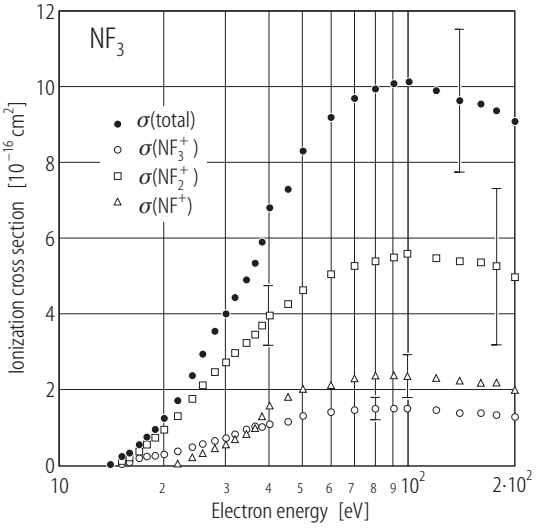

Fig. 5.1.16. NF_3 electron-impact ionization cross sections.

[24] Tarnovsky et al. [94Tar1] independently verified their $\sigma(NF_3^+)$ fast beam measurement using a double focusing mass spectrometric technique, indicating that no excited species were present in their fast neutral beam.
[25] A total cross section was estimated for the Tarnovsky et al. [94Tar1] study by summing their available partial cross sections.

Table 5.1.30. NF_3 partial and total electron-impact ionization cross sections.

Energy [eV]	$\sigma(NF_3^+)$ [10^{-17} cm^2]	$\sigma(NF_2^+)$ [10^{-16} cm^2]	$\sigma(NF^+)$ [10^{-17} cm^2]	$\sigma(N^+)$ [10^{-19} cm^2]	$\sigma(NF_3^{2+})$ [10^{-19} cm^2]	$\sigma(NF_2^{2+})$ [10^{-19} cm^2]	$\sigma(NF^{2+})$ [10^{-20} cm^2]	σ(total) [10^{-16} cm^2]
14	0.085							0.009
15	0.175	0.03						0.048
16	0.310	0.06						0.073
17	0.454	0.10						0.143
18	0.560	0.13						0.186
19	0.641	0.18						0.245
20	0.744	0.23						0.310
22	0.877	0.33	0.13					0.426
24	1.14	0.44	0.42					0.596
26	1.40	0.52	0.73					0.738
28	1.63	0.62	1.08					0.888
30	1.81	0.68	1.33			0.589		0.998
32	1.98	0.75	1.64			0.998		1.11
34	2.16	0.80	2.03			1.23		1.22
36	2.30	0.86	2.37	0.589		1.32		1.33
38	2.47	0.92	3.15	0.837		1.42		1.49
40	2.60	0.99	3.86	1.15		1.58		1.69
45	2.93	1.07	4.43	1.81	0.32	2.01		1.81
50	3.24	1.15	4.95	2.40	0.73	2.24		2.09
60	3.45	1.26	5.42	3.29	0.49	2.76		2.30
70	3.62	1.32	5.67	3.79	0.73	2.96	1.8	2.42
80	3.72	1.35	5.91	4.21	0.87	3.41	2.1	2.49
90	3.78	1.37	5.90	4.36	0.73	3.53	2.8	2.52
100	3.77	1.39	5.89	4.52	0.84	3.41	2.7	2.53
120	3.62	1.37	5.69	4.52	1.07	3.18	2.1	2.47
140	3.44	1.34	5.58	4.68	0.90	3.41	3.5	2.41
160	3.37	1.34	5.38	4.85	1.03	3.66	2.9	2.38
180	3.30	1.31	5.33	4.68	1.07	3.79	3.2	2.34
200	3.26	1.26	5.18	4.52	0.90	3.53	3.1	2.26

SiF_4 - Silicon tetrafluoride [7783-61-1]

Recommended data: Poll and Meichsner [87Pol1]

Technique used: Quadrupole mass spectrometer. The data are normalized to the argon total cross section of Rapp and Englander-Golden [65Rap2].

Comments: The only cross section which has been measured for this target is $\sigma(SiF_3^+)$. No uncertainty is reported for this cross section.

Table 5.1.31. SiF_4 electron-impact ionization cross sections.[26]

Energy [eV]	$\sigma(SiF_3^+)$ [10^{-16} cm^2]
15	0.09
18	0.30
20	0.56
25	1.44
30	2.56
35	3.34
40	4.10
45	4.71
50	5.20
55	5.58
60	5.88
65	6.12
70	6.30
80	6.51
90	6.61
100	6.65
110	6.63
120	6.57
130	6.48

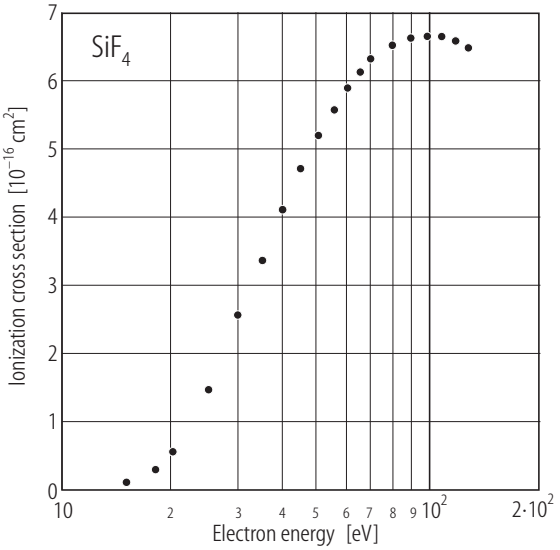

Fig. 5.1.17. SiF_3^+ partial electron-impact ionization cross section.

[26] The tabulated data were digitized from the graph given by Poll and Meichsner [87Pol1].

SF_6 - Sulfur hexafluoride [2551-62-4]

Recommended data: Rejoub et al. [01Rej1]

Technique used: Parallel plate apparatus with time-of-flight mass spectrometer and position-sensitive detection of product ions; independently absolute.

Comments: The absolute uncertainties in $\sigma(SF_5^+)$, $\sigma(SF_4^+)$, $\sigma(SF_3^+)$, $\sigma(SF_2^+)$, and $\sigma(SF^+ + SF_4^{2+})$ are ± 5 %. The uncertainties in $\sigma(S^+)$, $\sigma(SF_3^{2+})$, $\sigma(SF_2^{2+})$, and $\sigma(SF^{2+})$ are ± 8 %, ± 12 %, ± 15 %, and ± 12 %, respectively. The uncertainty in the measurement of $\sigma(F^+)$ is reported as ± 5 %, but it is noted that this may be a lower limit to the cross section because of the possibility of production of multiple F^+ ions in a single collision event. The uncertainty in the electron beam energy calibration is ± 0.5 eV. No observations of the SF_6^+ ion have been reported. The recommended total cross section is in excellent agreement with that of Rapp and Englander-Golden [65Rap2] which is reported to be accurate to within ± 7 %. Most of the SF_6 data have been reviewed recently by Christophorou and Olthoff [00Chr1].

Other data reviewed: [97Rao2, 90Mar1, 83Sta1]

Table 5.1.32. SF_6 partial electron-impact ionization cross sections.

Energy [eV]	$\sigma(SF_5^+)$ [10^{-16} cm^2]	$\sigma(SF_4^+)$ [10^{-17} cm^2]	$\sigma(SF_3^+)$ [10^{-17} cm^2]	$\sigma(SF_2^+)$ [10^{-17} cm^2]	$\sigma(SF^+ + SF_4^{2+})$ [10^{-17} cm^2]	$\sigma(S^+)$ [10^{-17} cm^2]	$\sigma(F^+)$ [10^{-17} cm^2]
18	0.06(2)						
20	0.19(3)						
22.5	0.46	0.13(7)	0.12(6)				
25	0.86	0.26(8)	0.56(7)				
27.5	1.18	0.42(5)	1.17(12)				
30	1.47	0.69(6)	2.21(13)				
32.5	1.84	1.11(7)	3.43	0.22(2)			
35	2.03	1.30	4.81	0.55(4)			
40	2.36	1.67	6.23	1.21	0.52(3)	0.11	
45	2.57	1.76	5.89	1.82	1.59	0.29	
50	2.74	1.97	6.76	2.27	2.75	0.70	0.49(12)
60	3.01	2.27	8.08	2.79	4.03	1.51	1.34(16)
70	3.12	2.52	8.69	3.02	4.89	2.11	2.39
80	3.23	2.67	8.92	2.94	5.30	2.54	2.94
90	3.23	2.68	9.26	3.08	5.94	2.88	3.96
100	3.34	2.86	9.71	3.14	6.34	3.32	5.01
120	3.31	2.83	9.59	2.95	6.50	3.92	6.33
140	3.34	2.89	9.79	2.95	6.49	4.17	7.32
160	3.32	2.70	9.55	2.74	6.61	4.24	7.85
200	3.23	2.67	9.35	2.66	6.27	4.31	8.45
250	3.03	2.43	8.68	2.34	5.69	3.90	8.17
300	2.93	2.38	8.17	2.18	5.17	3.71	7.62
400	2.62	2.08	7.17	1.72	4.25	3.00	6.27
500	2.42	1.99	6.60	1.54	3.83	2.63	5.38
600	2.21	1.72	5.98	1.40	3.42	2.33	4.81
800	1.86	1.46	4.93	1.13	2.67	1.73	3.72
1000	1.65	1.27	4.49	0.98	2.21	1.51	2.97

Table 5.1.33. Cross sections for production of doubly-charged ions by electron-impact ionization of SF_6.

Energy [eV]	$\sigma(SF_3^{2+})$ [10^{-18} cm^2]	$\sigma(SF_2^{2+})$ [10^{-17} cm^2]	$\sigma(SF^{2+})$ [10^{-18} cm^2]
60	0.32(10)	0.15(5)	0.35(7)
70	0.73(19)	0.32(9)	0.52(9)
80	0.89(18)	0.53(13)	1.11(17)
90	1.19(18)	0.72(16)	1.41
100	1.33	0.88(18)	1.75
120	1.54	1.08	2.29
140	1.72	1.19	2.71
160	1.67	1.17	2.87
200	1.54	1.24	2.87
250	1.41	1.16	2.45
300	1.39	1.08	2.00
400	1.17	0.90	1.72
500	1.04	0.78	1.39
600	0.98	0.68	1.16
800	0.72	0.51	1.02
1000	0.59	0.47	0.82

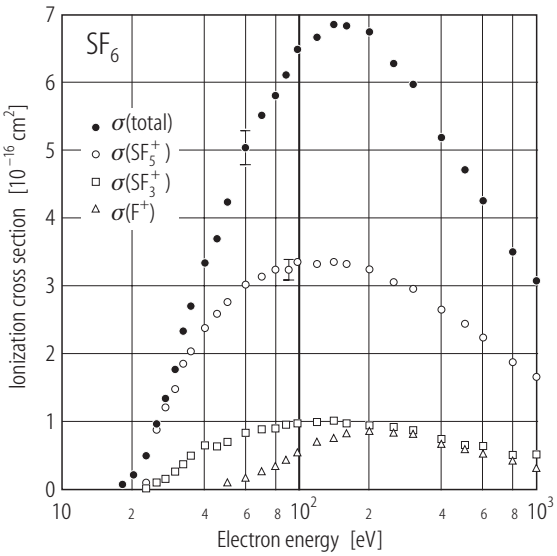

Fig. 5.1.18. SF_6 partial and total electron-impact ionization cross sections.

UF_6 - Uranium Hexafluoride [7783-81-5]

Recommended data: Compton [77Com1]
Technique used: A monoenergetic electron beam was passed through a cylindrical collision cell and the cross section was determined from the total positive charge collected. The reported data are independently absolute.
Comments: The major source of uncertainty in the Compton data is due to the pressure measurement (± 30 %).

Table 5.1.34. UF_6 total electron-impact ionization cross sections. [27]

Energy [eV]	σ (total) [10^{-15} cm^2]	Energy [eV]	σ (total) [10^{-15} cm^2]
15	0.00456	300	1.52
16	0.0341	320	1.46
17	0.0931	340	1.44
20	0.164	360	1.43
25	0.346	380	1.40
30	0.422	400	1.38
40	0.658	420	1.36
50	0.909	440	1.30
53	0.958	460	1.25
60	1.09	480	1.23
70	1.38	500	1.21
80	1.55	520	1.18
90	1.62	540	1.18
100	1.65	560	1.14
120	1.64	580	1.13
140	1.72	600	1.07
160	1.75	650	1.04
180	1.69	700	0.964
200	1.68	750	0.905
220	1.63	800	0.828
240	1.62	850	0.774
260	1.61	900	0.759
280	1.55	950	0.751

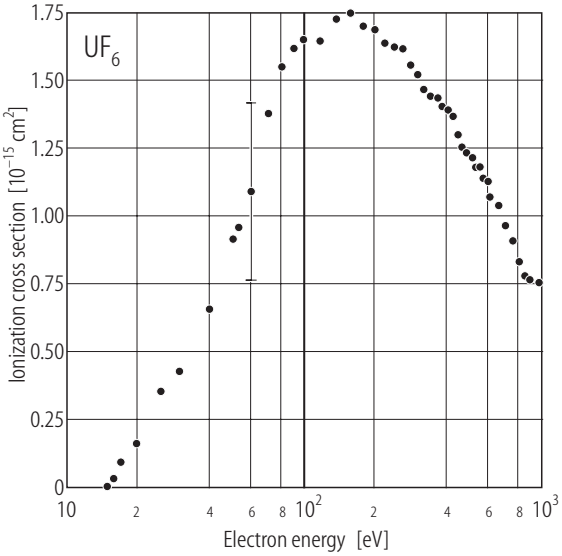

Fig. 5.1.19. UF_6 total electron-impact ionization cross section.

[27] The recommended data are for total charge production and were digitized from graphs given by Compton [77Com1].

H_2 - Hydrogen [1333-74-0]

Recommended data: Straub et al. [96Str1][28] for $\sigma(H^+)$, $\sigma(H_2^+)$, and σ(total) at energies greater than 25 eV; Krishnakumar and Srivastava [94Kri1] renormalized to Straub et al. [96Str1] for $\sigma(H^+)$, and $\sigma(H_2^+)$ at energies of 25 eV or less.
Rapp and Englander-Golden [65Rap2] for σ(total) at energies of 25 eV or less.

Technique used: Straub et al. [96Str1]: Parallel plate apparatus with time-of-flight mass spectrometer and position-sensitive detection of product ions; independently absolute.
Krishnakumar and Srivastava [94Kri1]: Crossed electron-molecular beam geometry. The ions were analyzed with a time-of-flight mass spectrometer. The data were put on an absolute scale using the relative flow technique and are normalized to known absolute cross sections [83Bel1].
Rapp and Englander-Golden [65Rap2]: Parallel plate apparatus with total ion collection; independently absolute.

Comments: At energies greater than 25 eV the absolute uncertainty in the cross sections is ± 5 %, the relative uncertainty is ± 2 % and the uncertainty in the energy is ± 1 eV. At energies of 25 eV or less the uncertainty in $\sigma(H_2^+)$ and $\sigma(H^+)$ is ± 15 %, the uncertainty in σ(total) is ± 4.5 % and the electron beam energy calibration is probably better than ± 0.5 eV. The total cross section of Straub et al. [96Str1] and that of Rapp and Englander-Golden [65Rap2] are in excellent agreement, however, the Straub et al. [96Str1] data have an uncertainty of ± 1 eV in the electron beam energy and there are few data points near threshold. In this range the data of Rapp et al. [65Rap2] and the energy dependence of Krishnakumar and Srivastava [94Kri1] are therefore preferred.

Other data reviewed: [73Cow1, 66Ada1, 66Sch2, 65Rap1, 65Sch1, 32Tat1]

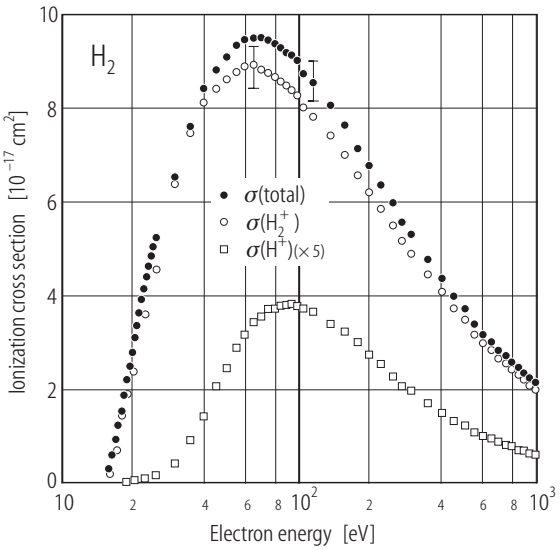

Fig. 5.1.20. H_2 partial and total electron-impact ionization cross sections.

[28] The data of Straub et al. [96Str1] reflect a recent recalibration of their apparatus and thus differ slightly from those given in their original paper.

Table 5.1.35. H_2 electron-impact ionization cross sections.

Energy [eV]	$\sigma(H_2^+)$ [10^{-17} cm^2]	$\sigma(H^+)$ [10^{-18} cm^2]	σ(total) [10^{-17} cm^2]	Energy [eV]	$\sigma(H_2^+)$ [10^{-17} cm^2]	$\sigma(H^+)$ [10^{-18} cm^2]	σ(total) [10^{-17} cm^2]
16	0.182		0.299	80	8.63	7.39	9.37
16.5			0.607	85	8.53	7.51	9.28
17	0.691		0.924	90	8.43	7.54	9.19
17.5			1.23	95	8.35	7.61	9.11
18	1.46		1.56	100	8.24	7.59	9.00
18.5			1.87	110	7.97	7.44	8.72
19	1.89	0.031	2.20	120	7.80	7.24	8.52
19.5			2.49	140	7.39	6.71	8.06
20	2.41	0.078	2.80	160	6.99	6.39	7.63
20.5			3.10	180	6.55	5.92	7.14
21			3.36	200	6.22	5.45	6.76
21.5			3.62	225	5.85	5.05	6.36
22			3.90	250	5.51	4.50	5.96
22.5	3.59	0.171	4.14	275	5.15	4.12	5.56
23			4.39	300	4.90	3.92	5.29
23.5			4.61	350	4.43	3.39	4.77
24			4.84	400	4.07	2.94	4.36
24.5			5.05	450	3.72	2.60	3.98
25	4.58	0.311	5.24	500	3.49	2.41	3.73
30	6.42	0.860	6.51	550	3.17	2.11	3.39
35	7.42	1.76	7.60	600	2.98	1.97	3.17
40	8.12	2.87	8.40	650	2.84	1.81	3.02
45	8.39	4.08	8.80	700	2.66	1.71	2.83
50	8.59	4.82	9.08	750	2.56	1.59	2.72
55	8.74	5.72	9.31	800	2.42	1.49	2.57
60	8.82	6.25	9.44	850	2.34	1.37	2.48
65	8.80	6.82	9.48	900	2.22	1.35	2.36
70	8.79	7.05	9.49	950	2.10	1.25	2.22
75	8.71	7.37	9.44	1000	1.99	1.17	2.11

H_2O - Water [7732-18-5]

D_2O - Deuterium oxide [7789-20-0]

Recommended data: Straub et al. [98Str1][29]

Technique used: Parallel plate apparatus with time-of-flight mass spectrometer and position-sensitive detection of product ions; independently absolute. Both H_2O and D_2O were studied.

Comments: It has been established by several workers that the H_2O and D_2O total and partial cross sections are essentially identical.[30] Therefore the cross sections below apply to either target. The uncertainties in $\sigma(H_2O^+)$, $\sigma(OH^+)$, $\sigma(O^+)$, $\sigma(H^+)$, and σ(total) are ± 6 %, ± 7 %, ± 9 %, ± 6.5 % and ± 6 %, respectively. The uncertainties in $\sigma(O^{2+})$ and $\sigma(H_2^+)$ are ± 13 % and ± 16 %, respectively. The uncertainty in the electron energy is ± 1 eV. The recommended partial cross sections agree well with the fast-neutral-beam D_2O measurements of Tarnovsky et al. [98Tar2]. The recommended total cross section is in good agreement with the measurements of Djuric et al. [88Dju1] and Schutten et al. [66Sch3] and in reasonable agreement with the calculations of Hwang et al. [96Hwa1].

Other data reviewed: [95Rao1, 87Ori1, 86Bol1, 76Mar1, 75Gom1]

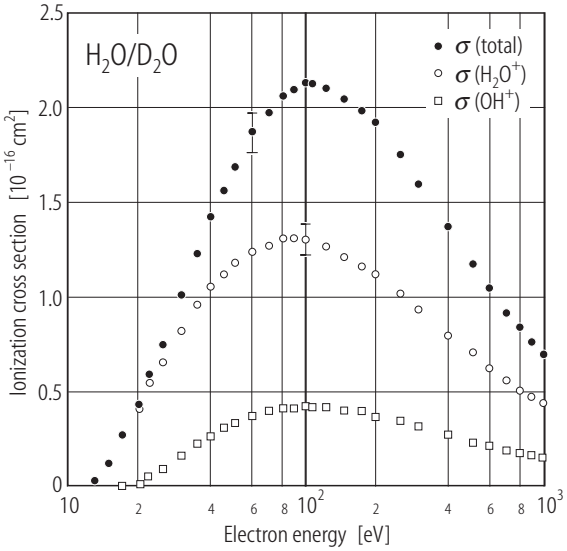

Fig. 5.1.21. H_2O/D_2O electron-impact ionization cross sections.

[29] The data of Straub et al. [98Str1] reflect a recent recalibration of their apparatus and thus differ slightly from those given in the original paper.

[30] The difference between $\sigma(H_2^+)$ and $\sigma(D_2^+)$ observed by Straub et al. [98Str1] was apparently an experimental artifact [01Rej2].

Table 5.1.36. H_2O/D_2O partial and total electron-impact ionization cross sections.[31]

Energy [eV]	$\sigma(H_2O^+)$ [10^{-16} cm^2]	$\sigma(OH^+)$ [10^{-17} cm^2]	$\sigma(O^+)$ [10^{-18} cm^2]	$\sigma(O^{2+})$ [10^{-19} cm^2]	$\sigma(H_2^+)$ [10^{-19} cm^2]	$\sigma(H^+)$ [10^{-17} cm^2]	σ(total) [10^{-16} cm^2]
13.5	0.025						0.025
15	0.126						0.126
17.5	0.272	0.013					0.274
20	0.411	0.145				0.024	0.428
22.5	0.549	0.500				0.091	0.609
25	0.652	0.855	0.22			0.207	0.761
30	0.815	1.60	0.37		0.18	0.433	1.02
35	0.958	2.22	0.70		0.39	0.759	1.26
40	1.05	2.64	1.32		0.57	1.10	1.43
45	1.12	3.00	2.07		0.70	1.45	1.59
50	1.18	3.29	2.75		0.65	1.78	1.72
60	1.24	3.64	3.94		0.66	2.35	1.88
70	1.27	3.89	4.84		0.69	2.79	1.99
80	1.31	4.09	5.94		0.63	3.17	2.09
90	1.31	4.12	6.66	0.08	0.78	3.43	2.13
100	1.31	4.18	6.95	0.19	0.75	3.60	2.16
110	1.29	4.15	7.38	0.46	0.73	3.70	2.15
125	1.27	4.12	7.63	0.69	0.64	3.75	2.13
150	1.21	3.93	7.52	1.16	0.77	3.71	2.05
175	1.16	3.81	7.31	1.78	0.71	3.66	1.99
200	1.12	3.63	7.07	1.79	0.54	3.51	1.90
250	1.01	3.34	6.34	1.95	0.50	3.16	1.73
300	0.921	3.11	5.51	1.79	0.45	2.84	1.57
400	0.789	2.66	4.34	1.34	0.40	2.37	1.34
500	0.696	2.30	3.73	1.05	0.32	1.98	1.16
600	0.618	2.03	3.13	0.96	0.29	1.72	1.02
700	0.555	1.85	2.71	0.80	0.33	1.49	0.917
800	0.502	1.69	2.40	0.80	0.22	1.35	0.830
900	0.465	1.56	2.20	0.60	0.32	1.20	0.763
1000	0.432	1.43	1.94	0.66	0.24	1.09	0.705

[31] The values of $\sigma(H_2O^+)$, $\sigma(OH^+)$, $\sigma(O^+)$, and $\sigma(H_2^+)$ are based on measurements with a D_2O target.

H_2S – Hydrogen sulfide [7783-06-4]

Recommended data: Lindsay et al. [03Lin1]
Technique used: Parallel plate apparatus with time-of-flight mass spectrometer and position sensitive detection of product ions; independently absolute..
Comments: The absolute uncertainties in $\sigma(H_nS^+)$, $\sigma(H^+)$, and σ(total) are ±6%, ±7%, and ±6% respectively. The uncertainty in the electron energy calibration is ±0.5 eV. The total cross section of Belic and Kurepa [85Bel1] agrees quite well with the recommended data.
Other data reviewed: [93Rao1, 57Lam1, 56Otv1]

Table 5.1.37. H_2S partial and total electron-impact ionization cross sections.

Energy [eV]	$\sigma(H_nS^+)$ [10^{-16} cm^2]	$\sigma(H^+)$ [10^{-17} cm^2]	σ(total) [10^{-16} cm^2]
16	2.11(53)		2.11(53)
18	2.92(44)		2.92(44)
20	3.87(31)		3.87(31)
25	4.51(32)	0.48(12)	4.56(32)
30	4.88(34)	1.93	5.08(35)
40	5.03	4.51	5.48
50	4.92	5.56	5.47
60	4.92	6.05	5.53
80	4.69	6.28	5.32
100	4.54	6.07	5.15
150	3.91	4.37	4.35
200	3.36	3.69	3.73
300	2.77	2.66	3.04
400	2.42	2.19	2.64
500	2.19	1.89	2.38
600	1.87(17)	1.44(14)	2.02(18)
800	1.52(18)	1.36(20)	1.65(20)
1000	1.29(15)	0.93(23)	1.39(17)

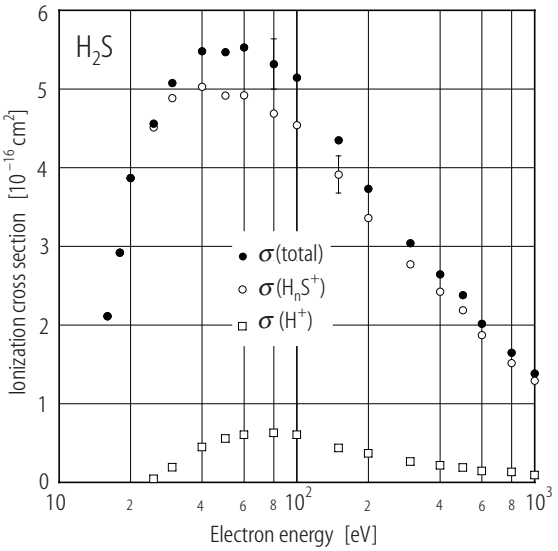

Fig. 5.1.22. H_2S electron-impact ionization cross sections.

NH_3 - Ammonia [7664-41-7]

ND_3 - Ammonia-d3 [84796-14-5]

Recommended data: Rejoub et al. [01Rej2]

Technique used: Parallel plate apparatus with time-of-flight mass spectrometer and position-sensitive detection of product ions; independently absolute. Both NH_3 and ND_3 were studied.

Comments: The NH_3 and ND_3 total and partial cross sections are essentially identical therefore the cross sections below apply to either target. The uncertainties in $\sigma(NH_3^+)$, $\sigma(NH_2^+)$, $\sigma(NH^+)$, $\sigma(N^+)$, $\sigma(H^+)$, $\sigma(H_2^+)$, and $\sigma(NH_3^{2+})$ are ± 6 %, ± 6 %, ± 12 %, ± 8 %, ± 6 %, ± 8 %, and ± 20 % respectively, unless otherwise indicated. The uncertainty in σ(total) is ± 6 %. The uncertainty in the electron energy is ± 0.5 eV. The recom-mended NH_3^+ and NH_2^+ partial cross sections are in agreement with the less precise data of Märk et al. [77Mar1], Rao and Srivastava [92Rao1], and Tarnovsky et al. [97Tar1]. The recommended total cross section is in very good agreement with the measurements of Djuric et al. [81Dju1] and with recent theoretical calculations [97Kim1].

Other data reviewed: [91Rao1, 88Sya1, 80Bed1, 77Cro1, 75Gom1, 66Mel1, 57Lam1]

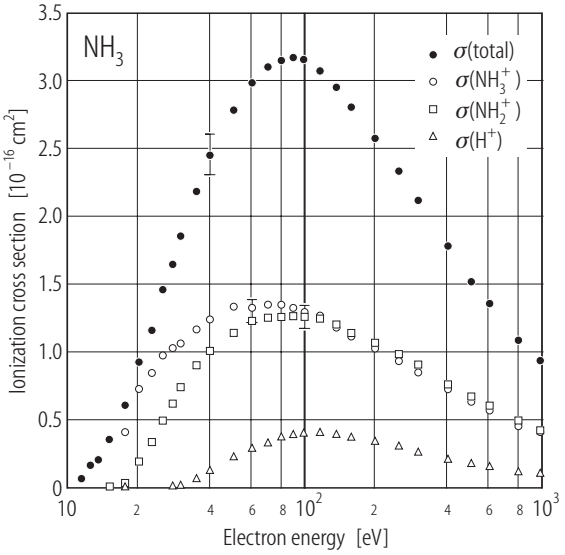

Fig. 5.1.23. NH_3/ND_3 electron-impact ionization cross sections.

Table 5.1.38a. NH_3/ND_3 partial electron-impact ionization cross sections.[32]

Energy [eV]	$\sigma(NH_3^+)$ [10^{-16} cm^2]	$\sigma(NH_2^+)$ [10^{-16} cm^2]	$\sigma(NH^+)$ [10^{-17} cm^2]	$\sigma(N^+)$ [10^{-18} cm^2]
11.5	0.065(7)			
12.5	0.159(13)			
13.5	0.202(14)			
15	0.344	0.0012(6)		
17.5	0.579	0.0253(21)		
20	0.725	0.185		
22.5	0.832	0.325		
25	0.965	0.486	0.0492	
27.5	1.03	0.604	0.102	
30	1.06	0.735	0.322	0.41(7)
35	1.16	0.891	0.635	0.88(8)
40	1.23	0.996	0.886	1.68
50	1.30	1.12	1.28	2.97
60	1.31	1.21	1.48	3.87
70	1.33	1.23	1.57	4.73
80	1.32	1.24	1.62	5.42
90	1.30	1.25	1.65	5.70
100	1.28	1.24	1.66	5.90
120	1.23	1.22	1.63	6.07
140	1.16	1.18	1.56	6.07
160	1.10	1.12	1.47	5.94
200	1.01	1.05	1.28	5.26
250	0.922	0.961	1.11	4.43
300	0.838	0.887	0.971	3.84
400	0.722	0.751	0.752	2.76
500	0.614	0.657	0.645	2.33
600	0.550	0.586	0.557	1.85
800	0.438	0.475	0.431	1.38
1000	0.390	0.401	0.371	1.15

[32] The values of $\sigma(NH_3^+)$, $\sigma(NH_2^+)$, $\sigma(NH^+)$, and $\sigma(N^+)$ are based on measurements with an ND_3 target.

Table 5.1.38b. NH_3/ND_3 partial and total electron-impact ionization cross sections.

Energy [eV]	$\sigma(H^+)$ [10^{-17} cm^2]	$\sigma(H_2^+)$ [10^{-18} cm^2]	$\sigma(NH_3^{2+})$ [10^{-19} cm^2]	σ(total) [10^{-16} cm^2]
11.5				0.065
12.5				0.159
13.5				0.202
15				0.345
17.5				0.605
20				0.911
22.5				1.16
25				1.46
27.5	0.065(7)			1.65
30	0.189	0.20(7)		1.86
35	0.573	0.438		2.18
40	1.09	0.636		2.45
50	1.93	0.839	0.42(21)	2.78
60	2.65	0.997	0.79(20)	2.98
70	3.17	1.06	0.95	3.10
80	3.56	1.07	1.08	3.15
90	3.75	1.08	1.02	3.16
100	3.85	1.08	1.25	3.14
120	3.83	1.01	1.25	3.07
140	3.74	0.969	1.44	2.95
160	3.55	0.844	1.35	2.80
200	3.17	0.756	1.15	2.56
250	2.83	0.668	0.75	2.33
300	2.37	0.560	0.67	2.10
400	1.84	0.405	0.67	1.77
500	1.49	0.363	0.53	1.51
600	1.28	0.293	0.48	1.34
800	0.964	0.240	0.46	1.07
1000	0.810	0.217	0.36	0.923

SiH_4 - Silane [7803-62-5]

Recommended data: Basner et al. [97Bas1] for energies from threshold to 100 eV; Chatham et al. [84Cha1] for energies greater than 100 eV.

Technique used: Basner et al. [97Bas1]: Double-focussing mass spectrometer. The data are normalized to the argon total cross section [65Rap2].
Chatham et al. [84Cha1]: Quadrupole mass spectrometer. The data are normalized to the argon total cross section [65Rap2].

Comments: The data of Basner et al. [97Bas1] and those of Chatham et al. [84Cha1] are in good agreement. The recommended total cross section is in agreement with the earlier measurement by Perrin et al. [82Per1] and with current theoretical calculations [97Bas1, 97Ali1]. The uncertainty given by Basner et al. [97Bas1] for $\sigma(SiH_3^+)$, $\sigma(SiH_2^+)$, $\sigma(SiH^+)$, and $\sigma(Si^+)$ is ± 18 %; that given by Chatham is ± 15 %. Note that the values of $\sigma(H^+)$, $\sigma(H_2^+)$ given in the table are reported by Basner et al. [97Bas1] as a lower limit only.

Other data reviewed: [95Kri1, 90Haa1]

Table 5.1.39. SiH_4 partial and total electron-impact ionization cross sections.

Energy [eV]	$\sigma(SiH_3^+)$ [10^{-16} cm^2]	$\sigma(SiH_2^+)$ [10^{-16} cm^2]	$\sigma(SiH^+)$ [10^{-17} cm^2]	$\sigma(Si^+)$ [10^{-17} cm^2]	$\sigma(H^+)$ [10^{-17} cm^2]	$\sigma(H_2^+)$ [10^{-18} cm^2]	σ(total) [10^{-16} cm^2]
12		0.06					0.06
13	0.07	0.15					0.22
14	0.20	0.31		0.1			0.52
15	0.36	0.55		0.3			0.94
16	0.57	0.86	0.2	0.4			1.49
17	0.81	1.09	0.3	0.5			1.98
18	0.96	1.35	0.7	0.6			2.44
19	1.11	1.58	1.2	0.8			2.89
20	1.22	1.69	1.8	1.0			3.19
22	1.36	1.87	2.8	1.4			3.65
24	1.40	1.93	4.1	1.9			3.93
26	1.41	1.97	5.1	2.7	0.2	0.3	4.18
28	1.44	2.00	5.5	3.3	0.6	0.5	4.39
30	1.46	2.03	5.7	3.9	0.8	0.7	4.54
32	1.48	2.06	5.9	4.3	1.3	0.9	4.70
34	1.49	2.07	6.1	4.7	1.7	1.1	4.81
36	1.51	2.08	6.1	4.9	1.9	1.4	4.89
38	1.51	2.09	6.2	5.1	2.2	1.7	4.97
40	1.52	2.09	6.2	5.2	2.4	2.0	5.01
45	1.54	2.08	6.4	5.4	2.7	2.4	5.09
50	1.56	2.11	6.5	5.6	2.8	2.8	5.19
55	1.59	2.14	6.5	5.8	2.8	3.1	5.27
60	1.61	2.16	6.5	5.8	2.8	3.3	5.31
70	1.67	2.18	6.4	5.9	2.8	3.5	5.40
80	1.66	2.14	6.3	5.9	2.8	3.5	5.34
90	1.63	2.08	6.0	5.7	2.7	3.5	5.19
100	1.59	2.05	5.8	5.5	2.7	3.5	5.08
200	1.40	1.75	4.1	2.1			4.19
300							3.42
400							2.85

Si_2H_6 - Disilane [1590-87-0]

Recommended data: Chatham et al. [84Cha1]
Technique used: Quadrupole mass spectrometer. The data are normalized to the argon total cross section [65Rap2].
Comments: The uncertainties in these cross sections are approximately ± 15 % for product ions containing two silicon atoms, and ± 25 % for the other cross sections.
Other data reviewed: [95Kri1]

Table 5.1.40. Si_2H_6 partial electron-impact ionization cross sections.

Energy [eV]	$\sigma(Si_2H_6^+)$ [10^{-16} cm^2]	$\sigma(Si_2H_5^+)$ [10^{-17} cm^2]	$\sigma(Si_2H_4^+)$ [10^{-16} cm^2]	$\sigma(Si_2H_3^+)$ [10^{-17} cm^2]	$\sigma(Si_2H_2^+)$ [10^{-16} cm^2]	$\sigma(Si_2H^+)$ [10^{-17} cm^2]
15	0.66	3.15	1.25	1.0	0.49	
20	0.85	5.6	1.83	3.0	0.98	2.1
30	0.99	7.0	2.17	4.2	1.40	8.4
50	1.10	7.6	2.47	4.8	1.10	7.6
100	1.07	7.2	2.35	4.9	1.42	8.2
200	0.76	5.9	1.78	4.2	1.07	6.4

Table 5.1.41. Si_2H_6 partial and total electron-impact ionization cross sections.

Energy [eV]	$\sigma(Si_2^+)$ [10^{-17} cm^2]	$\sigma(SiH_3^+)$ [10^{-17} cm^2]	$\sigma(SiH_2^+)$ [10^{-17} cm^2]	$\sigma(SiH^+)$ [10^{-17} cm^2]	$\sigma(Si^+)$ [10^{-17} cm^2]	σ(total) [10^{-15} cm^2]
15		3.2				0.325
20	0.2	5.7		1.3		0.58
30	4.4	6.6	4.4	4.0	2.4	0.87
50	6.1	7.0	4.7	5.6	4.9	1.01
100	5.7	6.8	4.2	5.0	4.6	0.94
200	4.1	5.3	2.9	3.4	3.9	0.71
300						0.585
400						0.50

NO - Nitric oxide [10102-43-9]

Recommended data: Lindsay et al. [00Lin1]

Technique used: Parallel plate apparatus with time-of-flight mass spectrometer and position-sensitive detection of product ions; independently absolute.

Comments: The uncertainties in $\sigma(NO^+)$, $\sigma(N^+ + O^+ + NO^{2+})$, $\sigma(N^+)$, $\sigma(O^+)$, $\sigma(NO^{2+})$, and σ (total) are ± 5 %, ± 5 %, ± 15 %, ± 20 %, ± 30 %, and ± 5 %, respectively, unless otherwise indicated in the table. Note that a fitting procedure was used to extract $\sigma(N^+)$ and $\sigma(O^+)$ and consequently the individual cross sections are not known with the same certainty as their sum, which is given separately.

Other data reviewed: [96Iga1, 81Kim1, 68Fiq1, 65Rap2, 32Tat1]

Table 5.1.42. NO partial and total electron-impact ionization cross sections.

Energy [eV]	$\sigma(NO^+)$ [10^{-16} cm^2]	$\sigma(N^+ + O^+ + NO^{2+})$ [10^{-17} cm^2]	$\sigma(N^+)$ [10^{-17} cm^2]	$\sigma(O^+)$ [10^{-17} cm^2]	$\sigma(NO^{2+})$ [10^{-18} cm^2]	σ (total) [10^{-16} cm^2]
12.5	0.048(12)					0.048(12)
15	0.21(3)					0.21(3)
17.5	0.48(5)					0.48(5)
20	0.59					0.59
22.5	0.75	0.035(7)				0.76
25	0.98	0.18(3)	0.14(4)	0.040(100)		0.99
30	1.20	0.67(6)	0.54	0.125		1.27
35	1.37	1.54	1.32	0.22		1.53
40	1.51	2.44	1.91	0.46		1.75
45	1.67	3.29	2.52	0.73		2.00
50	1.74	4.21	3.17	1.04		2.16
55	1.84	4.68	3.15	1.40		2.31
60	1.89	5.41	3.75	1.58	0.89	2.43
70	1.92	6.28	4.44	1.70	1.42	2.55
80	1.96	7.02	4.79	1.99	2.24	2.67
90	1.97	7.71	4.81	2.51	3.77	2.74
100	1.97	7.88	5.06	2.47	3.49	2.75
125	1.92	8.19	4.99	2.86	3.21	2.73
150	1.84	8.08	5.02	2.74	2.93	2.65
200	1.69	7.37	4.38	2.67	3.06	2.43
250	1.55	6.80	4.06	2.46	2.84	2.23
300	1.40	6.01	3.85	1.91	2.33	2.00
400	1.24	5.01	3.09	1.68	2.32	1.74
500	1.11	4.24	2.65	1.39	2.03	1.53
600	0.98	3.82	2.28	1.39	1.47	1.36
800	0.81	3.01	1.90	1.00	1.32	1.11
1000	0.70	2.52	1.69(42)	0.76(23)	0.69(35)	0.95

NO_2 - Nitrogen dioxide [10102-44-0]

Recommended data: Lindsay et al. [00Lin1]

Technique used: Parallel plate apparatus with time-of-flight mass spectrometer and position-sensitive detection of product ions; independently absolute.

Comments: The uncertainties in $\sigma(NO_2^+)$, $\sigma(NO^+)$, $\sigma(N^+ + O^+)$, $\sigma(N^+)$, $\sigma(O^+)$, $\sigma(N^{2+} + O^{2+})$, and σ(total) are ± 5 %, ± 5 %, ± 5 %, ± 20 %, ± 15 %, ± 12 %, and ± 5 %, respectively. The uncertainty in the electron energy is ± 1 eV. Note that a fitting procedure was used to extract $\sigma(N^+)$ and $\sigma(O^+)$ and consequently the individual cross sections are not known with the same certainty as their sum. The recommended total cross section is in excellent agreement with that of Luki´c et al. [01Luk1] for energies greater than 25 eV and with a recent theoretical calculation [97Kim1].

Other data reviewed: [80Ste1]

Table 5.1.43. NO_2 partial and total electron-impact ionization cross sections.

Energy [eV]	$\sigma(NO_2^+)$ [10^{-17} cm^2]	$\sigma(NO^+)$ [10^{-16} cm^2]	$\sigma(N^+ + O^+)$ [10^{-16} cm^2]	$\sigma(N^+)$ [10^{-17} cm^2]	$\sigma(O^+)$ [10^{-17} cm^2]	$\sigma(N^{2+} + O^{2+})$ [10^{-19} cm^2]	σ(total) [10^{-16} cm^2]
13.5	0.909	0.055					0.146
16	1.59	0.148					0.308
20	2.44	0.401	0.022		0.22		0.667
25	3.17	0.612	0.061		0.61		0.990
30	3.89	0.906	0.155	0.15	1.40		1.45
35	4.36	1.14	0.272	0.55	2.17		1.85
40	4.54	1.30	0.428	1.14	3.14		2.18
50	5.25	1.57	0.642	1.89	4.53		2.74
60	5.46	1.77	0.849	2.34	6.15		3.16
80	5.61	1.89	1.12	3.37	7.78		3.57
100	5.42	1.95	1.26	3.65	8.92	1.40	3.75
120	5.43	1.95	1.35	4.07	9.38	2.38	3.84
160	5.07	1.86	1.31	3.86	9.27	4.33	3.69
200	4.70	1.76	1.24	3.97	8.43	6.14	3.47
250	4.32	1.63	1.14	3.60	7.76	6.40	3.21
300	3.99	1.51	1.02	3.27	6.90	6.15	2.93
400	3.53	1.32	0.850	2.75	5.74	5.07	2.53
500	3.11	1.17	0.719	2.21	4.98	4.52	2.21
600	2.78	1.06	0.631	2.02	4.29	4.13	1.97
800	2.35	0.886	0.516	1.36	3.80	3.30	1.64
1000	2.01	0.756	0.422	1.17	3.05	2.11	1.38

N_2 - Nitrogen [7727-37-9]

Recommended data: Straub et al. [96Str1][33] for σ (N_2^+), σ ($N^+ + N_2^{2+}$), σ (N^{2+}), and σ (total) at energies greater than 25 eV.
Rapp and Englander-Golden [65Rap2] for σ (total) and σ (N_2^+) at energies of 25 eV or less.

Technique used: Straub et al. [96Str1]: Parallel plate apparatus with time-of-flight mass spectrometer and position-sensitive detection of product ions; independently absolute.
Rapp and Englander-Golden [65Rap2]: Parallel plate apparatus with total ion collection; independently absolute.

Comments: The absolute uncertainty in σ (N_2^+) and σ (total) is ± 5 %, the relative uncertainty is ± 2 %. The absolute uncertainty in σ (N^++N_2^{2+}) is ± 5 %, the relative uncertainty is ± 2.5 %; the absolute uncertainty in σ (N^{2+}) is ± 6 %, the relative uncertainty is ± 3.5 %. The uncertainty in the electron energy is ± 1 eV. The two data sets are in excellent agreement, however, the [96Str1] data have an uncertainty of ± 1 eV in the electron beam energy and there are few data points near threshold. In this range the total cross section of of Rapp and Englander-Golden [65Rap2] is therefore preferred. The only product ion of any significance below 25 eV is N_2^+, and σ (N_2^+) is therefore equal to σ(total) in this region. The N_2^+ cross section data of Freund et al. [90Fre1], which are of lower accuracy than those of Rapp and Englander-Golden, are in excellent agreement with the recommended values near threshold.

Other data reviewed: [98Tia5, 90Fre1, 90Kri1, 75Mar1, 73Cro1, 73Hal1, 73Mar1, 65Rap1]

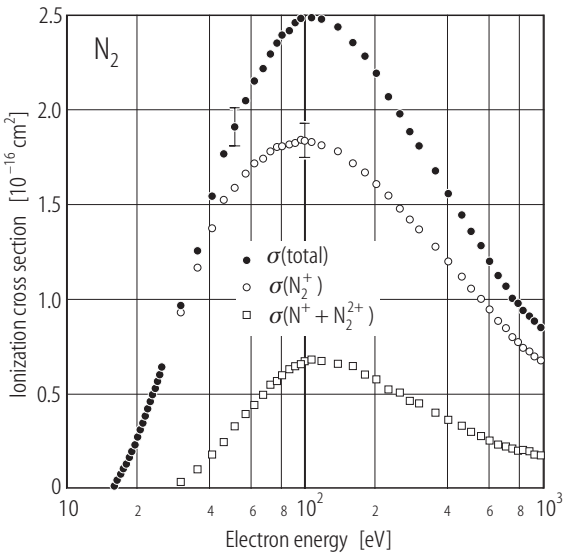

Fig. 5.1.24. N_2 partial and total electron-impact ionization cross sections.

[33] The data of Straub et al. reflect a recent recalibration of their apparatus and thus differ slightly from those given in their original paper.

Table 5.1.44. N_2 partial and total electron-impact ionization cross sections.

Energy [eV]	$\sigma(N_2^+)$ [10^{-16} cm^2]	$\sigma(N^+ + N_2^{2+})$ [10^{-17} cm^2]	$\sigma(N^{2+})$ [10^{-18} cm^2]	σ(total) [10^{-16} cm^2]
16	0.0211			0.0211
16.5	0.0466			0.0466
17	0.0713			0.0713
17.5	0.0985			0.0985
18	0.129			0.129
18.5	0.164			0.164
19	0.199			0.199
19.5	0.230			0.230
20	0.270			0.270
20.5	0.308			0.308
21	0.344			0.344
21.5	0.380			0.380
22	0.418			0.418
22.5	0.455			0.455
23	0.492			0.492
23.5	0.528			0.528
24	0.565			0.565
24.5	0.603			0.603
25	0.640			0.640
30	0.929	0.325		0.962
35	1.16	0.904		1.25
40	1.37	1.66		1.54
45	1.52	2.45		1.77
50	1.60	3.19		1.91
55	1.66	3.90		2.05
60	1.72	4.38		2.16
65	1.74	4.82		2.22
70	1.78	5.23	0.0171	2.30
75	1.80	5.61	0.0658	2.36
80	1.81	5.87	0.122	2.40
85	1.82	6.05	0.204	2.43
90	1.83	6.32	0.328	2.47
95	1.85	6.45	0.439	2.50
100	1.85	6.56	0.495	2.51
110	1.83	6.60	0.725	2.50
120	1.81	6.61	0.927	2.48
140	1.78	6.52	1.22	2.45
160	1.72	6.33	1.37	2.36
180	1.67	5.95	1.54	2.28
200	1.61	5.66	1.54	2.19
225	1.55	5.16	1.54	2.08
250	1.48	4.93	1.42	1.98
275	1.41	4.58	1.41	1.89
300	1.37	4.38	1.28	1.82
350	1.28	3.93	1.17	1.68
400	1.20	3.51	1.03	1.56
450	1.11	3.24	0.940	1.45
500	1.05	2.99	0.808	1.36

Table 5.1.44 (continued)

Energy [eV]	$\sigma(N_2^+)$ [10^{-16} cm^2]	$\sigma(N^+ + N_2^{2+})$ [10^{-17} cm^2]	$\sigma(N^{2+})$ [10^{-18} cm^2]	σ(total) [10^{-16} cm^2]
550	0.998	2.74	0.796	1.28
600	0.943	2.48	0.760	1.20
650	0.880	2.34	0.701	1.12
700	0.844	2.17	0.649	1.07
750	0.796	2.05	0.587	1.01
800	0.765	2.00	0.594	0.971
850	0.738	1.92	0.543	0.936
900	0.719	1.83	0.522	0.907
950	0.698	1.76	0.505	0.879
1000	0.676	1.67	0.485	0.847

N_2O - Nitrous oxide [10024-97-2]

Recommended data: Lindsay et al. [03Lin1]

Technique used: Parallel plate apparatus with time-of-flight mass spectrometer and position sensitive detection of product ions; independently absolute.

Comments: The absolute uncertainties in $\sigma(N_2O^+)$, $\sigma(N_2^+)$, $\sigma(NO^+)$, $\sigma(N^+)$, $\sigma(O^+)$, and σ(total) are ±6%, ±15%, ±10%, ±10%, ±15%, and ±6%, respectively, unless otherwise indicated in the table. The uncertainty in the electron beam energy is ±0.5 eV. Note that a fitting procedure was used to extract $\sigma(N_2^+)$ and $\sigma(NO^+)$, and $\sigma(N^+)$ and $\sigma(O^+)$, and consequently the sum of $\sigma(N_2^+)$ and $\sigma(NO^+)$ is accurate to ±6% as is the sum of $\sigma(N^+)$ and $\sigma(O^+)$. The recommended N_2O^+ cross section agrees well with that of Mark et al. [81Mar1] and the total cross section is in excellent agreement with that of Rapp and Englander-Golden [65Rap2].

Other data reviewed: [96Iga1, 76Ada1]

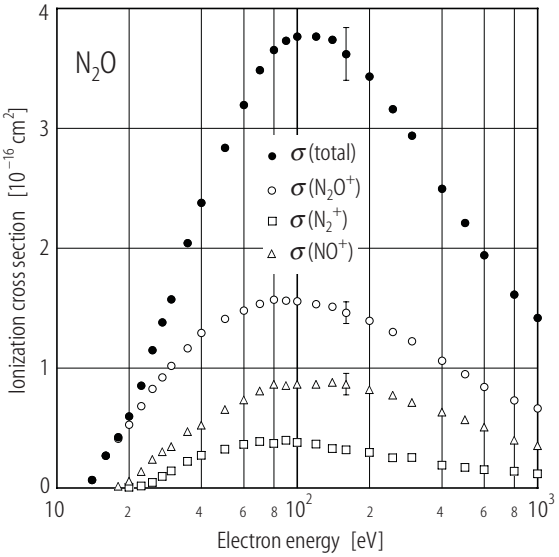

Fig. 5.1.25. N_2O partial and total electron-impact ionization cross sections.

Table 5.1.45. N_2O partial and total electron-impact ionization cross sections.

Energy [eV]	$\sigma(N_2O^+)$ [10^{-16} cm^2]	$\sigma(N_2^+)$ [10^{-17} cm^2]	$\sigma(NO^+)$ [10^{-17} cm^2]	$\sigma(N^+)$ [10^{-17} cm^2]	$\sigma(O^+)$ [10^{-17} cm^2]	σ(total) [10^{-16} cm^2]
14	0.067(8)					0.067(8)
16	0.269(22)					0.269(22)
18	0.411(29)		0.131(26)			0.424(32)
20	0.527	0.066(20)	0.564		0.066(26)	0.597
22.5	0.684	0.17(5)	1.36	0.023(6)	0.163(20)	0.855
25	0.827	0.47(12)	2.37	0.059(6)	0.315(32)	1.15
27.5	0.922	0.97(20)	3.03	0.187(19)	0.407(41)	1.38
30	1.02	1.41	3.44	0.237(24)	0.466(47)	1.57
35	1.17	2.23	4.71	0.958	0.860	2.04
40	1.29	2.72	5.23	1.73	1.15	2.38
50	1.41	3.23	6.54	2.82	1.67	2.84
60	1.48	3.63	7.35	3.75	2.40	3.20
70	1.54	3.87	8.09	4.67	2.85	3.49
80	1.57	3.72	8.64	5.26	3.19	3.65
90	1.56	3.98	8.54	5.96	3.20	3.73
100	1.56	3.79	8.65	6.18	3.47	3.77
120	1.53	3.65	8.65	6.63	3.41	3.77
140	1.51	3.30	8.82	6.57	3.57	3.74
160	1.46	3.18	8.66	6.27	3.47	3.62
200	1.39	2.97	8.19	5.85	3.37	3.43
250	1.30	2.52	7.75	5.25	3.05	3.16
300	1.22	2.53	7.12	4.86	2.65	2.94
400	1.06	1.91	6.34	3.77	2.32	2.50
500	0.950	1.71	5.69	3.20	2.02	2.21
600	0.844	1.52	5.07	2.69	1.71	1.94
800	0.731	1.38	4.00	2.28	1.17	1.61
1000	0.666	1.17	3.53	2.03	0.807	1.42

O_2 - Oxygen [7782-44-7]

Recommended data: Straub et al. [96Str1][34]

Technique used: Parallel plate apparatus with time-of-flight mass spectrometer and position-sensitive detection of product ions; independently absolute.

Comments: The absolute uncertainties in $\sigma(O_2^+)$, $\sigma(O^+ + O_2^{2+})$, $\sigma(O^{2+})$, and σ(total) are ± 5 %, ± 5 %, ± 6 %, and ± 5 % respectively. The uncertainty in the electron energy calibration is ± 1 eV. For the most part, the recommended data set is in agreement with the measurements of Tian and Vidal [98Tia5] and Krishnakumar and Srivastava [92Kri1] to within the combined uncertainties.

Other data reviewed: [75Mar1, 66Sch2, 65Rap1, 65Sch1, 63Asu1, 32Tat1]

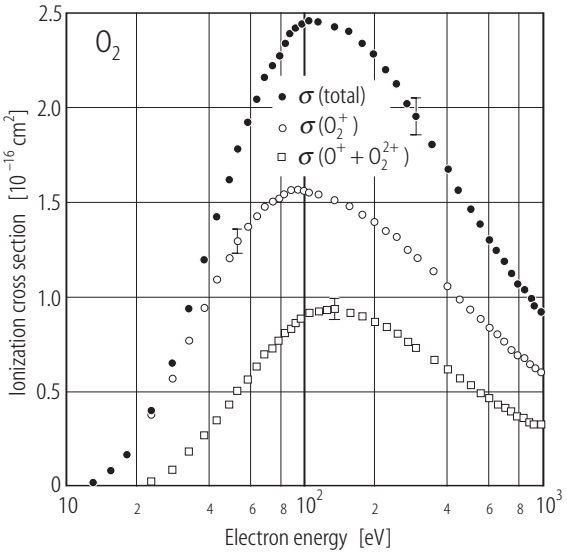

Fig. 5.1.26. O_2 electron-impact ionization cross sections.

[34] The data of Straub et al. [96Str1] reflect a recent recalibration of their apparatus and thus differ slightly from those given in their original paper.

Table 5.1.46. O_2 partial and total electron-impact ionization cross sections.

Energy [eV]	$\sigma(O_2^+)$ [10^{-16} cm^2]	$\sigma(O^+ + O_2^{2+})$ [10^{-17} cm^2]	$\sigma(O^{2+})$ [10^{-18} cm^2]	σ(total) [10^{-16} cm^2]
13	0.0117			0.0117
15.5	0.0730			0.0730
18	0.164			0.164
23	0.366	0.167		0.383
28	0.563	0.781		0.641
33	0.758	1.69		0.927
38	0.929	2.58		1.19
43	1.08	3.33		1.42
48	1.19	4.19		1.61
53	1.29	4.90		1.78
58	1.36	5.53		1.91
63	1.42	6.21		2.04
68	1.47	6.79		2.15
73	1.50	7.17	0.118	2.22
78	1.51	7.51	0.189	2.26
83	1.53	8.01	0.241	2.34
88	1.55	8.27	0.352	2.38
93	1.56	8.55	0.438	2.42
98	1.56	8.71	0.610	2.43
108	1.54	9.00	0.808	2.45
118	1.53	9.10	0.956	2.45
138	1.50	9.13	1.37	2.42
158	1.48	9.05	1.80	2.40
178	1.43	8.91	2.00	2.34
198	1.39	8.64	2.11	2.28
223	1.34	8.30	2.30	2.19
248	1.31	7.94	2.26	2.12
273	1.24	7.55	2.13	2.01
298	1.20	7.21	2.07	1.94
348	1.13	6.59	1.89	1.80
398	1.05	6.11	1.71	1.68
448	0.983	5.62	1.53	1.56
498	0.923	5.26	1.36	1.46
548	0.882	4.87	1.23	1.38
598	0.827	4.57	1.11	1.30
648	0.800	4.32	1.08	1.24
698	0.761	4.15	0.987	1.19
748	0.720	3.88	0.977	1.12
798	0.686	3.69	0.837	1.06
848	0.671	3.55	0.799	1.03
898	0.643	3.36	0.770	0.987
948	0.617	3.26	0.740	0.950
998	0.597	3.17	0.743	0.922

SO_2 - Sulphur dioxide [7446-09-5]

Recommended data: Lindsay et al. [96Lin1][35]

Technique used: Parallel plate apparatus with time-of-flight mass spectrometer and position-sensitive detection of product ions; independently absolute.

Comments: The absolute uncertainties in $\sigma(SO_2^+)$, $\sigma(SO^+)$, $\sigma(S^+ + O_2^+ + SO_2^{2+})$, $\sigma(O^+)$, $\sigma(SO^{2+})$ and σ(total) are ± 5 %, ± 6 %, ± 6 %, ± 6 %, ± 9 % and ± 5 %, respectively. The uncertainty in the electron energy calibration is ± 1 eV. The recommended values of $\sigma(SO_2^+)$ and $\sigma(SO^+)$ agree well with those measured by Basner et al. [95Bas1]. The recommended total cross section agrees well with the data of Basner et al. [95Bas1] and with that of Cadez et al. [83Cad1].

Other data reviewed: [81Smi1, 84Ori1]

Table 5.1.47. SO_2 partial and total electron-impact ionization cross sections.

Energy [eV]	$\sigma(SO_2^+)$ [10^{-16} cm^2]	$\sigma(SO^+)$ [10^{-16} cm^2]	$\sigma(S^+ + O_2^+ + SO_2^{2+})$ [10^{-17} cm^2]	$\sigma(O^+)$ [10^{-17} cm^2]	$\sigma(SO^{2+})$ [10^{-18} cm^2]	σ(total) [10^{-16} cm^2]
15	0.26	0.005				0.26
20	0.78	0.21				0.99
25	1.13	0.71	0.29	0.08		1.88
30	1.40	1.12	1.92	0.20		2.73
35	1.50	1.26	3.95	0.50		3.20
40	1.60	1.35	5.58	1.14	0.03	3.62
50	1.73	1.44	7.19	2.78	0.58	4.18
60	1.83	1.52	8.25	4.23	1.24	4.61
80	1.90	1.55	8.90	6.12	2.03	4.97
100	1.92	1.59	9.09	7.16	2.40	5.16
120	1.89	1.55	8.55	7.37	2.53	5.05
160	1.79	1.45	7.70	7.12	2.30	4.75
200	1.72	1.39	7.10	6.69	2.28	4.51
250	1.58	1.26	6.22	5.92	1.97	4.07
300	1.49	1.19	5.56	5.38	1.74	3.79
400	1.30	1.03	4.54	4.41	1.49	3.24
500	1.14	0.90	3.79	3.67	1.21	2.80
600	1.01	0.79	3.22	3.12	1.05	2.45
800	0.85	0.66	2.59	2.49	0.74	2.02
1000	0.73	0.56	2.18	2.04	0.62	1.72

[35] The data of Lindsay et al. [96Lin1] reflect a recent recalibration of their apparatus and thus differ slightly from those given in their original paper.

O_3 - Ozone [10028-15-6]

Recommended data: Siegel [82Sie1] and Newson et al. [95New1]

Technique used: Siegel [82Sie1]: Quadrupole mass spectrometer; normalized to absolute rare gas cross sections [73Kie1].
Newson et al. [95New1]: Time-of-flight mass spectrometer; data normalized to those of Siegel [82Sie1].

Comments: In the energy range where these two data sets overlap an average cross section value is given. σ (total) has been obtained by summing the partial ionization cross sections. No error estimates are available for the Siegel [82Sie1] data. As Newson et al. [95New1] normalized their data to those of Siegel [82Sie1], neither measurement can adequately be assigned an absolute uncertainty. Recent calculations suggest that these ozone cross sections may be too low [97Kim1, 00Deu1]. The uncertainty in the shape of the cross section appears to be of the order of ± 5-10 %.

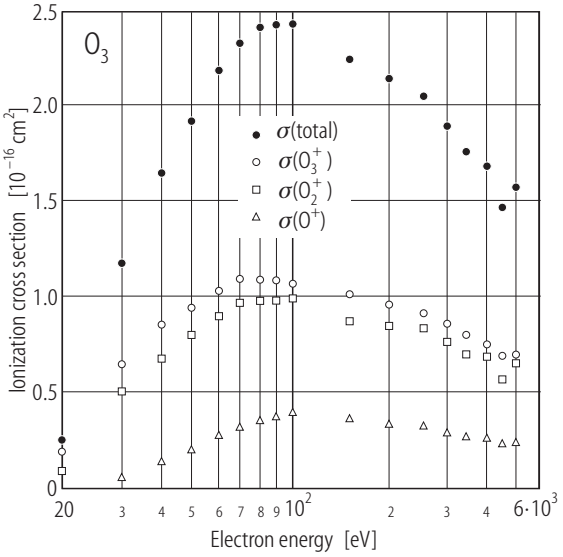

Fig. 5.1.27. O_3 electron-impact ionization cross sections.

Table 5.1.48. O_3 electron-impact ionization cross sections.

Energy [eV]	$\sigma(O_3^+)$ [10^{-16} cm^2]	$\sigma(O_2^+)$ [10^{-17} cm^2]	$\sigma(O^+)$ [10^{-17} cm^2]	σ(total) [10^{-16} cm^2]
20	0.179	0.74	-	0.25
30	0.636	4.88	0.51	1.17
40	0.848	6.75	1.20	1.64
50	0.936	7.92	1.95	1.92
60	1.03	8.98	2.59	2.18
70	1.07	9.60	3.07	2.33
80	1.09	9.80	3.43	2.41
90	1.08	9.79	3.67	2.42
100	1.06	9.92	3.79	2.43
152	1.01	8.66	3.65	2.24
200	0.959	8.44	3.34	2.14
259	0.911	8.27	3.14	2.05
306	0.854	7.61	2.81	1.90
355	0.797	7.00	2.60	1.76
413	0.757	6.79	2.50	1.69
462	0.682	5.65	2.21	1.47
509	0.690	6.49	2.31	1.57

S_2 - Sulfur dimer [23550-45-0]

Recommended data: Freund et al. [90Fre1]
Technique used: A beam of molecules was prepared by charge-transfer neutralization of a mass separated ion beam and then ionized by a well-characterized electron beam.
Comments: The uncertainty in $\sigma(S_2^+)$ is reported as ± 10 %.

Table 5.1.49. $\sigma(S_2^+)$ partial electron-impact ionization cross section.

Energy [eV]	$\sigma(S_2^+)$ [10^{-16} cm^2]	Energy [eV]	$\sigma(S_2^+)$ [10^{-16} cm^2]
7	0.00	55	5.63
8	0.04	60	5.67
9	0.17	65	5.64
10	0.46	70	5.68
11	0.91	75	5.65
12	1.53	80	5.64
13	2.23	85	5.63
14	2.84	90	5.59
15	3.44	95	5.55
16	3.95	100	5.51
17	4.32	105	5.48
18	4.67	110	5.43
19	4.93	115	5.42
20	5.04	120	5.36
21	5.16	125	5.32
22	5.28	130	5.22
23	5.36	135	5.21
24	5.43	140	5.14
25	5.45	145	5.11
26	5.39	150	5.04
27	5.37	155	5.01
28	5.37	160	4.95
29	5.38	165	4.89
30	5.37	170	4.83
32	5.33	175	4.77
34	5.32	180	4.69
36	5.34	185	4.59
38	5.41	190	4.47
40	5.42	195	4.44
45	5.48	200	4.41
50	5.59		

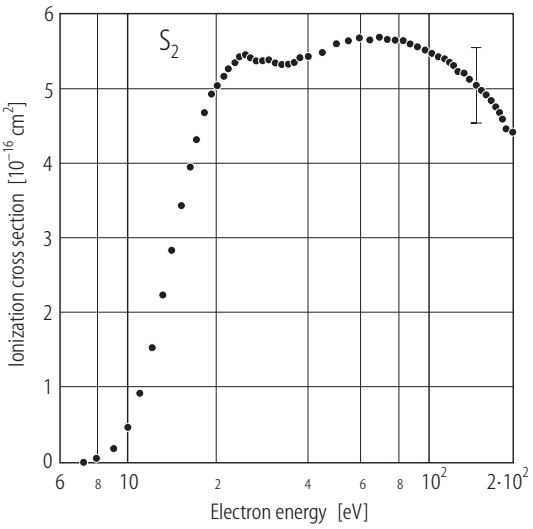

Fig. 5.1.28. $\sigma(S_2^+)$ partial electron-impact ionization cross section.

5.1.5 References for 5.1

24Hug1 Hughes, A.L., Klein, E.: Phys. Rev. **23** (1924) 450
30Smi1 Smith, P.T.: Phys. Rev. **36** (1930) 1293
31Vau1 Vaughan, A.L.: Phys. Rev. **38** (1931) 1687
32Tat1 Tate, J.T., Smith, P.T.: Phys. Rev. **39** (1932) 270
52Cra1 Craggs J.D., McDowell, C.A., Warren, J.W.: Trans. Faraday Soc. **48** (1952) 1093
56Otv1 Otvos, J.W., Stevenson, D.P.: J. Am. Chem. Soc. **78** (1956) 546
57Lam1 Lampe, F.W., Franklin, J.L., Field, F.H.: J. Am. Chem. Soc. **79** (1957) 6129
58Toz1 Tozer, B.A.: J. Electron. Control **4** (1958) 149
60Fro1 Frost D.C., McDowell, C.A.: Can. J. Chem. **38** (1960) 407
61Fox1 Fox, R.E., Curran, R.K.: J. Chem. Phys. **34** (1961) 1595
62Sch1 Schulz, G.J.: Phys. Rev. **128** (1962) 178
63Asu1 Asundi, R.K., Craggs, J.D., Kurepa, M.V.: Proc. Phys. Soc. **82** (1963) 967
63Bib1 Bibby, M.M., Carter, G.: Trans. Faraday Soc. **59** (1963) 2455
63Kur1 Kurepa, M.V. 3rd Czech. Conf. Electron. Vac. Transactions (1963)
65Rap1 Rapp, D., Englander-Golden, P., Briglia, D.: J. Chem. Phys. **42** (1965) 4081
65Rap2 Rapp, D., Englander-Golden, P.: J. Chem. Phys. **43** (1965) 1464
65Sch1 Schram, B.L., De Heer, F.J., Van der Wiel, M.J., Kistemaker, J.: Physica **31** (1965) 94
66Ada1 Adamczyk, B., Boerboom, A.J.H., Schram, B.L., Kistemaker, J.: J. Chem. Phys. **44** (1966) 4640
66Def1 Defrance, A., Gomet, J.C.: Methodes Phys. Anal. **3** (1966) 205
66Kie1 Kieffer, L.J., Dunn, G.H.: Rev. Mod. Phys. **38** (1966) 1
66Mel1 Melton, C.E.: J. Chem. Phys. **45** (1966) 4414
66Sch1 Schram, B.L., van der Wiel, M.J., de Heer, F.J., Moustafa, J.: J. Chem. Phys. **44** (1966) 49
66Sch2 Schram, B.L., Moustafa, H.R., Schutten, J., De Heer, F.J.: Physica **32** (1966) 734
66Sch3 Schutten, J., de Heer, F.J., Moustafa, H.R., Boerboom, A.J.H., Kistemaker, J.: J. Chem. Phys. **44** (1966) 3924
67Gau1 Gaudin, A., Hagemann, R.: J. Chim. Phys. **64** (1967) 1209
67Kie1 Kieffer, L.J.: Bibliography of Low Energy Electron Collision Cross Section Data. (1967) (Nat. Bur. Stand. Miscellaneous Publ. 289)
67Sri1 Srinivasan, V., Rees, J.A.: J. Appl. Phys. **18** (1967) 59
68Fiq1 Fiquet-Fayard, F., Chiari, J., Muller, F., Ziesel, J.: J. Chem. Phys. **48** (1968) 478
69Ber1 Beran, J.A., Kevan, L.: J. Phys. Chem. **73** (1969) 3866
72Ada1 Adamczyk, B., Boerboom, A.J.H., Lukasiewicz, M.: Int. J. Mass Spectrom. Ion Phys. **9** (1972) 407
72Cen1 Center, R.E., Mandl, A.: J. Chem. Phys. **57** (1972) 4104
73Cow1 Cowling, I.R., Fletcher, J.: J. Phys. B: At. Mol. Phys. **6** (1973) 665
73Cro1 Crowe, A., McConkey, J.W.: J. Phys. B: At. Mol. Phys. **6** (1973) 2108
73Hal1 Halas, S., Adamczyk, B.: Int. J. Mass Spectrom. Ion Phys. **10** (1973) 157
73Kie1 Kieffer, L.J.: University of Colorado, Boulder, Colorado; 1973 (JILA Information Center Report; 13)
73Mar1 Märk, T.D.: Acta Physica Austriaca **37** (1973) 381
74Cro1 Crowe, A., McConkey, J.W.: J. Phys. B: At. Mol. Phys. **7** (1974) 349
75Gom1 Gomet, J.C.: C. R. Acad. Sci. Ser. B **281** (1975) 627
75Mar1 Märk, T.D.: J. Chem. Phys. **63** (1975) 3731
75Win1 Winters, H.F.: J. Chem. Phys. **63** (1975) 3462
75Zie1 Ziesel, J.P., Schulz, G.J.: J. Chem. Phys. **62** (1975) 1936
76Ada1 Adamczyk, B., Bederski, K., Wojcik, L., Stanski, T.: Folio Scientatis Scientiarum Lublinensis Mat.-Fiz.-Chem. **18** (1976) 217
76Mar1 Märk, T.D., Egger, F.: Int. J. Mass Spectrom. Ion Phys. **20** (1976) 89
77Com1 Compton, R.N.: J. Chem. Phys. **66** (1977) 4478
77Cro1 Crowe, A., McConkey, J.W.: Int. J. Mass Spectrom. Ion Phys. **24** (1977) 181

77Mar1 Märk, T.D., Egger, F., Cheret, M.: J. Chem. Phys. **67** (1977) 3795
78Hil1 Hille, E., Märk, T.D.: J. Chem. Phys. **69** (1978) 4600
78Kur1 Kurepa, M.V., Belic, D.S.: J. Phys. B: At. Mol. Phys. **11** (1978) 3719
78Mar1 Märk, T.D., Hille, E.: J. Chem. Phys. **69** (1978) 2492
79Pej1 Pejcev, V.M., Kurepa, M.V., Cadez, I.M.: Chem. Phys. Lett. **63** (1979) 301
80Bed1 Bederski, K., Wojcik, L., Adamczyk, B.: Int. J. Mass Spectrom. Ion Phys. **35** (1980) 171
80Ste1 Stephan, K., Helm, H., Kim, Y.B., Seykora, G., Ramler, J., Grössl, M., Märk, E., Märk, T.D.: J. Chem. Phys. **73** (1980) 303
80Ste2 Stephan, K., Helm, H., Märk, T.D.: J. Chem. Phys. **73** (1980) 3763
81Dju1 Djuric, N., Belic, D., Kurepa, M., Mack, J.U., Rothleitner, J., Märk, T.D.: Proceedings of the XII International Conference on the Physics of Electronic and Atomic Collisions; Gatlinburg, Tenn. (1981) 384
81Kim1 Kim, Y.B., Stephan, K., Märk, E., Märk, T.D.: J. Chem. Phys. **74** (1981) 6771
81Kur1 Kurepa, M.V., Babic, D.S., Belic, D.S.: J. Phys. B: At. Mol. Phys. **14** (1981) 375
81Mar1 Märk, E., Märk, T.D., Kim, Y.B., Stephan, K.: J. Chem. Phys. **75** (1981) 4446
81Smi1 Smith, O.I., Stevenson, J.S.: J. Chem. Phys. **74** (1981) 6777
81Ste1 Stevie, F.A., Vasile, M.J.: J. Chem. Phys. **74** (1981) 5106
82Per1 Perrin, J., Schmidt, J.P.M., de Rosny, G., Drevillon, B., Huc, J., Loret, A.: Chem. Phys. **73** (1982) 383
82Sie1 Siegel, M.W.: Int. J. Mass Spectrom. Ion Phys. **44** (1982) 19
83Bel1 Bell, K.L., Gilbody, H.B., Hughes, J.G., Kingston, A.E., Smith, F.J.: J. Chem. Phys. Ref. Data **12** (1983) 891
83Cad1 Cadez, I.M., Pejcev, V.M., Kurepa, M.V.: J. Phys. D **16** (1983) 305
83Sta1 Stanski, T., Adamczyk, B.: Int. J. Mass Spectrom. Ion Phys. **46** (1983) 31
84Cha1 Chatham, H., Hils, D., Robertson, R., Gallagher, A.: J. Chem. Phys. **81** (1984) 1770
84Lei1 Leiter, K., Stephan, K., Märk, E., Märk, T.D.: Plasma Chemistry and Plasma Processing **4** (1984) 235
84Ori1 Orient, O.J., Srivastava, S.K.: J. Chem. Phys. **80** (1984) 140
85Bel1 Belic, D.S., Kurepa, M.V.: Fizika **17** (1985) 117
85deH1 de Heer, F.J., Inokuti, M., in: Electron Impact Ionization (Märk, T.D., Dunn, G. H., eds.), Wien New York: Springer (1985)
85Mar1 Märk, T.D., in: Electron Impact Ionization (Märk, T.D., Dunn, G. H., eds.), Wien New York: Springer (1985)
85Ste1 Stephan, K., Deutsch, H., Märk, T.D.: J. Chem. Phys. **83** (1985) 5712
86Bol1 Bolorizadeh, M.A., Rudd, M.E.: Phys. Rev. A **33** (1986) 882
87Ori1 Orient, O.J., Srivastava, S.K.: J. Phys. B: At. Mol. Phys. **20** (1987) 3923
87Pol1 Poll, H.U., Meichsner, J.: Contrib. Plasma Phys. **27** (1987) 359
87Wet1 Wetzel, R.C., Baiocchi, F.A., Hayes, T.R., Freund, R.S.: Phys. Rev. A **35** (1987) 559
88Dju1 Djuric, N., Lj., Cadez, I.M., Kurepa, M.V.: Int. J. Mass Spectrom. Ion Processes **83** (1988) R7
88Shu1 Shul, R.J., Hayes, T.R., Wetzel, R.C., Baiocchi, F.A., Freund, R.S.: J. Chem. Phys. **89** (1988) 4042
88Sya1 Syage, J.A.: Chem. Phys. Lett. **143** (1988) 19
89Cha1 Chantry, P.J., Chen, C.L.: J. Chem. Phys. **90** (1989) 2585
89Dur1 Duric, N., Cadez, I., Kurepa, M.: Fizika **21** (1989) 339
89Lei1 Leiter, K., Scheier, P., Walder, G., Märk, T.D.: Int. J. Mass Spectrom. Ion Processes **87** (1989) 209
90Fre1 Freund, R.S., Wetzel, R.C., Schul, R.J.: Phys. Rev. A **41** (1990) 5861
90Haa1 Haaland, P.: Chem. Phys. Lett. **170** (1990) 146
90Kri1 Krishnakumar, E., Srivastava, S.K.: J. Phys. B: At. Mol. Opt. Phys. **23** (1990) 1893
90Kri2 Krishnakumar, E.: Int. J. Mass Spectrom. Ion Processes **97** (1990) 283
90Mar1 Margreiter, D., Walder, G., Deutsch, H., Poll, H.U., Winkler, C., Stephan, K., Märk, T.D.: Int. J. Mass Spectrom. Ion Processes **100** (1990) 143

90Mar2 Margreiter, D., Deutsch H., Schmidt, M., Märk, T.D.: Int. J. Mass Spectrom. Ion Processes **100** (1990) 157
91Dur1 Duric, N., Cadez, I., Kurepa, M.: Int. J. Mass Spectrom. Ion Processes **108** (1991) R1-R10
91Ma1 Ma, C., Bruce, M.R., Bonham, R.A.: Phys. Rev. A **44** (1991) 2921
91Rao1 Rao, M.V.V.S., Srivastava, S.K.: J. Geophys. Res. **96** (1991) 17563
92Bab1 Baba, M.S., Narasimhan, T.S.L., Balasubramanian, R., Mathews, C.K.: Int. J. Mass Spectrom. Ion Processes **114** (1992) R1-R8
92Bru1 Bruce, M.R., Ma, C., Bonham, R.A.: Chem. Phys. Lett. **190** (1992) 285
92Kri1 Krishnakumar, E., Srivastava, S.K.: Int. J. Mass Spectrom. Ion Processes **113** (1992) 1
92Ma1 Ma, C., Bruce, M.R., Bonham, R.A.: Phys. Rev. A **45** (1992) 6932
92Mor1 Morgan, W.L.: Plasma Chem. Plasma Proc. **12** (1992) 449
92Pol1 Poll, H.U., Winkler, C., Margreiter, D., Grill, V., Märk, T.D.: Int. J. Mass Spectrom. Ion Processes **112** (1992) 1
92Rao1 Rao, M.V.V.S., Srivastava, S.K.: J. Phys. B: At. Mol. Opt. Phys. **25** (1992) 2175
93Bru1 Bruce, M.R., Bonham, R.A.: Int. J. Mass Spectrom. Ion Processes **123** (1993) 97
93Gri1 Grill, V., Walder, G., Scheier, P., Kurdel, M., Märk, T.D.: Int. J. Mass Spectrom. Ion Processes **129** (1993) 31
93Rao1 Rao, M.V.V.S., Srivastava, S.K.: J. Geophys. Res. **98** (1993) 13137
93Smi1 Smith, D., Spanel, P., Märk, T.D.: Chem. Phys. Lett. **213** (1993) 202
93Tar1 Tarnovsky, V., Becker, K.: J. Chem. Phys. **98** (1993) 7868
94Bon1 Bonham, R.A.: Jpn. J. Appl. Phys. Part I **33** (1994) 4157
94Bru1 Bruce, M.R., Mi, L., Sporleder, C.R., Bonham, R.A.: J. Phys. B: At. Mol. Opt. Phys. **27** (1994) 5773
94Kri1 Krishnakumar, E., Srivastava, S.K.: J. Phys. B: At. Mol. Opt. Phys. **27** (1994) L251
94Nis1 Nishimura, H., Tawara, H.: J. Phys. B: At. Mol. Opt. Phys. **27** (1994) 2063
94Tar1 Tarnovsky, V., Levin, A., Becker, K., Basner, R., Schmidt, M.: Int. J. Mass Spectrom. Ion Processes **133** (1994) 175
95Bas1 Basner, R., Schmidt, M., Deutsch, H., Tarnovsky, V., Levin, A., Becker, K.: J. Chem. Phys. **103** (1995) 211
95Bru1 Bruce, M.R., Bonham, R.A.: J. Mol. Struct. **352/353** (1995) 235
95Dun1 Dünser, B., Lezius, M., Scheier, P., Deutsch, H., Märk, T.D.: Phys. Rev. Lett. **74** (1995) 3364
95Kri1 Krishnakumar, E., Srivastava, S.K.: Contrib. Plasma Phys. **35** (1995) 395
95Mat1 Matejcik, S., Märk, T.D., Spanel, P., Smith, D., Jaffke, T., Illenberger, E.: J. Chem. Phys. **102** (1995) 2516
95New1 Newson, K.A., Luc, S.M., Price, S.D., Mason, N.J.: Int. J. Mass Spectrom. Ion Processes **148** (1995) 203
95Rao1 Rao, M.V.V.S., Iga, I., Srivastava, S.K.: J. Geophys. Res. **100** (1995) 26421
95Str1 Straub, H.C., Renault, P., Lindsay, B.G., Smith, K.A., Stebbings, R.F.: Phys. Rev. A **52** (1995) 1115
95Vos1 Vostrikov, A.A., Dubov, D.Y., Agarkov, A.A.: Tech. Phys. Lett. **21** (1995) 715
96Chr1 Christophorou, L.G., Olthoff, J.K., Rao, M.V.V.S.: J. Phys. Chem. Ref. Data **25** (1996) 1341
96Hwa1 Hwang, W., Kim, Y.-K., Rudd, M.E.: J. Chem. Phys. **104** (1996) 2956
96Iga1 Iga, I., Rao, M.V.V.S., Srivastava, S.K.: J. Geophys. Res. **101** (1996) 9261
96Lin1 Lindsay, B.G., Straub, H.C., Smith, K.A., Stebbings, R.F.: J. Geophys. Res. **101** (1996) 21151
96Mat1 Matt, S., Dünser, B., Lezius, M., Deutsch, H., Becker, K., Stamatovic, A., Scheier, P., Märk, T.D.: J. Chem. Phys. **105** (1996) 1880
96Rao1 Rao, M.V.V.S., Srivastava, S.K.: J. Phys. B: At. Mol. Opt. Phys. **29** (1996) 1841
96Sri1 Srivastava, S.K., Krishnakumar, E., Fucalora, A.F., van Note, T.: J. Geophys. Res. **101** (1996) 26155
96Str1 Straub, H.C., Renault, P., Lindsay, B.G., Smith, K.A., Stebbings, R.F.: Phys. Rev. A **54** (1996) 2146

96Str2 Straub, H.C., Lindsay, B.G., Smith, K.A., Stebbings, R.F.: J. Chem. Phys. **105** (1996) 4015
96Tar1 Tarnovsky, V., Levin, A., Deutsch, H., Becker, K.: J. Phys. B: At. Mol. Opt. Phys. **29** (1996) 139
96Zec1 Zecca, A., Karwasz, G.P., Brusa, R.S.: Riv. Nuovo Cimento **19** N. 3 (1996) 1
96Zhe1 Zheng, S.-H., Srivastava, S.K.: J. Phys. B: At. Mol. Opt. Phys. **29** (1996) 3235
97Ali1 Ali, M.A., Kim, Y.-K., Hwang, W., Weinberger, N.M., Rudd, M.E.: J. Chem. Phys. **106** (1997) 9602
97Bas1 Basner, R., Schmidt, M., Tarnovsky, V., Becker, K., Deutsch, H.: Int. J. Mass Spectrom. Ion Processes **171** (1997) 83
97Chr1 Christophorou, L.G., Olthoff, J.K., Wang, Y.: J. Phys. Chem. Ref. Data **26** (1997) 1205
97Kim1 Kim, Y.-K., Hwang, W., Weinberger, N.M., Ali, M.A., Rudd, M.E.: J. Chem. Phys. **106** (1997) 1026
97Rao1 Rao, M.V.V.S., Srivastava, S.K.: Proceedings of the Twentieth International Conference on the Physics of Electronic and Atomic Collisions; Vienna, Austria (1997) MO150
97Rao2 Rao, M.V.V.S., Srivastava, S.K.: Proceedings of the Twentieth International Conference on the Physics of Electronic and Atomic Collisions; Vienna, Austria (1997) MO151
97Sri1 Srivastava, S.K., Boivin, R.: Bull. Am. Phys. Soc. **42** (1997) 1738
97Sri2 Srivastava, S.K.: Unpublished, quoted in [97Kim1] (1997)
97Str1 Straub, H.C., Lin, D., Lindsay, B.G., Smith, K.A., Stebbings, R.F.: J. Chem. Phys. **106** (1997) 4430
97Tar1 Tarnovsky, V., Deutsch H., Becker, K.: Int. J. Mass Spectrom. Ion Processes **167/168** (1997) 69
97Tia1 Tian, C., Vidal, C.R.: Chem. Phys. **222** (1997) 105
97Val1 Vallance, C., Harris, S.A., Hudson, J.E., Harland, P.W.: J. Phys. B: At. Mol. Opt. Phys. **30** (1997) 2465
98Chr1 Christophorou, L.G., Olthoff, J.K.: J. Phys. Chem. Ref. Data **27** (1998) 1
98Chr2 Christophorou, L.G., Olthoff, J.K.: J. Phys. Chem. Ref. Data **27** (1998) 889
98Fol1 Foltin, V., Foltin, M., Matt, S., Scheier, P., Becker, K., Deutsch, H., Märk, T.D.: Chem. Phys. Lett. **289** (1998) 181
98Har1 Harland, P.W., Vallance, C., in: Advances in Gas-Phase Ion Chemistry (Adams, N.G., Babcock, L.M., eds.), Greenwich Connecticut: JAI Press (1998)
98Str1 Straub, H.C., Lindsay, B.G., Smith, K.A., Stebbings, R.F.: J. Chem. Phys. **108** (1998) 109
98Tar1 Tarnovsky, V., Kurunczi, P., Matt, S., Märk, T.D., Deutsch, H., Becker, K.: J. Phys. B: At. Mol. Opt. Phys. **31** (1998) 3043
98Tar2 Tarnovsky, V., Deutsch, H., Becker, K.: J. Chem. Phys. **109** (1998) 932
98Tia1 Tian, C., Vidal, C.R.: J. Phys. B: At. Mol. Opt. Phys. **31** (1998) 895
98Tia2 Tian, C., Vidal, C.R.: J. Chem. Phys. **108** (1998) 927
98Tia3 Tian, C., Vidal, C.R.: J. Chem. Phys. **109** (1998) 1704
98Tia4 Tian, C., Vidal, C.R.: Chem. Phys. Lett. **288** (1998) 499
98Tia5 Tian, C., Vidal, C.R.: J. Phys. B: At. Mol. Opt. Phys. **31** (1998) 5369
99Chr1 Christophorou, L.G., Olthoff, J.K.: J. Phys. Chem. Ref. Data **28** (1999) 131
99Chr2 Christophorou, L.G., Olthoff, J.K.: J. Phys. Chem. Ref. Data **28** (1999) 967
99Ito1 Itoh, A., Tsuchida, H., Miyabe, K., Majima, T., Imanishi, N.: J. Phys. B: At. Mol. Opt. Phys. **32** (1999) 277
99Jia1 Jiao, C.Q., Garscadden, A., Haaland, P.D.: Chem. Phys. Lett. **310** (1999) 52
99Lim1 Limão, Vieira P., Lobo, R.F.M.: Vacuum **52** (1999) 19
99Mat1 Matt, S., Scheier, P., Stamatovic, A., Deutsch, H., Becker, K., Märk, T.D.: Philos. Trans. R. Soc. London Ser. A **357** (1999) 1201
99Nis1 Nishimura, N., Huo, W.M., Ali, M.A., Kim, Y.-K.: J. Chem. Phys. **110** (1999) 3811
99Tia1 Tian, C., Vidal, C.R.: Phys. Rev. A **59** (1999) 1955
00Cal1 Calandra, P., O'Connor, C.S.S., Price, S.D.: J. Chem. Phys. **112** (2000) 10821
00Chr1 Christophorou, L.G., Olthoff, J.K.: J. Phys. Chem. Ref. Data **29** (2000) 267
00Deu1 Deutsch, H., Becker, K., Matt, S., Märk, T.D.: Int. J. Mass Spectrom. **197** (2000) 37

00Lin1 Lindsay, B.G., Mangan, M.A., Straub, H.C., Stebbings, R.F.: J. Chem. Phys. **112** (2000) 9404

00Man1 Mangan, M.A., Lindsay, B.G., Stebbings, R.F.: J. Phys. B: At. Mol. Opt. Phys. **33** (2000) 3225

01Haa1 Haaland, P.D., Jiao, C.Q., Garscadden, A.: Chem. Phys. Lett. **340** (2001) 479

01Hud1 Hudson, J.E., Vallance, C., Bart, M., Harland, P.W.: J. Phys. B: At. Mol. Opt. Phys. **34** (2001) 3025

01Kar1 Karwasz, G.P., Brusa, R.S., Zecca, A.: Riv. Nuovo Cimento **24** N. 1 (2001) 1

01Kar2 Karwasz, G.P., Brusa, R.S., Zecca, A.: Riv. Nuovo Cimento **24** N. 4 (2001) 1

01Lin1 Lindsay, B.G., Rejoub, R., Stebbings, R.F.: J. Chem. Phys. **114** (2001) 10225

01Luk1 Luki´c, D., Josifov, G., Kurepa, M.V.: Int. J. Mass Spectrom. **205** (2001) 1

01Rej1 Rejoub, R., Sieglaff, D.R., Lindsay, B.G., Stebbings, R.F.: J. Phys. B: At. Mol. Opt. Phys. **34** (2001) 1289

01Rej2 Rejoub, R., Lindsay, B.G., Stebbings, R.F.: J. Chem. Phys. **115** (2001) 5053

01Sie1 Sieglaff, D.R., Rejoub, R., Lindsay, B.G., Stebbings, R.F.: J. Phys. B: At. Mol. Opt. Phys. **34** (2001) 799

01Ste1 Stebbings, R.F., Lindsay, B.G.: J. Chem. Phys. **114** (2001) 4741

01Tor1 Torres, I., Martínez, R., Sánchez Rayo, M.N., Castaño, F.: J. Chem. Phys. **115** (2001) 4041

02Rej1 Rejoub, R., Lindsay, B.G., Stebbings, R.F.: Phys. Rev. A **65** (2002) 042713

02Rej2 Rejoub, R., Lindsay, B.G., Stebbings, R.F.: J. Chem. Phys. **117** (2002) 6450

03Lin1 Lindsay, B.G., Rejoub, R., Stebbings, R.F.: J. Chem. Phys. **118** (2003) 5894

03Rej1 Rejoub, R., Morton, C. D., Lindsay, B.G., Stebbings, R.F.: J. Chem. Phys. **118** (2003) 1756

5.2 Electron attachment

5.2.1 Introduction

When an electron collides with an atom or a molecule, it can often be attached to the atom or the molecule to form a negative ion. This process, called an electron attachment, has two roles of practical importance. First, it is the most effective way to produce negative ions. Negative ions play an important role in nature or laboratory. Since the attached electron can be readily detached, for instance, negative ions are used to produce a fast beam of neutral particles. Another feature of the electron attachment is to remove free electrons in a plasma. This enhances the breakdown voltage of the gas and hence the ability of insulation.

Compared to the atomic target, molecules are easier to capture electrons. An electron attachment to a molecule takes place mainly through

$$e + AB \rightarrow AB^- + \gamma \qquad \text{(radiative attachment)} \qquad (1)$$

or

$$e + AB \rightarrow A + B^- \qquad \text{(dissociative attachment)} \qquad (2)$$

Usually the radiative process (1) is very slow and can be ignored in the case of molecular target. The dissociative attachment (DA) is mediated mostly by the resonance state $AB^{-}**$. In other words, the process occurs mostly through a temporary capture of the incident electron to the metastable negative ion state of the target molecule. Thus the process is sensitive to molecular property and the cross section varies widely depending on the collision energy. In this sense, it is in contrast with the positive ion formation of the molecule, in which cross sections have almost the same energy dependence for all the molecules. If the state $AB^{-}**$ has a long lifetime (say, > 10 μs), the negative ion of the target molecule can be detected

$$e + AB \rightarrow AB^{-}** \qquad (3)$$

When the gas density is high, a 3-body reaction

$$e + AB + M \rightarrow AB^- + M \qquad \text{(3-body attachment)} \qquad (4)$$

may also be possible. In the laboratory experiment, the third body M can be a wall of the apparatus. Since reliable data are scarcely known for the 3-body reaction, the present chapter concentrates on the two-body processes, (2) and (3). For the 3-body attachment, a review article by Aleksandrov [88Ale1] contains useful information.

Because of its importance in various fields, electron attachment has been reviewed several times [75Cal1, 84Chr1, 85Ele1, 98Ill1]. They show many graphs of attachment cross section, but mostly for the purpose of discussion. No comprehensive compilation of the attachment cross section has been published.

Methods of measurement of the attachment cross section are divided into two categories: swarm method and beam method. In the swarm method, transport of electrons in a gas is investigated under an applied electric field. Attachment coefficient is measured as a function of the intensity of the electric field and the gas density. The coefficient is a kind of an average of the attachment cross section over the electron energy distribution. (The review papers mentioned above provide detailed information about the thermal attachment coefficient.) The cross section is unfolded from the attachment coefficient with the electron energy distribution function (EEDF). The latter quantity (EEDF) is derived by solving the Boltzmann equation to reproduce the measured values of the electron transport parameters, such as drift velocity. In this method an absolute value of the cross section is determined automatically. Sometimes, however, the deconvolution procedure to obtain the cross section has a large ambiguity. When two or more negative ions are produced upon dissociation, the branching ratio of them cannot be determined in the swarm method.

The principle behind the beam method is simple and essentially the same as in the case of positive ion production. An energy selected electron beam is passed through a target gas and the resulting negative

ions are collected with a certain detector. Here it is very important to accomplish a complete collection of the product ion. If the ion is mass-analyzed before detection, the branching ratio of the product ions is obtained. Several different methods are used for the mass separation: sector type magnet, time-of-flight (TOF) method, quadrupole mass filter. To obtain the correct value of the branching ratio, care should be taken not to discriminate different ions. This is essential, because different product ion has different kinetic energy. Generally speaking it is difficult to obtain an absolute cross section with the use of beam measurement. In many cases, the detection efficiency is determined from the positive ion production. In some cases, a normalization is made through a comparison to the cross section for a well-known process (so called relative-flow method). In certain molecules, attachment cross section increases with decreasing electron energy toward zero. In those cases, some special technique is necessary to prepare an electron beam with very slow velocity. The most successful method is to use photoelectrons produced upon photoionization of atoms at very near threshold. This and other methods for low energy experiments are reviewed by Chutjian et al [96Chu1].

For the present task of data compilation, literature has been surveyed through the end of 2001. Evaluation of the data has been made on the basis of the method to obtain those data. In many cases, two or more papers report cross sections for the same molecule. Normally the most recent data set is selected as recommended values, because usually it pays more attention to the experimental details to reduce inherent uncertainties. In many cases, different results agree with each other within the combined uncertainties. For some fundamental molecules, only very old data are available. However, when they have been scrutinized and found reliable in the review articles mentioned above, those data are recommended here.

Finally , there is one important point which users of the attachment cross section should have in their mind. The process of electron attachment is very much dependent on the internal state of the target molecule. That is, an attachment cross section for a molecule in its (say, vibrationally) excited state is very much different from (in most case, larger than) the cross section for the molecule in the ground state. Thus the cross section depends on the gaseous temperature. This subject has been discussed by many authors [84Chr1, 87Chr1, 01Chr2]. In the present chapter, data are collected from the measurement at room temperature.

Acknowledgements

During the work of the present data compilation, many colleagues have assisted the present author. Special thanks are due to Drs. H. Hotop, M.-W. Ruf, E. Krishnakumar, who kindly provided the numerical values of their cross section data. The digitization of the figures in the original literature has been made mostly by Mr. A. Tanogashira, to whom the author is grateful.

5.2.2 Attachment cross sections for individual molecule

H_2

Recommended data

Cross sections for the energy range 3 - 5 eV are from [01Dre1] and those for the higher energy region (7.7 - 18 eV) are from [65Rap2].

Comments

Rapp et al. [65Rap2] used the method of total ionization measurement. The electron energy spread was 0.3 eV. The absolute value of the cross section was obtained by a comparison with known total cross sections for positive ions. Drexel et al. [01Dre1] measured the attachment cross section using a high-resolution electron beam. They detected H^- with a quadrupole mass spectrometer. The absolute cross section was obtained by normalizing their ion current at 14 eV to the corresponding cross section obtained by Rapp et al. [65Rap2] at the energy. Due to the high energy-resolution (0.1 eV), the present cross section has a sharper peak with a larger maximum than that reported by Schulz and Asundi [67Sch1], which has been used as a standard for long time. The present cross sections are favorably compared with recent elaborate calculations (see [01Dre1]). It is well known that the dissociative attachment of H_2 is very sensitive to the internal excitation of the molecule. The dissociative attachment cross section is enhanced enormously as the gas temperature is increased (e.g., [78All1]).

Table 5.2.1. Production of H^- from H_2.

Energy [eV]	Cross section [10^{-16}cm^2]	Energy [eV]	Cross section [10^{-16}cm^2]	Energy [eV]	Cross section [10^{-16}cm^2]
3.56	9.7E–7	9.99	0.000122	13.8	0.000195
3.63	1.9E–6	10.2	0.000123	13.9	0.000198
3.69	8.09E–6	10.4	0.000123	13.9	0.000195
3.75	1.8E–05	10.6	0.00012	14.0	0.000189
3.76	2.07E–05	10.8	0.000116	14.1	0.000172
3.81	1.94E–5	11.0	0.000112	14.2	0.000155
3.88	1.29E–5	11.2	0.000108	14.3	0.000139
3.94	8.38E–06	11.4	0.000102	14.4	0.000126
4.0	6.21E–06	11.6	9.29E–05	14.5	0.000112
4.06	3.88E–06	11.8	8.27E–05	14.6	0.000102
4.13	2.8E–06	12.1	6.8E–05	14.7	9.33E–05
4.25	2.0E–06	12.4	5.57E–05	14.8	8.88E–05
4.375	9.7E–07	12.6	5.17E–05	15.9	8.31E–05
		12.9	5.01E–05	15.2	8.03E–05
7.67	1.94E–05	13.2	5.56E–05	15.4	7.89E–05
7.84	2.64E–05	13.2	6.92E–05	15.5	7.85E–05
8.08	3.76E–05	13.3	9.03E–05	15.6	7.86E–05
8.3	4.9E–05	13.5	0.000119	15.9	7.97E–05
8.59	6.51E–05	13.5	0.000132	16.4	8.29E–05
8.87	8.15E–05	13.5	0.000148	16.9	8.7E–05
9.17	9.74E–05	13.7	0.00017	17.4	9.41E–05
9.48	0.00011	13.7	0.00018	18.0	0.0001
9.78	0.000119	13.8	0.000189		

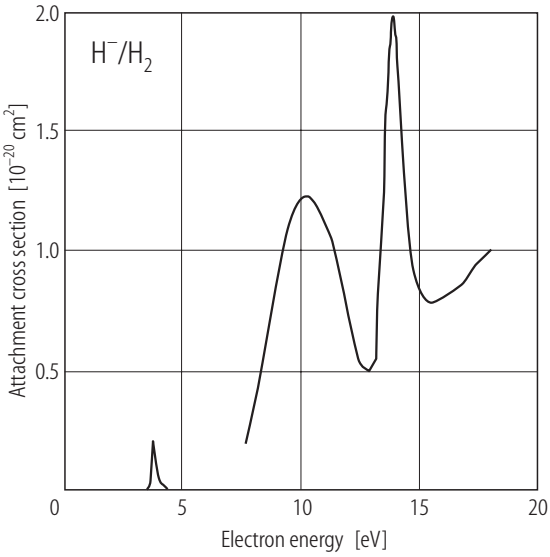

Fig. 5.2.1. Attachment cross section for the production of H^- from H_2.

O_2

Recommended data: [65Rap1]

Comments

Rapp and Briglia [65Rap1] used the method of total ionization measurement, which is essentially the same as that used for the positive ion measurement by the same group. Particular emphasis was placed on total collection of the product ions. Absolute values were obtained by a comparison with the positive ion cross section. With the use of a swarm-beam method, Christophorou et al. [65Chr1] measured the same cross sections, which are in agreement with the values of Rapp and Briglia. Spence and Schulz [69Spe1] found that the dissociative attachment cross section of O_2 greatly increases with increasing the gaseous temperature.

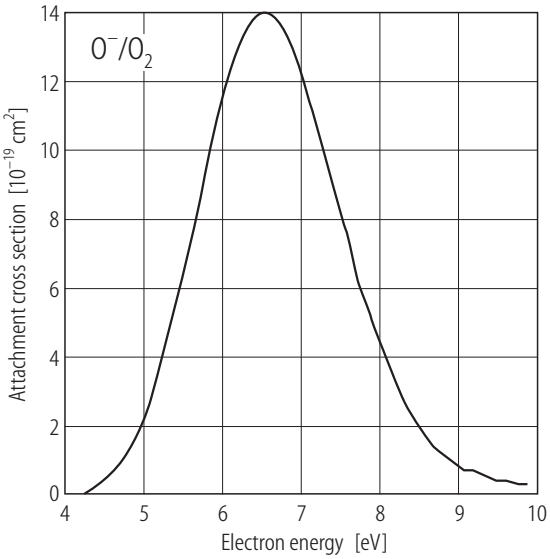

Fig. 5.2.2. Attachment cross section for the production of O^- from O_2.

Table 5.2.2. Production of O^- from O_2.

Energy [eV]	Cross section [10^{-16}cm^2]	Energy [eV]	Cross section [10^{-16}cm^2]	Energy [eV]	Cross section [10^{-16}cm^2]
4.2	0	6.1	0.0123	8.0	0.00449
4.3	8.80E–05	6.2	0.0131	8.1	0.00387
4.4	0.000264	6.3	0.0136	8.2	0.00334
4.5	0.000440	6.4	0.0131	8.3	0.00282
4.6	0.000704	6.5	0.0141	8.4	0.00238
4.7	0.000968	6.6	0.0140	8.5	0.00202
4.8	0.00132	6.7	0.0137	8.6	0.00167
4.9	0.00176	6.8	0.0134	8.7	0.00141
5.0	0.00220	6.9	0.0128	8.8	0.00123
5.1	0.00290	7.0	0.0122	8.9	0.00106
5.2	0.00361	7.1	0.0114	9.0	0.000880
5.3	0.00449	7.2	0.0106	9.1	0.000704
5.4	0.00537	7.3	0.00985	9.2	0.000704
5.5	0.00633	7.4	0.00897	9.3	0.000616
5.6	0.00748	7.5	0.00818	9.4	0.000528
5.7	0.00853	7.6	0.00739	9.5	0.000440
5.8	0.00959	7.7	0.00642	9.6	0.000440
5.9	0.0105	7.8	0.00572	9.8	0.000352
6.0	0.0114	7.9	0.00501	9.9	0.000352

F_2

Recommended data: [87Chu1]

Comments

Chutjian and Alajajian [87Chu1] obtained the cross section with the Kr-photoionization method. A mixture of Kr and F_2 was photoionized by narrow-band photons from a He–Hopfield lamp and 1 m VUV monochromator. The energy resolution of the resulting electrons (i.e., photoelectrons from Kr) was 6 meV. The energy dependence of the ion signal was analyzed assuming an analytic form of the attachment cross section. Absolute values were determined by comparing with the thermal rate of attachment measured by a swarm technique. It is not clear if the cross section has a peak at zero energy (see the discussion in [96Chu1]). The statistical error of the cross section is reported to be 25 %.

Table 5.2.3. Production of F^- from F_2.

Energy [eV]	Cross section [10^{-16}cm^2]	Energy [eV]	Cross section [10^{-16}cm^2]
0.001	176.7	0.02	22.62
0.002	120.5	0.03	19.17
0.003	88.75	0.04	16.24
0.005	51.21	0.05	13.77
0.006	40.90	0.06	11.67
0.008	30.65	0.07	9.885
0.01	27.24	0.08	8.377
0.015	24.57		

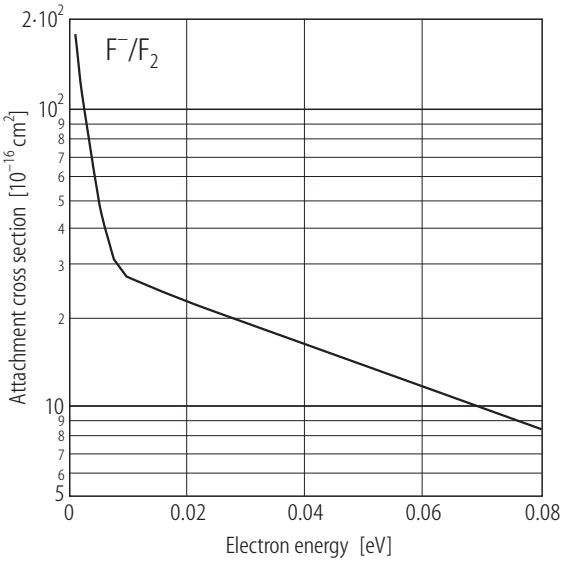

Fig. 5.2.3. Attachment cross section for the production of F^- from F_2.

Cl_2

Recommended data: [99Chr1]

Comments

Christophorou and Olthoff [99Chr1] compiled cross section data for various processes in electron collisions with Cl_2. Their recommended data on the attachment cross section are based on the beam-type measurement of Kurepa and Belic [78Kur1]. To be consistent with the thermal rate coefficients measured, the original cross section of [78Kur1] was increased by 30 % by Christophorou and Olthoff. Here the result of [99Chr1] is presented as the recommended values.

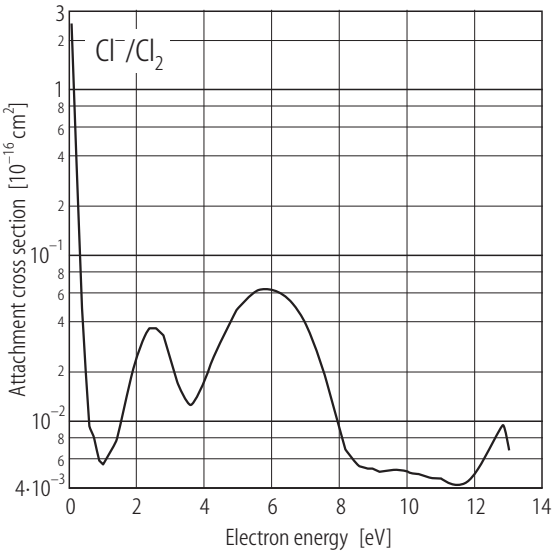

Fig. 5.2.4. Attachment cross section for the production of Cl^- from Cl_2.

Table 5.2.4. Production of Cl^- from Cl_2.

Energy [eV]	Cross section [$10^{-16}cm^2$]	Energy [eV]	Cross section [$10^{-16}cm^2$]	Energy [eV]	Cross section [$10^{-16}cm^2$]
0	2.621	3.8	0.01365	8.6	0.00533
0.1	1.04	4.0	0.01677	8.8	0.005135
0.2	0.3185	4.2	0.02197	9.0	0.005135
0.3	0.0806	4.4	0.02717	9.2	0.00494
0.4	0.026	4.6	0.03341	9.4	0.005018
0.5	0.01274	4.8	0.04004	9.6	0.005096
0.6	0.00884	5.0	0.04719	9.8	0.00507
0.7	0.00819	5.2	0.05304	10.0	0.00494
0.8	0.0065	5.4	0.05798	10.2	0.004836
0.9	0.00572	5.6	0.06162	10.4	0.004745
1.0	0.00546	5.8	0.06292	10.6	0.004615
1.2	0.00624	6.0	0.06214	10.8	0.004524
1.4	0.00767	6.2	0.06006	11.0	0.004472
1.6	0.01092	6.4	0.05694	11.2	0.004225
1.8	0.01716	6.6	0.05187	11.4	0.004108
2.0	0.02353	6.8	0.04615	11.6	0.004134
2.2	0.03146	7.0	0.03913	11.8	0.004264
2.4	0.03601	7.2	0.03003	12.0	0.004745
2.6	0.03627	7.4	0.02314	12.2	0.00572
2.8	0.03237	7.6	0.01794	12.4	0.00689
3.0	0.02496	7.8	0.013	12.6	0.008125
3.2	0.01768	8.0	0.009087	12.8	0.00936
3.4	0.01378	8.2	0.00663	13.0	0.00663
3.6	0.01235	8.4	0.00585		

CO

Recommended data

[65Rap1] for O^- production. For C^-, see the comments below.

Comments

The method of [65Rap1] is described in the comments for O_2. Considering the dissociation mechanism, Stamatovic and Schulz [70Sta1] suggested a vertical onset of the cross section at 9.65 eV. Because of a rather wide energy-resolution of the electron beam used, the experiment of [65Rap1] does not show the feature. Stamatovic and Schulz [70Sta1] detected also C^- ions. The cross section for the C^- production has two peaks at 10.4 and 10.9 eV and its maximum value is $(6 \pm 1.5) \cdot 10^{-23}$ cm^2 at the first 10.4 eV peak.

Table 5.2.5. Production of O^- from CO.

Energy [eV]	Cross section [$10^{-16}cm^2$]	Energy [eV]	Cross section [$10^{-16}cm^2$]	Energy [eV]	Cross section [$10^{-16}cm^2$]
9.2	8.80E–05	10.2	0.00190	11.6	0.000325
9.3	0.000185	10.3	0.00179	11.7	0.000282
9.35	0.000264	10.4	0.00170	11.8	0.000238
9.4	0.000343	10.5	0.00155	11.9	0.000194
9.45	0.000730	10.6	0.00138	12.0	0.000167
9.6	0.00113	10.7	0.00124	12.1	0.000141
9.65	0.00169	10.8	0.00112	12.2	0.000114
9.7	0.00183	10.9	0.00100	12.3	9.68E–05
9.75	0.00193	11.0	0.000880	12.4	8.80E–05
9.8	0.00199	11.1	0.000765	12.5	7.92E–05
9.85	0.00200	11.2	0.000651	12.6	7.04E–05
9.9	0.00202	11.3	0.000554	12.8	6.16E–05
10.0	0.00201	11.4	0.000466	13.0	6.16E–05
10.1	0.00198	11.5	0.000396		

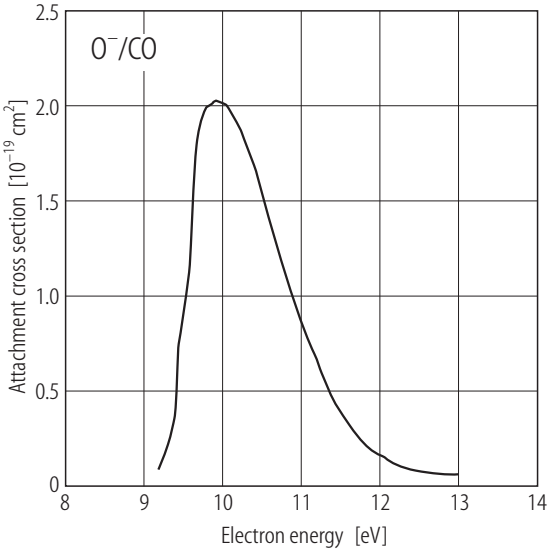

Fig. 5.2.5. Attachment cross section for the production of O^- from CO.

NO

Recommended data

[65Rap1] for O^- production.

Comments

See the comments for O_2 for the method of [65Rap1].

Table 5.2.6. Production of O^- from NO.

Energy [eV]	Cross section [10^{-16}cm^2]	Energy [eV]	Cross section [10^{-16}cm^2]	Energy [eV]	Cross section [10^{-16}cm^2]
6.5	0	8.2	0.01116	9.9	0.00440
6.6	0	8.3	0.01109	10.0	0.00378
6.7	8.80E–05	8.4	0.01100	10.1	0.00317
6.8	0.000176	8.5	0.01103	10.2	0.00264
6.9	0.000440	8.6	0.01106	10.3	0.00220
7.0	0.000792	8.7	0.01100	10.4	0.00176
7.1	0.00150	8.8	0.01088	10.5	0.00141
7.2	0.00334	8.9	0.01069	10.6	0.00114
7.3	0.00537	9.0	0.0104	10.7	0.000924
7.4	0.00713	9.1	0.0100	10.8	0.000792
7.5	0.00862	9.2	0.00950	10.9	0.000704
7.6	0.00959	9.3	0.00888	11.0	0.000616
7.7	0.0104	9.4	0.00827	11.5	0.000440
7.8	0.01076	9.5	0.00748	12.0	0.000440
7.9	0.01103	9.6	0.00651	12.5	0.000352
8.0	0.01115	9.7	0.00581	13.0	0.000352
8.1	0.01117	9.8	0.00510		

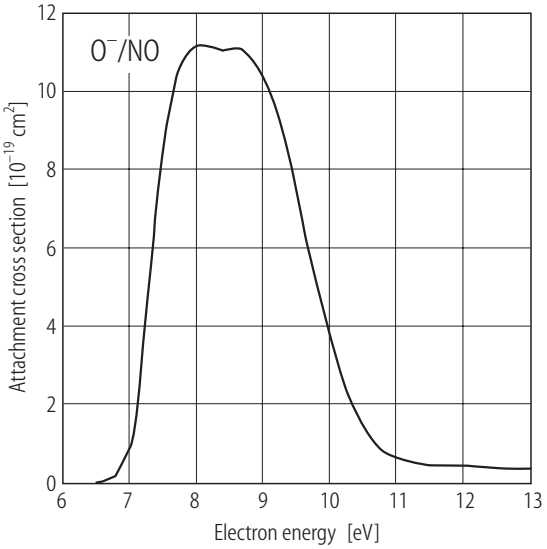

Fig. 5.2.6. Attachment cross section for the production of O^- from NO

HCl

Recommended data

[88Pet1] for Cl^- and [85Ori1] for H^-.

Comments

Petrovic et al. [88Pet1] obtained their cross sections with a swarm method. They used a mixture of HCl with Ar or N_2 for the measurement. The mixing ratio of HCl to Ar or N_2 was taken so small that the electron energy distribution was determined mainly by the electron collision with Ar or N_2 , for which reliable cross section data are available. Since the experiment was done at low energies of electrons, the product negative ion was ensured to be only Cl^-. Orient and Srivastava [85Ori1] employed a crossed beam method with mass analysis by a quadrupole filter and obtained cross sections both for Cl^- and for H^-. The absolute value was determined by a relative flow technique. Their cross section for Cl^- is, however, by almost a factor of two larger than the corresponding result of [88Pet1]. Hence the present H^- cross section may have a large uncertainty. The Cl^- formation is known to be much dependent on the gaseous temperature [81All1].

Table 5.2.7. Production of Cl^- from HCl.

Energy [eV]	Cross section [$10^{-16}cm^2$]
0.63	0.0024
0.678	0.004
0.70	0.008
0.715	0.0141
0.747	0.0296
0.772	0.0496
0.80	0.0707
0.8212	0.0892
0.854	0.113
0.877	0.124
0.891	0.127
0.90	0.127
0.914	0.125
0.9263	0.119
0.9463	0.1128
0.9679	0.103
1.0	0.097
1.042	0.0848
1.0972	0.074
1.1403	0.0672
1.2	0.056
1.244	0.045
1.3	0.033
1.35	0.028
1.4	0.023
1.5	0.018
1.7	0.0116
1.9	0.0048

Table 5.2.8. Production of H^- from HCl.

Energy [eV]	Cross section [$10^{-16}cm^2$]
5.0	0.00045
5.5	0.0027
6.0	0.00844
6.5	0.0168
7.0	0.0205
7.08	0.02067
7.5	0.0169
8.0	0.0116
8.5	0.0096
9.0	0.009
9.5	0.007
10.0	0.00462
10.5	0.00276
11.0	0.00124
11.5	0.0004
12.0	7E–05

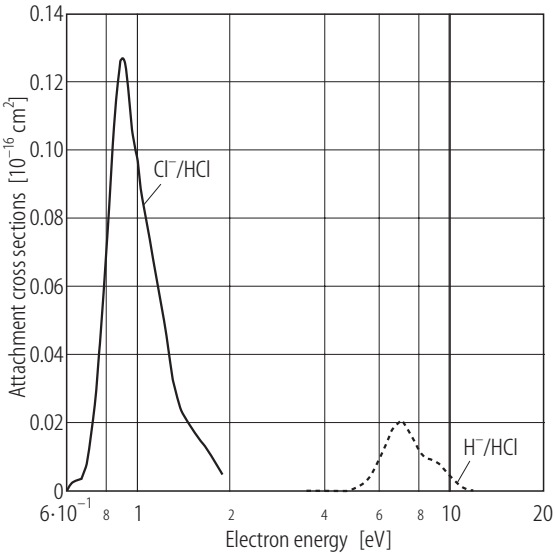

Fig. 5.2.7. Attachment cross sections for the productions of Cl^- and H^- from HCl.

HBr

Recommended data

[68Chr1] for Br^- production.

Comments

Christophorou et al. [68Chr1] obtained their cross section with the swarm-beam method (see, for details, [65Chr1]). Christophorou [84Chr1] reported qualitative information about the production of H^- from HBr.

Table 5.2.9. Production of Br^- from HBr.

Energy [eV]	Cross section [10^{-16}cm^2]	Energy [eV]	Cross section [10^{-16}cm^2]	Energy [eV]	Cross section [10^{-16}cm^2]
0.0791	0.0241	0.197	1.82	0.348	2.23
0.0976	0.129	0.204	2.01	0.367	1.96
0.114	0.246	0.215	2.19	0.393	1.71
0.135	0.363	0.227	2.36	0.427	1.36
0.15	0.468	0.244	2.53	0.464	1.04
0.158	0.579	0.261	2.63	0.515	0.698
0.166	0.749	0.278	2.69	0.578	0.459
0.172	0.909	0.293	2.71	0.624	0.408
0.175	1.05	0.306	2.68	0.668	0.355
0.181	1.29	0.316	2.61	0.696	0.324
0.189	1.55	0.326	2.49	0.715	0.297

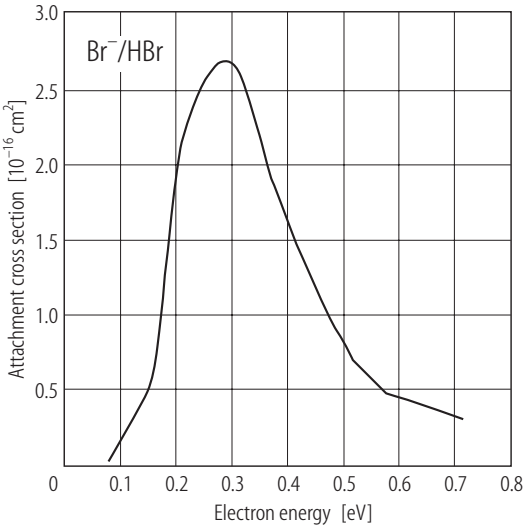

Fig. 5.2.8. Attachment cross section for the production of Br^- from HBr.

HI

Recommended data

Cross sections for the production of I^- at electron energies below 0.173 eV are from [01Kla2] and those for higher energies are from [97Hor1] (the numerical values of the latter being cited from [01Kla2]).

Comments

Klar et al. [01Kla2] measured the attachment cross section using the laser-photoionization technique (see the comments for CCl_4) at the electron energies 0.0008 - 0.173 eV. It is the very low energy and very high resolution measurement. Horáček et al. [97Hor1] applied the non-local resonance theory to obtain the attachment cross section. In so doing, they determined the adjustable parameters in their formula by a least-squares fit to the experimental data of Klar et al. at the energies 0.01 - 0.173 eV. Klar et al. combined their own measured cross sections with the theoretical ones of Horáček et al. to determine their recommended cross section. This recommended value is adopted here. It should be noted that the resulting cross section shows cusps at the threshold of vibrational excitation of the molecule.

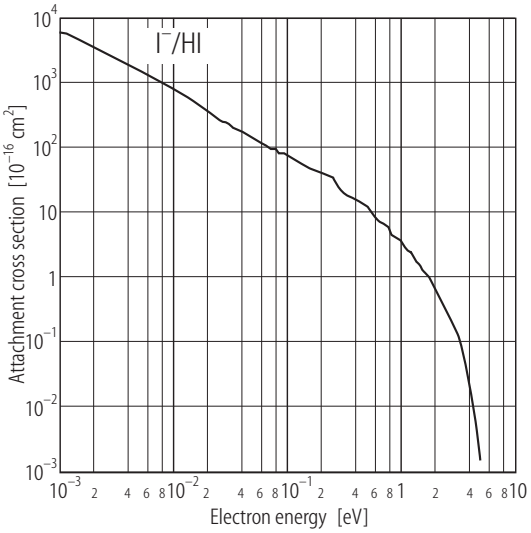

Fig. 5.2.9. Attachment cross section for the production of I^- from HI.

Table 5.2.10. Production of I^- from HI.

Energy [eV]	Cross section [10^{-16}cm^2]	Energy [eV]	Cross section [10^{-16}cm^2]	Energy [eV]	Cross section [10^{-16}cm^2]
0.0010	5940	0.22	39.25	1.18	2.494
0.0012	5192	0.24	36.43	1.20	2.450
0.0014	4446	0.26	33.62	1.22	2.415
0.0016	4100	0.28	26.59	1.24	2.398
0.0018	3709	0.30	22.68	1.26	2.178
0.0020	3446	0.32	20.37	1.28	2.066
0.0025	2822	0.34	18.69	1.30	1.983
0.0030	2439	0.36	17.37	1.32	1.916
0.0035	2131	0.38	16.29	1.34	1.859
0.0040	1831	0.40	15.39	1.36	1.810
0.0045	1659	0.42	14.63	1.38	1.768
0.0050	1501	0.44	13.97	1.40	1.732
0.0055	1404	0.46	13.41	1.42	1.701
0.0060	1282	0.48	12.92	1.44	1.677
0.0065	1171	0.50	12.49	1.46	1.589
0.0070	1096	0.52	12.14	1.48	1.506
0.0075	1016	0.54	11.06	1.50	1.450
0.0080	977.4	0.56	9.961	1.52	1.405
0.0085	908.7	0.58	9.251	1.54	1.367
0.0090	849.6	0.60	8.692	1.56	1.334
0.0095	814.6	0.62	8.227	1.58	1.305
0.0100	755.9	0.64	7.828	1.60	1.279
0.0120	627.4	0.66	7.479	1.62	1.257
0.0140	534.3	0.68	7.171	1.64	1.237
0.0160	460.4	0.70	6.896	1.66	1.163
0.0180	409.6	0.72	6.648	1.68	1.112
0.0200	362.2	0.74	6.422	1.70	1.075
0.0250	280.4	0.76	6.214	1.72	1.045
0.0300	239.6	0.78	5.969	1.74	1.020
0.0350	193.8	0.80	5.257	1.76	0.9983
0.0400	174.8	0.82	4.933	1.78	0.9790
0.0450	158.4	0.84	4.696	1.80	0.9620
0.0500	140.0	0.86	4.505	1.82	0.9471
0.0550	126.8	0.88	4.345	1.84	0.9020
0.0600	116.7	0.90	4.209	1.86	0.8593
0.0650	109.2	0.92	4.090	1.88	0.8304
0.0700	102.6	0.94	3.986	1.90	0.8072
0.0750	95.20	0.96	3.894	1.92	0.7875
0.0800	94.60	0.98	3.812	1.94	0.7705
0.0851	80.30	1.00	3.741	1.96	0.7557
0.0900	78.72	1.02	3.634	1.98	0.7427
0.0950	79.83	1.04	3.210	2.0	0.7322
0.100	74.47	1.06	3.023	2.5	0.3452
0.120	62.00	1.08	2.886	3.0	0.1870
0.140	55.63	1.10	2.777	3.5	0.0844
0.160	48.12	1.12	2.687	4.0	0.0273
0.180	45.80	1.14	2.612	4.5	0.0071
0.20	42.31	1.16	2.548	5.0	0.0015

H_2O

Recommended data

[72Mel1] for H^-, O^-, OH^- productions.

Comments

Melton [72Mel1] obtained his attachment cross sections using mass spectrometric method with a 90° sector magnet. The absolute values were determined by a comparison with positive ion (Ar^+) production. The result is almost in good agreement with the earlier measurement by Compton and Christophorou [67Com1], though the latter authors could not detect OH^-.

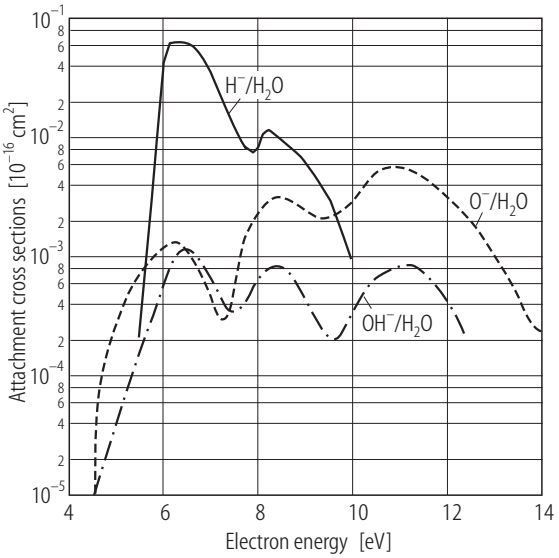

Fig. 5.2.10. Attachment cross sections for the productions of H^-, O^-, OH^- from H_2O.

Table 5.2.11. Production of H^- from H_2O.

Energy [eV]	Cross section [10^{-16}cm^2]	Energy [eV]	Cross section [10^{-16}cm^2]	Energy [eV]	Cross section [10^{-16}cm^2]
5.5	0.0002	6.65	0.0579	8.14	0.0109
5.74	0.0016	6.81	0.0489	8.235	0.01166
5.9	0.00985	7.0	0.0356	8.395	0.0104
6.01	0.043	7.465	0.0129	8.79	0.0076
6.165	0.0622	7.69	0.00877	9.01	0.0062
6.286	0.06317	7.89	0.0074	9.57	0.0028
6.4	0.0637	8.0	0.0079	9.8	0.0017
6.52	0.0625	8.09	0.00995	10.0	0.00098

Table 5.2.12. Production of O^- from H_2O.

Energy [eV]	Cross section [10^{-16}cm^2]	Energy [eV]	Cross section [10^{-16}cm^2]	Energy [eV]	Cross section [10^{-16}cm^2]
4.43	0	7.56	0.00062	10.138	0.00337
4.59	4.4E–05	7.7	0.00133	10.46	0.00493
4.71	0.00011	8.0	0.0023	10.66	0.0055
5.0	0.00025	8.21	0.00286	10.8	0.0057
5.29	0.0005	8.35	0.0031	10.9	0.00576
5.72	0.000913	8.44	0.00316	11.0	0.00576
6.0	0.00116	8.6	0.0031	11.18	0.00553
6.19	0.00128	8.76	0.00285	11.5	0.00466
6.32	0.00133	9.0	0.00244	12.0	0.00327
6.45	0.00122	9.22	0.00213	12.5	0.002
6.64	0.001	9.4	0.00208	13.0	0.00108
7.0	0.000485	9.56	0.00214	13.28	0.000688
7.186	0.000313	9.67	0.00226	13.625	0.00038
7.3	0.000287	9.89	0.00256	13.8	0.000264
7.43	0.00036	10.0	0.00285	14.0	0.00023

Table 5.2.13. Production of OH^- from H_2O.

Energy [eV]	Cross section [10^{-16}cm^2]	Energy [eV]	Cross section [10^{-16}cm^2]	Energy [eV]	Cross section [10^{-16}cm^2]
4.3	0	7.02	0.0006235	9.49	0.000201
4.51	9E–06	7.15	0.000489	9.57	0.000194
4.75	1.87E–05	7.32	0.000376	9.654	0.000202
5.0	4E–05	7.413	0.000356	9.78	0.000229
5.21	6.6E–05	7.49	0.000345	10.01	0.000358
5.39	0.000109	7.6	0.00036	10.26	0.00053
5.56	0.000165	7.73	0.000417	10.52	0.0006686
5.69	0.000246	7.83	0.00048	10.825	0.000775
5.836	0.000379	8.02	0.00067	11.0	0.0008235
6.0	0.000537	8.19	0.00078	11.13	0.000847
6.1	0.000757	8.31	0.00082	11.3	0.00083
6.27	0.001048	8.385	0.00083	11.45	0.000795
6.36	0.00114	8.53	0.00081	11.6	0.000699
6.437	0.00116	8.64	0.000756	11.87	0.0004818
6.536	0.001154	8.85	0.00057	12.0	0.000402
6.626	0.001105	9.0	0.000436	12.19	0.000311
6.77	0.00095	9.23	0.000304	12.47	0.000184
6.874	0.000763	9.36	0.000244		

H_2S

Recommended data

[72Azr1] for the total attachment cross section and [93Rao1] for SH^- and S^- productions.

Comments

Azria et al. [72Azr1] measured the total attachment cross sections using the total ionization method. They suggested that the first peak at 2.2 eV is essentially SH^-, the second one at 5.35 eV and the third one at around 8 eV are H^-, and the fourth one at around 10 eV is S^-. In 1993, Rao and Srivastava [93Rao1] made a mass spectrometric measurement with a quadrupole mass filter. They obtained the cross sections for the production of SH^- and S^-. They determined the absolute values with the use of relative flow technique. Their result confirmed the previous suggestion by Azria et al. Rao and Srivastava, however, could not detect H^-, because of the poor mass resolution of their method. The difference between the cross section of [72Azr1] and the sum of the cross sections of [93Rao1], therefore, can be attributed to the contribution of H^-.

Table 5.2.14. Production of S^- from H_2S.

Energy [eV]	Cross section [10^{-16}cm^2]	Energy [eV]	Cross section [10^{-16}cm^2]	Energy [eV]	Cross section [10^{-16}cm^2]
0	3E–05	5.0	0.00011	9.5	0.0048
1.0	3E–05	5.5	0.00023	9.6	0.00485
1.5	0.0001	5.83	0.000312	10.0	0.00392
2.0	0.000298	6.5	0.0002	10.5	0.00178
2.25	0.00034	7.2	0.00011	11.0	0.00072
2.5	0.00032	8.0	0.0002	11.5	0.0003
3.0	0.00025	8.5	0.00116	12.0	8.7E–05
4.0	9E–05	9.0	0.00297	13.0	2E–05

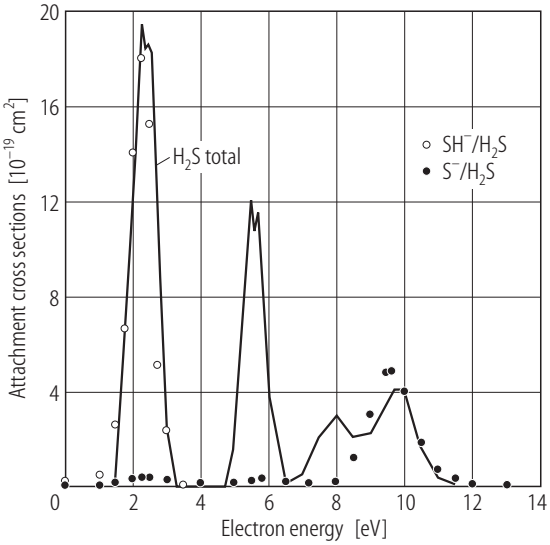

Fig. 5.2.11. Partial and total attachment cross sections of H_2S.

Table 5.2.15. Production of SH^- from H_2S.

Energy [eV]	Cross section [10^{-16}cm^2]
0	0.0002
1.0	0.00046
1.5	0.00257
1.75	0.00657
2.0	0.014
2.25	0.018
2.5	0.0152
2.75	0.00506
3.0	0.0023
3.5	0

Table 5.2.16. Total attachment cross section of H_2S.

Energy [eV]	Cross section [10^{-16}cm^2]	Energy [eV]	Cross section [10^{-16}cm^2]	Energy [eV]	Cross section [10^{-16}cm^2]
2.0	0.012	5.0	0.0015	8.5	0.002
2.25	0.0194	5.5	0.012	9.0	0.0022
2.35	0.0183	5.6	0.0106	9.5	0.0035
2.45	0.0186	5.7	0.0115	9.7	0.004
2.55	0.0181	6.0	0.004	10.0	0.004
3.0	0.0024	6.5	0	10.5	0.0015
3.3	0	7.0	0.0005	11.0	0.0004
4.0	0	7.5	0.002	11.5	0
4.75	0	8.0	0.003		

CO_2

Recommended data

[65Rap1] for O^-. For C^-, see the comments below.

Comments

The details of the method of [65Rap1] is described in the comments for O_2. In 1983, Orient and Srivastava [83Ori1] made a mass spectrometric measurement of O^- ions. Their values agree with the present recommended data within their uncertainties of the magnitude (20 %) and the energy scale (0.1 eV). They obtained small peaks of O^- also at 12, 17 and 19 eV. The cross sections at those peaks are of the order of 10^{-20}-10^{-21} cm^2. Spence and Schulz [74Spe1] measured the cross section for the C^- production. The cross section has a finite value at the electron energies 14 - 21 eV, but its maximum is as small as $2 \cdot 10^{-21}$ cm^2. Spence and Schulz [69Spe1] reported the temperature dependence of the attachment cross section of CO_2.

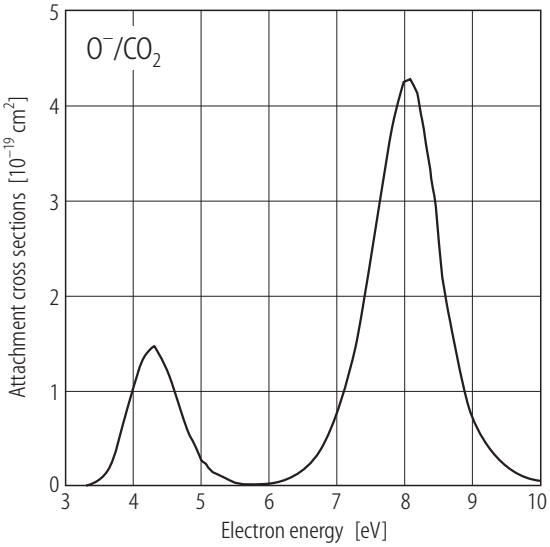

Fig. 5.2.12. Attachment cross section for the production of O^- from CO_2.

Table 5.2.17. Production of O^- from CO_2.

Energy [eV]	Cross section [10^{-16}cm^2]	Energy [eV]	Cross section [10^{-16}cm^2]	Energy [eV]	Cross section [10^{-16}cm^2]
3.3	0	5.6	1.76E–05	7.9	0.00396
3.4	1.76E–05	5.7	8.80E–06	8.0	0.00424
3.5	6.16E–05	5.8	0	8.1	0.00428
3.6	0.000141	5.9	8.80E–06	8.2	0.00413
3.7	0.000273	6.0	1.76E–05	8.3	0.00380
3.8	0.000528	6.1	2.64E–05	8.4	0.00336
3.9	0.000818	6.2	4.40E–05	8.5	0.00283
4.0	0.00106	6.3	6.16E–05	8.6	0.00215
4.1	0.00128	6.4	0.000106	8.7	0.00172
4.2	0.00141	6.5	0.000141	8.8	0.00136
4.3	0.00148	6.6	0.000202	8.9	0.00102
4.4	0.00136	6.7	0.000290	9.0	0.000783
4.5	0.00121	6.8	0.000387	9.1	0.000616
4.6	0.000976	6.9	0.000528	9.2	0.000484
4.7	0.000774	7.0	0.000686	9.3	0.000369
4.8	0.000598	7.1	0.000897	9.4	0.000290
4.9	0.000440	7.2	0.00114	9.5	0.000229
5.0	0.000282	7.3	0.00145	9.6	0.000176
5.1	0.000194	7.4	0.00178	9.7	0.000132
5.2	0.000132	7.5	0.00216	9.8	0.000106
5.3	9.68E–05	7.6	0.00267	9.9	7.92E–05
5.4	6.16E–05	7.7	0.00312	10.0	6.16E–05
5.5	2.64E–05	7.8	0.00357		

CS_2

Recommended data

[92Kri1] for S^-, CS^-, C^-, S_2^- productions.

Comments

Krishnakumar and Nagesha [92Kri1] obtained their cross sections with the use of a TOF mass spectrometer. The absolute magnitudes were determined with the relative flow technique, where a comparison was made with O^- production from O_2. Uncertainty of the result was 15 %.

Table 5.2.18. Productions of S^- and CS^- from CS_2.

Energy [eV]	Cross section for S^- [10^{-16}cm^2]	Cross section for CS^- [10^{-16}cm^2]
1.0	2E–05	0
1.25	0.00012	0
1.5	0.00014	0
1.75	0.00023	0
2.0	0.00033	0

Table 5.2.18 (continued)

Energy [eV]	Cross section for S^- [$10^{-16}cm^2$]	Cross section for CS^- [$10^{-16}cm^2$]
2.25	0.0004	0
2.5	0.00079	0
2.75	0.00142	2E–06
3.0	0.00256	2E–06
3.25	0.0033	4E–06
3.5	0.00351	1.8E–05
3.75	0.00274	3.1E–05
4.0	0.00223	3.9E–05
4.25	0.00121	4.5E–05
4.5	0.00065	4.9E–05
4.75	0.00042	8.1E–05
5.0	0.0006	0.00013
5.25	0.00084	0.000269
5.5	0.00123	0.000403
5.75	0.00202	0.000574
6.0	0.00221	0.00065
6.25	0.0023	0.00067
6.5	0.00165	0.000492
6.75	0.00126	0.000423
7.0	0.0006	0.000212
7.25	0.00049	8.8E–05
7.5	0.00048	3.9E–05
7.75	0.00049	2.2E–05
8.0	0.00045	1.4E–05
8.25	0.00034	1.2E–05
8.5	0.00023	1.2E–05
8.75	0.00014	1E–05
9.0	0.0001	8E–06
9.25	7E–05	8E–06
9.5	5E–05	6E–06
9.75	5E–05	6E–06
10.0	3E–05	5E–06
10.5	1E–05	6E–06
11.0	1E–05	6E–06
11.5	2E–05	7E–06
12.0	3E–05	4E–06
12.5	5E–05	3E–06
13.0	6E–05	2E–06
13.5	8E–05	2E–06
14.0	0.0001	4E–06
14.5	0.00015	1.6E–05
15.0	0.00022	2.8E–05
15.5	0.00028	4.7E–05
16.0	0.00034	6.1E–05
16.5	0.00037	7.9E–05
17.0	0.00041	0.0001
17.5	0.00048	0.000114
18.0	0.00051	0.00013

Table 5.2.18 (continued)

Energy [eV]	Cross section for S^- [$10^{-16}cm^2$]	Cross section for CS^- [$10^{-16}cm^2$]
18.5	0.00056	0.000138
19.0	0.00059	0.000149
19.5	0.00064	0.000153
20.0	0.00067	0.000157
20.5	0.00072	0.000161
21.0	0.00079	0.000163
21.5	0.00086	0.000165
22.0	0.00093	0.000163
22.5	0.00101	0.000161
23.0	0.00107	0.000159
23.5	0.00114	0.000157
24.0	0.00122	0.000155
24.5	0.00134	0.000153
25.0	0.00137	0.000149
25.5	0.00142	0.000144
26.0	0.00147	0.000142
26.5	0.0015	0.000138
27.0	0.00151	0.000134
27.5	0.00149	0.00013
28.0	0.00147	0.000126
28.5	0.00142	0.000122
29.0	0.0014	0.00012
29.5	0.00137	0.000116
30.0	0.00135	0.000112
30.5	0.00133	0.000108
31.0	0.0013	0.000104
31.5	0.00128	0.0001
32.0	0.00126	9.8E–05
32.5	0.00123	9.2E–05
33.0	0.00124	9E–05
33.5	0.00121	8.8E–05
34.0	0.00117	8.1E–05
34.5	0.00116	7.9E–05
35.0	0.00115	7.7E–05
35.5	0.00114	7.5E–05
36.0	0.00113	6.9E–05
36.5	0.00113	6.9E–05
37.0	0.00113	6.7E–05
37.5	0.00112	6.7E–05
38.0	0.00112	6.5E–05
38.5	0.00112	6.3E–05
39.0	0.00112	6.1E–05
39.5	0.00112	5.9E–05
40.0	0.00112	5.9E–05

Table 5.2.19. Production of C^- from CS_2.

Energy [eV]	Cross section [10^{-16}cm^2]	Energy [eV]	Cross section [10^{-16}cm^2]	Energy [eV]	Cross section [10^{-16}cm^2]
3.0	1E–06	19.0	1.6E–05	35.0	0.000144
3.5	2E–06	19.5	1.7E–05	35.5	0.000143
4.0	5E–06	20.0	1.8E–05	36.0	0.000143
4.5	7E–06	20.5	1.9E–05	36.5	0.000142
5.0	4E–06	21.0	2.1E–05	37.0	0.000142
5.5	9E–06	21.5	2.4E–05	37.5	0.000142
6.0	1.4E–05	22.0	2.9E–05	38.0	0.000142
6.5	2.2E–05	22.5	3.3E–05	38.5	0.000143
7.0	1.5E–05	23.0	3.6E–05	39.0	0.000145
7.5	1.7E–05	23.5	4.2E–05	39.5	0.000146
8.0	1.4E–05	24.0	4.6E–05	40.0	0.000147
8.5	9E–06	24.5	5.8E–05	40.5	0.000149
9.0	5E–06	25.0	6.8E–05	41.0	0.00015
9.5	4E–06	25.5	8.2E–05	41.5	0.000153
10.0	4E–06	26.0	9.1E–05	42.0	0.000155
10.5	4E–06	26.5	0.000102	42.5	0.000158
11.0	5E–06	27.0	0.000114	43.0	0.000162
11.5	5E–06	27.8	0.000123	43.5	0.000164
12.0	6E–06	28.0	0.000129	44.0	0.000167
12.5	8E–06	28.5	0.000137	44.5	0.00017
13.0	9E–06	29.0	0.000141	45.0	0.000172
13.5	8E–06	29.5	0.000144	45.5	0.000174
14.0	6E–06	30.0	0.000153	46.0	0.000176
14.5	6E–06	30.5	0.000157	46.5	0.000177
15.0	7E–06	31.0	0.000156	47.0	0.000179
15.5	8E–06	31.5	0.000154	47.5	0.000179
16.0	9E–06	32.0	0.000152	48.0	0.00018
16.5	1E–05	32.5	0.000151	48.5	0.00018
17.0	1.2E–05	33.0	0.000149	49.0	0.000181
17.5	1.3E–05	33.5	0.000148	49.5	0.000182
18.0	1.4E–05	34.0	0.000147	50.0	0.000182
18.5	1.5E–05	34.5	0.000145		

Table 5.2.20. Production of S_2^- from CS_2.

Energy [eV]	Cross section [10^{-16}cm^2]	Energy [eV]	Cross section [10^{-16}cm^2]	Energy [eV]	Cross section [10^{-16}cm^2]
3.0	4.34E–07	5.0	2.6E–05	7.0	9.7E–05
3.25	1E–06	5.25	4.3E–05	7.25	3.6E–05
3.5	3E–06	5.5	0.000116	7.5	2.6E–05
3.75	4E–06	5.75	0.000161	7.75	2.3E–05
4.0	8E–06	6.0	0.00021	8.0	1.6E–05
4.25	1E–05	6.25	0.000248	8.25	8E–06
4.5	1.2E–05	6.5	0.00023	8.5	4E–06
4.75	1.4E–05	6.75	0.00022	8.75	2E–06

COS

Recommended data: [75Zie1] for S^- production.

Comments

Ziesel et al. [75Zie1] used a mass spectrometric method with a quadrupole mass filter to obtain the energy dependence of the cross section for the S^- production. They employed an electron beam of high energy-resolution (0.06 eV). The absolute magnitude of the cross section was obtained with the total ionization measurement and a comparison to the positive ion production.

Table 5.2.21. Production of S^- from COS.

Energy [eV]	Cross section [10^{-16}cm^2]	Energy [eV]	Cross section [10^{-16}cm^2]	Energy [eV]	Cross section [10^{-16}cm^2]
0.8	0.003	1.2	0.172	1.743	0.1267
0.846	0.0043	1.293	0.2756	1.8	0.1
0.9	0.006	1.347	0.29	1.89	0.067
0.952	0.009	1.4	0.281	1.937	0.0543
1.0	0.0184	1.49	0.2654	2.0	0.042
1.042	0.035	1.524	0.2585	2.2	0.016
1.078	0.049	1.526	0.259	2.4	0.006
1.08	0.05	1.6	0.217		
1.152	0.111	1.644	0.191		

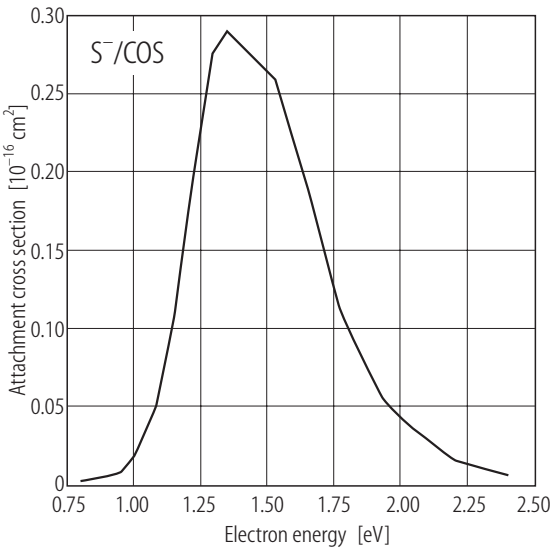

Fig. 5.2.13. Attachment cross section for the production of S^- from COS.

N_2O

Recommended data: [65Rap1] for O^- production.

Comments

The method of [65Rap1] is described in the comments for O_2. Recently Krishnakumar and Srivastava [90Kri1] obtained the O^- cross section using a mass spectrometric method with a quadrupole mass filter.

Their result is in reasonable agreement with the values of [65Rap1], except in the region of energy below 1.5 eV. They claimed that the difference arose from the sensitivity of the process to the gaseous temperature. More recently, Wan et al. [91Wan1] measured the O^- cross section to test their experiment for chlorosilane and chloromerthane. Their result agrees with the values of [65Rap1] within the uncertainty of 15 %. Krishnakumar and Srivastava made their measurement up to 50 eV. They found small peaks at 5.4, 8.1, 13.2, and 35.0 eV, but the magnitude of the peak cross section was by one or two orders of magnitude smaller than the value at the 2.25 eV peak.

Table 5.2.22. Production of O^- from N_2O.

Energy [eV]	Cross section [10^{-16}cm^2]	Energy [eV]	Cross section [10^{-16}cm^2]	Energy [eV]	Cross section [10^{-16}cm^2]
0.4	0.00457	1.8	0.0595	3.2	0.00968
0.5	0.0133	1.9	0.0663	3.3	0.00633
0.6	0.0173	2.0	0.0758	3.4	0.00466
0.7	0.0193	2.1	0.0828	3.5	0.00352
0.8	0.0204	2.2	0.0860	3.6	0.00282
0.9	0.0208	2.3	0.0857	3.7	0.00229
1.0	0.0216	2.4	0.0804	3.8	0.00194
1.1	0.0223	2.5	0.0710	3.9	0.00167
1.2	0.0233	2.6	0.0598	4.0	0.00132
1.3	0.0249	2.7	0.0484	4.1	0.00123
1.4	0.0279	2.8	0.0357	4.2	0.00106
1.5	0.0329	2.9	0.0260	4.3	0.000968
1.6	0.0392	3.0	0.0192	4.5	0.000968
1.7	0.0494	3.1	0.0139	5.0	0.000968

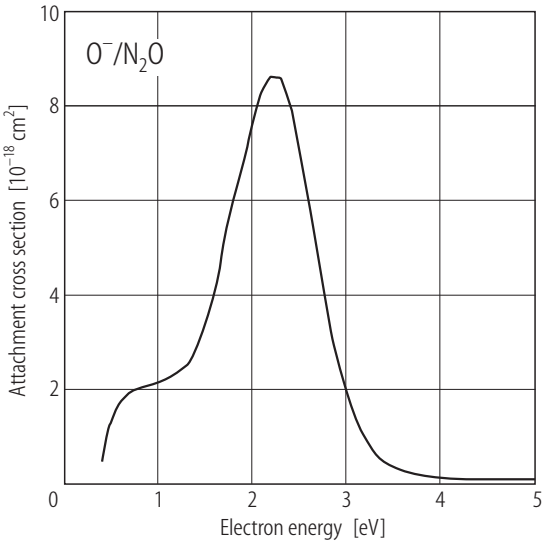

Fig. 5.2.14. Attachment cross section for the production of O^- from N_2O.

SO_2

Recommended data

[97Kri1] for O^-, S^-, SO^- productions.

Comments

There are four independent measurements of the attachment cross sections for each ion product from SO_2 [83Cad1, 83Ori2, 86Spy1, 97Kri1]. The peak positions of the respective cross section almost coincides with each other, but there are rather large disagreement among the absolute magnitudes of the cross sections. Here the most recent data by Krishnakumar et al. [97Kri1] are selected as recommended data. The total attachment cross section of [97Kri1] is in good agreement with the corresponding value of another recent measurement by Wan et al. [93Wan1], who reported only the total cross section. Krishnakumar et al. obtained their cross section with a TOF mass spectrometer. The absolute magnitude of the cross section was determined with a comparison to O^- production from O_2. The authors claimed an uncertainty of 15 %.

Table 5.2.23. Productions of O^-, S^-, SO^- from SO_2 and the total attachment cross section.

Energy [eV]	O^- [10^{-16}cm^2]	S^- [10^{-16}cm^2]	SO^- [10^{-16}cm^2]	total [10^{-16}cm^2]
2.6	0.0002	0	0.0002	0.0004
2.7	0.0004	0.0001	0.0002	0.0007
2.8	0.0009	0.0001	0.0003	0.0014
2.9	0.0007	0.0002	0.0004	0.0013
3.0	0.0011	0.0003	0.0007	0.0021
3.1	0.0014	0.0004	0.0005	0.0023
3.2	0.0023	0.0005	0.0005	0.0033
3.3	0.0043	0.0008	0.0009	0.006
3.4	0.0053	0.001	0.0013	0.0076
3.5	0.0082	0.0012	0.0019	0.0114
3.6	0.0122	0.0016	0.0036	0.0174
3.7	0.0164	0.0018	0.0045	0.0228
3.8	0.0218	0.0021	0.0072	0.0311
3.9	0.0285	0.0024	0.0092	0.0401
4.0	0.0365	0.0026	0.0126	0.0517
4.1	0.04	0.0028	0.0167	0.0595
4.2	0.0503	0.0028	0.0214	0.0745
4.3	0.0553	0.0027	0.026	0.084
4.4	0.0569	0.0027	0.0318	0.0915
4.5	0.0585	0.0024	0.0368	0.0977
4.6	0.059	0.0022	0.0404	0.1016
4.7	0.0566	0.0021	0.043	0.1017
4.8	0.0489	0.0019	0.0416	0.0923
4.9	0.0482	0.0017	0.0404	0.0903
5.0	0.0403	0.0014	0.0348	0.0765
5.1	0.0343	0.0012	0.0309	0.0664
5.2	0.0291	0.001	0.0246	0.0548
5.3	0.0253	0.0009	0.0202	0.0464
5.4	0.0202	0.0008	0.0156	0.0366
5.5	0.0171	0.0006	0.0127	0.0304

Table 5.2.23 (continued)

Energy [eV]	O^- [$10^{-16}cm^2$]	S^- [$10^{-16}cm^2$]	SO^- [$10^{-16}cm^2$]	total [$10^{-16}cm^2$]
5.6	0.0135	0.0005	0.0094	0.0234
5.7	0.0118	0.0004	0.0073	0.0195
5.8	0.0094	0.0004	0.0057	0.0155
5.9	0.0089	0.0003	0.0048	0.0141
6.0	0.0092	0.0003	0.0037	0.0131
6.1	0.0106	0.0003	0.0044	0.0153
6.2	0.0118	0.0003	0.0038	0.0159
6.3	0.0143	0.0003	0.0032	0.0178
6.4	0.0165	0.0004	0.0048	0.0217
6.5	0.0192	0.0004	0.0041	0.0237
6.6	0.0219	0.0005	0.0049	0.0273
6.7	0.0267	0.0005	0.0052	0.0324
6.8	0.0304	0.0005	0.005	0.036
6.9	0.0324	0.0005	0.0048	0.0378
7.0	0.0349	0.0006	0.0052	0.0407
7.1	0.037	0.0006	0.0046	0.0422
7.2	0.0381	0.0007	0.0047	0.0435
7.3	0.0364	0.0007	0.005	0.042
7.4	0.0345	0.0008	0.0051	0.0404
7.5	0.0339	0.0008	0.0047	0.0394
7.6	0.029	0.0007	0.0048	0.0345
7.7	0.0274	0.0007	0.0038	0.032
7.8	0.0226	0.0007	0.0042	0.0275
7.9	0.0184	0.0007	0.003	0.0221
8.0	0.0161	0.0006	0.0029	0.0196
8.1	0.012	0.0006	0.0022	0.0147
8.2	0.0097	0.0005	0.0018	0.012
8.3	0.0083	0.0004	0.0015	0.0102
8.4	0.0065	0.0004	0.0014	0.0083
8.5	0.0055	0.0003	0.0013	0.0071
8.6	0.0049	0.0003	0.0009	0.006
8.7	0.0034	0.0003	0.001	0.0047
8.8	0.0025	0.0003	0.0008	0.0036
8.9	0.002	0.0003	0.0008	0.0031
9.0	0.0016	0.0003	0.0008	0.0028
9.1	0.0009	0.0003	0.0008	0.002
9.2	0.0008	0.0003	0.0007	0.0018
9.3	0.0006	0.0002	0.0006	0.0015
9.4	0.0005	0.0002	0.0007	0.0013
9.5	0.0005	0.0001	0.0008	0.0014
9.6	0.0003	0.0001	0.0005	0.0009
9.7	0.0003	0.0001	0.0006	0.0009
9.8	0.0004	3.09E–05	0.0005	0.0009
9.9	0.0003	6.31E–06	0.0007	0.001
10.0	0.0004	1.4E–06	0.0009	0.0013
10.1	0.0003		0.0007	0.0009
10.2	0.0006		0.0007	0.0012

O_3

Recommended data

[99Ran1] for O^-, O_2^- productions.

Comments

Rangwala et al. [99Ran1] used a TOF method to obtain cross sections for the productions of O^- and O_2^-. Absolute values were determined by a comparison to the O^- production from O_2. They claimed uncertainty of 23 %. Another measurement was done by Senn et al. [99Sen1]. They detected the product ions by a quadrupole mass filter. They employed an electron beam of a very high energy-resolution (5 meV). They found a large but very sharp additional peak of O^- production at zero incident energy. Because of the finite resolution of the electron energy, the height of the peak could not be determined unambiguously. Other part of the cross sections of [99Sen1] is essentially in agreement with the data of [99Ran1], considering the possibility of a loss of fast ions in the experiment of [99Sen1].

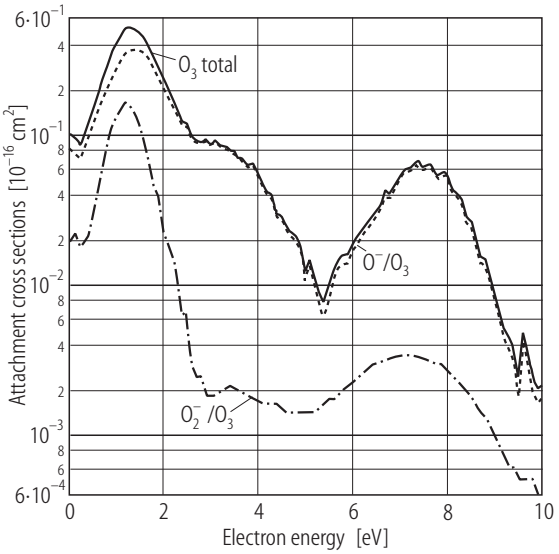

Fig. 5.2.15. Partial and total attachment cross sections of O_3.

Table 5.2.24. Productions of O^-, O_2^- from O_3 and the total attachment cross section.

Energy [eV]	O^- [10^{-16}cm^2]	O_2^- [10^{-16}cm^2]	total [10^{-16}cm^2]
0	0.0806	0.02	0.1006
0.1	0.075	0.0222	0.0972
0.2	0.0692	0.018	0.0872
0.3	0.082	0.02	0.102
0.4	0.1001	0.0216	0.1217
0.5	0.1194	0.0306	0.15
0.6	0.1469	0.0402	0.1871
0.7	0.187	0.0624	0.2494
0.8	0.2087	0.0864	0.2951
0.9	0.2488	0.1188	0.3676
1.0	0.2824	0.1326	0.415

Table 5.2.24 (continued)

Energy [eV]	O^- [$10^{-16}cm^2$]	O_2^- [$10^{-16}cm^2$]	total [$10^{-16}cm^2$]
1.1	0.3158	0.15	0.4658
1.2	0.3621	0.168	0.5301
1.3	0.3703	0.1548	0.5251
1.4	0.3721	0.1416	0.5137
1.5	0.3647	0.1152	0.4799
1.6	0.3467	0.093	0.4397
1.7	0.3129	0.0696	0.3825
1.8	0.2797	0.0468	0.3265
1.9	0.2378	0.0396	0.2774
2.0	0.2111	0.0228	0.2339
2.1	0.1905	0.0186	0.2091
2.2	0.1599	0.0156	0.1755
2.3	0.133	0.012	0.145
2.4	0.1151	0.006	0.1211
2.5	0.1125	0.0069	0.1194
2.6	0.0959	0.003	0.0989
2.7	0.0893	0.0024	0.0917
2.8	0.0863	0.0024	0.0887
2.9	0.0918	0.0018	0.0936
3.0	0.0847	0.0018	0.0865
3.1	0.0894	0.0018	0.0912
3.2	0.0825	0.0019	0.0844
3.3	0.082	0.002	0.084
3.4	0.0785	0.0021	0.0806
3.5	0.0766	0.002	0.0786
3.6	0.0686	0.002	0.0706
3.7	0.0662	0.0019	0.0681
3.8	0.0612	0.0018	0.063
3.9	0.0629	0.0018	0.0647
4.0	0.0553	0.0017	0.057
4.1	0.0462	0.0016	0.0478
4.2	0.04	0.0016	0.0416
4.3	0.0385	0.0016	0.0401
4.4	0.0284	0.0016	0.03
4.5	0.0277	0.0015	0.0292
4.6	0.0234	0.0014	0.0248
4.7	0.021	0.0014	0.0224
4.8	0.02	0.0014	0.0214
4.9	0.0177	0.0014	0.0191
5.0	0.0108	0.0014	0.0122
5.1	0.0131	0.0014	0.0145
5.2	0.0103	0.0014	0.0117
5.3	0.0072	0.0015	0.0087
5.4	0.0059	0.0016	0.0075
5.5	0.0076	0.0017	0.0093
5.6	0.0106	0.0017	0.0123
5.7	0.0127	0.0019	0.0146
5.8	0.0139	0.002	0.0159
5.9	0.0137	0.0021	0.0158

Table 5.2.24 (continued)

Energy [eV]	O^- [$10^{-16}cm^2$]	O_2^- [$10^{-16}cm^2$]	total [$10^{-16}cm^2$]
6.0	0.0167	0.0022	0.0189
6.1	0.0182	0.0024	0.0206
6.2	0.0212	0.0025	0.0237
6.3	0.0231	0.0027	0.0258
6.4	0.0256	0.0028	0.0284
6.5	0.0279	0.003	0.0309
6.6	0.0307	0.0031	0.0338
6.7	0.0392	0.0032	0.0424
6.8	0.0372	0.0032	0.0404
6.9	0.0436	0.0033	0.0469
7.0	0.0498	0.0034	0.0532
7.1	0.0556	0.0034	0.059
7.2	0.0571	0.0034	0.0605
7.3	0.0601	0.0033	0.0634
7.4	0.0631	0.0033	0.0664
7.5	0.0571	0.0032	0.0603
7.6	0.0608	0.0031	0.0639
7.7	0.0586	0.003	0.0616
7.8	0.0503	0.0029	0.0532
7.9	0.0535	0.0029	0.0564
8.0	0.053	0.0026	0.0556
8.1	0.0407	0.0025	0.0432
8.2	0.0389	0.0023	0.0412
8.3	0.0358	0.0022	0.038
8.4	0.0258	0.002	0.0278
8.5	0.0246	0.0018	0.0264
8.6	0.0181	0.0016	0.0197
8.7	0.0137	0.0014	0.0151
8.8	0.0135	0.0013	0.0148
8.9	0.0101	0.0011	0.0112
9.0	0.0079	0.001	0.0089
9.1	0.006	0.0008	0.0068
9.2	0.0043	0.0007	0.005
9.3	0.0038	0.0006	0.0044
9.4	0.0031	0.0006	0.0037
9.5	0.0019	0.0005	0.0024
9.6	0.0042	0.0005	0.0047
9.7	0.0031	0.0005	0.0036
9.8	0.0019	0.0005	0.0024
9.9	0.0016	0.0004	0.002
10.0	0.0017	0.0004	0.0021

NH_3

Recommended data

[69Sha1], but renormalized.

Comments

Sharp and Dowell [69Sha1] obtained their cross section with a beam-gas method and mass-analysis by a magnetic field. They determined absolute cross sections by comparing to the positive-ion cross section, which is by about 30 % too small compared with the recent value [92Rao1]. Here the original cross section of [69Sha1] is renormalized to the recent positive-ion cross section and shown as recommended data. Sharp and Dowell do not show the cross section for the H^- production, but the difference between the two sets of the cross sections shown here is attributed to the H^- production.

Table 5.2.25. Production of NH_2^- from NH_3.

Energy [eV]	Cross section [10^{-16}cm^2]	Energy [eV]	Cross section [10^{-16}cm^2]	Energy [eV]	Cross section [10^{-16}cm^2]
4.0	0	5.68	0.01976	8.5	1.98E–05
4.4	0.000127	5.81	0.01966	9.0	0.000348
4.5	0.000313	5.893	0.01861	9.7	0.000634
4.62	0.000905	6.0	0.01612	10.0	0.000554
4.72	0.00146	6.5	0.00509	10.5	0.000416
5.0	0.00578	6.813	0.00187	11.0	0.000277
5.186	0.01033	7.0	0.000907	11.5	0.000194
5.22	0.01109	7.193	0.000481	12.0	0
5.5	0.01784	7.5	0.000139		
5.593	0.01956	8.0	1.98E–05		

Table 5.2.26. Total attachment cross section for NH_3.

Energy [eV]	Cross section [10^{-16}cm^2]	Energy [eV]	Cross section [10^{-16}cm^2]	Energy [eV]	Cross section [10^{-16}cm^2]
4.5	0.000181	6.38	0.01270	10.714	0.00555
4.61	0.000635	6.5	0.00868	11.0	0.00505
4.77	0.00178	6.7	0.00411	11.255	0.00438
5.0	0.00756	7.0	0.00130	11.5	0.00360
5.25	0.02056	7.2	0.000635	11.76	0.00290
5.5	0.03386	8.0	0	12.0	0.00218
5.55	0.03555	9.0	0.000756	12.25	0.00145
5.59	0.03649	9.28	0.00168	12.5	0.00106
5.68	0.03697	9.5	0.00269	12.737	0.000665
5.76	0.03649	9.752	0.00408	13.0	0.000453
5.86	0.03446	10.0	0.00484	13.5	0.000302
6.0	0.02902	10.268	0.00550		
6.2	0.02056	10.5	0.00568		

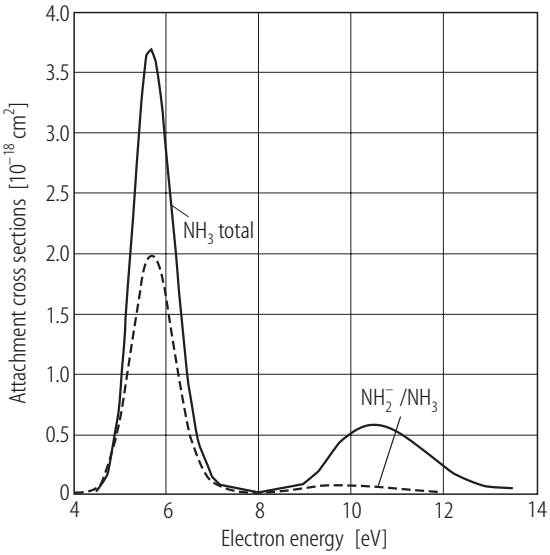

Fig. 5.2.16. Partial and total attachment cross section of NH_3.

CH_4

Recommended data [67Sha1]

Comments

Sharp and Dowell [67Sha1] measured the total attachment cross section using the total ionization method like the one used in [65Rap1]. They normalized their data to the positive ion cross section. The resulting cross section has two peaks. Sharp and Dowell assigned the lower-energy peak as the production of H^- and the higher one as CH_2^-.

Table 5.2.27. Total attachment cross section for CH_4.

Energy [eV]	Cross section [10^{-16}cm^2]	Energy [eV]	Cross section [10^{-16}cm^2]
6.0	0	10.0	0.000952
7.0	0	10.08	0.00096
7.5	1.8E–05	10.17	0.000956
7.571	2.3E–05	10.34	0.000937
7.773	4.8E–05	10.5	0.000913
7.924	9.4E–05	10.748	0.00082
8.015	0.00013	11.0	0.000705
8.13	0.000187	11.5	0.000495
8.5	0.0005	12.0	0.000278
8.915	0.000728	12.5	0.00014
9.0	0.000753	13.0	6.6E–05
9.5	0.000838	13.5	2.7E–05
9.86	0.000928		

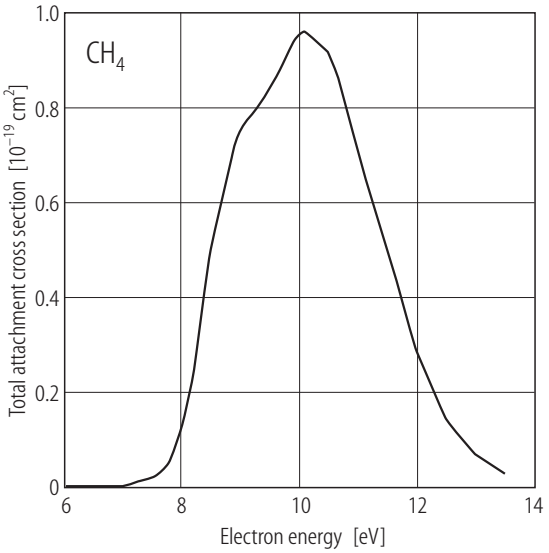

Fig. 5.2.17. Total attachment cross section of CH_4.

CF_4

Recommended data [96Chr1]

Comments

Christophorou et al. [96Chr1] surveyed all the cross section data for the electron collision with CF_4. Their recommended data on the total attachment cross section are presented here. They obtained these values by normalizing the relative values of Spyrou et al. [83Spy1] with the result of a swarm measurement of Hunter and Christophorou [84Hun1]. The former authors [83Spy1] measured the cross section with a beam method with a TOF mass spectrometer. Recently Iga et al. [92Iga1] reported their measurement of the partial cross sections for F^-, F_2^-, and CF_3^-. The sum of those cross sections is in good agreement with the total cross section recommended here. As for each partial cross section, however, there is a considerable disagreement between the results of [83Spy1] and [92Iga1]. No definite conclusion can be obtained about the preference of the two sets of data on the partial cross section.

Table 5.2.28. Total attachment cross section for CF_4.

Energy [eV]	Cross section [10^{-16}cm^2]	Energy [eV]	Cross section [10^{-16}cm^2]	Energy [eV]	Cross section [10^{-16}cm^2]
4.31	4E–05	6.52	0.0144	8.75	0.00389
4.6	0.00012	6.73	0.0157	8.93	0.00284
4.79	0.00048	6.91	0.0161	9.13	0.00213
5.0	0.00108	7.14	0.0158	9.35	0.00146
5.18	0.00202	7.32	0.0146	9.52	0.00099
5.38	0.00317	7.52	0.0131	9.76	0.00069
5.56	0.00486	7.72	0.0114	9.96	0.00043
5.77	0.00681	7.93	0.00977	10.2	0.00022
5.94	0.00881	8.1	0.00802	10.4	9E–05
6.15	0.0107	8.33	0.00656		
6.34	0.0126	8.51	0.00506		

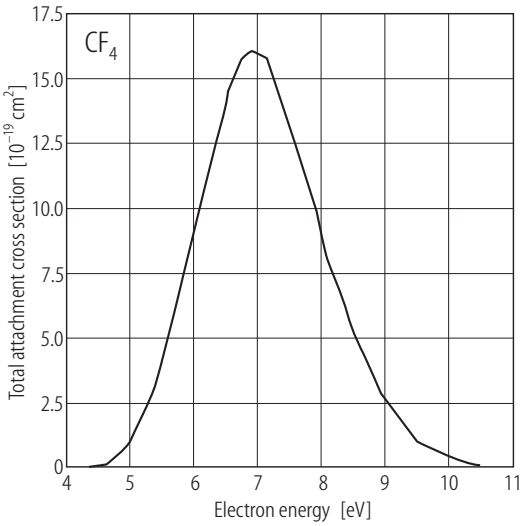

Fig. 5.2.18. Total attachment cross section of CF_4.

CCl_4

Recommended data

[01Kla1] for Cl^- production.

Comments

Klar et al. determined the recommended data for Cl^- production. Below about 173 meV, they based on their own measurement using the laser photoelectron method. The photoelectron from Ar, produced by a laser irradiation, was used for the attachment. The product ions were detected by a quadrupole mass filter. The absolute values were determined by comparing with thermal attachment coefficient. For the higher energy range, they employed the data obtained by Chu and Burrow [90Chu1], but renormalized the values so as to smoothly connect to the lower energy values. Chu and Burrow used the total ionization method. The present recommended data are consistent with the two recent measurements ([97Mat1] for 6 - 1200 meV and [95Fre1] for the energies less than 1 meV).

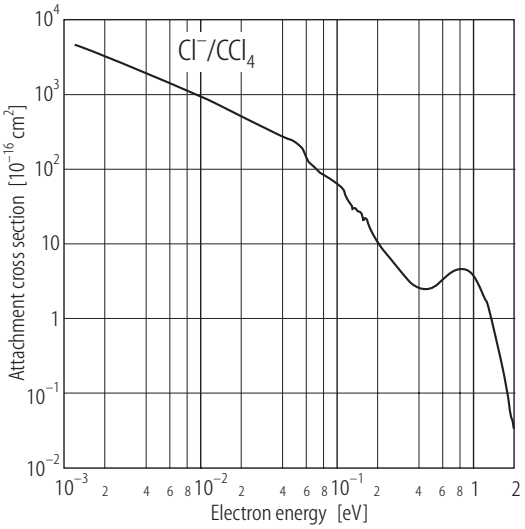

Fig. 5.2.19. Attachment cross section for the production of Cl^- from CCl_4.

Table 5.2.29. Production of Cl^- from CCl_4.

Energy [eV]	Cross section [$10^{-16}cm^2$]	Energy [eV]	Cross section [$10^{-16}cm^2$]	Energy [eV]	Cross section [$10^{-16}cm^2$]
0.001133	4612.2	0.09032	73.558	0.2964	4.4199
0.002001	3181.5	0.09351	70.873	0.355	3.0313
0.002976	2412.3	0.09663	67.859	0.4136	2.5878
0.005903	1428.8	0.09983	66.93	0.4722	2.5564
0.00901	1025.6	0.103	62.31	0.5308	2.838
0.01207	805.4	0.1061	58.917	0.5894	3.4739
0.01519	661.76	0.1093	57.323	0.648	4.0509
0.01826	560.69	0.1125	54.445	0.7066	4.5239
0.02137	486.3	0.1156	46.338	0.7652	4.7771
0.02445	432.13	0.1188	42.256	0.8238	4.9537
0.02756	388.25	0.122	39.266	0.8824	4.7957
0.03068	347.72	0.1251	35.199	0.941	4.31
0.03378	316.46	0.1283	33.58	0.9996	3.7614
0.03691	296.54	0.1314	30.416	1.058	3.3424
0.04002	270.85	0.1346	31.14	1.117	2.7251
0.04317	255.69	0.1377	30.698	1.175	2.1746
0.04627	244.99	0.1409	28.619	1.234	1.84
0.04942	226.41	0.1441	27.824	1.293	1.3719
0.05253	212.48	0.1472	28.015	1.351	1.0912
0.05567	192.79	0.1504	27.983	1.41	0.83217
0.05881	155.03	0.1534	26.01	1.468	0.60842
0.06194	131.79	0.1566	23.387	1.527	0.4573
0.06513	116.18	0.1597	21.598	1.586	0.33464
0.06824	109.87	0.1629	22.909	1.644	0.22375
0.07143	101.07	0.166	21.987	1.703	0.16585
0.07455	91.474	0.1691	21.959	1.761	0.11972
0.07772	88.143	0.1722	18.474	1.82	0.092249
0.08086	83.955	0.1843	13.897	1.878	0.053967
0.08401	79.776	0.2036	10.187	1.937	0.047105
0.08719	78.568	0.2378	7.3256	1.996	0.036309

SF_6

Recommended data

[01Chr1] (for numerical tables, see [00Chr1]).

Comments

Christophorou and Olthoff [01Chr1] critically assessed the published data on the electron attachment cross section for SF_6. For the production of SF_6^-, they combined the results of a very high-resolution, very low-energy measurement by Hotop et al. ([92Kla1, 98Sch1]), a conventional beam-type measurement of Kline et al. [79Kli1], and a swarm experiment using mixtures of SF_6 and N_2, Ar, and Xe by Hunter et al. [89Hun1]. The method of Hotop et al. is based on the laser-photoionization technique (see the comment for CCl_4). The cross sections for the production of SF_5^- are from the measurements of Kline et al. [79Kli1] and Hunter et al. [89Hun1]. Since the experimental data at the energy below 0.1 eV are likely to have a large uncertainty, no data are recommended for the SF_5^- production below 0.1 eV. Those cross sections, however, are very small compared to the cross sections for the production of SF_6^-. The

dissociative attachment cross sections for the productions of SF_4^-, SF_3^-, SF_2^-, F_2^-, and F^- are a compromise of three sets of measurements [70Leh1, 79Kli1, and 93Rao2]. Numerical tables of all the attachment cross sections recommended by Christophorou and Olthoff [01Chr1] are presented in their review article on the electron collisions with SF_6 molecules [00Chr1].

Table 5.2.30. Production of SF_6^- from SF_6.

Energy [eV]	Cross section [10^{-16}cm^2]	Energy [eV]	Cross section [10^{-16}cm^2]	Energy [eV]	Cross section [10^{-16}cm^2]
0.0001	7617	0.007	683	0.090	74.3
0.0002	5283	0.008	621	0.10	49.5
0.0003	4284	0.009	569	0.12	30.8
0.0004	3692	0.010	526	0.14	17.8
0.0005	3280	0.015	383	0.15	14.2
0.0006	2968	0.020	304	0.16	10.5
0.0007	2724	0.025	257	0.18	5.85
0.0008	2529	0.030	221	0.20	2.86
0.0009	2369	0.035	190	0.22	1.24
0.001	2237	0.040	171	0.25	0.52
0.002	1511	0.045	149	0.28	0.25
0.003	1202	0.050	132	0.30	0.16
0.004	993	0.060	109	0.35	0.05
0.005	859	0.070	92.7	0.40	0.01
0.006	760	0.080	82.9		

Table 5.2.31. Production of SF_5^- from SF_6.

Energy [eV]	Cross section [10^{-16}cm^2]	Energy [eV]	Cross section [10^{-16}cm^2]
0.10	1.85	0.40	3.45
0.12	2.09	0.45	2.75
0.14	2.36	0.50	2.15
0.15	2.48	0.60	1.25
0.16	2.61	0.70	0.72
0.18	2.87	0.80	0.42
0.20	3.15	0.90	0.25
0.22	3.45	1.0	0.15
0.25	3.86	1.2	0.06
0.28	4.15	1.5	0.02
0.30	4.24	1.9	0.005
0.35	4.07		

Table 5.2.32. Production of SF_4^- from SF_6.

Energy [eV]	Cross section [$10^{-16}cm^2$]	Energy [eV]	Cross section [$10^{-16}cm^2$]
3.5	8.4E–05	6.5	0.00251
4.0	0.00035	7.0	0.0013
4.5	0.00144	7.5	0.00046
5.0	0.00457	8.0	8.4E–05
5.5	0.00528	8.5	3.2E–05
6.0	0.00394		

Table 5.2.35. Production of F_2^- and F^- from SF_6.

Energy [eV]	F_2^- [$10^{-16}cm^2$]	F^- [$10^{-16}cm^2$]
1.5	3E–05	
2.0	8E–05	0.00022
2.25	7.5E–05	0.00075
2.5	6E–05	0.00149
2.75	4.2E–05	0.00162
3.0	2.6E–05	0.00098
3.5	2.6E–05	0.00171
4.0	0.000265	0.00856
4.5	0.000707	0.0269
5.0	0.000489	0.0463
5.5	0.000155	0.0439
6.0	3.8E–05	0.0278
6.5	1.9E–05	0.0137
7.0	1.5E–05	0.00749
7.5	1.5E–05	0.00615
8.0	1.8E–05	0.00977
8.5	3.1E–05	0.0142
9.0	6.5E–05	0.0157
9.5	0.000104	0.0139
10.0	0.000200	0.0113
10.25	0.000308	0.0114
10.5	0.000503	0.0131
11.0	0.000910	0.0210
11.5	0.000954	0.0235
12.0	0.000615	0.0195
12.5	0.000274	0.0122
13.0	0.000111	0.00629
13.5	5.0E–05	0.00400
14.0	3.2E–05	0.00340
14.5	1.8E–05	0.00310
15.0	1.2E–05	0.00300

Table 5.2.33. Production of SF_3^- from SF_6.

Energy [eV]	Cross section [10^{-16}cm^2]
8.0	1.4E–05
8.5	4.6E–05
9.0	0.00015
9.5	0.00033
10.0	0.00051
10.25	0.000577
10.5	0.00064
11.0	0.00075
11.5	0.00071
12.0	0.00049
12.5	0.00026
13.0	0.00011
13.5	3.1E–05
14.0	8E–06

Table 5.2.34. Production of SF_2^- from SF_6.

Energy [eV]	Cross section [10^{-16}cm^2]
10.25	1.9E–06
10.5	3.7E–06
11.0	1.4E–05
11.5	4.2E–05
12.0	7.6E–05
12.5	0.000106
13.0	8.7E–05
13.5	4.4E–05
14.0	1.7E–05
14.5	6.8E–06
15.0	2.8E–06

5.2.3 References for 5.2

65Chr1 Christophorou, L.G., Compton, R.N., Hurst, G.S., Reinhardt, P.W.: J. Chem. Phys. **43** (1965) 4273
65Rap1 Rapp, D., Briglia, D.D.: J. Chem. Phys. **43** (1965) 1480
65Rap2 Rapp, D., Sharp, T.E., Briglia, D.D.: Phys. Rev. Lett. **14** (1965) 533
67Com1 Compton, R.N., Christophorou, L.G.: Phys. Rev. **154** (1967) 110
67Sch1 Schulz, G.J., Asundi, R.K.: Phys. Rev. **158** (1967) 25
67Sha1 Sharp, T.E., Dowell, J.T.: J. Chem. Phys. **46** (1967) 1530
68Chr1 Christophorou, L.G., Compton, R.N., Dickson, H.W.: J. Chem. Phys. **48** (1968) 1949
69Sha1 Sharp, T.E., Dowell, J.T.: J. Chem. Phys. **50** (1969) 3024
69Spe1 Spence, D., Schulz, G.J.: Phys. Rev. **188** (1969) 280
70Leh1 Lehmann, B.: Z. Naturforsch. A **25** (1970) 1755
70Sta1 Stamatovic, A., Schulz, G.J.: J. Chem. Phys. **53** (1970) 2663
72Azr1 Azria, R., Tronc, M., Goursaud, S.: J. Chem. Phys. **56** (1972) 4234
72Mel1 Melton, C.E.: J. Chem. Phys. **57** (1972) 4218
74Spe1 Spence, D., Schulz, G.J.: J. Chem. Phys. **60** (1974) 216
75Cal1 Caledonia, G.E.: Chem. Rev. **75** (1975) 333
75Zie1 Ziesel, J.P., Schulz, G.J., Milhaud, J.: J. Chem. Phys. **62** (1975) 1936
78All1 Allan, M., Wong, S.F.: Phys. Rev. Lett. **41** (1978) 1791
78Kur1 Kurepa, M.V., Belić, D.S.: J. Phys. B: At. Mol. Phys. **11** (1978) 3719
79Kli1 Kline, L.E., Davies, D.K., Chen, C.L., Chantry, P.J.: J. Appl. Phys. **50** (1979) 6789
81All1 Allan, M., Wong, S.F.: J. Chem. Phys. **74** (1981) 1687
83Cad1 Čadež, I.M., Pejčev, V.M., Kurepa, M.V.: J. Phys. D: Appl. Phys. **16** (1983) 305
83Ori1 Orient, O.J., Srivastava, S.K.: Chem. Phys. Lett. **96** (1983) 681
83Ori2 Orient, O.J., Srivastava, S.K.: J. Chem. Phys. **78** (1983) 2949
83Spy1 Spyrou, S.M., Sauers, I., Chrisrtophorou, L.G.: J. Chem. Phys. **78** (1983) 7200
84Chr1 Christophorou, L.G., McCorkle, D.L., Christodoulides, A.A., in: Electron-Molecule Interactions and Their Applications, edited by L.G. Christophorou (Academic Press, 1984) vol. 1, p. 477
84Hun1 Hunter, S.R., Christophorou, L.G.: J. Chem. Phys. **80** (1984) 6150

85Ele1 Eletskii, A.V., Smirnov, B.M.: Sov. Phys. Usp. **28** (1985) 956
85Ori1 Orient, O.J., Srivastava, S.K.: Phys. Rev. A **32** (1985) 2678
86Spy1 Spyrou, S.M., Sauers, I., Christophorou, L.G.: J. Chem. Phys. **84** (1986) 239
87Chr1 Christophorou, L.G., Hunter, S.R., Carter, J.G., Spyrou, S.M., in: Swarm Studies and Inelastic Electron-Molecule Collisions, edited by L.C. Pitchford, B.V. McKoy, A. Chutjian, S. Trajmar (Springer, 1987) p. 303
87Chu1 Chutjian, A., Alajajian, S.H.: Phys. Rev. A **35** (1987) 4512
88Ale1 Aleksandrov, N.L.: Sov. Phys. Usp. **31** (1988) 101
88Pet1 Petrović, Z.L., Wang, W.C., Lee, L.C.: J. Appl. Phys. **64** (1988) 1625
89Hun1 Hunter, S.R., Carter, J.G., Christophorou, L.G.: J. Chem. Phys. **90** (1989) 4879
90Chu1 Chu, S.C., Burrow, P.D.: Chem. Phys. Lett. **172** (1990) 17
90Kri1 Krishnakumar, E., Srivastava, S.K.: Phys. Rev. A **41** (1990) 2445
91Wan1 Wan, H.-X., Moore, J.H., Tossell, A.: J. Chem. Phys. **94** (1991) 1868
92Iga1 Iga, I., Rao, M.V.V.S., Srivastava, S.K., Nogueira, J.C.: Z. Phys. D **24** (1992) 111
92Kla1 Klar, D., Ruf, M.-W., Hotop, H.: Aust. J. Phys. **45** (1992) 263
92Kri1 Krishnakumar, E., Nagesha, K.: J. Phys. B: At. Mol. Opt. Phys. **25** (1992) 1645
92Rao1 Rao, M.V.V.S., Srivastava, S.K.: J. Phys. B: At. Mol. Opt. Phys. **25** (1992) 2175
93Rao1 Rao, M.V.V.S., Srivastava, S.K.: J. Geophys. Res. **98** (1993) 13137
93Rao2 Rao, M.V.V.S., Srivastava, S.K., in: Proceedings of the 18th International Conference on the Physics of Electronic and Atomic Collisions, edited by T. Andersen, B. Fastrup, F. Folkmann, H. Knudsen, Abstracts of contributed papers (1993), p. 345
93Wan1 Wan, H.-X., Moore, J.H., Olthoff, J.K., van Brunt, R.J.: Plasma Chemistry and Plasma Processing **13** (1993) 1
95Fre1 Frey, M.T., Hill, S.B., Smith, K.A., Dunning, F.B., Fabrikant, I.I.: Phys. Rev. Lett. **75** (1995) 810
96Chr1 Christophorou, L.G., Olthoff, J.K., Rao, M.V.V.S.: J. Phys. Chem. Ref. Data **25** (1996) 1341
96Chu1 Chutjian, A., Garscadden, A., Wadehra, J.M.: Phys. Rep. **264** (1996) 393
97Hor1 Horáček, J., Domcke, W., Nakamura, H.: Z. Phys. D **42** (1997) 181
97Kri1 Krishnakumar, E., Kumar, S.V.K., Rangwala, S.A., Mitra, S.K.: Phys. Rev. A **56** (1997) 1945
97Mat1 Matejcik, S., Senn, G., Scheier, P., Kiendler, A., Stamatovic, A., Märk, T.D.: J. Chem. Phys. **107** (1997) 8955
98Ill1 Illenberger, E., Smirnov, B.M.: Physics - Uspekhi **41** (1998) 651
98Sch1 Schramm, A., Weber, J.M., Kreil, J., Klar, D., Ruf, M.-W., Hotop, H.: Phys. Rev. Lett. **81** (1998) 778
99Chr1 Christophorou, L.G., Olthoff, J.K.: J. Phys. Chem. Ref. Data **28** (1999) 131
99Ran1 Rangwala, S.A., Kumar, S.V.K., Krishnakumar, E.,Mason, N.J.: J. Phys. B: At. Mol. Opt. Phys. **32** (1999) 3795
99Sen1 Senn, G., Skalny, J.D., Stamatovic, A., Mason, N.J., Scheier, P., Märk, T.D.: Phys. Rev. Lett. **82** (1999) 5028
00Chr1 Christophorou, L.G., Olthoff, J.K.: J. Phys. Chem. Ref. Data **29** (2000) 267
01Chr1 Christophorou, L.G., Olthoff, J.K.: Int. J. Mass Spect. **205** (2001) 27
01Chr2 Christophorou, L.G., Olthoff, J.K.: Adv. At. Mol. Opt. Phys. **44** (2001) 155
01Dre1 Drexel, H., Senn, G., Fiegele, T., Scheier, P., Stamatovic, A., Mason, N.J., Märk, T.D.: J. Phys. B **34** (2001) 1415
01Kla1 Klar, D., Ruf, M.-W., Hotop, H.: Int. J. Mass Spect. **205** (2001) 93
01Kla2 Klar, D., Ruf, M.-W., Fabrikant, I.I., Hotop, H.: J. Phys. B **34** (2001) 3855

6 Cross sections for scattering- and excitation-processes in electron-molecule collisions

6.1 Total scattering cross sections

6.1.1 Introduction

6.1.1.1 Subject

This contribution presents a collection of total cross sections for electron scattering on molecules from the lowest energies examined experimentally up to 1000 eV. Some data at higher energies can be found, for example in [96Zec1, 01Kar1, 01Kar2]. Although the electron-atom scattering is not discussed explicitly, some references on electron-noble gases scattering are given while discussing experimental methods.

The bibliography mainly covers papers printed later than 1970. A description of experimental methods (on atoms) was given in [71Bed1], the list of early experiments in [33Bro1, 33Ram1], tabulated data for cross sections in [89Shi1], recommended cross sections in [92Hay1]. We quote also several other review articles and books on electron scattering [84Shi1, 84Chr1, 89McD1, 90Kau1, 94Ino1, 96Zec1, 00Kim1, 01Kar1, 01Kar2].

6.1.1.2 Measured quantities

6.1.1.2.1 Total cross section

Most of the total cross section (TCS) measurements on molecules have been performed by the transmission method. In this type of experiments the attenuation of an electron beam passing through a gas cell is monitored. The total cross section σ_{tot} is obtained from the deBeer-Lambert formula

$$I = I_0 \exp(-\frac{p}{kT} l\sigma_{tot}) \quad (1)$$

where I_0 and I stand for the electron current at the entrance and exit of the gas cell respectively, T and p for the gas temperature and pressure respectively, l -for the length of the scattering region and k for Boltzmann's constant.

The total cross section can be described as a sum of the cross sections for scattering into all channels opened at a given energy. In the case of molecules these channels are elastic scattering, rotational and vibrational excitation, electronic excitation, dissociative and non-dissociative attachment, dissociation into neutrals, dissociative and non-dissociative ionization. This definition has been used to check the quality of total cross sections by comparison with the sum of partial integral values [96Zec1, 01Kar1, 01Kar2]. Nevertheless the amount of data available as partial integral cross sections is rather sparse, and does not help in the assessment of total cross section recommended values.

6.1.1.2.2 Integral and momentum transfer cross sections

A few other experimental methods allow to evaluate the total cross sections whenever it is difficult to be measured by the transmission method. For example, below the threshold for inelastic processes, the total cross section coincides with the integral cross section for elastic scattering σ_{el} which can be obtained by integrating experimental differential cross sections $d\sigma_{el}/d\omega$ over the full solid angle

$$\sigma_{el} = 2\pi \int_0^{\pi} \frac{d\sigma_{el}}{d\omega} \cdot \sin\theta \cdot d\theta \tag{2}$$

where θ is the scattering angle.

Note that although the rotational excitation channel is opened also at the lowest energies experimentally achievable, the rotational excitation is usually not discriminated in the experiment. In this way the measured integral elastic cross section equals to the total one below the vibrational excitation thresholds, see section 6.2 in this volume. In some gases, like HCl, the rotational cross sections have been measured [89Rad1] and can be summed to check the total cross section.

In the limit of isotropic scattering (e.g. low energy scattering for non polar molecules) the total cross section can be evaluated by comparison with the momentum transfer cross section σ_m obtained from the analysis of diffusion coefficients (see section 6.4).

$$\sigma_m = 2\pi \int_0^{\pi} \frac{d\sigma_{el}}{d\omega} \cdot (1 - \cos\theta) \cdot \sin\theta \cdot d\theta \tag{3}$$

Practically, the total and momentum transfer cross sections coincide at low energies (say below 1 eV) for non polar molecules, like N_2. For molecules showing a Ramsauer-Townsend minimum, σ_{tot} and σ_m coincide only for energies below the minimum. The momentum transfer cross section at higher energies is lower than the total cross section.

6.1.1.2.3 Other measurements

Sporadically, other methods have been used to measure total cross sections. In the recoil method, the electron beam crosses at right angle the molecular beam and the current I_s of recoiled atoms is measured. The total cross section is determined from the formula

$$\sigma_{tot} = \frac{I_s}{I_m} \frac{hu}{I_e} \tag{4}$$

where u is the velocity of atoms in the beam, h is the height of the electron beam, I_m is the molecular beam intensity and I_e the electron beam intensity. Targets measured by this method are alkali atoms dimers [73Mil1, 82Mil1], alkali halides [74Sla1, 84Jad1, 89Vus1] and oxygen [67Sun1].

At very low energies (at meV range) the Rydberg atoms quenching method has been used to evaluate total cross section. Electrons in high Rydberg orbits can be considered as almost free so they scatter on perturbing gas molecules. Rydberg electrons with principal quantum numbers above 100 have mean kinetic energies below 1 meV [92Lin1]. Quenching rate constants in the presence of a perturbing gas are measured. The interpretation of these data is not straightforward. Quenching of the Rydberg atoms can be caused by such processes as electron attachment, like in CCl_4 [92Lin1]; by formation of intermediate molecular complexes, like in C_6H_6 [93Pop1]; by rotational excitation of the molecule, like in CH_3I [93Lin1].

In the limit of zero-energy $E = 0$, the Fermi method [34Fer1] can be used to evaluate the scattering length A_0:

$$\sigma_{tot}(E = 0) = 4\pi A_0^2 \quad (5)$$

The method consists in measurements of the shift in the optical emission from molecular gases (like C_6H_6, CH_3I) [90Rup1] in presence of a perturber. Targets for which the scattering length has been determined in this way are noble gases [90Rup1], CO_2 [91Asa1], CH_4, C_2H_6, C_3H_8 [91Mey1].

6.1.1.3 Experimental methods

6.1.1.3.1 Absolute measurements

In absolute measurements, all quantities in eq. (1) are monitored directly. The typical systematic error of most of the absolute measurements performed in the last decades (apart from the angular resolution error, see below), is less than 5 %. The most difficult is the pressure evaluation, which requires, for example, corrections for the temperature difference between the scattering cell and the pressure gauge (the thermal transpiration error). A few experiments used indirect methods of pressure evaluation, like ionization [78Szm1] or optical emission [86Gar1]. Indirect methods are likely to introduce additional errors.

In normalized measurements, some of the quantities (often the electron path length inside the gas cell) are unknown. Sometimes this uncertainty is related to gas outflow from the scattering through entrance and exit orifices [85Wag1]; for this reason long scattering cells are privileged. In other apparatuses the uncertainty is introduced by the use of electron-guiding magnetic fields [77Kau1, 80McM1, 84Sue1]. Here the real length of the electron path is determined by spiralling in the magnetic field. This is a difficult quantity to evaluate.

The normalized measurements can be useful to assess the shape of the cross section vs. energy curve, but are of no use for the evaluation of the recommended (absolute) values.

6.1.1.3.2 Angular resolution error

An inherent error of the transmission technique is due to the lack of discrimination for electrons scattered into small angles, within the angular acceptance of the detector. The absolute error $\Delta\sigma_\omega$, leading to underestimation of the measured cross section, depends on the angular acceptance $\Delta\omega(x)$ of the detector, as seen from the position x of the scattering event and on the small-angle differential cross section $d\sigma/d\omega$ for a specified scattering channel [80Win1, 83Laz1]

$$\Delta\sigma_\omega = \frac{1}{l}\int_0^l dx\, I'(x) \int_0^{\Delta\omega(x)} \frac{d\sigma}{d\omega} d\omega \ , \quad (6)$$

with $I'(x) = I(x)/I_0$, see eq. (1), and the first integral to be evaluated over the interaction region length (l). The angular resolution error, similarly as the total cross section, is a sum over all possible scattering processes. However, many experiments use retarding-field analyzers, preventing a part of the inelastically scattered electrons to reach the detector. The energy resolution of such detectors, in any case, hardly allows to discriminate the lowest inelastic channels, like the rotational and vibrational excitation.

The angular resolution error, for a given apparatus, rises if the differential cross section is forward peaked. For any given apparatus it depends also on the total cross section partitioning between elastic and inelastic channels. For the apparatuses used in the last decades, the angular resolution error becomes comparable with the remaining systematic errors essentially in two limits: at energies lower than a few eV for polar molecules (like H_2O and NH_3) [92Yua1, 94Ham2, 00Kim1] and at energies above several hundreds eV for all targets [92Zec1, 96Gar2].

Some authors correct the measured total cross sections for the angular resolution error [79Jos1, 82Nog1, 83Jos1, 00Kim1], using theoretical or extrapolated into zero-angle experimental differential cross sections. The reliability of such corrections is often limited.

6.1.1.3.3 Survey of the experimental methods

As stated in subsect. 6.1.1.2.1, reliable electron - molecule total cross section measurements have been performed using the attenuation method. The attenuation of an electron beam is measured when it passes through a region containing the sample gas. Other measurement principles have been occasionally proposed, but the few data produced are considered of low reliability (see subsect. 6.1.1.2.3). Fig. 6.1.1 is a block diagram of a transmission measurement showing all the possible functional blocks.

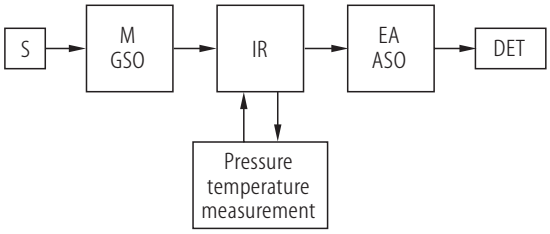

Fig. 6.1.1. Block diagram showing all the functional blocks of a transmission measurement.

Here S stands for the electron source. Electrons are then monochromatized (M) and geometrically selected (GSO) to form a beam. This beam is passed through an interaction region (IR) where the target gas is confined. The confinement is performed in a gas cell or by the use of a molecular beam. Different techniques are used to measure the gas density with the needed accuracy. Transmitted electrons are energy selected by an energy analyzer (EA) and geometrically selected by a suitable angular selection optics (ASO) to be admitted in the detector (DET). The beam forming and the monochromatization functions are often mixed in a single device; the same applies for the geometrical selection and the energy analysis functions. In real experimental set-ups some of these functional blocks can be absent. As an example, the monochromator function is sometimes missing: at energies higher than several tens of eV, this can be justified by the fact that $\Delta E/E$ is smaller than 1/100 for standard thermionic sources.

Attenuation measurements are performed with a variety of different set-ups. Among these, we can distinguish two broad classes: the time of flight techniques (TOF) and the beam techniques. The former rely on fast timing to obtain a velocity (energy) spectrum of transmitted electrons. TOF apparatuses cannot deconvolve energy losses introduced by the scattering event from the original electron energy distribution of the source; therefore they have been used mostly in the very low energy range, where inelastic channels are closed. TOF spectrometers are (typically) more difficult to operate than beam spectrometers: below 1 eV, difficulties in obtaining stable beams increase, rendering the TOF technique more interesting [80Ken1, 81Fer1, 86Buc2, 96All1].

Beam techniques can be implemented as linear apparatuses or as curved beams. The pioneering works of Ramsauer [21Ram1] and Ramsauer and Kollath [29Ram1], Brüche [27Bru1] and others in the twenties have been performed with a 180° magnetic spectrometer. This type of apparatus suffers from a poor energy discrimination of the inelastically scattered electrons [81Dal1]. Linear apparatuses [80Bla1] can more easily implement an energy analyzer (see Fig. 6.1.1) to improve this discrimination.

Errors affecting the measured cross section can arise mainly from:

1. Determination of the interaction region length; this is more difficult when axial magnetic fields are used.
2. Target density measurement.
3. Electron emission instabilities.

4. Poor energy and/or angle discrimination of the scattered electrons - at the high energy limit of each apparatus.
5. Apparatus instabilities - at the low energy limit of each apparatus.

Table 6.1.1 gives a short form description of the apparatuses used in the total cross section measurements referenced throughout this paper. Table 6.1.1 quotes those parameters which are more important for the assessment of the quality of the measured cross sections. This table does not give a detailed description of each apparatus: this is hindered by the fact that each apparatus has undergone continuous improvements during its life. The relevant parameters often change from one paper to the next. In particular, the errors quoted by the authors often change in the measurement of different gases. The energy range also changes frequently.

The order in which the apparatuses appear in the table is in accordance with the lower limit of the energy span. The symbols used in the table are listed in the table caption. The most relevant references are given in the last column and are listed in the reference list below the table.

Table 6.1.1. Overview of transmission-method experiments for total cross section measurements.

Laboratory	Method Monochr. Analyzer	Energy range [eV]	Energy resolution ΔE [eV]	Stat. error [%]	Syst. error [%]	L_{scat} L_{cell} [cm]	Ω_{geom} [10^{-4} sr]	Source	Ref.
LURE-ACO, Orsay (France)	LTE No RF	0.01 - 6	0.0055 - 0.015	NQ	NQ	3 3	NQ	Ph-S	A1, A2
SRS-SERC, Daresbury (UK)	LTE No SE	0.02 - 20	0.0035	ND Tot: 8		3 3	NQ	Ph-S	B1, B2
University of Bielefeld (Germany)	TOF	0.08 - 20	0.003 – 2.9, DoE	2 - 3	< 1	27.1 24.7	2.4 to 15	ThC	C
Australian National University, Canberra (Australia)	TOF	0.12 - 20	>0.003, DoE	3 - 3.75	2.2	25.5 NQ	7.0	WF	D
Forschungsinstitut der AEG	RT MAG MAG	1.16 - 2.2	0.09 at 0.5 eV	NQ		3.14 3.14	240	PhC	E
University of Maryland (USA)	LTM (axial) TR RF	0.2 - 12	0.05 - 0.08, DoE	< 10	10 - 43 DoE	NQ NQ	NQ	ThC	F
Technical University of Gdańsk (Poland)	LTE CE RF	0.25 - 250	0.07	< 1	4 - 10	3.05 3.05	10	WF	G
University of Trento (Italy)	LTE RPD RPD	0.3 - 100	0.5	ND Tot: 1.7 - 7 DoE		(a)	NQ	ThC	H
Indiana University Bloomington (USA)	TOF	0.5 - 100	0.06 - 2.8 DoE	ND Tot: 3-15		38 38	0.22 to 1.4	SE	I
Phys. Research Lab., Navrangpura Ahmedabad-India	LTE CE RF	0.7 - 10	NQ	1.5	5.3	2.37 NQ	NQ	Ph	J

Table 6.1.1 (continued)

Laboratory	Method Monochr. Analyzer	Energy range [eV]	Energy resolution ΔE [eV]	Stat. error [%]	Syst. error [%]	L_{scat} L_{cell} [cm]	Ω_{geom} [10^{-4} sr]	Source	Ref.
Technische Hochschule Danzig	RT MAG MAG	1 - 50	0.2 at 1.2 eV	NQ		1.8 1.8	$9 \cdot 10^2$	PhC	K
Tokyo-Yamaguchi, University (Japan)	RP-TOF +axial B field	1 - 400	1.8	ND Tot: 3 - 15		7.17 (b) 6.38	NQ	SE	L1, L2
Wayne State University, Detroit (USA)	LTM (axial) No RF	1 - 700	0.15 at 5 eV	1	5	109 109	NQ	ThC WF for O_2	M
Lockheed Research Laboratory, Palo Alto (USA)	RT MAG MAG	2 - 21	0.07 - 0.7, DoE	ND Tot: 3 - 10		NQ NQ	NQ	ThC WF	N
Jet Propulsion Lab., Pasadena, California (USA)	LTE-linear No RF	4 - 300	0.35	0.2 - 2	2	14.43 14.43	2.2	WF	O
Niigata University (Japan)	LTE No RF	7 - 500	1.25 at 100 eV	0.2 - 6	13 - 18	2.52 2.52	NQ	WF	P
University of Bielefeld (Germany)	LTE CE RF	5 - 400	> 0.5	> 5	3	51.8 51.5	NQ	ThC SE	Q
FOM-Inst. Atom. Mol. Phys., Amsterdam-Holland	LTE-linear No RF	16 - 700	0.4	Stat. 1 Tot: < 4		4.2 4.2	0.785	ThC	R
University of Trento (Italy)	RT MAG MAG	75 - 4000	NQ	< 1.5	2.4 - 3	14.02 14.02	3.4	ThC	S1, S2
Universitad Complutense Madrid (Spain)	LTE No SE	380 - 5200	1	Stat. 2 Tot: 3		7 – 12.7 7 - 12.7	0.35	WF	T1, T2
University of Science and Techn., Hefey (China)	LTE-linear No RF	400 - 4250	0.85	2.5 - 3	1 - 3	20.2 20.2	0.63	WF	U

Symbols

1st column: laboratories.

2nd column: *First line*, method, apparatuses used to measure TCS: **RT** Ramsauer-type; **TOF** time of flight; **RP-TOF** time of flight + retarding potential; linear transmission methods with (i) electrostatic transport **LTE** or with (ii) with magnetic transport **LTM**.
Second line, monochromator: **SE** spherical electrostatic, **CE** cylindrical electrostatic, **TR** trochoidal, **RPD** retarding potential difference, **MAG** magnetic 180°, **No** no monochromator.
Third line, analyser: **SE** spherical electrostatic; **RF** retarding field, **MAG** magnetic 180°, **No** no analyser.

3rd column: energy range of the measured TCS.

4th column: energy resolution of the apparatus.

5th and 6th columns: statistical and systematic errors. Where not distinguished, the total error is given.

7th column: length of the scattering path and of the scattering cell.

8th column: angular discrimination of the apparatus after the interaction region.

9th column: source: **ThC** thermoionic cathode, **WF** tungsten filament, **SE** secondary, electrons, **Ph** – photoionization, **Ph-S** photoionization with synchrotron radiation, **PhC** photocathode.

10th column: selected references regarding the gases measured with the corresponding apparatus.

ND: not distinguished; **NQ**: not quoted; **Do*E***: depends on energy

Notes

(a) A cell (and a scattering) length of (1.8 ± 0.02) cm and (5.0 ± 0.02) cm in the 0 - 10 eV and 10 - 100 eV energy range was respectively used.

(b) Obtained by normalization of positron-scattering TCS in N_2 with those of [82Hof1].

References and targets

A1 84Fie1 (CF_4, N_2,O_2); 94Lun1 (CH_4, C_2H_4, C_2H_6)

A2 LTE with an axial magnetic field: 93Zie1 (O_2); 93Ran1 (CF_3Cl, CF_2Cl_2, $CFCl_3$, CCl_4); 96Ran1 (CO)

B1 with crossed beam: 91Fie1; 88Fie1 (O_2); 91Fie2 (CO_2); 94Lun1 (CH_4, C_2H_4, C_2H_6)

B2 LTE with an axial magnetic field: 98Gul1 (C_6H_6, C_6D_6, C_6H_5D); 98Gul2 (O_3, ClO_2); 98Gul3 (Cl_2); 98Lun1 (CH_4, C_2H_6, C_3H_8, C_3H_6); 99Lun1 (C_6H_5F, C_6H_5Cl, C_6H_5Br, C_6H_5I)

C 80Fer1 (H_2, O_2); 81Fer1 (CO_2); 85Fer1 (Ar); 85Fer2 (CH_4); 89Fer1 (CO_2); 91Fer1 (N_2)

D 86Buc1 (CO); 86Buc2 (He, Ar); 86Loh1 (CH_4); 87Buc1 (CO_2); 95Sun1 (N_2); 94Gul1 (Ne); 96All1 (NO)

E 21Ram1 (He, Ne, Ar), 29Ram1 (He-Xe), 30Ram1 (H_2, N_2, O_2, CO, CO_2, CH_4); 30 Ram2 (H_2, N_2O)

F 88Ben1 (CH_3I, CH_3Br, CH_3F, CH_3Cl); 89Wan1 (SiH_4, SiH_2Cl_2, $SiHCl_3$, SiH_4, SiF_4, $SiCl_4$, $SiBr_4$, SiI_4); 91Wan1 (CCl_4, $CHCl_3$, CH_2Cl_2, $CHCl_3$, CH_4); 93Wan1 (SO_2); 94Und1 (CF_3Cl, CF_3Br, CF_3I, CF_2Cl_2, CF_2Br_2); 98San1 (CHF_3, C_2F_6, C_3F_8, c-C_4F_8)

G 78Szm1 (CO_2); 84Szm1 (N_2O, OCS); 86Zec1 (O_2); 86Szm1 (H_2S); 86Szm2 (SO_2); 87Szm1 (H_2O); 87Szm2 (CS_2); 87Szm3 (CO_2); 89Szm1 (NH_3, OCS, N_2O); 91Szm2 (D_2O); 91Szm1 (NO); 92Szm1 (NO_2); 92Szm2 (CF_4, CCl_4); 93Szm1 (CH_3I); 94Krz1 (CH_3Br); 95Krz1 (CH_3F, CH_3Cl); 95Szm1 (C_2H_6, CH_3OH, CH_3NH_2); 95Szm2 (CH_3SH); 96Moz1 (GeH_4); 96Moz2 (C_6H_6); 96Szm1 (He-Xe, H_2, N_2, O_2, CO, NO); 96Szm2 (SO_2); 96Szm3 (N_2O, OCS, SO_2); 97Szm1 (SiH_4, $GeCl_4$); 98Kar1 (SiF_4); 98Szm1 (GeF_4); 99Moz1 ($SiCl_4$)

H 80Dal1 (H_2); 86Zec1 (O_2)

I 78Ken1 (He); 79Ken1 (SF_6); 80Ken1 (N_2); 85Jon1 (H_2); 85Jon2 (CH_4); 86Jon1 (CF_4, CF_3Cl, CF_2Cl_2, $CFCl_3$, CCl_4)

J 87Kum1 (He); 89Sub1 (H_2); 90Sub1 (O_2)

K 27Bru1 (HCl), 27Bru2 (N_2, H_2), 27Bru3 (O_2, CO, NO, CO_2, N_2O, CH_4); 29Bru1 (C_2H_2, C_2H_4), 29Bru2 (NH_3, H_2O), 30Bru1 (CH_4, C_2H_6, C_3H_8, n-C_4H_{10}), 30Bru2 (n-C_4H_{10}, iso-C_4H_{10})

L1 different L_{cell} and L_{scatt} 84Sue1 (N_2, CO, CO_2)
L2 86Sue1 (CH_4, C_2H_4, C_2H_6); 86Sue2 (H_2O); 87Sue1 (NH_3); 88Sue1 (C_6H_6); 89Sue1 (C_2H_2); 94Ham1 (HCl); 94Ham2 (H_2O, NH_3); 94Sue1 (SiH_4, CF_4); 95Ham1 (CCl_4); 97Kim1 (CO_2); 98Sue1 (CHF_3); 99Sue1 (OCS); 99Tan1 (C_3F_8, C_3H_8); 00Kim1 (H_2O, HCl, CO, CO_2, OCS, CH_4, CH_2F_2, CF_4, CCl_4, SiH_4, C_2H_2, C_2H_4, C_2H_6, C_3H_8, C_3F_8, CH_3OH, HCOOH, CH_3COCH_3, C_6H_6, n-C_5H_{12}, n-C_6H_{14}, c-C_6H_{12})
M 77Kau1 (He, Ar); 82Hof1 (CO_2 ,N_2); 83Kwa1 (CO_2); 84Kwa1 (N_2O); 86Dab1 (OCS, SO_2); 88Dab1 (O_2, CH_4, SF_6)
N 65Gol1 (He); 66Gol1 (N_2); 66Gol2 (H_2,D_2); 70Sal1 (O_2, Ne)
O 85Nic1 (He, Ne, Ar, Xe); 90Sag1, 91Sag1 (H_2O); 92Kan1 (Kr, O_2, CO); 92Nic1 (H_2, N_2); 92Kan2 (CH_4)
P 88Nis1 (Ar, N_2, H_2O, D_2O); 90Nis1 (CH_4); 91Nis1 (C_2H_4, C_2H_6, C_3H_6, cyclo-C_3H_6, C_3H_8)
Q 83Deu1 (H_2) ; 85Flo1 (CH_4, C_2H_6, C_2H_4, C_3H_8, C_3H_6, C_4H_{10}, C_4H_8)
R 80Bla1 (N_2, He); 80Win1 (H_2)
S1 Ω_{geom} $1.6\cdot10^{-4}$ sr in the 250-3000 eV energy range, $3.4\cdot10^{-4}$ sr in the 100-360 eV energy range: 81Dal1 (He); 80Dal2 (O_2, N_2, NO); 87Zec2 (Ne, Ar)
S2 Ω_{geom} $3.4\cdot10^{-4}$ sr in the 75 - 4000 eV energy range: 87Zec1 (H_2O); 87Szm3 (CO_2); 91Zec1 (CH_4); 91Szm2 (D_2O); 92Zec1 (NH_3,SiH_4,H_2S); 92Zec2 (CF_4, $CClF_3$, CCl_2F_2, CCl_3F, CCl_4); 92Zec3 (SF_6); 93Kar1 (CO); 95Zec1 (NO_2, OCS, SO_2); 95Kar1 (GeH_4); 96Moz2 (C_6H_6); 98Kar1 (SiF_4); 99Kar1 (CH_3Cl, CH_2Cl_2, $CHCl_3$); 99Moz1 ($SiCl_4$); 00Kar1 (WF_6)
T1 different energy resolution and L_{cell} 88Gar1 (N_2)
T2 90Gar1 (CO); 96Gar1 (CO_2); 96Gar2 (NH_3); 98Gar1 (CH_4)
U 94Xin1 (N_2); 95Xin1 (C_2H_2, CO); 97Xin1 (N_2O)

6.1.1.4 Semiempirical methods

In some cases (very low or high-energies) semiempirical formulae have been used to extrapolate measured total cross sections. As far as these methods have been originally developed for atoms, numerous authors use them also for molecules. In the zero-energy limit, the modified effective-range theory [62OMa1, 89Buc1] gives for σ_{el} the following formula:

$$\sigma_{el} = 4\pi\left[A_0^2 + \frac{2\pi}{3a_0}\alpha A_0 k + \frac{8\pi}{3a_0}\alpha A_0^2 k^2 \ln(ka_0) + Bk^2 + \cdots\right] \quad (7)$$

where α is the electric polarizability, a_0 is the Bohr radius, A_0 the scattering length, E is the electron energy and k its wavenumber. The modified effective-range theory has been used to extrapolate towards zero-energy the elastic cross sections in targets like CF_4 [92Man1] and C_2H_6 [98Mer1]; below inelastic thresholds it is also used to extrapolate total cross sections [80Fer1].

In the high energy limit, the Born-Bethe approximation [71Ino1] is the most frequently used. For the elastic cross sections this approximation gives:

$$\sigma_{el} = A_1\frac{R}{E} + A_2\frac{R^2}{E^2} + \cdots \quad (8)$$

where R is the Rydberg energy and the coefficients A_i are related to the atomic number Z and atomic form factors [74Ino1]. For the inelastic cross section it yields:

$$\sigma_{in} = 4\pi a_0^2 R\left[M_{tot}^2\frac{\ln(E)}{E} + M_{tot}^2\frac{\ln(4C_{tot}/R)}{E} + \gamma_{tot}\frac{R}{E^2} + \cdots\right] \quad (9)$$

where the coefficients M^2_{tot}, C_{tot}, and γ_{tot} can be obtained theoretically from the distributions of electronic moments. The Born-Bethe formulae (eqs. 8 and 9) have been indicated as the very high energy (above 10 keV) limit for the total cross section in targets like N_2 [88Gar1], CH_4 [98Gar1], NH_3 [96Gar2].

Note that other approximating formulae have been given for total cross section in the few hundreds eV - few keV range. As an example we quote the one based on Born's scattering from a screened Coulomb potential [91Zec1]

$$\sigma_{\text{tot}} = \frac{\sigma_z b}{b + \sigma_z E} \tag{10}$$

where σ_z and b are found by a fitting procedure.

In the case of polyatomic molecules, like CF_3Cl [92Zec2] or WF_6 [00Kar1] a more complex formula, similar to the one giving the integral elastic cross section for scattering on a double Yukawa potential (see [92Zec2], [00Zec1]) was used to fit the observed total cross section energy dependence.

$$\sigma = \frac{1}{A(B+E)} + \frac{1}{C(D+E)} + \frac{2}{E}\sqrt{\frac{BD}{AC}}\frac{1}{|B-D|}\left|\ln\frac{E/D+1}{E/B+1}\right| \tag{11}$$

where A, B, C, D are fitting parameters.

In some cases, in particular at low energies, the TCS almost coincides with the integral cross section for inelastic processes, like vibrational and rotational excitation. In other molecules, like CCl_4 [92Lin1] $CFCl_3$, C_6F_6 [88Mar1], CH_3I [88Ala1] the zero-energy total cross section is governed by electron attachment processes. Some approximate formulae allow to evaluate the TCS in these cases. For the rotational and vibrational excitation cross sections, the Born approximation [66Tak1, 74Iti1] can be used:

$$\sigma_{\text{rot}}(J \to J \pm 1) = \frac{8\pi}{3k^2} D^2 \frac{J_>}{2J+1} \ln\frac{k+k'}{|k-k'|} \tag{12}$$

with k being the incident electron wavenumber and k' being the scattered electron wave number, J – initial rotational number; D is the permanent dipole moment of the molecule. For example, the TCS below 0.1 eV for polar molecules like NO and CO [96Ran1] is determined by the rotational excitation.

Similarly, the vibrational excitation cross section equals

$$\sigma_{\text{vib}}(v \to v') = \frac{8\pi}{3k^2} g' \left|\langle v'|D|v\rangle\right|^2 \ln\frac{k+k'}{|k-k'|} \tag{13}$$

with $<v'|D|v>$ being the transient dipole moment matrix element for the $v \to v'$ vibrational transition and g' being the degeneration factor for this transition. Vibrational excitation determines the total cross section at energies below 1 eV in targets like CF_4 [98Lun1] or SiF_4 [98Kar1].

For the electron attachment cross sections, the experiments in the few meV energy range [87Dun1, 92Lin1] showed the applicability of Wannier's [54Vog1] threshold law: $\sigma_{\text{att}} \propto E^{1/2}$ in the zero-energy limit for targets, like CCl_4 or SF_6 [92Lin1]. At energies in the few tens of meV other types of approximating formulae have been proposed [88Ala1].

Finally, for total cross sections at intermediate and high energies we quote numerous additivity rule formulations [96Jos1, 95Jia1, 96Liu1, 99Zec1, 99Kar1] which have been published in the last years. These allow to calculate molecular cross sections starting from those of the atomic constituents. At present, the reliability of such additivity rules has not been validated, mainly due to the noise present in total cross section measurements. In the future it is possible that these rules will become useful for the evaluation of total cross section for "exotic" targets where little experimental data exist.

6.1.1.5 Data selection and analysis criteria

In this section we list the criteria used to select the experimental cross section data. After this selection, the accepted data have been handled to obtain the recommended values. The handling procedure has been codified in order to obtain criteria as uniform and as objective as possible for the various gases and various authors.

The selection has been made according to the following criteria. Total cross section data sets have been rejected when:

1. The number of measured points was very small.
2. The energy span of the measurement was much less than a decade.
3. The measurements were performed with a relative method: i.e. when the cross section values were normalized or when the values of one key parameter were obtained through a normalization procedure.
4. The measurements were in large disagreement with the majority of other existing measurements in the same energy range.

In several instances isolated data points or groups of points were rejected when metadata obtained from more recent articles of the same research group or from more recent articles from competing groups give evidence of systematic errors limited to those points.

We note that in all the cases where we have found measurements from one group only, we have relaxed the above conditions giving those values as the recommended cross sections. Obviously, in such cases the error bar on the recommended values is at least as large as the error bars declared by the authors. We warn that sometimes these error bars have been underestimated.

The selected data have been handled to obtain the recommended values. We note here the different role of statistic and systematic errors. Systematic errors can be described as introducing an unknown multiplicative factor, so that the published values can be thought as the product of the "real" cross section times this factor. Statistic errors can be described as introducing an additional random noise on the "real" cross sections and thus in the published values. As a consequence of this distinction, we have first smoothed each published data set in order to reduce the random noise. The smoothing has been done by filtering the data or by fitting them with appropriate functions. Different filtering and fitting functions have been chosen for different gases and for different energy ranges according to the density of data points and to the behaviour of the cross section as a function of the energy. This smoothing operation results normally in a reduction of the statistical noise by a factor 5 to 10.

The smoothed data sets from different laboratories have been averaged giving a weight to each of them. Normally all data, for a given gas and a given energy range, had the same weight. A differentiated weighting has been used whenever the absolute errors published by the authors where significantly different. A differentiated weighting has been used in some instances when available metadata have evidenced the possibility of systematic errors larger than those declared by the authors.

We note here that different authors have measured cross sections at different energy values, so that only rarely it is possible to have data from different groups at the same given energy. The use of a smoothing procedure circumvents this difficulty, allowing us to make averages at any chosen energy and to give recommended values for different gases with the same "comb" on the energy axis.

The region of resonances (see for instance the N_2 molecule) has been handled in the following way. The recommended values have been obtained as averages over several measurements performed by different methods. Additionally, the resonant region has been presented with an extra table with values from a high resolution, low noise measurements, like [80Ken1] for N_2. An extra figure (Fig. 6.1.3, p. 6-13) with a resonant structure from "backward" scattering [93Zie1, 96Ran2] has been added for NO and O_2, for comparison reasons. Note that the data presented in Fig. 6.1.3 are not exactly total cross sections.

Recommended values obtained through this procedure are presented in numerical form in Tables 6.1.2 to 6.1.13. Figures 6.1.2 and 6.1.4 to 6.1.9 present the recommended values as bold continuous lines. In these figures also the original (uncorrected) experimental data are presented as data points or thin lines. The figures are intended to give a visual representation of the cross section dependence on the energy. The scatter of the points (where more than one measurement exist) allows an immediate evaluation of the probable error bar in each energy range.

We note that the grouping of targets in the figures does not follow the grouping in the tables. This has been done to optimize the use of printed space. We also note that Tables 6.1.11, 6.1.12 and 6.1.13 do not contain recommended values but rather the experimental data from a single group. These are the only data available for the targets and therefore can be considered as recommended data.

6.1.2 Diatomic molecules

Table 6.1.2. Recommended total cross sections for diatomic molecules.

Energy [eV]	Cross section [10^{-16} cm^2]				
	H_2	N_2	O_2	CO	NO
0.1	9.23	4.88	3.83 (c1)		
0.12	9.47	5.13	4.02	(d1)	
0.15	9.76	5.56	4.22		(e1)
0.17	9.93	5.85	4.33		
0.2	10.1	6.25	4.47		
0.25	10.5	6.84	4.65		
0.3	10.7	7.32	4.79	9.13	
0.35	11.0	7.72	4.91	9.69	
0.4	11.2	8.06	5.07	10.2	
0.45	11.4	8.33	5.20	10.6	
0.5	11.6	8.61	5.31 (c2)	10.9	
0.6	11.9	8.96	5.49	11.7	
0.7	12.3	9.25	5.64	12.2	
0.8	12.8	9.48	5.77	12.7	
0.9	13.2	9.66	5.87	13.3	
1.0	13.5 (a1)	9.85	5.97	14.1	
1.2	14.2	10.2	6.18	16.7	
1.5	15.0	11.2	6.36	29.1	
1.7	15.5	13.3	6.45	38.9	
2.0	16.0	25.7	6.56 (c3)	43.3 (d2)	
2.5	16.5	28.5 (b1)	6.68	33.3	9.70
3.0	16.6	21.0	6.84	23.8	9.47
3.5	16.6	14.6	7.01	18.9	9.32
4.0	16.3	13.2	7.18	16.4	9.25
4.5	15.9	12.3	7.36	15.2	9.22
5.0	15.4	11.8	7.55	14.5	9.23
6.0	14.4	11.4	7.93	13.7	9.32
7.0	13.3	11.4	8.39	13.5	9.48
8.0	12.4	11.5	9.16	13.6	9.68
9.0	11.6	11.7	9.91	13.5	9.92
10	10.9	12.0	10.4	13.2	10.2
12	9.61	12.4	10.8	13.3	11.0
15	8.19	13.2	10.7	13.9	11.5
17	7.46	13.5	10.7	14.3	11.6
20	6.60	13.7	10.8	14.5	11.4
25	5.61	13.5	11.0	14.1	11.1
30	4.97	13.0	11.0	13.6	10.7
35	4.54	12.4	10.9	13.2	10.3
40	4.19	12.0	10.7	12.7	9.97
45	3.91	11.6	10.5	12.3	9.73
50	3.68	11.3	10.3	11.9	9.53
60	3.36	10.7	9.87	11.2	9.18
70	3.06	10.2	9.52	10.7	8.89
80	2.86	9.72	9.23	10.2	8.64
90	2.68	9.30	8.98	9.69	8.42

Table 6.1.2 (continued)

Energy [eV]	Cross section [10^{-16} cm^2]				
	H_2	N_2	O_2	CO	NO
100	2.54	8.94	8.68	9.27	8.22
120	2.25	8.33	7.97	8.53	7.86
150	1.98	7.48	7.21	7.64	7.44
170	1.84	7.02	6.78	7.15	7.13
200	1.66	6.43	6.24	6.53	6.64
250	1.43	5.66	5.51	5.71	5.93
300	1.24	5.04	4.94	5.09	5.25
350	1.11	4.54	4.55	4.57	4.75
400	1.00	4.15	4.17	4.16	4.34
450	0.914	3.82	3.85	3.82	4.00
500	0.841	3.55	3.58	3.54	3.70
600	0.700	3.14	3.11	3.13	3.23
700	0.614	2.79	2.76	2.79	2.87
800	0.516	2.55	2.49	2.52	2.58
900	0.464	2.32	2.26	2.31	2.34
1000	0.422 (a2)	2.13	2.08 (c4)	2.13	2.15

Notes

The following sets of data (the energy ranges are given in brackets) have been used to obtain the recommended TCS.

H_2: [80Fer1] (0.02-1.0); [96Szm1] (0.4-250); [80Dal1] (0.6-100); [85Jon1] (1-50), corrected by 0 % at 4 eV up to + 3 % at 50 eV; [92Nic1] (4-300); [82Hof1] (4.9-500); [80Win1] (25-750); [96Kar1] (70-1000). See. Fig. 6.1.2.

N_2: [95Sun1] (0.1-10); [96Szm1] (1.0-250); [91Fer1] (0.1-1); [80Ken1] (0.5-50) corrected by 0 % at 5 eV up to + 7 % at 50 eV; [82Hof1] (3.8-700); [92Nic1] (4-300); [88Nis1] (10-500); [80Bla1] (100-750); [93Kar1] (121-1000); [94Xin1] (500-1000); [88Gar1] (600-1000). See. Fig. 6.1.2.

O_2: [90Sub1] (0.15-1.1); [96Szm1] (0.4-250); [70Sal1] (2.3-7); [86Zec1] (0.15-100), Trento data; [86Zec1] (2-15), Gdańsk data; [92Kan1] (5-300); [88Dab1] (51-500); [80Dal2] (100-1000); [96Kar1] (100-1000). See. Fig. 6.1.2 and Fig. 6.1.3.

CO: [86Buc1] (0.5-4.9); [96Szm1] (0.4-250); [83Kwa1] (4.8-500); [92Kan1] (5-300); [93Kar1] (80-1000); [95Xin1] (400-1000); [90Gar1] (380-1000). See. Fig. 6.1.2.

NO: [91Szm1] (2.5-160); [96Szm1] (2.5-250); [74Zec1] (2.5-9.5); [80Dal2] (144-1000). See. Fig. 6.1.2 and Fig. 6.1.3.

(a1) All different sets of data at low energies are in good agreement apart from data in [80Fer1] which are somewhat lower than the recommended set above 1 eV.

(a2) Note that scattering in H_2 at high energies is extremely forward centred; existing data [96Kar1] could be underestimated due to angular resolution error.

(b1) A vibrational structure due to the presence of $^2\Pi_g$ resonant state is visible in TCS in the 2 - 4 eV energy region. See Table 6.1.3a for detailed values of TCS in this range.

(c1) The 0.1 eV point has been extrapolated from data in [90Sub1] and [86Zec1]. The early TCS measurements in O_2 [30Ram1] indicated a rise of TCS below 0.1 eV up to about $6 \cdot 10^{-16}$ cm^2 at 0.04 eV [see 96Zec1].

(c2) A resonant structure is present in O_2 TCS between 0.2 - 1 eV [74Lan1, 80Fer1, 86Zec1]. A series of narrow peaks was observed also in other experiments [62Sch1, 70Bon1, 71Lin1, 88Fie1, 94Ran1, 95All1]. Only recent TCS measurements [99Buc1] have been performed with an energy resolution sufficient to distinguish the structure. See also Fig. 6.1.3.

(c3) Different TCS measurements [70Sal1, 86Zec1, 90Sub1, 96Szm1] in O_2 at 1.5 - 6 eV are in serious disagreement. Present recommended values are average of results quoted in the table caption above. They agree well with TCS from Tokyo lab [85Kat1]. The recent elastic cross sections between 1 - 5 eV [95Sul1, see also [97Gre1] are slightly higher than our recommended TCS, with differences remaining well within the declared [95Sul1] error bar. In this energy range the scattering into inelastic channels (vibrational and $a^1\Delta_g$, $b^1\Sigma_g^+$ electronic excitation) is in the 10^{-18} cm^2 range and contributes less than 1 % to TCS [71Lin1, 92Mid1, 93Shy1].

(c4) Present high energy TCS in O_2 are slightly lower than in N_2 and CO, being average values of only Trento TCS [80Dal2, 96Kar1]. Comparative measurements, say at 2500 eV, [93Kar1, 96Kar1] show that O_2 TCS is higher ($0.92 \cdot 10^{-16}$ cm^2) than the N_2 ($0.89 \cdot 10^{-16}$ cm^2) value.

(d1) The backward-scattering measurements from Daresbury lab [96Ran1] indicate a rise of TCS below 0.12 eV, attributed to the rotational excitation, see formula (eq.12) in the introduction.

(d2) A $^2\Pi$ resonant state is present between 1 and 4 eV. A maximum TCS is reached at 2 eV.

(e1) TCS at very low energies in NO is dominated by the presence of resonant states. See Table 6.1.3b for detailed values of TCS in the 0.16 - 2.0 eV energy region.

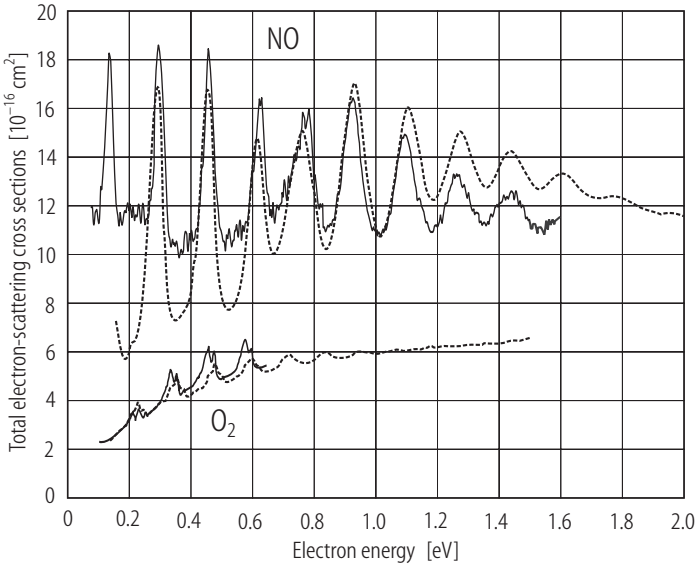

Fig. 6.1.3. Low-energy resonance region in O_2 and NO (solid lines: Orsay and Daresbury experiments using synchrotron-radiation electron sources; broken lines: total cross sections from Canberra lab).

Synchrotron radiation experiments:
O_2, total cross section obtained with use of a strong guiding magnetic field [93Zie1];
NO, signal of electrons elastically scattered into 60°-120° angle [96Ran2].

Total cross sections:
O_2 [99Buc1], NO [96All1].

Notes. A resonant structure in NO total cross section was observed in numerous measurements [74Zec1, 91Szm1] but only in Canberra lab it was measured with a high (3 meV) energy resolution [96All1]. Also in O_2, only the measurement from Canberra lab yielded a well-distinct structure [99Buc1]. Therefore, in this figure we compare two available "scattered electrons" measurements in NO and O_2 from a synchrotron-radiation electron-source spectrometer with the TCS data from Canberry laboratory. Note the above mentioned difference in the detection method in the experiments with the synchrotron-radiation electron source. Note also that the Orsay data show in O_2 a double structure of the peaks due to the spin-orbit coupling in the $^2\Pi_g$ O_2^- resonant state. Such a structure was observed, for example, also in time-of-flight measurements of [74Lan1].

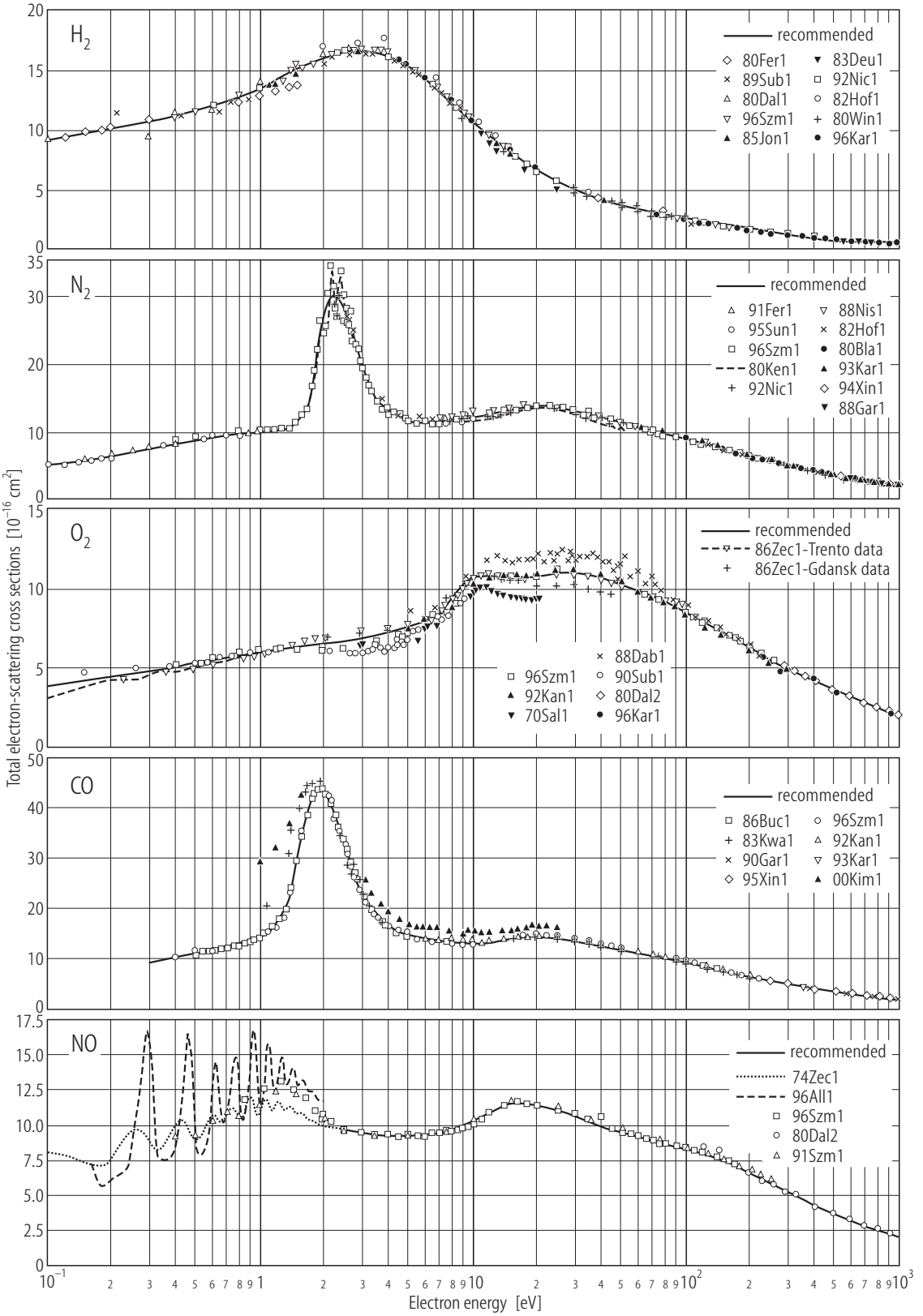

Fig. 6.1.2. Overview of experimental and recommended total cross sections for H_2, N_2, O_2, CO, NO.

Table 6.1.3a. Resonant structure in N_2 total cross section (from [80Ken1]).

Energy [eV]	σ [10^{-16} cm^2]	Energy [eV]	σ [10^{-16} cm^2]	Energy [eV]	σ [10^{-16} cm^2]	Energy [eV]	σ [10^{-16} cm^2]
1.002	9.91	1.584	11.79	2.290	28.32	3.267	16.75
1.012	9.88	1.604	11.86	2.308	27.14	3.298	16.69
1.023	9.86	1.625	12.04	2.326	26.19	3.328	16.60
1.033	9.96	1.647	12.30	2.345	26.36	3.360	16.51
1.044	10.05	1.668	12.66	2.364	27.64	3.391	16.02
1.055	10.04	1.691	13.00	2.383	28.82	3.423	15.90
1.066	10.01	1.713	13.51	2.403	30.79	3.456	15.37
1.078	10.21	1.736	13.79	2.422	32.06	3.489	15.16
1.089	10.10	1.760	14.44	2.463	31.80	3.523	15.05
1.101	10.17	1.784	15.28	2.483	30.85	3.557	15.05
1.113	10.07	1.809	16.36	2.504	29.19	3.591	14.55
1.125	10.06	1.834	17.46	2.525	27.25	3.626	14.51
1.137	9.95	1.853	18.61	2.546	25.83	3.662	14.16
1.150	10.03	1.866	19.12	2.567	25.18	3.698	14.14
1.162	10.22	1.879	20.23	2.589	25.19	3.734	13.86
1.175	10.31	1.892	21.19	2.611	25.63	3.772	13.71
1.188	10.15	1.906	22.26	2.633	27.03	3.809	13.63
1.202	10.14	1.922	23.23	2.656	27.90	3.848	13.34
1.215	10.34	1.936	24.26	2.679	27.78	3.886	13.50
1.229	10.27	1.951	25.40	2.702	26.74	3.926	13.31
1.243	10.33	1.965	25.95	2.725	25.90	3.966	13.09
1.258	10.32	1.980	25.88	2.749	24.33	4.007	13.21
1.272	10.43	1.994	25.84	2.773	22.95	4.048	12.92
1.287	10.42	2.009	25.61	2.798	22.19	4.090	12.89
1.302	10.31	2.024	25.37	2.822	22.32	4.132	12.88
1.317	10.44	2.039	24.52	2.848	22.49	4.176	12.48
1.333	10.36	2.055	23.81	2.873	22.84	4.220	12.44
1.349	10.61	2.070	23.69	2.899	23.28	4.264	12.54
1.365	10.66	2.086	23.83	2.925	22.39	4.310	12.34
1.381	10.55	2.102	24.13	2.951	21.64	4.356	12.31
1.398	10.75	2.118	25.26	2.978	20.51	4.402	12.25
1.415	10.76	2.134	27.18	3.005	19.73	4.450	12.19
1.432	10.80	2.151	29.13	3.033	19.29	4.498	12.15
1.450	10.96	2.167	30.77	3.061	19.30	4.547	11.95
1.468	10.97	2.184	32.78	3.089	19.17	4.597	12.00
1.487	10.98	2.201	33.22	3.118	19.24	4.648	11.99
1.505	11.24	2.219	33.58	3.147	18.69	4.700	11.89
1.524	11.29	2.236	32.62	3.176	18.22	4.752	11.90
1.544	11.40	2.254	31.11	3.206	17.46	4.806	11.79
1.563	11.58	2.272	29.75	3.236	16.95	4.860	11.74

Notes

This structure is due to the presence of $^2\Pi_g$ resonant state [62Sch2] which manifests itself in total, elastic and vibrational excitation cross sections, see e.g. [85All1]. Different recent TCS measurements [95Sun1, 96Szm1] agree on the position and height of the peaks. The resonant structure in N_2, in particular as measured in Ref. [80Ken1] is the most frequently used as standard in the energy scale calibration for low-energy electron scattering.

Table 6.1.3b. Resonant structure in NO total cross section (digitized from Fig. 1 in Ref. [96All1]).

Energy [eV]	σ [10^{-16} cm^2]	Energy [eV]	σ [10^{-16} cm^2]	Energy [eV]	σ [10^{-16} cm^2]	Energy [eV]	σ [10^{-16} cm^2]
0.160	7.28	0.445	14.52	0.785	14.73	1.160	13.21
0.165	6.74	0.452	16.03	0.792	13.97	1.177	12.46
0.170	6.20	0.454	16.28	0.799	13.40	1.197	12.13
0.174	5.67	0.458	16.79	0.803	12.79	1.217	12.53
0.191	5.63	0.460	16.25	0.814	11.68	1.224	12.89
0.207	6.42	0.465	15.93	0.818	11.17	1.237	13.47
0.224	6.42	0.470	15.60	0.821	10.78	1.240	13.72
0.234	6.71	0.475	15.42	0.831	10.35	1.253	14.26
0.241	7.25	0.480	14.09	0.838	10.31	1.260	14.65
0.247	7.79	0.483	12.51	0.855	10.49	1.273	14.91
0.250	8.65	0.488	10.86	0.861	11.18	1.290	14.91
0.253	9.52	0.492	9.64	0.868	11.54	1.301	14.55
0.259	10.34	0.499	8.89	0.874	11.82	1.311	14.08
0.268	11.64	0.503	8.02	0.884	12.29	1.325	13.54
0.274	13.15	0.520	7.77	0.890	13.44	1.335	13.15
0.277	13.72	0.547	7.88	0.900	14.02	1.352	12.79
0.284	14.51	0.553	8.24	0.903	14.52	1.379	12.87
0.286	15.55	0.569	9.32	0.910	15.06	1.396	13.26
0.288	15.81	0.582	10.37	0.916	16.14	1.412	13.77
0.290	15.99	0.592	11.62	0.942	17.00	1.432	14.09
0.292	16.20	0.598	12.31	0.949	16.57	1.445	14.24
0.294	16.52	0.601	12.95	0.953	16.14	1.469	13.84
0.296	16.88	0.607	13.60	0.960	15.60	1.490	13.31
0.298	16.42	0.614	14.21	0.964	14.92	1.513	12.91
0.300	16.20	0.620	14.75	0.971	14.27	1.527	12.73
0.302	15.95	0.634	14.29	0.982	12.59	1.557	12.84
0.304	15.77	0.638	13.64	0.992	11.69	1.574	13.06
0.306	15.52	0.641	12.88	1.000	11.19	1.587	13.24
0.308	15.09	0.649	12.02	1.030	10.94	1.601	13.35
0.310	14.94	0.653	11.23	1.039	11.62	1.652	12.92
0.320	9.59	0.660	10.66	1.053	12.05	1.675	12.60
0.327	8.48	0.663	10.16	1.062	13.09	1.713	12.35
0.331	7.72	0.683	10.09	1.068	13.92	1.753	12.43
0.348	7.26	0.693	10.59	1.078	14.43	1.793	12.43
0.385	7.76	0.696	10.84	1.085	14.93	1.830	12.14
0.402	8.45	0.706	11.49	1.088	15.32	1.868	11.90
0.411	9.46	0.716	11.92	1.101	15.79	1.912	11.75
0.414	10.21	0.726	12.68	1.114	16.01	1.935	11.68
0.420	10.89	0.739	13.54	1.125	15.51	1.949	11.79
0.430	11.76	0.745	14.26	1.128	15.36	1.996	11.65
0.433	12.65	0.752	14.73	1.135	14.97		
0.442	13.70	0.772	14.98	1.149	13.78		

Notes

This resonant structure in NO was detected with different methods [71Spe1, 75Tro1, 96Ran2]. Below 0.7 eV only one "shape" resonance state is present; at 0.7 - 2.0 eV it overlaps with two more states [77Tei1, 86Ten1]. The TCS measurements in ref. [96All1] were performed with a much better (± 3 meV at 0.3 eV) energy resolution than other TCS experiments in this range [74Zec1, 91Szm1, 96Szm1]. Differently than the N_2 data given in Table 6.1.3a, the resonant structure in NO is not an established standard.

6.1.3 Triatomic molecules

Table 6.1.4. Recommended total cross sections for triatomic molecules.

Energy [eV]	Cross section [10^{-16} cm^2]					
	CO_2	N_2O	NO_2	OCS	SO_2	CS_2
0.1	49.7					
0.12	44.3					
0.15	38.1	10.3				
0.17	34.9	9.69				
0.20	31.1	8.96		51.6 (d1)	40.3 (e1)	
0.25	26.4	8.08		48.0	38.9	
0.30	23.0	7.48		44.0	37.8	
0.35	20.5	7.06		39.9	36.8	
0.40	18.6	6.77		36.0	36.0	22.4 (f1)
0.45	17.0	6.58		32.7	35.2	21.1
0.5	15.7	6.48		29.8	34.5	20.0
0.6	13.6	6.57	16.9	25.8	33.3	18.4
0.7	11.9	6.70	16.4	25.7	32.3	17.6
0.8	10.5	6.98	16.0	29.0	31.2	17.6
0.9	9.25	7.37	15.6	34.3	30.3	18.1
1.0	8.29	8.08	15.3 (c1)	42.5	29.8	19.1
1.2	7.22	10.2	14.7	51.3 (d2)	29.4	22.0
1.5	6.32	14.2	14.1	31.8	29.9	27.7
1.7	6.02	18.1	13.7	24.4	30.6	30.8
2.0	5.94	25.6	13.3	20.3	31.8	33.4 (f2)
2.5	6.81	26.9 (b1)	12.9	19.4	33.0 (e2)	37.5
3.0	8.77	18.6	12.7	22.5	33.4	42.2
3.5	13.3	13.6	12.6	26.3	33.7	46.9
4.0	14.9 (a1)	11.0	12.6	27.5	33.8	50.0
4.5	11.3	9.73	12.7	27.5	33.8	51.1
5.0	9.06	9.24	12.8	27.5	33.6	51.8 (f2)
6.0	8.44	9.37	13.2	28.2	32.2	52.3
7.0	9.21	10.4	13.7	29.4	31.5	52.4
8.0	10.3	11.9	14.3	30.6	31.1	52.4
9.0	11.3	13.4	14.7	31.7	30.8	52.4
10	12.2	14.5	14.9	32.3	30.7	52.3
12	14.2	15.9	14.8	32.8	30.7	51.8
15	15.8	16.4	14.5	32.2	29.5	50.4
17	16.4	16.6	14.7	31.2	28.4	48.7
20	17.0	17.4	14.7	30.0	26.4	45.7
25	17.8	17.7	14.4	28.5	25.0	39.3
30	18.0 (a2)	17.6	14.1	27.4 (d3)	24.0 (e3)	34.7
35	17.6	17.2	13.9	26.5	23.2	32.0
40	17.0	16.7	13.7	25.7	22.7	30.8
45	16.4	16.3	13.6	24.8	22.3	29.9
50	15.8	15.8 (b2)	13.4	23.9	22.0	28.1
60	14.8	15.0	13.2	22.3	21.1	25.2
70	14.1	14.4	12.9	21.1	20.1	23.8
80	13.5	13.8	12.6	20.2	19.1	22.5 (f3)
90	13.1	13.2	12.2	19.2	18.1	

Table 6.1.4 (continued)

Energy [eV]	Cross section [10^{-16} cm^2]					
	CO_2	N_2O	NO_2	OCS	SO_2	CS_2
100	12.6	12.6	11.8	18.4	17.2	
120	11.8	11.6	10.9	16.9	15.7	
150	10.6	10.4	9.87	15.1	13.9	
170	10.0	9.78	9.28	14.2	13.1	
200	9.24	8.87	8.55	13.0	12.2	
250	8.20	7.80	7.65	11.5	11.0	
300	7.39	7.12	6.97	10.3	9.99	
350	6.73	6.46	6.40	9.39	9.16	
400	6.08	5.92	5.92	8.63	8.46	
450	5.62	5.47	5.50	7.98	7.87	
500	5.23	5.08	5.14	7.43	7.35	
600	4.63	4.44	4.55	6.58	6.51	
700	4.16	3.94	4.07	6.08	5.84	
800	3.78	3.56	3.69	5.50	5.30	
900	3.47	3.26	3.37	5.02	4.85	
1000	3.20	3.01	3.11	4.63	4.48	

Notes

The following sets of data (the energy ranges are given in brackets) have been used to obtain the recommended TCS.

CO_2 [87Buc1] (0.1-5); [81Fer1] (0.07-3); [97Kim1] (1.0-2.9, 4.8-90); [83Kwa1] (3-500); [87Szm3] (0.5-80) Gdańsk data; [87Szm3] (72-1000) Trento data; [96Gar1] (400-1000). See Fig. 6.1.4.

N_2O [30Ram2] (0.15-1.25), [84Szm1] (0.6-16.5), [96Szm3] (17-250), [84Kwa1] (1.2-500), [97Xin1] (600-1000). See Fig. 6.1.4.

NO_2 [92Szm1] (0.6-220), [95Zec1] (100-1000). See Fig. 6.1.4.

OCS [84Szm1] (0.2-40), [89Szm1](40-100), [86Dab1] (1.6-40), [99Sue1] (1.6-600) [95Zec1] (121-1000). See. Fig. 6.1.4.

SO_2 [96Szm3] (0.5-200); [93Wan1] (0.2-12); [95Zec1] (144-1000). See Fig. 6.1.4.

CS_2 [87Szm2] (0.4-80).

(a1) TCS between 2.5 - 5 eV is characterized by a $^2\Pi_u$ shape resonance. A maximum value of $15.8 \cdot 10^{-16}$ cm^2 is reached at 3.8 eV.

(a2) We note some discrepancy at intermediate energies where TCS from the Gdańsk lab [87Szm3] are lower than those from Detroit lab [83Kwa1] and TCS corrected for the angular resolution error from Tokyo lab [97Kim1]; the recommended TCS are averaged over all the three laboratories.

(b1) TCS between 1 - 4 eV is characterized by two resonances [84And1]. A maximum value of $28.4 \cdot 10^{-16}$ cm^2 is reached at 2.3 eV.

(b2) Earlier TCS from Gdańsk lab [84Szm1, 89Szm1] at 20 - 100 eV have not been included in the averaged values being lower than the successive data from the same group [96Szm3] and those from the Detroit lab [84Kwa1].

(c1) Electron transmission spectra [73San1] and vibrational excitation studies [91Ben1] indicate the presence of resonant states between 0.1 - 1.8 eV; no structures were seen in TCS [92Szm1].

(d1) The sum of elastic and vibrational excitation cross section [87Soh1] exceeds TCS from Gdańsk lab [84Szm1] and amounts to 57.2 at 0.4 eV and $39.4 \cdot 10^{-16}$ cm^2 at 0.6 eV. Note that Gdańsk data at very low energies could be effected by a high uncertainty in the electron current measurement, in the 10^{-13} A range.

(d2) TCS between 0.7 - 2 eV is characterized by a $^2\Pi$ resonance, seen also in the vibrational excitation [87Soh1] and dissociative attachment [75Zie1] channels. A maximum TCS of $52.8 \cdot 10^{-16} cm^2$ is reached at 1.15 eV.

(d3) Differently than in SO_2 and N_2O, the successive measurements in OCS at intermediate energies from Gdańsk lab [96Szm1] coincide with earlier data [84Szm1]. However, they disagree with the data in [86Dab1] and recent TCS from the Tokyo apparatus [99Sue1]; the recommended TCS are averaged over all three laboratories.

(e1) Low energy data in SO_2 show large discrepancies [86Szm2, 86Dab1, 93Wan1, 96Szm2].

(e2) Two resonant states are present in electron scattering on SO_2 at 2 - 5 eV [73San1, 83And1, 94Gul1].

(e3) More recent TCS from Gdańsk lab [96Szm2, 96Szm3] differ rather seriously at intermediate energies from the previous ones [86Szm1] but coincide with TCS from the Detroit lab [86Dab1].

(f1) The only existing TCS data [87Szm2] agree in shape with elastic cross sections [87Soh1] at 0.3 - 5 eV.

(f2) At low energies TCS shows two weak shoulder structures, at about 2 and 5 eV, probably due to resonant states, as seen in the dissociative attachment channel [87Dre1].

(f3) At 80 eV the TCS from [87Szm2] and therefore also our recommended values, can be underestimated, being lower than the theory [97Raj1].

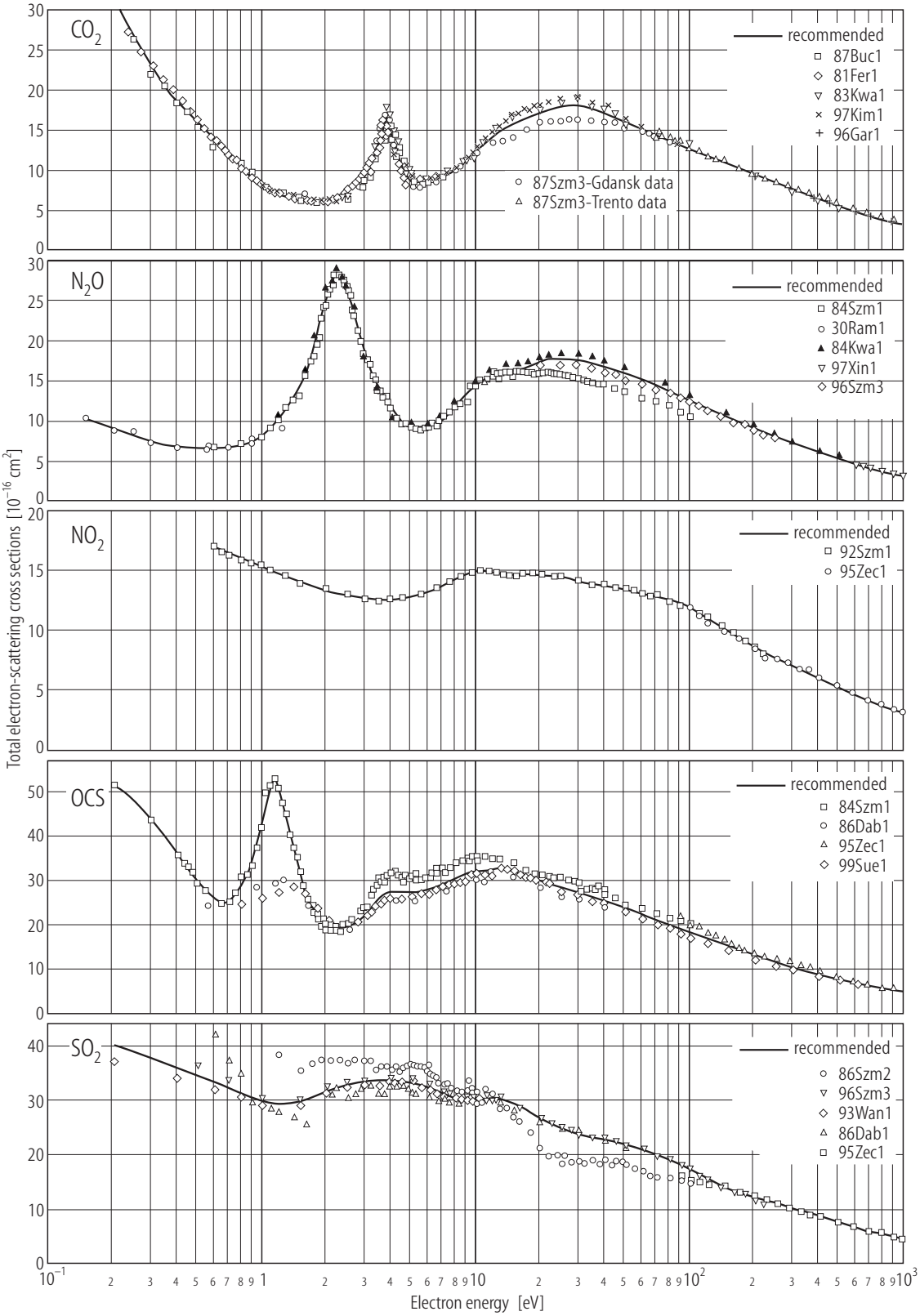

Fig. 6.1.4. Overview of experimental and recommended total cross sections for CO_2, N_2O, NO_2, OCS, SO_2.

6.1.4 Hydrides

Table 6.1.5. Recommended total cross sections for some hydrides.

Energy [eV]	Cross section [10^{-16} cm^2]			
	NH_3	H_2O (b1)	H_2S	HCl (d1)
0.5		71.4		
0.6		61.4		
0.7		53.8		
0.8		47.9		35.5
0.9		43.2		33.9
1.0	14.5 (a1)	39.4 (b2)	32.0	32.2
1.2	13.3	33.8	28.4	28.9
1.5	12.0	28.4	25.1	25.3
1.7	11.4	26.1	25.9	23.7
2.0	10.8	23.7	29.1 (c1)	22.4
2.5	10.5	21.6	31.8	22.1
3.0	10.7	20.5	31.7	23.1 (d2)
3.5	11.4	20.0	31.3	23.5
4.0	12.6	19.5	31.2	23.6
4.5	14.0	19.5	31.6	23.6
5.0	15.6	19.7	32.5	23.6
6.0	18.0	20.2	35.5	23.6
7.0	20.3	20.7	38.7	24.2
8.0	21.9	21.1	39.9 (c1)	25.6
9.0	22.8	21.2	39.8	27.4
10	22.9	20.9	39.0	28.0
12	21.8	19.1	36.4	28.0
15	20.1	17.3	32.1	26.6
17	19.1	16.5	30.9	24.9
20	17.8	15.6	30.0	22.2
25	16.1	14.0	28.0	20.5
30	14.8	12.7	25.0	19.0
35	13.8	11.7	22.1	17.2
40	13.0	10.9	20.4	15.9
45	12.3	10.3	19.1	14.9
50	11.8	9.78	18.2	14.0
60	10.9	8.98	17.3	12.7
70	10.3	8.37	16.1	11.7
80	9.68	7.89	15.0	10.9
90	9.10	7.56	14.0	10.2
100	8.57	7.17	13.1	9.67
120	7.64	6.50	11.7	8.79
150	6.67	5.74	10.3	7.81
170	6.17	5.34	9.57	7.29
200	5.55	4.83	8.71	6.66
250	4.76	4.17	7.61	5.85
300	4.21	3.68	6.79	5.23
350	3.75	3.26	6.14	4.74
400	3.38	2.95	5.61	4.34
450	3.13	2.71	5.17	
500	2.88	2.50	4.80	

Table 6.1.5 (continued)

Energy [eV]	Cross section [10^{-16} cm^2]			
	NH_3	H_2O (b1)	H_2S	HCl (d1)
600	2.50	2.19	4.20	
700	2.21	1.93	3.74	
800	1.99	1.73	3.37	
900	1.81	1.56	3.06	
1000	1.66	1.43	2.81	

Notes

The following sets of data (the energy ranges are given in brackets) have been used to obtain the recommended TCS.

H_2O [87Szm1] (0.5-80), [90Sag1] (25-300), [88Nis1] (40-500), [87Zec2] (80-1000). See Fig. 6.1.5.
NH_3 [89Szm1] (1-100), [92Zec1] (75-1000), [96Gar2] (300-1000). See Fig. 6.1.5.
H_2S [86Szm1] (1-100), [92Zec1] (75-1000). See Fig. 6.1.5.
HCl [94Ham1] (0.8-400). See Fig. 6.1.5.

(a1) At low energies two sets of TCS in NH_3 from Tokyo lab – those uncorrected for forward scattering [87Sue1] and the corrected ones [94Ham2] differ substantially. The data in [87Sue1] agree well in shape with the data in [87Szm3] and differ by 0 % at 4 eV, 28 % at 8 eV and 0 % at 400 eV. The TCS in [94Ham2] does not show a maximum and rises towards the zero energy reaching 29.0 at 5 eV, 45.7 at 2 eV and $76.2 \cdot 10^{-16}$cm^2 at 1 eV.

(b1) D_2O total cross sections as measured by [91Szm2] and [88Nis1] practically coincide with the H_2O data from the same laboratories, [87Szm1] and [88Nis1], respectively.

(b2) Low energy TCS in H_2O is subject to a big uncertainty. Two sets of data from Tokyo lab, the uncorrected for forward scattering [86Sue2] and the corrected one [94Ham2, 00Kim1], differ substantially, see Fig. 6.1.5. The TCS in [94Ham2] does not show a maximum and rises towards the zero energy reaching 30.2 at 5 eV, 54.2 at 2 eV and $110 \cdot 10^{-16}$ cm^2 at 1 eV. These data are in agreement with the theory [92Yua1] who suggested that maxima observed in H_2O [29Bru2, 87Szm1, 91Sag1] and NH_3 could be experimental artifacts due to angular resolution errors.

(c1) Structures in TCS in H_2S at about 2.5 and 8 eV are due to resonant scattering. An enhancement of the cross section was seen at 2-3 eV in the vibrational channel [78Roh1, 93Gul1]. Several maxima between 2 eV and 10 eV were observed in the dissociative attachment channel [72Azr1, 73Tro1, 85Bel1, 93Rao1].

(d1) Recommended TCS in HCl are based exclusively on the Tokyo lab results [94Ham1]. We note, that these experimental data are lower than the early TCS measurements [27Bru1] in the 4 - 35 eV range and lower than the sum of elastic + rotational excitation cross [89Rad1, 95Got1], by 20 - 30 % in the 0.8 - 20 eV energy range.

(d2) The hump in TCS at about 3 eV reflects the presence of a $^2\Sigma^+$ resonant state [89Rad1], seen also in the vibrational [75Roh1, 89Kno1, 89Kno2] and rotational [89Rad1] excitation channels.

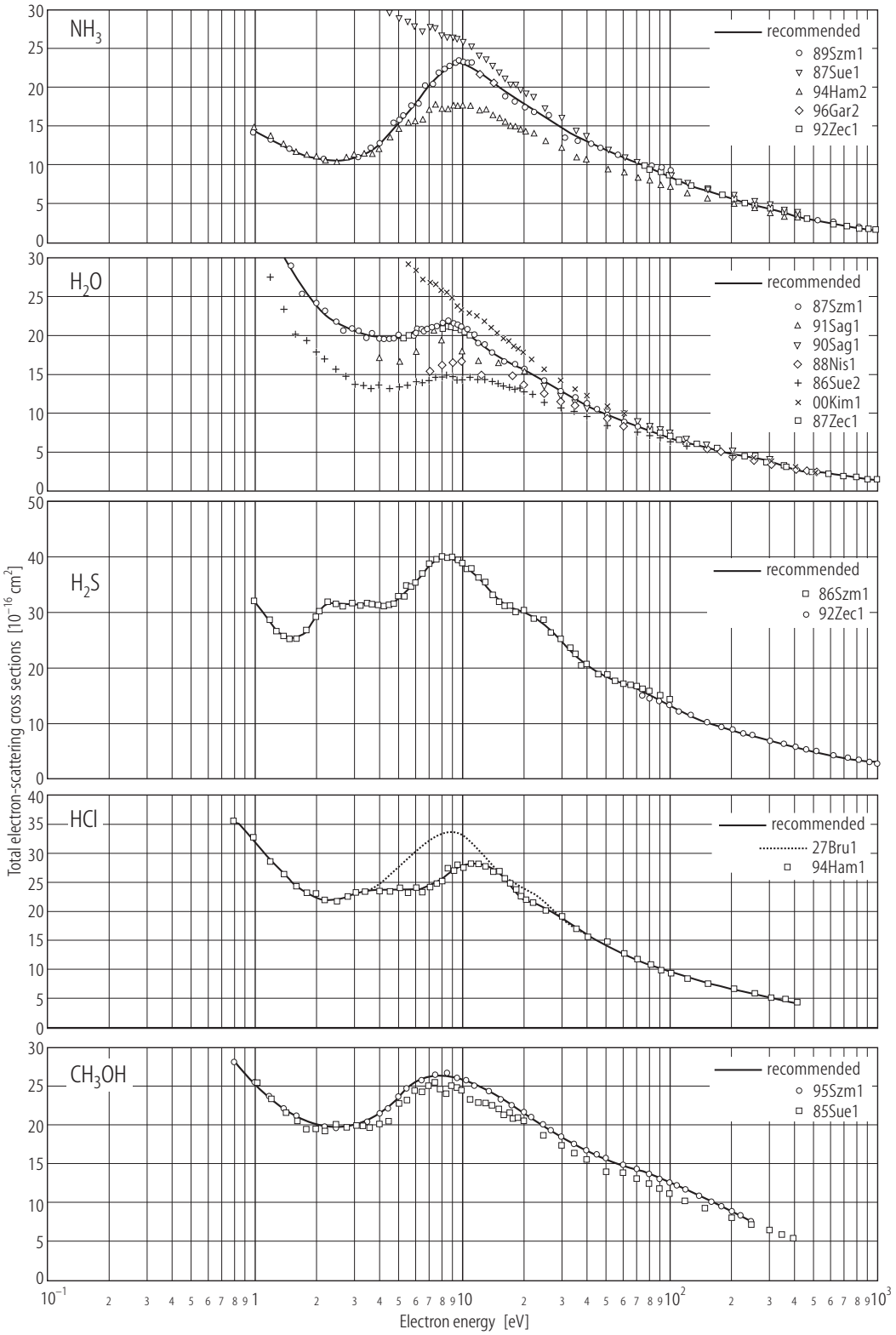

Fig. 6.1.5. Overview of experimental and recommended total cross sections for NH_3, H_2O, H_2S, HCl, CH_3OH.

6.1.5 Hydrocarbons

Table 6.1.6. Recommended total cross sections for hydrocarbons.

Energy [eV]	Cross section [10^{-16} cm^2]					
	CH_4	C_2H_2	C_2H_4	C_2H_6	C_3H_8	C_6H_6
0.1	4.20	9.41 (b1)			(e1)	
0.12	3.45	9.20				
0.15	2.72	9.50				
0.17	2.46	9.90				
0.2	2.13	10.6				
0.25	1.77	11.7				
0.3	1.55	12.7				
0.35	1.42	13.4				
0.4	1.39	14.0				
0.45	1.40	14.5				
0.5	1.41	15.0				
0.6	1.51	15.7		3.18 (d1)		32.7
0.7	1.64	16.2		4.19		32.5
0.8	1.81	16.7		5.10	15.3	32.3
0.9	2.01	17.3		5.92	15.6	32.3
1	2.23	17.8	14.6	6.86	15.9	32.5
1.2	2.76	19.2	17.2	8.03	16.4	33.1 (f1)
1.5	3.73	22.4	22.0	9.50	17.2	33.2
1.7	4.42	25.4	23.7	10.3	17.7	32.8
2	5.64	30.4	24.2	11.6	18.5	34.0
2.5	7.43	35.4 (b2)	20.8	13.8	20.0	35.7
3	9.60	34.9	19.0	16.0	22.0	37.5
3.5	12.0	31.9	18.7	18.2	24.6	40.7
4	14.5	29.2	19.7	20.0	28.1	44.6
4.5	16.9	27.2	21.4	22.2	31.4	48.1 (f2)
5	19.3	25.1	22.7	24.6	33.9	50.5
6	23.4	24.1	25.3	29.4	38.3	52.2
7	25.6	24.8	27.2	32.5	42.3	55.6
8	26.2 (a1)	24.7	28.0	33.4	44.9	57.7
9	26.1	23.7	28.3	33.0	45.4	57.9
10	25.7	23.0	28.3 (c1)	31.9 (d2)	43.3 (e2)	56.8
12	24.3	22.2	27.9	29.6	40.6	54.1
15	22.3	20.6	26.5	28.9	38.9	50.3
17	21.2	19.6	25.6	28.4	38.4	48.2
20	19.6	18.4	24.4	27.4	37.5	45.9
25	17.6	16.8	22.5	25.5	35.8	43.3
30	16.2	15.9	21.1	23.9	34.0	41.7
35	15.1	15.2	20.0	22.7	32.4	40.5
40	14.2	14.7	19.1	21.8	31.1	39.5
45	13.5	14.2	18.4	20.9	29.9	38.6
50	12.8	13.7	17.7	20.2	28.9	37.7 (f3)
60	11.8	13.0	16.6	18.9	27.0	35.9
70	11.0	12.4	15.7	17.8	25.4	34.1
80	10.3	11.8	14.9	16.9	24.1	31.8
90	9.75	11.3	14.2	16.1	22.9	30.2

Table 6.1.6 (continued)

Energy [eV]	Cross section [10^{-16} cm^2]					
	CH_4	C_2H_2	C_2H_4	C_2H_6	C_3H_8	C_6H_6
100	9.24	10.9	13.6	15.3	21.8	29.0
120	8.38	10.1	12.5	14.1	19.9	26.9
150	7.37	9.15	11.2	12.5	17.7	24.3
170	6.83	8.62	10.5	11.7	16.4	22.9
200	6.16	7.93	9.62	10.6	14.9	21.0
250	5.30	7.00	8.43	9.25	12.9	18.5
300	4.66	6.28	7.51	8.24	11.4	16.4
350	4.10	5.73	6.78	7.41	10.2	14.8
400	3.71	5.30	6.18	6.73	9.19	13.5
450	3.38	4.94	5.67	6.15	8.38	12.4
500	3.11	4.60	5.25	5.65	7.71	11.4
600	2.74	4.01				9.94
700	2.42	3.56				8.79
800	2.17	3.19				7.88
900	1.97	2.90				7.13
1000	1.81	2.65				6.52

Notes

The following sets of data (the energy ranges are given in brackets) have been used to obtain the recommended TCS.

CH_4 [85Fer2] (0.09-12); [86Loh1] (0.1-20); [88Dab1] (1.4-500); [85Jon2] (1.3-50), corrected linearly from 0 % at 4 eV to +7 % at 50 eV; [91Zec1] (1.2-100) Gdańsk data; [91Zec1] (77-1000) Trento data; [90Nis1] (5-500); [92Kan2] (5-300); [98Gar1] (400-1000). See Fig. 6.1.6.

C_2H_2 [87Dre1] (0.1-4.8) normalized to [89Sue1] at 2.5 eV, [89Sue1] (1-400), energy scale corrected linearly by + 10 % at 1 eV down to 0 % at 20 eV, TCS corrected by 0 % at 5 eV up to + 14 % at 400 eV; [95Xin1] (400-1000). See Fig. 6.1.7.

C_2H_4 [86Sue1] (1-400); [91Nis1] (4-500), [85Flo1] (5-400). See Fig. 6.1.7.

C_2H_6 [95Szm1] (0.6-250); [86Sue1] (1-400); [91Nis1] (4-500), [85Flo1] (5-400). See Fig. 6.1.7.

C_3H_8 [99Tan1] (0.8-500); [91Nis1] (4-500). See Fig. 6.1.7.

C_6H_6 [96Moz2] (0.6-250) Gdańsk data; [96Moz2] (90-3500) Trento data. See Fig. 6.1.7.

(a1) The agreement between all used sets of data is very good. At the TCS maximum, five sets of TCS [85Jon2, 90Nis1, 91Zec1, 92Kan2, 00Kim1] agree within 4 %.

(b1) [87Dre2] reported a "total" transmission spectrum between 0.07 - 4.8 eV in arbitrary units. These data normalized to TCS in [89Sue1] at 2.5 eV agree very well in shape with [89Sue1] in the whole energy range of overlap.

(b2) Early data [29Bru1], not included in the averaged values, are above 2 eV slightly (about 10 %) higher than those in [89Sue1]. TCS maximum in [29Bru1] amounts to about $40 \cdot 10^{-16}$cm^2.

(c1) The agreement between existing data is rather bad above 5 eV. At 10 eV, measurements performed with a guiding magnetic field [86Sue1, 85Flo1] are 15 % lower than the data obtained in [91Nis1].

(d1) Present recommended values below 2 eV are based on TCS in [95Szm1] and [86Sue1], in good mutual agreement. A quick fall of TCS below 2 eV with a Ramsauer-Townsend minimum at about 0.15 eV [98Lun1] is indicated also by relative TCS measurements from Daresbury and Orsay labs [94Lun1, 98Lun1]. However, TCS measurements [95Szm1, 86Sue1] below 2 eV are not compatible with the elastic cross sections in [98Mer1].

(d2) The agreement between different data [86Sue1, 91Nis1, 95Szm1] is very good up to 6 eV. At higher energies the agreement is poor: at 10 eV the data in [85Flo1] are 25 % lower than those in [91Nis1].

(e1) "Backward scattering" from Orsay lab indicates a Ramsauer-Townsend minimum at about 0.1 eV [98Lun1].

(e2) The TCS from Tokyo lab corrected [99Tan1] for the angular resolution error are slightly (7 % at 10 eV) higher than TCS in [91Nis1]. TCS in [85Flo1], much lower than the two other sets of data [99Tan1, 91Nis1], have not been included in the averaged values.

(f1) A $^2E_{2u}$ resonant state is present in the 1.2 - 1.6 eV energy region [75Won1]. In TCS measurements with a moderate energy-resolution [88Sue1, 96Moz2, 00Kim1] only an enhancement of TCS was observed (reproduced in the present table). A resonant structure, seen in TCS measurements [98Gul1] performed with a high energy resolution (3.5 meV) is reported in Table 6.1.12.

(f2) The shoulder in TCS at about 4.8 eV is attributed to a short-lived $^2B_{2g}$ resonant state, seen also in the vibrational excitation channel [75Azr1, 89All1] and in electron-transmission spectra [73San1].

(f3) The recommended data for C_6H_6 are based on two sets (Gdańsk and Trento labs) of TCS from [96Moz2], in good agreement in the energy overlap region. The more recent set of TCS from Tokyo lab [00Kim1] agrees within the error bar with results in [96Moz2] up to 10 eV but is 15 % lower at 50 eV. These data [00Kim1] are higher than previous results from the Tokyo lab [88Sue1] by 20 % at 10 eV and 6 % at 50 eV.

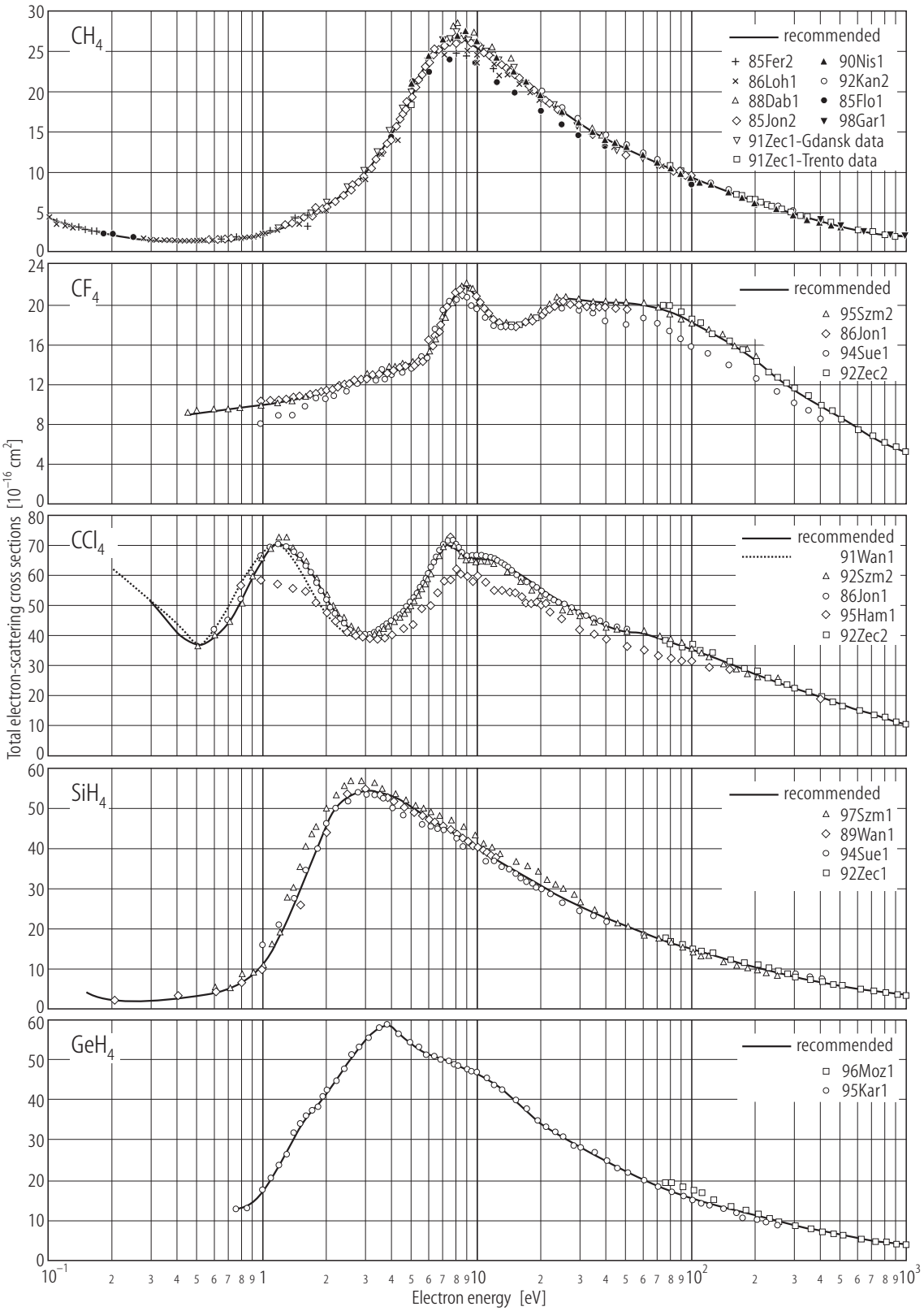

Fig. 6.1.6. Overview of experimental and recommended total cross sections for CH_4, CF_4, CCl_4, SiH_4, GeH_4.

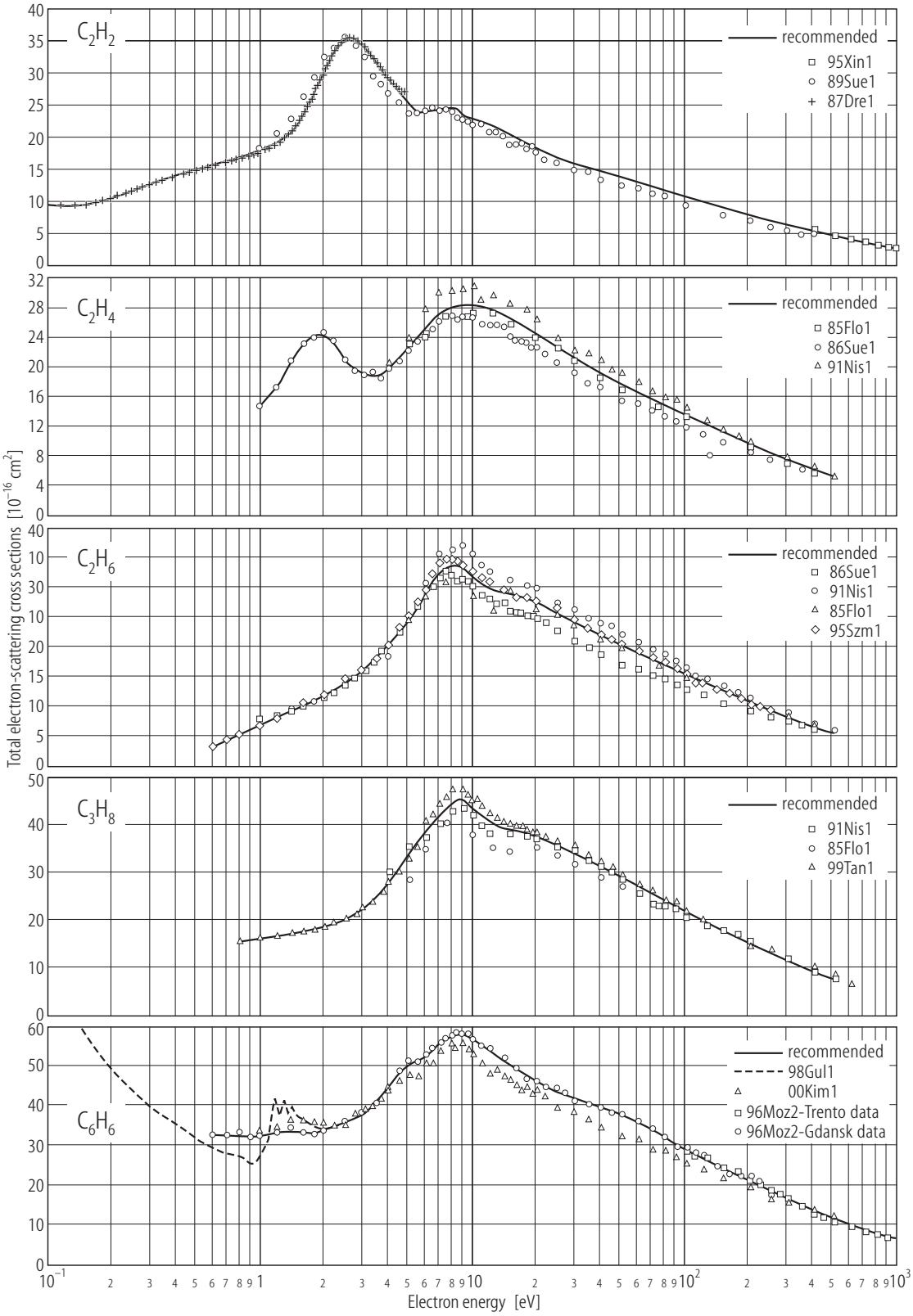

Fig. 6.1.7. Overview of experimental and recommended total cross sections for C_2H_2, C_2H_4, C_2H_6, C_3H_8, C_6H_6.

6.1.6 Halomethanes

Table 6.1.7. Recommended total cross sections for some halomethanes.

Energy [eV]	Cross section [10^{-16} cm^2]					
	CHF_3 (a1)	CF_4	CF_3Cl	CF_2Cl_2	$CFCl_3$	CCl_4
0.10	(a2)	(b1)	(c1)	(d1)	96.7 (e1)	(f1)
0.12					88.4	
0.15					78.9	
0.17					74.4	
0.20				73.3	69.4	
0.25			41.9	60.7	64.0	
0.30			31.7	53.0	60.5	51.7
0.35			25.7	47.2	57.4	45.7
0.40			22.1	42.4	55.2	41.2
0.45		8.97	19.8	38.6	53.2	38.3
0.5		9.15	18.4	35.6	51.3	36.5
0.6		9.35	17.3	32.2	47.3	39.5
0.7		9.47	17.2	32.9	43.6	44.0
0.8	32.1	9.59	17.3	36.6	40.2	51.4
0.9	30.9	9.73	17.6	40.0	36.8	58.9
1.0	30.2	9.87	18.2	41.4 (d2)	34.8	65.0 (f2)
1.2	29.5	10.2	20.3	38.3	39.6	71.0 (f3)
1.5	29.1	10.6	25.5	30.3	51.2	66.5
1.7	28.6	10.9	29.2	29.4	53.9 (e2)	60.6
2.0	27.4	11.3	31.8 (c2)	32.4	52.5	52.0
2.5	25.8	12.0	27.2	38.5 (d2)	46.1	42.5
3.0	24.8	12.6	23.6	38.0	42.4	39.6
3.5	24.2	13.1	23.2	38.2	44.1	41.4
4.0	24.0	13.5	24.9	39.9 (d2)	44.9 (e2)	44.1
4.5	24.1	13.8	27.8	40.6	44.7	47.7
5.0	24.5	14.0	31.3	41.7	45.2	51.9
6.0	26.1 (a3)	15.2	33.7 (c2)	43.6	49.8	61.3
7.0	26.7	18.6	33.1	44.3	56.4	69.8 (f3)
8.0	26.7	21.2	33.8	46.6	59.9	69.1
9.0	26.3	21.9 (b2)	34.6	49.0	60.4	65.7
10	25.4	21.0	35.0	50.8	60.5	65.2
12	23.2	18.6	36.1	50.6	59.7	64.2
15	22.8	18.0	33.9	46.0	54.5	59.9
17	22.7	18.3	32.2	43.8	51.8	56.9
20	23.3	19.3	30.8	41.4	48.9	53.5
25	23.3	20.6	30.0	39.2	45.6	49.4
30	22.8	20.4 (b3)	28.6	37.3	43.4	46.6
35	22.2	20.3	28.0	36.1	41.7	44.6
40	21.6	20.3	27.4	35.1	40.3	43.2
45	21.0	20.3	26.9	34.2	39.1	42.2
50	20.5	20.2	26.3	33.4	38.1	41.5
60	19.6	20.0	25.4	32.0	36.3	40.8
70	18.4	19.7	24.5	30.7	34.8	39.4
80	17.4	19.4	23.7	29.5	33.6	37.8
90	16.4	18.8	23.0	28.4	32.4	36.5

Table 6.1.7 (continued)

Energy [eV]	Cross section [10^{-16} cm^2]					
	CHF_3 (a1)	CF_4	CF_3Cl	CF_2Cl_2	$CFCl_3$	CCl_4
100	15.6	18.3	22.3	27.4	31.4	35.4
120	14.3	17.3	21.0	25.7	29.6	33.3
150	12.7	16.3	19.3	23.4	27.3	30.5
170	11.9	15.6	18.4	22.1	26.0	29.0
200	10.8	14.4	17.1	20.5	24.2	27.1
250	9.48	12.8	15.1	18.4	21.5	24.6
300	8.49	11.6	13.6	16.7	19.6	22.4
350	7.72	10.7	12.5	15.3	18.0	20.6
400	7.12	9.87	11.5	14.1	16.7	19.1
450	6.64	9.18	10.7	13.2	15.6	17.9
500	6.26	8.59	10.1	12.3	14.6	16.7
600	5.70	7.60	8.98	10.9	13.0	14.9
700		6.83	8.13	9.80	11.7	13.4
800		6.19	7.43	8.91	10.7	12.2
900		5.67	6.86	8.16	9.83	11.3
1000		5.22	6.36	7.53	9.09	10.4

Notes

The following sets of data (the energy ranges are given in brackets) have been used to obtain the recommended TCS.

CHF_3 [98Sue1] (0.8-600).

CF_4 [92Szm2] (0.45-200); [86Jon1] (1-50) corrected linearly from 0 % at 4 eV to 5 % at 50 eV, according to the angular resolution error; [92Zec2] (75-1000). See Fig. 6.1.6 (p. 6-27).

CF_3Cl [94Und1] (0.2-1.8); [86Jon1] (0.6-50) corrected linearly from 0 % at 4 eV to +7 % at 50 eV, according to the angular resolution error given in [86Jon1]; [92Zec2] (75-1000). See Fig. 6.1.8.

CF_2Cl_2 [94Und1] (0.2-2); [86Jon1] (0.6-50) corrected linearly from 0 % at 4 eV to +7 % at 50 eV, according to the angular resolution error given in [86Jon1]; [92Zec2] (75-1000). See Fig. 6.1.8.

$CFCl_3$ [93Ran1] (0.1-0.9) backward scattering, normalized to [86Jon1] at 0.9 eV; [86Jon1] (0.6-50) corrected linearly from 0 % at 4 eV to +7 % at 50 eV, according to the angular resolution error given in [86Jon1]; [92Zec2] (75-1000). See Fig. 6.1.8.

CCl_4 [86Jon1] (0.6-50), corrected linearly from 0 % at 4 eV to +7 % at 50 eV, according to the angular resolution error given in [86Jon1]; [92Szm2] (0.5-200); [91Wan1] (0.2-9); [92Zec2] (75-1000). See Fig. 6.1.6 (p. 6-27).

(a1) The recommended TCS are based on the recent data from the Tokyo lab [98Sue1]. Note that the recent TCS from this lab in CH_4 and CF_4, cited together with CHF_3 [98Sue1] are in a very good agreement with recommended values.

(a2) Low energy measurements indicate a rise TCS in the limit of zero energy: from about $20 \cdot 10^{-16}$ cm^2 at 1 eV to $45 \cdot 10^{-16}$ cm^2 at about 0.1 eV [98San1].

(a3) Measurements from Maryland lab [98San1] at 0.1 - 20 eV are generally lower in the energy overlap region than the TCS in [98Sue1] and at the 6.5 eV maximum amount to about $17.5 \cdot 10^{-16}$ cm^2.

(b1) The "backward-scattering" measurements from the Orsay lab [84Fie1, 98Lun1] indicate a fall of TCS below 0.2 eV and a Ramsauer minimum at about 0.15 eV. Normalizing the data from [84Fie1] at 0.4 eV to the TCS in [92Szm2] one gets a good agreement of this fall with the Born approximation for the vibrational excitation (see eq. 13).

(b2) The peak in TCS at 8.87 eV [86Jon1] is due to resonant scattering, seen as a dip structure in elastic cross section [92Boe1, 92Man1], as an enhancement in the vibrational [92Boe1, 92Man2] and in the dissociative attachment cross sections [92Iga1].

(b3) The recent measurements from Tokyo lab [94Sue1] are very close to the recommended data, being at 30 eV only 5 % lower.

(c1) The measurements from the Maryland lab [94Und1], lower by 25 % on the average than those in [86Jon1], indicate a rise of TCS in the low energy limit. These data [94Und1] normalized at 1 eV by a factor of 1.25 to the TCS from [86Jon1] yield a value of about $42 \cdot 10^{-16}$ cm^2 at 0.25 eV.

(c2) The TCS maxima at 2.0 and 5.94 eV [86Jon1] are due to the presence of resonances, which have been observed at about the same energies in the vibrational excitation [92Man3] and electron attachment [89Ost1, 95Und1] channels.

(d1) TCS from the Maryland lab [94Und1] show a rise below 0.5 eV, see Fig. 6.1.8. These data normalized at 1 eV by a factor of 1.33 to the TCS in [86Jon1] reach about $73 \cdot 10^{-16}$ cm^2 at 0.2 eV. We note also that a peak at 0.2 eV was observed in the dissociative attachment cross section [95Und1].

(d2) Two peaks and a shoulder at 1.02, 2.64 and 4.0 eV were reported in [86Jon1]. Resonances were observed at about the same energies in the vibrational excitation [92Man4] and dissociative attachment cross sections [79Pej1, 89Ost1, 95Und1].

(e1) The "backward scattering" measurements [93Ran1] indicate a rise of TCS below 1 eV. This rise is due to electron attachment [80McC1, 87Dun1]. In Fig. 6.1.8 relative data from [93Ran1] have been normalized to TCS from [86Jon1] at 0.8 eV.

(e2) Maxima in TCS were observed at 1.76 and 4.0 eV in [86Jon1]. Peaks in electron attachment cross sections were observed at slightly lower energies, 1.6 and 3.3 eV [89Ost1].

(f1) The measurements from the Maryland lab [91Wan1] indicate a rise of TCS in the limit of zero-energy, up to approximately $120 \cdot 10^{-16}$ cm^2 at 0.1 eV (data digitized from Fig. 3. in [91Wan1]). This rise is due to electron attachment [85Chu1, 92Lin1, 95Mat1].

(f2) Different sets of TCS in CCl_4 [86Jon1, 91Wan1, 92Szm2, 95Ham1] are in good agreement. TCS in [95Ham1] are somewhat lower at the low-energy maximum at 1 eV, probably due to a poorer energy resolution.

(f3) The TCS maxima at 1.22 and 7.51 eV [86Jon1] are due to resonant scattering. These maxima were also seen in dissociative attachment [91Wan1, 90Chu1, 89Ost1].

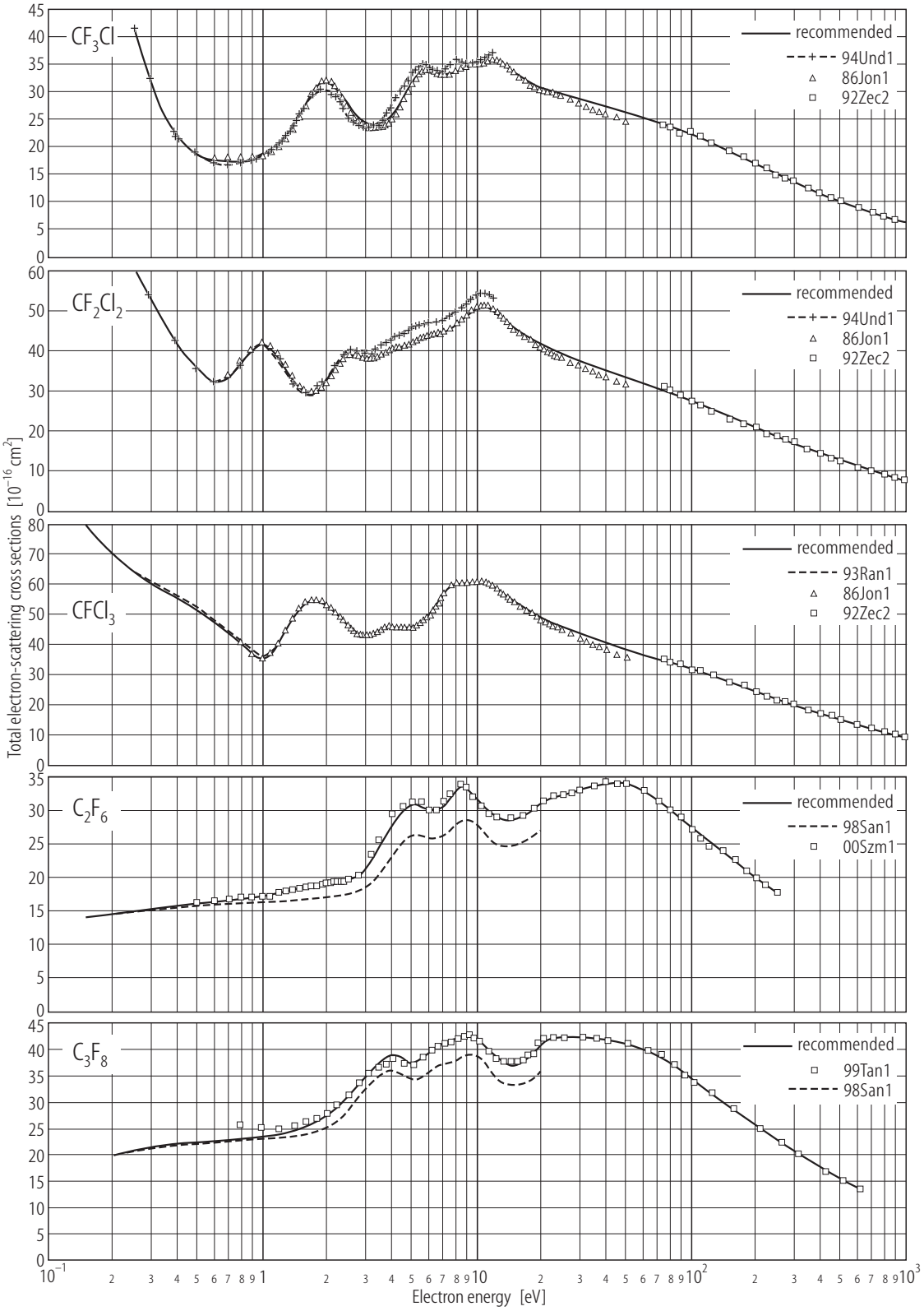

Fig. 6.1.8. Overview of experimental and recommended total cross sections for CF_3Cl, CF_2Cl_2, $CFCl_3$, C_2F_6, C_3F_8.

6.1.7 Methyl compounds

Table 6.1.8. Recommended total cross sections for some methyl compounds.

Energy [eV]	Cross section [10^{-16} cm^2]				
	CH_3OH	CH_3F	CH_3Cl	CH_3Br	CH_3I
0.25			58.4 (c1)		
0.30			54.4		
0.35		38.8 (b1)	51.0		
0.40		37.5	48.1	62.4 (d1)	
0.45		36.3	45.6	60.3	95.6 (e1)
0.5		35.1	43.5	58.4	90.6
0.6		32.8	40.2	55.4	82.9
0.7		30.8	37.7	52.9	76.9
0.8	28.2	29.0	35.9	51.0	72.0
0.9	26.8	27.4	34.6	49.4	67.8
1.0	25.6	25.9	33.6	48.1	64.2
1.2	23.6	23.6	32.4	46.1	58.4
1.5	21.6	21.1	31.7	45.2	52.6
1.7	20.7	19.9	31.6	44.5	50.7
2.0	19.9	19.2	31.9	42.9 (d2)	49.9
2.5	19.5	19.2	32.6	39.8	49.8
3.0	19.7	19.8	33.5	39.0	49.8
3.5	20.5	20.6	34.2	38.8	50.4
4.0	21.4 (a1)	21.4	34.7	38.9	52.0
4.5	22.5	22.3	34.6	39.1	53.7
5	23.6	23.2	34.6	39.4	55.0
6	25.4	24.1	35.0	40.0	57.2
7	26.3 (a2)	24.4	35.5	40.3	58.0
8	26.6	24.1	35.5	40.1	56.0
9	26.5	23.5	34.3	39.4	54.4
10	26.1	22.8	33.1	38.2	53.4
12	24.8	21.8	31.7	36.1	52.1
15	23.4	20.2	30.3	33.6	50.7
17	22.7	19.4	29.4	32.6	49.2
20	21.6	18.6	28.0	31.4	46.2
25	20.0	17.5	25.9	29.6	42.5
30	18.5	16.8	24.4	28.4	39.8
35	17.4	16.2	23.5	27.3	37.6
40	16.6	15.7	22.6	26.3	35.9
45	16.2	15.3	21.9	25.3	34.4
50	15.7	14.9	21.2	24.4	33.0
60	14.9	14.1	20.1	22.7	30.8
70	14.2	13.5	19.1	21.3	29.0
80	13.5	12.9	18.2	20.1	27.4
90	12.9	12.4	17.4	19.0	26.0
100	12.4	11.9	16.6 (c2)	18.0	24.8
120	11.5	11.0	15.4	16.4	22.6
150	10.3	9.79	13.8	14.4	19.7
170	9.70	9.07	12.9	13.4	18.1
200	8.83	8.10	11.8	11.9	15.8

Table 6.1.8 (continued)

Energy [eV]	Cross section [10^{-16} cm^2]				
	CH_3OH	CH_3F	CH_3Cl	CH_3Br	CH_3I
250	7.55	6.70	10.4	9.91	
300			9.22		
350			8.30		
400			7.55		
450			6.93		
500			6.40		
600			5.55		
700			4.90		
800			4.39		
900			3.98		
1000			3.63		

Notes

The following sets of data (the energy ranges are given in brackets) have been used to obtain the recommended TCS**.**

CH_3OH [95Szm1] (0.8-250). See Fig. 6.1.5 (p. 6-23)
CH_3F [95Krz1] (0.35-250).
CH_3Cl [95Krz1] (0.25-250); [99Kar1] (75-1000).
CH_3Br [94Krz1] (0.4-250).
CH_3I [93Szm1] (0.45-220).

(a1) TCS in [85Sue1] agree well with those in [95Szm1] up to 4 eV, are lower by 10 -15 % at 7 - 150 eV and merge again in the 250 eV limit.
(a2) The more recent TCS from the Tokyo lab [00Kim1] are higher than the previous data [85Sue1] and amount to $31 \cdot 10^{-16}$ cm^2 at 7 eV. The recent data [00Kim1] report also a narrow maximum at 2 eV.
(b1) TCS in [95Krz1] agree well in shape with TCS in [88Ben1] at 0.35 - 7 eV but are up to 20 % higher.
(c1) TCS from Maryland lab [88Ben1, 91Wan1] agree well in shape with those from Gdańsk lab [95Krz1] in the whole energy overlap region up to 12 eV but are 30 % lower on the average.
(c2) TCS from Gdańsk lab [95Krz1] and Trento lab [99Kar1] merge poorly in the 75 - 250 eV region with differences up to 15 %. A fit with formula (eq. 11) on both sets of data together was used to get recommended values.
(d1) TCS in [94Krz1] agree well in shape with TCS measurements from the Maryland lab [88Ben1] in the whole energy region of overlap (0.4 - 7 eV). Absolute values in these two sets of data differ by less than 10 %.
(d2) A shoulder structure at about 2 eV [94Krz1] was seen as a weak maximum in TCS measurements presented in [88Ben1]. A weak resonant state was predicted theoretically at this energy [92Mod1].
(e1) TCS measurements from the Maryland lab [88Ben1] are higher than in [93Szm1] by 10 - 15 % in the whole energy region of overlap (0.45 - 7 eV) but agree well in shape.

6.1.8 Fluorides

Table 6.1.9. Recommended total cross sections for some fluorides.

Energy [eV]	Cross section [10^{-16} cm^2]				
	C_2F_6	C_3F_8	C_6F_6	SF_6	WF_6
0.10				156 (d1)	
0.12				131	
0.15	14.1 (a1)			106	
0.17	14.2			94.6	
0.20	14.5	19.7 (b1)	(c1)	81.4	
0.25	14.9	20.7		66.4	
0.30	15.2	21.2		56.5	
0.35	15.5	21.6		49.5	
0.40	15.7	21.9		44.3	
0.45	15.9	22.1		40.3	
0.5	16.1	22.2		37.1	
0.6	16.3	22.5	31.6	32.7	
0.7	16.5	22.7	32.8	29.7	
0.8	16.7	22.9	33.2	27.0	
0.9	16.9	23.1	33.2	24.9	
1.0	17.1	23.3	33.1 (c2)	23.5	
1.2	17.4	23.7	32.6	22.4	21.7
1.5	17.9	25.0	31.8	21.9	22.1
1.7	18.2	25.8	31.4	22.1	22.3
2.0	18.7	27.2 (b2)	30.8	22.6	23.3
2.5	19.5	30.8	29.9	23.3 (d2)	29.4
3.0	21.1	34.8	29.1	23.1	30.8 (e1)
3.5	24.7	37.7	29.0	22.8	27.9
4.0	27.9	38.8	29.8	22.4	26.1
4.5	29.9 (a2)	38.0	31.0	22.5	24.5
5.0	30.7	37.4	32.5	23.5	23.4
6.0	29.9	39.6	36.0	27.9	22.7
7.0	30.7	41.1	39.9	31.3 (d2)	23.1
8.0	33.0 (a2)	41.7	44.1	28.9	23.5
9.0	33.1	42.9	48.4 (c3)	27.0	24.4
10	31.6 (a3)	42.2	47.7	27.1	26.7 (e1)
12	29.2	38.8	53.4	33.3 (d2)	28.1
15	28.6	36.9	56.2 (c3)	26.3	30.6
17	29.5	37.9	56.3	26.2	34.7
20	31.1	41.1	57.7	27.3	36.5
25	32.4	42.4	59.7	29.1	36.6
30	33.1	42.4	60.5	29.3	37.1
35	33.6	42.2	60.4	29.3	37.9
40	34.0	42.0	59.5	29.3	37.8
45	34.2	41.6	58.2	29.4	37.5
50	34.1	41.2	56.7	29.3	37.0
60	33.0	40.2	53.7	28.8	36.1
70	31.5	38.9	51.2	28.0	35.2
80	30.0	37.5	49.0	27.3	34.4
90	28.6	35.8	47.0	26.4	33.5

Table 6.1.9 (continued)

Energy [eV]	Cross section [10^{-16} cm^2]				
	C_2F_6	C_3F_8	C_6F_6	SF_6	WF_6
100	27.3	34.1	45.2	25.6	32.6
120	25.2	31.9	42.1	24.3	30.9
150	22.9	29.2	38.3	22.5	28.9 (e2)
170	21.7	27.6	36.1	21.5	27.8
200	20.1	25.6	33.3	20.1	26.3
250	17.7	22.8	29.5	18.1	24.2
300		20.6		16.4	22.4
350		18.8		15.2	20.9
400		17.3		14.2	19.6
450		16.1		13.3	18.3
500		15.1		12.6	16.8
600		13.5		11.5	14.8
700				10.4	13.3
800				9.47	12.2
900				8.69	11.3
1000				8.04	10.6

Notes

The following sets of data (the energy ranges are given in brackets) have been used to obtain the recommended TCS.

C_2F_6 [00Szm1] (0.5-250); [98San1] (0.15-20) corrected linearly from 0 % at 0.15 up to +15 % at 3.4 eV and then by 15 % at 3.4 - 20 eV. See Fig. 6.1.8 (p. 6-32).

C_3F_8 [99Tan1] (1.4-600); [98San1] (0.2-20), corrected linearly from 0 % at 0.2 eV to +10 % at 20 eV. See Fig. 6.1.8 (p. 6-32).

C_6F_6 [97Kas1] (0.6-250).

SF_6 [82Fer1] (0.1-1); [97Kas1] (0.6-250); [88Dab1] (2.8-500); [79Ken1] (0.5-95), corrected linearly from 0 % at 1 eV up to +10 % at 100 eV (angular resolution error); [92Zec3] (75-1000). See Fig. 6.1.9.

WF_6 [00Szm1] (1.2-250), [00Kar1] (150-3500). See Fig. 6.1.9.

(a1) The "backward scattering" measurement from Orsay lab indicates a quick fall of the cross section below 0.15 eV, with a Ramsauer-Townsend minimum at 0.08 eV [98Lun1].

(a2) The C_2F_6 TCS [00Szm1, 97Sue1, 98San1] shows two maxima: of about $31 \cdot 10^{-16}$ cm^2 at 5 eV and $34 \cdot 10^{-16}$ cm^2 at 8 eV [00Szm1]. The vibrational excitation [94Tak1] shows resonances at 4.3 and 8.5 eV. The data in [98San1] are probably underestimated, see note (b1).

(a3) The TCS from the Tokyo lab [97Sue1] show the same shape as our recommended values, but are somewhat (15 % at 10 eV) lower.

(b1) The data in [98San1] obtained with a trochoidal spectrometer are possibly underestimated due to the uncertainty in determining the effective length of the scattering cell. We have corrected data in [98San1] by a factor linearly rising from 0 % at 0.2 eV to 10 % at 20 eV. Below 1.5 eV our recommended values follow the data of of [98San1] which extend down to 0.2 eV. Low energy data in [99Tan1] amount to: 25.4 at 0.8 eV, 25.0 at 1 eV, 24.7 at 1.2 eV, $25.2 \cdot 10^{-16}$ cm^2 at 1.4 eV.

(b2) The large discrepancy between the two sets of data suggest a large error bar on the recommended values. The data in [98San1] agree in shape with those in [99Tan1] but are systematically lower; we have corrected them by a factor linearly rising with energy from 0 % at 0.2 eV to 10 % at 20 eV.

(c1) The "backward scattering" measurement from Orsay lab indicates a slowly diminishing cross section down to 0.2 eV then a quick fall, with a Ramsauer-Townsend minimum at 0.08 eV [98Lun1].
(c2) An enhancement of electron attachment was observed around 1 eV [94Shi1].
(c3) Two weak structures can be discerned in the TCS at 9.5 and 14 eV [97Kas1]. Peaks in dissociative attachment have been seen at 4.5 and 8 - 12 eV [89Fen1].
(d1) The rise of TCS below 1 eV is caused both by vibrational excitation [79Roh1, 92Ran1] and electron attachment [85Chu1, 92Lin1, 92Shi1].
(d2) TCS in SF_6 below 20 eV shows three maxima: a weak one of 23.3 at 2.5 eV and two distinct of 31.3 and $33.5 \cdot 10^{-16}$ cm^2 at 7.1 and 11.9 eV, respectively. Electron transmission spectra [79Ken1] evidenced resonant states at 2.52, 7.05, 11.87 eV; their symmetries were discussed in [78Deh1].
(e1) TCS in WF_6 [00Szm1] shows a maximum of $31.4 \cdot 10^{-16}$ cm^2 at 3.0 eV and a shoulder structure at 8 - 10 eV on the slope of the low-energy edge of the very broad hump. An enhancement of the electron attachment has been seen at 2.8 eV and 10 eV [73Thy1].
(e2) The two existing sets of TCS [00Szm1, 00Kar1] are in rather serious disagreement in the overlap region. For this reason an unique fit with formula (eq. 11), extending from 100 to 450 eV was used.

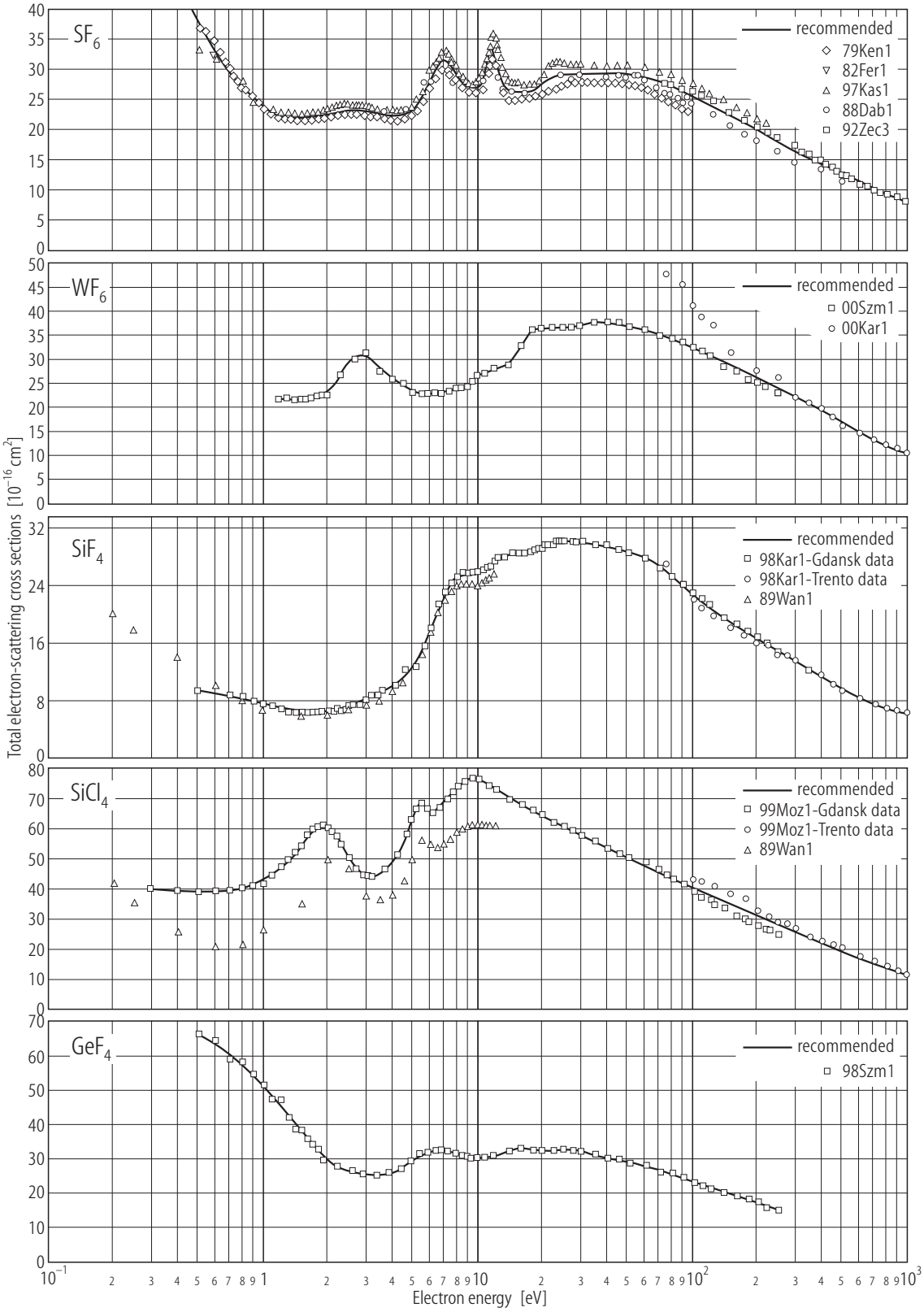

Fig. 6.1.9. Overview of experimental and recommended total cross sections for SF_6, WF_6, SiF_4, $SiCl_4$, GeF_4.

6.1.9 Silicon and germanium compounds

Table 6.1.10. Recommended total cross sections for silicon and germanium compounds.

Energy [eV]	Cross section [10^{-16} cm^2]					
	SiH_4	SiF_4	$SiCl_4$	GeH_4	GeF_4	$GeCl_4$
0.15	3.86					
0.17	2.84					
0.20	2.00					
0.25	1.53					
0.30	1.55		39.7			
0.35	1.77		39.6			
0.40	2.08		39.3			
0.45	2.45		39.1			
0.5	2.87	9.26	38.9		66.4	
0.6	4.00	8.97	38.9		63.3	36.9
0.7	5.05	8.65	39.2		60.3	42.3
0.8	6.13	8.30	40.0	12.7	57.3	45.5
0.9	7.81	7.93	41.2	14.2	54.2	47.8
1.0	11.0	7.55 (b1)	42.7	16.7	51.1	49.8
1.2	17.9	6.81	46.8	23.6	45.3	53.2
1.5	29.3	6.23	54.8	33.7	37.7	56.3
1.7	36.4	6.22	59.9	37.4	33.7	57.0 (f1)
2.0	46.1	6.44	60.2 (c1)	41.9	29.4	57.0
2.5	53.1 (a1)	7.11	50.1	49.2	26.6	50.9
3.0	54.6 (a2)	7.99	44.3	55.0	25.4	47.5
3.5	54.1	9.04	45.0	58.0	25.2	48.3
4.0	52.9	10.1	49.2	57.9 (d1)	26.2	50.1
4.5	51.4	11.1	55.5	55.4	27.8	53.0
5.0	49.9	12.8	64.3 (c2)	53.5	30.0	57.9 (f2)
6.0	47.3	17.7	65.4	51.1	32.4 (e1)	70.6
7.0	45.2	22.7	68.5	49.6	32.4	74.2
8.0	43.5	25.2 (b2)	73.6	48.4	31.6	75.3
9.0	42.0	25.7	76.4	47.3	30.7	77.8
10	40.7	25.9	76.5	46.1	30.1	79.6
12	38.0	27.3	73.2	43.7	30.9	78.3
15	34.4	28.5	68.6	39.9	32.9	73.9
17	32.6	28.7	66.9	37.3	32.8	71.1
20	30.5	29.3	64.3	34.0	32.4	67.3
25	27.8	30.2	60.7	30.5	32.7	63.0
30	25.7	30.1	57.8	28.1	32.2	60.3
35	24.1	29.8	55.5	26.1	31.3	58.0
40	22.7	29.4	53.6	24.5	30.5	55.9
45	21.6	29.1	51.8	23.0	29.7	53.8
50	20.6	28.8	50.0	21.7	29.0	52.2
60	18.8	27.8	47.4	19.6	27.7	49.3
70	17.4	26.6	45.2	18.0	26.5	46.7
80	16.4	25.4	43.4	16.8	25.5	44.2
90	15.4	23.9	41.8	15.9	24.5	41.9
100	14.6	22.7	40.4 (c3)	15.2	23.5	39.9
120	13.6	20.7	37.9	14.1	21.9	36.5

Table 6.1.10 (continued)

Energy [eV]	Cross section [10^{-16} cm^2]					
	SiH_4	SiF_4	$SiCl_4$	GeH_4	GeF_4	$GeCl_4$
150	12.1	18.7	34.9	12.7	19.9	32.8
170	11.3	17.7	33.3	11.9	18.7	30.8
200	10.2	16.5	31.1	10.8	17.2	28.4
250	8.86	14.7	28.1	9.46	15.3	25.1
300	7.82	13.2	25.6	8.47		
350	7.01	12.0	23.6	7.66		
400	6.35	11.0	21.9	7.01		
450	5.91	10.2	20.4	6.48		
500	5.44	9.58	19.1	6.03		
600	4.70	8.51	16.9	5.32		
700	4.14	7.68	15.2	4.76		
800	3.70	7.01	13.8	4.32		
900	3.34	6.46	12.8	3.96		
1000	3.05	5.99	12.0	3.66		

Notes

The following sets of data (the energy is given in brackets) have been used to obtain the recommended TCS.

SiH_4 [89Wan1] (0.15-12); [97Szm1] (0.6-100); [94Sue1] (1-400); [92Zec1] (75-1000); Fig. 6.1.6 (p. 6-27).
SiF_4 [98Kar1] (0.5-250) Gdańsk data, (80-1000) Trento data. See Fig. 6.1.9 (p. 6-38).
$SiCl_4$ [99Moz1] (0.3-250) Gdańsk data, (100-1000) Trento data. See Fig. 6.1.9 (p. 6-38).
GeH_4 [96Moz1] (0.75-200); [95Kar1] (150-1000). See Fig. 6.1.6 (p. 6-27).
GeF_4 [98Szm1] (0.5-200). See Fig. 6.1.9 (p. 6-38).
$GeCl_4$ [97Szm1] (0.6-250).

(a1) An enhancement of the dissociative attachment [69Pot1] and the vibrational excitation [90Tan1] cross sections at 2.5 eV suggest the existence of a resonance state at about this energy.
(a2) The TCS from the Tokyo lab [94Sue1] are generally higher, at 3 eV by 15 %, than the preliminary measurements [85Mor1] from the same laboratory.
(b1) A rise of TCS below 2 eV was also observed in the data from the Maryland lab [89Wan1], see Table 6.1.11.
(b2) A shoulder structure in TCS at 8 eV has been also observed in [89Wan1], see Fig. 6.1.9 (p. 6-38).
(c1) The TCS reaches a sharp maximum of about $62 \cdot 10^{-16}$ cm^2 at 1.9 eV [99Moz1]. A resonant state at 2.07 eV has been seen in electron transmission spectra [98Mod1]; an enhancement of the dissociative attachment cross section has been observed around 2 eV [74Wan1, 90Moy1].
(c2) The TCS reaches a weak maximum of $68 \cdot 10^{-16}$ cm^2 at 5.5 eV and a broader one ($77 \cdot 10^{-16}$ cm^2) at about 9.5 eV. A resonant state has been seen in electron transmission spectra at 5.4 eV [98Mod1]; an enhancement of the dissociative attachment has been seen between 8 - 12 eV [74Wan, 90Moy1].
(c3) The TCS from Gdańsk and Trento labs [99Moz1] merge poorly in the 100 - 200 eV region. For this reason the recommended data were obtained by fitting formula (eq. 11) to all data points from 30 to 3000 eV.
(d1) The maximum of TCS ($59 \cdot 10^{-16}$ cm^2) has been reported [96Moz1] at 3.8 eV, while the elastic cross section reaches a maximum at about 5 eV and the vibrational one a maximum at 2 - 2.5 eV [93Dil1].
(e1) A maximum of $33 \cdot 10^{-16}$ cm^2 has been observed at 6.5 eV [98Szm1]. We are not aware of resonances in GeF_4.
(f1) TCS reaches a maximum of $57.8 \cdot 10^{-16}$ cm^2 at 2.0 eV [97Szm1]. Electron transmission spectra [96Gui1, 98Mod1] indicate the presence of a resonant state at 1.7 eV.
(f2) Electron transmission and electron attachment spectra [98Mod1] indicate the presence of a resonant state at 5.6 eV; a shoulder is visible in TCS [97Szm1] at about this energy.

6.1.10 Halogen substituted silanes

Table 6.1.11. Experimental total cross section for halogen substituted silanes (a1).

Energy [eV]	Cross section 10^{-16} cm^2						
	SiH_4 (a2)	SiH_2Cl_2	$SiHCl_3$	$SiCl_4$ (a2)	SiF_4 (a2)	$SiBr_4$	SiI_4
0.2	1.9	36.6	26.5	41.2	19.9 (c1)	87.9	95.6
0.4	2.7	33.9	23.7	24.9	13.7	50.1	82.6
0.6	4.0	45.9	32.0	20.1 (b1)	9.9	34.7	61.2
0.8	6.2	55.2	39.0	21.1	7.7	36.9	39.7
1.0	9.5	60.8	45.4	25.7	6.5	48.6 (b1)	35.0
1.5	25.7	64.1 (b1)	58.0 (b1)	34.4	5.6 (b1)	45.5	42.7
2.0	44.0	60.8	58.5	49.1 (b1)	5.7	25.9	59.0
2.5	53.4	57.6	51.8	45.9	6.4	22.9	73.8
3.0	54.7 (b1)	57.2 (b1)	48.1	36.9	7.2	26.8	95.4
3.5	53.1	53.5	46.6	35.9	7.7	33.2	108.0 (b1)
4.0	51.6	50.7	46.8	37.9	8.9	42.3	104.4
4.5	50.1	49.7	48.1	41.9	10.1	53.7	102.0
5.0	48.9	50.5	51.6	49.3	12.4	58.4 (b1)	100.4
5.5	48.0	51.5 (b1)	56.0 (b1)	55.7 (b1)	14.3	57.1	100.9
6.0	47.1	51.5	56.5	54.3	17.4	54.9	100.3
6.5	45.7	51.1	55.0	53.3	19.8	55.6	101.9
7.0	45.2	51.1	54.8	54.5	21.6 (b1)	58.3	103.3
7.5	44.1	51.2	55.4	56.2	22.9	59.8	102.0
8.0	43.3	51.1	56.1	58.2	23.7	61.0	100.3
8.5	42.4	51.0	56.7	59.4	24.0	61.8	100.0
9.0	41.5	51.2 (b1)	57.1	60.1	24.0	60.5	99.9
9.5	40.5	51.4	57.4 (b1)	60.8	23.9	60.3	99.3
10.0	40.2	51.6	57.5	60.7	23.8	61.4	99.0
10.5	39.6	51.1	57.7	60.5	24.2	61.7	99.9
11.0	39.0	51.0	58.1	60.9	24.6	61.3	100.3
11.5	38.3	51.0	57.8	60.6	24.9	60.1	100.0
12.0	38.0	51.6	57.9	60.7	25.6	59.9	100.3

Notes

(a1) All data are from Table 1 in [89Wan1]; for recommended data in SiH_4, SiF_4, $SiCl_4$ see Table 6.1.10. Electron transmission spectra in all seven gases were given in the same reference [89Wan1].

(a2) The data in [89Wan1] for SiH_4, SiF_4 and $SiCl_4$ given in this table are slightly different from recommended values given in table 10. In particular in SiF_4 and $SiCl_4$ at the minima of the TCS (1.5 and 0.6 eV respectively) the measurements from the trochoidal spectrometer [89Wan1] are lower than the recommended data; the difference amounts to 15 % in SiF_4 and 50 % in $SiCl_4$. This is probably due to non-complete discrimination of forward scattered electrons in the Maryland apparatus [89Wan1]. The data for SiH_4, SiF_4 and $SiCl_4$ are given again in Table 6.1.11 in order to give a hint about the quality of TCS for other halosilanes in [89Wan1].

(b1) These maxima and shoulders in TCS can be caused by resonances; see a detailed discussion in [89Wan1].

(c1) The rise of TCS in SiF_4 below 1.0 eV can be well reproduced [98Kar1] by the Born approximation for the vibrational excitation, see eq. 13 in the introduction.

6.1.11 Very low energy (0.01 - 10 eV) TCS for some targets

Table 6.1.12. Experimental total cross sections for Cl_2, ClO_2, O_3 and C_6H_6.

Energy [eV]	σ [10^{-16} cm^2]			Energy [eV]	σ [10^{-16} cm^2]
	Cl_2	ClO_2	O_3		C_6H_6
0.010			117	0.040	153
0.012			108	0.045	145
0.015			99.0	0.05	135
0.017			93.9	0.06	109
0.020	40.3	308 (b1)	87.6	0.07	91.9
0.022	39.9	277	84.0	0.08	86.0
0.025	38.8	227	79.4	0.09	90.3
0.030	35.6	131	73.1	0.10	89.7 (d1)
0.035	31.2	55.0	68.1	0.12	74.0
0.040	26.3	42.2	63.9	0.15	61.9
0.045	21.6	85.3	60.3	0.17	56.5
0.05	17.2	117	57.3	0.20	50.7
0.06	10.6	132 (b2)	52.3	0.25	44.7
0.07	7.5 (a1)	121	48.2	0.30	40.9
0.08	8.2	116	45.0	0.35	38.3
0.09	10.3	109	42.2	0.40	36.4
0.10	9.74	101	39.8	0.45	34.8
0.12	8.96	88.2	35.9	0.50	33.5
0.15	9.08	76.3	31.6	0.60	31.2
0.17	7.25	70.5	29.4	0.70	29.1
0.20	5.19	62.8	26.7	0.80	27.2
0.22	4.56	58.1	25.2	0.90	25.6
0.25	3.99	52.2	23.4	1.00	26.8
0.30	3.63	44.9	21.0	1.05	29.0
0.35	3.64	40.0	19.2	1.10	32.5
0.40	3.84	36.4	17.8	1.15	40.5 (d2)
0.45	4.11	33.4	16.7	1.17	42.0
0.5	4.43	30.8	15.8	1.19	40.2
0.6	5.12	25.8	14.5	1.21	37.7
0.7	5.81	22.3	13.7	1.23	37.3
0.8	6.50	20.1	13.1	1.25	38.5
0.9	7.18	18.5	12.8	1.27	40.8
1.0	7.87	17.5	12.6	1.29	41.8
1.2	9.14	16.0	12.2	1.31	40.8
1.5	10.9	14.8	12.0	1.34	38.3
1.7	12.2	14.2	12.1	1.37	39.4
2.0	13.8	13.6 (b2)	12.3	1.40	39.9
2.2	14.7	13.4	12.6	1.42	39.3
2.5	16.0 (a2)	12.9	13.0	1.45	38.0
3.0	17.8	12.0	13.8	1.47	37.1
3.5	19.7	11.0	14.8	1.50	37.8
4.0	21.8	9.94	15.4	1.52	38.1
4.5	24.3	8.97	14.6	1.55	37.8
5	27.1	8.11	14.1 (c1)	1.60	37.4
6	34.1	7.50	14.2	1.65	36.9

Table 6.1.12 (continued)

Energy [eV]	σ [10^{-16} cm^2]			Energy [eV]	σ [10^{-16} cm^2]
	Cl_2	ClO_2	O_3		C_6H_6
7	40.8	7.85	14.7	1.70	36.2
8	42.5	8.05	15.3	1.8	35.1
9	41.1	8.19	15.9	1.9	34.7
10	39.6 (a3)	8.32	16.5	2.0	35.1

Notes

All the data in Table 6.1.12 are based on TCS measurements with the transmission method from a joint Daresbury and Aarhus laboratories experiment using synchrotron radiation electron sources. The original experimental points have been smoothed and fitted numerically in the present work. Recommended data for C_6H_6 above 0.6 eV are given in Table 6.1.6.

Cl_2 [98Gul3]
ClO_2 [98Gul2]
O_3 [98Gul2]
C_6H_6 [98Gul1]. See Fig. 6.1.7 (p. 6-28).

(a1) A two-maxima structure, with onset at the threshold of first vibrational level (70 meV) has been attributed in [98Gul3] to a resonant state.
(a2) No interpretation was attributed in [98Gul3] to a shoulder structure in TCS at about 2.5 eV.
(a3) Measurements from a trochoidal spectrometer [99Coo1] at 0.3 - 23 eV agree well in shape with those in [98Gul3]; the absolute values coincide at 1 eV while at 10 eV the data in [99Coo1] are 20 % lower. Following a recent review [99Chr1] we have adopted results from [98Gul3] as recommended values.
(b1) The very large cross-section at low energy most probably arises from rotationally inelastic scattering [98Gul2], see eq. 13 in the introduction.
(b2) The nature of the maximum at 55 - 60 meV and of a weak shoulder structure at 2 - 3 eV is not clear [98Gul2].
(c1) The TCS in [98Gul2] at 3 - 10 eV are compatible with the integral elastic cross section measurements [93Shy2], within the declared [93Shy2] error bar.
(d1) A weak maximum at 0.1 eV remains outside the experimental noise and could correspond to a vibrational excitation through a direct (non-resonant) process (see [75Won1]).
(d2) A resonant structure, with onset at 1.14 eV, vibrational spacing of 123 meV and – 6 mV anharmonicity [75Nen1] was observed in the transmission spectra [72Lar1, 73San1, 75Nen1, 87Bur1]. Measurements in [98Gul1] with 3.5 - 8 meV energy resolution are, to our knowledge, the only results which evidenced such a structure also in TCS.

6.1.12 Alkali metal dimers and alkali halides

Table 6.1.13. Experimental total cross sections for alkali metal dimers and alkali halides.

Energy [eV]	Cross section $[10^{-16}\,cm^2]$				
	Li_2 (1,a)	Na_2 (1,b)	K_2 (1,c)	LiBr (2,d)	CsCl (2,d)
0.5	543	305	430		
1	308	242	318		
2	200	195	251		
3	159	175	202		
4		169	174		
5		145	169	350	729
6	133	150	158		
7		127	149		
8		135	138		
9		109	149		
10	98	120	140		
20		100	117	99	178
50		85	97		

Notes

All the data in Table 6.1.13 are based on TCS measurements with a recoil-beam method, see subsect. 6.1.1.2.3.

The main difficulty of this method lies in the determination of the interaction-region geometry. Big discrepancies can be generated from wrong evaluations of these parameters, compare for example [72Sla1, 74Sla1, 83Jad1, 84Jad1].

(1) The alkali metal dimmers are targets with high polarizability values (α = 34, 30, $60\cdot10^{-30}$ m^3 for Li_2, Na_2, K_2, respectively [86Wea1]). The classical theory [89McD1] for scattering on a polarization potential predicts an $(\alpha/E)^{1/2}$ scaling of the cross sections. The data in Table 6.1.13 follow this scaling only in a very approximate way (see [96Zec1]).

(2) The alkali metal halides are targets with high dipole moments D, see [86Wea1]). Various theories, see [78Iti1], predict a (D^2/E) scaling of the cross sections for scattering on polar targets.

Li_2 [82Mil1]
Na_2 and **K_2** [73Mil1]
LiBr and **CsCl** [89Vus1]

(a) The declared [82Mil1] uncertainty of these data is ± 16 %.

(b) The declared [73Mil1] uncertainty is 16 % below 4 eV and 14 % above 4 eV.

(c) The declared [73Mil1] uncertainty is 20 % below 4 eV and 15 % above 4 eV.

(d) The data for the alkali halides in Table 6.1.13 are from the more recent measurements by the recoil method [89Vus1]. These data show approximately a D^2/E scaling of the TCS [96Zec1]. Earlier data from recoil experiments, for CsF [74Sla1], CsCl [74Bec1], KI [74Sla1] and for CsBr, RbBr, CsCl, RbCl, KI [84Jad1] do not show such an energy dependence, and in the case of CsCl differ by a factor of 4 from the data of [89Vus1].

6.1.13 References for 6.1

21Ram1 Ramsauer, C.: Ann. Phys. (Leipzig) **66** (1921) 546
27Bru1 Brüche, E.: Ann. Phys. (Leipzig) **82** (1927) 25
27Bru2 Brüche, E.: Ann. Phys. (Leipzig) **82** (1927) 912
27Bru3 Brüche, E.: Ann. Phys. (Leipzig) **83** (1927) 1065
29Bru1 Brüche, E.: Ann. Phys. (Leipzig) **2** (1929) 909
29Bru2 Brüche, E.: Ann. Phys. (Leipzig) **1** (1929) 93
29Ram1 Ramsauer, C., Kollath, R.: Ann. Phys. (Leipzig) **3** (1929) 536
30Bru1 Brüche, E.: Ann. Phys. (Leipzig) **4** (1930) 387
30Bru2 Brüche, E.: Ann. Phys. (Leipzig) **5** (1930) 281
30Ram1 Ramsauer, C., Kollath, R.: Ann. Phys. (Leipzig) **4** (1930) 91
30Ram2 Ramsauer, C., Kollath, R.: Ann. Phys. (Leipzig) **7** (1930) 176
33Bro1 Brode, R.B.: Rev. Mod. Phys. **5** (1933) 257
33Ram1 Ramsauer C., Kollath R.: Der Wirkungsquerschnitt von Gasmolekülen gegenüber langsamen Elektronen und langsamen Ionen, in: Handbuch der Physik, 2nd edition, Berlin: Springer 1933, Vol. 22, Part 2, pp. 16-312
34Fer1 Fermi, E.: Nuovo Cimento **11** (1934) 157
54Vog1 Vogt, E., Wannier, G.H.: Phys. Rev. **95** (1954) 1190
62OMa1 O'Malley, T.F., Spruch, L., Rosenberg, L.: Phys. Rev. **125** (1962) 1300
62Sch1 Schulz, G.J., Dowell, J.T.: Phys. Rev. **128** (1962) 174
62Sch2 Schulz, G.J.: Phys. Rev. **125** (1962) 229
65Gol1 Golden, D.E., Bandel, H.W.: Phys. Rev. A **138** (1965) 14
66Gol1 Golden, D.E.: Phys. Rev. Lett. **17** (1966) 847
66Gol2 Golden, D.E., Bandel, H.W., Salerno, J.A.: Phys. Rev. **146** (1966) 40
66Tak1 Takayanagi, K.: J. Phys. Soc. Jpn. **21** (1966) 507
67Sun1 Sunshine, G., Aubrey, B.B., Bederson, B.: Phys. Rev. **154** (1967) 1
69Pot1 Potzinger, P., Lampe, F.W.: J. Phys. Chem. **73** (1969) 3912
70Bon1 Boness, M.J.W., Schulz, G.J.: Phys. Rev. A **2** (1970) 2182
70Gol1 Golden, D.E., Zecca, A.: Phys. Rev. A **1** (1970) 241
70Sal1 Salop, A., Nakano, H.H.: Phys. Rev. A **2** (1970) 127
71Bed1 Bederson, B., Kieffer, L.J.: Rev. Mod. Phys. **43** (1971) 601
71Ino1 Inokuti, M.: Rev. Mod. Phys. **43** (1971) 297
71Lin1 Linder, F., Schmidt, H.: Z. Naturforsch. A **26** (1971) 1617
71Spe1 Spence, D., Schulz, G.J.: Phys. Rev. A **3** (1971) 1968
72Azr1 Azria, R., Tronc, M., Goursaud, S.: J. Chem. Phys. **56** (1972) 4234
72Lar1 Larkin, I.W., Hasted, J.B.: J. Phys. B **5** (1972) 95
72Sla1 Slater, R.C., Fickes, M.G., Stern, R.C.: Phys. Rev. Lett. **29** (1972) 333
73Mil1 Miller, T.M., Kasdan, A.: J. Chem. Phys. **59** (1973) 3913
73San1 Sanche, L., Schulz, G.J.: J. Chem. Phys. **58** (1973) 479
73Thy1 Thynne, J.C.J., Harland, P.W.: Int. J. Mass Spectrom. Ion Phys. **11** (1973) 137
73Tro1 Tronc, M., Goursaud, S., Azria, R., Fiquet-Fayard, F.: J. Phys. (Paris) **34** (1973) 381
74Bec1 Becker, W.G., Fickes, M.G., Slater, R.C., Stern, R.C.: J.Chem.Phys. **61** (1974) 2283
74Ino1 Inokuti, M., McDowell, M.R.C.: J. Phys. B **7** (1974) 2382
74Iti1 Itikawa, Y.: J. Phys. Soc. Jpn. **36** (1974) 1121
74Lan1 Land, J.E., Raith, W.: Phys. Rev. A **9** (1974) 1592
74Sla1 Slater, R.C., Fickes, M.G., Becker, W.G., Stern, R.C.: J. Chem. Phys. **60** (1974) 4697
74Sla2 Slater, R.C., Fickes, M.G., Becker, W.G., Stern, R.C.: J. Chem. Phys. **61** (1974) 2290
74Wan1 Wang, J.L.-F., Margrave J.L., Franklin, J.L.: J. Chem. Phys. **61** (1974) 1357
74Zec1 Zecca, A., Lazzizzera, I., Krauss, M., Kuyatt, C.E.: J. Chem. Phys. **61** (1974) 4560
75Azr1 Azria, R., Schulz, G.J.: J. Chem. Phys. **62** (1975) 573
75Nen1 Nenner, I., Schulz, G.J.: J. Chem. Phys. **62** (1975) 1547
75Roh1 Rohr, K., Linder, F.: J. Phys. B **8** (1975) L200

75Tro1 Tronc, M., Huetz, A., Landau, M., Pichou, F., Reinhardt, J.: J. Phys. B **8** (1975) 1160
75Won1 Wong, S.F., Schulz, G.J.: Phys. Rev. Lett. **35** (1975) 1429
75Zie1 Ziesel, A., Nenner, I., Schulz, G.J.: J. Chem. Phys. **63** (1075) 1943
77Kau1 Kauppila, W.E., Stein, T.S., Jesion, G., Dababneh, M.S., Pol, V.: Rev. Sci. Instrum. **48** (1977) 822
77Tei1 Teillet-Billy, D., Fiquet-Fayard, F.: J. Phys. B **10** (1977) L111
78Deh1 Dehmer, J.L., Siegel, J., Dill, D.: J. Chem. Phys. **69** (1978) 5205
78Iti1 Itikawa, Y.: Phys. Rep. **46** (1978) 117
78Ken1 Kennerly, R.E., Bonham, R.A.: Phys. Rev. A **17** (1978) 1844
78Roh1 Rohr, K.: J. Phys. B **11** (1978) 4109
78Szm1 Szmytkowski, Cz., Zubek, M.: Chem. Phys. Lett. **57** (1978) 105
79Jos1 Jost, K., Ohnemus, B.: Phys. Rev. A **19** (1979) 641
79Ken1 Kennerly, R.E., Bonham, R.A., McMillan, M.: J. Chem. Phys. **70** (1979) 2039
79Pej1 Pejčev, V.M., Kurepa, M.V., Čadež, I.M.: Chem. Phys. Lett. **63** (1979) 301
79Roh1 Rohr, K.: J. Phys. B **12** (1979) L185
80Bla1 Blaauw, H.J., Wagenaar, R.W., Barends, D.H., de Heer, F.J.: J. Phys.B **13** (1980) 359
80Dal1 Dalba, G., Fornasini, P., Lazzizzera, I., Ranieri, G., Zecca, A.: J. Phys. B **13** (1980) 2839
80Dal2 Dalba, G., Fornasini, P., Grisenti, R., Ranieri, G., Zecca, A.: J. Phys. B **13** (1980) 4695
80Fer1 Ferch, J., Raith, W., Schröder, K.: J. Phys. B **13** (1980) 1481
80Ken1 Kennerly, R.E.: Phys. Rev. A **21** (1980) 1876
80McC1 McCorkle, D.L., Christodoulides, A.A., Christophorou, L.G., Szamrej, I.: J. Chem. Phys. **72** (1980) 4049, corrigendum in: J. Chem. Phys. **76** (1982) 753
80McM1 McMillan, M.R., Moore, J.H.: Rev. Sci. Instrum. **51** (1980) 944
80Win1 van Wingerden, B., Wagenaar, R.W., de Heer, F.J.: J. Phys. B **13** (1980) 3481
81Dal1 Dalba, G., Fornasini, P., Grisenti, R., Lazzizzera, I., Ranieri, G., Zecca, A.: Rev. Sci. Instrum. **52** (1981) 979
81Fer1 Ferch, J., Masche, C., Raith, W.: J. Phys. B **14** (1981) L97
82Fer1 Ferch, J., Raith, W., Schröder, K.: J. Phys. B **15** (1982) L15
82Hof1 Hoffman, K.R., Dababneh, M.S., Hsieh, Y.-F., Kauppila, W.E., Pol, V., Smart, J.H., Stein, T.S.: Phys. Rev. A **25** (1982) 1393
82Mil1 Miller, T.M., Kasdan, A., Bederson, B.: Phys. Rev. A **25** (1982) 1777
82Nog1 Nogueira, J.C., Iga, I., Lee, M.-T.: J. Phys. B **15** (1982) 2539
83And1 Andrić, L., Čadež, I., Hall, R.I., Zubek, M.: J. Phys. B **16** (1983) 1837
83Deu1 Deuring, A., Floeder, K., Fromme, D., Raith, W., Schwab, A., Sinapius, G., Zitzewitz, P.W., Krug, J.: J. Phys. B **16** (1983) 1633
83Jad1 Jaduszliwer, B., Tino, A., Bederson, B.: Phys. Rev. Lett. **51** (1983) 1644
83Jos1 Jost, K., Bisling, P.G., Eschen, F., Felsmann, M., Walther, L.: XIIIth Int. Conf. on Physics of Electronic and Atomic Collisions (Berlin), Abstracts p. 91 (Eichler, J. et al., eds.), Amsterdam: North-Holland 1983
83Kwa1 Kwan, C.K., Hsieh, Y.-F., Kauppila, W.E., Smith, S.J., Stein, T.S., Uddin, M.N., Dababneh, M.S.: Phys. Rev. A **27** (1983) 1328
83Laz1 Lazzizzera, I., Zecca, A.: Rev. Sci. Instrum. **54** (1983) 541
84And1 Andrić, L., Hall, R.I.: J. Phys. B **17** (1984) 2713
84Chr1 Christophurou, L.G. (ed.): Electron- Molecule Interactions and their Applications, New York: Academic Press 1984, Vol. 1
84Fie1 Field D., Ziesel, J.P., Guyon, P.M., Govers, T.R.: J. Phys. B **17** (1984) 4565
84Jad1 Jaduszliwer, B., Tino, A., Bederson, B.: Phys. Rev. A **30** (1984) 1269
84Jon1 Jones, R.J.: J. Chem. Phys. **82** (1984) 5424
84Kwa1 Kwan, C.K., Hsieh, Y.-F., Kauppila, W.E., Smith, S.J., Stein, T.S., Uddin, M.N.: Phys. Rev. Lett. **52** (1984)1417
84Shi1 Shimamura, I., Takayanagi, K., eds., Electron-Molecule Collisions, New York: Plenum 1984
84Sue1 Sueoka, O., Mori, S.: J. Phys. Soc. Jpn. **53** (1984) 2491
84Szm1 Szmytkowski, Cz., Karwasz, G., Maciąg, K.: Chem. Phys. Lett. **107** (1984) 481

85All1 Allan, M.: J.Phys. B **18** (1985) 4511
85Bel1 Belić, D.S., Kurepa, M.V.: Fizika **17** (1985) 117
85Chu1 Chutjian, A., Alajajian, S.H.: Phys. Rev. A **31** (1985) 2885
85Fer1 Ferch, J., Granitza, B., Masche, C., Raith, W.: J. Phys. B **18** (1985) 967
85Fer2 Ferch, J., Granitza, B., Raith, W.: J. Phys. B **18** (1985) L445
85Flo1 Floeder, K., Fromme, D., Raith, W., Schwab, A., Sinapius, G.: J. Phys. B **18** (1985) 3347
85Jon1 Jones, R.K.: Phys. Rev. A **31** (1985) 2898
85Jon2 Jones, R.K.: J. Chem. Phys. **82** (1985) 5424
85Kat1 Katayama, Y., Mori, S., Sueoka, O.: Atom. Coll. Research Japan **11** (1985) 22
85Mor1 Mori, S., Katayama, Y., Sueoka, O.: Atom. Coll. Research Japan **11** (1985) 19
85Nic1 Nickel, J.C., Imre, K., Register, D.F., Trajmar, S.: J. Phys. B **18** (1985) 125
85Sue1 Sueoka, O., Katayama, Y., Mori, S.: Atom. Coll. Research Japan **11** (1985) 17
85Wag1 Wagenaar, R.W., de Heer, F.J.: J. Phys. B **18** (1985) 2021
86Buc1 Buckman, S.J., Lohmann, B.: Phys. Rev. A **34** (1986) 1561
86Buc2 Buckman, S.J., Lohmann, B.: J. Phys. B **19** (1986) 2547
86Dab1 Dababneh, M.S., Hsieh, Y.F., Kauppila, W.E., Kwan, Ch.K., Stein, T.S. 1986 Proc. III Int.Workshop on Positron (Electron) - Gas Scattering, Detroit (Kauppila,W.E. et al., eds.), World Scientific 1986, p.251
86Gar1 García, G., Arqueros, F., Campos, J.: J. Phys. B **19** (1986) 3777
86Jon1 Jones, R.K.: J. Chem. Phys. **84** (1986) 813
86Loh1 Lohmann, B., Buckman, S.J.: J. Phys. B **19** (1986) 2565
86Ran1 Randell, J., Lunt, S.L., Mrotzek, G., Field, D., Ziesel, J.P.: Chem. Phys. Lett. **252** (1986) 253
86Szm1 Szmytkowski, Cz., Maciąg, K.: Chem. Phys. Lett **129** (1986) 321
86Szm2 Szmytkowski, Cz., Maciąg, K.: Chem. Phys. Lett. **124** (1986) 463
86Sue1 Sueoka, O., Mori, S.: J. Phys. B **19** (1986) 4035
86Sue2 Sueoka, O., Mori, S., Katayama, Y.: J. Phys. B **19** (1986) L373
86Ten1 Tennyson, J., Noble, C.J.: J. Phys. B **19** (1986) 4025
86Wea1 Weast, R.C.: CRC Handbook of Chemistry and Physics, 67th ed., Boca Raton, Florida, 1986
86Zec1 Zecca, A., Brusa, R.S., Grisenti, R., Oss, S., Szmytkowski, Cz.: J. Phys. B **19** (1986) 3353
87Buc1 Buckman, S.J., Elfordt, M.T., Newman, D.S.: J. Phys .B **20** (1987) 5178
87Bur1 Burrow, P.D., Machejda, J.A., Jordan, K.D.: J. Chem. Phys. **86** (1987) 9
87Dre1 Dressler, R., Allan, M., Tronc, M.: J. Phys. B **20** (1987) 393
87Dre2 Dressler, R., Allan, M.: J. Chem. Phys. **87** (1987) 4510
87Dun1 Dunning, F.B.: J. Phys. Chem. **91** (1987) 2244
87Kum1 Kumar, V., Krishnakumar, E., Subramanian, K.P.: J. Phys. B **20** (1987) 2899
87Soh1 Sohn, W., Kochem, K.-H., Scheuerlein, K.M., Jung, K., Ehrhardt, H.: J. Phys. B **20** (1987) 3217
87Sue1 Sueoka, O., Mori, S., Katayama, Y.: J. Phys. B **20** (1987) 3237
87Szm1 Szmytkowski, Cz.: Chem. Phys. Lett. **136** (1987) 363
87Szm2 Szmytkowski, Cz.: J. Phys. B **20** (1987) 6613
87Szm3 Szmytkowski, Cz., Zecca, A., Karwasz, G., Oss, S., Maciąg, K., Marinković, B., Brusa, R.S., Grisenti, R.: J. Phys. B **20** (1987) 5817
87Zec1 Zecca, A., Karwasz, G., Oss, S., Grisenti, R., Brusa, R.S.: J. Phys. B **20** (1987) L133
87Zec2 Zecca, A., Oss, S., Karwasz, G., Grisenti, R., Brusa, R.S.: J. Phys. B **20** (1987) 5157
88Ala1 Alajajian, S.H., Bernius, M.T., Chutjian, A.: J. Phys. B **21** (1988) 4021, corrigendum in: J. Phys. B **29** (1996) 1283
88Ben1 Benitez, A., Moore, J.H., Tossell, J.A.: J. Chem. Phys. **88** (1988) 6691
88Dab1 Dababneh, M.S., Hsieh, Y.-F., Kauppila, W.E., Kwan, C.K., Smith, S.J., Stein, T.S., Uddin, M.N.: Phys. Rev. A **38** (1988) 1207
88Fie1 Field, D., Mrotzek, G., Knight, D.W., Lunt, S., Ziesel, J.P.: J. Phys. B **21** (1988) 171
88Gar1 García, G., Pérez, A., Campos, J.: Phys. Rev. A **38** (1988) 654
88Mar1 Marawar, R.W., Walter, C.W., Smith, K.A., Dunning, F.B.: J. Chem. Phys. **88** (1988) 2853

88Nis1 Nishimura, H., Yano, K.: J. Phys. Soc. Jpn. **57** (1988) 1951
88Sue1 Sueoka, O.: J. Phys. B **21** (1988) L631
89All1 Allan, M.: J. Electron Spectrosc. Relat. Phenom. **48** (1989) 219
89Ben1 Benitez, A., Moore, J.H., Tossell, J.A.: J. Chem. Phys. **88** (1988) 6691
89Buc1 Buckman, S.J., Mitroy, J.: J. Phys. B **22** (1989) 1365
89Fen1 Fenzlaff, H.-P., Illenberger, E.: Chem. Phys. **136** (1989) 443
89Fer1 Ferch, J., Masche, C., Raith, W., Wiemann, L.: Phys. Rev. A **40** (1989) 5407
89Kno1 Knoth, G., Rädle, M., Gote, M., Ehrhardt, H., Jung, K.: J. Phys. B **22** (1989) 299
89Kno2 Knoth, G., Gote, M., Rädle, M., Leber, F., Jung, K., Ehrhardt, H.: J. Phys. B **22** (1989) 2797
89McD1 McDaniel, E.W.: Atomic Collisions, Electron and Photon Projectiles, New York: Wiley, 1989
89Ost1 Oster, T., Kühn, A., Illenberger, E.: Int. J. Mass Spectrom. Ion Processes **89** (1989) 1
89Rad1 Rädle, M., Knoth, K., Jung, K., Ehrhardt, H.: J. Phys. B **22** (1989) 1455
89Shi1 Shimamura, I.: Sci. Pap. Inst. Phys. Chem. Res. (Jpn.) **82** (1989) 1
89Sub1 Subramanian, K.P., Kumar, V.: J. Phys. B **22** (1989) 2387
89Sue1 Sueoka, O., Mori, S.: J. Phys. B **22** (1989) 963
89Szm1 Szmytkowski, Cz., Maciąg, K., Karwasz, G., Filipović, D.: J. Phys. B **22** (1989) 525
89Vus1 Vušković, L., Zuo, M., Shen, G.F., Stumpf, B., Bederson, B.: Phys. Rev. A **40** (1989) 133
89Wan1 Wan, H.-X., Moore, J.H., Tossell, J.A.: J. Chem. Phys. **91** (1989) 7340
90Chu1 Chu, S.C., Burrow, P.D.: Chem. Phys. Lett. **171** (1990) 17
90Gar1 García, G., Aragón, C., Campos, J.: Phys. Rev. A **42** (1990) 4400
90Kau1 Kauppila, W.E., Stein, T.S.: Adv. At. Mol. Phys. **26** (1990) 1
90Nis1 Nishimura, H., Sakae, T.: Jpn. J. Appl. Phys. **29** (1990) 1372
90Moy1 Moylan, C.R., Baer Green, S., Brauman, J.I.: Int. J. Mass Spcetrom. Ion Processes **96** (1990) 299
90Rup1 Rupnik, K., Asaf, U., McGlynn, S.P.: J. Chem. Phys. **92** (1990) 2303
90Sag1 Sağlam, Z., Aktekin, N.: J. Phys. B **23** (1990) 1529
90Sub1 Subramanian, K.P., Kumar, V.: J. Phys. B **23** (1990) 745
90Tan1 Tanaka, H., Boesten, L., Sato, H., Kimura, M., Dillon, M.A., Spence, D.: J. Phys. B **23** (1990) 577
91Asa1 Asaf, U., Steinberger, I.T., Meyer, J., Reininger, R.: J. Chem. Phys. **95** (1991) 4070
91Ben1 Benoit, C., Abouaf, R.: Chem. Phys. Lett. **177** (1991) 573
91Fer1 Ferch, J., Raith, W., Schweiker, A.: XVII Int.Conf. on Physics of Electronic and Atomic Collisions, Brisbane (McCarthy, I. E. et al., eds.), Griffith University 1991, Abstract p. 211
91Fie1 Field, D. , Knight, D.W., Mrotzek, G., Randell, J., Lunt, S.L., Ozenne, J.B., Ziesel, J.P.: Meas. Sci. Technol. **2** (1991) 757
91Fie2 Field, D., Lunt., S.L., Mrotzek, G., Randell, J., Ziesel, J.P.: J. Phys. B **24** (1991) 3497
91Mey1 Meyer, J., Reininger, R., Asaf, U., Steinberger, I.T.: J. Chem. Phys. **94** (1991) 1820
91Nis1 Nishimura, H., Tawara, H.: J. Phys. B **24** (1991) L363
91Sag1 Sağlam, Z., Aktekin, N.: J. Phys. B **24** (1991) 3491
91Szm1 Szmytkowski, Cz, Maciąg, K :J. Phys. B **24** (1991) 4273
91Szm2 Szmytkowski, Cz., Maciąg, K., Koenig, P., Zecca, A., Oss, S., Grisenti, R.: Chem. Phys. Lett. **179** (1991)114
91Wan1 Wan, H.-X., Moore, J.H., Tossell, J.A.: J. Chem. Phys. **94** (1991) 1868
91Zec1 Zecca, A., Karwasz, G., Brusa, R.S., Szmytkowski, Cz.: J. Phys. B **24** (1991) 2747
92Boe1 Boesten, L., Tanaka, H., Kobayashi, A., Dillon, M.A., Kimura, M.: J. Phys. B **24** (1992) 1607
92Hay1 Hayashi, M.: 1992 Electron Collision Cross Sections, Handbook on Plasma Material Science, Vol. 4 (1992) No 9, Jap. Soc. Promotion Science (Ohm-sha)
92Iga1 Iga, I., Rao, M.V.V.S., Srivastava, S.K., Nogueira, J.C.: Z. Phys. D **24** (1992) 111
92Kan1 Kanik, I., Nickel, J.C., Trajmar, S.: J. Phys. B **25** (1992) 2189
92Kan2 Kanik, I., Trajmar, S., Nickel, J.C.: Chem. Phys. Lett. **193** (1992) 281
92Lin1 Ling, X., Lindsay, B.G., Smith, K.A., Dunning, F.B.: Phys. Rev. A **45** (1992) 242

92Man1 Mann, A., Linder, F.: J. Phys. B **25** (1992) 533
92Man2 Mann, A., Linder, F.: J. Phys. B **25** (1992) 545
92Man3 Mann, A., Linder, F.: J. Phys. B **25** (1992) 1621
92Man4 Mann, A., Linder, F.: J. Phys. B **25** (1992) 1633
92Mid1 Middleton, A.G., Teubner, P.J.O., Brunger, M.J.L.: Phys. Rev. Lett. **69** (1992) 2495
92Mod1 Modelli, A., Scagnaroli, F., Distefano, G., Jones, D., Guerra, M.: J. Chem. Phys. **96** (1992) 2061
92Nic1 Nickel, J.C., Kanik, I., Trajmar, S., Imre, K.: J. Phys. B **25** (1992) 2427
92Ran1 Randell, J., Field, D., Lunt, S.L., Mrotzek, G., Ziesel, J.P.: J. Phys. B **25** (1992) 2899
92Shi1 Shimamori, H., Tatsumi, Y., Ogawa, Y., Sunagawa, T.: J. Chem. Phys. **97** (1992) 6335
92Szm1 Szmytkowski, Cz., Maciąg, K., Krzysztofowicz, A.M.: Chem. Phys. Lett. **190** (1992) 141
92Szm2 Szmytkowski, Cz., Krzysztofowicz, A.M., Janicki, P., Rosenthal, L.: Chem. Phys. Lett. **199** (1992) 191
92Yua1 Yuan, J., Zhang, Z.: Phys. Rev. A **45** (1992) 4565
92Zec1 Zecca, A., Karwasz, G.P., Brusa, R.S.: Phys. Rev. A **45** (1992) 2777
92Zec2 Zecca, A., Karwasz, G.P., Brusa, R.S.: Phys. Rev. A **46** (1992) 3877
92Zec3 Zecca, A., Karwasz, G.P., Brusa, R.S.: Chem. Phys. Lett. **199** (1992) 423
93Dil1 Dillon, M.A., Boesten, L., Tanaka, H., Kimura, M., Sato, H.: J. Phys. B **26** (1993) 3147
93Gul1 Gulley, R.J., Brunger, M.J., Buckman, S.J.: J. Phys. B **26** (1993) 2913
93Kar1 Karwasz, G., Brusa, R.S., Gasparoli, A., Zecca, A.: Chem. Phys. Lett. **211** (1993) 529
93Lin1 Ling, X., Smith, K.A., Dunning, F.B.: Phys. Rev. A **47** (1993) R1
93Pop1 Popple, R., Smith, K.A., Dunning, F.B.: J. Chem. Phys. **99** (1993) 184
93Ran1 Randell, J., Ziesel, J.P., Lunt, S.L., Mrotzek, G., Field, D.: J. Phys. B **26** (1993) 3423
93Rao1 Rao, M.V.V.S., Srivastava, S.K.: J. Geophys. Res. **98** (1993) 13137
93Szm1 Szmytkowski, Cz., Krzysztofowicz, A.: Chem. Phys. Lett. **209** (1993) 474
93Shy1 Shyn, T.W., Sweeney, C.J.: Phys. Rev. A **47** (1993) 1006
93Shy2 Shyn, T.W., Sweeney, C.J.: Phys. Rev. A **47** (1993) 2919
93Wan1 Wan, H.-X., Moore, J.H., Olthoff, J.K., Van Brunt, R.J.: Plasma Chem.Plasma Process. **13** (1993) 1
93Zie1 Ziesel, J.P., Randell, J., Field, D., Lunt, S.L., Mrotzek, G., Martin, P.: J. Phys. B **26** (1993) 527
94Gul1 Gulley, R.J., Buckman, S.: J. Phys. B **27** (1994) 1833
94Ham1 Hamada, A., Sueoka, O.: J. Phys. B **27** (1994) 5055
94Ham2 Hamada, A.: PhD Thesis, Yamaguchi University, Ube, Japan (1994)
94Ino1 Inokuti, M. (ed.): Adv. At. Mol. Phys. **33** (1994) 1-473
94Krz1 Krzysztofowicz, A.M., Szmytkowski, Cz.: Chem. Phys. Lett. **219** (1994) 86
94Lun1 Lunt, S.L., Randell, J., Ziesel, J.P., Mrotzek, G., Field, D.: J. Phys. B **27** (1994) 1407
94Ran1 Randell, J., Lunt, S.L., Mrotzek, G., Ziesel, J.-P., Field, D.: J. Phys. B **27** (1994) 2369
94Shi1 Shimamori, H., Sunagawa, T., Ogawa, Y., Tatsumi, Y.: Chem. Phys. Lett. **227** (1994) 609
94Sue1 Sueoka, O., Mori, S., Hamada, A.: J. Phys. B **27** (1994)1453
94Tak1 Takagi, T., Boesten, L., Tanaka, H., Dillon, M.A.: J. Phys. B **27** (1994) 5398
94Und1 Underwood-Lemons, T., Winkler, D.C., Tossell, J.A., Moore, J.H.: J. Chem. Phys. **100** (1994) 9117
94Xin1 Xing, S.-L., Xu, K.-Z., Chen, X.-J., Yang, B.-X., Wang, Y.-G., Pang, W.-N., Zhang, F., Shi, Q.-C.: Acta Phys. Sin. **43** (1994) 1077
95All1 Allan, M.: J. Phys. B **28** (1995) 5163
95Got1 Gote, M., Ehrhardt, H.: J. Phys. B **28** (1995) 3957
95Ham1 Hamada, A., Sueoka, O.: Appl. Surface Sci. **85** (1995) 64
95Jia1 Jiang, Y., Sun, J., Wan, L.: Phys. Rev. A **52** (1995) 398
95Kar1 Karwasz, G.P.: J. Phys. B **28** (1995) 1301
95Krz1 Krzysztofowicz, A.M., Szmytkowski, Cz.: J. Phys. B **28** (1995)1593
95Mat1 Matejcik, S., Kiendler, A., Stamatovic, A., Märk, T.D.: Int. J. Mass Spectrom. Ion Processes **149/150** (1995) 311
95Szm1 Szmytkowski, Cz., Krzysztofowicz, A.: J. Phys. B **28** (1995) 4291

95Szm2 Szmytkowski, Cz., Kasperski, G., Możejko, P.: J. Phys. B **28** (1995) L629
95Sul1 Sullivan, J.P., Gibson, J.C., Gulley, R.J., Buckman, S.J.: J. Phys. B **28** (1995) 4319
95Sun1 Sun, W., Morrison, M.A., Isaacs, W.A., Trail, W.K., Alle, D.T., Gulley, R.J., Brennan, M.J., Buckman, S.J.: Phys. Rev. A **52** (1995) 1229
95Und1 Underwood-Lemons, T., Gergel, T.J., Moore, J.H.: J. Chem. Phys. **102** (1995) 119
95Xin1 Xing, S.L., Shi, Q.C., Chen, X.J., Xu, K.Z., Yang, B.X., Wu, S.L., Feng, R.F.: Phys. Rev. A **51** (1995) 414
95Zec1 Zecca, A., Nogueira, J.C., Karwasz, G.P., Brusa, R.S.: J. Phys. B **28** (1995) 477
96All1 Alle, D.T, Brennan, M.J., Buckman, S.J.: J. Phys. B **29** (1996) L277
96Gar1 García, G., Manero, F.: Phys. Rev. A **53** (1996) 250
96Gar2 García, G., Manero, F.: J. Phys. B **29** (1996) 4017
96Gui1 Guillot, F., Dézarnaud-Dandine, C., Tronc, M., Modelli, A., Lisini, A., Declava, P., Fronzoni, G.: Chem. Phys. **205** (1996) 359
96Jos1 Joshipura, K.N., Patel, P.M.: J. Phys. B **29** (1996) 3925
96Kar1 Karwasz, G.P., Piazza, A., Brusa, R.S., Zecca, A.: XVIII International Symposium on Physics of Ionized Gases (Kotor), Abstracts (Vujičić, B., Djurović, S., eds.), Novi Sad, Yugoslavia, 1996, p. 62
96Liu1 Liu, Y., Sun, J.: Phys. Lett. A **222** (1996) 233
96Moz1 Możejko, P., Kasperski, G., Szmytkowski, Cz.: J. Phys. B **29** (1996) L571
96Moz2 Możejko, P., Kasperski, G., Szmytkowski, Cz., Karwasz, G.P., Brusa, R.S., Zecca, A.: Chem. Phys. Lett. **257** (1996) 309
96Ran1 Randell, J., Gulley, R.J., Lunt, S.L., Ziesel, J.-P., Field, D.: J. Phys. B **29** (1996) 2049
96Ran2 Randell, J., Lunt, S.L., Mrotzek, G., Field, D., Ziesel, J.-P.: Chem. Phys. Lett. **252** (1996) 252
96Szm1 Szmytkowski, Cz., Maciąg, K., Karwasz, G.: Physica Sripta **54** (1996) 271
96Szm2 Szmytkowski, Cz., Możejko, P., Kasperski, G.: XXVIII European Group for Atomic Spectroscopy Conference (Graz), Abstract (Windholz, L., ed.), Graz, Austria, 1996, p. 576
96Szm3 Szmytkowski, Cz., Możejko, P., Kasperski, G.: XVIII International Symposium on Physics of Ionized Gases (Kotor), Abstracts (Vujičić, B., Djurović, S., eds.), Novi Sad, Yugoslavia, 1996, p. 66
96Zec1 Zecca, A., Karwasz, G.P., Brusa, R.S.: One century of experiments on electron-atom and molecule scattering: a critical review of integral cross sections. I Atoms and diatomic molecules, La Rivista del Nuovo Cimento **19** (1996) No3
97Gre1 Green, M.A., Teubner, P.J.O., Mojarrabi, B., Brunger, M.J.: J. Phys. B **30** (1997) 1813
97Kas1 Kasperski, G., Możejko, P., Szmytkowski, Cz.: Z. Phys. D **42** (1997) 187
97Kim1 Kimura, M., Sueoka, O., Hamada, A., Takekawa, M., Itikawa, Y., Tanaka, H., Boesten, L.: J. Chem. Phys. **107** (1997) 6616
97Raj1 Raj, D., Tomar, S.: J. Phys. B **30** (1997) 1989
97Sue1 Sueoka, O., Takaki, H., Hamada, A., Kimura, M.: XXth Int.Conf. on Physics of Electronic and Atomic Collisions (Vienna), Abstracts of Contributed Papers, p. WE057, (Aumayer, F., Betz, G., Winter, H.P., eds.), Vienna, 1997
97Szm1 Szmytkowski, Cz., Możejko, P., Kasperski, G.: J. Phys. B **30** (1997) 4363
97Xin1 Xing, S., Zhang, F., Yao, L., Yu, C., Xu, K.: J. Phys. B **30** (1997) 2867
98Gar1 García, G., Manero, F.: Phys. Rev. A **57** (1998) 1069
98Gul1 Gulley, R.J., Lunt, S.L., Ziesel, J.-P., Field, D.: J. Phys. B **31** (1998) 2735
98Gul2 Gulley, R.J., Field, T.A., Steer, W.A., Mason, N.J., Lunt, S.L., Ziesel, J.-P., Field, D.: J. Phys. B **31** (1998) 5197
98Gul3 Gulley, R.J., Field, T.A., Steer, W.A., Mason, N.J., Lunt, S.L., Ziesel, J.-P., Field, D.: J. Phys. B **31** (1998) 2971
98Kar1 Karwasz, G.P., Brusa R.S., Piazza A., Zecca, A., Możejko, P., Kasperski, G., Szmytkowski, Cz.: Chem. Phys. Lett. **284** (1998) 128
98Lun1 Lunt, S.L., Randell, J., Ziesel, J.-P., Mrotzek, G., Field, D.: J. Phys. B **31** (1998) 4225
98Mer1 Merz, R., Linder, F.: J. Phys. B **31** (1998) 4663

98Mod1 Modelli, A., Guerra, M., Jones, D., Distefano, G., Tronc, M.: J. Chem. Phys. **108** (1998) 9004
98San1 Sanabia, J.E., Cooper, G.D., Tossell, J.A., Moore, J.H.: J. Chem. Phys. **198** (1998) 389
98Sue1 Sueoka, O., Takaki, H., Hamada, A., Sato, H., Kimura, M.: Chem. Phys. Lett. **288** (1998) 124
98Szm1 Szmytkowski, Cz., Możejko, P., Kasperski, G.: J. Phys. B **31** (1998) 3917
99Buc1 Buckman, S.J., Alle, D.T., Brennan, M.J., Burrow, P.D., Gibson, J.C., Gulley, R.J., Jacka, M., Newman, D.S., Rau, A.R.P., Sullivan, J.P., Trantham, K.W.: Austr. J. Phys. **52** (1999) 473
99Chr1 Christophorou, L.G., Olthoff, J.K.: J. Phys. Chem. Ref. Data **28** (1999) 131
99Coo1 Cooper, G.D., Sanabia, J.E., Moore, J.H., Olthoff, J.K., Christophorou, L.G.: J. Chem. Phys. **110** (1999) 682
99Kar1 Karwasz, G.P., Brusa, R.S., Piazza, A., Zecca, A.: Phys. Rev. A **59** (1999) 1341
99Lun1 Lunt, S.L., Field, D., Hoffmann, S.V., Gulley, R.J., Ziesel, J.-P.: J. Phys. B **32** (1999) 2707
99Moz1 Możejko, P., Kasperski, G., Szmytkowski, Cz., Zecca, A., Karwasz, G.P., Del Longo, L., Brusa, R.S.: Eur. Phys. J D **6** (1999) 481
99Sue1 Sueoka, O., Hamada, A., Kimura, M., Tanaka, H., Kitajima, M.: J. Chem. Phys. **111** (1999) 245
99Tan1 Tanaka, H., Tachibana, Y., Kitajima, M., Sueoka, O., Takaki, H., Hamada, A., Kimura, M.: Phys. Rev. A **59** (1999) 2006
99Zec1 Zecca, A., Melissa, R., Brusa, R.S., Karwasz, G.P.: Phys. Lett. A **257** (1999) 75
00Kar1 Karwasz, G.P., Brusa, R.S., Del Longo, L., Zecca, A.: Phys. Rev. A **61** (2000) 024701-1-4
00Kim1 Kimura, M., Sueoka, M., Hamada, A., Itikawa, Y.: Adv. Chem. Phys. **111** (2000) 537
00Szm1 Szmytkowski, Cz., Możejko, P., Kasperski, G., Ptasińska-Denga, E.: J. Phys. B **33** (2000) 15
00Zec1 Zecca, A., Karwasz, G.P, Brusa, R.S: J. Phys. B **33** (2000) 843
01Kar1 Karwasz, G.P., Brusa, R.S., Zecca, A.: One century of experiments on electron-atom and molecule scattering: a critical review of integral cross sections. II Polyatomic molecules, La Rivista del Nuovo Cimento **24** (2001), No. 1
01Kar2 Karwasz, G.P., Brusa, R.S., Zecca, A.: One century of experiments on electron-atom and molecule scattering: a critical review of integral cross sections. III Hydrocarbons and halides, La Rivista del Nuovo Cimento **24** (2001), No. 4

6.2 Integral elastic cross sections

6.2.1 Introduction

6.2.1.1 Definition in terms of the differential cross section

The integral elastic cross section, σ_i, for electron scattering is defined as

$$\sigma_i(\varepsilon) = 2\pi \int_0^{\pi} \frac{d\sigma}{d\Omega} \sin\theta \, d\theta \tag{1}$$

where $d\sigma/d\Omega$ differential elastic scattering cross section, is defined as that fraction of a beam of electrons of energy ε which are scattered at an angle θ into the element of solid angle $d\Omega = 2\pi \sin\theta d\theta$.

6.2.1.2 Definition in terms of the scattering phase shifts

In the quantum mechanical description of elastic scattering the wave function of an electron, at a distance r from a scattering centre, after being scattered at an angle θ is given (in its simplest form) by

$$\psi = e^{ikz} + \frac{f(\theta)}{r} e^{ikr} \tag{2}$$

where $f(\theta)$ is the amplitude of the scattered wave, k is the wavevector and the z axis is in the direction of the incoming particle. The angular part of the outgoing wave may be expressed in partial waves corresponding to specific values of the angular momentum quantum number l. The differential cross section is given by

$$\frac{d\sigma}{d\Omega} = |f(\theta)|^2 \tag{3}$$

where

$$f(\theta) = \frac{1}{2ik} \sum_l (2l+1)[\exp(2i\eta_l) - 1] P_l(\cos\theta) \tag{4}$$

from which it follows that

$$\sigma_i(\varepsilon) = \frac{4\pi}{k^2} \sum_l (l+1) \sin^2(\eta_l - \eta_{l+1}) \tag{5}$$

where η_l is the additional shift introduced into the asymptotic phase of the l*th* partial wave by the scattering. $P_l(\cos\theta)$ are the Legendre polynomials.

For elastic electron scattering from targets without permanent electric dipole moments O'Malley and co-workers [62OMa1, 63OMa1] have shown that the phase shifts at low energies may be expanded in terms of the wave number (the resulting relations are known as modified effective range (MERT) formulae). These formulae have been used in fitting routines to derive the integral elastic cross section at low energies and the scattering length A. An extended version of their formulae (see for example [89Buc1, 95Pet1]) is as follows (atomic units are used):

$$\tan\eta_0 = -Ak[1 + \frac{4}{3}\alpha k^2 \ln(ka_0)] - \frac{\pi}{3}\alpha k^2 + Dk^3 + Fk^4 \tag{6}$$

$$\tan\eta_1 = \frac{\pi}{15}\alpha k^2 - A_1 k^3 \tag{7}$$

where A, A_1, D and F are fitting parameters, a_0 is the Bohr radius and α is the dipole polarizability. For higher order phaseshifts ($l \geq 2$) the Born expansion is used

$$\tan\eta_l = \frac{\pi\alpha k^2}{(2l+3)(2l+1)(2l-1)} \tag{8}$$

The scattering length is also related to the zero energy integral and momentum transfer (σ_m) cross sections via the relation

$$\sigma_i = \sigma_m = 4\pi A^2 \tag{9}$$

Whilst the application of phaseshift approaches are not, strictly speaking, appropriate in electron-molecule scattering, the above technique, or variations of it, have been applied to a number of non-polar molecules which exhibit a high degree of spherical symmetry, such as the hydrocarbons. Examples of these applications can be found in [92Man1, 94Lun1, 98Mer1].

6.2.2 Experimental determinations

6.2.2.1 From attenuation experiments

In some circumstances attenuation techniques, which are widely used for the measurement of grand total scattering cross sections (see section 6.1), can provide a measurement of the integral elastic cross section. Strictly speaking this is only the case where there are no inelastic scattering channels open, which in the case of the overwhelming majority of molecules, is only for very low energies below the first rotational excitation threshold. However in practice, for some molecular systems, the low energy inelastic cross sections are small compared to the elastic such that an attenuation measurement (e.g. using the Beer-Lambert law) will provide a reasonable upper limit on the total elastic cross section. However, in general, this is not the case and almost all of the experimental total elastic cross sections in the literature for electron-molecule scattering have been derived from crossed beam experiments of the differential cross section.

6.2.2.2 From crossed beam experiments

The integral elastic cross section, $\sigma_i(\varepsilon)$, can be derived from absolute measurements of $d\sigma/d\Omega$ via eq. (1). The main complication with this technique is that most measurements of $d\sigma/d\Omega$ cannot cover the entire range of scattering angles between 0 and π due to the presence of the primary beam at forward angles and other geometrical constraints at backward angles. Whilst a recent technique has been developed to overcome this problem at large scattering angles [96Zub1], most of the data in the literature has been derived by the use of some extrapolation procedure to extend the differential measurements to 0 and π. Various techniques have been applied to enable this extrapolation and they, and the uncertainties involved have been discussed by various authors (e.g. [83Tra1]). One common technique which has been applied to many atomic, and some molecular species, is the so-called phaseshift analysis. In this technique, the experimental differential cross sections are fitted with expressions such as (3) and (4), where the first few (perhaps 2 - 4) phaseshifts (expressions (6) and (7)) are treated as free parameters. Higher-order phaseshifts are obtained by the use of (8). The results of the fitting process can then be used to calculate the elastic differential cross section over the entire angular range as well as the integral elastic cross section. This process has been applied, for instance, in electron-rare-gas atom colisions for energies up to the first inelastic threshold (see for example [75And1, 80Reg1, 96Gib1]). Once again, the application of

phaseshift analysis techniques to molecular systems at the differential scattering level has not been used extensively. However, several variations on this process have proved useful in a number of cases for deriving integral elastic cross sections for molecules, e.g. [91Boe1, 95Sun1, 96Boe1].

Most of the experimental data which is used in deriving the preferred integral elastic cross sections in the following section is from crossed beam measurements of differential elastic scattering. As a result of the difficulties, outlined above, in extracting accurate integral cross sections by integrating the differential cross section, it is not uncommon for the the uncertainties on the derived integral cross sections to exceed 20 %. This is particularly true for polar molecules where strong forward scattering, as a result of the long-range dipole interaction, can dominate the differential cross section.

References for 6.2.1 and 6.2.2

62OMa1 O'Malley, T.F., Rosenberg, L., Spruch, L.: Phys. Rev. **125** (1962) 1300

63OMa1 O'Malley, T.F.: Phys. Rev. **130** (1963) 1020

75And1 Andrick, D. and Bitsch, A.: J. Phys. B: At. Mol. Phys. **8** (1975) 393

80Reg1 Register, D.F., Trajmar, S., Srivastava, S.K.: Phys. Rev. A **21** (1980) 1134

83Tra1 Trajmar, S., Register, D.F., Chutjian, A.: Phys. Rep. **97** (1983) 219

89Buc1 Buckman, S.J., Mitroy, J.: J. Phys. B: At. Mol. Opt. Phys. **22** (1989) 1365

91Boe1 Boesten, L., Tanaka, H.: J. Phys. B: At. Mol. Opt. Phys. **24** (1991) 821

92Man1 Mann, A., Linder, F.: J. Phys. B: At. Mol. Opt. Phys. **25** (1992) 533

94Lun1 Lunt, S.L., Randell, J., Ziesel, J.P., Mrotzek, G., Field, D.: J. Phys. B: At. Mol. Opt. Phys. **27** (1994) 1407

95Sun1 Sun, W., Morrison, M.A., Isaacs, W.A., Trail, W.K., Alle, D.T., Gulley, R.J., Brennan, M.J., Buckman, S.J.: Phys. Rev. A **52** (1995) 1229

95Pet1 Petrovic, Z.Lj., O'Malley, T.F., Crompton, R.W.: J. Phys. B: At. Mol. Opt. Phys. **28** (1995) 3309

96Gib1 Gibson, J.C., Gulley, R.J., Sullivan, J.P., Buckman, S.J., Chan, V., Burrow, P.D.: J. Phys. B: At. Mol. Opt. Phys. **29** (1996) 3177

96Boe1 Boesten, L., Tachibana, Y., Nakano, Y., Shinohara, T., Tanaka, H., Dillon, M.A.: J. Phys. B: At. Mol. Opt. Phys. **29** (1996) 5475

96Zub1 Zubek, M., Gulley, N., King, G.C., Read, F.H. J. Phys. B: At. Mol. Opt. Phys. **29** (1996) L239

98Mer1 Merz, R., Linder, F.: J. Phys. B: At. Mol. Opt. Phys. **31** (1998) 4663

6.2.3 Determination of preferred cross sections

The preferred integral elastic cross section for each molecule in this section has been derived from a consideration of all available (published) experimental and, in some cases, theoretical work. In general, we do not consider those cases where only theoretical values exist, unless there is substantial corroboration between two or more diffferent calculations. More weight has been placed on recent measurements which have realistic and well quantified uncertainties. In some cases it is also possible to exclude certain data sets on the basis that the integral elastic cross sections are *larger* than reliable, and more accurate, grand total cross section determinations. The uncertainty estimates on the preferred cross sections indicate the level of concurrence between the various individual measurements and calculations.

6.2.4 Units

Cross sections are given in square Ångström (1 $Å^2 = 10^{-16}$ cm^2) and electron energies in electron volt (eV). Where applicable, scattering lengths are given in atomic units (1 a.u. = $5.2918 \cdot 10^{-9}$ cm) as is customary.

6.2.5 Diatomic molecules

6.2.5.1 Hydrogen (H_2)

The preferred cross sections, listed in Table 6.2.5.1 and shown in Fig. 6.2.5.1, are obtained using the data of [71Lin1, 75Sri1, 80Fer1, 85Nis1, 86Kha1, 91Bru1]. With the exception of [80Fer1], which are grand total cross section measurements but are equivalent to the integral elastic cross section below 50 meV, all of the above cross sections were derived from differential scattering measurements. These experimental values are in reasonable agreement with a vibrational close coupling calculation of [90Sni1].

Table 6.2.5.1. Preferred values of the integral elastic cross section (σ_i) for electrons scattered from hydrogen. The estimated uncertainty is ± 20 % across the entire energy range.

Energy [eV]	σ_i [$Å^2$]	Energy [eV]	σ_i [$Å^2$]	Energy [eV]	σ_i [$Å^2$]
0.020	7.41	0.50	10.95	12	7.61
0.030	7.77	0.60	11.28	14	6.92
0.040	8.08	0.70	11.59	16	6.32
0.050	8.32	0.80	11.88	18	5.78
0.060	8.51	0.90	12.16	20	5.26
0.070	8.69	1.0	12.36	25	4.23
0.080	8.84	1.25	13.0	30	3.40
0.090	8.99	1.50	13.55	35	2.81
0.10	9.13	2.0	14.11	40	2.36
0.12	9.33	3.0	14.12	50	1.73
0.15	9.55	4.0	13.2	60	1.31
0.20	9.83	5.0	12.51	70	1.06
0.25	10.04	6.0	11.45	80	0.89
0.30	10.24	8.0	9.85	90	0.81
0.40	10.61	10	8.58	100	0.74

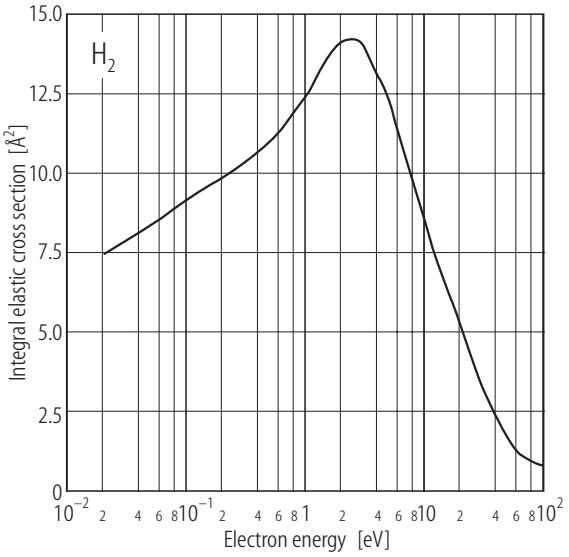

Fig. 6.2.5.1. Integral elastic scattering cross section for H_2 for energies below 100 eV.

References for 6.2.5.1

71Lin1 Linder, F., Schmidt, H.: Z. Naturforsch. **26** A (1971) 1603

75Sri1 Srivastava, S., Chutjian, A., Trajmar, S.: J. Chem. Phys. **63** (1975) 2659

80Fer1 Ferch, J., Raith, W. and Schroder, K.: J. Phys. B: At. Mol. Phys. **13** (1980) 148

85Nis1 Nishimura, H., Danjo, A., Sugahara, H.: J. Phys. Soc. Jpn. **54** (1985) 1757

86Kha1 Khakoo, M., Trajmar, S.: Phys. Rev. A **34** (1986) 138

90Sni1 Snitchler, G., Alston, S., Norcross, D., Saha, B., Danby, G., Trail, W., Morrison, M.A.: Private communication, shown in [91Bru1]

91Bru1 Brunger, M.J., Buckman, S.J., Newman, D.S., Alle, D.T.: J. Phys. B: At. Mol. Opt. Phys. **24** (1991) 1435

6.2.5.2 Nitrogen (N_2)

The preferred cross section, listed in Table 6.2.5.2 and shown in Fig. 6.2.5.2, was obtained using the data of [76Sri1, 80Shy1, 86Soh1, 92Bre1, 93Shi1, 95Sun1]. All of these cross sections were derived from differential scattering measurements. A previous cross section compilation has been presented by [86Iti1]. Note that at low energies, in the region of the dominant $^2\Pi$ resonance, the level of detail in the DCS measurements does not permit the fine details of the resonance profile to be extracted. A broad envelope of the resonance enhanced cross section is thus provided. There is good general agreement between the preferred cross section and the calculations of (for example) [76Cha1, 95Sun1].

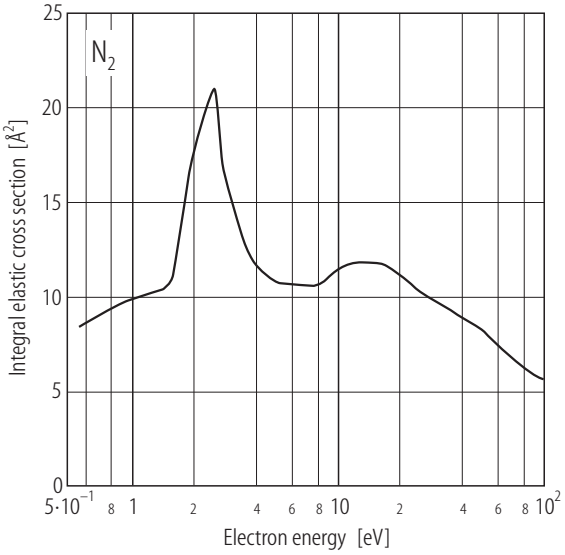

Fig. 6.2.5.2. Integral elastic scattering cross section for N_2 for energies below 100 eV.

Table 6.2.5.2. Preferred values of the integral elastic cross section (σ_i) for electrons scattered from nitrogen. The uncertainty in the cross section is estimated to be of the order of ± 20 %.

Energy [eV]	σ_i [Å^2]	Energy [eV]	σ_i [Å^2]	Energy [eV]	σ_i [Å^2]
0.55	8.39	2.7	17.5	25	10.25
0.70	9.03	3.0	15.0	30	9.65
0.90	9.62	4.0	11.6	40	8.85
1.0	9.83	5.0	10.75	50	8.2
1.5	10.53	6.0	10.6	60	7.4
2.0	17.93	8.0	10.6	80	6.25
2.2	19.5	10	11.4	100	5.6
2.35	20.5	15	11.8		
2.5	21.0	20	11.15		

References for 6.2.5.2

76Sri1 Srivastava, S., Chutjian, A., Trajmar, S.: J. Chem. Phys. **64** (1976) 1340

76Cha1 Chandra, N., Temkin, A.: Phys. Rev. A **13** (1976) 188

80Shy1 Shyn, T.W., Carignan, G.R.: Phys. Rev. A **22** (1980) 923

86Soh1 Sohn, W., Kochem, K-H., Scheuerlein, K-M., Jung, K., Ehrhardt, H.: J. Phys. B: At. Mol. Phys. **19** (1986) 4017

86Iti1 Itikawa, Y., Hayashi, M., Ichimura, A., Onda, K., Sakimoto, K., Takayanagi, K., Nakamura, M., Nishimura, H., Takayanagi, T.: J. Phys. Chem. Ref. Data **15** (1986) 985

92Bre1 Brennan, M.J., Alle, D.T., Euripides, P., Buckman, S.J., Brunger, M.J.: J. Phys. B: At. Mol. Opt. Phys. **25** (1992) 2669

93Shi1 Shi, X., Stephen, T.M., Burrow, P.D.: J. Phys. B: At. Mol. Opt. Phys. **26** (1993) 121

95Sun1 Sun, W., Morrison, M.A., Isaacs, W.A., Trail, W.K., Alle, D.T., Gulley, R.J., Brennan, M.J., Buckman, S.J.: Phys. Rev. A **52** (1995) 1229

6.2.5.3 Oxygen (O_2)

The preferred cross section, listed in Table 6.2.5.3 and shown in Fig. 6.2.5.3, was obtained using the data of [71Tra1, 82Shy1, 93Kan1, 95Sul1]. All of these cross sections were derived from differential elastic scattering measurements.

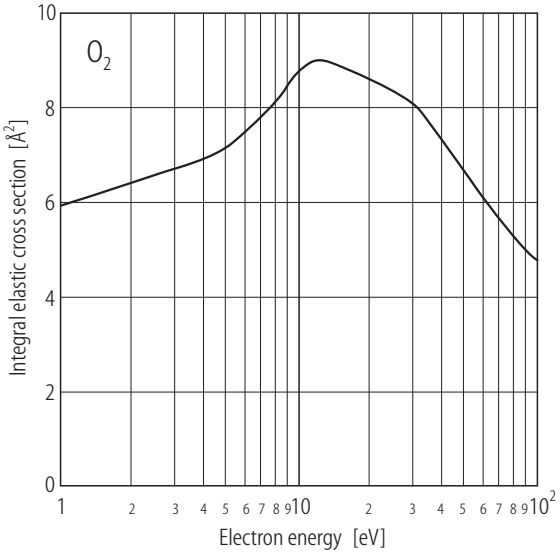

Fig. 6.2.5.3. Integral elastic scattering cross section for O_2 for energies below 100 eV.

Table 6.2.5.3. Preferred values of the integral elastic cross section (σ_i) for electrons scattered from molecular oxygen. The uncertainty in the cross section is estimated to be of the order of ± 20 %.

Energy [eV]	σ_i [Å^2]	Energy [eV]	σ_i [Å^2]	Energy [eV]	σ_i [Å^2]
1.0	5.97	8.0	8.21	40	7.30
2.0	6.45	9.0	8.49	50	6.59
3.0	6.74	10	8.80	60	6.08
4.0	6.93	12	9.00	70	5.63
5.0	7.20	15	8.89	80	5.29
6.0	7.52	20	8.60	90	5.01
7.0	7.86	30	8.09	100	4.78

References for 6.2.5.3

71Tra1 Trajmar, S., Cartwright, D.W., Williams, W.: J. Chem. Phys. **56** (1971) 1482
82Shy1 Shyn, T.W., Sharp, W.E.: Phys. Rev. A **26** (1982) 1369
93Kan1 Kanik, I., Trajmar, S., Nickel, J.C.: J. Geophys. Res. **98** (1993) 7447
95Sul1 Sullivan, J.P., Gibson, J.C., Gulley, R.J., Buckman, S.J.: J. Phys. B: At. Mol. Opt. Phys. **28** (1995) 4319

6.2.5.4 Carbon monoxide (CO)

The preferred cross section, listed in Table 6.2.5.4 and shown in Fig. 6.2.5.4, was obtained using the data of [78Tan1, 88Nic1, 93Kan1, 96Gib1]. The cross section of [93Kan1] is their preferred cross section based on an analysis of previous work. The present preferred cross section, which includes the more recent work of [96Gib1], is very similar to that of [93Kan1]. All of the other cross sections cited here were derived from differential elastic scattering measurements. There is a good level of agreement between the preferred cross section and the close-coupling SCF calculation of [80Ond1].

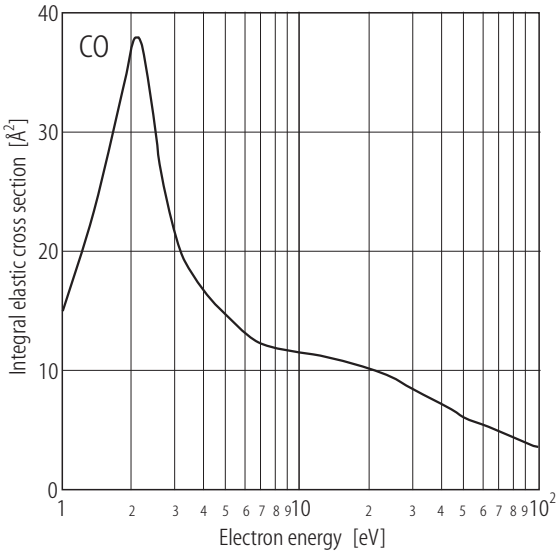

Fig. 6.2.5.4. Integral elastic scattering cross section for CO for energies below 100 eV.

Table 6.2.5.4. Preferred values of the integral elastic cross section (σ_i) for electrons scattered from carbon monoxide. The uncertainty in the cross section is estimated to be of the order of ± 15 %.

Energy [eV]	σ_i [Å^2]	Energy [eV]	σ_i [Å^2]	Energy [eV]	σ_i [Å^2]
1.0	14.72	3.0	21.22	20	10.19
1.2	19.39	3.5	18.11	30	8.49
1.4	24.33	4.0	16.56	40	7.08
1.6	29.29	4.5	15.42	50	5.94
1.8	33.5	5.0	14.43	60	5.38
2.0	37.78	6.0	13.02	70	4.81
2.1	37.92	7.0	12.17	80	4.25
2.2	36.65	8.0	11.89	90	3.96
2.4	31.55	9.0	11.60	100	3.68
2.6	26.46	10	11.46		
2.8	23.49	15	10.89		

References for 6.2.5.4

78Tan1 Tanaka, H., Srivastava, S.K., Chutjian, A.: J. Chem. Phys. **69** (1978) 5329

80Ond1 Onda, K., Truhlar, D.G.: J. Phys. C **72** (1980) 5249

88Nic1 Nickel, J.C., Mott, C., Kanik, I., McCollum, D.C.: J. Phys. B: At. Mol. Opt. Phys. **21** (1988) 1867

93Kan1 Kanik, I., Trajmar, S., Nickel, J.C.: J. Geophys. Res. **98** (1993) 7447

96Gib1 Gibson, J.C., Morgan, L.A., Gulley, R.J., Brunger, M.J., Bundschu, C.T., Buckman, S.J.: J. Phys. B: At. Mol. Opt. Phys. **29** (1996) 3197

6.2.5.5 Nitric oxide (NO)

The preferred cross section, listed in Table 6.2.5.5 and shown in Fig. 6.2.5.5, was obtained using the only data available in the literature, the differential elastic scattering data of [95Moj1].

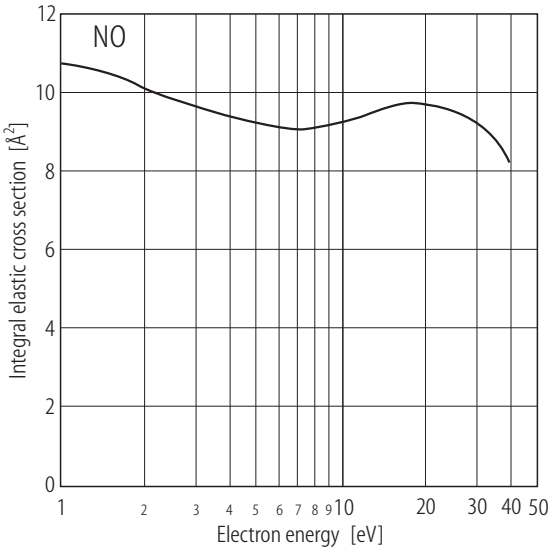

Fig. 6.2.5.5. Integral elastic scattering cross section for NO for energies below 50 eV.

Table 6.2.5.5. Preferred values of the integral elastic cross section (σ_i) for electrons scattered from nitric oxide. The uncertainty in the cross section is estimated to be of the order of ± 25 %.

Energy [eV]	σ_i [Å^2]
1.0	10.75
1.5	10.45
2.0	10.10
3.0	9.65
4.0	9.40
5.0	9.25
7.5	9.05
10	9.25
15	9.65
20	9.70
30	9.25
40	8.21

References for 6.2.5.5

95Moj1 Mojarrabi, B., Gulley, R.J., Middleton, A.G., Cartwright, D.C., Teubner, P.J.O., Buckman, S.J., Brunger, M.J.: J. Phys. B: At. Mol. Opt. Phys. **28** (1995) 487

6.2.6 Polyatomic molecules

6.2.6.1 Methane (CH_4)

The preferred cross section, listed in Table 6.2.6.1 and shown in Fig. 6.2.6.1, is obtained using the cross sections of [83Soh1, 85Fer1, 86Loh1, 86Soh1, 90Shy1, 91Boe1, 94Lun1, 97Bun1, 98Lun1]. This cross section is in reasonable agreement with the calculated cross section of [95Alt1], particularly at energies above 2 eV.

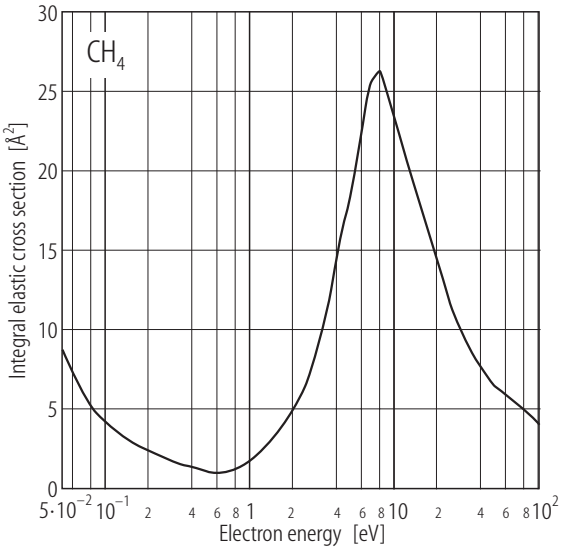

Fig. 6.2.6.1. Integral elastic scattering cross section for CH_4 for energies below 100 eV.

Table 6.2.6.1. Preferred values of the integral elastic cross section (σ_i) for electrons scattered from methane. The estimated uncertainty is ± 35 % below 1 eV and ± 25 % above 1 eV.

Energy [eV]	σ_i [Å^2]	Energy [eV]	σ_i [Å^2]	Energy [eV]	σ_i [Å^2]
0	21.1	0.80	1.16	9.0	25.0
0.05	8.80	0.9	1.42	10	23.3
0.1	4.16	1.0	1.72	15	18.1
0.15	2.88	1.5	3.12	20	14.22
0.20	2.33	2.0	4.88	30	9.65
0.25	1.93	3.0	8.69	40	7.63
0.30	1.59	4.0	14.2	50	6.47
0.40	1.31	5.0	18.4	75	5.25
0.50	1.09	6.0	22.8	100	4.0
0.60	0.96	7.0	25.6		
0.70	1.01	8.0	26.2		

References for 6.2.6.1

83Soh1 Sohn, W., Jung, K., Ehrhardt, H.: J. Phys. B: At. Mol. Phys. **16** (1983) 891
85Fer1 Ferch, J., Granitza, B., Raith, W.: J. Phys. B: At. Mol. Phys. **18** (1985) L445
86Loh1 Lohmann, B., Buckman, S.J.: J. Phys. B: At. Mol. Phys. **19** (1986) 2565
86Soh1 Sohn, W., Kochem, K.H., Scheuerlein, K.M, Jung, K., Ehrhardt, H.: J. Phys. B: At. Mol. Phys. **19** (1986) 3625
90Shy1 Shyn, T.W., Cravens, T.E.: J. Phys. B: At. Mol. Opt. Phys. **23** (1990) 293
91Boe1 Boesten, L., Tanaka, H.: J. Phys. B: At. Mol. Opt. Phys. **24** (1991) 821
94Lun1 Lunt, S.L., Randell, J., Ziesel, J.P., Mrotzek, G., Field, D.: J. Phys. B: At. Mol. Opt. Phys. **27** (1994) 1407
95Alt1 Althorpe, S.C., Gianturco, F.A., Sanna, N.: J. Phys. B: At. Mol. Opt. Phys. **28** (1995) 4165
97Bun1 Bundschu, C.T., Gibson, J.C., Gulley, R.J., Brunger, M.J., Buckman, S.J., Sanna, N., Gianturco, F.A.: J. Phys. B: At. Mol. Opt. Phys. **30** (1997) 2239
98Lun1 Lunt, S.L., Randell, J., Ziesel, J.P., Mrotzek, G., Field, D.: J. Phys. B: At. Mol. Opt. Phys. **31** (1998) 4225

6.2.6.2 Ammonia (NH_3)

There has only been one experiment where absolute elastic scattering cross sections for ammonia have been determined. The preferred cross section is thus based on the sole differential scattering measurement of [92All1] at energies between 2 and 30 eV. This cross section is given in Table 6.2.6.2 and shown in Fig. 6.2.6.2. Due to the large dipole moment of this molecule and the subsequently strong forward scattering, the estimated uncertainty in the cross section is ± 40 %. At energies above 5 eV there is good agreement between this cross section and the Kohn variational calculation of [92Res1].

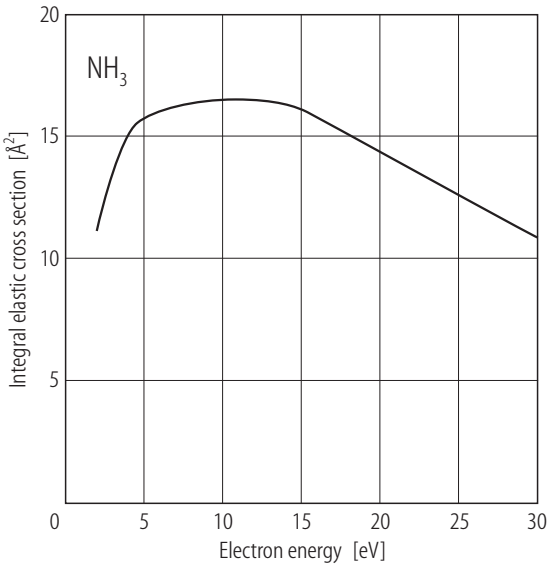

Fig. 6.2.6.2. Integral elastic scattering cross section for NH_3 for energies below 30 eV.

Table 6.2.6.2. Preferred values of the integral elastic cross section (σ_i) for electrons scattered from ammonia. The uncertainty in the cross section is estimated to be of the order of ± 40 %.

Energy [eV]	σ_i [Å^2]
2.0	11.2
3.0	13.5
4.0	15.1
5.0	15.8
7.5	16.3
10	16.5
15	16.1
20	14.4
30	10.9

References for 6.2.6.2

92All1 Alle, D.T., Gulley, R.J., Buckman, S.J., Brunger, M.J.: J. Phys. B: At. Mol. Opt. Phys. **25** (1992) 1533
92Res1 Rescigno, T.N., Lengsfield, B.H., McCurdy, C.W., Parker, S.D.: Phys. Rev. A **45** (1992) 7800

6.2.6.3 Water vapour (H_2O)

The preferred cross section, listed in Table 6.2.6.3 and shown in Fig. 6.2.6.3, was obtained from an analysis of the differential scattering data of [85Dan1, 86Kat1, 87Shy1, 91Joh1, 92Shy1]. As there are substantial differences between these cross sections the estimated uncertainty on the preferred cross section is ± 40 %. There is reasonable agreement between the preferred cross section and the theoretical calculations of (for example) [88Jai1] and [93Oka1].

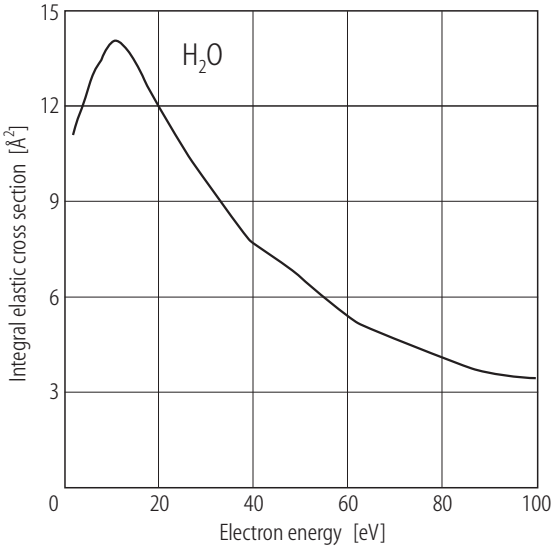

Fig. 6.2.6.3. Integral elastic scattering cross section for H_2O for energies below 100 eV.

Table 6.2.6.3. Preferred values of the integral elastic cross section (σ_i) for electrons scattered from water vapour. The uncertainty in the cross section is estimated to be of the order of ± 40 %.

Energy [eV]	σ_i [Å^2]	Energy [eV]	σ_i [Å^2]	Energy [eV]	σ_i [Å^2]
2.0	11.1	9.0	13.8	50	6.62
3.0	11.6	10	14.0	60	5.37
4.0	11.9	12	14.0	70	4.72
5.0	12.4	15	13.4	80	4.13
6.0	12.9	20	12.0	90	3.60
7.0	13.2	30	9.65	100	3.43
8.0	13.5	40	7.70		

References for 6.2.6.3

85Dan1 Danjo, A., Nishimura, H.: J. Phys. Soc. Jpn. **54** (1985) 1224
86Kat1 Katase, A., Ishibashi, K., Matsuomoto, Y., Sakae, T., Maezono, S., Murakami, E., Watanabe, K., Makai, H.: J. Phys. B: At. Mol. Phys. **19** (1986) 2715
87Shy1 Shyn, T.W, Cho, S.Y.: Phys. Rev. A **36** (1987) 5138
88Jai1 Jain, A.: J. Phys. B: At. Mol. Opt. Phys. **21** (1988) 905
91Joh1 Johnstone, W.M., Newell, W.R.: J. Phys. B: At. Mol. Opt. Phys. **24** (1991) 3633
92Shy1 Shyn, T.W., Grafe, A.: Phys. Rev. A **46** (1992) 4406
93Oka1 Okamoto, Y., Onda, K., Itikawa, Y.: J. Phys. B: At. Mol. Opt. Phys. **26** (1993) 745

6.2.6.4 Acetylene (C_2H_2)

There have been two absolute measurements of differential elastic scattering in acetylene, those of [85Koc1] and [93Kha1]. The preferred elastic cross section for C_2H_2 is given in Table 6.2.6.4 and shown in Fig. 6.2.6.4.

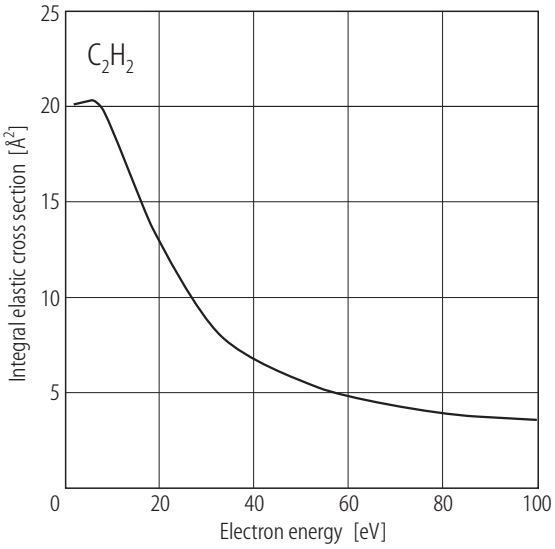

Fig. 6.2.6.4. Integral elastic scattering cross section for C_2H_2 for energies below 100 eV.

Table 6.2.6.4. Preferred values of the integral elastic cross section (σ_i) for electrons scattered from acetylene. The uncertainty in the cross section is estimated to be of the order of ± 25 %.

Energy [eV]	σ_i [Å^2]
2	20
5	20.3
10	20.3
15	15.1
20	12.8
30	8.5
50	5.6
100	3.7

References for 6.2.6.4

85Koc1 Kochem, K-H., Sohn, W., Jung, K., Ehrhardt, H., Chang, E.S.: J. Phys. B: At. Mol. Phys. **18** (1985) 1253
93Kha1 Khakoo, M.A, Jayaweera, T., Wang, S., Trajmar, S.: J. Phys. B: At. Mol. Opt. Phys. **26** (1993) 4845

6.2.6.5 Ethane (C_2H_6)

The preferred integral elastic scattering cross section for ethane is given in Table 6.2.6.5 and is shown in Fig. 6.2.6.5. It has been derived from the differential elastic scattering cross sections of [88Tan1] and [98Mer1].

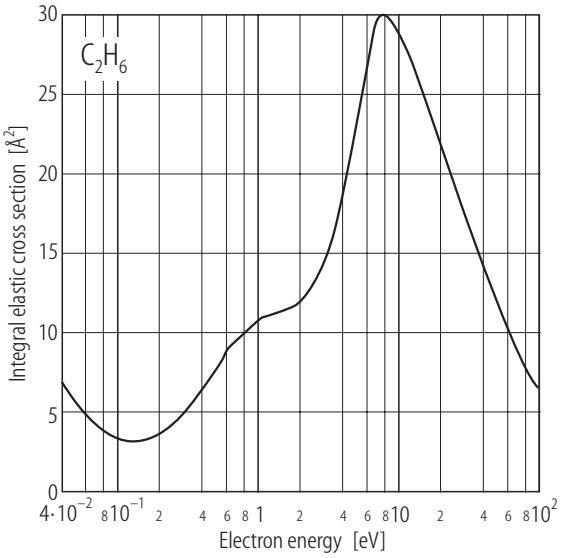

Fig. 6.2.6.5. Integral elastic scattering cross section for C_2H_6 for energies below 100 eV.

Table 6.2.6.5. Preferred values of the integral elastic cross section (σ_i) for electrons scattered from ethane. The uncertainty in the cross section is estimated to be of the order of ± 25 %.

Energy [eV]	σ_i [Å^2]	Energy [eV]	σ_i [Å^2]	Energy [eV]	σ_i [Å^2]
0	31.9	0.4	6.5	6.0	27.4
0.02	11.2	0.5	7.7	7.0	29.9
0.04	6.8	0.6	8.9	8.0	30.3
0.06	4.8	0.8	9.95	10	28.8
0.08	3.7	1.0	10.8	15	25.3
0.1	3.25	1.5	11.4	20	21.8
0.12	3.12	2.0	11.9	30	17.2
0.14	3.17	3.0	14.7	50	11.7
0.2	3.7	4.0	19.1	75	8.3
0.3	5.0	5.0	23.7	100	6.6

References for 6.2.6.5

88Tan1 Tanaka, H., Boesten, L., Matsunaga, D., Kudo, T.: J. Phys. B: At. Mol. Opt. Phys. **21** (1988) 1255

98Mer1 Merz, R., Linder, F.: J. Phys. B: At. Mol. Opt. Phys. **31** (1998) 4663

6.2.6.6 Silane (SiH_4)

The preferred integral elastic scattering cross section for silane is given in Table 6.2.6.6 and is shown in Fig. 6.2.6.6. It is derived from the differential scattering measurements of [90Tan1].

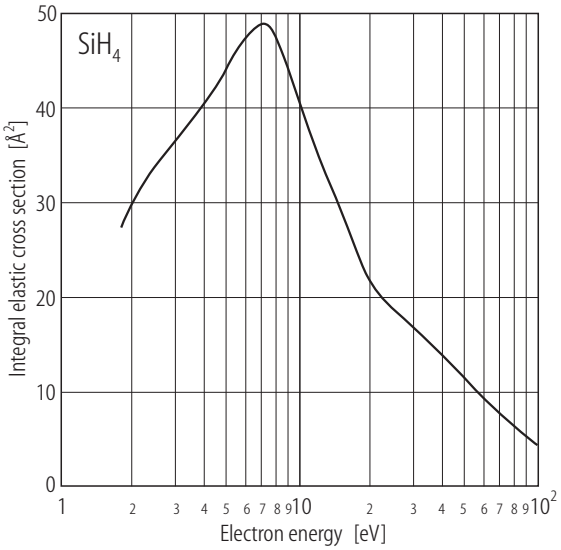

Fig. 6.2.6.6. Integral elastic scattering cross section for SiH_4 for energies below 100 eV.

Table 6.2.6.6. Preferred values of the integral elastic cross section (σ_i) for electrons scattered from silane. The uncertainty in the cross section is estimated to be of the order of ± 25 %.

Energy [eV]	σ_i [Å^2]
1.8	27.5
2.15	31.6
2.65	34.8
3	36.5
4	40.1
5	44.4
7.5	49.9
10	39.4
15	28.7
20	20.7
40	14
100	4.3

References for 6.2.6.6

90Tan1 Tanaka, H., Boesten, L., Sato, H., Kimura, M., Dillon, M.A., Spence, D.: J. Phys. B: At. Mol. Opt. Phys. **23** (1990) 577

6.2.6.7 Hydrogen sulphide (H_2S)

There has only been one measurement of elastic differential scattering for H_2S, that of [93Gul1]. The preferred integral elastic cross section derived from this work is given in Table 6.2.6.7. and is shown in Fig. 6.2.6.7. Due to the strong forward scattering, resulting from the large dipole moment, it is difficult to determine the small angle scattering cross section and as a result the uncertainty on the integral cross section is estimated to be ± 40 %. At energies above 5 eV there is reasonably good agreement between the preferred cross section, the close coupling calculation of [91Gia1] and the Kohn variational calculation of [92Len1].

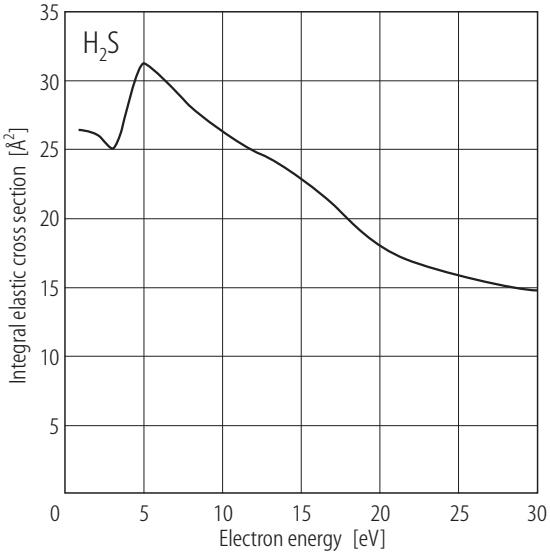

Fig. 6.2.6.7. Integral elastic scattering cross section for H_2S for energies below 30 eV.

Table 6.2.6.7. Preferred values of the integral elastic cross section (σ_i) for electrons scattered from hydrogen sulphide. The uncertainty in the cross section is estimated to be of the order of ± 40 %.

Energy [eV]	σ_i [Å^2]
1.0	26.3
2.0	26.0
3.0	25.1
5.0	31.1
10	26.2
15	22.9
20	18.0
30	14.8

References for 6.2.6.7

91Gia1 Gianturco, F.A.: J. Phys. B: At. Mol. Opt. Phys. **24** (1991) 4627
92Len1 Lengsfield, B.H. Rescigno, T.N., McCurdy, C.W., Parker, S.D.: Private communication, shown in [93Gul1]
93Gul1 Gulley, R.J., Brunger, M.J., Buckman, S.J.: J. Phys. B: At. Mol. Opt. Phys. **26** (1993) 1533

6.2.6.8 Carbon dioxide (CO_2)

The preferred integral elastic cross section for carbon dioxide at energies between 1 and 100 eV is given in Table 6.2.6.8 and shown in Fig. 6.2.6.8. It is based on the differential elastic scattering measurements of [80Reg1, 98Tan1, 99Gib1]. There is reasonable accord between this cross section and the calculations of [77Mor1, 96Tak1, 99Lee1].

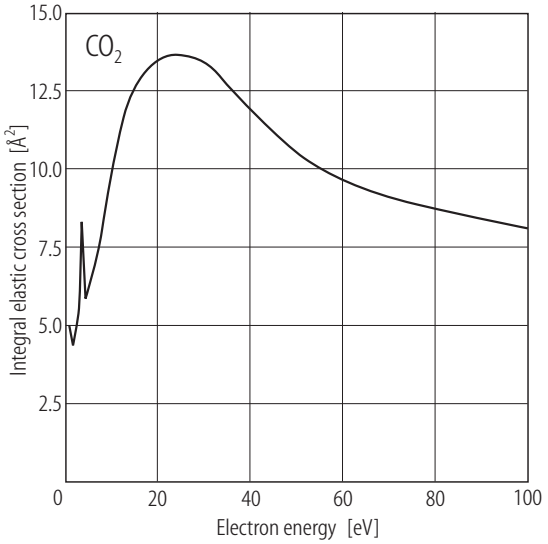

Fig. 6.2.6.8. Integral elastic scattering cross section for CO_2 for energies below 100 eV.

Table 6.2.6.8. Preferred values of the integral elastic cross section (σ_i) for electrons scattered from carbon dioxide. The uncertainty in the cross section is estimated to be of the order of ± 30 %.

Energy [eV]	σ_i [Å^2]	Energy [eV]	σ_i [Å^2]	Energy [eV]	σ_i [Å^2]
1.0	5.00	4.5	5.80	25	13.6
1.5	4.73	5.0	6.00	30	13.4
2.0	4.37	6.0	6.60	40	11.9
2.5	4.70	7.0	7.25	50	10.5
3.0	5.25	8.0	8.06	60	9.6
3.5	6.40	10.0	9.95	70	9.1
3.8	8.20	15	12.5	80	8.7
4.0	8.15	20	13.4	100	8.1

References for 6.2.6.8

77Mor1 Morrison, M.A., Lane, N.F., Collins, L.A.: Phys. Rev. A **15** (1977) 2186
80Reg1 Register, D.F., Nishimura, H., Trajmar, S.: J. Phys. B: At. Mol. Phys. **13** (1980) 1651
96Tak1 Takekawa, M., Itikawa, Y.: J. Phys. B: At. Mol. Opt. Phys. **29** (1996) 4227
98Tan1 Tanaka, H., Ishikawa, T., Masai, T., Sagara, T., Boesten, L., Takekawa, M., Itikawa, Y., Kimura, M.: Phys. Rev. A **57** (1998) 1798
99Gib1 Gibson, J.C., Green, M.A., Trantham, K.W., Buckman, S.J., Teubner, P.J.O., Brunger, M.J.: J. Phys. B: At. Mol. Opt. Phys. **32** (1999) 213
99Lee1 Lee, C.H., Winstead, C., McKoy, V.: J. Chem. Phys. **111** (1999) 5056

6.2.6.9 Nitrous oxide (N_2O)

The preferred integral elastic cross section for Nitrous oxide at energies between 1 and 100 eV is given in Table 6.2.6.9. and shown in Fig. 6.2.6.9. It is based on the differential elastic scattering measurements of [93Joh1, 99Kit1, 00Kit1]. At energies above a few eV there is good agreement between this cross section and the recent variational calculation of [98Win1].

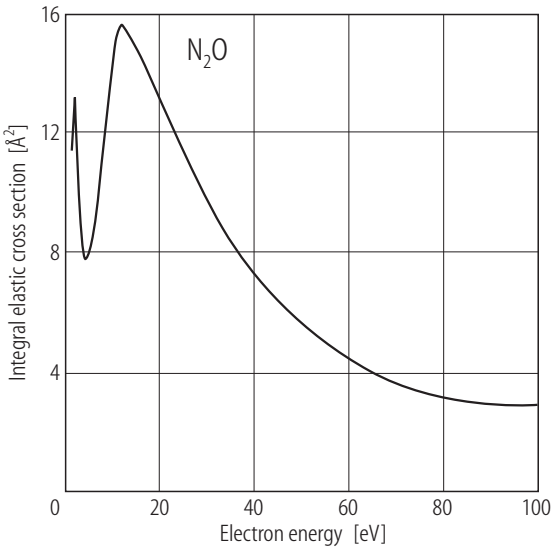

Fig. 6.2.6.9. Integral elastic scattering cross section for N_2O for energies below 100 eV.

Table 6.2.6.9. Preferred values of the integral elastic cross section (σ_i) for electrons scattered from nitrous oxide. The uncertainty in the cross section is estimated to be of the order of ± 25 %.

Energy [eV]	σ_i [Å^2]	Energy [eV]	σ_i [Å^2]
2.0	11.4	10	13.9
2.2	12.1	12	15.6
2.4	13.2	15	15.0
2.6	12.2	20	13.2
3.0	10.3	30	9.8
4.0	7.9	50	5.6
5.0	7.8	75	3.4
6.0	8.5	100	2.9
8.0	10.8		

References for 6.2.6.9

93Joh1 Johnstone, W.M., Newell, W.R.: J. Phys. B: At. Mol. Opt. Phys. **26** (1993) 129
98Win1 Winstead, C., McKoy, V: Phys. Rev. A **57** (1998) 3589
99Kit1 Kitajima, M., Sakamoto, Y., Watanabe, S., Suzuki, T., Ishikawa, T., Tanaka, H., Kimura, M.: Chem. Phys. Lett. **309** (1999) 414
00Kit1 Kitajima, M., Sakamoto, Y., Gulley R.J., Hoshino, M., Gibson, J.C., Tanaka, H., Buckman, S.J.: J. Phys. B: At. Mol. Opt. Phys. **33** (2000) 1687

6.2.6.10 Propane (C_3H_8)

The only measurements of the integral elastic scattering cross section for propane are those of [94Boe1, 99Tan1], both from the same laboratory and both derived from differential elastic scattering measurements at energies between 1.5 and 100 eV. The latter measurements, which are somewhat larger than the former, are taken as the preferred values. The preferred cross section for propane is given in Table 6.2.6.10 and shown in Fig. 6.2.6.10.

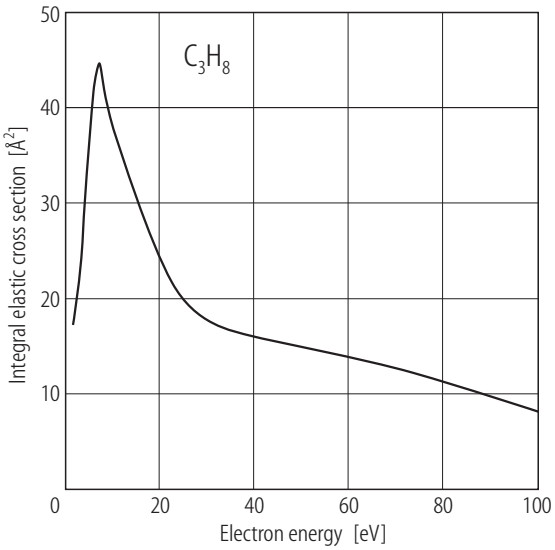

Fig. 6.2.6.10. Integral elastic scattering cross section for C_3H_8 at energies below 100 eV.

Table 6.2.6.10. Preferred values of the integral elastic cross section (σ_i) for electrons scattered from propane. The uncertainty in the cross section is estimated to be of the order of ± 35 %.

Energy [eV]	σ_i [Å^2]	Energy [eV]	σ_i [Å^2]
1.5	19.8	10	44.3
2.0	20.8	12	42.4
3.0	27.4	15	39.2
4.0	35.3	20	37.6
5.0	37.5	25	36.3
6.5	42.9	30	32.9
7.0	44.4	60	18.8
8.0	44.5	100	13.0
9.0	44.9		

References for 6.2.6.10

94Boe1 Boesten, L., Dillon , M.A., Tanaka, H., Kimura, M., Sato, H.: J. Phys. B: At. Mol. Opt. Phys. **27** (1994) 1845

99Tan1 Tanaka, H., Tachibana, Y., Kitajima, M., Sueoka, O, Takaki, H., Hamada, A., Kimura, M.: Phys. Rev. A **59** (1999) 2006

6.2.6.11 Carbonyl sulphide (OCS)

The preferred integral elastic cross section for carbonyl sulphide at energies between 0.4 and 5 eV is given in Table 6.2.6.11 and shown in Fig. 6.2.6.11. It is based on the only elastic differential scattering measurement available in the literature, those of [87Soh1].

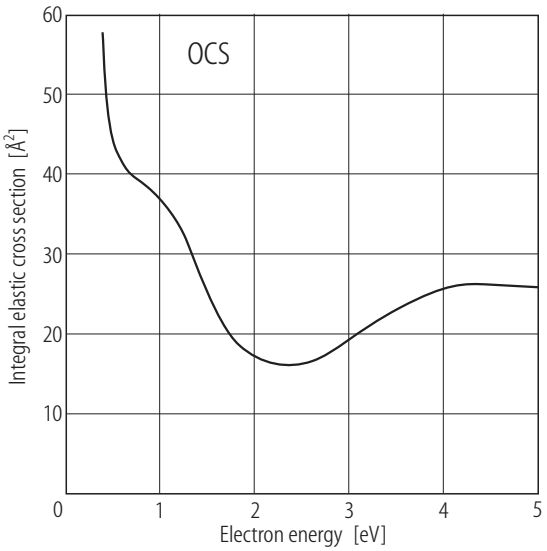

Fig. 6.2.6.11. Integral elastic scattering cross section for OCS at energies below 5 eV.

Table 6.2.6.11. Preferred values of the integral elastic cross section (σ_i) for electrons scattered from carbonyl sulphide. The uncertainty in the cross section is estimated to be of the order of ± 40 % below 1 eV and ± 30 % above 1 eV.

Energy [eV]	σ_i Å^2]
0.4	57.2
0.6	39.4
1.15	36.1
1.7	18.9
2	16.9
2.5	15.3
3	19.6
3.5	23.0
4	26.3
5	25.8

References for 6.2.6.11

87Soh1 Sohn, W., Kochem, H-H., Scheuerlein, K.M., Jung, K., Ehrhardt, H.: J. Phys. B: At. Mol. Phys. **20** (1987) 3217

6.2.6.12 Disilane (Si_2H_6)

The preferred integral elastic scattering cross section for Si_2H_6 is given in Table 6.2.6.12 and it is shown in Fig. 6.2.6.12. This cross section has been derived from the differential scattering measurements of [94Dil1].

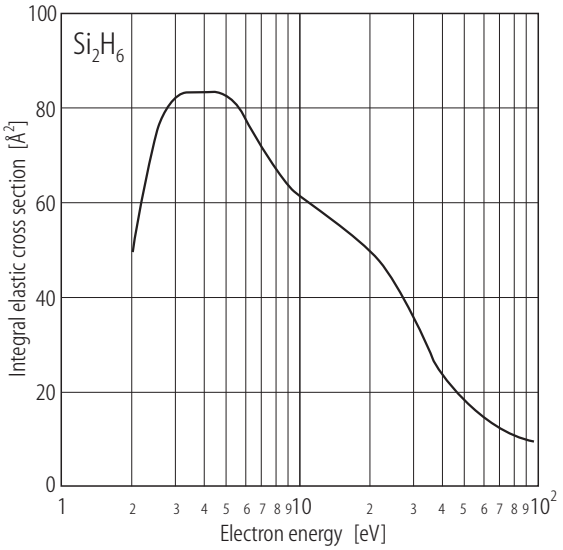

Fig. 6.2.6.12. Integral elastic scattering cross section for Si_2H_6 at energies below 100 eV.

Table 6.2.6.12. Preferred values of the integral elastic cross section (σ_i) for electrons scattered from disilane. The uncertainty in the cross section is estimated to be of the order of ± 30 %.

Energy [eV]	σ_i [Å^2]	Energy [eV]	σ_i [Å^2]
2	49.3	10	61.4
3	82.8	15	54.6
4	83.2	20	50.0
5	83.1	40	23.7
7.5	68.8	100	9.6

References for 6.2.6.12

94Dil1 Dillon, M.A., Boesten, L., Tanaka, H., Kimura, M. and Sato, H.: J. Phys. B: At. Mol. Opt. Phys. **27** (1994) 1209

6.2.6.13 Sulphur dioxide (SO_2)

The preferred integral elastic cross section for sulphur dioxide, for energies between 1 and 100 eV, is provided in Table 6.2.6.13 and shown in Fig. 6.2.6.13. This cross section is based on the differential elastic scattering measurements [89Tra1] and [94Gul1]. Due to the large dipole moment of this molecule, and the resultant strong forward scattering, the estimated uncertainty in this cross section is ± 45 %.

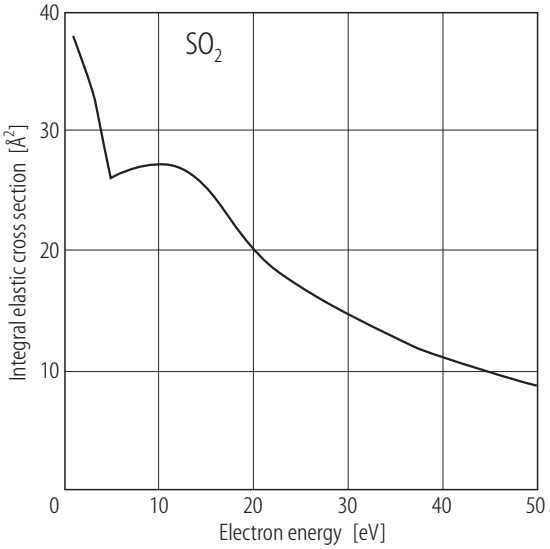

Fig. 6.2.6.13. Integral elastic scattering cross section for SO_2 at energies below 50 eV.

Table 6.2.6.13. Preferred values of the integral elastic cross section (σ_i) for electrons scattered from sulphur dioxide. The uncertainty in the cross section is estimated to be of the order of ± 45 %.

Energy [eV]	σ_i [Å^2]	Energy [eV]	σ_i [Å^2]
1.0	38.0	12	27.1
2.0	36.1	15	25.4
3.4	32.1	20	20.0
4.0	29.8	30	14.6
5.0	26.2	40	11.1
7.5	26.9	50	8.7
10	27.3		

References for 6.2.6.13

89Tra1 Trajmar, S., Shyn, T.W.: J. Phys. B: At. Mol. Opt. Phys. **22** (1989) 2911
94Gul1 Gulley, R.J., Buckman, S.J.: J. Phys. B: At. Mol. Opt. Phys. **27** (1994) 1833

6.2.6.14 Nitogen trifluoride (NF_3)

The preferred integral elastic cross section for nitrogen trifluoride, for energies between 1.5 and 100 eV, is provided in Table 6.2.6.14 and shown in Fig. 6.2.6.14. This cross section is based on the only published elastic scattering measurements, those of [96Boe1].

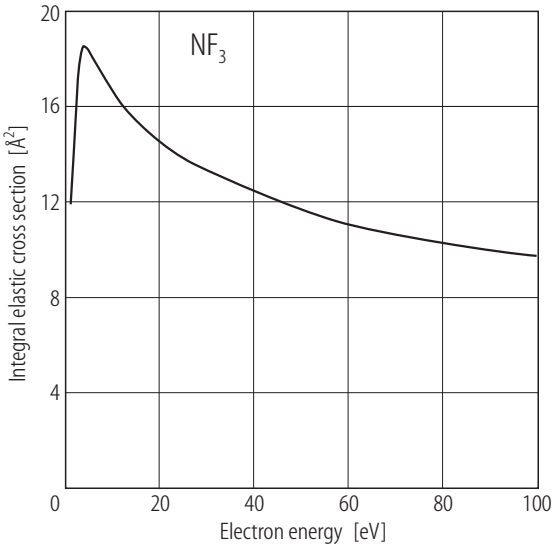

Fig. 6.2.6.14. Integral elastic scattering cross section for NF_3 at energies below 100 eV.

Table 6.2.6.14. Preferred values of the integral elastic cross section (σ_i) for electrons scattered from nitrogen trifluoride. The uncertainties in the cross section are estimated to be of the order of ± 25 %.

Energy [eV]	σ_i [Å^2]	Energy [eV]	σ_i [Å^2]
1.5	11.9	15	15.4
2.0	13.0	20	14.5
3.0	17.2	25	13.8
4.0	18.4	30	13.3
5.0	18.4	50	11.6
6.0	17.9	60	11
7.5	17.5	100	9.7
10	16.7		

References for 6.2.6.14

96Boe1 Boesten, L., Tachibana, Y., Nakano, Y., Shinohara, T., Tanaka, H., Dillon, M A.: J. Phys. B: At. Mol. Opt. Phys. **27** (1994) 1845

6.2.6.15 Carbon disulphide (CS_2)

The preferred integral elastic scattering cross section for carbon disulphide is given in Table 6.2.6.15 and is shown in Fig. 6.2.6.15. The only measurements for this molecule are the differential elastic scattering cross sections of [87Soh1] at energies between 0.3 and 5 eV.

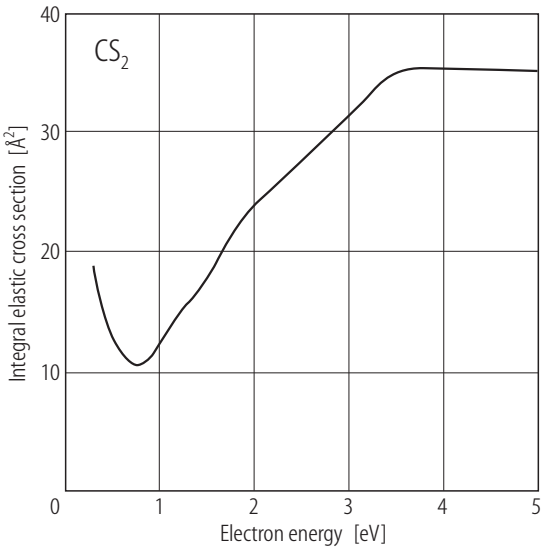

Fig. 6.2.6.15. Integral elastic scattering cross section for CS_2 at energies below 5 eV.

Table 6.2.6.15. Preferred values of the integral elastic cross section (σ_i) for electrons scattered from carbon disulphide. The uncertainty in the cross section is estimated to be of the order of ± 40 % below 1 eV and ± 30 % above 1 eV.

Energy [eV]	σ_i [Å^2]	Energy [eV]	σ_i [Å^2]
0.3	18.7	1.8	22.4
0.5	12.8	2.2	25.4
0.8	9.5	3	31.6
1	12.3	3.5	35.5
1.2	14.9	5	35.1
1.5	17.3		

References for 6.2.6.15

87Soh1 Sohn, W., Kochem, H-H., Scheuerlein, K.M., Jung, K., Ehrhardt, H.: J. Phys. B: At. Mol. Phys. **20** (1987) 3217

6.2.6.16 Germane (GeH_4)

The preferred integral elastic scattering cross section for germane is given in Table 6.2.6.16 and is shown in Fig. 6.2.6.16. The only measurements for this molecule are the differential elastic scattering cross sections of [93Dil1] at energies between 1 and 100 eV.

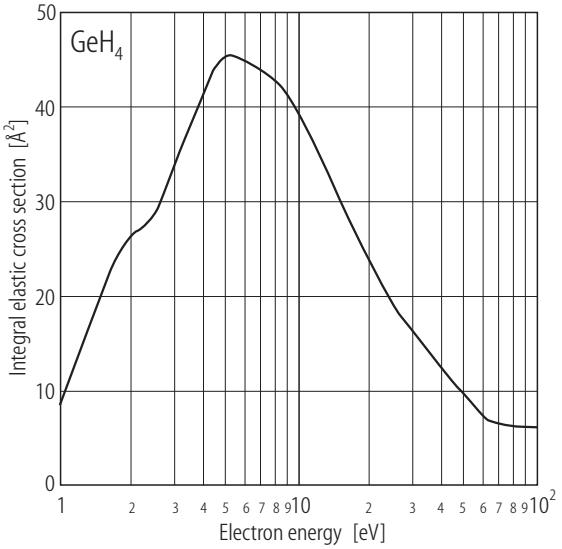

Fig. 6.2.6.16. Integral elastic scattering cross section for GeH_4 at energies below 100 eV.

Table 6.2.6.16. Preferred values of the integral elastic cross section (σ_i) for electrons scattered from germane. The uncertainty in the cross section is estimated to be of the order of ± 30 %.

Energy [eV]	σ_i [Å^2]	Energy [eV]	σ_i [Å^2]
1	8.4	10	39.42
2	26.45	15	30.14
2.5	28.76	20	23.63
3	34.07	60	7.47
5	45.48	100	6.36
7.5	43.4		

References for 6.2.6.16

93Dil1 Dillon, M.A., Boesten, L., Tanaka, H., Kimura, M., Sato, H.: J. Phys. B: At. Mol. Opt. Phys. **26** (1993) 3147

6.2.6.17 Benzene (C_6H_6)

The preferred values of the integral elastic scattering cross section for benzene are given in Table 6.2.6.17 and shown in Fig. 6.2.6.17. These have been derived from the differential elastic scattering measurements of [99 Gul1] and [01Cho1].

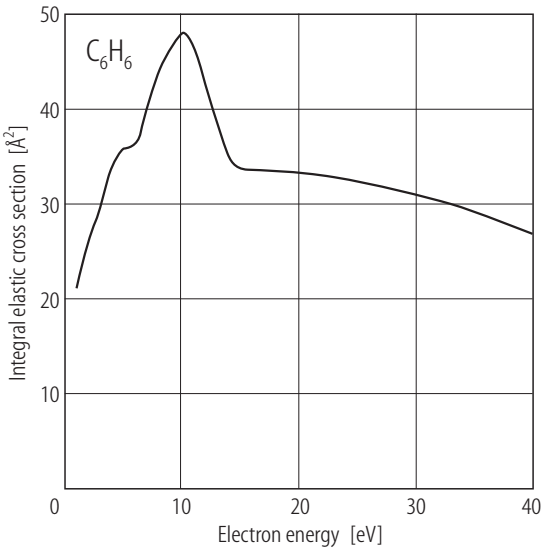

Fig. 6.2.6.17. Integral elastic scattering cross section for C_6H_6 at energies below 40 eV.

Table 6.2.6.17. Preferred values of the integral elastic cross section (σ_i) for electrons scattered from benzene. The estimated uncertainty is ± 25 %.

Energy [eV]	σ_i [Å^2]	Energy [eV]	σ_i [Å^2]
1.1	21.2	8.5	44.9
2.0	25.7	10	47.8
3.0	29.0	15	33.8
3.5	24.7	20	33.3
4.0	33.4	30	31.1
4.9	35.6	40	26.9
6.0	36.1		

References for 6.2.6.17

99Gul1 Gulley, R.J., Buckman, S.J.: J. Phys. B: At. Mol. Opt. Phys. **32** (1999) L405
01Cho1 Cho, H., Gulley, R.J., Sunohara, K., Kitajima, M., Uhlmann, L.J., Tanaka, H., Buckman, S.J.: J. Phys. B: At. Mol. Opt. Phys. **34** (2001) 1019

6.2.6.18 Carbon tetrafluoride (CF_4)

The preferred integral elastic scattering cross section for CF_4 is given in Table 6.2.6.18 and it is shown in Fig. 6.2.6.18. This cross section has been derived from the measurements of [89Sak1, 92Man1, 92Boe1], and a previous analysis of the CF_4 cross sections by [94Bon1].

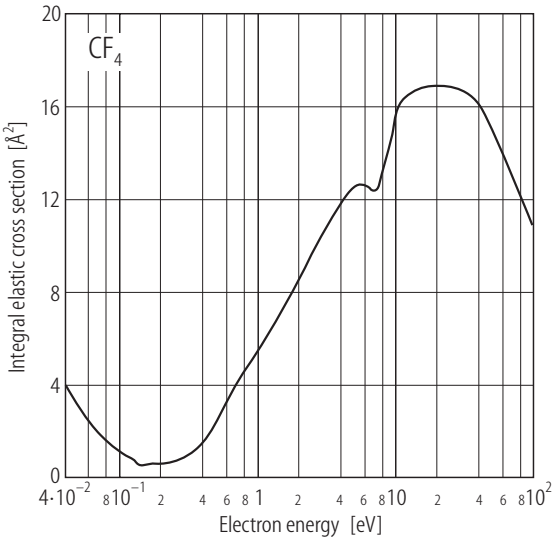

Fig. 6.2.6.18. Integral elastic scattering cross section for CF_4 at energies below 100 eV.

Table 6.2.6.18. Preferred values of the integral elastic cross section (σ_i) for electrons scattered from carbon tetrafluoride. The uncertainty in the cross section is estimated to be of the order of ± 25 %.

Energy [eV]	σ_i [Å^2]	Energy [eV]	σ_i [Å^2]	Energy [eV]	σ_i [Å^2]
0	20	0.30	0.90	8	13.1
0.02	6.5	0.40	1.6	9	14.3
0.04	4.0	0.50	2.6	10	15.8
0.06	2.3	0.75	4.3	15	16.8
0.08	1.6	1.0	5.5	20	16.9
0.10	1.1	1.5	7.2	30	16.7
0.12	0.85	2	8.6	40	16.0
0.14	0.53	3	10.6	50	15.1
0.16	0.62	4	11.9	75	12.6
0.18	0.58	5	12.5	100	10.9
0.20	0.60	6	12.6		
0.25	0.7	7	12.3		

References for 6.2.6.18

89Sak1 Sakae, T., Sumiyoshi, E., Murakami, E., Matsumoto, Y., Ishibashi, K., Katase, A.: J. Phys. B: At. Mol. Opt. Phys. **27** (1989) 1385

92Man1 Mann, A., Linder, F.: J. Phys. B: At. Mol. Opt. Phys. **25** (1992) 533

92Boe1 Boesten, L., Tanaka, H., Kobayashi, A., Dillon, M.A., Kimura, M.: J. Phys. B: At. Mol. Opt. Phys. **25** (1992) 1607

94Bon1 Bonham, R.A.: Jpn. J. Appl. Phys. **33** (1994) 4157
96Chr1 Christophorou, L.G., Olthoff, J.K., Rao, M.V.V.S.: J. Phys. Chem. Ref. Data **25** (1996) 1341

6.2.6.19 Trifluorochloromethane (CF_3Cl)

The preferred integral elastic scattering cross section for CF_3Cl is given in Table 6.2.6.19 and is shown in Fig. 6.2.6.19. It is derived from the elastic differential cross section measurements of [92Man1] which span the energy range from 1 to 10 eV.

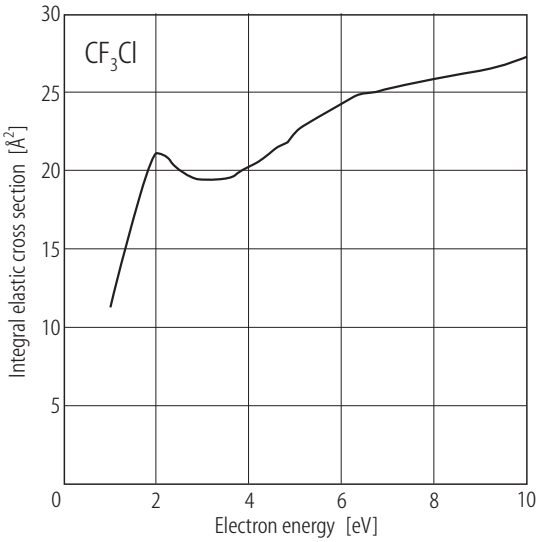

Fig. 6.2.6.19. Integral elastic scattering cross section for CF_3Cl at energies below 10 eV.

Table 6.2.6.19. Preferred values of the integral elastic cross section (σ_i) for electrons scattered from CF_3Cl. The estimated uncertainty is ± 40 %.

Energy [eV]	σ_i [Å^2]	Energy [eV]	σ_i [Å^2]	Energy [eV]	σ_i [Å^2]
1	11.3	3.2	19.4	6.0	24.3
1.2	13.5	3.4	19.4	6.5	25.0
1.4	15.9	3.6	19.6	7.0	25.2
1.6	18.1	3.8	19.7	7.5	25.5
1.8	19.7	4.0	20.3	8.0	25.8
2.0	21.2	4.2	20.6	8.5	26.1
2.2	21.0	4.4	21.0	9	26.4
2.4	20.4	4.6	21.5	9.5	26.8
2.6	19.8	4.8	21.8	10	27.3
2.8	19.5	5	22.4		
3	19.4	5.5	23.5		

References for 6.2.6.19

92Man1 Mann, A. and Linder, F.: J. Phys. B: At. Mol. Opt. Phys. **25** (1992) 1621

6.2.6.20 Difluorodichloromethane (CF_2Cl_2)

The preferred integral elastic scattering cross section for CF_2Cl_2 is given in Table 6.2.6.20 and is shown in Fig. 6.2.6.20. It is derived from the elastic differential cross section measurements of [92Man2] which span the energy range from 0.5 - 9.5 eV. These data have also been considered by [97Chr1] who have derived a cross section set for this molecule.

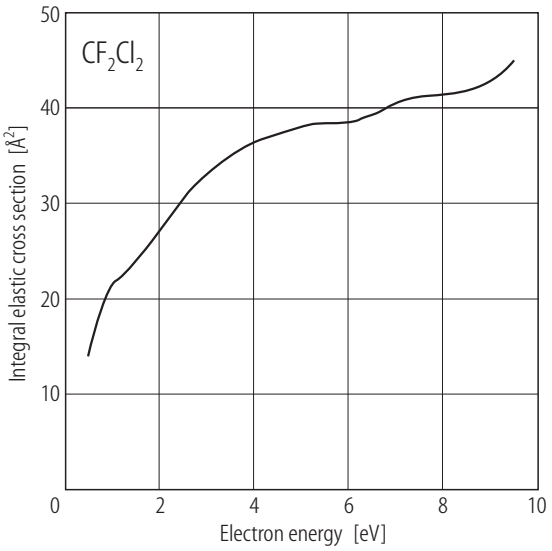

Fig. 6.2.6.20. Integral elastic scattering cross section for CF_2Cl_2 at energies below 10 eV.

Table 6.2.6.20. Preferred values of the integral elastic cross section (σ_i) for electrons scattered from CF_2Cl_2. The estimated uncertainty is ± 40 %.

Energy [eV]	σ_i [Å^2]	Energy [eV]	σ_i [Å^2]	Energy [eV]	σ_i [Å^2]
0.5	14.2	4.0	36.4	7.5	41.2
1.0	21.4	4.5	37.2	8.0	41.3
1.5	23.9	5.0	38.0	8.5	41.8
2.0	27.2	5.5	38.5	9.0	42.9
2.5	30.6	6.0	38.5	9.5	44.9
3.0	33.1	6.5	39.4		
3.5	34.9	7.0	40.6		

References for 6.2.6.20

92Man2 Mann, A., Linder, F.: J. Phys. B: At. Mol. Opt. Phys. **25** (1992) 1633
97Chr1 Christophorou, L.G., Olthoff, J.K., Wang, Y.: J. Phys. Chem. Ref. Data **26** (1997) 1205

6.2.6.21 Hexafluoroethane (C_2F_6)

The preferred integral elastic scattering cross section for hexafluoroethane is given in Table 6.2.6.21 and is shown in Fig. 6.2.6.21. This cross section is based on the differential scattering measurements of [94Tak1] and the extensive review of [98Chr1], who propose a suggested cross section based on additional, unpublished, differential scattering results of [97Mer1]. The tabulated values below are thus taken from the work of [98Chr1].

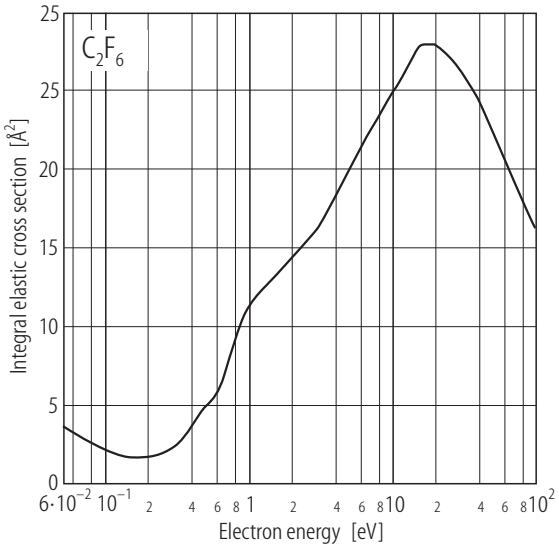

Fig. 6.2.6.21. Integral elastic scattering cross section for C_2F_6 at energies below 100 eV.

Table 6.2.6.21. Preferred values of the integral elastic cross section (σ_i) for electrons scattered from hexafluoroethane. The estimated uncertainty is ± 40 %.

Energy [eV]	σ_i [Å^2]	Energy [eV]	σ_i [Å^2]	Energy [eV]	σ_i [Å^2]
0.01	12.2	0.50	4.9	8.0	23.5
0.02	7.9	0.60	5.71	9.0	24.3
0.04	4.4	0.80	9.39	10	24.9
0.06	3.1	1.0	11.3	15	27.9
0.08	2.4	1.5	13.2	20	28.0
0.10	2.07	2.0	14.5	30	26.3
0.15	1.69	3.0	16.3	40	24.4
0.20	1.66	4.0	18.3	60	20.9
0.25	1.99	5.0	20.1	80	18.4
0.30	2.4	6.0	21.4	100	16.4
0.40	3.7	7.0	22.5		

References for 6.2.6.21

94Tak1 Takagi, T., Boesten, L., Tanaka, H., Dillon, M.A.: J. Phys. B: At. Mol. Opt. Phys. **27** (1994) 5389
97Mer1 Merz, R., Linder, F.: Private communication to L.G. Christophorou and J.K. Olthoff 1997
98Chr1 Christophorou, L.G., Olthoff, J.K.: J. Phys. Chem. Ref. Data **27** (1998) 1

6.2.6.22 Sulphur hexafluoride (SF_6)

The preferred integral elastic cross section for SF_6 is given in Table 6.2.6.22 and is shown in Fig. 6.2.6.22. It is based on the differential elastic scattering measurements of [76Sri1, 79Roh1, 89Sak1, 91Joh1, 00Cho1]. We also note the recent, extensive review of [00Chr1] in which a similar preferred cross section is provided.

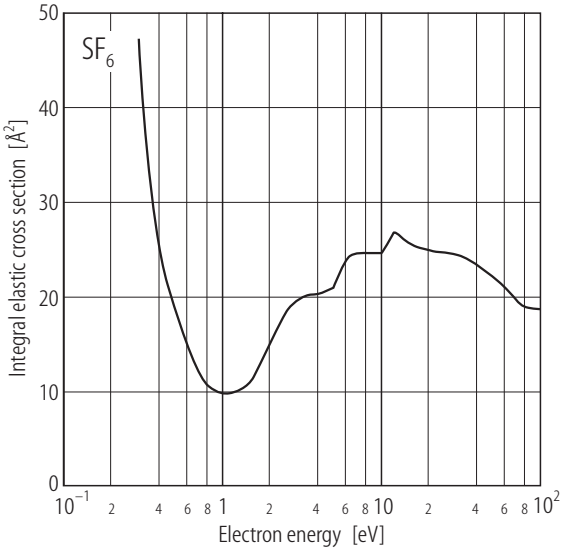

Fig. 6.2.6.22. Integral elastic scattering cross section for SF_6 at energies below 100 eV.

Table 6.2.6.22. Preferred values of the integral elastic cross section (σ_i) for electrons scattered from SF_6. The estimated uncertainty is ± 25 %.

Energy [eV]	σ_i [Å^2]	Energy [eV]	σ_i [Å^2]	Energy [eV]	σ_i [Å^2]
0.30	47.0	1.5	10.8	8.0	24.5
0.35	32.0	2.0	14.8	9.0	24.5
0.40	25.7	2.5	17.9	10	24.5
0.45	21.8	3.0	19.5	12	26.7
0.50	18.8	3.5	20.0	15	25.5
0.60	14.8	4.0	20.1	20	24.8
0.70	12.6	4.5	20.5	30	24.3
0.80	10.9	5.0	20.8	50	22.1
0.90	10.0	5.5	22.5	75	19.1
1.0	9.7	6.0	23.8	100	18.5
1.25	9.8	7.0	24.4		

References for 6.2.6.22

76Sri1 Srivastava, S.K., Trajmar, S., Chutjian, A., Williams, W.: J. Chem. Phys. **64** (1976) 2767
79Roh1 Rohr, K.: J. Phys. B: At. Mol. Phys. **12** (1979) L185
89Sak1 Sakae, T., Sumiyoshi, S., Murakami, E., Matsumoto, Y., Ishibashi, K., Katase, J.: J. Phys. B: At. Mol. Opt. Phys. **22** (1989) 1385

91Joh1 Johnstone, W.M., Newell, W.R.: J. Phys. B: At. Mol. Opt. Phys. **24** (1991) 473
00Cho1 Cho, H., Gulley, R.J., Trantham, K.W., Uhlmann, L.J., Dedman, C.J., Buckman, S.J.: J. Phys. B: At. Mol. Opt. Phys. **33** (2000) 3531
00Chr1 Christophorou, L.G., Olthoff, J.K.: J. Phys. Chem. Ref. Data **29** (2000) 267

6.2.6.23 Hexafluorobenzene (C_6F_6)

The preferred integral elastic scattering cross section for hexafluorobenzene is given in Table 6.2.6.23 and is shown in Fig. 6.2.6.23. This cross section is based on the differential scattering measurements of [01Cho1].

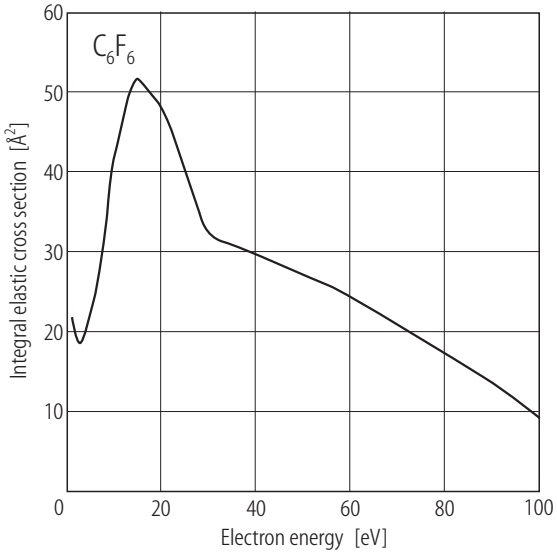

Fig. 6.2.6.23. Integral elastic scattering cross section for C_6F_6 at energies below 100 eV.

Table 6.2.6.23. Preferred values of the integral elastic cross section (σ_i) for electrons scattered from hexafluoro-benzene. The estimated uncertainty is ± 30 %.

Energy [eV]	σ_i [Å^2]	Energy [eV]	σ_i [Å^2]
1.5	21.8	15	51.6
3	18.6	20	48.0
5	21.5	30	32.7
8	31.0	60	24.3
10	41.1	100	9.0

References for 6.2.6.23

[01Cho1] Cho, H., Gulley, R.J., Sunohara, K., Kitajima, M., Uhlmann, L.J., Tanaka, H., Buckman, S.J.: J. Phys. B: At. Mol. Opt. Phys. **34** (2001) 1019

6.2.6.24 Perfluoropropane (C_3F_8)

The preferred integral elastic scattering cross section for perfluoropropane is given in Table 6.2.6.24 and is shown in Fig. 6.2.6.24. [98Chr1] constructed a set of preferred cross sections for this molecule based on the differential elastic scattering cross sections of [97Shi1]. These measurements have since been updated by [99Tan1] but tabulated results were not published. The tabulated values of [98Chr1], are reproduced below.

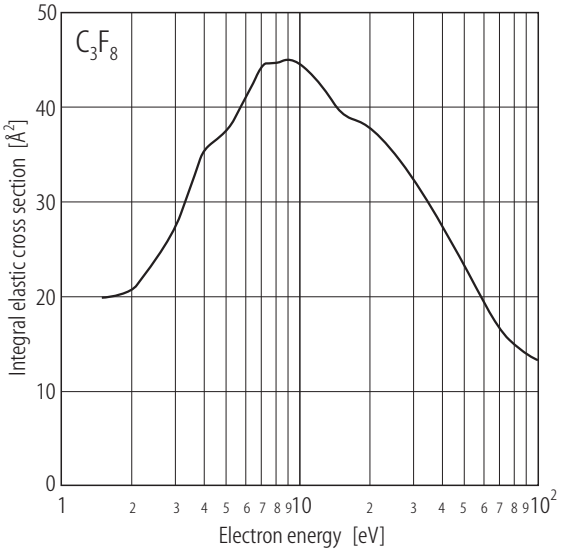

Fig. 6.2.6.24. Integral elastic scattering cross section for C_3F_8 at energies below 100 eV.

Table 6.2.6.24. Preferred values of the integral elastic cross section (σ_i) for electrons scattered from perfluoropropane. The estimated uncertainty is ± 30 %.

Energy [eV]	σ_i [Å^2]	Energy [eV]	σ_i [Å^2]
1.5	19.6	9.0	45.0
2.0	20.7	10	44.4
3.0	27.4	12	42.4
4.0	35.4	15	39.1
5.0	37.5	20	37.6
6.5	42.9	30	32.3
7.0	44.4	60	18.7
8.0	44.6	100	12.9

References for 6.2.6.24

97Shi1 Shinohara, T., Tachibana, Y., Yuri, M., Tanaka, H., Boesten, L.: Abstracts of XIX ICPEAC, Whistler (Mitchell, J.B.A., McConkey, J.W., Brion, C.E., eds.), 1995, p. 13

98Chr1 Christophorou, L.G., Olthoff, J.K.: J. Phys. Chem. Ref. Data **27** (1998) 889

99Tan1 Tanaka, H., Tachibana, Y., Kitajima, M., Sueoka, O, Takaki, H., Hamada, A., Kimura, M.: Phys. Rev. A **59** (1999) 2006

6.3 Elastic momentum transfer cross sections

6.3.1 Introduction

6.3.1.1 Definition in terms of the differential cross section

The momentum transfer cross section, σ_m, for electron scattering is defined as

$$\sigma_m(\varepsilon) = 2\pi \int_0^\pi \frac{d\sigma}{d\Omega}(1 - \frac{c'}{c}\cos\theta)\sin\theta d\theta \quad (1)$$

where $d\sigma/d\Omega$, the differential cross section, is defined as that fraction of a beam of electrons of energy ε which are scattered at an angle θ into the element of solid angle $d\Omega = 2\pi\sin\theta d\theta$; c and c' are the electron speeds before and after the collision respectively. The name of this cross section arises from the fact that the term $(1 - (c'/c)\cos\theta)$ is the fractional loss of directed momentum of the electron in a collision. More accurately, the speeds c and c' should be the relative speeds in the centre of mass system, g, before the collision and g' after the collision. However because of the small mass ratio m/M, where m is the electron mass and M the mass of the target particle, the replacement of g and g' by c and c' does not result in significant error.

In general electron collisions may be elastic, inelastic or superelastic. Relation (1) can thus be written as the sum of the momentum transfer cross sections for specific scattering processes, i.e.

$$\sigma_m(\varepsilon) = \sigma_m(\varepsilon)^{el} + \sum_k \sigma_m^k(\varepsilon)^{in} + \sum_k \sigma_m^k(\varepsilon)^{sup} \quad (2)$$

where $\sigma_m(\varepsilon)^{el}$ is the elastic momentum transfer cross section and $\sigma_m^k(\varepsilon)^{in}$ and $\sigma_m^k(\varepsilon)^{sup}$ are the momentum transfer cross sections for the k^{th} inelastic and superelastic scattering processes, respectively.

There are a number of special cases:

(a) if the scattering is isotropic (i.e. $d\sigma/d\Omega$ is independent of θ) then

$$\sigma_m(\varepsilon) = \sigma(\varepsilon) \quad (3)$$

where $\sigma(\varepsilon)$ is the integral elastic cross section, defined in subsect. 6.2.1.1, as

$$\sigma(\varepsilon) = 2\pi \int_0^\pi \frac{d\sigma}{d\Omega}\sin\theta \, d\theta \quad (4)$$

(b) if the scattering is elastic only, then

$$\sigma_m(\varepsilon) = \sigma_m(\varepsilon)^{el} = 2\pi \int_0^\pi \frac{d\sigma}{d\Omega}(1 - \cos\theta)\sin\theta \, d\theta \quad (5)$$

The entries in the accompanying tables of momentum transfer cross sections are values of $\sigma_m(\varepsilon)^{el}$ i.e. the elastic component of $\sigma_m(\varepsilon)$. In cases where the momentum transfer cross section is derived from crossed beam studies the elastic component should be understood as usually consisting of the sum of $\sigma_m(\varepsilon)^{el}$ and rotational excitation cross sections (suitably weighted for the relative abundances in the lower rotational state), the molecule being in its ground vibrational and electronic state. There is also a contribution from super elastic rotational de-excitation processes. In those cases where the elastic component is derived from an analysis of swarm experiments using multiterm solutions of the Boltzmann equation (see 6.3.2.1 below), the elastic component does not contain any contribution due to rotational excitation.

The momentum transfer cross section arises most often, but not exclusively, in the description of the motion of electrons in a gas at a given temperature and number density, usually in the presence of electric and/or magnetic fields. For a detailed description of the electron motion see Huxley and Crompton [74Hux1].

6.3.1.2 Definition in terms of the scattering phase shifts

The application of the phaseshift approaches described in subsect. 6.2.1.2 for elastic scattering are not, strictly speaking, appropriate in electron molecule scattering. However the technique, or variations of it, have been applied to a number of non-polar molecules which exhibit a high degree of spherical symmetry, such as the hydrocarbons.

6.3.2 Experimental determinations

6.3.2.1 From swarm experiments

The momentum transfer cross section, $\sigma_m(\varepsilon)$, can be obtained from transport coefficients measured in electron swarm experiments by using a solution of the Boltzmann equation, and an iterative procedure, to match calculated values of the transport coefficients (commonly the drift velocity, v_{dr}, and the ratio of the lateral diffusion coefficient, D_T, to the electron mobility, μ, i.e. D_T/μ) to the experimental data. Problems involving non-uniqueness of the fitted cross sections, due to the form of $\sigma_m(\varepsilon)$ or the presence of inelastic processes, have been discussed by Huxley and Crompton [74Hux1]. The energy range over which $\sigma_m(\varepsilon)$ can be derived from swarm data is limited by the range of values of E/N (E is the electric field strength and N the gas number density) for which transport coefficient data are available. This range is restricted by the onset of electric discharge.

Two types of solution of the Boltzman equation have been used:

(a) the "two term" solution:

The "two term" solution involves the assumption that the electron velocity distribution can be expanded in spherical harmonics and truncated after two terms. If the cross section for elastic scattering is very much greater than those for inelastic collisions then the angular scattering in such collisions does not significantly affect $\sigma_m(\varepsilon)$. In these circumstances the inelastic scattering may be assumed to be isotropic without significant error and thus

$$\sigma_m(\varepsilon) = \sigma_m(\varepsilon)^{el} + \sum_k \sigma^k(\varepsilon)^{in} + \sum_k \sigma^k(\varepsilon)^{sup} \qquad (6)$$

where $\sigma^k(\varepsilon)^{in}$ and $\sigma^k(\varepsilon)^{sup}$ are the integral cross sections for the k^{th} inelastic and superelastic collision processes, respectively.

(b) "multiterm" solutions

In certain cases (e.g. D_T/μ calculations for methane [91Sch1]) the two term representation of the velocity distribution function is inadequate and a more complex representation is required. In multiterm solutions the isotropic scattering assumption for all the inelastic processes is not made and the differential scattering cross sections are entered separately. In many cases however the transport coefficient calculations are not sensitive to the angular scattering for specific inelastic scattering processes and isotropic scattering may be assumed.

There is often ambiguity in the literature concerning the exact designation of the momentum transfer cross section. Unless otherwise specified, it is probable that the $\sigma^m(\varepsilon)$ derived using a "two term" solution is the cross section defined by (6), whereas the momentum transfer cross section listed in analyses using a "multiterm solution" are values of $\sigma^m(\varepsilon)^{el}$. However considerable care should be exercised to avoid confusion on this point.

6.3.2.2 From crossed beam experiments

The elastic momentum transfer cross section, $\sigma_m(\varepsilon)^{el}$, can be derived from absolute measurements of the elastic differential scattering cross section, $d\sigma/d\Omega$, via eq. (1). The main complication with this technique is that most measurements of $d\sigma/d\Omega$ cannot cover the entire range of scattering angles between 0 and π, due to the presence of the primary beam at forward angles and other geometrical constraints at backward angles. Procedures for carrying out the extrapolations to 0 and π and the uncertainties involved are discussed in subsect. 6.2.2.2. Methods for increasing the angular range of the experimental measurements are also discussed in this section. Much of the experimental data which is used in deriving the preferred elastic momentum transfer cross sections in the following section is from crossed beam measurements of differential elastic scattering. As a result of the difficulties in extracting accurate elastic momentum transfer cross sections by integrating the differential cross section, it is not uncommon for the the uncertainties on the derived $\sigma_m(\varepsilon)^{el}$ cross sections to exceed 20 %. In general swarm experiments provide the most accurate values at low electron energies (where freqently there are no beam derived values available) and are complementary to the beam-derived values at higher energies.

References for 6.3.1 and 6.3.2

74Hux1 Huxley, L.G.H., Crompton, R.W.: The Diffusion and Drift of Electrons in Gases, New York: Wiley 1974

91Sch1 Schmidt, B: J. Phys. B: At. Mol. Opt. Phys. **28** (1991) 4809

6.3.3 Determination of preferred cross sections

The preferred elastic momentum transfer cross section for each molecule in this section has been derived from a consideration of all available (published) experimental and, in some cases, theoretical work. In general, we do not consider those cases where only theoretical values exist, unless there is substantial corroboration between two or more diffferent calculations. More weight has been placed on recent measurements which have realistic and well quantified uncertainties. The uncertainty estimates on the preferred cross sections indicate the level of concurrence between the various individual measurements and calculations.

6.3.4 Units

Cross sections are given in square Ångström ($1 Å^2 = 10^{-16}$ cm^2) and electron energies in electron volt (eV).

6.3.5 Molecules

6.3.5.1 Hydrogen (H_2)

The preferred cross section is listed in Table 6.3.5.1 and shown in Fig. 6.3.5.1. From 0.001 to 2 eV the preferred cross section is taken to be that of [94Sch1]. From 2 to 4 eV the preferred cross section follows closely the *ab initio* theoretical values of [87Mor1] which agree with [94Sch1] to within 4 % over the range to 4 eV. For the remainder of the energy range to 100 eV the preferred cross section is based on the experimental beam-derived values of [81Shy1, 85Nis1, 86Kha1, 91Bru1].

The uncertainty limits are estimated to be $< \pm 5$ % for 0.001 eV $\leq \varepsilon < 4$ eV and $< \pm 15$ % for 4 eV $\leq \varepsilon \leq 100$ eV.

Table 6.3.5.1. Preferred values of the elastic momentum transfer cross section (σ_m^{el}) for electrons scattered from hydrogen (H_2).

Energy [eV]	σ_m^{el} [Å^2]	Energy [eV]	σ_m^{el} [Å^2]	Energy [eV]	σ_m^{el} [Å^2]
0.0010	7.25	0.06	9.54	2.5	17.40
0.0012	7.26	0.07	9.79	3	16.28
0.0015	7.26	0.08	10.04	4	13.70
0.0018	7.27	0.09	10.25	5	11.59
0.0020	7.28	0.10	10.47	6	10.00
0.0025	7.30	0.12	10.86	7	8.59
0.0030	7.35	0.15	11.35	8	7.48
0.004	7.38	0.18	11.78	9	6.58
0.005	7.45	0.20	12.02	10	5.78
0.006	7.48	0.25	12.54	12	4.396
0.007	7.54	0.30	13.00	15	3.275
0.008	7.59	0.40	13.81	18	2.529
0.009	7.64	0.50	14.52	20	2.154
0.010	7.70	0.60	15.16	25	1.476
0.012	7.78	0.70	15.66	30	1.077
0.015	7.90	0.80	16.17	40	0.636
0.018	8.04	0.90	16.58	50	0.417
0.020	8.14	1.0	17.01	60	0.311
0.025	8.33	1.2	17.70	70	0.243
0.03	8.56	1.5	18.15	80	0.200
0.04	8.93	1.8	18.22	90	0.169
0.05	9.27	2.0	18.11	100	0.149

References for 6.3.5.1

81Shy1 Shyn, T.W., Sharp, W.E.: Phys. Rev. A **24** (1981) 1734
85Nis1 Nishimura, H., Danjo, A., Sugahara, H.J.: Phys. Soc. Jpn. **54** (1985) 1757
86Kha1 Khakoo, M.A., Trajmar, S.: Phys. Rev. A **34** (1986) 138
87Mor1 Morrison, M.A., Crompton, R.W., Saha, B.C., Petrovic, Z.Lj.: Aust. J. Phys. **40** (1987) 239
91Bru1 Brunger, M.J., Buckman, S.J., Newman, D.S., Alle, D.T.: J. Phys. B: At. Mol. Opt. Phys. **24** (1991) 1435
94Sch1 Schmidt, B., Berkhan, K., Gotz, B., Muller, M.: Phys. Scripta T **53** (1994) 30

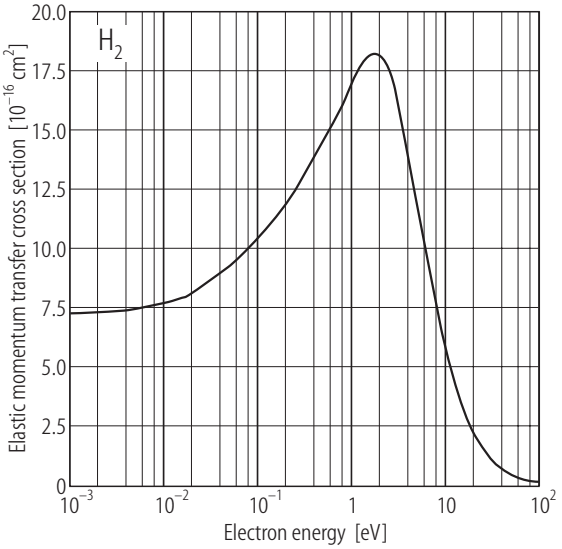

Fig. 6.3.5.1. Preferred values of the elastic momentum transfer cross section for electrons scattered from hydrogen (H_2).

6.3.5.2 Deuterium (D_2)

The preferred cross section is listed in Table 6.3.5.2 and shown in Fig. 6.3.5.2. The preferred σ_m^{el} is derived from the σ_m cross section of [89Pet1] by subtracting the v = 0 - 1 vibrational excitation cross section which they used in their calculations of transport coefficients. The [89Pet1] cross section is the same as the "reference set" cross section of [85Buc1], with minor variations and has been taken from the thesis by Z. Petrovic [87Pet1].

The uncertainty limits are estimated to be ≤ 5 % from 0.1 to 1.4 eV. No uncertainty limit is quoted for energies greater than 1.4 eV due to non-uniqueness problems.

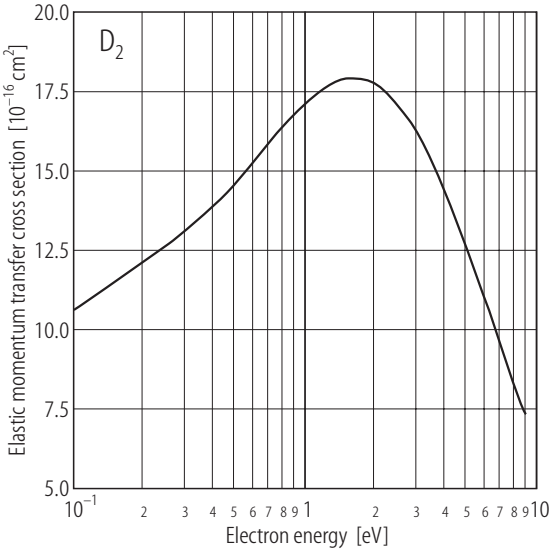

Fig. 6.3.5.2. Preferred values of the elastic momentum transfer cross section for electrons scattered from deuterium (D_2).

Table 6.3.5.2. Preferred values of the elastic momentum transfer cross section (σ_m^{el}) for electrons scattered from deuterium (D_2).

Energy [eV]	σ_m^{el} [Å^2]	Energy [eV]	σ_m^{el} [Å^2]	Energy [eV]	σ_m^{el} [Å^2]
0.1	10.6	0.6	15.2	2.5	17.3
0.12	10.9	0.7	15.8	3	16.4
0.15	11.5	0.8	16.4	4	14.5
0.18	11.9	0.9	16.8	5	12.6
0.2	12.1	1	17.1	6	10.9
0.25	12.6	1.2	17.6	7	9.50
0.3	13.0	1.5	18.0	8	8.28
0.4	13.8	1.8	18.0	9	7.34
0.5	14.5	2	17.9		

References for 6.3.5.2

85Buc1 Buckman, S.J., Phelps, A.V.: J. Chem. Phys. **82** (1985) 499l
87Pet1 Petrovic, Z.Lj.: PhD thesis (1987), Australian National University, Canberra
89Pet1 Petrovic, Z.Lj., Crompton, R.W.: Aust. J. Phys. **42** (1989) 609

6.3.5.3 Nitrogen (N_2)

The preferred cross section is listed in Table 6.3.5.3 and shown in Figs. 6.3.5.3.1 and 6.3.5.3.2. From 0.001 to 0.5 eV the preferred σ_m^{el} is taken to be that of [84Had1]. From 0.5 eV to 1.9 eV the preferred cross section is based on [95Sun1] (tabled in [97Rob1]) and from 1.8 to 3.5 eV on [95Sun1] alone.

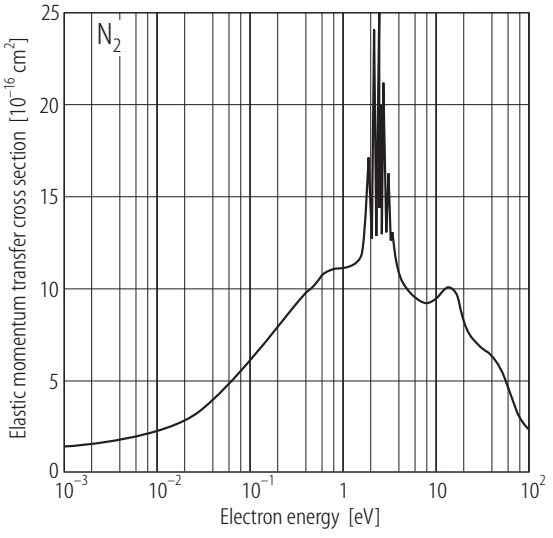

Fig. 6.3.5.3.1. Preferred values of the elastic momentum transfer cross section for electrons scattered from nitrogen (N_2).

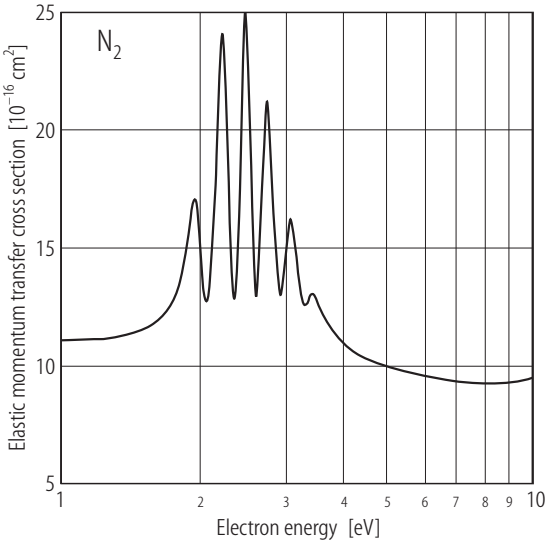

Fig. 6.3.5.3.2. Preferred values of the elastic momentum transfer cross section for electrons scattered from nitrogen (N_2), showing the region of the resonance on an expanded energy scale.

For the remainder of the energy range to 100 eV the preferred cross section is based on the beam-derived values of [95Sun1] and [76Sri1]. Fig. 6.3.5.3.2. shows details of the resonance calculated by [97Rob1] and which is generally supported by beam studies.

The uncertainty limits are estimated to be $< \pm 5$ % for $0.001 \leq \varepsilon < 0.5$ eV, $< \pm 10$ % for $0.5 \leq \varepsilon < 1.9$ eV and $< \pm 20$ % for $3.5 \leq \varepsilon < 100$ eV. No uncertainty limit is quoted for the range 1.9 to 3.5 eV.

Table 6.3.5.3. Preferred values of the elastic momentum transfer cross section (σ_m^{el}) for electrons scattered from nitrogen (N_2).

Energy [eV]	σ_m^{el} [Å^2]	Energy [eV]	σ_m^{el} [Å^2]	Energy [eV]	σ_m^{el} [Å^2]
0.001	1.357	1.5	11.52	2.85	15.59
0.0015	1.426	1.6	11.84	2.86	15.05
0.0018	1.464	1.7	12.42	2.9	13.48
0.002	1.490	1.8	13.63	2.925	13.04
0.0025	1.550	1.85	14.92	2.95	13.05
0.003	1.620	1.9	16.54	3	14.28
0.004	1.718	1.95	16.71	3.033	15.43
0.005	1.810	1.98	14.96	3.066	16.13
0.006	1.908	2	13.65	3.1	16.11
0.007	2.000	2.04	12.63	3.115	15.90
0.008	2.062	2.05	12.72	3.2	13.93
0.009	2.131	2.067	13.15	3.25	12.98
0.01	2.190	2.084	13.85	3.3	12.55
0.012	2.342	2.1	14.75	3.34	12.61
0.015	2.550	2.16	20.00	3.35	12.67
0.018	2.729	2.2	23.88	3.4	12.98
0.02	2.850	2.3	14.91	3.42	13.04
0.025	3.12	2.35	12.79	3.45	13.02
0.03	3.40	2.4	16.10	3.5	12.75
0.04	3.85	2.41	17.37	4	10.90
0.05	4.33	2.415	18.07	5	9.90
0.06	4.72	2.42	18.80	6	9.45
0.07	5.10	2.423	19.26	7	9.29
0.08	5.41	2.425	19.56	8	9.19
0.09	5.69	2.43	20.34	9	9.29
0.1	5.95	2.45	23.29	10	9.45
0.12	6.45	2.46	24.38	12	9.84
0.15	7.10	2.467	24.88	15	9.97
0.18	7.59	2.484	24.95	18	9.07
0.2	7.90	2.487	24.79	20	8.20
0.25	8.50	2.49	24.58	25	7.25
0.3	9.00	2.494	24.23	30	6.80
0.4	9.70	2.495	24.14	40	6.31
0.5	10.16	2.5	23.59	50	5.60
0.6	10.65	2.6	13.06	60	4.51
0.7	10.87	2.7	18.59	70	3.59
0.8	11.00	2.733	20.91	80	2.94
0.9	11.03	2.766	20.82	90	2.50
1	11.07	2.77	20.66	100	2.19
1.2	11.10	2.8	18.88		

References for 6.3.5.3

76Sri1 Srivastava, S.K., Chutjian, A., Trajmar, S.: J. Chem. Phys. **64** (1976) 1340

84Had1 Haddad, G.N.: Aust. J. Phys. **37** (1984) 487

95Sun1 Sun, W., Morrison, M.A., Isaacs, W.A., Trail, W.K., Alle, D.T., Gulley, R.J., Brennan, M.J., Buckman, S.J.: Phys. Rev. A **52** (1995) 1229

97Rob1 Robertson, A.G., Elford, M.T., Crompton, R.W., Morrison, M.A., Sun, W., Trail, W.K.: Aust. J. Phys. **50** (1997) 441

6.3.5.4 Carbon monoxide (CO)

The preferred cross section is listed in Table 6.3.5.4 and shown in Fig. 6.3.5.4. Below 0.4 eV there appear to be no experimental values available and over the range 0.1 to 0.4 eV the preferred σ_m^{el} has been assumed to be that given by the theoretical values of [92Jai1] reduced by 15 %. The reduced values of [92Jai1] are in good agreement with the preferred cross section over the common energy range (up to 10 eV), except at the maximum. From 0.4 to 20 eV the preferred values are based on [83Had1] and [96Gib1]. It should be noted that the σ_m of [83Had1] includes both elastic and inelastic components. The σ_m^{el} cross section was obtained by subtracting the sum of the $v = 0$ to $v = 0$ - 7 vibrational excitation cross sections measured by [68Ehr1] and multiplying by a factor of 1.35, as suggested by [89Pet1]. The maximum in σ_m^{el}, which occurs at about 1.8 eV, was assumed to be that given by [83Had1] (the σ_m^{el} component) and is supported by the theoretical values of [95Mor1]. At energies greater than 30 eV the cross section is based on the beam derived values of [78Tan1].

The uncertainty is considered to be < ± 20 % except in the vicinity of the maximum at about 1.8 eV where no estimate is given. No uncertainty limit is also estimated for the range 0.1 to 0.4 eV.

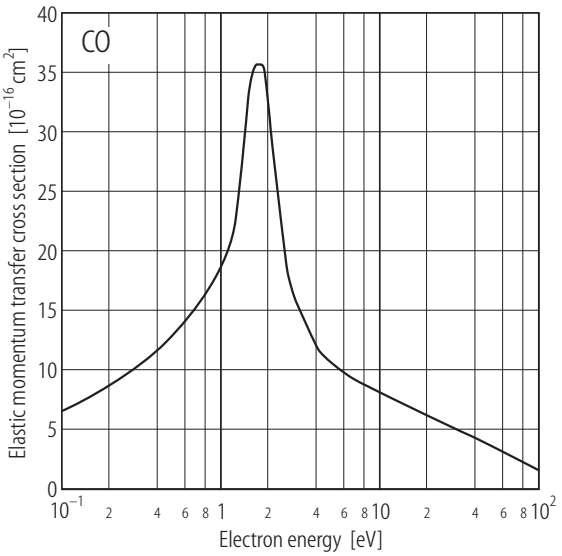

Fig. 6.3.5.4. Preferred values of the elastic momentum transfer cross section for electrons scattered from carbon monoxide (CO).

Table 6.3.5.4. Preferred values of the elastic momentum transfer cross section (σ_m^{el}) for electrons scattered from carbon monoxide (CO).

Energy [eV]	σ_m^{el} [Å^2]	Energy [eV]	σ_m^{el} [Å^2]	Energy [eV]	σ_m^{el} [Å^2]
0.1	6.51	1.4	29.1	8	8.87
0.12	6.99	1.5	33.2	9	8.53
0.15	7.64	1.6	35.2	10	8.17
0.18	8.23	1.7	35.6	12	7.64
0.2	8.60	1.8	35.5	15	7.07
0.25	9.43	1.9	34.7	18	6.50
0.3	10.16	2	32.1	20	6.27
0.4	11.58	2.1	28.9	25	5.59
0.5	12.90	2.2	26.5	30	5.11
0.6	14.03	2.3	24.4	40	4.27
0.7	15.16	2.4	22.3	50	3.66
0.8	16.24	2.5	20.3	60	3.17
0.9	17.31	3	15.8	70	2.69
1	18.55	4	12.1	80	2.31
1.1	19.79	5	10.7	90	1.97
1.2	21.6	6	9.79	100	1.69
1.3	25.0	7	9.25		

References for 6.3.5.4

68Ehr1 Ehrhardt, H., Langhans, L., Linder, F., Taylor, H.S.: Phys. Rev. **173** (1968) 222
78Tan1 Tanaka, H., Srivastava, S.K., Chutjian, A.: J. Chem. Phys. **69** (1978) 5329
83Had1 Haddad, G.N., Milloy, H.B.: Aust. J. Phys. **36** (1983) 473
89Pet1 Petrovic, Z.Lj., Crompton, R.W.: Aust. J. Phys. **42** (1989) 609
92Jai1 Jain, A., Norcross, D.W.: Phys. Rev. A **45** (1992) 1644
95Mor1 Morgan, L.A.: Private communication to S.J. Buckman, 1995
96Gib1 Gibson, J.C., Morgan, L.A., Gulley, R.J., Brunger, M.J., Bundschu, C.T., Buckman, S.J.: J. Phys. B: At. Mol. Opt. Phys. **29** (1996) 3197

6.3.5.5 Nitric oxide (NO)

The preferred cross section is listed in Table 6.3.5.5 and shown in Fig. 6.3.5.5. The preferred cross section for NO is based on that of [95Moj1] and covers the energy range 1.5 to 40 eV.

The uncertainty is estimated to be < ± 20 % for 5 eV ≤ ε ≤30 eV and < ± 30 % for values at energies outside this range.

Table 6.3.5.5. Preferred values of the elastic momentum transfer cross section (σ_m^{el}) for electrons scattered from nitric oxide (NO).

Energy [eV]	σ_m^{el} [Å^2]	Energy [eV]	σ_m^{el} [Å^2]
1.5	7.03	9	4.69
1.8	6.82	10	4.5
2	6.67	12	4.24
2.5	6.37	15	3.85
3	6.15	18	3.55
4	5.78	20	3.33
5	5.51	25	2.9
6	5.27	30	2.52
7	5.03	40	1.8
8	4.84		

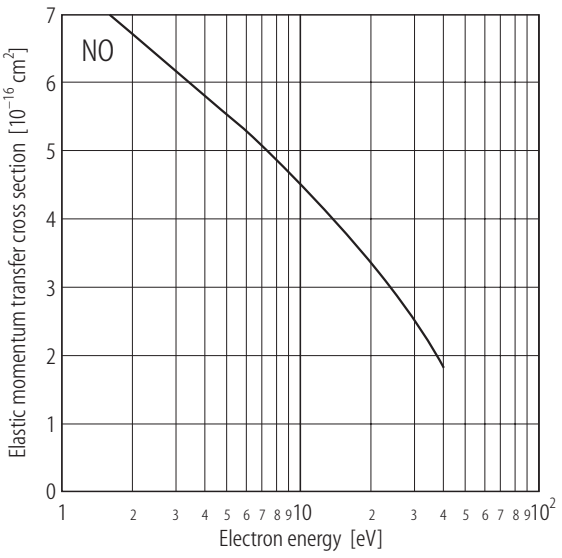

Fig. 6.3.5.5. Preferred values of the elastic momentum transfer cross section for electrons scattered from nitric oxide (NO).

References for 6.3.5.5

95Moj1 Mojarrabi, B., Gulley, R.J., Middleton, A.G., Cartwright, D.C., Teubner, P.J.O., Buckman, S.J., Brunger, M.J.: J. Phys. B: At. Mol. Opt. Phys. **28** (1995) 487

6.3.5.6 Oxygen (O_2)

The preferred cross section is listed in Table 6.3.5.6 and shown in Fig. 6.3.5.6. Values of σ_m^{el} in the low energy range (< 0.3 eV) are based on the analysis of electron transport coefficient data by [87You1]. At higher energies the preferred cross section follows that derived by [89Iti1] from beam data but has been modified in the energy range 2 to 20 eV to take into account the more recent experimental values obtained by [95Sul1]. The modifications were within the stated uncertainty of these beam measurements.

The uncertainty is estimated to be ≤ ± 20 %.

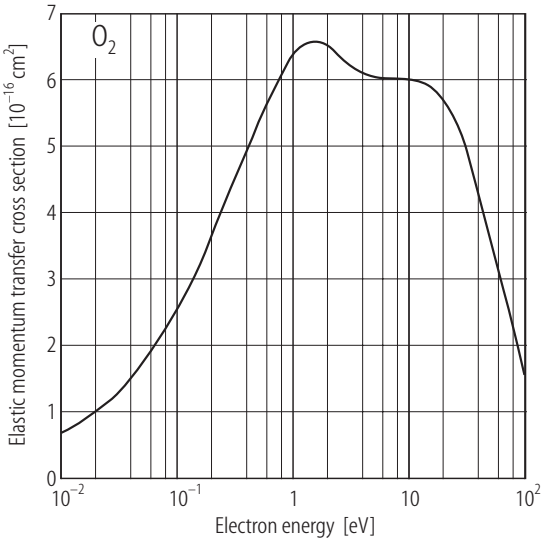

Fig. 6.3.5.6. Preferred values of the elastic momentum transfer cross section for electrons scattered from oxygen (O_2).

Table 6.3.5.6. Preferred values of the elastic momentum transfer cross section (σ_m^{el}) for electrons scattered from oxygen (O_2).

Energy [eV]	σ_m^{el} [Å^2]	Energy [eV]	σ_m^{el} [Å^2]	Energy [eV]	σ_m^{el} [Å^2]
0.01	0.69	0.25	4.02	7	6.01
0.012	0.75	0.3	4.37	8	6.01
0.015	0.86	0.4	4.91	9	6.01
0.018	0.92	0.5	5.36	10	6.01
0.02	0.96	0.6	5.7	12	6.01
0.025	1.1	0.7	5.98	15	6.01
0.03	1.23	0.8	6.17	18	5.97
0.04	1.42	0.9	6.32	20	5.91
0.05	1.63	1	6.49	25	5.60
0.06	1.85	1.2	6.71	30	5.17
0.07	2.04	1.5	6.82	40	4.37
0.08	2.19	1.8	6.69	50	3.66
0.09	2.38	2	6.58	60	3.05
0.1	2.51	2.5	6.32	70	2.58
0.12	2.77	3	6.14	80	2.22
0.15	3.1	4	6.01	90	1.91
0.18	3.42	5	6.01	100	1.44
0.2	3.61	6	6.01		

References for 6.3.5.6

87You1 Yousfi, M., Azzi, N., Segur, P., Gallimberti, I., Stangherlin, S.: Personal communication, 1987

89Iti1 Itikawa, Y., Ichimura, K., Onda, K., Sakimoto, K., Takayanagi, K., Hatano, Y., Hayashi, M., Nishimura, H., Tsurubuchi, S.: J. Phys. Chem. Ref. Data **18** (1989) 23

95Sul1 Sullivan, J.P., Gibson, J.C., Gulley, R.J., Buckman, S.J.: J. Phys. B: At. Mol. Opt. Phys. **28** (1995) 4319

6.3.5.7 Methane (CH_4)

The preferred cross section is listed in Table 6.3.5.7 and shown in Fig. 6.3.5.7. The preferred values of σ_m^{el} in the low energy range 0.01 to 0.2 eV are based on the analysis of electron transport coefficient data by [91Sch1]. Between 0.2 and 0.6 eV the preferred cross section is based on the shape of the cross section of [86Soh1] but is about 25 % larger. At energies greater than 0.6 eV the preferred cross section is based on those of [97Bun1] and [91Boe1].

The uncertainty is estimated to be $\leq \pm$ 20 % except in the region of the Ramsauer-Townsend minimum (0.2 to 0.6 eV) where no estimate is given.

Table 6.3.5.7. Preferred values of the elastic momentum transfer cross section (σ_m^{el}) for electrons scattered from methane (CH_4).

Energy [eV]	σ_m^{el} [Å^2]	Energy [eV]	σ_m^{el} [Å^2]	Energy [eV]	σ_m^{el} [Å^2]
0.01	15.6	0.25	0.535	7	21.80
0.012	14.5	0.3	0.504	8	22.01
0.015	13.3	0.4	0.579	9	21.69
0.018	12.2	0.5	0.769	10	20.43
0.02	11.5	0.6	0.985	12	15.94
0.025	10.0	0.7	1.172	15	10.88
0.03	8.79	0.8	1.429	18	8.20
0.04	6.93	0.9	1.675	20	6.93
0.05	5.62	1	1.916	25	4.99
0.06	4.70	1.2	2.40	30	3.92
0.07	3.90	1.5	3.24	40	2.81
0.08	3.31	1.8	4.11	50	2.21
0.09	2.77	2	4.77	60	1.81
0.1	2.30	2.5	6.34	70	1.55
0.12	1.74	3	8.12	80	1.35
0.15	1.21	4	11.78	90	1.20
0.18	0.919	5	15.86	100	1.07
0.2	0.750	6	20.03		

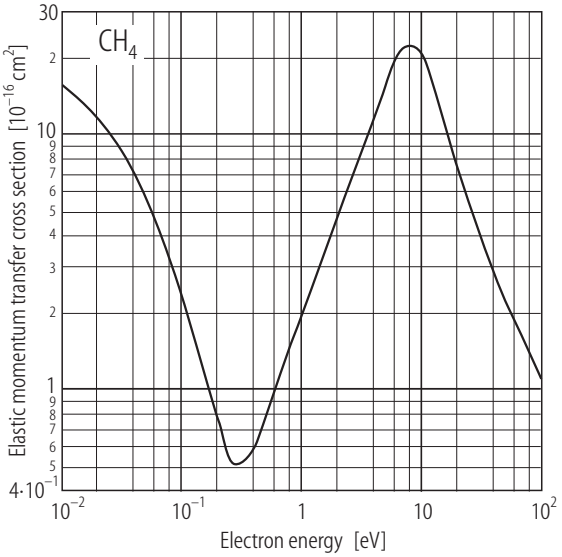

Fig. 6.3.5.7. Preferred values of the elastic momentum transfer cross section for electrons scattered from methane (CH_4).

References for 6.3.5.7

86Soh1 Sohn, W., Kochem, K-H., Scheurlein, K.M., Jung, K., Ehrhardt, H.: J. Phys. B: At. Mol. Phys. **19** (1986) 3625

91Boe1 Boesten, L., Tanaka, H.: J. Phys. B: At. Mol. Opt. Phys. **24** (1991) 821

91Sch1 Schmidt, B.: J. Phys. B: At. Mol. Opt. Phys. **28** (1991) 4809

97Bun1 Bundschu, C.T., Gibson, J.C., Gulley, R.J., Brunger, M.J., Buckman, S.J., Sanna, N., Gianturco, F.A.: J. Phys. B: At. Mol. Opt. Phys. **30** (1997) 2239

6.3.5.8 Ammonia (NH_3)

The preferred cross section is listed in Table 6.3.5.8 and shown in Fig. 6.3.5.8. The preferred cross section is based on the beam-derived values of [92All1] and takes into account the theoretical cross section of [91Gia1].

The estimated uncertainty is < ± 20 %.

Table 6.3.5.8. Preferred values of the elastic momentum transfer cross section (σ_m^{el}) for electrons scattered from ammonia (NH_3).

Energy [eV]	σ_m^{el} [Å^2]	Energy [eV]	σ_m^{el} [Å^2]
2	1.73	9	10
2.5	2.63	10	10.1
3	3.69	12	9.90
4	5.91	15	9.15
5	7.88	18	8.16
6	8.97	20	7.46
7	9.56	25	6.00
8	9.90	30	4.89

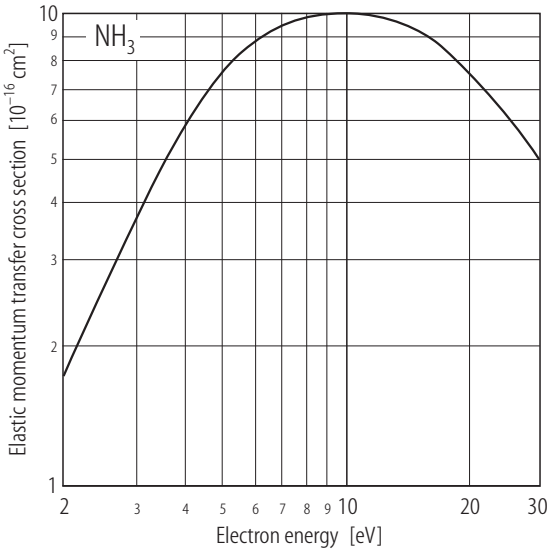

Fig. 6.3.5.8. Preferred values of the elastic momentum transfer cross section for electrons scattered from ammonia (NH_3).

References for 6.3.5.8

91Gia1 Gianturco, F.A.: J. Phys. B: At. Mol. Opt. Phys. **24** (1991) 4627

92All1 Alle, D.T., Gulley, R.J., Buckman, S.J., Brunger, M.J.: J. Phys. B: At. Mol. Opt. Phys. **25** (1992) 1533

6.3.5.9 Water vapour (H_2O)

The preferred cross section is listed in Table 6.3.5.9 and shown in Fig. 6.3.5.9. The preferred values of σ_m^{el} over the energy range 0.01 to 1eV are based on the swarm derived cross section of [87You1]. For energies greater than 1eV the preferred cross section is based on the beam derived cross sections of [79Sen1, 87Shy1, 91Joh1]. No data point from each of these three sets of data differs from the preferred values by more than 20 %.

Below 1 eV no estimate of the uncertainty is given, but at higher energies the uncertainty is estimated to be $< \pm 20$ %.

References for 6.3.5.9

79Sen1 Seng, G., Linder, F.: quoted by Gianturco, F.A, Thompson, D.G.: J. Phys. B: At. Mol. Phys. **13** (1980) 613

87Shy1 Shyn, T.W., Cho, S.Y.: Phys. Rev. A **36** (1987) 5138

87You1 Yousfi, M., Azzi, N., Segur, P., Gallimberti, I., Stangherlin, S.: Private communication, 1987

91Joh1 Johnstone, W.M., Newell, W.R.: J. Phys. B: At. Mol. Opt. Phys. **24** (1991) 3633

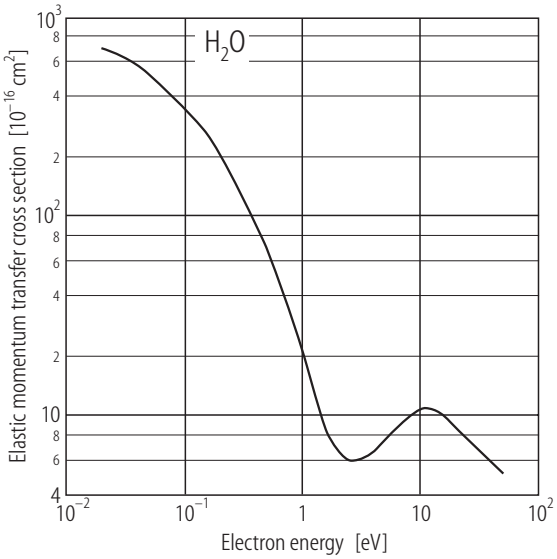

Fig. 6.3.5.9. Preferred values of the elastic momentum transfer cross section for electrons scattered from water vapour (H_2O).

Table 6.3.5.9. Preferred values of the elastic momentum transfer cross section (σ_m^{el}) for electrons scattered from water vapour (H_2O).

Energy [eV]	σ_m^{el} [Å^2]	Energy [eV]	σ_m^{el} [Å^2]	Energy [eV]	σ_m^{el} [Å^2]
0.02	700	0.9	25	8	9.56
0.03	640	1	21	9	10.15
0.05	505	1.2	13.73	10	10.50
0.07	430	1.5	9.38	12	10.77
0.1	350	1.8	7.39	15	10.00
0.14	280	2	6.66	18	9.01
0.2	200	2.5	5.91	20	8.45
0.3	130	3	5.95	25	7.54
0.5	66	4	6.56	30	6.80
0.6	50	5	7.43	40	5.83
0.7	40	6	8.24	50	5.07
0.8	32	7	8.92		

6.3.5.10 Ethane (C_2H_6)

The preferred cross section is listed in Table 6.3.5.10 and shown in Fig. 6.3.5.10. The preferred cross section σ_m^{el} for C_2H_6 is based primarily on the swarm-derived cross sections of [97Shi1] and [97Sch1] but includes consideration of the beam-derived cross sections of [88Tan1] and [98Mer1].

The estimated uncertainty is < ± 10 % at energies < 10 eV with the exception of values at energies in the vicinity of the minimum where no estimate is given. For energies of 10 eV and higher the estimated uncertainty is < ± 15 %.

Fig. 6.3.5.10. Preferred values of the elastic momentum transfer cross section for electrons scattered from ethane (C_2H_6).

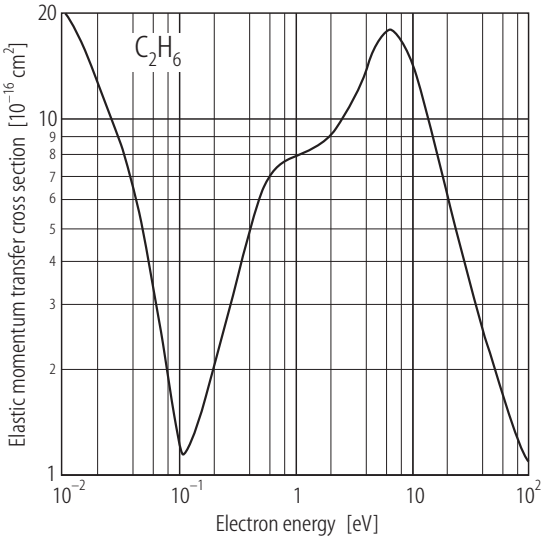

Table 6.3.5.10. Preferred values of the elastic momentum transfer cross section (σ_m^{el}) for electrons scattered from ethane (C_2H_6).

Energy [eV]	σ_m^{el} [Å^2]	Energy [eV]	σ_m^{el} [Å^2]	Energy [eV]	σ_m^{el} [Å^2]
0.01	20.65	0.25	2.66	7	17.83
0.012	18.91	0.3	3.24	8	16.97
0.015	16.00	0.4	4.82	9	15.77
0.018	14.01	0.5	6.04	10	14.58
0.02	12.65	0.6	6.89	12	12.05
0.025	10.61	0.7	7.35	15	9.20
0.03	9.10	0.8	7.56	18	7.17
0.04	6.76	0.9	7.79	20	6.13
0.05	4.80	1	7.90	25	4.61
0.06	3.42	1.2	8.18	30	3.63
0.07	2.56	1.5	8.34	40	2.57
0.08	1.96	1.8	8.76	50	2.01
0.09	1.48	2	9.07	60	1.68
0.1	1.204	2.5	10.02	70	1.451
0.12	1.204	3	11.03	80	1.296
0.15	1.444	4	13.55	90	1.164
0.18	1.783	5	16.08	100	1.076
0.2	1.99	6	17.65		

References for 6.3.5.10

88Tan1 Tanaka, H., Boesten, L., Matsunaga, D., Kudo, T.: J. Phys. B: At. Mol. Opt. Phys. **21** (1988) 1255
97Sch1 Schmidt, B.: Private communication (1997) to [98Mer1]
97Shi1 Shisikura, Y., Asano, K., Nakamura, Y.: J. Phys. D **30** (1997) 1610
98Mer1 Merz, R., Linder, F.: J. Phys. B: At. Mol. Opt. Phys. **31** (1998) 4663

6.3.5.11 Silane (SiH_4)

The preferred cross section for silane is listed in Table 6.3.5.11 and shown in Fig. 6.3.5.11. The preferred cross section for SiH_4 at energies less than 1 eV is based on that derived by [94Nag1] from the analysis of electron swarm data. At energies between 1.8 and 20 eV the preferred cross section is a smooth fit to the beam-derived values of [90Tan1] and follows closely the swarm-derived cross section of [87Mat1]. No cross section is suggested for energies greater than 20 eV as beam and swarm-derived cross sections diverge significantly.

No uncertainty is estimated for $\varepsilon < 1.8$ eV. The uncertainty in the region for 1.8 eV $\leq \varepsilon \leq 20$ eV is estimated to be < ± 25 %.

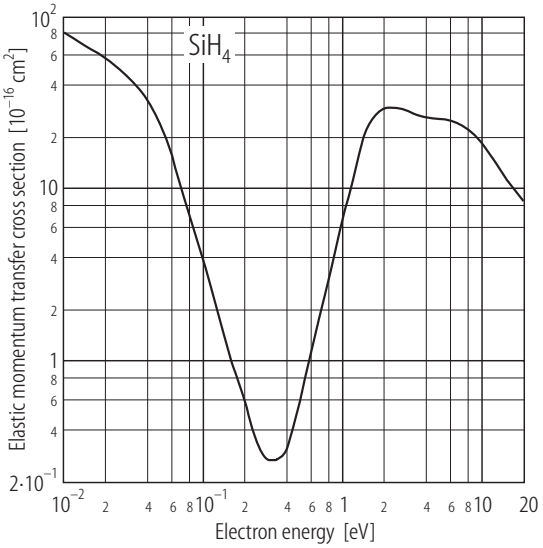

Fig. 6.3.5.11. Preferred values of the elastic momentum transfer cross section for electrons scattered from silane (SiH_4).

Table 6.3.5.11. Preferred values of the elastic momentum transfer cross section (σ_m^{el}) for electrons scattered from silane (SiH_4).

Energy [eV]	σ_m^{el} [Å^2]	Energy [eV]	σ_m^{el} [Å^2]	Energy [eV]	σ_m^{el} [Å^2]
0.01	80.8	0.15	1.17	1.8	27.38
0.012	73.5	0.18	0.739	2	28.78
0.015	64.9	0.2	0.554	2.5	29.50
0.018	59.7	0.25	0.310	3	28.07
0.02	56.2	0.3	0.268	4	26.06
0.025	48.7	0.35	0.271	5	25.42
0.03	42.7	0.4	0.319	6	24.80
0.04	32.4	0.5	0.633	7	23.83
0.05	23.1	0.6	1.161	8	22.34
0.06	15.7	0.7	1.983	9	20.23
0.07	10.00	0.8	3.07	10	18.14
0.08	6.89	0.9	4.66	12	14.95
0.09	5.01	1	6.49	15	11.32
0.1	3.76	1.2	11.21	18	9.28
0.12	2.30	1.5	21.37	20	8.24

References for 6.3.5.11

87Mat1 Mathieson, K.J., Millican, P.G., Walker, I.C., Curtis, M.G.: J. Chem. Soc. Faraday Trans. II **83** (1987) 1041
90Tan1 Tanaka, H., Boesten, L., Sato, H., Kimura, M., Dillon, M.A., Spence, D.: J. Phys. B: At. Mol. Opt. Phys. **23** (1990) 577
94 Nag1 Nagpal, R., Garscadden, A.: J. Appl. Phys.**75** (1994) 703

6.3.5.12 Hydrogen sulphide (H_2S)

The preferred cross section is listed in Table 6.3.5.12 and shown in Fig. 6.3.5.12. The preferred values of σ_m^{el} are based on the beam-derived values of [93Gul1] and take into account the form of the theoretical cross sections of [92Len1] and [99Var1].

The estimated uncertainty is < ± 20 %.

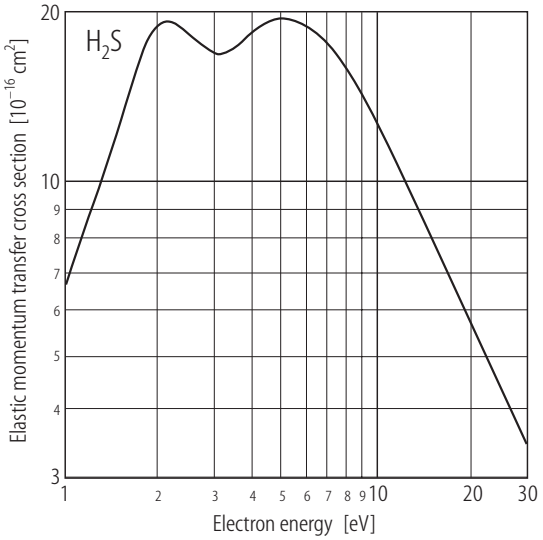

Fig. 6.3.5.12. Preferred values of the elastic momentum transfer cross section for electrons scattered from hydrogen sulphide (H_2S).

Table 6.3.5.12. Preferred values of the elastic momentum transfer cross section (σ_m^{el}) for electrons scattered from hydrogen sulphide (H_2S).

Energy [eV]	σ_m^{el} [Å^2]	Energy [eV]	σ_m^{el} [Å^2]
1.2	8.83	8	15.79
1.5	12.69	9	14.22
1.8	17.34	10	12.75
2	18.87	12	10.25
2.5	18.14	15	7.92
3	16.84	18	6.33
4	18.41	20	5.57
5	19.35	25	4.28
6	18.69	30	3.44
7	17.35		

References for 6.3.5.12

92Len1 Lengsfield, B.H., Rescigno, T.N., McCurdy, C.W., Parker, S.: cited by [93Gul1] as private communication
93Gul1 Gulley, R.J., Brunger, M.J., Buckman, S.J.: J. Phys. B: At. Mol. Opt. Phys. **26** (1993) 2913
99Var1 Varella, M.T.do N., Bettega, M.H.F., Lima, M.A.P., Ferreira, L.G.: J. Chem. Phys. **111** (1999) 6396

6.3.5.13 Carbon dioxide (CO_2)

The preferred cross section is listed in Table 6.3.5.13 and shown in Fig. 6.3.5.13. Below 1 eV there are no beam derived data and the preferred σ_m^{el} cross section is taken to be that of [95Nak1] derived from an analysis of swarm data. In the range 1 to 20 eV the preferred cross section follows the general form of the [95Nak1] cross section but with some modifications in the region of the 3.8 eV resonance and at values in the region of 15 eV. The beam derived cross section values of [99Gib1] generally agree with the preferred cross section to within 10 % over their energy range of 1 to 10 eV. There is also good agreement with values of [98Tan1] at energies greater than 7 eV and at energies from 20 to 100 eV the preferred curve values follow a smooth curve through their data points. Other beam derived values [80Reg1] (with the exception of their lowest energy point) and [99Iga1] agree with the preferred curve to within their stated uncertainties.

The uncertainty limits are estimated to be $< \pm 5$ % for $0.04 \leq \varepsilon < 0.5$ eV, $< \pm 10$ % for $0.5 \leq \varepsilon < 20$ and $< \pm 20$ % for $20 \leq \varepsilon \leq 100$ eV.

References for 6.3.5.13

80Reg1 Register, D.F., Nishimura, H., Trajmar, S.J.: J. Phys. B: At. Mol. Opt. Phys. **13** (1980) 1651
95Nak1 Nakamura, Y.: Aust. J. Phys. **48** (1995) 357
98Tan1 Tanaka, H., Ishikawa, T., Masai, T., Sagara, T., Boesten, L., Takekawa, M., Itikawa, Y., Kimura, M.: Phys. Rev. A **57** (1998) 1798
99Gib1 Gibson, J.C., Green, M.A., Trantham, K.W., Buckman, S.J., Teubner, P.J.O., Brunger, M.J.: J. Phys. B: At. Mol. Opt. Phys. **32** (1999) 213
99Iga1 Iga, I., Homem, M.G.P., Mazon, K.T., Lee. M-T.: J. Phys. B: At. Mol. Opt. Phys. **32** (1999) 4373

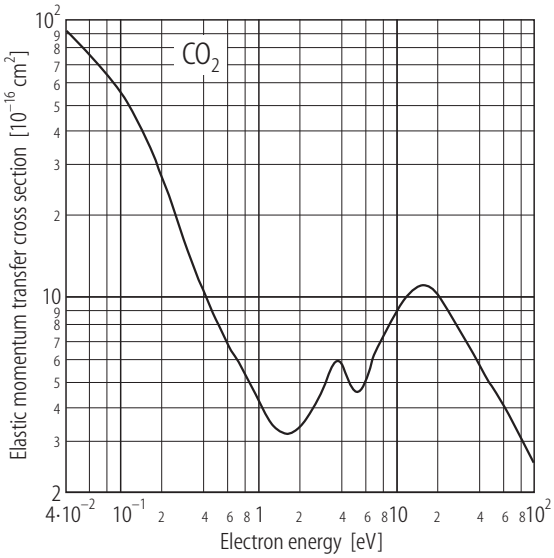

Fig. 6.3.5.13. Preferred values of the elastic momentum transfer cross section for electrons scattered from carbon dioxide (CO_2).

Table 6.3.5.13. Preferred values of the elastic momentum transfer cross section (σ_m^{el}) for electrons scattered from carbon dioxide (CO_2).

Energy [eV]	σ_m^{el} [Å^2]	Energy [eV]	σ_m^{el} [Å^2]	Energy [eV]	σ_m^{el} [Å^2]
0.04	90.0	0.7	5.69	8	7.40
0.05	80.6	0.8	5.18	9	8.09
0.06	73.2	0.9	4.69	10	9.02
0.07	66.8	1	4.25	12	10.00
0.08	61.9	1.2	3.59	15	10.86
0.09	56.8	1.5	3.24	18	10.76
0.1	53.6	1.8	3.24	20	10.17
0.12	46.4	2	3.39	25	8.74
0.15	37.2	2.5	3.91	30	7.51
0.18	30.1	3	4.67	40	5.84
0.2	26.2	3.5	5.64	50	4.79
0.25	19.8	4	5.79	60	4.15
0.3	15.05	4.5	5.02	70	3.61
0.4	10.48	5	4.58	80	3.19
0.5	8.09	6	4.91	90	2.83
0.6	6.77	7	6.08	100	2.53

6.3.5.14 Propane (C_3H_8)

The preferred cross section for propane is listed in Table 6.3.5.14 and shown in Fig. 6.3.5.14. The preferred cross section σ_m^{el} is based on that of [94Boe1].

The uncertainty is estimated to be < ± 30 %.

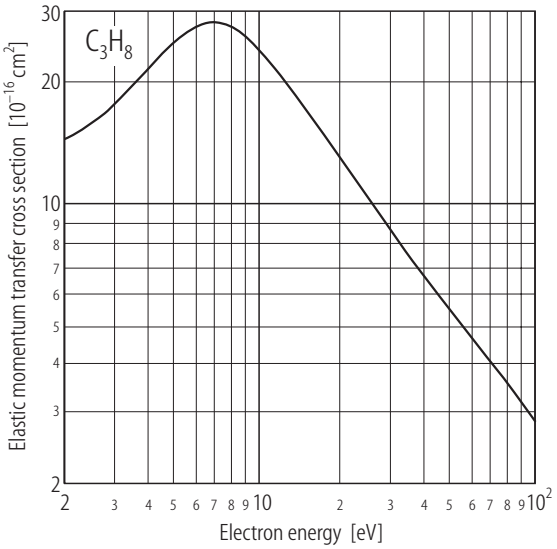

Fig. 6.3.5.14. Preferred values of the elastic momentum transfer cross section for electrons scattered from propane (C_3H_8).

Table 6.3.5.14. Preferred values of the elastic momentum transfer cross section (σ_m^{el}) for electrons scattered from propane (C_3H_8).

Energy [eV]	σ_m^{el} [Å^2]	Energy [eV]	σ_m^{el} [Å^2]	Energy [eV]	σ_m^{el} [Å^2]
2.5	15.9	10	24.4	50	5.25
3	17.6	12	20.43	60	4.52
4	21.9	15	16.66	70	3.93
5	25.4	18	13.74	80	3.53
6	28.6	20	12.44	90	3.16
7	29.2	25	10.00	100	2.86
8	28.4	30	8.45		
9	26.5	40	6.40		

Reference for 6.3.5.14

94Boe1 Boesten, L., Dillon, M.A., Tanaka, H., Kimura, M., Sato, H.: J. Phys. B: At. Mol. Opt. Phys. **27** (1994) 1845

6.3.5.15 Nitrous oxide (N_2O)

The preferred cross section is listed in Table 6.3.5.15 and shown in Fig. 6.3.5.15. The preferred cross section for N_2O is based on the beam-derived values of [86Mar1, 93Joh1, 00Kit1].

The uncertainty is estimated to be < ± 25 % over the whole energy range 2 to 80 eV.

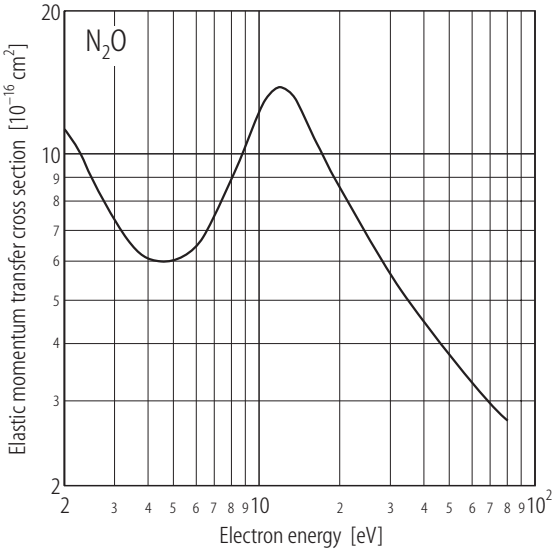

Fig. 6.3.5.15. Preferred values of the elastic momentum transfer cross section for electrons scattered from nitrous oxide (N_2O).

Table 6.3.5.15. The preferred values of the elastic momentum transfer cross section (σ_m^{el}) for electrons scattered from nitrous oxide (N_2O).

Energy [eV]	σ_m^{el} [Å^2]	Energy [eV]	σ_m^{el} [Å^2]	Energy [eV]	σ_m^{el} [Å^2]
2	11.18	8	8.88	25	6.62
2.5	8.81	9	10.4	30	5.60
3	7.22	10	12.13	40	4.36
4	5.97	12	13.74	50	3.71
5	5.97	15	11.18	60	3.29
6	6.41	18	9.31	70	2.97
7	7.57	20	8.33	80	2.73

References for 6.3.5.15

86Mar1 Marinkovic, B., Szmytkowski, Cz., Pejcev, V., Filipovic, D., Vuskovic, L.: J. Phys. B: At. Mol. Phys. **19** (1986) 2365

93Joh1 Johnstone, W.M., Newell, W.R.: J. Phys. B: At. Mol. Opt. Phys. **26** (1993) 129

00Kit1 Kitajima, M., Sakamoto, Y., Gulley, R.J., Hoshino, M., Gibson, J.C., Tanaka, H., Buckman, S.J.: Private communication, 2000

6.3.5.16 Disilane (Si_2H_6)

The preferred cross section for disilane is listed in Table 6.3.5.16 and shown in Fig. 6.3.5.16. The preferred cross section for disilane is taken to be a curve of best fit to the beam derived values of [94Dil1].

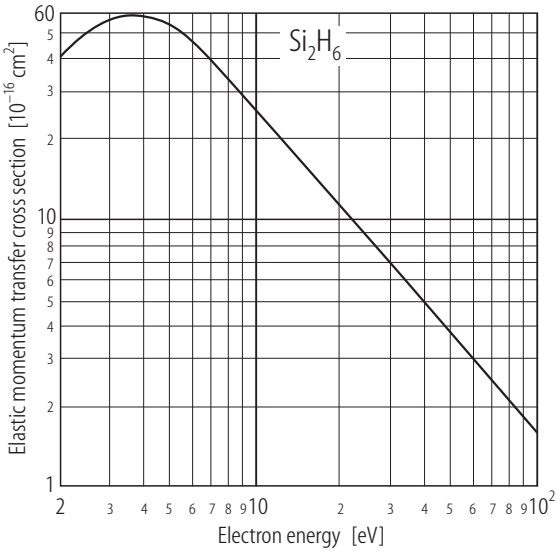

Fig. 6.3.5.16. Preferred values of the elastic momentum transfer cross section for electrons scattered from disilane (Si_2H_6).

Table 6.3.5.216. Preferred values of the elastic momentum transfer cross section (σ_m^{el}) for electrons scattered from disilane (Si_2H_6).

Energy [eV]	σ_m^{el} [Å^2]	Energy [eV]	σ_m^{el} [Å^2]	Energy [eV]	σ_m^{el} [Å^2]
2	40.1	9	28.3	40	4.77
2.5	50.8	10	24.9	50	3.64
3	57.1	12	19.75	60	2.95
4	59.7	15	15.17	70	2.44
5	54.5	18	12.22	80	2.08
6	45.6	20	10.94	90	1.81
7	38.3	25	8.35	100	1.60
8	32.6	30	6.70		

Reference for 6.3.5.16

94Dil1 Dillon, M.A., Boesten, L., Tanaka, H., Kimura, M., Sato, H.: J. Phys. B: At. Mol. Opt. Phys. **27** (1994) 1209

6.3.5.17 Sulphur dioxide (SO_2)

The preferred cross section is listed in Table 6.3.5.17 and shown in Fig. 6.3.5.17. The preferred values of σ_m^{el} are based on the beam-derived values of [89Tra1] and [94Gul1].

The estimated uncertainty is < ± 30 %.

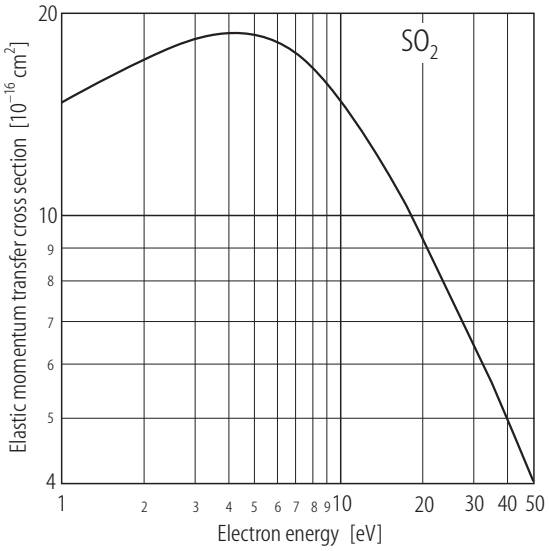

Fig. 6.3.5.17. Preferred values of the elastic momentum transfer cross section for electrons scattered from sulphur dioxide (SO_2).

Table 6.3.5.17. Preferred values of the elastic momentum transfer cross section (σ_m^{el}) for electrons scattered from sulphur dioxide (SO_2).

Energy [eV]	σ_m^{el} [Å^2]	Energy [eV]	σ_m^{el} [Å^2]	Energy [eV]	σ_m^{el} [Å^2]
1	14.7	5	18.8	18	10.0
1.2	15.4	6	18.2	20	9.15
1.5	16.2	7	17.4	25	7.61
1.8	16.8	8	16.6	30	6.46
2	17.2	9	15.8	40	4.97
2.5	17.9	10	15.0	50	4.05
3	18.3	12	13.5		
4	18.8	15	11.5		

References for 6.3.5.17

89Tra1 Trajmar, S., Shyn, T.W.: J. Phys. B: At. Mol. Opt. Phys. **22** (1989) 2911
94Gul1 Gulley, R.J., Buckman, S.J.: J. Phys. B: At. Mol. Opt. Phys. **27** (1994) 1833

6.3.5.18 Trifluoromethane (CHF_3)

The preferred cross section is listed in Table 6.3.5.18 and shown in Fig. 6.3.5.18. The preferred cross section, σ_m^{el}, is that calculated by [99Nat1].

No uncertainty is estimated.

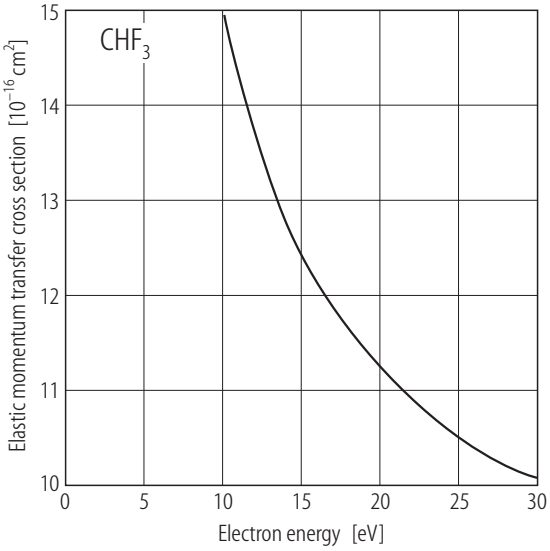

Fig. 6.3.5.18. Preferred values of the elastic momentum transfer cross section for electrons scattered from trifluoromethane (CHF_3).

Table 6.3.5.18. Preferred values of the elastic momentum transfer cross section (σ_m^{el}) for electrons scattered from trifluoroethane (CHF_3).

Energy [eV]	σ_m^{el} [Å^2]
10	14.9
12	13.7
15	12.4
18	11.6
20	11.2
25	10.5
30	10.1

References for 6.3.5.18

99Nat1 Natalense, A.P.P., Bettega, M.H.F., Ferreira, L.G., Lima, M.A.P.: Phys. Rev. A **59** (1999) 879

6.3.5.19 Nitrogen trifluoride (NF_3)

The preferred cross section for nitrogen trifluoride is listed in Table 6.3.5.19 and shown in Fig. 6.3.5.19. The preferred cross section is based on a curve of best fit to the only set of data available for this gas. These data are those of [96Boe1] and cover the energy range 1.5 to 100 eV.

No estimate of the uncertainty is made.

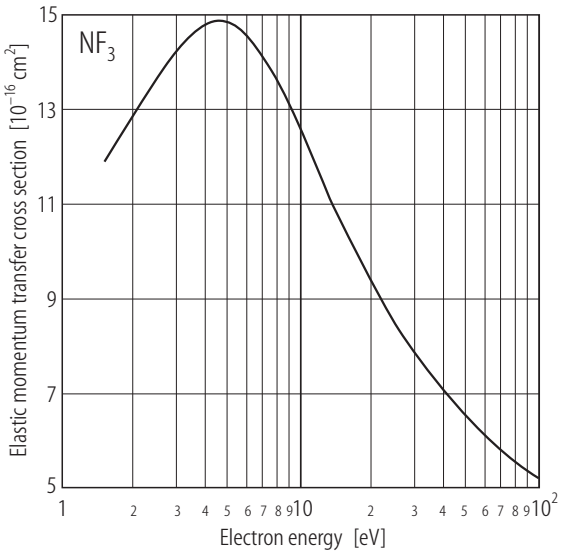

Fig. 6.3.5.19. Preferred values of the elastic momentum transfer cross section for electrons scattered from nitrogen trifluoride (NF_3).

Table 6.3.5.19. Preferred values of the elastic momentum transfer cross section (σ_m^{el}) for electrons scattered from nitrogen trifluoride (NF_3).

Energy [eV]	σ_m^{el} [Å^2]	Energy [eV]	σ_m^{el} [Å^2]	Energy [eV]	σ_m^{el} [Å^2]
1.5	11.90	8	13.62	40	6.98
1.8	12.57	9	12.99	50	6.45
2	12.93	10	12.46	60	6.08
2.5	13.71	12	11.57	70	5.78
3	14.27	15	10.45	80	5.56
4	14.94	18	9.72	90	5.39
5	14.94	20	9.29	100	5.22
6	14.61	25	8.41		
7	14.22	30	7.80		

Reference for 6.3.5.19

96Boe1 Boesten, L., Tachibana, Y., Nakano, Y., Shinohara, T., Tanaka, H., Dillon, M.A.: J. Phys. B: At. Mol. Opt. Phys. **29** (1996) 5475

6.3.5.20 Benzene (C_6H_6)

The preferred cross section is listed in Table 6.3.5.20 and shown in Fig. 6 3.5.20. There appears to be only two sets of beam-derived elastic momentum transfer cross section values, those of [99Gul1] and [00Cho1]. The preferred cross section has been taken as the best fit curve to these two data sets.

The uncertainty is estimated to be < ± 25 %.

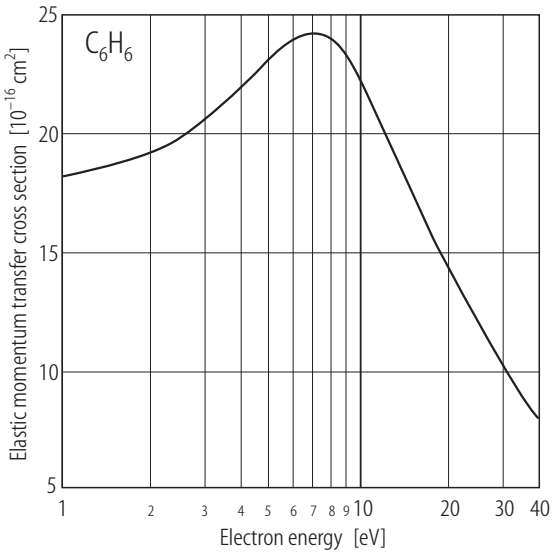

Fig. 6.3.5.20. Preferred values of the elastic momentum transfer cross section for electrons scattered from benzene (C_6H_6).

Table 6.3.5.20. Preferred values of the elastic momentum transfer cross section (σ_m^{el}) for electrons scattered from benzene (C_6H_6).

Energy [eV]	σ_m^{el} [Å^2]	Energy [eV]	σ_m^{el} [Å^2]
1	18.19	8	24.483
1.2	18.362	9	23.879
1.5	18.621	10	22.413
1.8	18.966	12	20.258
2	19.138	15	17.414
2.5	19.741	18	15.345
3	20.517	20	14.052
4	21.897	25	11.948
5	23.19	30	10.172
6	24.138	40	7.931
7	24.482		

References for 6.3.5.20

99Gul1 Gulley, R.J., Buckman, S.J.: J. Phys. B: At. Mol. Opt. Phys. **32** (1999) L405

00Ch01 Cho, H., Gulley, R.J., Sunohara, K., Kitajima, M., Uhlmann, L.J., Tanaka, H., Buckman, S.J.: Private communication, 2000

6.3.5.21 Carbon tetrafluoride (CF_4)

The preferred cross section is listed in Table 6.3.5.21 and shown in Fig. 6.3.5.21. The preferred values of σ_m^{el} are those determined by [99Chr1] after an extensive review of the literature up to 1999.

No uncertainty limits are quoted.

Table 6.3.5.21. Preferred values of the elastic momentum transfer cross section (σ_m^{el}) for electrons scattered from carbon tetrafluoride (CF_4).

Energy [eV]	σ_m^{el} [Å^2]	Energy [eV]	σ_m^{el} [Å^2]	Energy [eV]	σ_m^{el} [Å^2]
0.001	13.03	0.1	0.26	8	8.96
0.0015	12.30	0.125	0.14	9	10.06
0.002	11.76	0.15	0.13	10	11.23
0.0025	11.30	0.175	0.18	15	13.41
0.003	10.92	0.2	0.27	20	14.10
0.0035	10.55	0.25	0.48	25	12.50
0.004	10.22	0.3	0.76	30	10.38
0.0045	9.93	0.35	1.05	35	8.80
0.005	9.65	0.4	1.39	40	7.80
0.006	9.14	0.45	1.76	45	7.24
0.007	8.67	0.5	2.13	50	6.66
0.008	8.25	0.6	2.82	60	5.80
0.009	7.85	0.7	3.45	70	5.28
0.01	7.52	0.8	4.01	80	4.77
0.015	6.15	0.9	4.48	90	4.37
0.02	5.06	1	4.92	100	4.03
0.025	4.16	1.5	6.26	150	2.74
0.03	3.44	2	6.92	200	1.92
0.035	2.82	2.5	7.3	250	1.46
0.04	2.29	3	7.53	300	1.17
0.045	1.90	3.5	7.72	350	0.97
0.05	1.54	4	7.89	400	0.82
0.06	1.10	4.5	8.04	450	0.71
0.07	0.78	5	8.21	500	0.62
0.08	0.55	6	8.55	600	0.5
0.09	0.39	7	8.68	700	0.41

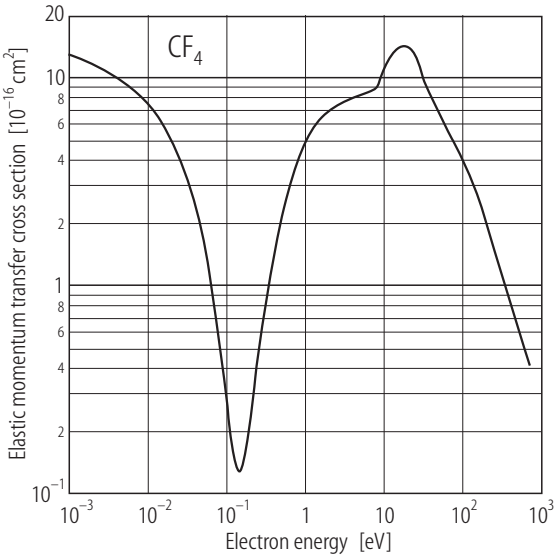

Fig. 6.3.5.21. Preferred values of the elastic momentum transfer cross section for electrons scattered from carbon tetrafluoride (CF_4).

Reference for 6.3.5.21

99Chr1 Christophorou, L.G.: J. Phys. Chem. Ref. Data **28** (1999) 1

6.3.5.22 Perfluoroethane (C_2F_6)

The preferred cross section is listed in Table 6.3.5.22 and shown in Fig. 6.3.5.22. The preferred cross section σ_m^{el}, is that determined by [98Chr1] from an assessment of the literature to 1997.

The uncertainty is estimated to be < ± 35 %.

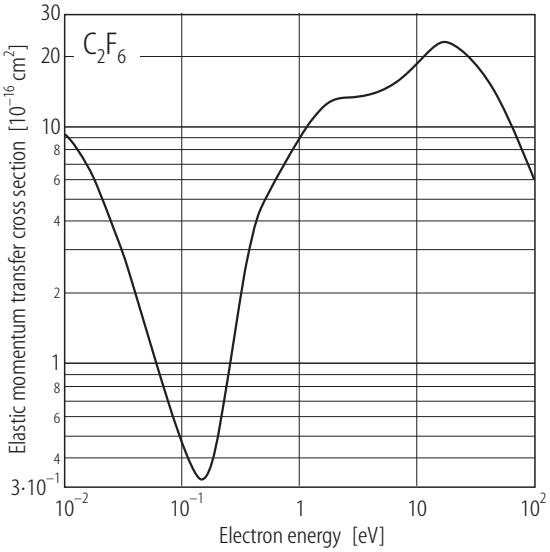

Fig. 6.3.5.22. Preferred values of the elastic momentum transfer cross section for electrons scattered from perfluoroethane (C_2F_6).

Table 6.3.5.22. Preferred values of the elastic momentum transfer cross section (σ_m^{el}) for electrons scattered from perfluoroethane (C_2F_6).

Energy [eV]	σ_m^{el} [Å^2]	Energy [eV]	σ_m^{el} [Å^2]	Energy [eV]	σ_m^{el} [Å^2]
0.01	9.47	0.4	3.45	8	17.9
0.02	5.08	0.45	4.24	9	18.4
0.03	3.06	0.5	4.82	10	18.8
0.04	1.99	0.6	5.71	15	22.7
0.05	1.38	0.7	6.55	20	22.5
0.06	1.01	0.8	7.39	30	18.9
0.07	0.78	0.9	8.21	40	15.5
0.08	0.63	1	8.98	50	12.8
0.09	0.53	1.5	11.8	60	10.6
0.1	0.46	2	13	70	8.96
0.15	0.32	3	13.2	80	7.66
0.2	0.47	4	14.1	90	6.66
0.25	0.93	5	14.6	100	5.86
0.3	1.66	6	15.2		
0.35	2.55	7	16.4		

References for 6.3.5.22

98Chr1 Christophorou, L.G. and Olthoff, J.K.: J. Phys. Chem. Ref. Data **27** (1998) 1

6.3.5.23 Sulphur hexafluoride (SF_6)

The preferred cross section is listed in Table 6.3.5.23 and shown in Fig. 6.3.5.23. The preferred values of σ_m^{el} are those of [00Chr1] which cover the energy range 2.75 to 700 eV. This cross section agrees to within the stated error limits with the beam derived values of [83Tra1, 89Sak1 91Joh1, 00Cho1].

The uncertainty is estimated to be < ± 20 %.

References for 6.3.5.23

83Tra1 Trajmar, S., Register, D.F., Chutjian, A.: Phys. Rep. **97** (1983) 216
89Sak1 Sakae, T., Sumiyoshi, S., Murakami, E., Matsumoto, Y., Ishibashi, K., Katase, A.: J. Phys. B: At. Mol. Opt. Phys.: **22** (1989) 1385
91Joh1 Johnstone, W.M., Newell, W.R.: J. Phys. B: At. Mol. Opt. Phys. **24** (1991) 473
00Cho1 Cho, H., Gulley, R.J., Buckman, S.J.: J. Phys. B: At. Mol. Opt. Phys. **33** (2000) L309
00Chr1 Christophorou, L.G., Olthoff, J.K.: J. Phys. Chem. Ref. Data **29** (20009 267

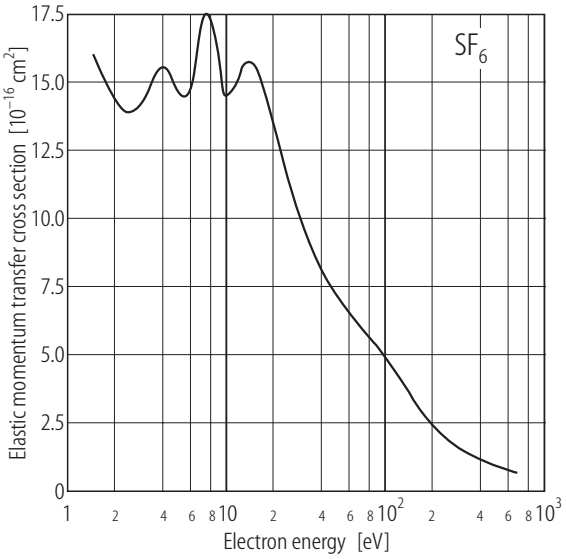

Fig. 6.3.5.23. Preferred values of the elastic momentum transfer cross section for electrons scattered from sulphur hexafluoride (SF_6).

Table 6.3.5.23. Preferred values of the elastic momentum transfer cross section (σ_m^{el}) for electrons scattered from sulphur hexafluoride (SF_6).

Energy [eV]	σ_m [Å^2]	Energy [eV]	σ_m [Å^2]
2.75	16	30	13.2
3	15.4	35	11.4
3.5	14.5	40	10.3
4	14.00	45	9.37
4.5	13.9	50	8.65
5	14.1	60	7.69
6	15.1	70	7.06
7	15.5	75	6.74
8	14.8	80	6.46
9	14.4	90	6.03
10	15.1	100	5.70
11	16.7	125	4.92
12	17.6	150	4.16
13	17.1	200	2.98
14	15.8	250	2.23
15	14.9	300	1.76
16	14.5	350	1.47
17	14.7	400	1.28
18	15.00	450	1.13
19	15.4	500	1.02
20	15.7	600	0.82
22	15.7	700	0.66
25	15.00		

6.3.5.24 Hexafluorobenzene (C_6F_6)

The preferred cross section is listed in Table 6.3.5.24 and shown in Fig. 6.3.5.24.
The preferred cross section is a best fit curve to the only available data, the beam-derived values of [00Cho1].

The uncertainty is estimated to be < ± 25 %.

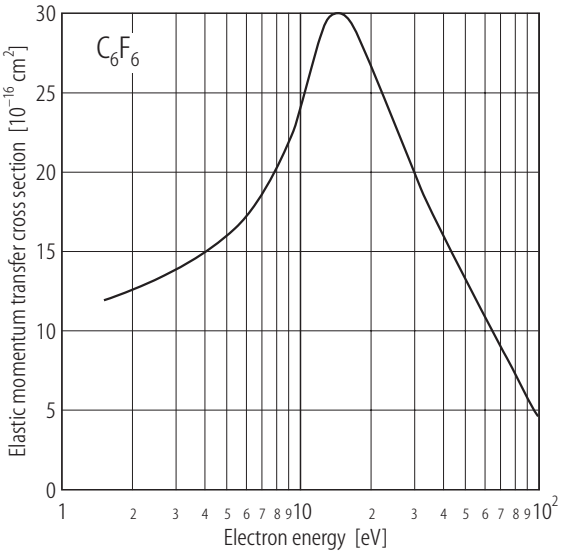

Fig. 6.3.5.24. Preferred values of the elastic momentum transfer cross section for electrons scattered from hexafluorobenzene (C_6F_6).

Table 6.3.5.24. Preferred values of the elastic momentum transfer cross section (σ_m^{el}) for electrons scattered from hexafluorobenzene (C_6F_6).

Energy [eV]	σ_m^{el} [Å^2]	Energy [eV]	σ_m^{el} [Å^2]	Energy [eV]	σ_m^{el} [Å^2]
1.5	11.9	8	20.34	40	15.86
1.8	12.33	9	21.98	50	12.93
2	12.59	10	23.97	60	10.603
2.5	13.28	12	28.36	70	8.879
3	13.79	15	29.91	80	7.155
4	14.914	18	28.05	90	5.69
5	16.12	20	26.38	100	4.569
6	17.41	25	22.5		
7	18.79	30	19.74		

References for 6.3.5.24

00Cho1 Cho, H., Gulley, R.J., Sunohara, K., Kitajima, M., Uhlmann, L.J., Tanaka, H., Buckman, S.J.: Private communication, 2000

6.3.5.25 Perfluoropropane (C_3F_8)

The preferred cross section is listed in Table 6.3.5.25 and shown in Fig. 6.3.5.25. The preferred cross section, σ_m^{el} is based on that determined by [99Tan1] (erroneously tabled in this paper as being for C_3H_8).

The uncertainty is estimated to be < ± 30 %.

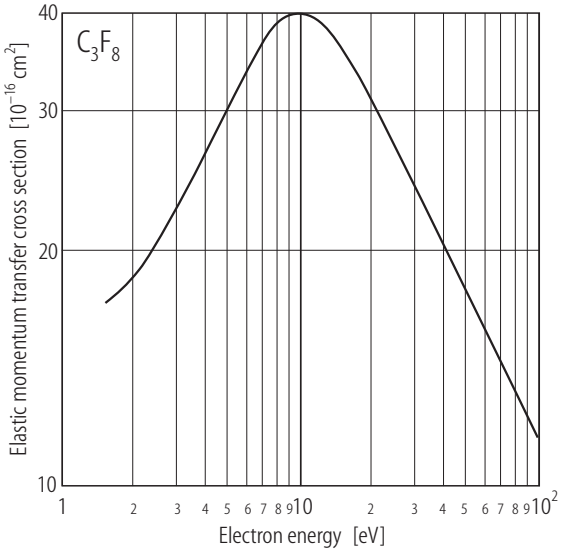

Fig. 6.3.5.25. Preferred values of the elastic momentum transfer cross section for electrons scattered from perfluoropropane (C_3F_8).

Table 6.3.5.25. Preferred values of the elastic momentum transfer cross section (σ_m^{el}) for electrons scattered from perfluoropropane (C_3F_8).

Energy [eV]	σ_m^{el} [Å^2]	Energy [eV]	σ_m^{el} [Å^2]	Energy [eV]	σ_m^{el} [Å^2]
1.5	17.1	8	39.7	40	19.8
1.8	17.9	9	40.7	50	17.3
2	18.4	10	41.1	60	15.5
2.5	20.1	12	39.5	70	14.2
3	22.2	15	35.9	80	13.1
4	26.7	18	32.3	90	12.2
5	30.4	20	30.2	100	11.5
6	33.9	25	26.6		
7	37.3	30	23.6		

References for 6.3.5.25

99Tan1 Tanaka, H., Tachibana, Y., Kitajima, M., Sueoka, O., Takaki, H., Hamada, A., Kimura, M.: Phys. Rev. A **59** (1999) 2006

6.4 Excitation cross sections

6.4.1 Introduction

In this section of Chapter 6 preferred integral cross sections for discrete inelastic (i.e. rotation, vibration and electronic) excitation for a wide range of molecules are presented. Ionisation, dissociation and attachment phenomena are not considered. If a molecule does not appear in this section then its omission reflects either the absence of any relevant cross section data, or that there was insufficient data available for us to construct a preferred set.

Definition of the integral cross section in terms of the differential cross section and the scattering phase shifts was given previously in 6.2. Consequently those details are not repeated again here.

6.4.2 Experimental determinations

6.4.2.1 From swarm experiments

The technique involves high precision measurements of characteristic transport properties, the transport coefficients, of an ensemble or swarm of electrons as they drift and diffuse through a gas under the influence of an applied electric (***E***), or crossed electric and magnetic (***B***), fields at pressures ranging from a few torr to many atmospheres.

Procedures for measurement of these transport coefficients (commonly the drift velocity, v_{dr}, ratio of the lateral diffusion coefficient D_T, to the electron mobility, μ, and when there is a magnetic field transverse to ***E***, the ratio $v_\perp/v_{dr}$, where $v_\perp$ is the drift velocity at right angles to ***E*** and ***B***) include the Bradbury-Nielsen [74Hux1], photon flux [89Kel1] and voltage transient [89Pur1] techniques. For a given gas, in the hydrodynamic regime, all these transport coefficients are functions only of the ratio E/N, the gas temperature T, and when a magnetic field is present, of B/N.

The macroscopic transport coefficients are related to the desired microscopic quantities (integral cross sections as a function of energy) through an energy distribution function which is usually non-Maxwellian and often complex in form. The microscopic properties have to be determined in a complicated and somewhat cumbersome [74Hux1] unfolding procedure by seeking a self-consistent set of cross sections which produce the experimental coefficients via an appropriate (either "two term" or "multiterm", see 6.3.2.1 for more details) formulation of the Boltzmann transport equation [84Kum1]. Alternatively, one can use Monte Carlo simulation to describe the kinetics of the swarm, from which the same transport coefficients can be derived. The beauty of this approach is that it is mathematically very simple and also versatile in its applicability; its weakness is the computational overhead associated with the repetitive calculations required for statistical accuracy [97Nol1].

When applied to atomic systems at low "mean energies" swarm experiments can provide very accurate integral and momentum transfer cross sections. However in molecular systems there are particular problems in obtaining a unique set of cross sections from swarm experiments [84Kum1, 93Bren1], as is evidenced by the molecular hydrogen (H_2) $\nu = 0 \rightarrow 1$ rotationally-averaged vibrational integral cross section of Schmidt et al. [94Sch1]. Here they [94Sch1] derived a H_2 $\nu = 0 \rightarrow 1$ integral cross section which is some 14 % different to that which had hitherto been considered the definitive swarm result for this process [88Eng1]. This discrepancy between [88Eng1] and [94Sch1] is probably due to [94Sch1] being able to measure a more extensive set of transport parameters with their $\boldsymbol{E} \times \boldsymbol{B}$ technique. Consequently a more rigorous constraint is placed on the integral cross sections derived from their Boltzmann analysis. However, the point here is not that the cross section of Schmidt et al. [94Sch1] is arguably in better agreement with theory [90Buc1, 93Res1] and beam experiments [91Bru1] than was the earlier swarm data [88Eng1], but that two quite similar analyses of swarm data produced two significantly different results for the $0 \rightarrow 1$ H_2 integral cross section. This lack of uniqueness problem

with the swarm technique, which grows as more inelastic channels become open, is a major limitation in its application to deriving integral excitation cross sections in molecules. Consequently, we have been very circumspect in using swarm-derived excitation integral cross sections when constructing our preferred cross section sets.

Nonetheless we note that the power of the swarm technique, in electron scattering from molecular systems, is its ability to test the consistency of a proposed set of cross sections with accurately measured transport data.

6.4.2.2 From crossed beam experiments

The integral excitation cross section $\sigma(\varepsilon)$ can be derived from absolute measurements of the corresponding differential cross section $d\sigma/d\Omega$ from:

$$\sigma(\varepsilon) = 2\pi \int_0^{\pi} \frac{d\sigma}{d\Omega} \sin\theta \, d\theta \tag{1}$$

There are several complications with this technique. Firstly, in the measurement of the absolute excitation differential cross section the establishment of the relative detector response function for the energy loss range corresponding to the elastic and inelastic events can be problematic [94Traj1]. Secondly, the excitation processes of interest may be strongly overlapping in energy loss, thereby requiring the use of spectral deconvolution procedures [97Cam1]. Finally in most measurements of $d\sigma/d\Omega$ the entire range of scattering angles between 0 and π, due to the presence of primary beam and other geometrical constraints, cannot be covered. Consequently some extrapolation procedure is required to extend these measurements to 0 and π. Various techniques have been applied to enable this extrapolation and they, and the uncertainties involved, have been discused by various authors (e.g. [83Tra1]). We note that the recent experimental development of Read and Channing [96Rea1], in which a localised magnetic field is added to the interaction region of a conventional electrostatic electron spectrometer to increase the angular range of electrons that the analyser receives, provides a possible solution to the extrapolation problem.

Integral excitation cross sections, for optically allowed transitions, can also be determined by measurement of the number of emitted photons as a function of the incident electron energy i.e. the so-called optical excitation function. Normalisation to an absolute scale is usually achieved by application of the Bethe-Born approximation [30Bet1] at a high enough energy at which the Born approximation is expected to be valid [71Ino1]. There are also several complications with this technique. They include that the emitted radiation is polarised, so that there will be some angular distribution of the intensity of the photons. In addition cascade effects can be a serious problem.

References for 6.4.2

30Bet1 Bethe, H.A.: Ann. Phys. **5** (1930) 325

71Ino1 Inokuti, M.: Rev. Mod. Phys. **43** (1971) 297

74Hux1 Huxley, L.G.H., Crompton, R.W.: The diffusion and drift of electrons in gases, NewYork: Wiley-Interscience, 1974

83Traj1 Trajmar, S., Register, D.F., Chutjian, A.: Phys. Rep. **97** (1983) 219

84Kum1 Kumar, K.: Phys. Rep. **112** (1984) 319

88Eng1 England, J.P., Elford, M.T., Crompton, R.W.: Aust. J. Phys. **41** (1988) 573

89Kel1 Kelly, L.J., Brennan, M.J., Wedding, A.B.: Aust. J. Phys. **42** (1989) 365

89Pur1 Purdie, P.H., Fletcher, J.: J. Phys. D **22** (1989) 759

90Buc1 Buckman, S.J., Brunger, M.J., Newman, D.S., Snitchler, G., Alston, S., Norcross, D.W., Morrison, M.A., Saha, B.C., Danby, G., Trail, W.K.: Phys. Rev. Lett. **65** (1990) 3253

91Bru1 Brunger, M.J. Buckman, S.J., Newman, D.S., Alle, D.T.: J. Phys. B: At. Mol. Opt. Phys. **24** (1991) 1435

93Bren1 Brennan, M.J., Ness, K.F.: Aust. J. Phys. **45** (1993) 249
93Res1 Rescigno, T.N., Elza, B.K., Lengsfield III, B.H.: J. Phys. B: At. Mol. Opt. Phys. **26** (1993) L567
94Sch1 Schmidt, B., Berkhan, K., Götz, B., Möller, M.: Phys. Scr. **53** (1994) 30
94Traj1 Trajmar, S., McConkey, J.W.: Adv. At. Mol. Opt. Phys. **33** (1994) 63
96Rea1 Read, F.H., Channing, J.M.: Rev. Sci. Instrum. **67** (1996) 2372
97Cam1 Campbell, L., Brunger, M.J., Teubner, P.J.O., Mojarrabi, B., Cartwright, D.C.: Aust. J. Phys. **50** (1997) 525
97Nol1 Nolan, A.M., Brennan, M.J. Ness, K.F., Wedding, A.B.: J. Phys. D: Appl. Phys. **30** (1997) 2865

6.4.3 Determination of preferred cross sections

The preferred integral excitation cross sections for each molecule have been derived from a consideration of all available (published) experimental and theoretical work. In general, we do not consider those cases where only theoretical values exist, unless there is substantial corroboration between two or more different calculations. More weight has been placed on recent measurements which have realistic and well quantified uncertainties. The uncertainty estimates on the preferred cross sections indicate the level of concurrence between the various individual measurements and calculations.

6.4.4 Units

Cross sections are given in square Ångström ($1 Å^2 = 10^{-16}$ cm^2) and electron energies in electron volt (eV).

6.4.5 Molecules

6.4.5.1 Hydrogen (H_2)

6.4.5.1.1 $J = 0 \rightarrow 2$

Below the threshold for vibrational excitation ($\Delta E \approx 0.5$ eV), accurate integral cross sections for the $J = 0 \rightarrow 2$ rotational excitation process in H_2 can be found in the electron swarm work of [70Crom1, 70Gib1, 88Eng1]. The relatively recent work of [88Eng1] is considered to be the definitive swarm measurement and it forms the basis for our preferred integral cross section set, as tabulated in Table 6.4.1 and plotted in Fig. 6.4.1

The uncertainty on the cross sections is estimated to be ± 5 %.

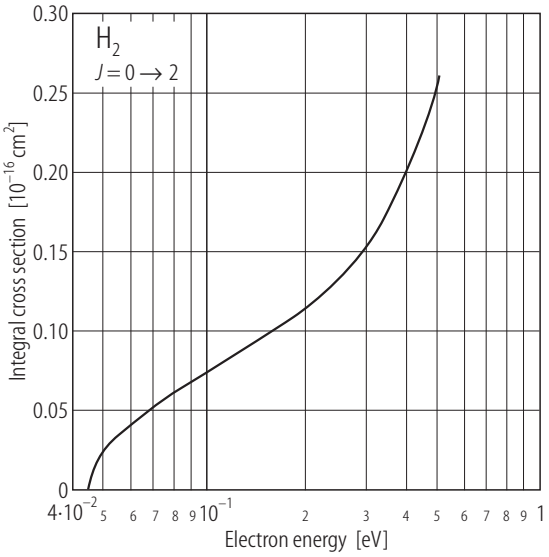

Fig. 6.4.1. Recommended integral cross section for $J = 0 \rightarrow 2$ in H_2.

Table 6.4.1. Preferred values of the integral $J = 0 \rightarrow 2$ rotational excitation cross section ($\sigma_{0\text{-}2}$) for electrons in molecular hydrogen.

Energy [eV]	$\sigma_{0\text{-}2}$ [Å^2]	Energy [eV]	$\sigma_{0\text{-}2}$ [Å^2]
0.044	0	0.13	0.088
0.047	0.0185	0.15	0.097
0.050	0.027	0.20	0.115
0.060	0.042	0.25	0.132
0.065	0.048	0.30	0.152
0.070	0.053	0.35	0.175
0.080	0.062	0.40	0.200
0.090	0.068	0.45	0.228
0.10	0.074	0.50	0.260
0.11	0.079		

References for 6.4.5.1.1

70Crom1 Crompton, R.W., Gibson, D.K., Robertson, A.G.: Phys. Rev. A **2** (1970) 1386
70Gib1 Gibson, D.K.: Aust. J. Phys. **23** (1970) 683
88Eng1 England, J.P., Elford, M.T., Crompton, R.W.: Aust. J. Phys. **41** (1988) 573

6.4.5.1.2 $J = 1 \rightarrow 3$

The preferred integral cross section for electron impact excitation of the $J = 1 \rightarrow 3$ rotational transition is presented over the energy range from threshold to 0.5 eV. The data are tabulated in Table 6.4.2 and plotted in Fig. 6.4.2. For the $J = 1 \rightarrow 3$ transition there are swarm cross sections due to [88Eng1] and beam cross sections due to [71Lin1]. The accurate calculation of [87Mor1] favours the swarm determination over that of the beam measurements, in the energy range considered, and so our preferred cross section is based on the work of [88Eng1].

The uncertainty is estimated to be ± 10 %.

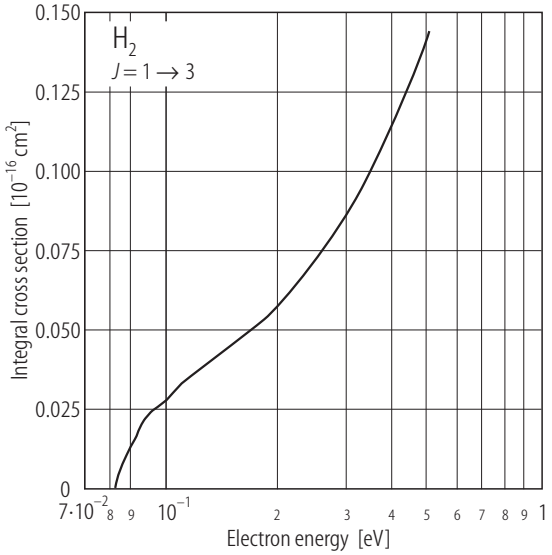

Fig. 6.4.2. Recommended integral cross section for $J = 1 \rightarrow 3$ in H_2.

Table 6.4.2. Preferred values of the integral $J = 1 \rightarrow 3$ rotational excitation cross section ($\sigma_{1\text{-}3}$) for electrons in molecular hydrogen.

Energy [eV]	$\sigma_{1\text{-}3}$ [Å^2]	Energy [eV]	$\sigma_{1\text{-}3}$ [Å^2]	Energy [eV]	$\sigma_{1\text{-}3}$ [Å^2]
0.073	0	0.10	0.028	0.25	0.072
0.075	0.007	0.11	0.033	0.3	0.086
0.08	0.014	0.12	0.0364	0.35	0.10
0.085	0.0198	0.13	0.039	0.40	0.114
0.09	0.0237	0.15	0.045	0.45	0.129
0.095	0.0265	0.20	0.058	0.50	0.144

References for 6.4.5.1.2

71Lin1 Linder, F., Schmidt, H.: Z. Naturforsch A **26** (1971) 1603
87Mor1 Morrison, M.A., Crompton, R.W., Saha, B.C., Petrovic, Z.Lj.: Aust. J. Phys. **40** (1987) 239
88Eng1 England, J.P., Elford, M.T., Crompton, R.W.: Aust. J. Phys. **41** (1988) 573

6.4.5.1.3 $\nu' = 0 \rightarrow 1$

There have been several experimental, both swarm and crossed beam, determinations of integral cross sections for the $\nu' = 0 \rightarrow 1$ vibrational excitation in molecular hydrogen. These include [70Cro1, 88Eng1, 68Ehr1, 71Lin1, 85Nis1, 90Buc1, 91Bru1, 94Sch1]. The differential cross section measurements of [85Nis1] are in poor agreement with the other crossed beam determinations [68Ehr1, 71Lin1, 91Bru1] and with theory [90Buc1, 93Res1], and so we do not use their [85Nis1] integral cross sections in determining our preferred integral cross section set.

The preferred cross section set was constructed in the following manner. For $\varepsilon < 1$ eV an average of the integral cross sections from [68Ehr1, 88Eng1, 94Sch1] was used. For 1 eV $\leq \varepsilon \leq$ 2.4 eV an average of the integral cross sections from [68Ehr1, 88Eng1, 91Bru1, 94Sch1] was employed, while for 2.4 eV $\leq \varepsilon \leq$ 5 eV an average of the integral cross sections from [68Ehr1, 71Lin1, 88Eng1, 91Bru1] was used. Finally, for 5 eV $< \varepsilon \leq$ 7 eV the preferred integral cross section was formed from an average of the measurements of [68Ehr1] and [88Eng1]. The preferred cross sections are listed in Table 6.4.3 and plotted in Fig. 6.4.3.

The uncertainty on the cross sections is estimated to be: ± 50 % for $\varepsilon < 0.60$ eV, ± 30 % for 0.60 eV $\leq \varepsilon < 1.25$ eV, ± 20 % for 1.25 eV $\leq \varepsilon \leq 2$ eV and ± 15 % for $\varepsilon > 2$ eV.

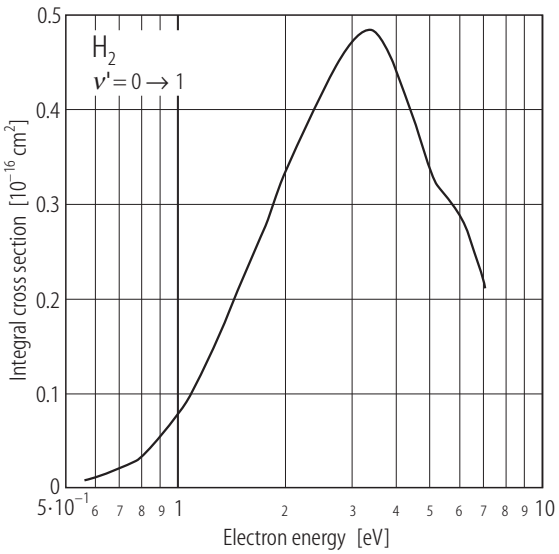

Fig. 6.4.3. Recommended integral cross section for $\nu' = 0 \rightarrow 1$ in H_2.

Table 6.4.3. Preferred values of the integral $\nu' = 0 \rightarrow 1$ vibrational excitation cross section ($\sigma_{0\text{-}1}$) for electrons in molecular hydrogen.

Energy [eV]	$\sigma_{0\text{-}1}$ [Å^2]	Energy [eV]	$\sigma_{0\text{-}1}$ [Å^2]	Energy [eV]	$\sigma_{0\text{-}1}$ [Å^2]
0.56	0.0065	1	0.073	3.4	0.483
0.60	0.0097	1.25	0.141	3.8	0.458
0.65	0.0138	1.5	0.211	4.5	0.382
0.75	0.0261	2	0.339	5	0.330
0.85	0.040	2.5	0.419	6	0.284
0.95	0.062	3	0.470	7	0.210

References for 6.4.5.1.3

68Ehr1 Ehrhardt, H., Langhans, L., Linder, F., Taylor, H.S.: Phys. Rev. **173** (1968) 222
70Cro1 Crompton, R.W., Gibson, D.K., Robertson, A.G.: Phys. Rev. A **2** (1970) 1386
71Lin1 Linder, F., Schmidt, H.: Z. Naturforsch A **26** (1971) 1603
85Nis1 Nishimura, H., Danjo, A., Sugahara, H.: J. Phys. Soc. Jpn. **54** (1985) 1757
88Eng1 England, J.P., Elford, M.T., Crompton, R.W.: Aust. J. Phys. **41** (1988) 573
90Buc1 Buckman, S.J., Brunger, M.J., Newman, D.S., Snitchler, G., Alston, S., Norcross, D.W., Morrison, M.A., Saha, B.C., Danby, G., Trail, W.K.: Phys. Rev. Lett. **65** (1990) 3253
91Bru1 Brunger, M.J., Buckman, S.J., Newman, D.S., Alle, D.T.: J. Phys. B: At. Mol. Opt. Phys. **24** (1991) 1435
93Res1 Rescigno, T.N., Elza, B.K., Lengsfield III, B.H.: J. Phys. B: At. Mol. Opt. Phys. **26** (1993) L567
94Sch1 Schmidt, B., Berkhan, K., Götz, B., Möller, M.: Phys. Scr. **53** (1994) 30

6.4.5.1.4 $X^1\Sigma_g^+ \rightarrow B^1\Sigma_u^+$

There appears to be three experimental determinations of integral cross sections for excitation of the $B^1\Sigma_u^+$ electronic-state of molecular hydrogen. The first, from 15 to 60 eV, is due to [77Sri1] while the second, from 20 to 60 eV is due to [86Kha1]. Both [77Sri1] and [86Kha1] are crossed beam measurements. The final determination is an optical emission cross section from [85She1], at energies from near-threshold to around 300 eV. All three sets of integral cross sections appear to be in fair agreement with one another, and as such they form the basis for our preferred cross section set. This set is tabulated in Table 6.4.4 and plotted in Fig. 6.4.4.

The uncertainty on the integral cross section is estimated to be ± 20 % over the entire range of electron energies.

Table 6.4.4. Preferred values of the integral $X^1\Sigma_g^+ \rightarrow B^1\Sigma_u^+$ electronic-state excitation cross section ($\sigma_{X\text{-}B}$) for electrons in molecular hydrogen.

Energy [eV]	$\sigma_{X\text{-}B}$ [Å^2]	Energy [eV]	$\sigma_{X\text{-}B}$ [Å^2]	Energy [eV]	$\sigma_{X\text{-}B}$ [Å^2]
13.00	0.010	16.1	0.082	32	0.309
13.15	0.013	16.9	0.104	41	0.331
13.41	0.015	17.6	0.125	47	0.338
13.55	0.020	18.2	0.144	55	0.331
13.83	0.026	18.5	0.153	70	0.318
13.97	0.032	19.9	0.187	90	0.291
14.4	0.040	21.3	0.213	101	0.279
15.0	0.053	23.9	0.248		
15.6	0.067	27.2	0.279		

References for 6.4.5.1.4

77Sri1 Srivastava, S.K., Jansen, S.: J. Phys. B: At. Mol. Phys. **10** (1977) 3341
85She1 Shemansky, D.E., Ajello, J.M., Hall, D.T.: Astrophys. J. **296** (1985) 765
86Kha1 Khakoo, M.A., Trajmar, S.: Phys. Rev. A **34** (1986) 146

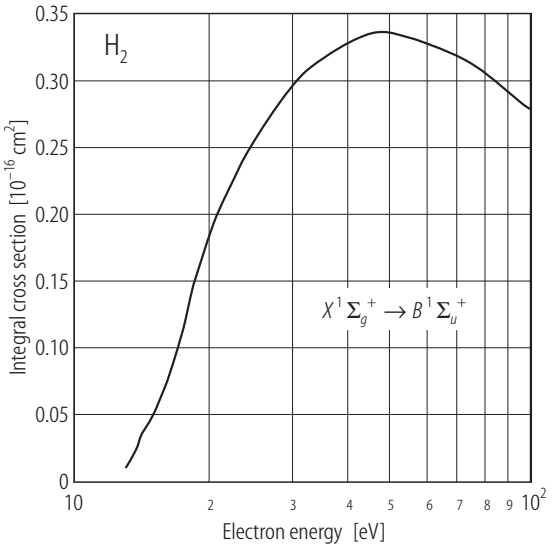

Fig. 6.4.4. Recommended integral cross section for $X^1\Sigma^+_g \rightarrow B^1\Sigma_u^+$ in H_2.

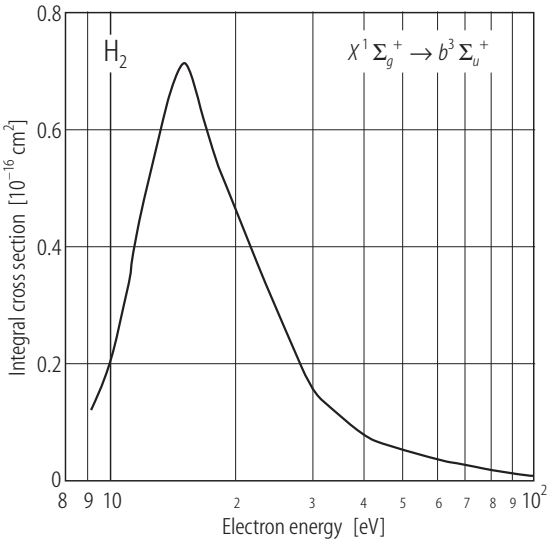

Fig. 6.4.5. Recommended integral cross section for $X^1\Sigma_g^+ \rightarrow b^3\Sigma_u^+$ in H_2.

6.4.5.1.5 $X^1\Sigma_g^+ \rightarrow b^3\Sigma_u^+$

There are four sets of crossed beam measurements of integral cross sections for excitation of the $b^3\Sigma_u^+$ electronic state of molecular hydrogen. These are due to [84Hal1, 86Nis1, 87Kha1, 94Kha1] and in general, to within their respective uncertainty of measurement, they are in fair agreement with one another. Our preferred cross section set is constructed using all four of these measurements and it covers the energy range 9.2 to 100 eV. This data is plotted in Fig. 6.4.5 and tabulated in Table 6.4.5.

The uncertainty on the integral cross section is estimated to be ± 20 % over the entire range of electron energies.

Table 6.4.5. Preferred values of the integral $X^1\Sigma^+_g \rightarrow b^3\Sigma^+_u$ electronic-state excitation cross section ($\sigma_{X\text{-}b}$) for electrons in molecular hydrogen.

Energy [eV]	$\sigma_{X\text{-}b}$ [Å^2]	Energy [eV]	$\sigma_{X\text{-}b}$ [Å^2]	Energy [eV]	$\sigma_{X\text{-}b}$ [Å^2]
9.2	0.121	15.1	0.717	40	0.080
10.2	0.208	17.2	0.573	60	0.038
12	0.470	20	0.456	100	0.007
12.2	0.494	30	0.164		

References for 6.4.5.1.5

84Hal1 Hall, R.I., Andric, L.: J. Phys. B: At. Mol. Phys. **17** (1984) 3815
86Nis1 Nishimura, H., Danjo, A.: J. Phys. Soc. Jpn. **55** (1986) 3031
87Kha1 Khakoo, M.A., Trajmar, S., McAdams, R., Shyn, T.: Phys. Rev. A **35** (1987) 2832
94Kha1 Khakoo, M.A., Segura, J.: J. Phys. B: At. Mol. Opt. Phys. **27** (1994) 2355

6.4.5.1.6 $X^1\Sigma_g^+ \rightarrow c^3\Pi_u$

Integral cross sections for electron impact excitation of the $c^3\Pi_u$ electronic-state of H_2 have been reported by [86Kha1] and [86Mas1]. The crossed beam measurement of [86Kha1] covers the energy range 20 to 60 eV, while the metastable time-of-flight study of [86Mas1] is from threshold to about 60 eV. Note that the relative data of [86Mas1] were put on an absolute scale by normalisation to the 20 eV integral cross section of [86Kha1]. For $\varepsilon > 20$ eV the data of Mason and Newell [86Mas1] is significantly higher in magnitude than that of [86Kha1], perhaps due to cascade contributions in the formers work. Our preferred cross section is constructed from the data of [86Mas1] for $\varepsilon < 20$ eV and from [86Kha1] for 20 eV $\leq \varepsilon \leq$ 60 eV. It is tabulated in Table 6.4.6 and plotted in Fig. 6.4.6.

The uncertainty in the integral cross section is estimated to be ± 30 % for $\varepsilon < 20$ eV and ± 25 % for $\varepsilon \geq 20$ eV.

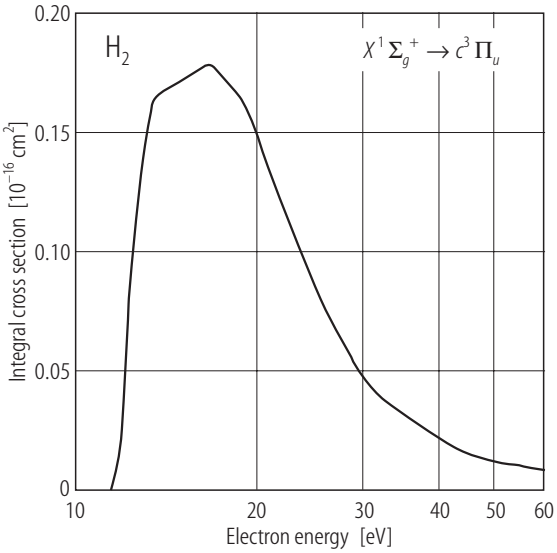

Fig. 6.4.6. Recommended integral cross section for $X^1\Sigma_g^+ \rightarrow c^3\Pi_u$ in H_2.

Table 6.4.6. Preferred values of the integral $X^1\Sigma_g^+ \rightarrow c^3\Pi_u$ electronic-state excitation cross section ($\sigma_{X\text{-}c}$) for electrons in molecular hydrogen.

Energy [eV]	$\sigma_{X\text{-}c}$ [Å^2]
11.52	0.001
11.91	0.021
12.28	0.080
13.4	0.162
15.7	0.174
16.6	0.178
17.4	0.173
18.6	0.164
19.5	0.155
20.0	0.147
30.0	0.046
40.0	0.021
50.0	0.008

References for 6.4.5.1.6

86Kha1 Khakoo, M.A., Trajmar, S.: Phys. Rev. A **34** (1986) 146
86Mas1 Mason, N.J., Newell, W.R.: J. Phys. B: At. Mol. Phys. **19** (1986) L587

6.4.5.1.7 $X^1\Sigma_g^+ \rightarrow a^3\Sigma_g^+$

Integral cross sections for electron impact excitation of the $a^3\Sigma_g^+$ electronic-state of H_2 have been reported by [86Kha1] and [85Aje1]. The crossed beam measurement of [86Kha1] covers the energy range 20 to 60 eV, while the optical emission cross section data of [85Aje1] is from threshold to about 60 eV. Note that the relative data of [85Aje1] were put on an absolute scale by normalisation to the 20 eV integral cross

section of [86Kha1]. Except at 60 eV, the cross sections of [86Kha1] and [85Aje1] are in good agreement, with our preferred set being constructed from the data of [85Aje1] for $\varepsilon \leq 30$ eV and from [86Kha1] for 30 eV $< \varepsilon \leq 60$ eV. Our preferred integral cross section is plotted in Fig. 6.4.7 and tabulated in Table 6.4.7.

The uncertainty in the integral cross section is estimated to be ± 20 % over the entire range of electron energies.

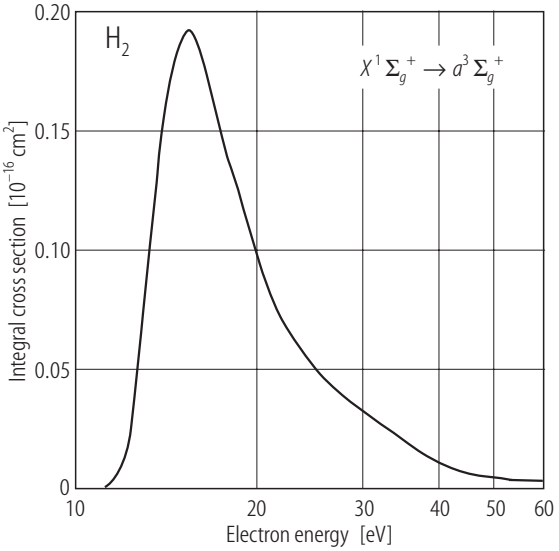

Fig. 6.4.7. Recommended integral cross section for $X^1\Sigma_g^+ \rightarrow a^3\Sigma_g^+$ in H_2.

Table 6.4.7. Preferred values of the integral $X^1\Sigma_g^+ \rightarrow a^3\Sigma_g^+$ electronic-state excitation cross section ($\sigma_{X\text{-}a}$) for electrons in molecular hydrogen.

Energy [eV]	$\sigma_{X\text{-}a}$ [Å^2]	Energy [eV]	$\sigma_{X\text{-}a}$ [Å^2]	Energy [eV]	$\sigma_{X\text{-}a}$ [Å^2]
11.29	0.001	15.2	0.193	21.6	0.076
11.5	0.002	15.5	0.193	22.5	0.068
11.75	0.005	15.6	0.193	23.6	0.060
12.1	0.013	15.8	0.190	24.5	0.054
12.5	0.028	16.2	0.183	25.8	0.047
12.8	0.056	16.8	0.169	26.8	0.043
13.2	0.087	17.7	0.145	27.8	0.039
13.5	0.118	18.5	0.129	29.2	0.035
14.0	0.152	19.4	0.110	30.0	0.033
14.3	0.167	20.0	0.100	40.0	0.011
14.8	0.184	20.5	0.092	60.0	0.003

References for 6.4.5.1.7

85Aje1 Ajello, J.M., Pang, K.D., Franklin, B., Fram, F.: EOS Transactions, Am. Geophys. Union **66** (1985) 989

86Kha1 Khakoo, M.A., Trajmar, S.: Phys. Rev. A **34** (1986) 146

6.4.5.1.8 $X^1\Sigma_g^+ \rightarrow C^1\Pi_u$

There appears to be only two experimental determinations of integral cross sections for excitation of the $C^1\Pi_u$ electronic-state of molecular hydrogen. The first, from near-threshold to about 300 eV, is an optical emission cross section from [85She1], while the other is a crossed beam measurement from [86Kha1] for energies in the range 20 eV to 60 eV. At 30 eV and 40 eV the integral cross sections of [85She1] and [86Kha1] are in fair agreement. However, at 20 eV and 60 eV there is an important discrepancy between them. In this case our preferred cross section set is drawn largely from the optical study of [85She1]. It is tabulated in Table 6.4.8 and plotted in Fig. 6.4.8.

The uncertainty in the integral cross section is estimated to be ± 25 % over the entire range of electron energies.

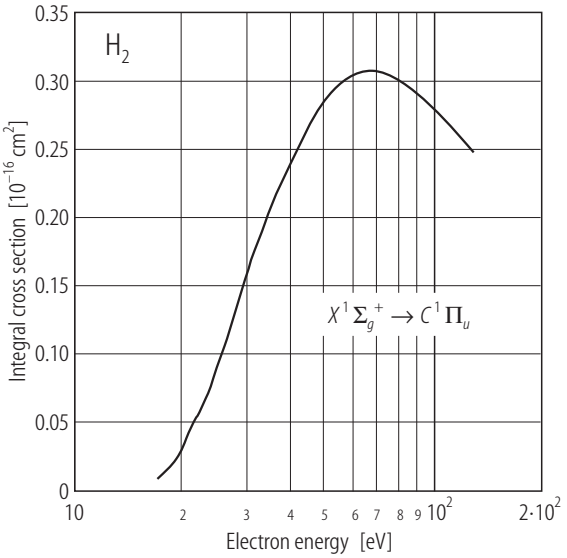

Fig. 6.4.8. Recommended integral cross section for $X^1\Sigma_g^+ \rightarrow C^1\Pi_u$ in H_2.

Table 6.4.8. Preferred values of the integral $X^1\Sigma_g^+ \rightarrow C^1\Pi_u$ electronic-state excitation cross section ($\sigma_{X\text{-}C}$) for electrons in molecular hydrogen.

Energy [eV]	$\sigma_{X\text{-}C}$ [Å^2]	Energy [eV]	$\sigma_{X\text{-}C}$ [Å^2]	Energy [eV]	$\sigma_{X\text{-}C}$ [Å^2]
16.9	0.010	24.6	0.090	53.5	0.294
17.4	0.013	26.4	0.112	66.1	0.306
18.2	0.017	28.6	0.140	76.1	0.303
18.9	0.023	29.2	0.149	99.0	0.279
19.7	0.030	31.6	0.176	129	0.248
20.5	0.041	35.0	0.207		
22.2	0.059	39.9	0.240		
23.6	0.074	44.6	0.266		

References for 6.4.5.1.8

85She1 Shemansky, D.E., Ajello, J.M., Hall, D.T.: Astrophys. J. **296** (1985) 765
86Kha1 Khakoo, M.A., Trajmar, S.: Phys. Rev. A **34** (1986) 146

6.4.5.2 Molecular nitrogen (N_2)

6.4.5.2.1a $J = 0 \rightarrow 2$

Integral cross sections for the $J = 0 \rightarrow 2$ rotational excitation process in N_2 were originally devised by [84Had1]. The validity of these cross sections and their agreement with the quadrupole Born approximation were recently reassessed by [97Rob1]. These swarm-derived ICS form the basis of our preferred integral cross section set, as tabulated in Table 6.4.9a and plotted in Fig. 6.4.9a. We also note the crossed beam study of [82Jun1] at the single electron energy of 2.47 eV ($\nu' = 0 \rightarrow 0$).

The uncertainty on the cross sections is estimated to be ± 10 %.

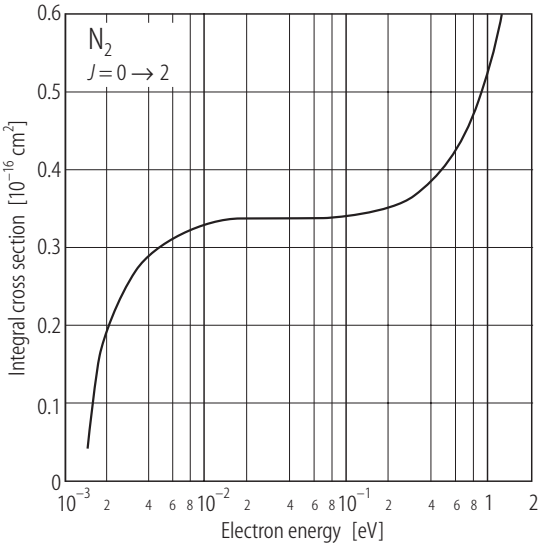

Fig. 6.4.9a. Recommended integral cross section for $J = 0 \rightarrow 2$ in N_2.

Table 6.4.9a. Preferred values of the integral $J = 0 \rightarrow 2$ rotational excitation cross section ($\sigma_{0\text{-}2}$) for electrons in molecular nitrogen.

Energy [eV]	$\sigma_{0\text{-}2}$ [Å^2]	Energy [eV]	$\sigma_{0\text{-}2}$ [Å^2]	Energy [eV]	$\sigma_{0\text{-}2}$ [Å^2]
0.0015	0.043	0.0070	0.319	0.120	0.342
0.0017	0.134	0.0080	0.324	0.140	0.344
0.0020	0.190	0.009	0.327	0.160	0.346
0.0025	0.236	0.010	0.329	0.200	0.351
0.0030	0.262	0.015	0.335	0.350	0.375
0.0035	0.278	0.020	0.337	0.550	0.415
0.0040	0.290	0.030	0.338	0.700	0.450
0.0045	0.298	0.040	0.338	0.800	0.475
0.0050	0.305	0.060	0.338	1.000	0.529
0.0055	0.309	0.080	0.339	1.250	0.608
0.0060	0.313	0.100	0.340		

References for 6.4.5.2.1a

82Jun1 Jung, K., Antoni, Th., Müller, R., Kochem, K-H., Ehrhardt, H.: J. Phys. B: At. Mol. Phys. **15** (1982) 3535

84Had1 Haddad, G.N.: Aust. J. Phys. **37** (1984) 487

97Rob1 Robertson, A.G., Elford, M.T., Crompton, R.W., Morrison, M.M., Sun, W., Trail, W.K.: Aust. J. Phys. **50** (1997) 441

6.4.5.2.1b $\nu' = 0 \rightarrow 1$

Integral cross sections for electron impact excitation of the first vibrational quantum ($\nu' = 0 \rightarrow 1$) in N_2 have been measured by [81Tan1, 86Soh1, 92Bre1, 95Sun1]. We have used all these data sets in constructing our preferred cross section, which is tabulated in Table 6.4.9b and plotted in Fig. 6.4.9b. Specifically, for $\varepsilon \leq 1$ eV we have employed the data of [86Soh1], for 1.5 eV $\leq \varepsilon \leq$ 5 eV we have used the integral cross sections of [92Bre1] and [95Sun1] and, finally, for 7.5 eV $\leq \varepsilon \leq$ 30 eV we have made use of the work of [81Tan1].

The uncertainties in the integral cross sections are estimated to be ± 30 % for $\varepsilon \leq 1$ eV, ± 25 % for 1.5 eV $\leq \varepsilon \leq$ 5 eV and ± 26 % for 7.5 eV $\leq \varepsilon \leq$ 30 eV.

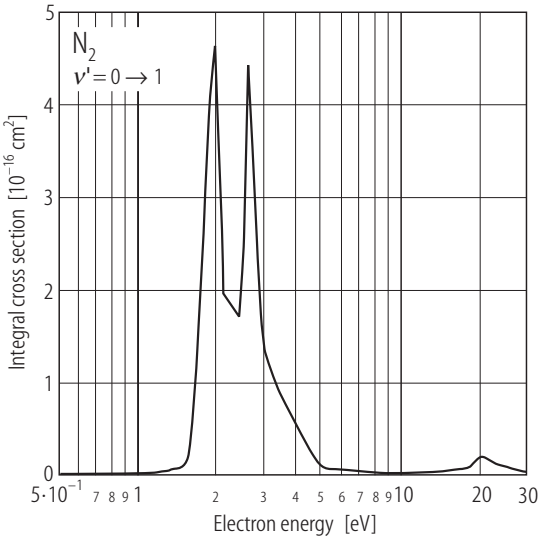

Fig. 6.4.9b. Recommended integral cross section for $\nu' = 0 \rightarrow 1$ in N_2.

Table 6.4.9b. Preferred values of the integral $\nu' = 0 \rightarrow 1$ vibrational excitation cross section ($\sigma_{0\text{-}1}$) for electrons in molecular nitrogen.

Energy [eV]	$\sigma_{0\text{-}1}$ [Å^2]	Energy [eV]	$\sigma_{0\text{-}1}$ [Å^2]	Energy [eV]	$\sigma_{0\text{-}1}$ [Å^2]
0.5	0.005	2.605	4.400	18	0.076
1.0	0.009	3.0	1.370	20	0.195
1.5	0.089	5.0	0.080	22.5	0.126
1.98	4.560	7.5	0.031	25	0.082
2.1	1.970	10	0.015	30	0.027
2.46	1.650	15	0.039		

References for 6.4.5.2.1b

81Tan1 Tanaka, H., Yamamoto, T., Okada, T.: J. Phys. B: At. Mol. Phys. **14** (1981) 2081

86Soh1 Sohn, W., Kochem, K-H., Scheuerlein, K-M., Jung, K., Ehrhardt, H.: J. Phys. B: At. Mol. Phys. **19** (1986) 4017

92Bre1 Brennan, M.J., Alle, D.T., Euripides, P., Buckman, S.J., Brunger, M.J.: J. Phys. B: At. Mol. Opt. Phys. **25** (1992) 2669

95Sun1 Sun, W., Morrison, M.A., Isaacs, W.A., Trail, W.K., Alle, D.T., Gulley, R.J., Brennan, M.J., Buckman, S.J.: Phys. Rev. A **52** (1995) 1229

6.4.5.2.2 $\nu' = 0 \rightarrow 2$

Integral cross sections for electron impact excitation of the second vibrational quantum ($\nu' = 0 \rightarrow 2$) in N_2 have only been reported by [92Bre1]. Furthermore, this data is only given for two energies (ε = 2.1 and 3.0 eV) in the region where the effects of the $^2\Pi_g$ resonance are important. Our preferred integral cross section is taken directly from the data of [92Bre1] and it is tabulated in Table 6.4.10.

The uncertainty in the preferred integral cross section is estimated to be ± 26 %.

Table 6.4.10. Preferred values of the integral $\nu' = 0 \rightarrow 2$ vibrational excitation cross section ($\sigma_{0\text{-}2}$) for electrons in molecular nitrogen.

Energy [eV]	$\sigma_{0\text{-}2}$ [Å^2]
2.1	1.32
3.0	0.90

References for 6.4.5.2.2

92Bre1 Brennan, M.J., Alle, D.T., Euripides, P., Buckman, S.J., Brunger, M.J.: J. Phys. B: At. Mol. Opt. Phys. **25** (1992) 2669

6.4.5.2.3 $\nu' = 0 \rightarrow 3$

Integral cross sections for electron impact excitation of the third vibrational quantum ($\nu' = 0 \rightarrow 3$) in N_2 have also only been reported by [92Bre1], and again only for two energies (ε = 2.1 and 3.0 eV). Our preferred integral cross section is thus taken directly from the data of [92Bre1] and it is tabulated in Table 6.4.11.

The uncertainty in the preferred integral cross section is estimated to be ± 27 %.

Table 6.4.11. Preferred values of the integral v' = 0 → 3 vibrational excitation cross section ($\sigma_{0\text{-}3}$) for electrons in molecular nitrogen.

Energy [eV]	$\sigma_{0\text{-}3}$ [Å^2]
2.1	0.34
3.0	0.26

References for 6.4.5.2.3

92Bre1 Brennan, M.J., Alle, D.T., Euripides, P., Buckman, S.J., Brunger, M.J.: J. Phys. B: At. Mol. Opt. Phys. **25** (1992) 2669

6.4.5.2.4 $X^1\Sigma_g^+ \rightarrow A^3\Sigma_u^+$

The electron impact excitation of the $A^3\Sigma_u^+$ electronic-state of molecular nitrogen ($X^1\Sigma_g^+ \rightarrow A^3\Sigma_u^+$) has been studied in crossed beam measurements by [77Car1] and [01Cam1]. The integral cross sections of [77Car1] were later renormalised by [83Tra1] and it is these latter cross sections that we consider here. The integral cross sections of [01Cam1] were derived from the original differential cross section data of [90Bru1] using a molecular phase shift analysis procedure from [91Boe1]. In addition there are several swarm-based derivations we could consider, with one of the more recent ones by [88Ohm1] being employed in our deliberations in constructing the preferred cross section set. Finally there are two calculations, an R-matrix type from [96Gil1] and a Z-matrix type from [99Huo1], which while not being in perfect agreement with one another, both indicate important near-threshold structure in the integral cross section. The calculations of [96Gil1] and [99Huo1] are both in good agreement with the data of [01Cam1] at the higher overlap energies of 15 eV and 17.5 eV and so we have, for $\varepsilon < 15$ eV, adopted the

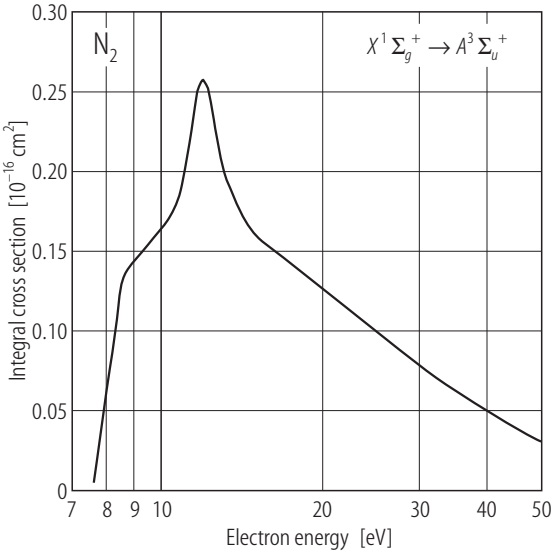

Fig. 6.4.10. Recommended integral cross section for $X^1\Sigma_g^+ \rightarrow A^3\Sigma_u^+$ in N_2.

calculation of [96Gil1] as our preferred cross section set. For $\varepsilon \geq 15$ eV we avoid any potential personal bias by performing a polynomial least squares fit to all the data of [83Tra1, 88Ohm1, 01Cam1] to determine our preferred integral cross section. This preferred cross section is tabulated in Table 6.4.12 and plotted in Fig. 6.4.10.

The uncertainties in the integral cross sections are estimated to be ± 40 % for $\varepsilon < 15$ eV and ± 35 % for 15 eV $\leq \varepsilon \leq$ 50 eV.

Table 6.4.12. Preferred values of the integral $X^1\Sigma_g^+ \rightarrow A^3\Sigma_u^+$ electronic-state excitation cross section ($\sigma_{X\text{-}A}$) for electrons in molecular nitrogen.

Energy [eV]	$\sigma_{X\text{-}A}$ [Å^2]	Energy [eV]	$\sigma_{X\text{-}A}$ [Å^2]	Energy [eV]	$\sigma_{X\text{-}A}$ [Å^2]
7.65	0.005	11.97	0.254	18.0	0.138
7.96	0.048	12.10	0.257	19.0	0.132
8.26	0.085	12.23	0.254	20.0	0.126
8.52	0.125	12.54	0.239	25.0	0.099
8.74	0.137	13.15	0.202	30.0	0.078
9.57	0.153	13.90	0.180	35.0	0.062
10.40	0.168	14.85	0.162	40.0	0.049
10.96	0.183	15.0	0.160	45.0	0.038
11.53	0.226	16.0	0.152	50.0	0.030
11.88	0.251	17.0	0.145		

References for 6.4.5.2.4

77Car1 Cartwright, D.C., Trajmar, S., Chutjian, A., Williams, W.: Phys. Rev. A **16** (1977) 1041
83Tra1 Trajmar, S., Register, D.F., Chutjian, A.: Phys. Rep. **97** (1983) 219
88Ohm1 Ohmori, Y., Shimozuma, M., Tagashira, H.: J. Phys. D: Appl. Phys. **21** (1988) 724
90Bru1 Brunger, M.J., Teubner, P.J.O.: Phys. Rev. A **41** (1990) 1413
91Boe1 Boesten, L., Tanaka, H.: J. Phys. B: At. Mol. Opt. Phys. **24** (1991) 821
96Gil1 Gillan, C.J., Tennyson, J., McLaughlin, B.M., Burke, P.G.: J. Phys. B: At. Mol. Opt. Phys. **29** (1996) 1531
99Huo1 Huo, W.M., Dateo, C.E.: Proc. 21st ICPEAC (1999) 294
01Cam1 Campbell, L., Cartwright, D.C., Harrison, J., Brunger, M.J., Teubner, P.J.O.: J. Phys. B: At. Mol. Opt. Phys. **34** (2001) 1185

6.4.5.2.5 $X^1\Sigma_g^+ \rightarrow B^3\Pi_g$

Integral cross sections for electron impact excitation of the $B^3\Pi_g$ electronic-state of molecular nitrogen ($X^1\Sigma_g^+ \rightarrow B^3\Pi_g$) have been reported by [77Car1, 83Tra1, 88Ohm1, 01Cam1] and an optical measurement by [69Sta1]. In addition, there is a R-matrix theory result from [96Gil1]. With the exception of the work of [77Car1], which was renormalised in [83Tra1], and the optical measurement of [69Sta1], which contained a significant cascade contribution, all of the above were considered when constructing our preferred $B^3\Pi_g$ cross section. Again, to avoid any possible bias, a polynomial least squares fit was made to the available integral cross section data in order to derive our preferred integral cross section. Note that the value of the integral cross section at threshold (7.353 eV) was assumed to be zero. Our preferred integral cross section is tabulated in Table 6.4.13 and plotted in Fig. 6.4.11.

The uncertainty in the integral cross section is estimated to be ± 35 % over the entire energy range considered.

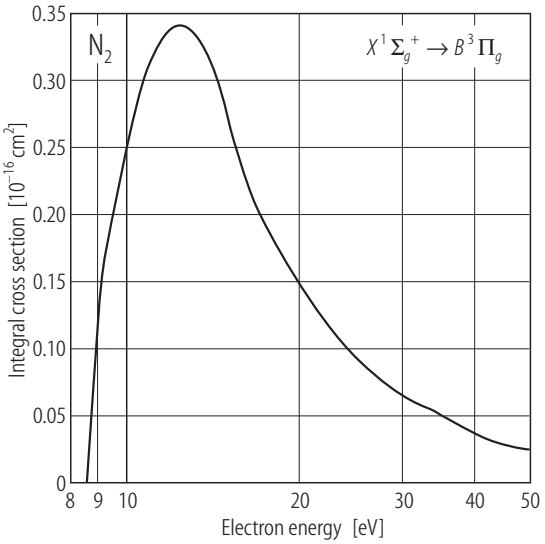

Fig. 6.4.11. Recommended integral cross section for $X^1\Sigma_g^+ \rightarrow B^3\Pi_g$ in N_2.

Table 6.4.13. Preferred values of the integral $X^1\Sigma_g^+ \rightarrow B^3\Pi_g$ electronic-state excitation cross section ($\sigma_{X\text{-}B}$) for electrons in molecular nitrogen.

Energy [eV]	$\sigma_{X\text{-}B}$ [Å^2]	Energy [eV]	$\sigma_{X\text{-}B}$ [Å^2]	Energy [eV]	$\sigma_{X\text{-}B}$ [Å^2]
8.55	0.002	13	0.333	20	0.144
9.0	0.141	13.5	0.323	25	0.092
9.5	0.202	14	0.308	30	0.064
10	0.250	14.5	0.290	35	0.049
10.5	0.287	15	0.270	40	0.036
11	0.313	16	0.224	45	0.028
11.5	0.330	17	0.199	50	0.023
12	0.338	18	0.177		
12.5	0.339	19	0.159		

References for 6.4.5.2.5

69Sta1 Stanton, P.N., St. John, R.M.: J. Opt. Soc. Am. **59** (1969) 252
77Car1 Cartwright, D.C., Trajmar, S., Chutjian, A., Williams, W.: Phys. Rev. A **16** (1977) 1041
83Tra1 Trajmar, S., Register, D.F., Chutjian, A.: Phys. Rep. **97** (1983) 219
88Ohm1 Ohmori, Y., Shimozuma, M., Tagashira, H.: J. Phys. D: Appl. Phys. **21** (1988) 724
96Gil1 Gillan, C.J., Tennyson, J., McLaughlin, B.M., Burke, P.G.: J. Phys. B: At. Mol. Opt. Phys. **29** (1996) 1531
01Cam1 Campbell, L., Cartwright, D.C., Harrison, J., Brunger, M.J., Teubner, P.J.O.: J. Phys. B: At. Mol. Opt. Phys. **34** (2001) 1185

6.4.5.2.6 $X^1\Sigma_g^+ \rightarrow W^3\Delta_u$

The electron impact excitation of the $W^3\Delta_u$ electronic-state of molecular nitrogen ($X^1\Sigma_g^+ \rightarrow W^3\Delta_u$) has been studied in crossed beam measurements by [77Car1] and [01Cam1]. The integral cross sections of [77Car1] were later renormalised by [83Tra1] and it is these latter cross sections that we consider here. Note that the cross sections in [01Cam1] were derived from the original differential cross section measurements of [90Bru1]. There are also several swarm-based cross sections we could consider, with the one from [88Ohm1] being employed in our deliverations in constructing the preferred cross section set. Finally there is an R-matrix calculation from [96Gil1] which, being in excellent agreement with [01Cam1] at ε = 15 and 17.5 eV, we have used to aid us in constructing the near-threshold behaviour of the $W^3\Delta_u$ integral cross section. Our preferred cross section is tabulated in Table 6.4.14 and plotted in Fig. 6.4.12. Note that once again, to avoid any possible potential bias, for $\varepsilon \geq 15$ eV we have used a polynomial least squares fit to the available data to determine our preferred integral cross section.

The uncertainty in the integral cross section is estimated to be ± 35 % over the entire energy range considered.

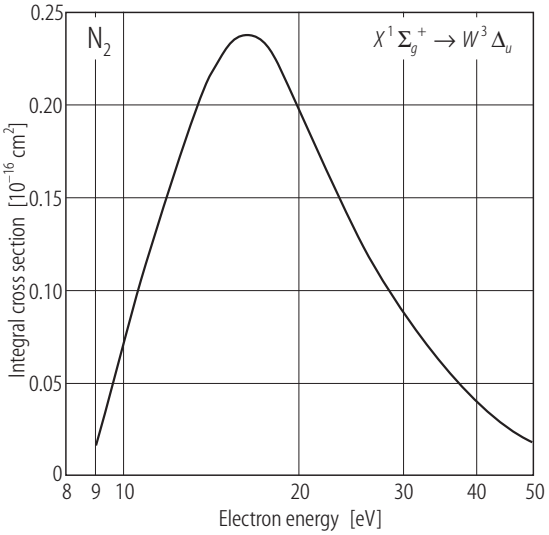

Fig. 6.4.12. Recommended integral cross section for $X^1\Sigma_g^+ \rightarrow W^3\Delta_u$ in N_2.

Table 6.4.14. Preferred values of the integral $X^1\Sigma_g^+ \rightarrow W^3\Delta_u$ electronic-state excitation cross section ($\sigma_{X\text{-}W}$) for electrons in molecular nitrogen.

Energy [eV]	$\sigma_{X\text{-}W}$ [Å^2]	Energy [eV]	$\sigma_{X\text{-}W}$ [Å^2]	Energy [eV]	$\sigma_{X\text{-}W}$ [Å^2]
9	0.017	13.5	0.205	20	0.194
9.5	0.045	14	0.216	25	0.131
10	0.072	14.5	0.224	30	0.088
10.5	0.096	15	0.231	35	0.059
11	0.119	16	0.238	40	0.040
11.5	0.140	16.5	0.238	45	0.027
12	0.159	17	0.236	50	0.018
12.5	0.176	18	0.227		
13	0.191	19	0.209		

References for 6.4.5.2.6

77Car1 Cartwright, D.C., Trajmar, S., Chutjian, A., Williams, W.: Phys. Rev. A **16** (1977) 1041
83Tra1 Trajmar, S., Register, D.F., Chutjian, A.: Phys. Rep. **97** (1983) 219
88Ohm1 Ohmori, Y., Shimozuma, M., Tagashira, H.: J. Phys. D: Appl. Phys. **21** (1988) 724
90Bru1 Brunger, M.J., Teubner, P.J.O.: Phys. Rev. A **41** (1990) 1413
96Gil1 Gillan, C.J., Tennyson, J., McLaughlin, B.M., Burke, P.G.: J. Phys. B: At. Mol. Opt. Phys. **29** (1996) 1531
01Cam1 Campbell, L., Cartwright, D.C., Harrison, J., Brunger, M.J., Teubner, P.J.O.: J. Phys. B: At. Mol. Opt. Phys. **34** (2001) 1185

6.4.5.2.7 $X^1\Sigma_g^+ \rightarrow B'^3\Sigma_u^-$

Integral cross sections for electron impact excitation of the $B'^3\Sigma_u^-$ electronic-state of molecular nitrogen ($X^1\Sigma_g^+ \rightarrow B'^3\Sigma_u^-$) have been reported by [77Car1, 83Tra1, 88Ohm1, 01Cam1]. In addition, there is an R-matrix theory result from [96Gil1]. With the exception of the work of [77Car1], which was renormalised by [83Tra1], all of the above were considered when constructing our preferred $B'^3\Sigma_u^-$ cross section. To avoid any possible bias, a polynomial least squares fit was made to the available integral cross section data in order to derive our preferred integral cross section. Our preferred cross section is tabulated in Table 6.4.15 and plotted in Fig. 6.4.13.

The uncertainty in the integral cross section is estimated to be ± 40 % over the entire energy range considered.

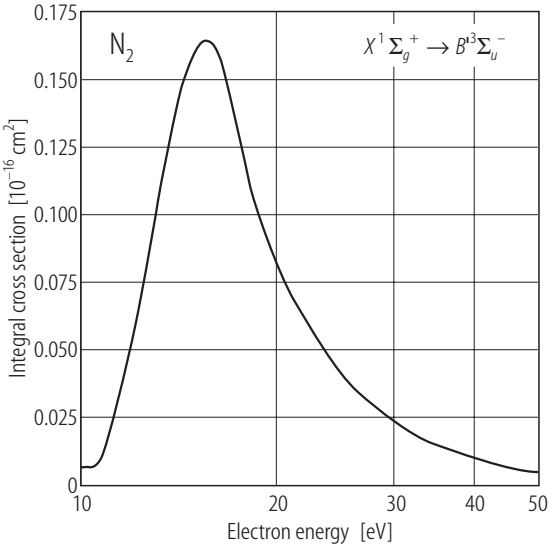

Fig. 6.4.13. Recommended integral cross section for $X^1\Sigma_g^+ \rightarrow B'^3\Sigma_u^-$ in N_2.

Table 6.4.15. Preferred values of the integral $X^1\Sigma_g^+ \rightarrow B'^3\Sigma_u^-$ electronic-state excitation cross section ($\sigma_{X\text{-}B'}$) for electrons in molecular nitrogen.

Energy [eV]	$\sigma_{X\text{-}B'}$ [Å^2]	Energy [eV]	$\sigma_{X\text{-}B'}$ [Å^2]	Energy [eV]	$\sigma_{X\text{-}B'}$ [Å^2]
10	0.007	14.5	0.155	19	0.093
10.5	0.008	15	0.163	19.5	0.086
11	0.019	15.5	0.165	20	0.080
11.5	0.037	16	0.162	25	0.041
12	0.058	16.5	0.153	30	0.024
12.5	0.082	17	0.140	35	0.015
13	0.105	17.5	0.124	40	0.010
13.5	0.125	18	0.110	45	0.007
14	0.143	18.5	0.101	50	0.005

References for 6.4.5.2.7

77Car1 Cartwright, D.C., Trajmar, S., Chutjian, A., Williams, W.: Phys. Rev. A **16** (1977) 1041
83Tra1 Trajmar, S., Register, D.F., Chutjian, A.: Phys. Rep. **97** (1983) 219
88Ohm1 Ohmori, Y., Shimozuma, M., Tagashira, H.: J. Phys. D: Appl. Phys. **21** (1988) 724
96Gil1 Gillan, C.J., Tennyson, J., McLaughlin, B.M., Burke, P.G.: J. Phys. B: At. Mol. Opt. Phys. **29** (1996) 1531
01Cam1 Campbell, L., Cartwright, D.C., Harrison, J., Brunger, M.J., Teubner, P.J.O.: J. Phys. B: At. Mol. Opt. Phys. **34** (2001) 1185

6.4.5.2.8 $X^1\Sigma_g^+ \rightarrow a'^1\Sigma_u^-$

There is a very good level of agreement between all the reported integral cross sections for electron impact excitation of the $a'^1\Sigma_u^-$ electronic-state of molecular nitrogen ($X^1\Sigma_g^+ \rightarrow a'^1\Sigma_u^-$). This work is due to [83Tra1, 88Ohm1, 01Cam1]. Nonetheless, a polynomial least squares fit was still made to the available data in order to derive our preferred integral $a'^1\Sigma_u^-$ cross section. This cross section is tabulated in Table 6.4.16 and plotted in Fig. 6.4.14. Note that the value of the integral cross section at threshold (8.398 eV) was assumed to be zero.

The uncertainty in the integral cross section is estimated to be ± 30 % over the entire energy range considered.

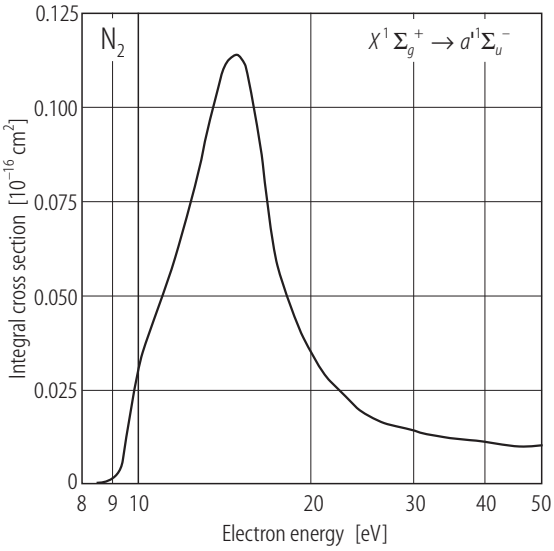

Fig. 6.4.14. Recommended integral cross section for $X^1\Sigma_g^+ \rightarrow a'^1\Sigma_u^-$ in N_2.

Table 6.4.16. Preferred values of the integral $X^1\Sigma_g^+ \rightarrow a'^1\Sigma_u^-$ electronic-state excitation cross section ($\sigma_{X\text{-}a'}$) for electrons in molecular nitrogen.

Energy [eV]	$\sigma_{X\text{-}a'}$ [Å^2]	Energy [eV]	$\sigma_{X\text{-}a'}$ [Å^2]	Energy [eV]	$\sigma_{X\text{-}a'}$ [Å^2]
8.4	0.000	13.5	0.101	18.5	0.045
9.4	0.006	14	0.110	19	0.041
9.5	0.011	14.5	0.113	20	0.034
10	0.031	15	0.113	25	0.018
10.5	0.042	15.5	0.107	30	0.014
11	0.051	16	0.095	35	0.012
11.5	0.059	16.5	0.079	40	0.011
12	0.069	17	0.063	45	0.010
12.5	0.080	17.5	0.056	50	0.010
13	0.091	18	0.050		

References for 6.4.5.2.8

83Tra1 Trajmar, S., Register, D.F., Chutjian, A.: Phys. Rep. **97** (1983) 219
88Ohm1 Ohmori, Y., Shimozuma, M., Tagashira, H.: J. Phys. D: Appl. Phys. **21** (1988) 724
01Cam1 Campbell, L., Cartwright, D.C., Harrison, J., Brunger, M.J., Teubner, P.J.O.: J. Phys. B: At. Mol. Opt. Phys.**34** (2001) 1185

6.4.5.2.9 $X^1\Sigma_g^+ \rightarrow a^1\Pi_g$

The electron impact excitation of the $a^1\Pi_g$ electronic-state of molecular nitrogen ($X^1\Sigma_g^+ \rightarrow a^1\Pi_g$) has been studied in detail by the crossed beam measurements of [77Car1, 76Fin1, 83Tra1, 87Mas1, 01Cam1]. We also note the swarm-based determination from [88Ohm1]. With the exception of the work of [77Car1], which was renormalised by [83Tra1], all of the above integral cross section determinations were considered by us in constructing our preferred cross section set. As before, we avoid any possible bias by employing a polynomial least squares fit to the available data to determine our preferred integral cross section. This cross section is tabulated in Table 6.4.17 and plotted in Fig. 6.4.15.

The uncertainty in the integral cross section is estimated to be ± 25 % over the entire energy range considered.

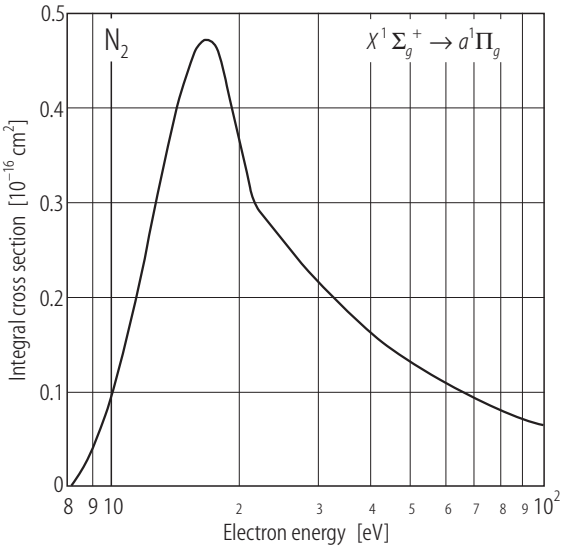

Fig. 6.4.15. Recommended integral cross section for $X^1\Sigma_g^+ \rightarrow a^1\Pi_g$ in N_2.

Table 6.4.17. Preferred values of the integral $X^1\Sigma_g^+ \rightarrow a^1\Pi_g$ electronic-state excitation cross section ($\sigma_{X\text{-}a}$) for electrons in molecular nitrogen.

Energy [eV]	$\sigma_{X\text{-}a}$ [Å^2]	Energy [eV]	$\sigma_{X\text{-}a}$ [Å^2]	Energy [eV]	$\sigma_{X\text{-}a}$ [Å^2]
8	0.001	15.5	0.459	35	0.185
8.5	0.016	16	0.469	40	0.161
9	0.038	16.5	0.473	45	0.144
9.5	0.066	17	0.471	50	0.129
10	0.099	17.5	0.462	60	0.108
11	0.174	18	0.446	70	0.092
12	0.254	19	0.394	80	0.081
13	0.329	21.5	0.300	90	0.072
14	0.394	25	0.258	100	0.065
15	0.443	30	0.215		

References for 6.4.5.2.9

76Fin1 Finn, T.G., Doering, J.P.: J. Chem. Phys. **64** (1976) 4490
77Car1 Cartwright, D.C., Trajmar, S., Chutjian, A., Williams, W.: Phys. Rev. A **16** (1977) 1041
83Tra1 Trajmar, S., Register, D.F., Chutjian, A.: Phys. Rep. **97** (1983) 219
87Mas1 Mason, N.J., Newell, W.R.: J. Phys. B **20** (1987) 3913
88Ohm1 Ohmori, Y., Shimozuma, M., Tagashira, H.: J. Phys. D: Appl. Phys. **21** (1988) 724
01Cam1 Campbell, L., Cartwright, D.C., Harrison, J., Brunger, M.J., Teubner, P.J.O.: J. Phys. B: At. Mol. Opt. Phys. **34** (2001) 1185

6.4.5.2.10 $X^1\Sigma_g^+ \rightarrow w^1\Delta_u$

There is a very good level of agreement between all the available integral cross sections for electron impact excitation of the $w^1\Delta_u$ electronic-state of molecular nitrogen ($X^1\Sigma_g^+ \rightarrow w^1\Delta_u$). Specifically we refer to the work of [83Tra1, 88Ohm1, 01Cam1]. A polynomial least squares fit to this data is again used to construct our preferred integral cross section, which is tabulated in Table 6.4.18 and plotted in Fig. 6.4.16.

The uncertainty in the integral cross section is estimated to be ± 30 % over the entire energy range considered.

Table 6.4.18. Preferred values of the integral $X^1\Sigma_g^+ \rightarrow w^1\Delta_u$ electronic-state excitation cross section ($\sigma_{X\text{-}w}$) for electrons in molecular nitrogen.

Energy [eV]	$\sigma_{X\text{-}w}$ [Å^2]	Energy [eV]	$\sigma_{X\text{-}w}$ [Å^2]	Energy [eV]	$\sigma_{X\text{-}w}$ [Å^2]
8.9	0.0001	13.0	0.105	19.0	0.044
9.0	0.002	13.5	0.105	20.0	0.040
9.5	0.024	14.0	0.103	25.0	0.026
10.0	0.043	14.5	0.099	30.0	0.018
10.5	0.061	15.0	0.093	35.0	0.013
11.0	0.076	15.5	0.086	40.0	0.010
11.5	0.088	16.0	0.078	45.0	0.008
12.0	0.096	17.0	0.062	50.0	0.006
12.5	0.102	18.0	0.049		

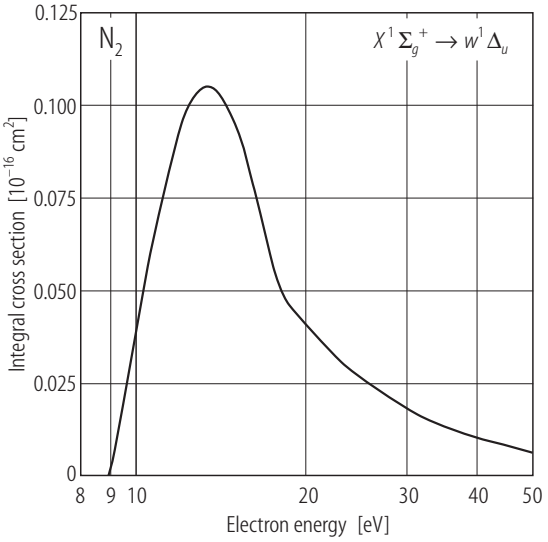

Fig. 6.4.16. Recommended integral cross section for $X^1\Sigma_g^+ \rightarrow w^1\Delta_u$ in N_2.

References for 6.4.5.2.10

83Tra1 Trajmar, S., Register, D.F., Chutjian, A.: Phys. Rep. **97** (1983) 219

88Ohm1 Ohmori, Y., Shimozuma, M., Tagashira, H.: J. Phys. D: Appl. Phys. **21** (1988) 724

01Cam1 Campbell, L., Cartwright, D.C., Harrison, J., Brunger, M.J., Teubner, P.J.O.: J. Phys. B: At. Mol. Opt. Phys. **34** (2001) 1185

6.4.5.2.11 $X^1\Sigma_g^+ \rightarrow C^3\Pi_u$

Integral cross sections for electron impact excitation of the $C^3\Pi_u$ electronic-state of molecular nitrogen ($X^1\Sigma_g^+ \rightarrow C^3\Pi_u$) have been reported by [77Car1, 83Tra1, 88Ohm1 94Zub1, 99Pop1, 01Cam1]. With the exception of the work of [77Car1], which was renormalised by [83Tra1], all of the above were considered when constructing our preferred $C^3\Pi_u$ cross section. This is particularly the case for $\varepsilon \geq 20$ eV where [83Tra1, 94Zub1, 01Cam1] are all in good accord with one another. On the other hand, for $\varepsilon < 20$ eV the data of [94Zub1, 99Pop1, 01Cam1] are in better agreement with one another than with [83Tra1]. Consequently for $\varepsilon < 20$ eV only the data of [94Zub1, 99Pop1, 01Cam1] were employed in our polynomial least squares fit procedure. Indeed we note that for $\varepsilon < 15$ eV the preferred integral cross section was essentially constructed entirely from the recent measurement of [99Pop1]. Our preferred integral cross section is tabulated in Table 6.4.19 and plotted in Fig. 6.4.17.

The uncertainty in the integral cross section is estimated to be ± 30 % over the entire energy range considered.

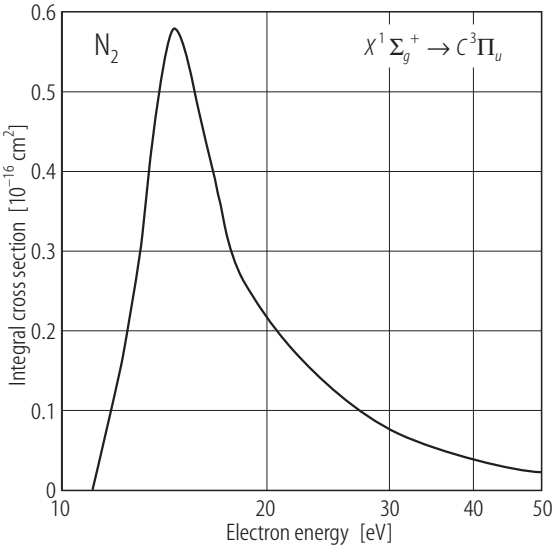

Fig. 6.4.17. Recommended integral cross section for $X^1\Sigma_g^+ \rightarrow C^3\Pi_u$ in N_2.

Table 6.4.19. Preferred values of the integral $X^1\Sigma_g^+ \rightarrow C^3\Pi_u$ electronic-state excitation cross section ($\sigma_{X\text{-}C}$) for electrons in molecular nitrogen.

Energy [eV]	$\sigma_{X\text{-}C}$ [Å^2]	Energy [eV]	$\sigma_{X\text{-}C}$ [Å^2]	Energy [eV]	$\sigma_{X\text{-}C}$ [Å^2]
11.0	0.001	15.7	0.478	20.0	0.212
11.5	0.074	16.0	0.447	25.0	0.122
12.0	0.147	16.5	0.403	30.0	0.077
12.5	0.229	17.0	0.353	35.0	0.052
13.0	0.335	17.5	0.302	40.0	0.038
13.5	0.455	18.0	0.276	45.0	0.028
14.0	0.551	18.5	0.258	50.0	0.022
14.5	0.583	19.0	0.242		
15.0	0.551	19.5	0.226		

References for 6.4.5.2.11

77Car1 Cartwright, D.C., Trajmar, S., Chutjian, A., Williams, W.: Phys. Rev. A **16** (1977) 1041
83Tra1 Trajmar, S., Register, D.F., Chutjian, A.: Phys. Rep. **97** (1983) 219
88Ohm1 Ohmori, Y., Shimozuma, M., Tagashira, H.: J. Phys. D: Appl. Phys. **21** (1988) 724
94Zub1 Zubek, M., King, G.C.: J. Phys. B: At. Mol. Opt. Phys. **27** (1994) 2613
99Pop1 Poparic, G., Vicic, M., Belic, D.S.: Chem. Phys. **240** (1999) 283
01Cam1 Campbell, L., Cartwright, D.C., Harrison, J., Brunger, M.J., Teubner, P.J.O.: J. Phys. B: At. Mol. Opt. Phys. **34** (2001) 1185

6.4.5.2.12 $X^1\Sigma_g^+ \rightarrow E^3\Sigma_g^+$

For $\varepsilon \geq 15$ eV there is a quite good level of agreement between the crossed-beam measurements of [83Tra1, 94Zub1, 01Cam1], for electron impact excitation of the $E^3\Sigma_g^+$ electronic-state of molecular nitrogen ($X^1\Sigma_g^+ \rightarrow E^3\Sigma_g^+$). Consequently a polynomial least squares fit was made to all this data in order, for $\varepsilon \geq 15$ eV, to derive our preferred $E^3\Sigma_g^+$ integral cross section. Near-threshold, however, there had been a serious discrepancy between [72Bor1] and [88Bru1] as to the magnitude and position of the resonance-enhanced cross section. This discrepancy was recently resolved by [99Pop2] in favour of [88Bru1]. Thus the near-threshold behaviour of our preferred integral cross section was constructed from [88Bru1] and [99Pop2]. Our preferred integral cross section is tabulated in Table 6.4.20 and plotted in Fig. 6.4.18.

The uncertainty in the integral cross section is estimated to be ± 40 % over the entire energy range considered.

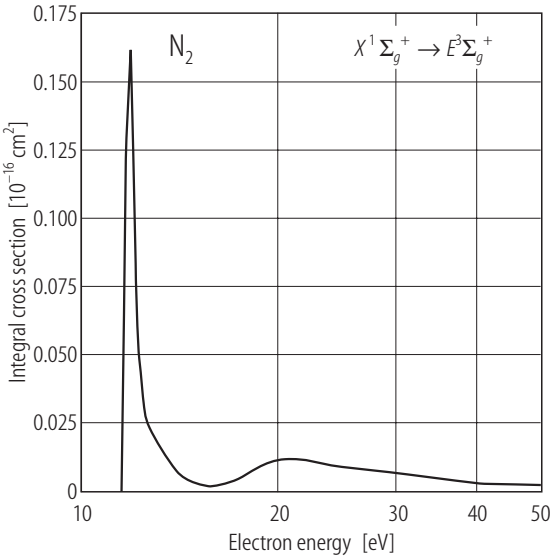

Fig. 6.4.18. Recommended integral cross section for $X^1\Sigma_g^+ \rightarrow E^3\Sigma_g^+$ in N_2.

Table 6.4.20. Preferred values of the integral $X^1\Sigma_g^+ \rightarrow E^3\Sigma_g^+$ electronic-state excitation cross section ($\sigma_{X\text{-}E}$) for electrons in molecular nitrogen.

Energy [eV]	$\sigma_{X\text{-}E}$ [Å^2]	Energy [eV]	$\sigma_{X\text{-}E}$ [Å^2]	Energy [eV]	$\sigma_{X\text{-}E}$ [Å^2]
11.5	0.000	15.0	0.003	25.0	0.009
11.9	0.148	16.0	0.002	30.0	0.007
11.95	0.120	17.0	0.004	35.0	0.005
12.0	0.095	18.0	0.007	40.0	0.003
12.5	0.029	19.0	0.010	45.0	0.0025
13.0	0.020	20.0	0.012	50.0	0.0018
14.0	0.008	21.0	0.012		

References for 6.4.5.2.12

72Bor1 Borst, W.L., Wells, W.C., Zipf, E.: Phys. Rev. A **5** (1972) 1744
83Tra1 Trajmar, S., Register, D.F., Chutjian, A.: Phys. Rep. **97** (1983) 219
88Bru1 Brunger, M.J., Teubner, P.J.O., Buckman, S.J.: Phys. Rev. A **37** (1988) 3570
88Ohm1 Ohmori, Y., Shimozuma, M., Tagashira, H.: J. Phys. D: Appl. Phys. **21** (1988) 724
94Zub1 Zubek, M., King, G.C.: J. Phys. B: At. Mol. Opt. Phys. **27** (1994) 2613
99Pop2 Poparic, G., Vicic, M., Belic, D.S.: Phys. Rev. A **60** (1999) 4542
01Cam1 Campbell, L., Cartwright, D.C., Harrison, J., Brunger, M.J., Teubner, P.J.O.: J. Phys. B: At. Mol. Opt. Phys. **34** (2001) 1185

6.4.5.2.13 $X^1\Sigma_g^+ \rightarrow a''^1\Sigma_g^+$

Integral cross sections for electron impact excitation of the $a''^1\Sigma_g^+$ electronic-state in N_2 ($X^1\Sigma_g^+ \rightarrow a''^1\Sigma_g^+$) have been reported by [83Tra1, 88Ohm1, 01Cam1]. The crossed-beam data of [83Tra1] and [01Cam1] are generally in good agreement with each other, although both are somewhat stronger in magnitude than the swarm-derived result from [88Ohm1]. We have employed a least squares polynomial fit to the integral cross sections of [83Tra1] and [01Cam1] in order to derive our preferred $a''^1\Sigma_g^+$ cross section, with the result being tabulated in Table 6.4.21 and plotted in Fig. 6.4.19.

The uncertainty in the integral cross section is estimated to be ± 33 % over the entire energy range considered.

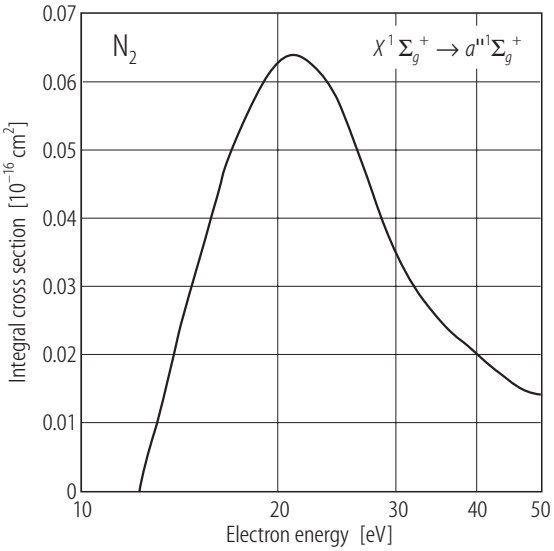

Fig. 6.4.19. Recommended integral cross section for $X^1\Sigma_g^+ \rightarrow a''^1\Sigma_g^+$ in N_2.

Table 6.4.21. Preferred values of the integral $X^1\Sigma_g^+ \rightarrow a''^1\Sigma_g^+$ electronic-state excitation cross section ($\sigma_{X\text{-}a''}$) for electrons in molecular nitrogen.

Energy [eV]	$\sigma_{X\text{-}a''}$ [Å^2]	Energy [eV]	$\sigma_{X\text{-}a''}$ [Å^2]
12.25	0.000	22.0	0.063
13.0	0.009	23.0	0.062
14.0	0.022	24.0	0.059
15.0	0.033	25.0	0.055
16.0	0.042	27.5	0.044
17.0	0.050	30.0	0.035
18.0	0.056	35.0	0.025
19.0	0.060	40.0	0.020
20.0	0.063	45.0	0.016
21.0	0.064	50.0	0.014

References for 6.4.5.2.13

83Tra1 Trajmar, S., Register, D.F., Chutjian, A.: Phys. Rep. **97** (1983) 219
88Ohm1 Ohmori, Y., Shimozuma, M., Tagashira, H.: J. Phys. D: Appl. Phys. **21** (1988) 724
01Cam1 Campbell, L., Cartwright, D.C., Harrison, J., Brunger, M.J., Teubner, P.J.O.: J. Phys. B: At. Mol. Opt. Phys. **34** (2001) 1185

6.4.5.3 Oxygen (O_2)

6.4.5.3.1 $\nu' = 0 \rightarrow 1$

There are two integral cross section measurements for $\nu' = 0 \rightarrow 1$ rovibrational excitation in O_2 available in the literature. They are due to [93Shy1], at 5, 7, 10 and 15 eV, and [96Nob1] at 10 energies in the range 5 eV to 20 eV. The agreement between these two measurements, in terms of the magnitude of the ICS at common energies, is generally fair. Consequently, we have constructed our preferred set from the more extensive measurements of [96Nob1]. These data are tabulated in Table 6.4.22 and plotted in Fig. 6.4.20.

The uncertainty in the integral cross section is estimated to be ± 20 % over the entire range of electron energies.

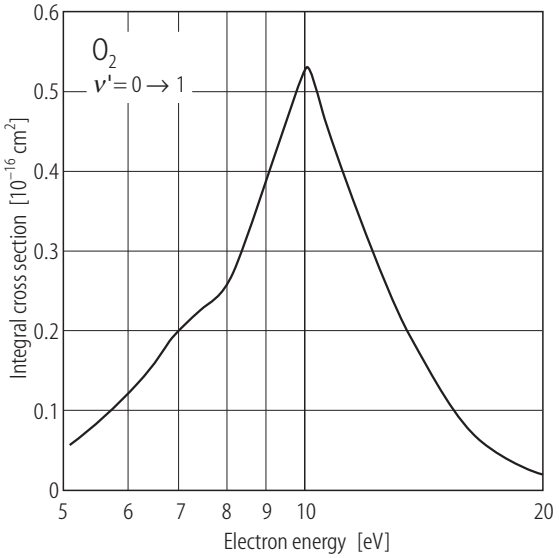

Fig. 6.4.20. Recommended integral cross section for $\nu' = 0 \rightarrow 1$ in O_2.

Table 6.4.22. Preferred values of the integral $\nu' = 0 \rightarrow 1$ vibrational excitation cross section ($\sigma_{0\text{-}1}$) for electrons in molecular oxygen.

Energy [eV]	$\sigma_{0\text{-}1}$ [Å^2]	Energy [eV]	$\sigma_{0\text{-}1}$ [Å^2]
5	0.052	9.5	0.464
6	0.116	10	0.536
7	0.202	11	0.406
8	0.256	15	0.116
9	0.403	20	0.018

References for 6.4.5.3.1

93Shy1 Shyn, T.W., Sweeney, C.J.: Phys. Rev. A **48** (1993) 1214
96Nob1 Noble, C.J., Higgins, K., Wöste, G., Duddy, P., Burke, P.G., Teubner, P.J.O., Middleton, A.G., Brunger, M.J.: Phys. Rev. Lett. **76** (1996) 3534

6.4.5.3.2 $\nu' = 0 \rightarrow 2$

The available integral cross section measurements for $\nu' = 0 \rightarrow 2$ rovibrational excitation in O_2 are again due to [93Shy1] and [96Nob1]. In this case the ICS of [96Nob1] were measured at eight energies in the range 6 - 15 eV, while [93Shy1] reported data at 5 eV, 7 eV, 10 eV, 15 eV. Agreement between the two measurements is not so good in this case, the R-matrix calculation of [96Nob1] indicating their data has the more physical shape. Thus we have constructed our preferred set (see Table 6.4.23 and Fig. 6.4.21) from the measurements of [96Nob1].

The uncertainty in the integral cross section is estimated to be ± 22 % over the entire range of electron energies.

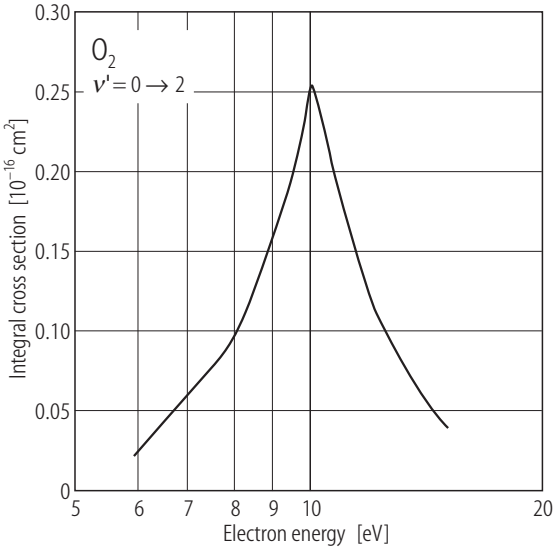

Fig. 6.4.21. Recommended integral cross section for $\nu' = 0 \rightarrow 2$ in O_2.

Table 6.4.23. Preferred values of the integral $\nu' = 0 \rightarrow 2$ vibrational excitation cross section ($\sigma_{0\text{-}2}$) for electrons in molecular oxygen.

Energy [eV]	$\sigma_{0\text{-}2}$ [Å^2]
6	0.023
7	0.060
8	0.096
9	0.163
9.5	0.201
10	0.255
11	0.175
15	0.039

References for 6.4.5.3.2

93Shy1 Shyn, T.W., Sweeney, C.J.: Phys. Rev. A **48** (1993) 1214

96Nob1 Noble, C.J., Higgins, K., Wöste, G., Duddy, P., Burke, P.G., Teubner, P.J.O., Middleton, A.G., Brunger, M.J.: Phys. Rev. Lett. **76** (1996) 3534

6.4.5.3.3 $\nu' = 0 \rightarrow 3$

The integral cross section measurements for $\nu' = 0 \rightarrow 3$ rovibrational excitation in O_2 are due to [93Shy1] and [96Nob1] and both are restricted to the energy range 7 - 15 eV. In this case [93Shy1] and [96Nob1] are in fair agreement with one another and so we have used the more comprehensive data base of [96Nob1] to construct our preferred integral cross section set. These data are tabulated in Table 6.4.24 and plotted in Fig. 6.4.22.

The uncertainty in the integral cross section is estimated to be ± 24 % over the entire range of electron energies.

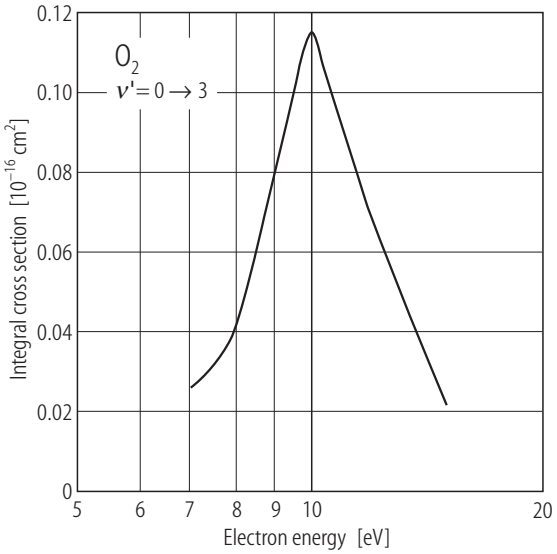

Fig. 6.4.22. Recommended integral cross section for $\nu' = 0 \rightarrow 3$ in O_2.

Table 6.4.24. Preferred values of the integral $\nu' = 0 \rightarrow 3$ vibrational excitation cross section ($\sigma_{0\text{-}3}$) for electrons in molecular oxygen.

Energy [eV]	$\sigma_{0\text{-}3}$ [Å^2]
7	0.026
8	0.041
9	0.081
9.5	0.101
10	0.115
11	0.090
15	0.022

References for 6.4.5.3.3

93Shy1 Shyn, T.W., Sweeney, C.J.: Phys. Rev. A **48** (1993) 1214
96Nob1 Noble, C.J., Higgins, K., Wöste, G., Duddy, P., Burke, P.G., Teubner, P.J.O., Middleton, A.G., Brunger, M.J.: Phys. Rev. Lett. **76** (1996) 3534

6.4.5.3.4 $\nu' = 0 \rightarrow 4$

Our preferred integral cross section set for $\nu' = 0 \rightarrow 4$ rovibrational excitation in O_2 is taken from [96Nob1]. These data are tabulated in Table 6.4.25 and plotted in Fig. 6.4.23.

The uncertainty in the integral cross section is estimated to be ± 26 % over the entire range of electron energies.

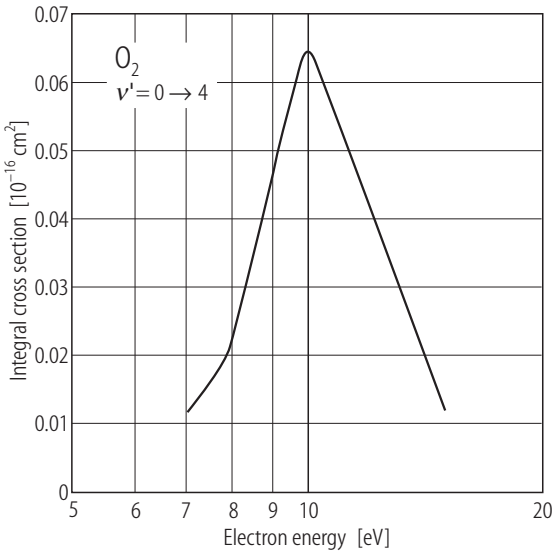

Fig. 6.4.23. Recommended integral cross section for $\nu' = 0 \rightarrow 4$ in O_2.

Table 6.4.25. Preferred values of the integral $\nu' = 0 \rightarrow 4$ vibrational excitation cross section ($\sigma_{0\text{-}4}$) for electrons in molecular oxygen.

Energy [eV]	$\sigma_{0\text{-}4}$ [Å^2]
7	0.012
8	0.023
9	0.047
9.5	0.058
10	0.065
11	0.053
15	0.012

References for 6.4.5.3.4

96Nob1 Noble, C.J., Higgins, K., Wöste, G., Duddy, P., Burke, P.G., Teubner, P.J.O., Middleton, A.G., Brunger, M.J.: Phys. Rev. Lett. 76 (1996) 3534

6.4.5.3.5 $X^3\Sigma_g^- \rightarrow a^1\Delta_g$

Experimental integral cross sections for electron impact excitation of the $a^1\Delta_g$ electronic state of O_2 have been reported by many groups. These include [71Lin2, 71Traj1, 70Kon1, 78Wak1, 92Doe1, 93Shy2, 92Mid1]. Away from the characteristic $^2\Pi_u$ resonance the data of [71Traj1] and [92Mid1] are in quite good agreement, although their agreement with the other measurements is "patchy". This observation is, at least in part, reflected in the uncertainty estimates we provide for our preferred integral cross section set. At and near resonance only the data of [92Mid1] provides a fine enough energy grid for the structure to be observed. Consequently our preferred integral cross section set for 5 eV < $\varepsilon \leq$ 20 eV is largely drawn from the work of [92Mid1]. Below 5 eV our preferred cross section, given the limited availability of experimental data, is taken from the reliable R-matrix calculation of [92Nob1]. The recommended integral cross section for $X^3\Sigma_g^- \rightarrow a^1\Delta_g$ is tabulated in Table 6.4.26 and plotted in Fig. 6.4.24.

The uncertainty in the integral cross section is estimated to be ± 30 % for ε < 5 eV and ± 28 % for 5 eV ≤ $\varepsilon \leq$ 20 eV.

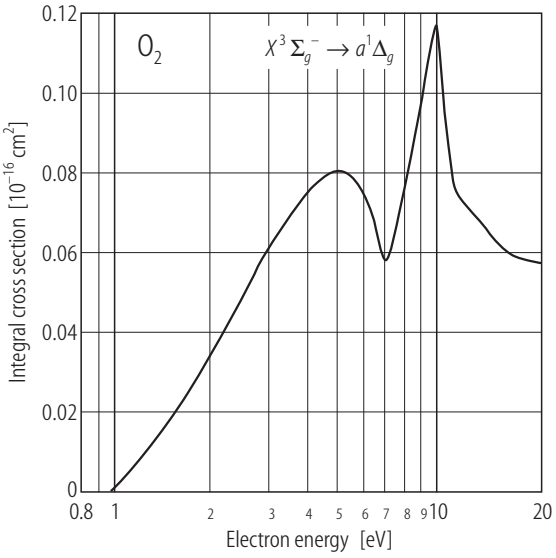

Fig. 6.4.24. Recommended integral cross section for $X^3\Sigma_g^- \rightarrow a^1\Delta_g$ in O_2.

Table 6.4.26. Preferred values of the integral $X^3\Sigma_g^- \rightarrow a^1\Delta_g$ electronic-state excitation cross section ($\sigma_{X\text{-}a}$) for electrons in molecular oxygen.

Energy [eV]	$\sigma_{X\text{-}a}$ [Å^2]	Energy [eV]	$\sigma_{X\text{-}a}$ [Å^2]
0.98	0.000	8	0.078
2	0.034	9	0.098
3	0.061	9.5	0.111
4	0.075	10	0.117
5	0.080	11	0.081
6	0.073	15	0.063
7	0.057	20	0.057

References for 6.4.5.3.5

70Kon1 Konishi, A., Wakiya, K., Yamamoto, M., Suzuki, H.: J. Phys. Soc. Jpn. **29** (1970) 526
71Lin2 Linder, F., Schmidt, H.: Z. Naturforsch. A **26** (1971) 1617
71Traj1 Trajmar, S., Cartwright, D.C., Williams, W.: Phys. Rev. A **4** (1971) 1482
78Wak1 Wakiya, K.: J. Phys. B: At. Mol. Phys. **11** (1978) 3931
92Doe1 Doering, J.P.: J. Geophys. Res. **97** (1992) 12267
92Mid1 Middleton, A.G., Teubner, P.J.O., Brunger, M.J.: Phys. Rev. Lett. **69** (1992) 2495
92Nob1 Noble, C.J., Burke, P.G.: Phys. Rev. Lett. **68** (1992) 2011
93Shy2 Shyn, T.W., Sweeney, C.J.: Phys. Rev. A **47** (1993), 1006

6.4.5.3.6 $X^3\Sigma_g^- \rightarrow b^1\Sigma_g^+$

Measurements of integral cross sections for electron impact excitation of the $b^1\Sigma_g^+$ electronic state of O_2 are due to [71Lin2, 71Traj1, 70Kon1, 78Wak1, 92Doe1, 93Shy2, 92Mid1]. Agreement between these various measurements ranges from very good to marginal, with perhaps best accord being found between the data of [71Traj1] and [92Mid1]. This scatter in the available data has led to somewhat larger estimates in the uncertainties on our preferred integral cross sections than would otherwise be the case. Our preferred integral cross section, for $\varepsilon \geq 7$ eV, is largely drawn from the work of [92Mid1], with some modest adjustments. For $\varepsilon < 7$ eV we have employed the R-matrix calculation of [92Nob1]. These data are tabulated in Table 6.4.27 and plotted in Fig. 6.4.25.

The uncertainty in the integral cross section is estimated to be ± 35 % for $\varepsilon < 7$ eV and ± 31 % for 7 eV $\leq \varepsilon \leq$ 20 eV.

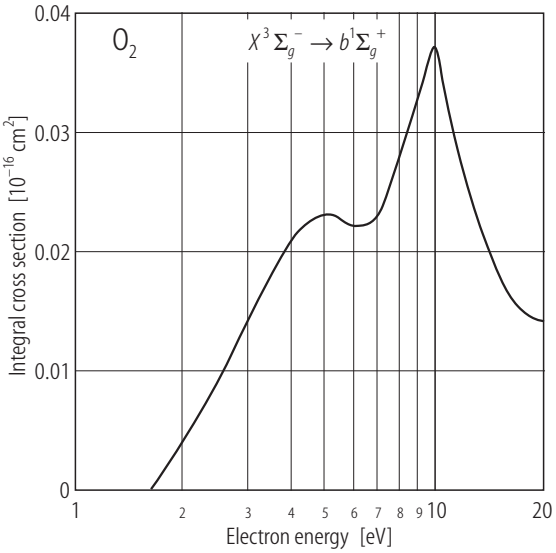

Fig. 6.4.25. Recommended integral cross section for $X^3\Sigma_g \rightarrow b^1\Sigma_g^+$ in O_2.

Table 6.4.27. Preferred values of the integral $X^3\Sigma_g^- \rightarrow b^1\Sigma_g^+$ electronic-state excitation cross section ($\sigma_{X\text{-}b}$) for electrons in molecular oxygen.

Energy [eV]	$\sigma_{X\text{-}b}$ [Å^2]	Energy [eV]	$\sigma_{X\text{-}b}$ [Å^2]
1.63	0	8	0.028
2	0.004	9	0.033
3	0.014	9.5	0.036
4	0.021	10	0.037
5	0.023	11	0.031
6	0.022	15	0.018
7	0.023	20	0.014

References for 6.4.5.3.6

70Kon1 Konishi, A., Wakiya, K., Yamamoto, M., Suzuki, H.: J. Phys. Soc. Jpn. **29** (1970) 526
71Lin2 Linder, F., Schmidt, H.: Z. Naturforsch. A **26** (1971) 1617
71Traj1 Trajmar, S., Cartwright, D.C., Williams, W.: Phys. Rev. A **4** (1971) 1482
78Wak1 Wakiya, K.: J. Phys. B: At. Mol. Phys. **11** (1978) 3931
92Doe1 Doering, J.P.: J. Geophys. Res. **97** (1992) 12267
92Mid1 Middleton, A.G., Teubner, P.J.O., Brunger, M.J.: Phys. Rev. Lett. **69** (1992) 2495
92Nob1 Noble, C.J., Burke, P.G.: Phys. Rev. Lett. **68** (1992) 2011
93Shy2 Shyn, T.W., Sweeney, C.J.: Phys. Rev. A **47** (1993) 1006

6.4.5.3.7 $c^1\Sigma_u^- + A'^3\Delta_u + A^3\Sigma_u^+$

The summed integral cross section for electron impact excitation of the three electronic states that comprise the Herzberg continuum have been measured by [70Kon1, 72Tra1, 00Cam1, 01Gre1]. Our preferred cross section set for the excitation of the $c^1\Sigma_u^- + A'^3\Delta_u + A^3\Sigma_u^+$ states is constructed from the data of [72Tra1, 00Cam1, 00Gre1]. They are tabulated in Table 6.4.28 and plotted in Fig. 6.4.26.

The uncertainty in the integral cross section is estimated to be ± 38 % over the entire range of electron energies.

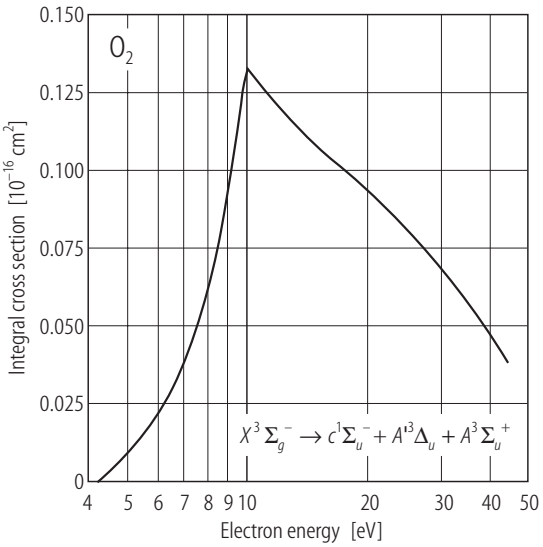

Fig. 6.4.26. Recommended integral cross section for $X^3\Sigma_g^- \rightarrow c^1\Sigma_u^- + A'^3\Delta_u + A^3\Sigma_u^+$ in O_2.

Table 6.4.28. Preferred values of the integral $c^1\Sigma_u^- + A'^3\Delta_u + A^3\Sigma_u^+$ electronic-states excitation cross section ($\sigma_{X\text{-}c+A'+A}$) for electrons in molecular oxygen.

Energy [eV]	$\sigma_{X\text{-}c+A'+A}$ [Å^2]
4.23	0.000
9	0.092
10	0.132
12	0.120
15	0.107
20	0.094
45	0.038

References for 6.4.5.3.7

70Kon1 Konishi, A., Wakiya, K., Yamamoto, M., Suzuki, H.: J. Phys. Soc. Jpn. **29** (1970) 526
72Tra1 Trajmar, S., Williams, W., Kuppermann, A.: J. Chem. Phys. **56** (1972) 3759
00Cam1 Campbell, L., Green, M.A., Brunger, M.J., Teubner, P.J.O., Cartwright, D.C.: Phys. Rev. A **61** (2000) 022706
01Gre1 Green, M.A., Campbell, L., Cartwright, D.C., Teunber, P.J.O., Brunger, M.J., J. Phys. B **34** (2001) L157

6.4.5.4 Carbon monoxide (CO)

6.4.5.4.1 $J = 0 \rightarrow 1$

Our preferred integral cross sections for the $J = 0 \rightarrow 1$ rotationally inelastic excitation of the CO ground molecular state are taken from [96Ran1]. These data are tabulated in Table 6.4.29 and plotted in Fig. 6.4.27.

The uncertainty on these cross sections is estimated to be ± 30 %.

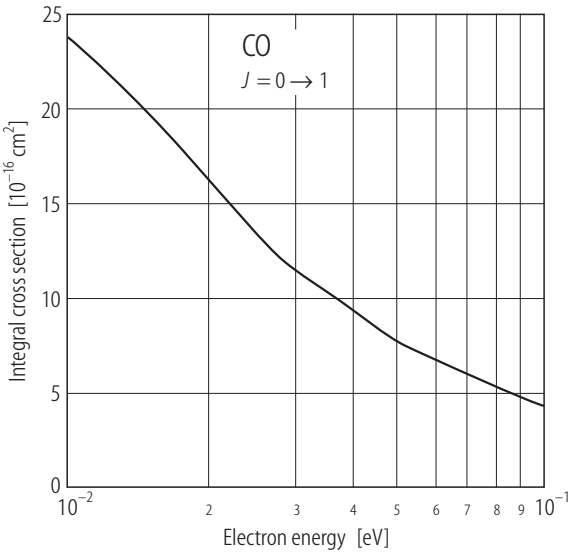

Fig. 6.4.27. Recommended integral cross section for $J = 0 \rightarrow 1$ in CO.

Table 6.4.29. Preferred values of the integral $J = 0 \rightarrow 1$ rotationally inelastic cross section ($\sigma_{0\text{-}1}$) for electron impact excitation of the ground molecular state in carbon monoxide.

Energy [eV]	$\sigma_{0\text{-}1}$ [Å^2]
0.002	34.6
0.003	31.5
0.004	30.2
0.005	29.4
0.010	23.8
0.030	11.4
0.050	7.5
0.100	4.2

References for 6.4.5.4.1

96Ran1 Randell, J., Gulley, R.J., Lunt, S.L., Ziesel, J.P., Field, D.: J. Phys. B: At. Mol. Opt. Phys. **29** (1996) 2049

6.4.5.4.2 $J = 1 \rightarrow 2$

Our preferred integral cross sections for the $J = 1 \rightarrow 2$ rotationally inelastic excitation of the CO ground molecular state are also taken from [96Ran1]. These data are tabulated in Table 6.4.30 and plotted in Fig. 6.4.28.

The uncertainty on these cross sections is estimated to be ± 30 %.

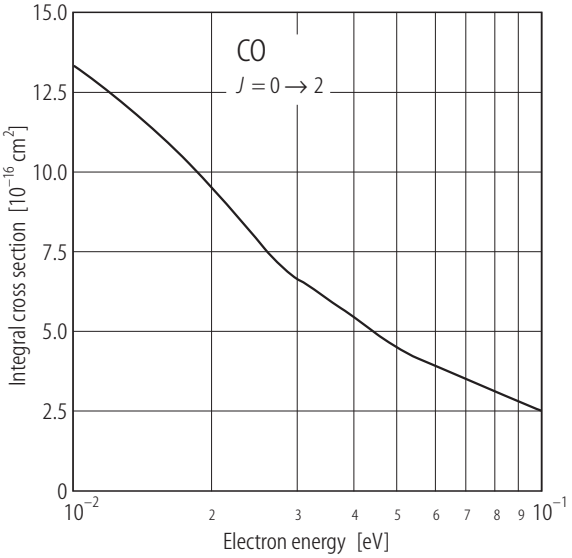

Fig. 6.4.28. Recommended integral cross section for $J = 1 \rightarrow 2$ in CO.

Table 6.4.30. Preferred values of the integral $J = 1 \rightarrow 2$ rotationally inelastic cross section ($\sigma_{1\text{-}2}$) for electron impact excitation of the ground molecular state in carbon monoxide.

Energy [eV]	$\sigma_{1\text{-}2}$ [Å^2]
0.003	15.7
0.004	15.7
0.005	15.6
0.010	13.3
0.030	6.6
0.050	4.4
0.100	2.5

References for 6.4.5.4.2

96Ran1 Randell, J., Gulley, R.J., Lunt, S.L., Ziesel, J.P., Field, D.: J. Phys. B: At. Mol. Opt. Phys. **29** (1996) 2049.

6.4.5.4.3 $\nu' = 0 \rightarrow 1$

Experimental integral cross sections for electron impact excitation of the first vibrational quantum ($\nu' = 0 \rightarrow 1$) in carbon monoxide are due to [78Lan1, 80Chu1, 85Soh1, 96Gib1]. Theoretical calculations include a Born Dipole approximation result from [85Soh1], and an R-matrix result from [96Gib1]. In constructing our preferred integral cross section we have employed all of the available experimental data except that from the swarm-based measurement of [78Lan1]. Specifically, for 0.37 eV $\leq \varepsilon \leq$ 30 eV we used [96Gib1] and for ε = 5 and 9 eV we have used [80Chu1]. Our preferred $\nu' = 0 \rightarrow 1$ integral cross section is tabulated in Table 6.4.31 and plotted in Fig. 6.4.29.

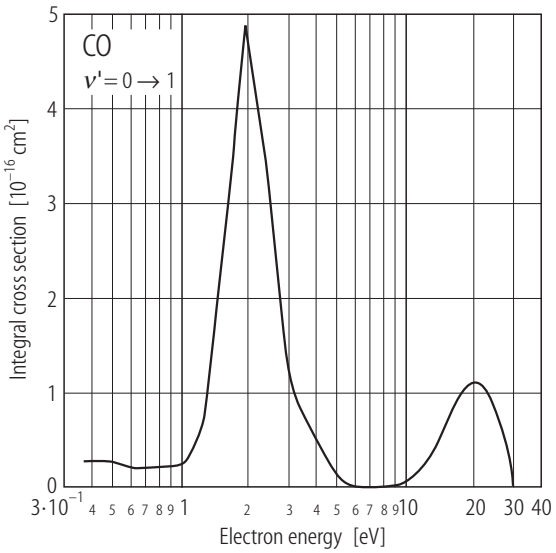

Fig. 6.4.29. Recommended integral cross section for $v' = 0 \rightarrow 1$ in CO.

Table 6.4.31. Preferred values of the integral $v' = 0 \rightarrow 1$ vibrational excitation cross section ($\sigma_{0\text{-}1}$) for electron impact excitation in carbon monoxide.

Energy [eV]	$\sigma_{0\text{-}1}$ [Å^2]	Energy [eV]	$\sigma_{0\text{-}1}$ [Å^2]
0.37	0.274	1.91	4.874
0.45	0.276	2.45	3.131
0.64	0.189	3	1.200
0.85	0.215	5	0.104
1.00	0.240	9	0.024
1.25	0.654	20	1.107
1.50	2.361	30	0.035

References for 6.4.5.4.3

78Lan1 Land, J.E.: J. Appl. Phys. **49** (1978) 5716
80Chu1 Chutjian, A., Tanaka, H.: J. Phys. B: At. Mol. Phys. **13** (1980) 1901
85Soh1 Sohn, W., Kochem, K-H., Jung, K., Ehrhardt, H., Chang, E.S.: J. Phys. B: At. Mol. Phys. **18** (1985) 2049
96Gib1 Gibson, J.C., Morgan, L.A., Gulley, R.J., Brunger, M.J., Bundschu, C.T., Buckman, S.J.: J. Phys. B: At. Mol. Opt. Phys. **29** (1996) 3197

6.4.5.4.4 $X^1\Sigma^+ \rightarrow a^3\Pi$

The preferred integral cross section for the electron impact excitation of the $a^3\Pi$ electronic-state is presented over the energy range 6 to 50 eV. The data are tabulated in Table 6.4.32 and plotted in Fig. 6.4.30. For 6 eV $\leq \varepsilon \leq$ 9.5 eV we have used the measurement of [96Zob1], for ε = 12.5 and 15 eV we have employed the integral cross sections of [98Zet1], while for $\varepsilon \geq$ 20 eV we have used the data of [94Liu1], as derived by them from the differential measurements of [93Mid1], to construct our preferred set.

The only other available data in the literature is due to [96Fur1]. This work was not considered when we constructed our preferred cross section because its shape and absolute magnitude are very different to those of [96Zob1], [98Zet1] and [94Liu1].

The uncertainty on our preferred integral cross section is estimated to be ± 25 % for ε < 20 eV and ± 35 % for $\varepsilon \geq$ 20 eV.

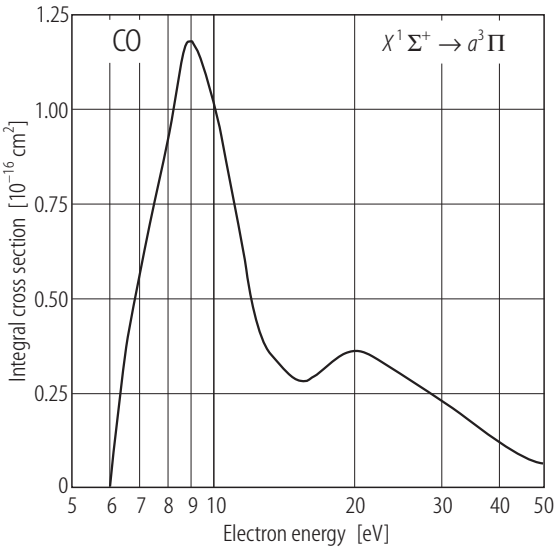

Fig. 6.4.30. Recommended integral cross section for $X^1\Sigma^+ \rightarrow a^3\Pi$ in CO.

Table 6.4.32. Preferred values of the integral $X^1\Sigma^+ \rightarrow a^3\Pi$ electronic state cross section ($\sigma_{a^3\Pi}$) for electron impact excitation in carbon monoxide.

Energy [eV]	$\sigma_{a^3\Pi}$ [Å^2]	Energy [eV]	$\sigma_{a^3\Pi}$ [Å^2]
6.01	0.000	9.5	1.110
6.5	0.355	12.5	0.417
7.0	0.595	15.0	0.285
7.5	0.760	20.0	0.369
8.0	0.915	30.0	0.237
8.5	1.130	40.0	0.119
9.0	1.190	50.0	0.065

References for 6.4.5.4.4

93Mid1 Middleton, A.G., Brunger, M.J., Teubner, P.J.O.: J. Phys. B: At. Mol. Opt. Phys. **26** (1993) 1743
94Liu1 Liu, W., Victor, G.A.: Astrophys. J. **435** (1994) 909
96Fur1 Furlong, J.M., Newell, W.R.: J. Phys. B: At. Mol. Opt. Phys. **29** (1996) 331
96Zob1 Zobel, J., Mayer, U., Jung, K., Ehrhardt, H.: J. Phys. B: At. Mol. Opt. Phys. **29** (1996) 813
98Zet1 Zetner, P.W., Kanik, I., Trajmar, S.: J. Phys. B: At. Mol. Opt. Phys. **31** (1998) 2395

6.4.5.4.5 $X^1\Sigma^+ \rightarrow a'^3\Sigma^+$

Integral cross sections for the electron impact excitation of the $a'^3\Sigma^+$ electronic-state of carbon monoxide have been reported by [94Liu1, 96Zob1, 98Zet1]. We note that the data of [94Liu1] was derived from the differential cross section measurements of [93Mid1]. All of these three sets of integral cross sections have been used to derive our preferred integral cross section, which is tabulated in Table 6.4.33 and plotted in Fig. 6.4.31.

The uncertainty on our preferred integral cross section is estimated to be ± 25 % for $\varepsilon < 20$ eV and ± 35 % for $\varepsilon \geq 20$ eV.

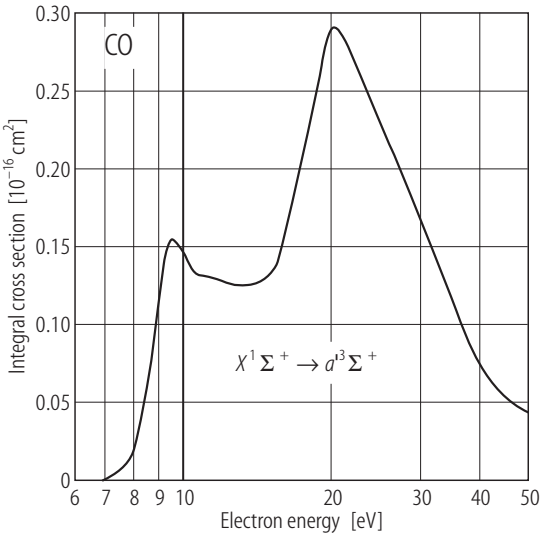

Fig. 6.4.31. Recommended integral cross section for $X^1\Sigma^+ \rightarrow a'^3\Sigma^+$ in CO.

Table 6.4.33. Preferred values of the integral $X^1\Sigma^+ \rightarrow a'^3\Sigma^+$ electronic-state cross section ($\sigma_{a'^3\Sigma^+}$) for electron impact excitation in carbon monoxide.

Energy [eV]	$\sigma_{a'^3\Sigma^+}$ [Å^2]	Energy [eV]	$\sigma_{a'^3\Sigma^+}$ [Å^2]	Energy [eV]	$\sigma_{a'^3\Sigma^+}$ [Å^2]
6.863	0.000	10.0	0.145	20.0	0.289
8.0	0.020	10.5	0.132	30.0	0.170
8.5	0.055	11.0	0.131	40.0	0.073
9.0	0.120	12.5	0.125	50.0	0.043
9.5	0.155	15.0	0.131		

References for 6.4.5.4.5

93Mid1 Middleton, A.G., Brunger, M.J., Teubner, P.J.O.: J. Phys. B: At. Mol. Opt. Phys. **26** (1993) 1743
94Liu1 Liu, W., Victor, G.A.: Astrophys. J. **435** (1994) 909
96Zob1 Zobel, J., Mayer, U., Jung, K., Ehrhardt, H.: J. Phys. B: At. Mol. Opt. Phys. **29** (1996) 813
98Zet1 Zetner, P.W., Kanik, I., Trajmar, S.: J. Phys. B: At. Mol. Opt. Phys. **31** (1998) 2395

6.4.5.4.6 $X^1\Sigma^+ \rightarrow d^3\Delta + e^3\Sigma^- + I^1\Sigma^- + D^1\Delta$

There is only one integral cross section for the unresolved sum of the $d^3\Delta$, $e^3\Sigma^-$, $I^1\Sigma^-$ and $D^1\Delta$ electronic-states in carbon monoxide. This is due to [94Liu1] and again note their values were derived from the differential cross section measurements of [93Mid1]. Our preferred integral cross section is taken directly from [94Liu1] and it is tabulated in Table 6.4.34.

For completeness we note the resolved $d^3\Delta$ integral cross section measurement of [96Zob1] and the resolved $I^1\Sigma$-integral cross section data of [88Mas1], neither of which are considered further here.

The uncertainty on our preferred integral cross section is estimated to be ± 35 % over the entire measured energy range.

Table 6.4.34. Preferred values of the integral $X^1\Sigma^+ \rightarrow d^3\Delta + e^3\Sigma^- + I^1\Sigma^- + D^1\Delta$ electronic-states cross section ($\sigma_{d^3\Delta+e^3\Sigma^-+I^1\Sigma^-+D^1\Delta}$) for electron impact excitation in carbon monoxide.

Energy [eV]	$\sigma_{d^3\Delta+e^3\Sigma^-+I^1\Sigma^-+D^1\Delta}$ [Å^2]
20	0.092
30	0.051
40	0.029
50	0.021

References for 6.4.5.4.6

88Mas1 Mason, N.J., Newell, W.R.: J. Phys. B: At. Mol. Opt. Phys. **21** (1988) 1293
93Mid1 Middleton, A.G., Brunger, M.J., Teubner, P.J.O.: J. Phys. B: At. Mol. Opt. Phys. **26** (1993) 1743
94Liu1 Liu, W., Victor, G.A.: Astrophys. J. **435** (1994) 909
96Zob1 Zobel, J., Mayer, U., Jung, K., Ehrhardt, H.: J. Phys. B: At. Mol. Opt. Phys. **29** (1996) 813

6.4.5.4.7 $X^1\Sigma^+ \rightarrow A^1\Pi$

The preferred integral cross section for the electron impact excitation of the $A^1\Pi$ electronic-state is presented over the energy range 8 to 50 eV. The data are tabulated in Table 6.4.35 and plotted in Fig. 6.4.32. For 8 eV ≤ ε ≤ 11.5 eV we have used the data of [96Zob1], for ε = 12.5 and 15 eV we have

employed the measurement of [98Zet1], while for $\varepsilon \geq 20$ eV we have used the data of [94Liu1], as derived by them from the differential measurements of [93Mid1], to construct our preferred set.

The uncertainty on our preferred integral cross section set is estimated to be ± 25 % for $\varepsilon < 20$ eV and ± 35 % for $\varepsilon \geq 20$ eV.

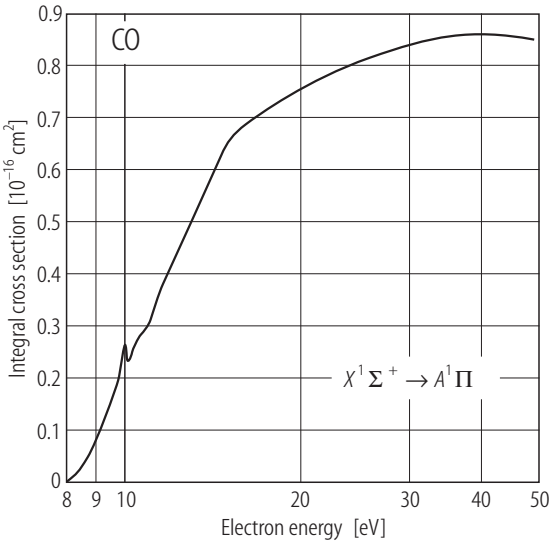

Fig. 6.4.32. Recommended integral cross section for $X^1\Sigma^+ \rightarrow A^1\Pi$ in CO.

Table 6.4.35. Preferred values of the integral $X^1\Sigma^+ \rightarrow A^1\Pi$ electronic-state cross section ($\sigma_{A^1\Pi}$) for electron impact excitation in carbon monoxide.

Energy [eV]	$\sigma_{A^1\Pi}$ [Å^2]	Energy [eV]	$\sigma_{A^1\Pi}$ [Å^2]
8.028	0.000	11.0	0.300
8.5	0.025	11.5	0.365
9.0	0.082	12.5	0.453
9.5	0.150	15.0	0.650
10.0	0.230	20.0	0.756
10.04	0.290	30.0	0.837
10.15	0.230	40.0	0.859
10.5	0.270	50.0	0.847

References for 6.4.5.4.7

93Mid1 Middleton, A.G., Brunger, M.J., Teubner, P.J.O.: J. Phys. B: At. Mol. Opt. Phys. **26** (1993) 1743
94Liu1 Liu, W., Victor, G.A.: G.A.: Astrophys. J. **435** (1994) 909
96Zob1 Zobel, J., Mayer, U., Jung, K., Ehrhardt, H.: J. Phys. B: At. Mol. Opt. Phys. **29** (1996) 813
98Zet1 Zetner, P.W., Kanik, I., Trajmar, S.: J. Phys. B: At. Mol. Opt. Phys. **31** (1998) 2395

6.4.5.4.8 $X^1\Sigma^+ \rightarrow b^3\Sigma^+$

Integral cross sections for the electron impact excitation of the $b^3\Sigma^+$ electronic-state of carbon monoxide have been reported by [94Liu1, 96Zob2, 97Zub1]. We again note that the data of [94Liu1] was derived from the differential cross section measurements of [93Mid1]. All of these three sets of integral cross sections have been used to derive our preferred integral cross section, which is tabulated in Table 6.4.36 and plotted in Fig. 6.4.33.

The uncertainty on our preferred integral cross section set is estimated to be ± 25 % for $\varepsilon \leq 14$ eV and ± 35 % for $\varepsilon > 14$ eV.

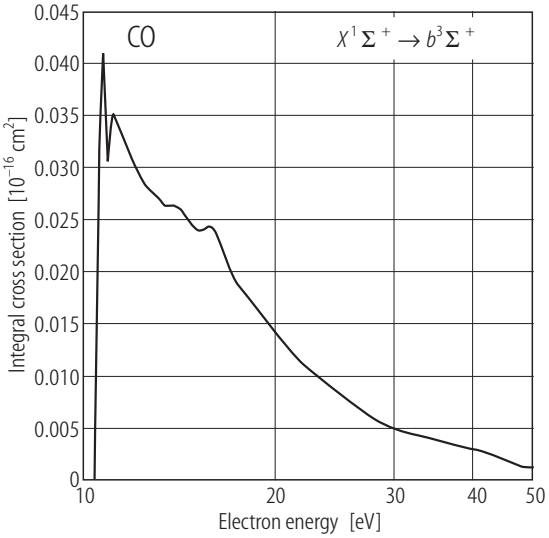

Fig. 6.4.33. Recommended integral cross section for $X^1\Sigma^+ \rightarrow b^3\Sigma^+$ in CO.

Table 6.4.36. Preferred values of the integral $X^1\Sigma^+ \rightarrow b^3\Sigma^+$ electronic-state cross section ($\sigma_{b^3\Sigma^+}$) for electron impact excitation in carbon monoxide.

Energy [eV]	$\sigma_{b^3\Sigma^+}$ [Å^2]	Energy [eV]	$\sigma_{b^3\Sigma^+}$ [Å^2]	Energy [eV]	$\sigma_{b^3\Sigma^+}$ [Å^2]
10.394	0.000	12.0	0.030	16.0	0.024
10.5	0.025	12.5	0.028	17.0	0.020
10.75	0.040	13.0	0.027	20.0	0.014
10.875	0.030	13.5	0.026	30.0	0.005
11.0	0.035	14.0	0.026	40.0	0.003
11.5	0.033	15.0	0.024	50.0	0.001

References for 6.4.5.4.8

93Mid1 Middleton, A.G., Brunger, M.J. and Teubner, P.J.O.: J. Phys. B: At. Mol. Opt. Phys. **26** (1993) 1743

94Liu1 Liu, W. and Victor, G.A.: G.A.: Astrophys. J. **435** (1994) 909

96Zob2 Zobel, J., Mayer, U., Jung, K., Ehrhardt, H., Pritchard, H., Winstead, C. and McKoy, V.: J. Phys. B: At. Mol. Opt. Phys. **29** (1996) 839

97Zub1 Zubek, M., Olszewski, R. and Wolinski, P.: J. Phys. B: At. Mol. Opt. Phys. **30** (1997) L791

6.4.5.4.9 $X^1\Sigma^+ \rightarrow B^1\Sigma^+$

Integral cross sections for the electron impact excitation of the $B^1\Sigma^+$ electronic-state of carbon monoxide have been reported by [94Liu1] for 20 eV ≤ ε ≤ 50 eV, [96Zob2] for 10.77 6 eV ≤ ε ≤ 14.5 eV and by [93Kan1] at ε = 100 eV. We once again note that the data of [94Liu1] was derived from the differential cross section measurements of [93Mid1]. All of the above three sets of integral cross sections have been used to derive our preferred integral cross section, which is tabulated in Table 6.4.37 and plotted in Fig. 6.4.34.

The uncertainty on our preferred integral cross section set is estimated to be ± 25 % for ε ≤ 14.5 eV, ± 35 % for 14 eV < ε ≤ 50 eV and ± 30 % at ε = 100 eV.

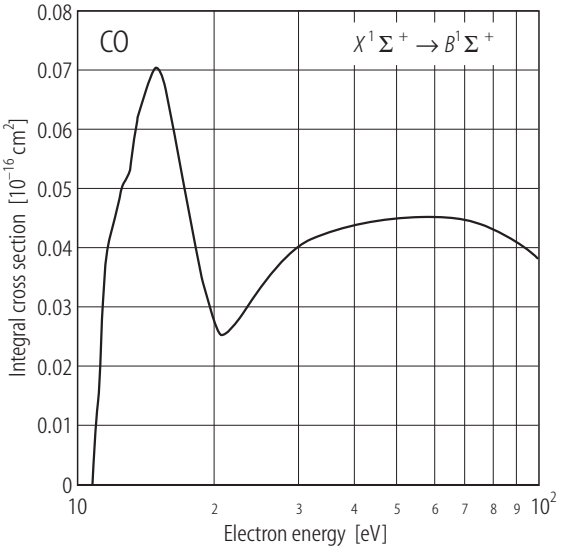

Fig. 6.4.34. Recommended integral cross section for $X^1\Sigma^+ \rightarrow B^1\Sigma^+$ in CO.

Table 6.4.37. Preferred values of the integral $X^1\Sigma^+ \rightarrow B^1\Sigma^+$ electronic-state cross section ($\sigma_{B^1\Sigma^+}$) for electron impact excitation in carbon monoxide.

Energy [eV]	$\sigma_{B^1\Sigma^+}$ [Å^2]	Energy [eV]	$\sigma_{B^1\Sigma^+}$ [Å^2]
10.776	0.000	14.0	0.066
11.0	0.010	14.5	0.070
11.5	0.038	20	0.026
12.0	0.045	30	0.040
12.5	0.050	40	0.044
13.0	0.053	50	0.045
13.5	0.062	100	0.038

References for 6.4.5.4.9

93Kan1 Kanik, I., Ratliff, M. and Trajmar, S.: Chem. Phys. Lett. **208** (1993) 341

93Mid1 Middleton, A.G., Brunger, M.J. and Teubner, P.J.O.: J. Phys. B: At. Mol. Opt. Phys. **26** (1993) 1743

94Liu1 Liu, W. and Victor, G.A.: G.A.: Astrophys. J. **435** (1994) 909

96Zob2 Zobel, J., Mayer, U., Jung, K., Ehrhardt, H., Pritchard, H., Winstead, C. and McKoy, V.: J. Phys. B: At. Mol. Opt. Phys. **29** (1996) 839

6.4.5.4.10 $X^1\Sigma^+ \rightarrow (C^1\Sigma^+ + c^3\Pi)$

The preferred integral cross section for the electron impact excitation of the unresolved $C^1\Sigma^+ + c^3\Pi$ electronic-states is presented over the energy range 20 to 100 eV. The data are tabulated in Table 6.4.38 and plotted in Fig. 6.4.35. For 20 eV $\leq \varepsilon \leq$ 50 eV we have employed the data of [94Liu1], as derived from the differential cross section measurements of [93Mid1], while at ε = 100 eV we have used the integral cross section of [93Kan1], to construct our preferred set.

The uncertainty on our preferred integral cross section is estimated to be ± 35 % for 20 eV $\leq \varepsilon \leq$ 50 eV and ± 25 % at ε = 100 eV.

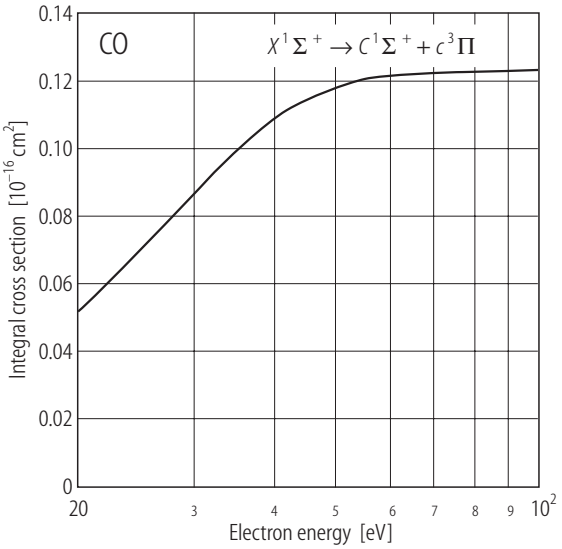

Fig. 6.4.35. Recommended integral cross section for $X^1\Sigma^+ \rightarrow C^1\Sigma^+ + c^3\Pi$ in CO.

Table 6.4.38. Preferred values of the integral $X^1\Sigma^+ \rightarrow C^1\Sigma^+ + c^3\Pi$ electronic-states cross section ($\sigma_{C^1\Sigma^+ + c^3\Pi}$) for electron impact excitation in carbon monoxide.

Energy [eV]	$\sigma_{C^1\Sigma^+ + c^3\Pi}$ [Å^2]
20.0	0.051
30.0	0.086
40.0	0.109
50.0	0.118
100.0	0.123

References for 6.4.5.4.10

93Mid1 Middleton, A.G., Brunger, M.J. and Teubner, P.J.O.: J. Phys. B: At. Mol. Opt. Phys. **26** (1993) 1743

93Kan1 Kanik, I., Ratliff, M. and Trajmar, S.: Chem. Phys. Lett. **208** (1993) 341

94Liu1 Liu, W. and Victor, G.A.: G.A.: Astrophys. J. **435** (1994) 909

6.4.5.4.11 $X^1\Sigma^+ \rightarrow E^1\Pi$

Integral cross sections for the electron impact excitation of the $E^1\Pi$ electronic-state of carbon monoxide have been reported by [94Liu1, 96Zob2, 93Kan1]. We note that the data of [94Liu1] was derived from the differential cross section measurements of [93Mid1]. All of these three sets of integral cross sections have been used to derive our preferred integral cross section, which is tabulated in Table 6.4.39 and plotted in Fig. 6.4.36.

The uncertainty on our preferred integral cross section set is estimated to be ± 25 % for $\varepsilon \leq 15$ eV and at $\varepsilon = 100$ eV and ± 35 % for 20 eV $\leq \varepsilon \leq$ 50 eV.

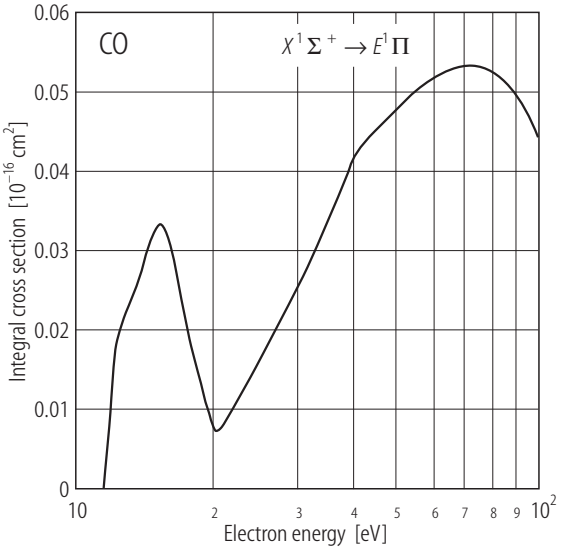

Fig. 6.4.36. Recommended integral cross section for $X^1\Sigma^+ \rightarrow E^1\Pi$ in CO.

Table 6.4.39. Preferred values of the integral $X^1\Sigma^+ \rightarrow E^1\Pi$ electronic-state cross section ($\sigma_{E^1\Pi}$) for electron impact excitation in carbon monoxide.

Energy [eV]	$\sigma_{E^1\Pi}$ [Å^2]	Energy [eV]	$\sigma_{E^1\Pi}$ [Å^2]
11.522	0.000	14.5	0.031
11.75	0.005	15.0	0.033
12.0	0.013	20.0	0.007
12.5	0.020	30.0	0.025
13.0	0.023	40.0	0.042
13.5	0.025	50.0	0.048
14.0	0.028	100.0	0.044

References for 6.4.5.4.11

93Kan1 Kanik, I., Ratliff, M. and Trajmar, S.: Chem. Phys. Lett. **208** (1993) 341

93Mid1 Middleton, A.G., Brunger, M.J. and Teubner, P.J.O.: J. Phys. B: At. Mol. Opt. Phys. **26** (1993) 1743

94Liu1 Liu, W. and Victor, G.A.: Astrophys. J. **435** (1994) 909

96Zob2 Zobel, J., Mayer, U., Jung, K., Ehrhardt, H., Pritchard, H., Winstead, C. and McKoy, V.: J. Phys. B: At. Mol. Opt. Phys. **29** (1996) 839

6.4.5.5 Nitric oxide (NO)

6.4.5.5.1 $\nu' = 0 \rightarrow 1$

There appears to be only one experimental determination for the $\nu' = 0 \rightarrow 1$ integral cross section of NO. This measurement is due to Mojarrabi et al. [95Moj1] and it forms the basis of our preferred cross section set for energies in the range 7.5 to 40 eV. The preferred cross sections are listed in Table 6.4.40 and shown in Fig. 6.4.37.

The uncertainty on the cross sections is estimated to be ± 25 %.

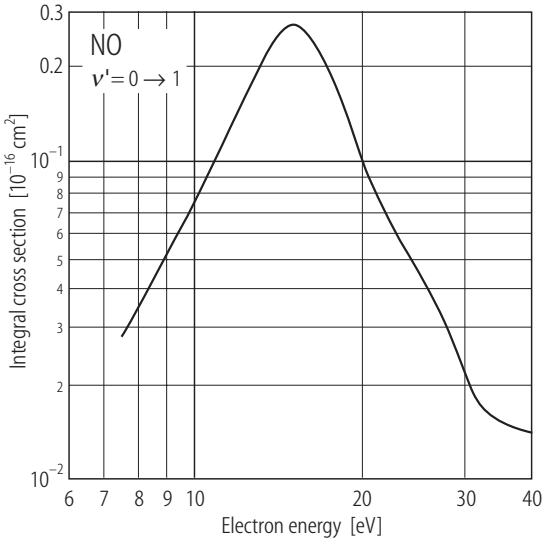

Fig. 6.4.37. Recommended integral cross section for $\nu' = 0 \rightarrow 1$ in NO.

Table 6.4.40. Preferred values of the integral $\nu' = 0 \rightarrow 1$ rovibration excitation cross section ($\sigma_{0\text{-}1}$) for electrons in nitric oxide.

Energy [eV]	$\sigma_{0\text{-}1}$ [Å^2]
7.5	0.028
10	0.074
15	0.270
20	0.097
30	0.022
40	0.014

References for 6.4.5.5.1

95Moj1 Mojarrabi, B., Gulley, R.J., Middleton, A.G., Cartwright, D.C., Teubner, P.J.O., Buckman, S.J., Brunger, M.J.: J. Phys. B: At. Mol. Opt. Phys. **28** (1995) 487

6.4.5.5.2 $\nu' = 0 \rightarrow 2$

There also appears to be only one experimental determination for the $\nu' = 0 \rightarrow 2$ integral cross section of NO. Again this measurement is due to Mojarrabi et al. [95Moj1] and it forms the basis of our preferred cross section set for energies in the range 10 to 20 eV. The preferred cross sections are listed in Table 6.4.41.

The uncertainty on the cross sections is estimated to be ± 30 %.

Table 6.4.41. Preferred values of the integral $\nu' = 0 \rightarrow 2$ rovibration excitation cross section ($\sigma_{0\text{-}2}$) for electrons in nitric oxide.

Energy [eV]	$\sigma_{0\text{-}2}$ [Å^2]
10	0.014
15	0.073
20	0.022

References for 6.4.5.5.2

95Moj1 Mojarrabi, B., Gulley, R.J., Middleton, A.G., Cartwright, D.C., Teubner, P.J.O., Buckman, S.J., Brunger, M.J.: J. Phys. B: At. Mol. Opt. Phys. **28** (1995) 487

6.4.5.5.3 $X^2\Pi \rightarrow A^2\Sigma^+$

The preferred integral cross section for the electron impact excitation of the $A^2\Sigma^+$ electronic state is presented over the energy range 15 to 50 eV. The data are tabulated in Table 6.4.42 and plotted in Fig. 6.4.38. At lower energies (ε < 15 eV) two emission cross sections due to [77Sku1] and [99Ols1] are in poor agreement, as to the existence of a strong near-threshold resonance, with one another. Hence no preferred cross section data are recommended below 15 eV. At higher energies (15 to 50 eV) the preferred cross section is based on the crossed beam measurements of Brunger et al. [00Bru1].

The uncertainty is estimated to be: ± 35 % at 15 and 50 eV, ± 30 % at 30 and 40 eV and ± 33 % at 20 eV.

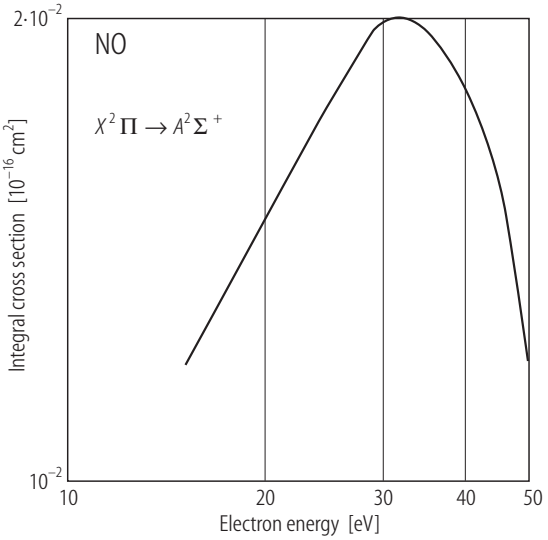

Fig. 6.4.38. Recommended integral cross section for $X^2\Pi \rightarrow A^2\Sigma^+$ in NO.

Table 6.4.42. Preferred values of the integral cross section ($\sigma_{X\text{-}A}$) for electron impact excitation of the $A^2\Sigma^+$ electronic state of nitric oxide.

Energy [eV]	$\sigma_{X\text{-}A}$ [Å^2]
15	0.012
20	0.015
30	0.020
40	0.018
50	0.012

References for 6.4.5.5.3

77Sku1 Skubenich, V.V., Povch, M.M., Zapesochnyi, I.P.: High Energy Chem. (USSR) **11** (1977) 92
99Ols1 Olszewski, R., Zubek, M.: Proc. 20th ICPEAC (Itikawa Y., Okuno, K., Tanaka, H., Yagishita, A., Matsuzawa, M., eds.), Sendai, Japan: 1999, p. 292
00Bru1 Brunger, M.J., Campbell, L., Cartwright, D.C., Middleton, A.G., Mojarrabi, B., Teubner, P.J.O.: J. Phys. B: At. Mol. Opt. Phys. **33** (2000) 809

6.4.5.5.4 $X^2\Pi \rightarrow C^2\Pi_r$

The only published values of integral cross sections for electron impact excitation of the $C^2\Pi_r$ electronic state are due to Brunger et al. [00Bru1] and Mojarrabi et al. [96Moj1]. In both cases the energy range was 15 to 50 eV, and we note their respective integral cross sections are identical. Consequently our preferred cross section is based on the recent crossed beam measurements of [00Bru1]. It can be found in Table 6.4.43.

The uncertainty is estimated to be: ± 27 % at 15 eV, ± 25 % at 20 eV, ± 23 % at 30 and 40 eV and ± 26 % at 50 eV.

Table 6.4.43. Preferred values of the integral cross section ($\sigma_{X\text{-}C}$) for electron impact excitation of the $C^2\Pi_r$ electronic state of nitric oxide.

Energy [eV]	$\sigma_{X\text{-}C}$ [Å^2]
15	0.023
20	0.033
30	0.041
40	0.047
50	0.033

References for 6.4.5.5.4

96Moj1 Mojarrabi, B., Campbell, L., Teubner, P.J.O., Brunger, M.J., Cartwright, D.C.: Phys. Rev. A **54** (1996) 2977
00Bru1 Brunger, M.J., Campbell, L., Cartwright, D.C., Middleton, A.G., Mojarrabi, B., Teubner, P.J.O.: J. Phys. B: At. Mol. Opt. Phys. **33** (2000) 809

6.4.5.5.5 $X^2\Pi \rightarrow F^2\Delta$

There appears to be only two experimental determinations of integral cross sections for the excitation of the $F^2\Delta$ electronic state of nitric oxide. The first, from threshold to 50 eV, is due to [77Sku1] while the second, from 15 to 50 eV is due to [00Bru1]. In this case the integral cross sections of [77Sku1] and [00Bru1] are in excellent agreement, at all common energies, between 15 and 50 eV. As such they form the basis for our preferred cross sections in this energy regime, as can be found in Table 6.4.44. Below 15 eV there is only the data of [77Sku1]. As this group's near-threshold measurements for the $A^2\Sigma^+$

electronic state (see 6.4.5.5.3) are in question, we do not incorporate their measurements of the $F^2\Delta$ electronic state integral cross sections, for $\varepsilon < 15$ eV, into our preferred set.

The uncertainty is estimated to be: ± 46 % at 15 eV, ± 44 % at 20 and 30 eV, ± 43 % at 40 eV and ± 45 % at 50 eV.

Table 6.4.44. Preferred values of the integral cross section ($\sigma_{X\text{-}F}$) for electron impact excitation of the $F^2\Delta$ electronic state of nitric oxide.

Energy [eV]	$\sigma_{X\text{-}F}$ [Å^2]
15	0.004
20	0.006
30	0.009
40	0.013
50	0.008

References for 6.4.5.5.5

77Sku1 Skubenich, V.V., Povch, M.M., Zapesochnyi, I.P.: High Energy Chem. (USSR) **11** (1977) 92

00Bru1 Brunger, M.J., Campbell, L., Cartwright, D.C., Middleton, A.G., Mojarrabi, B., Teubner, P.J.O.: J. Phys. B: At. Mol. Opt. Phys. **33** (2000) 809

6.4.5.5.6 $X^2\Pi \rightarrow B^2\Pi_r$

The preferred integral cross section for electron impact excitation of the $B^2\Pi$ valence electronic state of nitric oxide is presented over the energy range 15 to 50 eV. The data are tabulated in Table 6.4.45 and plotted in Fig. 6.4.39. The cross section of [00Bru1], at 30 eV, is in excellent agreement with the corresponding emission cross section of Schappe et al. [97Sch1], with both these data being a factor of 1.5 stronger in magnitude then that of [77Sku1]. Consequently our preferred cross section is based on the crossed beam measurement of [00Bru1].

The uncertainty is estimated to be: ± 56 % at 15 eV, ± 55 % at 20 eV, ± 53 % at 30 eV, ± 58 % at 40 eV and ± 60 % at 50 eV.

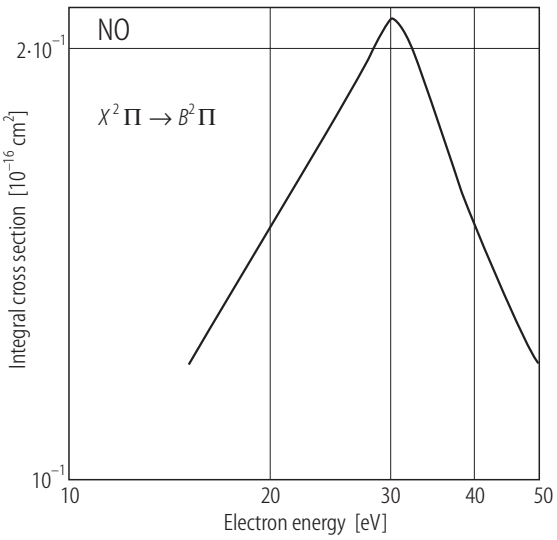

Fig. 6.4.39. Recommended integral cross section for $X^2\Pi \rightarrow B^2\Pi$ in NO.

Table 6.4.45. Preferred values of the integral cross section ($\sigma_{X\text{-}B}$) for electron impact excitation of the $B^2\Pi$ electronic state of nitric oxide.

Energy [eV]	$\sigma_{X\text{-}B}$ [Å^2]
15	0.012
20	0.015
30	0.021
40	0.015
50	0.012

References for 6.4.5.5.6

77Sku1 Skubenich, V.V., Povch, M.M., Zapesochnyi, I.P.: High Energy Chem. (USSR) **11** (1977) 92
97Sch1 Schappe, R.S., Hall, L., Wawrzyniak, M.: Bull. Am. Phys. Soc. **42** (1997) 1710
00Bru1 Brunger, M.J., Campbell, L., Cartwright, D.C., Middleton, A.G., Mojarrabi, B., Teubner, P.J.O.: J. Phys. B: At. Mol. Opt. Phys. **33** (2000) 809

6.4.5.5.7 $X^2\Pi \rightarrow b^4\Sigma^-$

The only published values of integral cross sections for electron impact excitation of the $b^4\Sigma^-$ valence electronic state are due to [00Bru1] and [77Sku1]. The measurement of [77Sku1] is restricted to near threshold energies and we do not consider it to be reliable. Thus our preferred cross section is again based solely on the recent crossed beam measurements of [00Bru1]. It can be found in Table 6.4.46.

The uncertainty is estimated to be: ± 45 % at 15 and 30 eV, ± 47 % at 40 eV and ± 49 % at 20 and 50 eV.

Table 6.4.46. Preferred values of the integral cross section ($\sigma_{X\text{-}b}$) for electron impact excitation of the $b^4\Sigma^-$ electronic state of nitric oxide.

Energy [eV]	$\sigma_{X\text{-}b}$ [Å^2]
15	0.047
20	0.047
30	0.041
40	0.020
50	0.009

References for 6.4.5.5.7

77Sku1 Skubenich, V.V., Povch, M.M., Zapesochnyi, I.P.: High Energy Chem. (USSR) **11** (1977) 92
00Bru1 Brunger, M.J., Campbell, L., Cartwright, D.C., Middleton, A.G., Mojarrabi, B., Teubner, P.J.O.: J. Phys. B: At. Mol. Opt. Phys. **33** (2000) 809

6.4.5.5.8 $X^2\Pi \rightarrow B'^2\Delta$

The level of agreement between the published integral cross sections of [00Bru1] and [77Sku1], for electron impact excitation of the $B'^2\Delta$ valence electronic state of NO, is quite poor in the 15 to 50 eV energy range. Given some of the problems, highlighted in earlier sections of this chapter, with the emission results of [77Sku1], our preferred cross section is taken from the data of [00Bru1] and is tabulated in Table 6.4.47.

The uncertainty is estimated to be: ± 35 % at 15 eV, ± 33 % at 20 eV, ± 30 % at 30 eV, ± 31 % at 40 eV and ± 34 % at 50 eV.

Table 6.4.47. Preferred values of the integral cross section ($\sigma_{X\text{-}B'}$) for electron impact excitation of the $B'^2\Delta$ electronic state of nitric oxide.

Energy [eV]	$\sigma_{X\text{-}B'}$ [Å^2]
15	0.032
20	0.065
30	0.084
40	0.058
50	0.022

References for 6.4.5.5.8

77Sku1 Skubenich, V.V., Povch, M.M., Zapesochnyi, I.P.: High Energy Chem. (USSR) **11** (1977) 92
00Bru1 Brunger, M.J., Campbell, L., Cartwright, D.C., Middleton, A.G., Mojarrabi, B., Teubner, P.J.O.: J. Phys. B: At. Mol. Opt. Phys. **33** (2000) 809

6.4.5.5.9 $X^2\Pi \rightarrow D^2\Sigma^+$

The only available data for electron impact excitation of the $D^2\Sigma^+$ electronic state of nitric oxide is from the crossed beam measurements of [00Bru1]. The energy range was 15 to 50 eV. It is from this data that the present preferred integral cross section of Table 6.4.48 was constructed.

The uncertainty is estimated to be: ± 35 % at 15 eV, ± 33 % at 20 eV, ± 30 % at 30 eV, ± 31 % at 40 eV and ± 34 % at 50 eV.

Table 6.4.48. Preferred values of the integral cross section ($\sigma_{X\text{-}D}$) for electron impact excitation of the $D^2\Sigma^+$ electronic state of nitric oxide.

Energy [eV]	$\sigma_{X\text{-}D}$ [Å^2]
15	0.014
20	0.019
30	0.025
40	0.030
50	0.022

References for 6.4.5.5.9

00Bru1 Brunger, M.J., Campbell, L., Cartwright, D.C., Middleton, A.G., Mojarrabi, B., Teubner, P.J.O.: J. Phys. B: At. Mol. Opt. Phys. **33** (2000) 809

6.4.5.5.10 $X^2\Pi \rightarrow a^4\Pi$

The preferred integral cross section for electron impact excitation of the $a^4\Pi$ electronic state of nitric oxide is presented over the energy range 15 to 50 eV. The data are tabulated in Table 6.4.49. As the crossed beam measurement of [00Bru1] is the only one available in the literature, our preferred set is taken directly from it.

The uncertainty is estimated to be: ± 65 % at 15, 30 and 40 eV and ± 63 % at 20 and 50 eV.

Table 6.4.49. Preferred values of the integral cross section ($\sigma_{X\text{-}a}$) for electron impact excitation of the $a^4\Pi$ valence electronic state of nitric oxide.

Energy [eV]	$\sigma_{X\text{-}a}$ [Å^2]
15	0.008
20	0.010
30	0.014
40	0.010
50	0.007

References for 6.4.5.5.10

00Bru1 Brunger, M.J., Campbell, L., Cartwright, D.C., Middleton, A.G., Mojarrabi, B., Teubner, P.J.O.: J. Phys. B: At. Mol. Opt. Phys. **33** (2000) 809

6.4.5.5.11 $X^2\Pi \rightarrow L'^2\Phi$

The only available data for electron excitation of the $L'^2\Phi$ valence electronic state of nitric oxide is from the crossed beam measurements of [00Bru1]. The energy range was 15 to 50 eV. It is from this data set that the present preferred integral cross section of Table 6.4.50 was constructed.

The uncertainty is estimated to be: ± 57 % at 15 and 50 eV, ± 62 % at 20 eV, ±55 % at 30 eV and ± 52 % at 40 eV.

Table 6.4.50. Preferred values of the integral cross section ($\sigma_{X\text{-}L'}$) for electron impact excitation of the $L'^2\Phi$ valence electronic state of nitric oxide.

Energy [eV]	$\sigma_{X\text{-}L'}$ [Å^2]
15	0.027
20	0.023
30	0.018
40	0.021
50	0.020

References for 6.4.5.5.11

00Bru1 Brunger, M.J., Campbell, L., Cartwright, D.C., Middleton, A.G., Mojarrabi, B., Teubner, P.J.O.: J. Phys. B: At. Mol. Opt. Phys. **33** (2000) 809

6.4.5.5.12 $X^2\Pi \rightarrow L^2\Pi$

The preferred integral cross section for electron impact excitation of the $L^2\Pi$ valence electronic state was constructed entirely from the crossed beam result of [00Bru1]. The data are tabulated, for energies between 15 and 50 eV, in Table 6.4.51 and plotted in Fig. 6.4.40.

The uncertainty is estimated to be: ± 42 % at 15 and 50 eV, ± 38 % at 20 and 30 eV and ± 39 % at 40 eV.

Table 6.4.51. Preferred values of the integral cross section ($\sigma_{X\text{-}L}$) for electron impact excitation of the $L^2\Pi$ valence electronic state of nitric oxide.

Energy [eV]	$\sigma_{X\text{-}L}$ [Å^2]
15	0.036
20	0.055
30	0.118
40	0.139
50	0.118

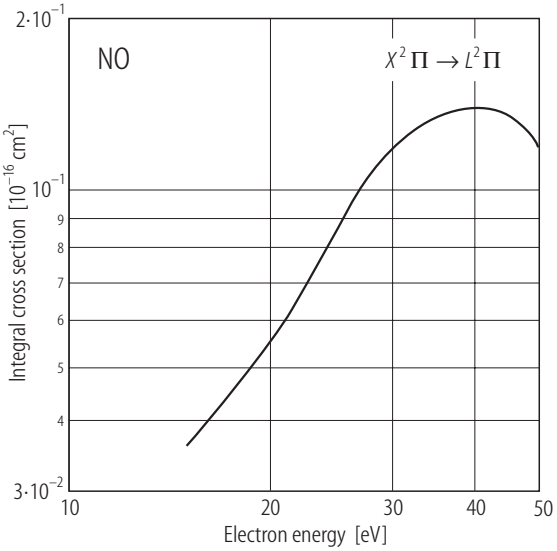

Fig. 6.4.40. Recommended integral cross section for $X^2\Pi \rightarrow L^2\Pi$ in NO.

References for 6.4.5.5.12

00Bru1 Brunger, M.J., Campbell, L., Cartwright, D.C., Middleton, A.G., Mojarrabi, B., Teubner, P.J.O.: J. Phys. B: At. Mol. Opt. Phys. **33** (2000) 809

6.4.5.5.13 $X^2\Pi \rightarrow K^2\Pi$

The preferred integral cross section for electron impact excitation of the $K^2\Pi$ electronic state of nitric oxide is presented over the energy range 15 to 50 eV. The data are tabulated in Table 6.4.52. As the crossed beam measurement of [00Bru1] is the only one available in the literature, our preferred set is taken directly from it.

The uncertainty is estimated to be: ± 38 % at 15 eV, ± 36 % at 20 eV, ± 34 % at 30 and 40 eV and ± 36 % at 50 eV.

Table 6.4.52. Preferred values of the integral cross section ($\sigma_{X\text{-}K}$) for electron impact excitation of the $K^2\Pi$ valence electronic state of nitric oxide.

Energy [eV]	$\sigma_{X\text{-}K}$ [Å^2]
15	0.006
20	0.008
30	0.016
40	0.019
50	0.010

References for 6.4.5.5.13

00Bru1 Brunger, M.J., Campbell, L., Cartwright, D.C., Middleton, A.G., Mojarrabi, B., Teubner, P.J.O.: J. Phys. B: At. Mol. Opt. Phys. **33** (2000) 809

6.4.5.5.14 $X^2\Pi \rightarrow E^2\Sigma^+$

The only available data for electron impact excitation of the $E^2\Sigma^+$ electronic state of nitric oxide is from the crossed beam measurements of [00Bru1]. The energy range was 15 to 50 eV. It is from this data set that the present preferred integral cross section of Table 6.4.53 was constructed.

The uncertainty is estimated to be: ± 65 % at 15 eV, ± 63 % at 20 eV, ± 60 % at 30 and 40 eV and ± 62 % at 50 eV.

Table 6.4.53. Preferred values of the integral cross section ($\sigma_{X\text{-}E}$) for electron impact excitation of the $E^2\Sigma^+$ electronic state of nitric oxide.

Energy [eV]	$\sigma_{X\text{-}E}$ [Å^2]
15	0.002
20	0.003
30	0.003
40	0.004
50	0.003

References for 6.4.5.5.14

00Bru1 Brunger, M.J., Campbell, L., Cartwright, D.C., Middleton, A.G., Mojarrabi, B., Teubner, P.J.O.: J. Phys. B: At. Mol. Opt. Phys. **33** (2000) 809

6.4.5.5.15 $X^2\Pi \rightarrow Q^2\Pi$

The preferred integral cross section for electron impact excitation of the $Q^2\Pi$ electronic state was constructed entirely from the crossed beam measurement of [00Bru1]. The data are tabulated in Table 6.4.54.

The uncertainty is estimated to be: ± 43 % at 15 eV, ± 40 % at 20, 30 and 40 eV and ± 42 % at 50 eV.

Table 6.4.54. Preferred values of the integral cross section ($\sigma_{X\text{-}Q}$) for electron impact excitation of the $Q^2\Pi$ electronic state of nitric oxide.

Energy [eV]	$\sigma_{X\text{-}Q}$ [Å^2]
15	0.005
20	0.007
30	0.012
40	0.015
50	0.009

References for 6.4.5.5.15

00Bru1 Brunger, M.J., Campbell, L., Cartwright, D.C., Middleton, A.G., Mojarrabi, B., Teubner, P.J.O.: J. Phys. B: At. Mol. Opt. Phys. **33** (2000) 809

6.4.5.5.16 $X^2\Pi \rightarrow S^2\Sigma^+$

The preferred integral cross section for electron impact excitation of the $S^2\Sigma^+$ electronic state of nitric oxide is presented over the energy range 15 to 50 eV. The data are tabulated in Table 6.4.55. As the crossed beam measurement of [00Bru1] is the only one available in the literature, our preferred set is taken directly from it.

The uncertainty is estimated to be: ± 55 % at 15 eV, ± 53 % at 20 eV, ± 50 % at 30 and 40 eV and ± 51 % at 50 eV.

Table 6.4.55. Preferred values of the integral cross section ($\sigma_{X\text{-}S}$) for electron impact excitation of the $S^2\Sigma^+$ electronic state of nitric oxide.

Energy [eV]	$\sigma_{X\text{-}S}$ [Å^2]
15	0.004
20	0.009
30	0.015
40	0.011
50	0.007

References for 6.4.5.5.16

00Bru1 Brunger, M.J., Campbell, L., Cartwright, D.C., Middleton, A.G., Mojarrabi, B., Teubner, P.J.O.: J. Phys. B: At. Mol. Opt. Phys. **33** (2000) 809

6.4.5.5.17 $X^2\Pi \rightarrow M^2\Sigma^+$

The only available data for electron impact excitation of the $M^2\Sigma^+$ electronic state of nitric oxide is from the crossed beam measurement of [00Bru1]. The energy range was 15 to 50 eV. It is from this data set that the present preferred integral cross section of Table 6.4.56 was constructed.

The uncertainty is estimated to be: ± 43 % at 15 eV, ± 40 % at 20, 30 and 40 eV and ± 42 % at 50 eV.

Table 6.4.56. Preferred values of the integral cross section ($\sigma_{X\text{-}M}$) for electron impact excitation of the $M^2\Sigma^+$ electronic state of nitric oxide.

Energy [eV]	$\sigma_{X\text{-}M}$ [Å^2]
15	0.004
20	0.006
30	0.010
40	0.011
50	0.006

References for 6.4.5.5.17

00Bru1 Brunger, M.J., Campbell, L., Cartwright, D.C., Middleton, A.G., Mojarrabi, B., Teubner, P.J.O.: J. Phys. B: At. Mol. Opt. Phys. **33** (2000) 809

6.4.5.5.18 $X^2\Pi \rightarrow H'^2\Pi$

The preferred integral cross section for electron impact excitation of the $H'^2\Pi$ electronic state was constructed entirely from the crossed beam measurement of [00Bru1]. The data are tabulated in Table 6.4.57.

The uncertainty is estimated to be: ± 57 % at 15 and 20 eV, ± 53 % at 30 and 40 eV and ± 56 % at 50 eV.

Table 6.4.57. Preferred values of the integral cross section ($\sigma_{X\text{-}H'}$) for electron impact excitation of the $H'^2\Pi$ electronic state of nitric oxide.

Energy [eV]	$\sigma_{X\text{-}H'}$ [Å^2]
15	0.004
20	0.006
30	0.007
40	0.009
50	0.006

References for 6.4.5.5.18

00Bru1 Brunger, M.J., Campbell, L., Cartwright, D.C., Middleton, A.G., Mojarrabi, B., Teubner, P.J.O.: J. Phys. B: At. Mol. Opt. Phys. **33** (2000) 809

6.4.5.5.19 $X^2\Pi \rightarrow H^2\Sigma^+$

The preferred integral cross section for electron impact excitation of the $H^2\Sigma^+$ electronic state of nitric oxide is presented over the energy range 15 to 50 eV. The data are tabulated in Table 6.4.58 and plotted in Fig. 6.4.41. As the crossed beam measurement of [00Bru1] is the only one available in the literature, our preferred set is taken directly from it.

The uncertainty is estimated to be: ± 57 % at 15 eV, ± 54 % at 20 eV, ± 52 % at 30 eV, ± 50 % at 40 eV and ± 55 % at 50 eV.

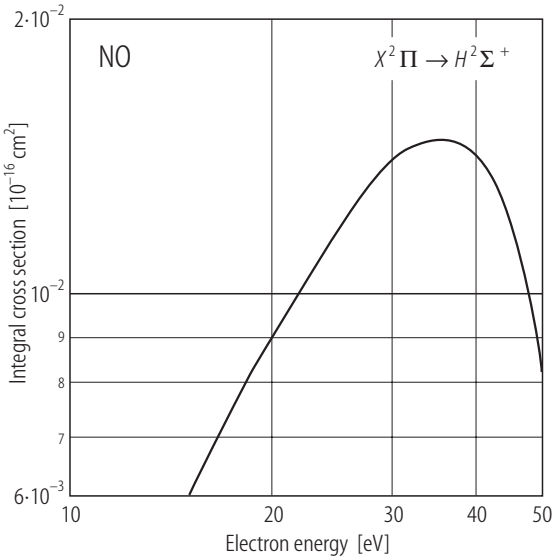

Fig. 6.4.41. Recommended integral cross section for $X^2\Pi \rightarrow H^2\Sigma^+$ in NO.

Table 6.4.58. Preferred values of the integral cross section ($\sigma_{X\text{-}H}$) for electron impact excitation of the $H^2\Sigma^+$ electronic state of nitric oxide.

Energy [eV]	$\sigma_{X\text{-}H}$ [Å^2]
15	0.006
20	0.009
30	0.014
40	0.014
50	0.008

References for 6.4.5.5.19

00Bru1 Brunger, M.J., Campbell, L., Cartwright, D.C., Middleton, A.G., Mojarrabi, B., Teubner, P.J.O.: J. Phys. B: At. Mol. Opt. Phys. **33** (2000) 809

6.4.5.5.20 $X^2\Pi \rightarrow N^2\Delta$

The only available data for electron impact excitation of the $N^2\Delta$ electronic state of nitric oxide is from the crossed beam measurement of [00Bru1]. The energy range was 15 to 50 eV. It is from this data set that the present preferred integral cross section of Table 6.4.59 was constructed.

The uncertainty is estimated to be: ± 117 % at 15 eV, ± 100 % at 30 eV and 40 eV and ± 90 % at 50 eV.

Table 6.4.59. Preferred values of the integral cross section ($\sigma_{X\text{-}N}$) for electron impact excitation of the $N^2\Delta$ electronic state of nitric oxide.

Energy [eV]	$\sigma_{X\text{-}N}$ [Å^2]
15	0.003
20	-
30	0.005
40	0.006
50	0.006

References for 6.4.5.5.20

00Bru1 Brunger, M.J., Campbell, L., Cartwright, D.C., Middleton, A.G., Mojarrabi, B., Teubner, P.J.O.: J. Phys. B: At. Mol. Opt. Phys. **33** (2000) 809

6.4.5.5.21 $X^2\Pi \rightarrow O'^2\Pi + O^2\Sigma^+$

At higher values of energy loss the unique spectral deconvolution of strongly overlapping electronic states becomes problematic. Under these circumstances cross sections are often expressed as a sum of two or more of these electronic states. The preferred integral cross section for electron impact excitation of the $O'^2\Pi + O^2\Sigma^+$ electronic states was constructed entirely from the crossed beam measurement of [00Bru1]. The data are tabulated in Table 6.4.60.

The uncertainty is estimated to be: ± 46 % at 15 and 20 eV, ± 43 % at 30 eV and 50 eV and ± 42 % at 40 eV.

Table 6.4.60. Preferred values of the integral cross section ($\sigma_{X\text{-}O'+O}$) for electron impact excitation of the $O'^2\Pi + O^2\Sigma^+$ electronic states of nitric oxide.

Energy [eV]	$\sigma_{X\text{-}O'+O}$ [Å^2]
15	0.005
20	0.007
30	0.015
40	0.013
50	0.009

References for 6.4.5.5.21

00Bru1 Brunger, M.J., Campbell, L., Cartwright, D.C., Middleton, A.G., Mojarrabi, B., Teubner, P.J.O.: J. Phys. B: At. Mol. Opt. Phys. **33** (2000) 809

6.4.5.5.22 $X^2\Pi \rightarrow W^2\Pi + Y^2\Sigma^+$

The preferred integral cross section for electron impact excitation of the $W^2\Pi + Y^2\Sigma^+$ electronic states of nitric oxide is presented over the energy range 15 to 50 eV. The data are tabulated in Table 6.4.61. Again the presented cross section is a sum for two strongly overlapping electronic states, due to uniqueness problems in the spectral deconvolution. As the crossed beam measurement of [00Bru1] is the only one available in the literature, our preferred set is taken directly from it.

The uncertainty is estimated to be: ± 36 % at 15 eV, ± 33 % at 20 eV, ± 30 % at 30 eV and 40 eV and ± 32 % at 50 eV.

Table 6.4.61. Preferred values of the integral cross section (σ_{X-W+Y}) for electron impact excitation of the $W^2\Pi + Y^2\Sigma^+$ electronic states of nitric oxide.

Energy [eV]	σ_{X+W+Y} [Å^2]
15	0.009
20	0.013
30	0.023
40	0.022
50	0.013

References for 6.4.5.5.22

00Bru1 Brunger, M.J., Campbell, L., Cartwright, D.C., Middleton, A.G., Mojarrabi, B., Teubner, P.J.O.: J. Phys. B: At. Mol. Opt. Phys. **33** (2000) 809

6.4.5.5.23 $X^2\Pi \rightarrow T^2\Sigma + U^2\Delta + 5f$

At higher values of energy loss the unique spectral deconvolution of strongly overlapping electronic states becomes problematic. Under these conditions cross sections are often expressed as a sum of two or more of these electronic states. The only available data for electron impact excitation of the $T^2\Sigma^+ + U^2\Delta +$ 5f electronic states of nitric oxide is from the crossed beam measurement of [00Bru1]. The energy range was 15 to 50 eV. It is from this data set that the present preferred integral cross section of Table 6.4.62 was constructed

The uncertainty is estimated to be: ± 65 % at 15 eV, ± 63 % at 20 eV and ± 60 % at 30, 40 and 50 eV.

Table 6.4.62. Preferred values of the integral cross section ($\sigma_{X\text{-}T+U+5f}$) for electron impact excitation of the $T^2\Sigma^+ + U^2\Delta + 5f$ electronic states of nitric oxide.

Energy [eV]	$\sigma_{X\text{-}T+U+5f}$ [Å^2]
15	0.002
20	0.002
30	0.005
40	0.004
50	0.002

References for 6.4.5.5.23

00Bru1 Brunger, M.J., Campbell, L., Cartwright, D.C., Middleton, A.G., Mojarrabi, B., Teubner, P.J.O.: J. Phys. B: At. Mol. Opt. Phys. **33** (2000) 809

6.4.5.5.24 $X^2\Pi \rightarrow Z^2\Sigma^+ + 6d\delta + 6f$

The preferred integral cross section for electron impact excitation of the $Z^2\Sigma^+ + 6d\delta + 6f$ electronic states was constructed entirely from the crossed beam measurement of [00Bru1]. The data are tabulated in Table 6.4.63. Again the presented cross section is a sum for three strongly overlapping electronic states, due to uniqueness problems in the spectral deconvolution.

The uncertainty is estimated to be: ± 69 % at 15 eV, ± 68 % at 20 eV and ± 65 % at 30, 40 and 50 eV.

Table 6.4.63. Preferred values of the integral cross section ($\sigma_{X\text{-}Z+6d+6f}$) for electron impact excitation of the $Z^2\Sigma^+ + 6d\delta + 6f$ electronic states of nitric oxide.

Energy [eV]	$\sigma_{X\text{-}Z+6d+6f}$ [Å^2]
15	0.001
20	0.001
30	0.002
40	0.002
50	0.002

References for 6.4.5.5.24

00Bru1 Brunger, M.J., Campbell, L., Cartwright, D.C., Middleton, A.G., Mojarrabi, B., Teubner, P.J.O.: J. Phys. B: At. Mol. Opt. Phys. **33** (2000) 809

6.4.5.6 Carbon dioxide (CO_2)

6.4.5.6.1 (000) → (010)

There are three integral cross section measurements for electron impact excitation of the bending mode of CO_2 ((000) → (010)), that are available to the community. They are due to [80Reg1, 70Dan1, 86Ant1] and we have used all of them in constructing our preferred set. These data are tabulated in Table 6.4.64 and plotted in Fig. 6.4.42.

The uncertainty in the integral cross sections is estimated to be ± 25 %.

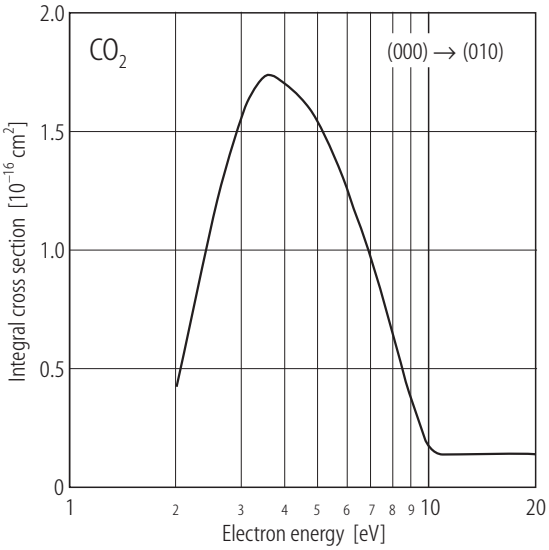

Fig. 6.4.42. Recommended integral cross section for (000) → (010) in CO_2.

Table 6.4.64. Preferred values of the integral (000) → (010) bending mode cross section (σ_{010}) for electron impact excitation in carbon dioxide.

Energy [eV]	σ_{010} [Å^2]
2	0.425
3.6	1.740
4	1.700
10	0.171
20	0.135

References for 6.4.5.6.1

70Dan1 Danner, D.: Diplomarbeit (unpublished), University of Freiburg, Germany, 1970
80Reg1 Register, D.F., Nishimura, H., Trajmar, S.: J. Phys. B: At. Mol. Phys. **13** (1980) 1651
86Ant1 Antoni, Th., Jung, K., Ehrhardt, H., Chang, E.S.: J. Phys. B: At. Mol. Opt. Phys. **19** (1986) 1377

6.4.5.6.2 (000) → (100)

There are only two integral cross section measurements for electron impact excitation of the symmetric stretch mode of CO_2 ((000) → (100)), that are currently available in the literature. They are due to [80Reg1] and [86Ant1] and we have used them both in constructing our preferred set. These data are tabulated in Table 6.4.65.

The uncertainty in the integral cross sections is estimated to be ± 25 %.

Table 6.4.65. Preferred values of the integral (000) → (100) symmetric stretch mode cross section (σ_{100}) for electron impact excitation in carbon dioxide.

Energy [eV]	σ_{100} [Å^2]
2	0.430
3.8	1.000
4	0.800
10	0.077

References for 6.4.5.6.2

80Reg1 Register, D.F., Nishimura, H., Trajmar, S.: J. Phys. B: At. Mol. Phys. **13** (1980) 1651

86Ant1 Antoni, Th., Jung, K., Ehrhardt, H., Chang, E.S.: J. Phys. B: At. Mol. Opt. Phys. **19** (1986) 1377

6.4.5.6.3 (000) → (001)

As for the bending mode, there are three integral cross section measurements for electron impact excitation of the asymmetric stretch mode of CO_2 ((000) → (001)), that are currently available to the community. They are due to [80Reg1, 70Dan1, 86Ant1] and we have used all of them in constructing our preferred set. These data are tabulated in Table 6.4.66 and plotted in Fig. 6.4.43.

The uncertainty in the integral cross sections is estimated to be ± 25 % fo $\varepsilon \leq$ 10eV, ± 30 % at ε = 20 eV and ± 50 % at ε = 50 eV.

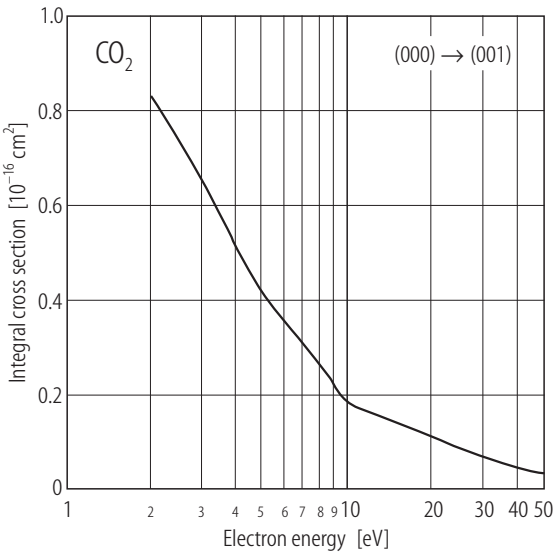

Fig. 6.4.43. Recommended integral cross section for (000) → (001) in CO_2.

Table 6.4.66. Preferred values of the integral (000) → (001) asymmetric stretch mode cross section (σ_{001}) for electron impact excitation in carbon dioxide.

Energy [eV]	σ_{001} [Å^2]
2	0.830
3.8	0.540
4	0.511
10	0.185
20	0.110
50	0.033

References for 6.4.5.6.3

70Dan1 Danner, D.: Diplomarbeit (unpublished), University of Freiburg (Germany, 1970)
80Reg1 Register, D.F., Nishimura, H., Trajmar, S.: J. Phys. B: At. Mol. Phys. **13** (1980) 1651
86Ant1 Antoni, Th., Jung, K., Ehrhardt, H., Chang, E.S.: J. Phys. B: At. Mol. Opt. Phys. **19** (1986) 1377

6.4.5.7 Nitrous oxide (N_2O)

6.4.5.7.1 (000) → (010)

The only available data, for excitation of the bending (010) mode of nitrous oxide by electron impact, is due to [00Kit1]. These integral cross sections are tabulated in Table 6.4.67.

The uncertainty in the integral cross sections is estimated to be ± 30 %.

Table 6.4.67. Preferred values of the integral (000) → (010) bending mode cross section (σ_{010}) for electron impact excitation in nitrous oxide.

Energy [eV]	σ_{010} [Å^2]
2.4	2.67
8.0	0.11

References for 6.4.5.7.1

00Kit1 Kitajima, M., Sakamoto, Y., Gulley, R.J., Hoshino, M., Gibson, J.C., Tanaka, H., Buckman, S.J.: J. Phys. B: At. Mol. Opt. Phys. **33** (2000) 1687

6.4.5.7.2 (000) → (100)

The only available data, for excitation of the symmetric stretch (100) mode of nitrous oxide by electron impact, is also due to due to [00Kit1]. These integral cross sections are tabulated in Table 6.4.68.

The uncertainty on the cross sections is estimated to be ± 30 %.

Table 6.4.68. Preferred values of the integral (000) → (100) symmetric stretch mode cross section (σ_{100}) for electron impact excitation in nitrous oxide.

Energy [eV]	σ_{100} [Å^2]
2.4	2.92
8.0	0.74

References for 6.4.5.7.2

00Kit1 Kitajima, M., Sakamoto, Y., Gulley, R.J., Hoshino, M., Gibson, J.C., Tanaka, H., Buckman, S.J.: J. Phys. B: At. Mol. Opt. Phys. **33** (2000) 1687

6.4.5.7.3 (000) → (001)

The only available data, for excitation of the asymmetric stretch (001) mode of nitrous oxide by electron impact, is again due to due to [00Kit1]. These integral cross sections are tabulated in Table 6.4.69.

The uncertainty on the cross sections is estimated to be ± 50 %.

Table 6.4.69. Preferred values of the integral (000) → (001) asymmetric stretch mode cross section (σ_{001}) for electron impact excitation in nitrous oxide.

Energy [eV]	σ_{001} [Å^2]
2.4	0.45
8.0	0.14

References for 6.4.5.7.3

00Kit1 Kitajima, M., Sakamoto, Y., Gulley, R.J., Hoshino, M., Gibson, J.C., Tanaka, H., Buckman, S.J.: J. Phys. B: At. Mol. Opt. Phys. **33** (2000) 1687

6.4.5.7.4 $2^1\Sigma^+$

Absolute differential cross sections for electron impact excitation of the $2^1\Sigma^+$ valence electronic state of nitrous oxide have been reported by [99Mar1]. To derive integral cross sections from these differential measurements we have used a Molecular Phase Shift Analysis procedure, with these results being presented in Table 6.4.70 and plotted in Fig. 6.4.44.

The uncertainty on the cross sections is estimated to be ± 50 %.

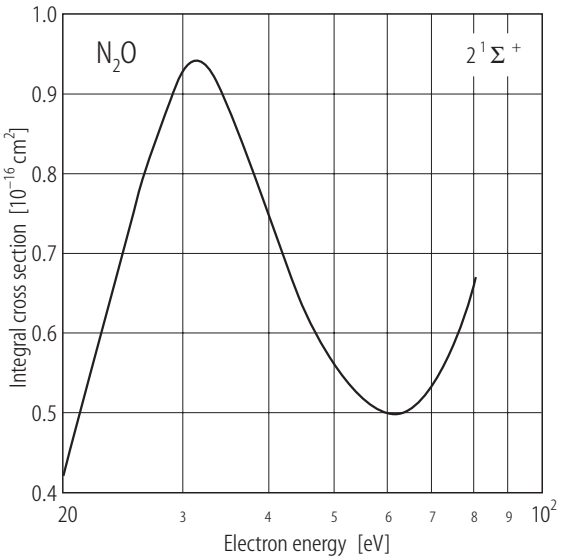

Fig. 6.4.44. Recommended integral cross section for $2^1\Sigma^+$ in N_2O.

Table 6.4.70. Preferred values of the integral cross section for the electron impact excitation of the $2^1\Sigma^+$ electronic state ($\sigma_{2^1\Sigma^+}$) of nitrous oxide.

Energy [eV]	$\sigma_{2^1\Sigma^+}$ [Å^2]
20	0.42
30	0.93
50	0.55
80	0.67

References for 6.4.5.7.4

99Mar1 Marinkovic, B., Panajotovic, R., R., Pesic, Z.D., Filipovic, D.M., Felfli, Z., Msezane, A.Z.: J. Phys. B: At. Mol. Opt. Phys. **32** (1999) 1949

6.4.5.7.5 $^1\Pi$

Absolute differential cross sections for electron impact excitation of the ($^2\Pi$) 3sσ $^1\Pi$ Rydberg electronic state of nitrous oxide have been reported by [99Mar1]. To derive integral cross sections from these differential measurements we have used a Molecular Phase Shift Analysis procedure, with these results being presented in Table 6.4.71 and plotted in Fig. 6.4.45.

The uncertainty on the cross sections is estimated to be ± 50 %.

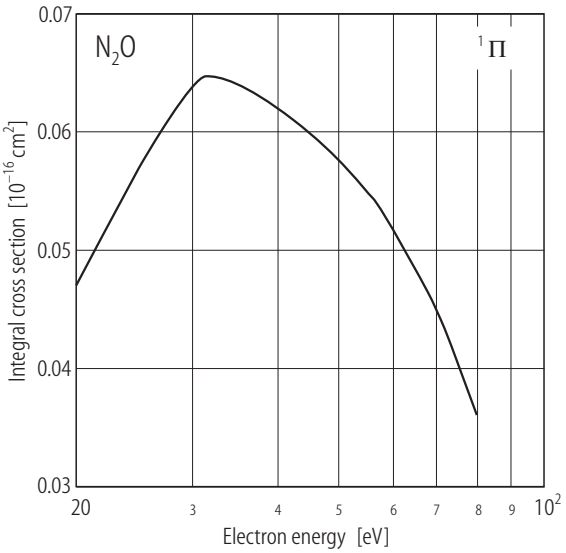

Fig. 6.4.45. Recommended integral cross section for $^1\Pi$ in N_2O.

Table 6.4.71. Preferred values of the integral cross section for the electron impact excitation of the $^1\Pi$ electronic state ($\sigma_{^1\Pi}$) of nitrous oxide.

Energy [eV]	($\sigma_{^1\Pi}$) [Å^2]
20	0.047
30	0.064
50	0.057
80	0.036

References for 6.4.5.7.5

99Mar1 Marinkovic, B., Panajotovic, R., Pesic, Z.D., Filipovic, D.M., Felfli, Z., Msezane, A.Z.: J. Phys. B: At. Mol. Opt. Phys. **32** (1999) 1949

6.4.5.8 Water (H_2O)

6.4.5.8.1 (000) → (010)

The available integral cross section data for electron impact excitation of the bending mode ((000) - (010)) of H_2O are due to [76Sen1, 88Shy1, 00Zei1]. There are some discrepancies between all three sets of results, and so our preferred cross section set was constructed from [76Sen1] for $\varepsilon < 6$ eV, from [00Zei1] for 6 eV $\leq \varepsilon \leq$ 10 eV and from [88Shy1] for ε = 15 and 20 eV where no other data exists. Our preferred set is tabulated in Table 6.4.72 and plotted in Fig. 6.4.46.

The uncertainty in the cross section is estimated to be ± 25 %.

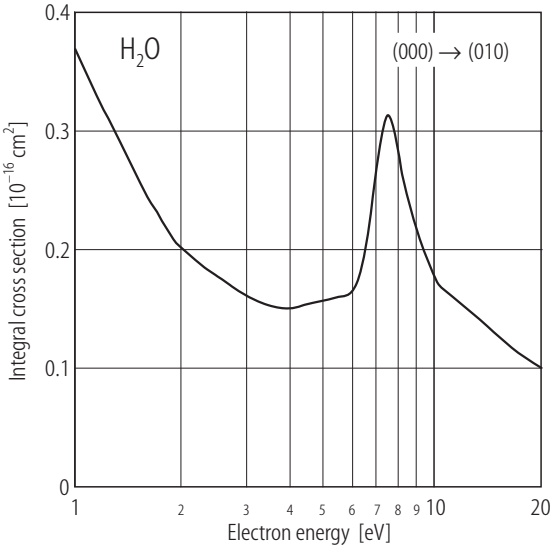

Fig. 6.4.46. Recommended integral cross section for (000) → (010) in H_2O.

Table 6.4.72. Preferred values of the integral (000) → (010) bending mode cross section (σ_{010}) for electron impact excitation in water.

Energy [eV]	σ_{010} [Å^2]	Energy [eV]	σ_{010} [Å^2]
1	0.370	6	0.163
2	0.200	7.5	0.317
2.2	0.190	8.75	0.227
3	0.160	10	0.180
4	0.150	15	0.130
5	0.157	20	0.100

References for 6.4.5.8.1

76Sen1 Seng, G., Linder, F.: J. Phys. B: At. Mol. Phys. **9** (1976) 2539
88Shy1 Shyn, T., Cho, S.Y., Cravens, T.E.: Phys. Rev. A **38** (1988) 678
00Zei1 El-Zein, A., Brunger, M.J., Newell, W.R.: Chem. Phys. Lett. **319** (2000) 701

6.4.5.8.2 (000) → (100 + 001)

The stretch modes of H_2O are essentially degenerate and so integral cross sections for their sum, (000) → (100 + 001) are usually reported in the literature. In this case the available electron impact integral cross sections are due to [76Sen1, 88Shy1, 00Zei1] and we note that in this case they are all in fair agreement with one another. Consequently all three data sets have been used to construct our preferred integral cross section. These data are tabulated in Table 6.4.73 and plotted in Fig. 6.4.47.

The uncertainty in the cross section is estimated to be ± 25 %.

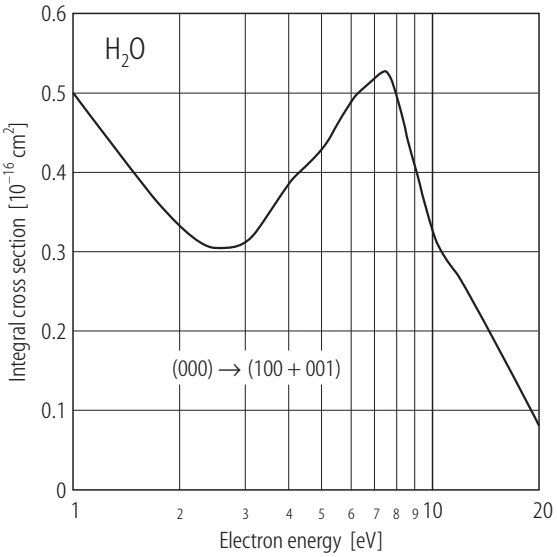

Fig. 6.4.47. Recommended integral cross section for (000) → (100 + 001) in H_2O.

Table 6.4.73. Preferred values of the integral (000) → (100 + 001) stretch mode cross section ($\sigma_{100+001}$) for electron impact excitation in water.

Energy [eV]	$\sigma_{100+001}$ [Å^2]	Energy [eV]	$\sigma_{100+001}$ [Å^2]
1	0.500	7.5	0.529
2.1	0.320	8	0.495
3	0.310	8.875	0.413
4	0.385	10	0.325
5	0.430	15	0.190
6	0.489	20	0.080
7	0.520		

References for 6.4.5.8.2

76Sen1 Seng, G., Linder, F.: J. Phys. B: At. Mol. Phys. **9** (1976) 2539
88Shy1 Shyn, T., Cho, S.Y., Cravens, T.E.: Phys. Rev. A **38** (1988) 678
00Zei1 El-Zein, A., Brunger, M.J., Newell, W.R.: Chem. Phys. Lett. **319** (2000) 701

6.4.5.9 Ammonia (NH_3)

6.4.5.9.1 $\nu_1 + \nu_3$ vibrational composite

Integral cross sections for electron impact excitation of the unresolved ν_1 symmetric stretch mode (ΔE = 414 meV) and ν_3 asymmetric stretch mode (ΔE = 427 meV) have been reported by [88Ben1] and [92Gul1]. The integral cross section of [88Ben1] was reported at ε = 7.3 eV, and that of [92Gul] at ε = 7.5 eV, with both values, allowing for the slight mismatch in energy near the peak of the ^{2}E shape resonance, being in good agreement with one another. We therefore report a single preferred integral cross section for $\nu_1 + \nu_3$ at ε = 7.5 eV, with this value being given in Table 6.4.74.

The uncertainty on this cross section is estimated to be ± 20 %.

Table 6.4.74. Preferred values of the integral $\nu_1 + \nu_3$ stretch mode composite cross section ($\sigma_{\nu_1+\nu_3}$) for electron impact excitation in ammonia.

Energy [eV]	($\sigma_{\nu_1+\nu_3}$) [Å^2]
7.5	0.67

References for 6.4.5.9.1

88Ben1 Ben Arfa, M., Tronc, M.: J. Chim. Physique **85** (1988) 889
92Gul1 Gulley, R.J., Brunger, M.J., Buckman, S.J.: J. Phys. B: At. Mol. Opt. Phys. **25** (1992) 2433

6.4.5.10 Ozone (O_3)

6.4.5.10.1 Hartley band electronic-states

The only integral cross section for electron impact excitation of the Hartley band electronic states in ozone is due to [96Swe1]. It therefore forms the basis for our preferred cross section which is tabulated in Table 6.4.75 and plotted in Fig. 6.4.48.

The uncertainty on these cross sections is estimated to be ± 26 % at ε = 7 and 10 eV and ± 22 % at ε = 15 and 20 eV.

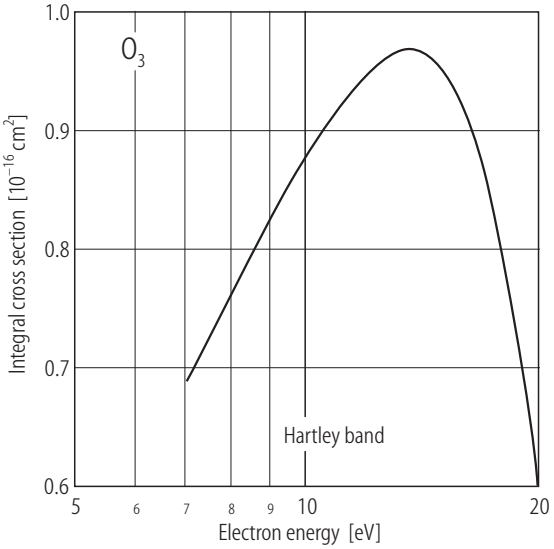

Fig. 6.4.48. Recommended integral cross section for the Hartley band in O_3.

Table 6.4.75. Preferred values of the integral cross section (σ_{HB}) for electron impact excitation of the Hartley band electronic-states of ozone.

Energy [eV]	σ_{HB} [Å^2]
7	0.69
10	0.88
15	0.95
20	0.60

References for 6.4.5.10.1

96Swe1 Sweeney, C.J., Shyn, T.W.: Phys. Rev. A **53** (1996) 1576

6.4.5.11 Carbonyl sulfide (OCS)

6.4.5.11.1 (000) → (010)

The only integral cross section measured for excitation of the bending mode in OCS ((000) → (010)) is due to [87Soh1]. Consequently our preferred cross section, as tabulated in Table 6.4.76 and plotted in Fig. 6.4.49, is taken directly from [87Soh1].

The uncertainty on these cross sections is estimated to be ± 20 %.

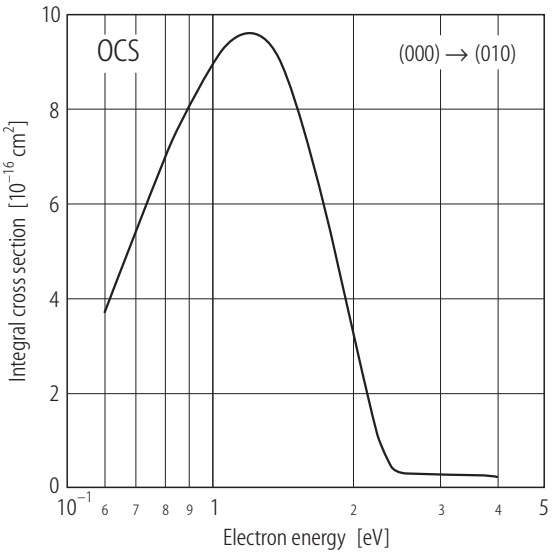

Fig. 6.4.49. Recommended integral cross section for (000) → (010) in OCS.

Table 6.4.76. Preferred values of the integral (000) → (010) bending mode cross section (σ_{010}) for electron impact excitation in carbonyl sulfide.

Energy [eV]	σ_{010} [Å^2]
0.6	3.65
1.15	9.6
2.5	0.3
3.0	0.27
3.5	0.28
4.0	0.25

References for 6.4.5.11.1

87Soh1 Sohn, W., Kochem, K-H., Scheuerlein, K.M., Jung, K., Ehrhardt, H.: J. Phys. B: At. Mol. Phys. **20** (1987) 3217

6.4.5.11.2 (000) → (100)

The only integral cross section measurement for excitation of the symmetric stretch mode in OCS ((000) → (100)) is also due to [87Soh1]. Thus our preferred cross section, as tabulated in Table 6.4.77 and plotted in Fig. 6.4.50, is taken directly from [87Soh1].

The uncertainty on these cross sections is estimated to be ± 20 %.

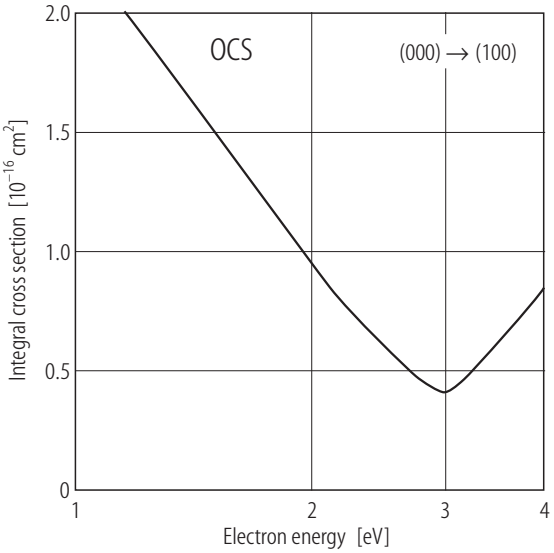

Fig. 6.4.50. Recommended integral cross section for (000) → (100) in OCS.

Table 6.4.77. Preferred values of the integral (000) → (100) symmetric stretch mode cross section (σ_{100}) for electron impact excitation in carbonyl sulfide.

Energy [eV]	σ_{100} [Å^2]
1.15	2.0
2.5	0.6
3.0	0.4
3.5	0.6
4.0	0.84

References for 6.4.5.11.2

87Soh1 Sohn, W., Kochem, K-H., Scheuerlein, K.M., Jung, K., Ehrhardt, H.: J. Phys. B: At. Mol. Phys. **20** (1987) 3217

6.4.5.11.3 (000) → (001)

Once again, the only integral cross section measurement for excitation of the asymmetric stretch mode in OCS ((000) → (001)) is also due to [87Soh1]. Thus our preferred cross section, as tabulated in Table 6.4.78 and plotted in Fig. 6.4.51, is taken directly from [87Soh1].

The uncertainty on these cross sections is estimated to be ± 20 %.

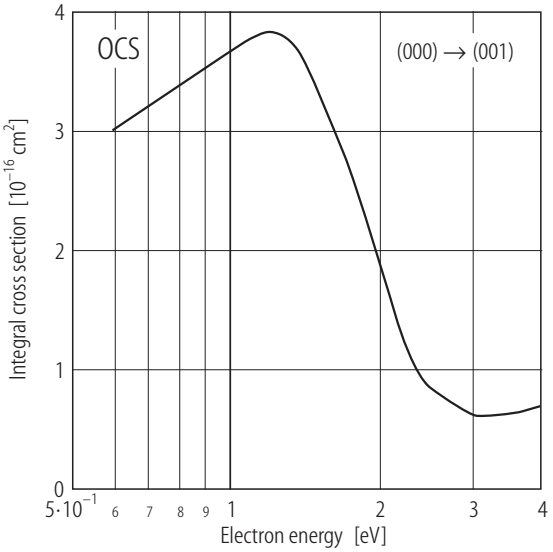

Fig. 6.4.51. Recommended integral cross section for (000) → (001) in OCS.

Table 6.4.78. Preferred values of the integral (000) → (001) asymmetric stretch mode cross section (σ_{001}) for electron impact excitation in carbonyl sulfide.

Energy [eV]	σ_{001} [Å^2]
0.6	3
1.15	3.8
2.5	0.82
3.0	0.62
3.5	0.63
4.0	0.69

References for 6.4.5.11.3

87Soh1 Sohn, W., Kochem, K-H., Scheuerlein, K.M., Jung, K., Ehrhardt, H.: J. Phys. B: At. Mol. Phys. **20** (1987) 3217

6.4.5.12 Methane (CH_4)

6.4.5.12.1 $\nu_{1,3}$ vibrational composite

Integral cross sections for excitation of the hybrid (unresolved) $\nu_{1,3}$ modes in CH_4 have been reported by [83Tan1, 91Shy1, 97Bun1]. The data of [83Tan1], for $\varepsilon \leq 7.5$ eV, tends to be somewhat systematically lower in magnitude than either [91Shy1] or [97Bun1]. Nonetheless, in our polynomial least squares fitting procedure we have used all three data sets to determine our preferred integral cross section for the $\nu_{1,3}$ modes. This cross section is tabulated in Table 6.4.79 and plotted in Fig. 6.4.52.

The uncertainty on these cross sections is estimated to be ± 25 %.

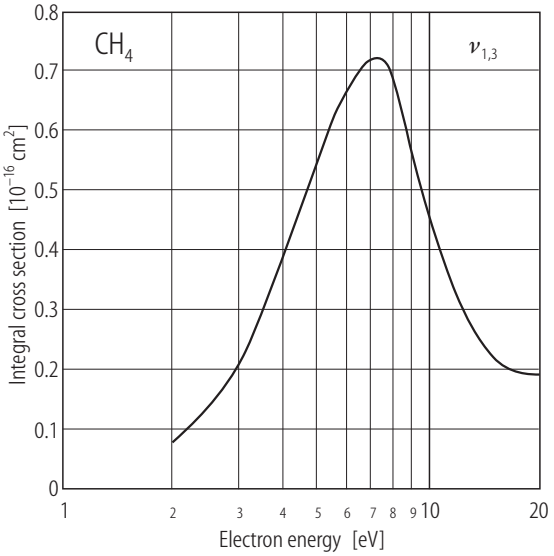

Fig. 6.4.52. Recommended integral cross section for the $\nu_{1,3}$ mode in CH_4.

Table 6.4.79. Preferred values of the integral $\nu_{1,3}$ hybrid vibrational mode cross section ($\sigma_{\nu_{1,3}}$) for electron impact excitation in methane.

Energy [eV]	$\sigma_{\nu_{1,3}}$ [Å^2]	Energy [eV]	$\sigma_{\nu_{1,3}}$ [Å^2]
2.0	0.080	10.0	0.450
3.0	0.204	12.5	0.291
4.0	0.384	15.0	0.220
5.0	0.558	20.0	0.190
7.5	0.716		

References for 6.4.5.12.1

83Tan1 Tanaka, H., Kubo, M., Onodera, N., Suzuki, A.: J. Phys. B: At. Mol. Phys. **16** (1983) 2861
91Shy1 Shyn, T.W.: J. Phys. B: At. Mol. Opt. Phys. **24** (1991) 5169
97Bun1 Bundschu, C.T., Gibson, J.C., Gulley, R.J., Brunger, M.J., Buckman, S.J., Sanna, N., Gianturco, F.A.: J. Phys. B: At. Mol. Opt. Phys. **30** (1997) 2239

6.4.5.12.2 $\nu_{2,4}$ vibrational composite

Integral cross sections for excitation of the hybrid (unresolved) $\nu_{2,4}$ modes in CH_4 have been reported by [83Tan1, 91Shy1, 97Bun1]. At 3 eV the data of [83Tan1] is significantly smaller in magnitude than that of [97Bun1], while at 5 eV the cross sections of [83Tan1] and [91Shy1] are also smaller in magnitude than that of [97Bun1]. Whilst we believe the more recent measurement [97Bun1] is the most reliable, we have nonetheless incorporated all three cross section sets in our polynomial least squares fit to determine the preferred integral cross section for the $\nu_{2,4}$ modes. This cross section is tabulated in Table 6.4.80 and plotted in Fig. 6.4.53.

The uncertainty on these cross sections is estimated to be ± 25 %.

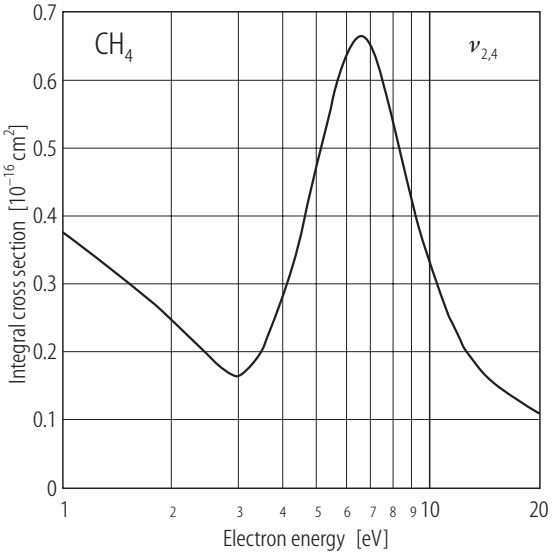

Fig. 6.4.53. Recommended integral cross section for the $\nu_{2,4}$ mode in CH_4.

Table 6.4.80. Preferred values of the integral $\nu_{2,4}$ hybrid vibrational mode cross section ($\sigma_{\nu_{2,4}}$) for electron impact excitation in methane.

Energy [eV]	$\sigma_{\nu_{2,4}}$ [Å^2]	Energy [eV]	$\sigma_{\nu_{2,4}}$ [Å^2]	Energy [eV]	$\sigma_{\nu_{2,4}}$ [Å^2]
1.0	0.377	6.0	0.644	10.0	0.333
2.0	0.242	7.0	0.647	12.5	0.203
3.0	0.163	7.5	0.591	15.0	0.153
4.0	0.284	8.0	0.527	17.5	0.128
5.0	0.495	9.0	0.418	20.0	0.109

References for 6.4.5.12.2

83Tan1 Tanaka, H., Kubo, M., Onodera, N., Suzuki, A.: J. Phys. B: At. Mol. Phys. **16** (1983) 2861
91Shy1 Shyn, T.W.: J. Phys. B: At. Mol. Opt. Phys. **24** (1991) 5169
97Bun1 Bundschu, C.T., Gibson, J.C., Gulley, R.J., Brunger, M.J., Buckman, S.J., Sanna, N., Gianturco, F.A.: J. Phys. B: At. Mol. Opt. Phys. **30** (1997) 2239

6.4.5.13 Ethane (C_2H_6)

6.4.5.13.1 ν_b bending vibrational composite

The only integral cross section measurement for electron impact excitation of the bending composite vibrational modes in C_2H_6 (ν_b) is due to [90Boe1]. Consequently our preferred cross section, as tabulated in Table 6.4.81 and plotted in Fig. 6.4.54, is taken directly from [90Boe1].

The uncertainty on these cross sections is estimated to be ± 25 %.

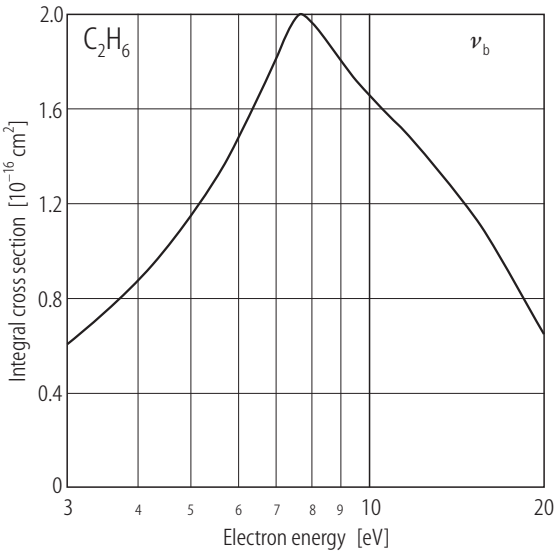

Fig. 6.4.54. Recommended integral cross section for the ν_b mode in C_2H_6.

Table 6.4.81. Preferred values of the integral ν_b bending composite mode cross section (σ_{ν_b}) for electron impact excitation in ethane.

Energy [eV]	σ_{ν_b} [Å^2]
3	0.604
5	1.185
7.5	2.012
10	1.651
15	1.158
20	0.648

References for 6.4.5.13.1

90Boe1 Boesten, L., Tanaka, H., Kubo, M., Sato, H., Kimura, M., Dillon, M.A., Spence, D.: J. Phys. B: At. Mol. Opt. Phys. **23** (1990) 1905

6.4.5.13.2 ν_s stretching vibrational composite

The only integral cross section measurement for electron impact excitation of the stretching composite vibrational modes in C_2H_6 (ν_s) is also due to [90Boe1]. Thus our preferred cross section, as tabulated in Table 6.4.82 and plotted in Fig. 6.4.55, is taken directly from [90Boe1].

The uncertainty on these cross sections is estimated to be ± 27 %.

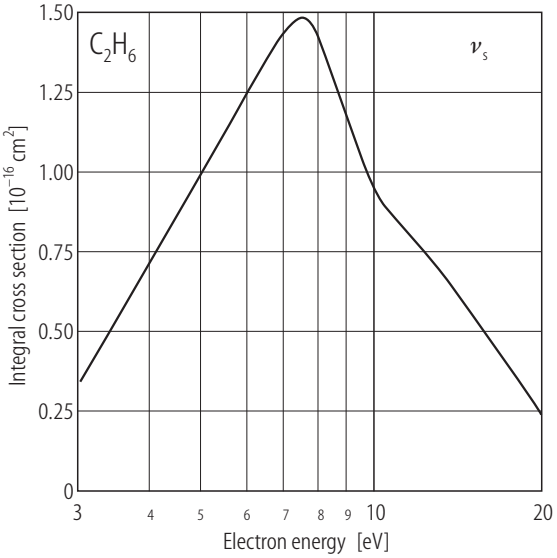

Fig. 6.4.55. Recommended integral cross section for the ν_s mode in C_2H_6.

Table 6.4.82. Preferred values of the integral ν_s stetching composite mode cross section (σ_{ν_s}) for electron impact excitation in ethane.

Energy [eV]	σ_{ν_a} [Å^2]
3	0.344
5	1.022
7.5	1.483
10	0.952
15	0.552
20	0.234

References for 6.4.5.13.2

90Boe1 Boesten, L., Tanaka, H., Kubo, M., Sato, H., Kimura, M., Dillon, M.A., Spence, D.: J. Phys. B: At. Mol. Opt. Phys. **23** (1990) 1905

6.4.5.14 Ethyne (C_2H_2)

6.4.5.14.1 $\nu_{1,3}$ vibrational composite

Integral cross sections for excitation of the composite (unresolved) $\nu_{1,3}$ modes in C_2H_2 have been reported by [85Koc1] and [93Kha1]. These data sets do not overlap in energy and so we have employed them both in constructing our preferred cross section. This preferred integral cross section is tabulated in Table 6.4.83 and plotted in Fig. 6.4.56.

The uncertainty on these cross sections is estimated to be ± 35 %.

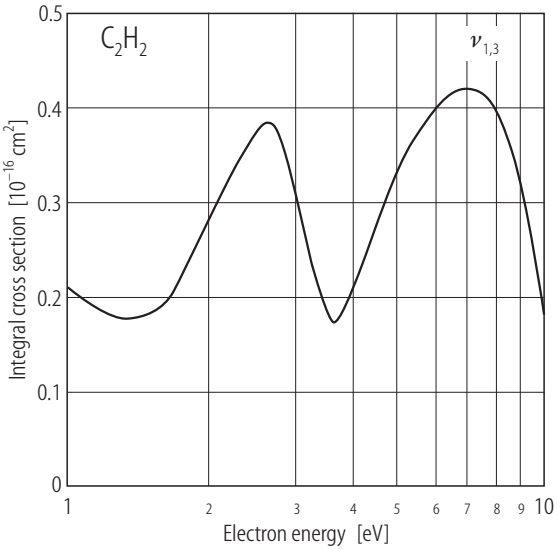

Fig. 6.4.56. Recommended integral cross section for the $\nu_{1,3}$ mode in C_2H_2.

Table 6.4.83. Preferred values of the integral $\nu_{1,3}$ composite mode cross section ($\sigma_{\nu_{1,3}}$) for electron impact excitation in ethyne.

Energy [eV]	$\sigma_{\nu_{1,3}}$ [Å^2]
1.0	0.21
1.6	0.192
2.0	0.287
2.6	0.383
3.6	0.172
5.0	0.340
10.0	0.180

References for 6.4.5.14.1

85Koc1 Kochem, K-H., Sohn, W., Jung, K., Ehrhardt, H., Chang, E.S.: J. Phys. B: At. Mol. Phys. **18** (1985) 1253

93Kha1 Khakoo, M.A., Jayaweera, T., Wang, S., Trajmar, S.: J. Phys. B: At. Mol. Opt. Phys. **26** (1993) 4845

6.4.5.14.2 ν_2 vibrational mode

Integral cross sections for excitation of the ν_2 normal vibrational mode in C_2H_2 have also been reported by [85Koc1] and [93Kha1]. These data sets do not overlap in energy and so once again we have employed them both when constructing our preferred cross section. This preferred integral cross section is tabulated in Table 6.4.84 and plotted in Fig. 6.4.57.

The uncertainty on these cross sections is estimated to be ± 35 %.

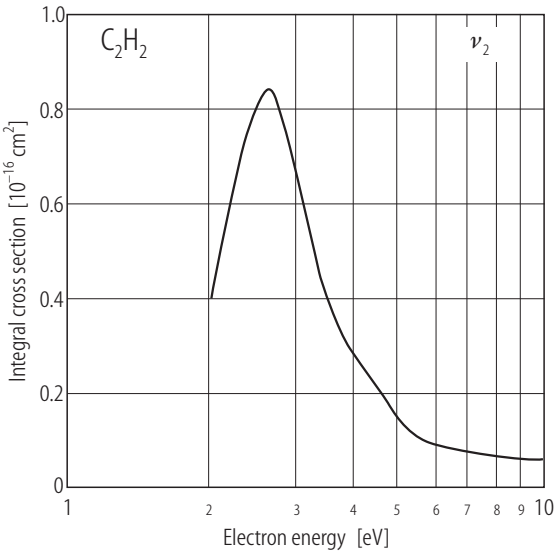

Fig. 6.4.57. Recommended integral cross section for the ν_2 mode in C_2H_2.

Table 6.4.84. Preferred values of the integral ν_2 normal vibrational mode cross section (σ_{ν_2}) for electron impact excitation in ethyne.

Energy [eV]	σ_{ν_2} [Å^2]
2.0	0.400
2.6	0.840
3.6	0.370
5.0	0.140
10.0	0.059

References for 6.4.5.14.2

85Koc1 Kochem, K-H., Sohn, W., Jung, K., Ehrhardt, H., Chang, E.S.: J. Phys. B: At. Mol. Phys. **18** (1985) 1253

93Kha1 Khakoo, M.A., Jayaweera, T., Wang, S., Trajmar, S.: J. Phys. B: At. Mol. Opt. Phys. **26** (1993) 4845

6.4.5.14.3 $\nu_{4,5}$ vibrational composite

Once again, integral cross sections for excitation of the composite (unresolved) $\nu_{4,5}$ modes in C_2H_2 have been reported by [85Koc1] and [93Kha1]. These data sets have both been used in determining our preferred cross section, which is tabulated in Table 6.4.85 and plotted in Fig. 6.4.58.

The uncertainty on these cross sections is estimated to be ± 35 %.

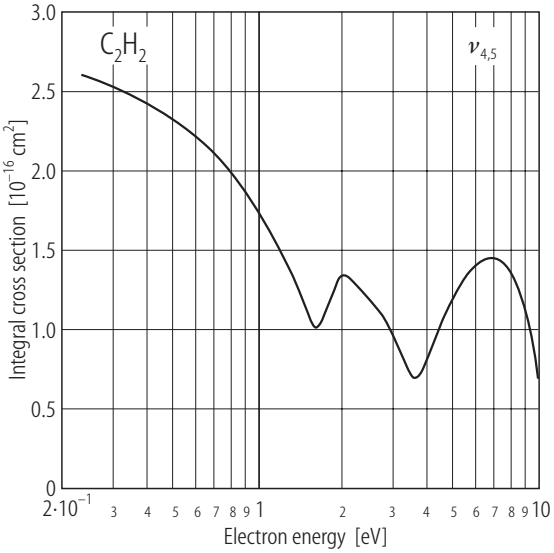

Fig. 6.4.58. Recommended integral cross section for the $\nu_{4,5}$ mode in C_2H_2.

Table 6.4.85. Preferred values of the integral $\nu_{4,5}$ composite mode cross section ($\sigma_{\nu_{4,5}}$) for electron impact excitation in ethyne.

Energy [eV]	$\sigma_{\nu_{4,5}}$ [Å^2]
0.235	2.600
1.0	1.740
1.6	1.000
2.0	1.340
2.6	1.150
3.6	0.690
5.0	1.220
10.0	0.690

References for 6.4.5.14.3

85Koc1 Kochem, K-H., Sohn, W., Jung, K., Ehrhardt, H., Chang, E.S.: J. Phys. B: At. Mol. Phys. **18** (1985) 1253

93Kha1 Khakoo, M.A., Jayaweera, T., Wang, S., Trajmar, S.: J. Phys. B: At. Mol. Opt. Phys. **26** (1993) 4845

6.4.5.15 Carbon tetrafluoride (CF_4)

6.4.5.15.1 $\nu_1 + \nu_2 + \nu_3 + \nu_4$ vibrational excitation

Differential cross sections for electron impact excitation of the ν_1, ν_2, ν_3 and ν_4 fundamental modes of vibration for CF_4 have been reported by [92Man1] and [92Boe1]. However, they did not report integral cross sections in these studies. Nonetheless, [94Bon1] derived integral cross sections, for energies in the range ε = 1.5 - 20 eV, from the work of [92Man1] and [94Boe1] and reported them as an integral cross section for the sum $\nu_1 + \nu_2 + \nu_3 + \nu_4$ of the fundamental modes. We have taken this experimentally-based integral cross section (for $\nu_1 + \nu_2 + \nu_3 + \nu_4$) as our preferred integral cross section. It is tabulated in Table 6.4.86 and plotted in Fig. 6.4.59.

The uncertainty on these cross sections is estimated to be ± 35 %.

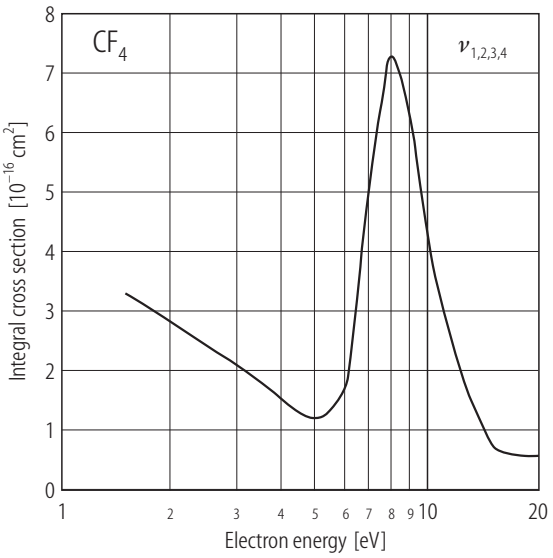

Fig. 6.4.59. Recommended integral cross section for the $\nu_{1,2,3,4}$ mode in CF_4.

Table 6.4.86. Preferred values of the integral $\nu_1 + \nu_2 + \nu_3 + \nu_4$ composite mode cross section ($\sigma_{\nu_1+\nu_2+\nu_3+\nu_4}$) for electron impact excitation in carbon tetrafloride.

Energy [eV]	$\sigma_{\nu_1+\nu_2+\nu_3+\nu_4}$ [Å^2]	Energy [eV]	$\sigma_{\nu_1+\nu_2+\nu_3+\nu_4}$ [Å^2]
1.5	3.30	8.0	7.30
2.0	2.80	9.0	6.30
3.0	2.10	10.0	4.30
5.0	1.20	15.0	0.76
6.0	1.70	20.0	0.55
7.0	5.30		

References for 6.4.5.15.1

92Man1 Mann, A., Linder, F.: J. Phys. B: At. Mol. Opt. Phys. **25** (1992) 545
92Boe1 Boesten, L., Tanaka, H., Kobayashi, A., Dillon, M.A., Kimura, M.: J. Phys. B: At. Mol. Opt. Phys. **25** (1992) 1607
94Bon1 Bonham, R.A.: Jpn. J. Appl. Phys. **33** (1994) 4157

6.4.6 Concluding remarks

After an extensive and critical search of the literature we have presented recommended inelastic cross sections for 15 important molecules. Great care was taken when applying our procedure for deriving each of the recommended cross section sets presented in this paper. In spite of this attention to detail we feel it important to note that there is no guarantee that our recommended cross section sets, when subjected to a Boltzmann or Monte Carlo analysis, will exactly reproduce the relevant transport parameters. We would hope, however, that when subjected to such an analysis our recommended sets would be largely consistent with the transport data, to within the uncertainties we quote.

Appendix

Index by molecular species

A list of the molecules included in volume I/17C is given below. The 2nd to 8th columns correspond to the collision processes dealt with in the volume: photo-absorption, -ionization and -dissociation (P), electron-impact ionization (E/ion), electron attachment (E/att), total scattering cross section for electron collision (E/tot), electron elastic scattering (E/elas), electron momentum transfer cross section (E/mom), and electron-impact excitation (E/exc), respectively. When cross section data are given for the respective process involving the respective molecule, the corresponding page number is indicated in the corresponding column on the line for the relevant molecule. The molecules are listed in the ascending order of the number of constituent atoms.

	P	E/ion	E/att	E/tot	E/elas	E/mom	E/exc
2 atoms							
CO	4-17	5-19	5-85	6-11	6-59	6-92	6-153
CS		5-25					
HBr			5-88				
HCl	4-35		5-87	6-21			
HF	4-36						
HI			5-89				
LiBr				6-44			
CsCl				6-44			
NO	4-44	5-60	5-86	6-11	6-60	6-94	6-164
Br_2		5-7					
Cl_2	4-32	5-42	5-83	6-42			
D_2						6-89	
F_2		5-43	5-82				
H_2	4-38	5-50	5-80	6-11	6-55	6-88	6-120
K_2				6-44			
Li_2				6-44			
N_2	4-45	5-62		6-11	6-56	6-90	6-129
Na_2				6-44			
O_2	4-50	5-67	5-81	6-11	6-58	6-95	6-146
S_2		5-72					

	P	E/ion	E/att	E/tot	E/elas	E/mom	E/exc
3 atoms							
CO_2	4-19	5-22	5-94	6-17	6-68	6-103	6-180
CS_2	4-20	5-26	5-95	6-17	6-75		
ClO_2				6-42			
H_2O	4-40	5-52	5-91	6-21	6-63	6-98	6-186
H_2S	4-41	5-54	5-93	6-21	6-67	6-102	
NO_2		5-61		6-17			
N_2O	4-47	5-65	5-99	6-17	6-69	6-106	6-182
OCS	4-48	5-21	5-99	6-17	6-71		6-190
SO_2	4-53	5-69	5-101	6-17	6-73	6-108	
O_3		5-70	5-103	6-42			6-189
4 atoms							
C_2H_2	4-21	5-29		6-24	6-64		6-197
NF_3		5-44			6-74	6-110	
NH_3	4-42	5-55	5-106	6-21	6-62	6-97	6-188
5 atoms							
CCl_4	4-7	5-10	5-109	6-29			
$CFCl_3$				6-29			
CF_2Cl_2		5-8		6-29	6-80		
CF_3Cl				6-29	6-79		
CF_3H				6-29		6-109	
CF_4	4-9	5-15	5-108	6-29	6-78	6-112	6-200
CH_3Br		5-5		6-33			
CH_3Cl		5-11		6-33			
CH_3F		5-11		6-33			
CH_3I		5-11		6-33			
CH_4	4-15	5-17	5-107	6-24	6-61	6-96	6-193
$GeCl_4$				6-39			
GeF_4				6-39			
GeH_4				6-39	6-76		
$SiBr_4$				6-41			
$SiCl_4$				6-39, 6-41			
SiF_4		5-46		6-39, 6-41			

	P	E/ion	E/att	E/tot	E/elas	E/mom	E/exc
$SiHCl_3$				6-41			
SiH_2Cl_2				6-41			
SiH_4	4-55	5-58		6-39, 6-41	6-66	6-101	
SiI_4				6-41			
6 atoms or more							
CH_3OH	4-13	5-16		6-33			
C_2F_6		5-27		6-35	6-81	6-113	
C_2H_4	4-23	5-30		6-24			
C_2H_6	4-24	5-34		6-24	6-65	6-99	6-195
C_3F_8		5-37		6-35	6-84	6-117	
C_3H_4	4-26						
C_3H_6	4-33						
C_3H_8	4-27	5-39		6-24	6-70	6-105	
CH_3OCH_3	4-10						
$CH_3OC_2H_5$	4-11						
C_6F_6				6-35	6-83	6-116	
C_6H_6	4-29			6-24, 6-42	6-77	6-111	
SF_6	4-51	5-47	5-110	6-35	6-82	6-114	
UF_6		5-49					
WF_6				6-35			
Si_2H_6	4-57	5-59			6-72	6-107	
C_{60}		5-40					